THE DEVELOPMENT OF TRANSITION METAL COMPLEXES TO TARGET HYPOXIC CELLS

Emma Louise Dux

A thesis submitted for the degree of

Doctor of Philosophy

University of York

Department of Chemistry

September

2011

Abstract

Hypoxic regions (areas of subnormal oxygen levels) are a common feature with solid tumours that have reached a size of 2-3 mm in diameter. Such regions have characteristically responded poorly to conventional anti-cancer treatments such as radiation or chemotherapeutics. It has been previously demonstrated that the specific targeting of these cells is possible with compounds of specific properties, such as tirapazamine.

This thesis describes an exploration of using transition metal complexes of cobalt(III) and copper(II) as hypoxia-selective prodrugs for use in cancer chemotherapy. The aim has been to use both the lowered pH and lowered oxygen levels found within hypoxic regions to activate prodrugs into their cytotoxic active form. Through doing this, the coordination chemistry of medicinally active *N*-oxide ligands has been expanded upon, including the first transition metal complexes of tirapazamine and the development of a novel series of heteroleptic complexes featuring an *N*-oxide and 2,2'-dipyridylamine ligand. The solution properties of the prepared complexes and their uncoordinated ligands have been studied so that their behaviour in biological systems can be better understood. The cobalt(III) heteroleptic complexes are shown to have promise for the purpose of improving delivery of *N*-oxide based drugs, improving their solubility and altering their delivery and release. The complex of a tirapazamine analogue $[Co(tpz\text{-}CN)(dpHa)_2]^{2+}$ was shown to release the cytotoxic *N*-oxide rapidly under hypoxic conditions, but promisingly, this dissociation appears to be hindered in the presence of oxygen. *In vitro* cytotoxicity studies on this complex showed it to have the same IC_{50} value as its *N*-oxide ligand, providing promise for the heteroleptic system as prodrugs.

Contents

List of Tables

1. Chapter One Tables

2. Chapter Two Tables

List of Figures

1. Chapter One Figures

2. Chapter Two Figures

4. Chapter Four Figures

List of Schemes

1. Chapter One Schemes

2. Chapter Two Schemes

3. Chapter Three Schemes

Acknowledgements

I would like to thank my supervisors Prof. Paul Walton and Dr. Anne-K. Duhme-Klair for providing the opportunity to carry out this project, and Prof. Ian Fairlamb for his many pieces of advice and support. I would especially like to thank Paul for all his endless help and patience in helping sort myself out whenever I needed 'super-gluing' back together on all the many occasions over the past 8 years. Thank you to Sentinel Oncology for their funding of this project. The following people have all made the working of the project possible: Helen Burrell for the training in cell culturing, Shirley Roberts, Sally Lewis, Jared Cartwright and Simon Grist for helping with fixing bits of kit and helping sorting out any biological problems that inevitably turned up, Adrian and Rob of the 'Whitwood-Thatcher Centre of Excellence' for putting on my crystals and finalising the solving of crystal structures when the disorder got too much for me and last but not least Naser and Iman for all their general advice, help and being the 'parents' of the group. A big thank you to all those who keep everything functioning and working in the department; Heather and Amanda (NMR), Karl (MS) and Steve and Mike in stores.

Thank you to all the people who have helped make the Chemistry Department a friendly, caring and enjoyable place to work in; especially Cath, Maria, Aimee, Abeda, Luisa, Áine, Christine, James, Sara and Tom. I wouldn't be here today with all the help and enthusiasm of the people who have taught me over the years, starting from when Chemistry was my least favourite pre-GCSE's right up to making me determined keep going with it after graduating. Thanks to all the people who have helped keep me sane(ish) over the pas t four years by providing great company at the bar-containing institution down the road on a Friday night and Deb for providing me with entertaining phone calls when late night writing desperation was starting to set in. Thanks to Helen, Phil, Julia, Sue and Dave in teaching labs for helping keep me sane (as is possible for me) leading up to the viva and for the all the much needed cups of tea and coffee!!

Thank you to my parents and brother for always being supportive when things didn't go my way and for always believing that I could achieve what I wanted as long as I stuck at it long enough.

Declaration

All the work reported in this thesis was carried out by the author apart from the following:

- Synthesis of py-dpHa-CN was carried out by Sentinel Oncology
- 700 MHz NMR spectroscopy was performed by Dr David Williamson
- 500 NMR spectroscopy was performed by Dr Naseralla Jasim
- Mass spectra were obtained by the MS service at the University of York
- CHN analyses were performed by Drs Phil Helliwell and Graeme McAllister
- Data collection for XRD experiments carried out by Dr Adrain Whitwood and Robert Thatcher

Structures and names of ligands reported within this thesis

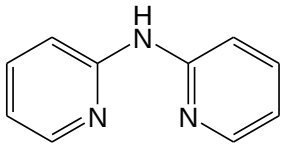

dpHa

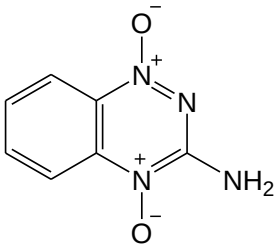

tpzH

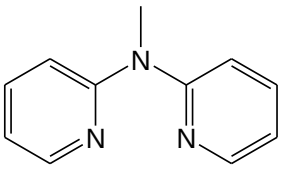

dpma

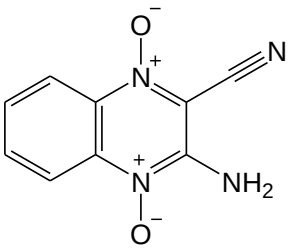

tpzH-CN

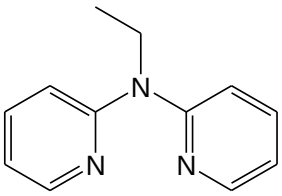

dpea

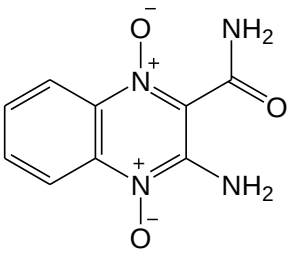

tpzH-CONH$_2$

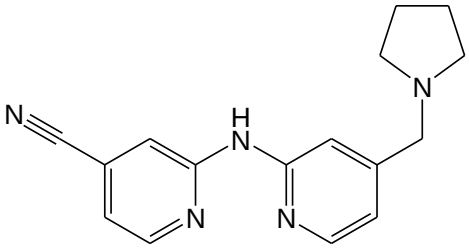

py-dpHa-CN

1. Introduction

1.1. Preamble

Cancer is a term used to describe over two hundred diseases which affect various organs, systems and tissues throughout the body but share several characteristics which include uncontrolled cellular growth.[1] Most forms of cancer involve the formation of neoplasms (new growths) more commonly known as tumours, with notable exceptions including leukaemias. Cancer is said to be a complex disease, in that there is a connection between genotype (characteristics arising from genetic coding) and phenotype (characteristics expressed by an organism) but the correlation was found to be weak. Cancer is a complex disease in that it is the result of a multitude of factors, ranging from genetic to environmental factors. Due to the large range of contributing factors, the occurrence of the disease is hard to predict.

Statistically one in three people in the UK will be diagnosed with a form of cancer during their life. In 2009, one in four of all deaths involved cancer, accounting for around 156 000 deaths.[2] Cancer, along with other non-communable (non-infectious) diseases such as cardiac disease, neurodegenerative disorders and diabetes are the major causes of death in the western world owing to its aging population (**Figure 1.1**), hence why the amount of research devoted to finding new treatments for these conditions has grown over the past few decades.[3]

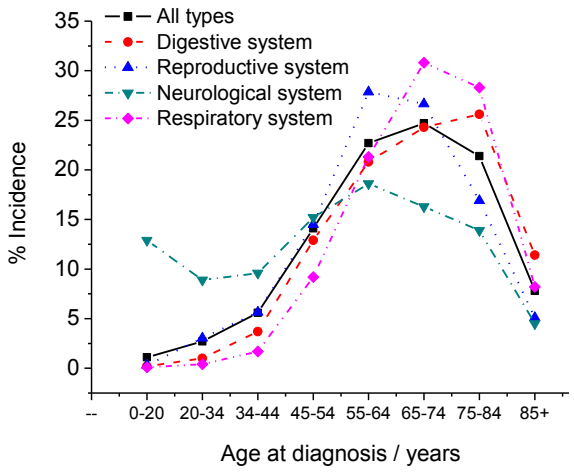

Figure 1.1: Age distribution of the incidence of cancer according to age group between 2004 and 2008 in the USA.[3]

Developments into anticancer agents such as cisplatin, along with earlier diagnoses, which use increasingly sensitive techniques, have vastly improved the prognosis for many cancer patients. However, despite these advances, there still remain several types of cancers which are problematic to treat such as brain tumours and prostate cancer, providing the need to develop improved anticancer agents with improved properties.[2] There is also the desire to develop agents which can selectively target cancer cells, with techniques such as targeting specific genes or enzymes specifically expressed within tumours. The need for this is driven by the unpleasant side effects that accompany many anticancer chemotherapy agents such as cell loss, nausea and diminished immunological strength, brought about by their lack of selectivity in targeting cancer cells.

1.2. Hypoxia in tumours

Cancerous cells are set apart from normal healthy cells by several characteristics.[4] These six hallmarks of sustained angiogenesis, unlimited replication potential, ability to metastasise, evasion of apoptosis, evasion of anti-growth and self-sufficiency in growth signals enable cancer cells to escape the normal cellular control mechanisms which act within healthy cells. Angiogenesis is an important factor in tumour growth as it allows the tumour to develop a new vascular network in the surrounding tissue from a pre-existing blood vessel.

Cell growth within normal tissues is a carefully controlled process, being regulated by several ‘checkpoints’ which occur throughout the cell cycle (**Figure 1.2**). The eukaryotic cell cycle consists of two main stages; interphase where the cell prepares itself for replication and mitosis where the division of the cell’s nucleus occurs. The interphase stage can be further subdivided into three stages; G_1, synthesis and G_2.[5]

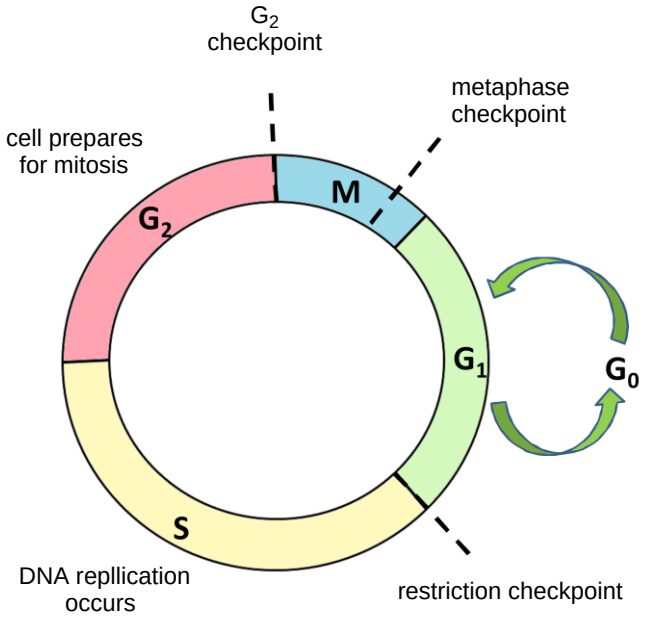

Figure 1.2: Schematic representation of the cell cycle

The G_1 phase involves the preparation of the enzymes needed for the DNA replication which occurs during the synthesis phase. During the G_2 phase, several proteins are synthesised including the production of microtubule structures essential to the cell division process of mitosis. The G_0 phase (cell quiescence) is when the cell is dormant, making no preparations for replication.[6]

In order for replication to take place, the cell must successfully pass through the various checkpoints. To pass the G_1 restriction checkpoint, the cell must be in a favourable environment and suitable condition for cell division to begin. Passage through the G_2 checkpoint requires the entire cellular DNA to have been successfully replicated so that a chain of reactions can then take place which signal for the mitosis process to begin. There is also a checkpoint to ensure all chromosomes are attached to the cell's spindle which occurs during mitosis before the metaphase where the cell division begins.[6]

Deregulation of the cell cycle through loss of checkpoint control causes a decreased genetic stability and uncontrolled cellular growth, facilitating tumour progression. The overall result of these characteristics is that cancer cells grow in a rapid, disordered, unstructured and unregulated manner quite like that of healthy tissue.

1.2.1. Tumour vasculature

The vascular network within solid tumours is remarkably different to that found within normal tissue. Two types of vasculature are found within tumours; one being the vessels which existed in the tissue before the cancer invaded and the other being the vessels which have grown as a result of the malignant tissue's increased angiogenic capability.[7] The latter are prone to structural abnormalities such as swollen capillaries and incomplete endothelial lining of the vessel walls which causes them to leak.[8] Both types are suspect to the development of blockages and blind ends as a result of the tissue's uncontrolled growth putting an increased pressure onto the vessel walls.[9, 10]

The poorly defined structure of a tumour's vascular network can lead to cells being remote from any fully functioning blood vessels. Oxygen can typically diffuse 150 μm through tissue but cells located at a distance greater than this from a functioning vessel have a lower partial pressure of oxygen within them (**Figure 1.3**).[11]

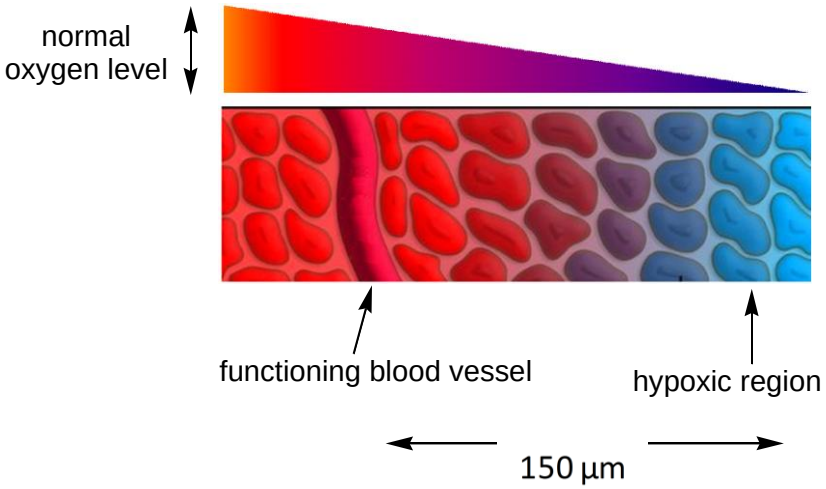

Figure 1.3: The occurrence of hypoxia as a result of increasing distance from functioning blood vessels in tumours.[12]

Cells with lowered oxygen levels are said to be hypoxic, and regions of such conditions were first recognised to occur within solid tumours during the mid 1950's.[9] The development of hypoxic regions has been found to occur in the early stages of tumour development and can typically be found in any solid tumour which

has reached over 2–3 mm in diameter.[13] There are two general types of hypoxia which have been found to occur within solid tumours. Chronic hypoxia is brought about by the cells being too far from a functioning blood vessel whilst intermittent hypoxia occurs when the irregular blood flow through vessels leaves regions of the tumour under-perfused for a temporary period of time.[14]

1.2.2. Cellular effects of tumour hypoxia

Hypoxia-inducible factor 1 (HIF-1) is a transcription factor continually produced in all cells. Under normally oxygenated conditions, HIF-1 is hydroxylated by a prolyl hydroxylase enzyme (PHD) in the presence of ascorbate, iron(II), oxygen and α-ketoglutarate (**Scheme 1.1**).[13] The hydroxylated HIF-1 is then recognised as a substrate by a ubiquitin-ligase enzyme which degrades the transcription factor.[13]

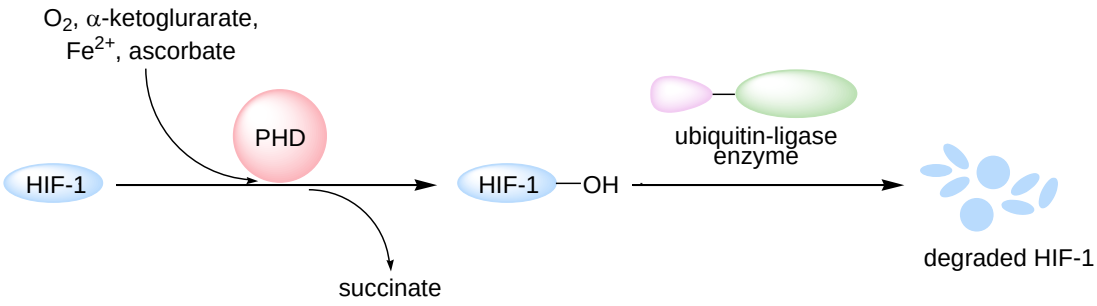

Scheme 1.1: The cellular degradation of HIF-1 (Hypoxia-inducible factor 1) under normally oxygenated conditions.[13]

Under hypoxic conditions, the degradation of HIF-1 is inhibited, causing it to accumulate within the cell's nucleus where it interacts with an aryl hydrocarbon receptor nuclear translocator (ARNT). This causes the ARNT to become transcriptionally active and results in either the initiation of the cells process to adapt to survival under the hypoxic conditions or cell death.[15] If the adaptation mechanism is activated, the cell increases its expression of glycolytic enzymes such as hexokinase, and protein pyruvate kinase-1.[15, 16] It also codes for the over-expression of proteins to aid increased glycolysis, such as the glucose transporter GLUT1 which facilitates glucose uptake.[15, 16] These combined alterations allow for an increased rate in anaerobic respiration, greater than that which occurs in normally oxygenated

tumour tissue, to produce sufficient amounts of ATP to meet the cell's energy requirements. As in normal tissue, the increased glycolytic rate results in the formation of acidic by-products.

The activation of ARNT by HIF-1 gives rise to an increased expression of vascular endothelial growth factor (VEGF) which signals for increased angiogenesis. This results in the regions of hypoxia within tumours to be transient, as once an area becomes hypoxic the increased expression of VEGF is signalled for so that more blood vessels are formed to improve the oxygen supply, but as the tumour grows other hypoxic regions develop.[17, 18]

The occurrence of hypoxia in tumours has been correlated with an increasingly aggressive phenotype due to the higher rate of mutations, with an increased occurrence of metastasis. The greater potential for metastasis is also believed to be due to the tumour cell having already adapted to a hostile environment, so the hypoxic cell is more adapted to breaking off from the main tumour and invading elsewhere.[19]

Another chemical difference which sets hypoxic regions apart from normoxic regions is pH. It was initially assumed that the intracellular pH of hypoxic cells was more acidic than normoxic tumour cells. This was chiefly based on measurements made with pH microelectrodes, but it was only later realised that these electrodes were only measuring the extracellular pH rather than that inside the cell.[20] It was with the use of techniques such as ^{31}P NMR spectroscopy which allowed the measurement of chemical shifts of the species within the cell against that of the equivalent compound at known pH values.

Figure 1.4 shows that in a normally oxygenated cell, glucose is transported into the cell by glucose transporter proteins (GLUT) where it is converted to pyruvate. It is then transferred to the cell's mitochondria where it is reacted with oxygen in the Kreb's cycle to produce energy, forming CO_2 as a waste product. The CO_2 can leave the cell by diffusing through the cell membrane and into the blood stream or can be hydrated by carbonic anyhydrase enzyme to form bicarbonate and a proton.

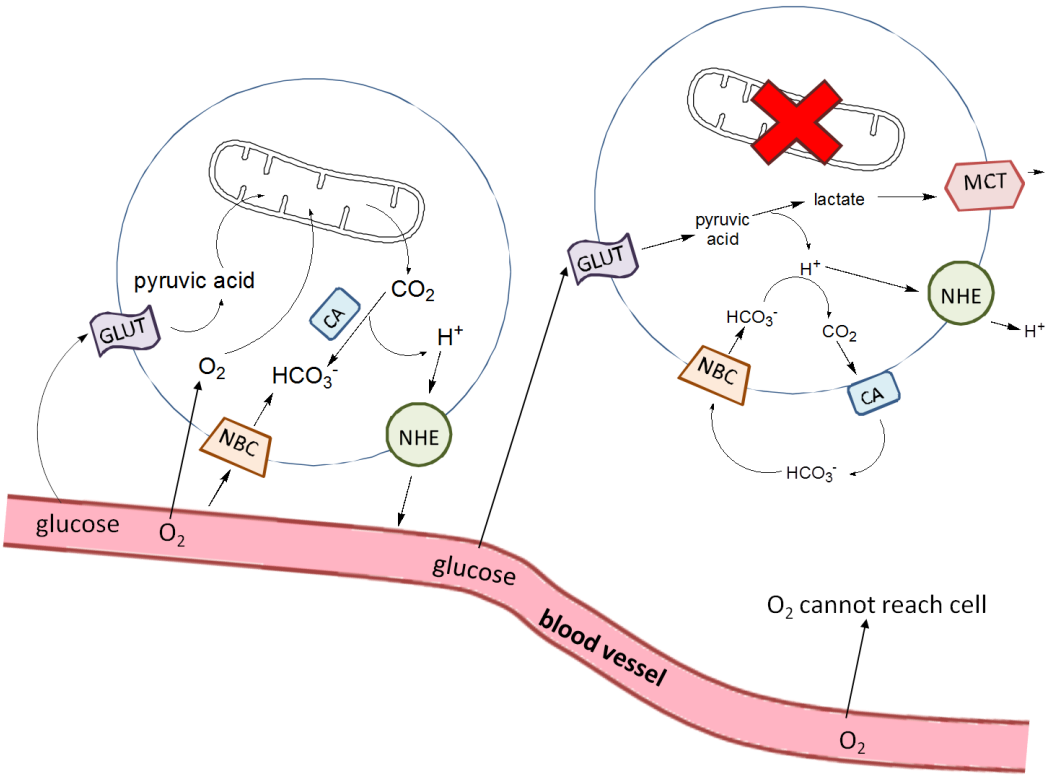

Figure 1.4: The adaptations made by hypoxic tumour cells to control their intracellular pH (*right*) compared with a normally oxygenated cell (*left*). Key: CA (carbonic anhydrase enzyme), NBC (Na^+-HCO_3^- co-transporter protein), GLUT (glucose transporter protein), NHE (Na^+-H^+ membrane transporter protein), MCT (monocarboxylate transporter protein).[21]

Transport proteins such as NBC (Na^+-HCO_3^- co-transporter protein) and NHE (Na^+-H^+ membrane transporter protein) help maintain the cellular pH by exporting protons out of the cell where they can diffuse into the blood and be removed. The limited blood supply of tumour cells causes several problems with this regulation of pH which the cell has to adapt to in order to survive. Firstly, the lack of oxygen supply means that the cell has to provide its energy through anaerobic rather than aerobic respiration, meaning that imported glucose is converted to lactic acid. The accumulation of lactic acid within the cell would cause a decrease in pH, so the cell removes it directly by using MCT (monocarboxylate transporter) proteins. The cell

can also neutralise the lactic acid with HCO_3^- which it imports into the cell using protein transporters such as NBC (**Scheme 1.2**).

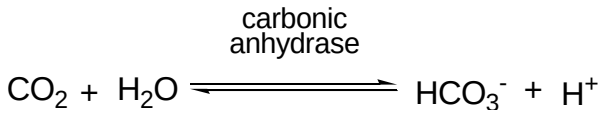

Scheme 1.2: The hydration of carbon dioxide catalysed by carbonic anyhydrase enzymes

The CO_2 formed by this neutralisation can then diffuse out of the cell as with aerobic cells. Once outside the cell, the CO_2 can be rehydrated to form bicarbonate, and be transported back into the cell again if needed. These mechanisms maintain the intracellular pH, but result in the exporting of species into the extracellular space. In a cell with an adequate blood supply, these ions can be removed by the vascular network. Within regions with poor blood supply, the acidic species accumulate outside the cell as they are unable to be carried away by the blood supply, resulting in a sub-normal extracellular pH (**Table 1.1**).[21-24]

Table 1.1: Extracellular and intracellular pH values of normally oxygenated and hypoxic cells.[21]

	Normally oxygenated cells	**Hypoxic cells**
pH_i (intracellular)	7.2	7.2
pH_e (extracellular)	7.4	6.9-5.5

1.2.3. The therapeutic resistance of hypoxic tumour cells

Unfortunately, the occurrence of hypoxia in tumours is problematic in anticancer treatments, being strongly correlated with a poorer patient prognosis.[25] Hypoxic tumour cells have an increased resistance to radiotherapy, chiefly owing to the cytotoxicity of this treatment relying on the radiation generated formation of dioxygen radicals (**Scheme 1.3)**. In hypoxic cells, the DNA based radicals can be formed in the same way as when under aerobic conditions, except that without

oxygen to react with, the DNA radical can abstract a hydrogen from a molecule such as glutathione (GSH) and thereby avoid damage.[10]

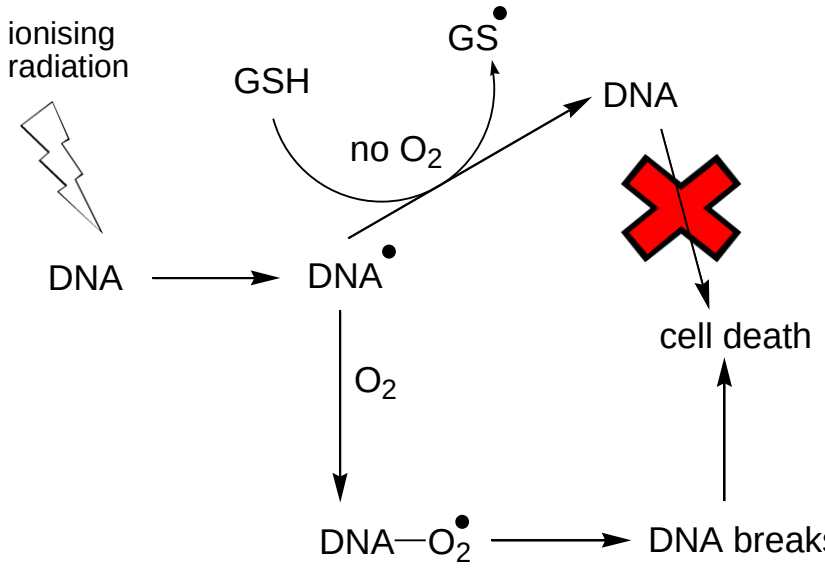

Scheme 1.3: The resistance of hypoxic tumour cells to radiotherapy.[10]

Hypoxic tumour cells also exhibit an increased resistance to many chemotherapeutic treatments. One reason for this is limited drug delivery; the poor blood supply to the hypoxic regions of tumours means that any chemotherapeutic agent would have to be able to diffuse over a relatively long distance from the nearest functional blood vessel to reach the area. Another reason is that many anticancer chemotherapeutic agents take effect through anti-proliferative mechanisms, proving effective by the general assumption of malignant cells having a greater proliferative rate than healthy cells. The onset of hypoxia in tumours causes the rate of cell proliferation to decrease owing to the cells becoming stationary at the G_1/S checkpoint because of the unfavourable environment the cell is within.[26, 27] Anti-proliferative agents therefore often prove ineffective against hypoxic tumour cells whilst they are stationary in the cell cycle. A third reason is that several agents such as bleomycin rely on a mechanism similar to that of radiation in that oxygen is used to generate the cytotoxic species.[28] There is also the potential for the more acidic extracellular environment of hypoxic tumour regions to change the protonated state of chemotherapeutic species, resulting reduced cell membrane diffusion.

1.3. Hypoxia selective agents

1.3.1. Cytotoxic agents

There is much interest in the development of anticancer agents which are able to be cytotoxic only when in the environment of a hypoxic tumour region. The differing cellular conditions found within hypoxic tumour regions; namely low oxygen levels and lowered pH, provide an opportunity to selectively target tumours.[29] There are three general classes of compounds which have been shown to have the capability of selectively targeting hypoxic cells; quinones, nitroaromatics and *N*-oxides.[30, 31] The general strategy used to achieve hypoxic selectivity is for the compound to be a non-toxic prodrug which can undergo selective reduction within hypoxic tumour cells. The reduced species ideally needs to be stable enough to enable it to be re-oxidised back to the prodrug species in the presence of oxygen (**Scheme 1.4**). Under hypoxic conditions, the reduced species can then go on to form the desired cytotoxic species

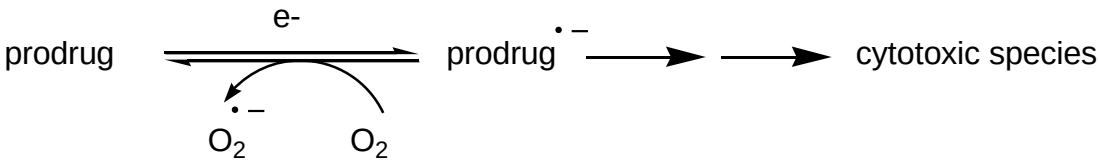

Scheme 1.4: Chemotherapeutic strategy for hypoxia-selective cytotoxic agents

1.3.1.1. Quinones

The naturally occurring quinone derivative Mitomycin C (**Figure 1.5**) became one of the first hypoxia-selective cytotoxic agents.[32]

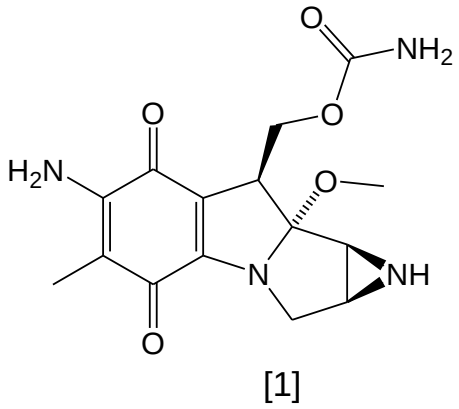

[1]

Figure 1.5: Structure of Mitomycin C (compound [**1**]).[32]

Quinones themselves generally have low toxicity but their functionality can be used to selectively activate cytotoxic groups.[33] Under hypoxic conditions, quinones can be reduced by a multi-step mechanism which proceeds via the formation of a semi-quinone one-electron reduction product or hydroquinone which is the result of a two electron reduction. These species undergo further reductions which yield the cytotoxic DNA alkylating species which can cause the formation of guanine-guanine cross links (**Scheme 1.5**).[34-36]

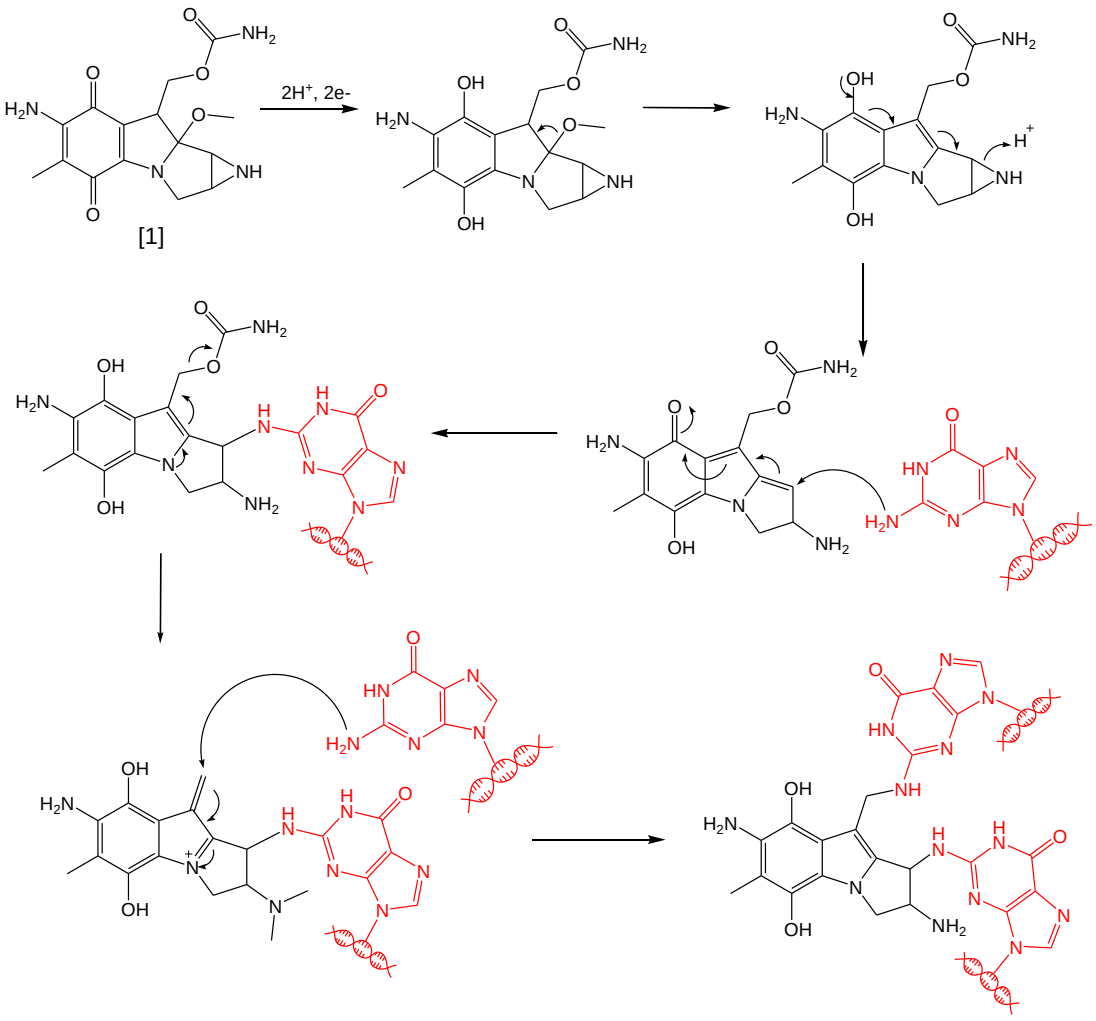

Scheme 1.5: Proposed mechanism for the formation of DNA cross-links between Mitomycin C [**1**] and guanine bases.[34-38]

1.3.1.2. Nitroaromatics

The nitroaromatic nitracrine (**Figure 1.6**), an analogue of the widely-studied acridines, was found to be one of several nitroaromatic compounds to show some selectivity towards hypoxic tumour cells.[37]

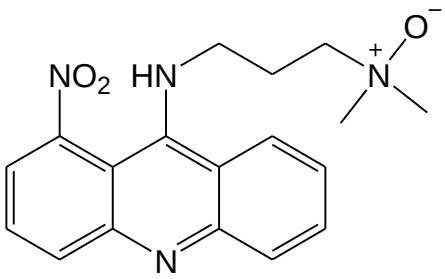

[2]

Figure 1.6: Structure of nitracrine (compound [**2**]).[39]

Acridines, a class of DNA chelating agents, have been long known for their medicinal properties, first finding use as anti-bacterial and anti-parasitic agents.[38] Initial *in vitro* experiments of nitracrine ([**2**]) showed a highly selectivity for AA8 (Chinese hamster ovarian) cells under hypoxic conditions compared to under aerobic conditions although the active cytotoxic species is yet to be fully identified.[39-41] Nitracrine has two bio-reducible groups; a nitro group and an *N*-oxide, which both need to be reduced before the molecule is transformed into its active form.[42]

Nitro reduction was investigated as a means of selectively activating a phosphoramidate mustard prodrug.[44] One of the investigated compounds provided highly promising results with 1-methyl-2-nitro-1*H*-imidazol-5-yl)methyl *N*,*N*-*bis*-(2-bromoethyl)phosphordiami-date (**Figure 1.7)**.

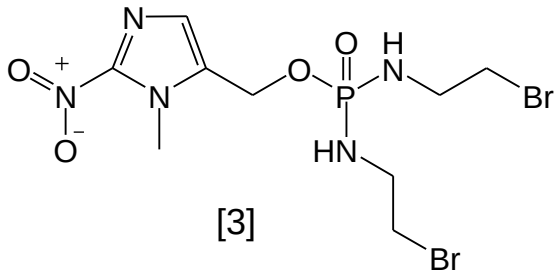

[3]

Figure 1.7: Structure of the phosphoramidate mustard [**3**].[44]

[3] demonstrated a 300-fold increase in potency against H460 (human lung cancer) cells when under hypoxic conditions compared to aerobic conditions, and a 200-fold increase against HT29 (human colon adenocarcinoma) cells (**Table 1.2**).[43]

Table 1.2: IC_{90} data for compound [**3**] against H460 and HT 29 cells.[44]

Cell line	IC_{90} (N_2) / µM	IC_{90} (air) / µM
H460	0.1	30
HT29	0.2	40

The proposed mechanism for the selective activation of the compound under hypoxic conditions is shown in **Scheme 1.6**.

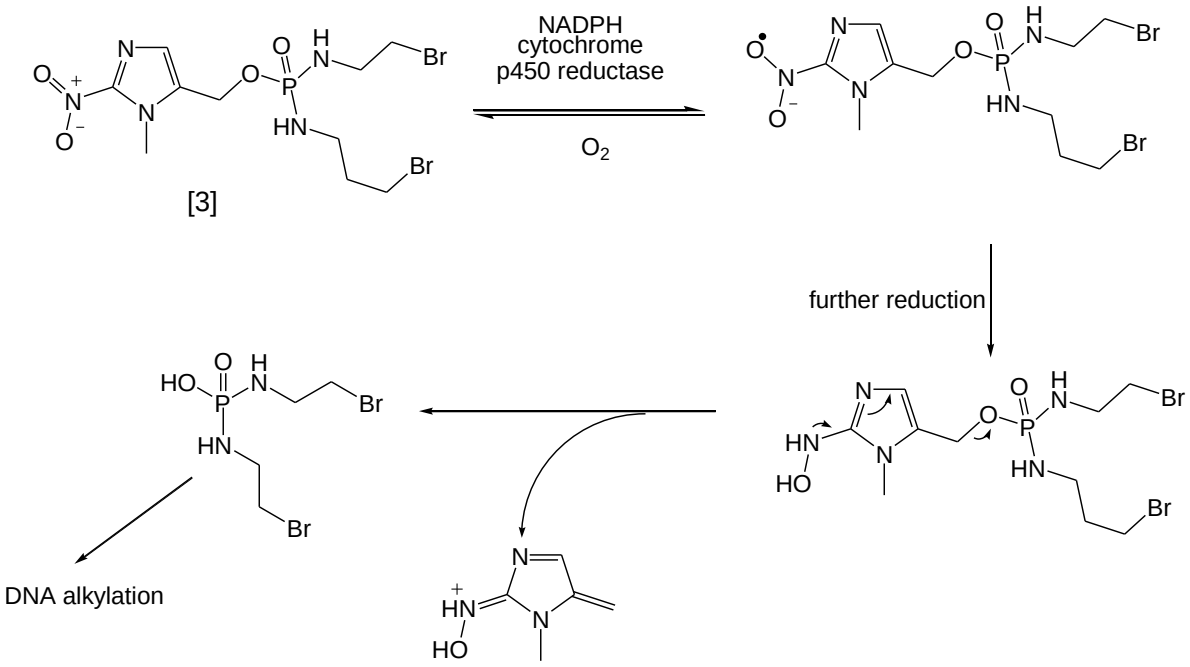

Scheme 1.6: The selective bio-reductive activation of [**3**] under hypoxic conditions.[44]

Fluorine-18 fluoromisonidazole ([^{18}F]FMISO) (**Figure 1.8**) is the most widely used nitroimadazole-based PET imaging agent, and is also one of the prototype hypoxia-

selective radiotracers.[44] The selective retention of **[4]** within hypoxic cells is due to the nitro group undergoing reduction by nitroreductase enzymes, forming a reactive species which can then alkylate intracellular macromolecules.[45]

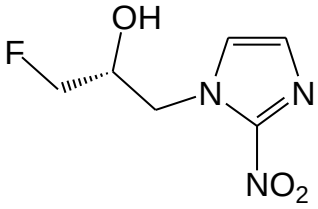

[4]

Figure 1.8: Structure of [^{18}F]FMISO

1.3.1.3. *N*-oxides

N-oxides represent a class of compounds which have undergone extensive research for use as hypoxia-selective agents, with one particular example having undergone phase II and phase III clinical trials.[46] 3-Amino-1,2,4-benzotraizine-*N*1,*N*4-oxide (**Figure 1.9**), commonly known as tirapazamine, has undergone clinical trials in combination with other anticancer treatments such as cisplatin and radiotherapy, where it was found to sensitise platinum-resistant cells to treatment.[47, 48]

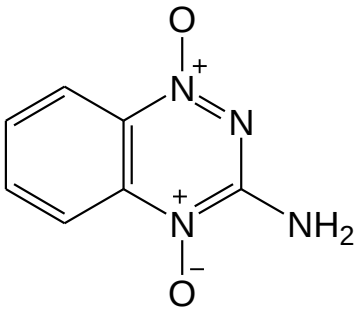

Figure 1.9: Structure of tirapazamine (tpzH)

In vitro studies have demonstrated that tirapazamine (tpzH) has a promising 100-200 fold selective cytotoxicity toward hypoxic cells over normally oxygenated cells.[36] **Table 1.3** shows the IC_{50} values against selected cell lines under both aerobic and anaerobic conditions. For all of these cell lines, a 15-fold increase or above is

observed in the IC_{50} values of tpzH when under hypoxia compared to aerobic conditions, with the greatest selectivity observed against the H226 (human lung squamous carcinoma) cell line.

Table 1:3: IC_{50} of tpzH against selected cell lines under both aerobic and hypoxic conditions.[49]

Cell line	IC_{50} / µM after 3 hours exposure		Differential toxicity
	Aerobic	Hypoxic	
A549	247.0 ± 44	7.4 ± 0.5	33.2
H322	980 ± 24	54.3 ± 1.7	18.1
H358	1231.0 ± 62	48.1 ± 5.6	25.6
H460	110.0 ± 10	4.2 ± 2.0	26.2
H522	141.0 ± 12	8.9 ± 0.6	15.8
H647	135.0 ± 22	6.3 ± 2.0	21.4
H226	941.0 ± 189	22.8 ± 4.6	41.3

Despite extensive studies, the mechanism responsible for tpzH's selective cytotoxicity is still a subject of great debate between two different mechanisms which propose the cytotoxic species to be either a hydroxyl radical or a tpzH-based radical species. However, there is general agreement on the tpzH undergoing a one electron enzymatic reduction to form a radical based active species.[50] Although the identity of the responsible biological reducing agents remains elusive, many have reported evidence for the reduction being carried out by cytochrome P450 reductase.[51, 52] The one-electron reductive enzyme xanthine oxidase has also been used to reduce tpzH into its active species for *in vitro* experiments.[53]

Gates *et al*. proposed that the cytotoxicity of tpzH arises from the generation of hydroxyl radicals (**Scheme 1.7**). This proposal was based upon characterisation studies of the products arising from tpzH-mediated DNA damage found that the strand breakage was non-sequence specific and matched the strand damage formed by hydroxyl radicals.[54] The mechanism involves the one electron reduction of tpzH followed by protonation of the *N*4-oxide oxygen. This then allows the elimination of this protonated oxygen as a hydroxyl radical which can then go on to cause DNA damage.

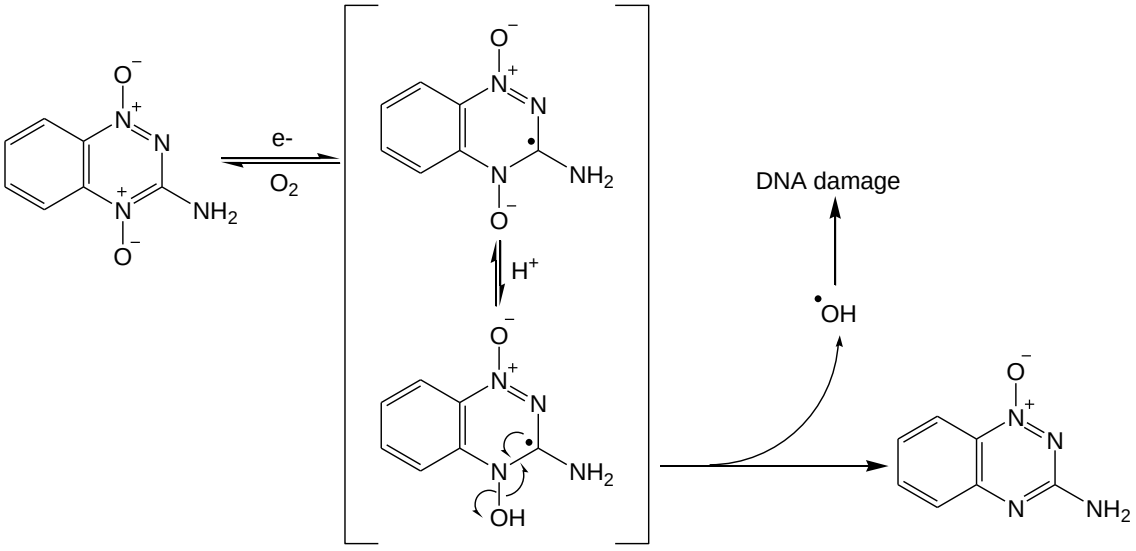

Scheme 1.7: Proposed mechanism of activity for tpzH where the cytotoxic species is a hydroxyl radical.[54]

Anderson *et al*. reported spectral evidence which disfavoured the hydroxyl radical elimination or mechanism that involving the formation of a charged species. They proposed the formation of a benzotriazinyl radical (**Scheme 1.8**). The benzotriazinyl species is a nitrogen-centred radical which would be more oxidising in nature than a carbon-based radical species so would be more likely to cause the DNA damage caused by tpzH.[55] They proposed that such a species could be generated via the elimination of water from the species from the one electron protonated product. This hypothesised mechanism was further supported by the results of spin-trapping experiments, where EPR spectroscopy indicated the formation of a carbon-centred radical after the one electron reduction of tpzH. The authors' interpretation of these

results concluded that the nitrogen-centred radical had poor stability, and therefore a short life time, so went on to form the detected carbon-centred radical.[56] Pulse radiolysis studies supported this hypothesis by demonstrating the occurrence of short-lived chain reaction occurring upon the one electron reduction of tpzH.[56]

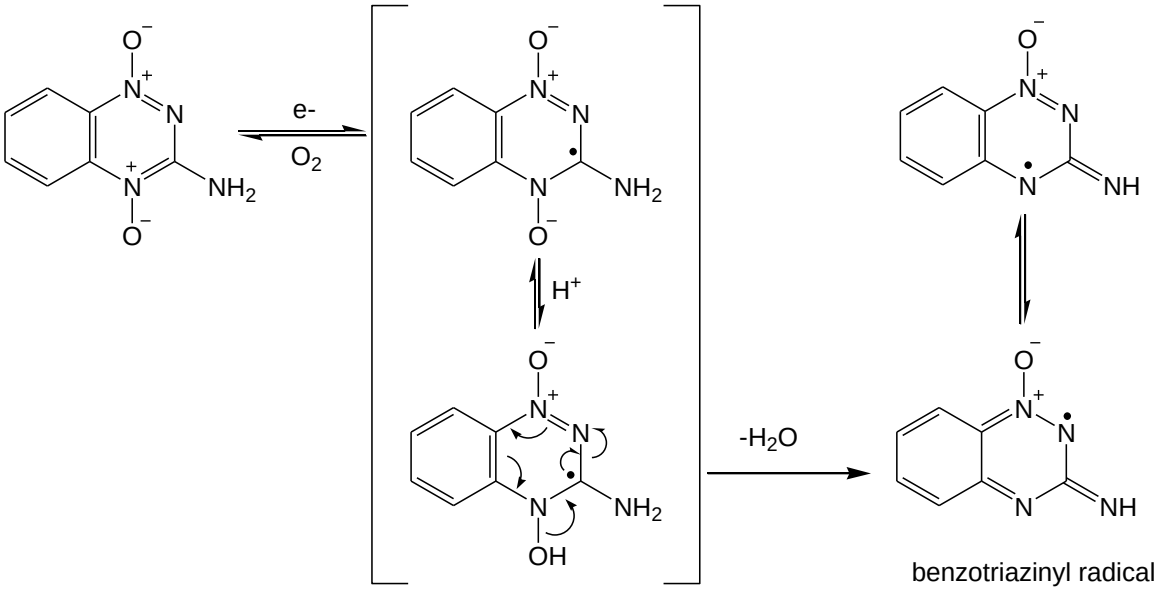

Scheme 1.8: Proposed mechanism of activity for tpzH involving the elimination of water to form a benzotriazinyl radical.[49]

Whilst highly effective *in vitro*, this success has not translated into immediate clinical success. This has been partly attributed to the distribution of tpzH outside the bloodstream being too poor, preventing it from penetrating deep into the tumour to the hypoxic regions where it would be most potent.[57] It has also been suggested that tpzH is metabolised too quickly upon reaching the reducing environment of hypoxic reagents, preventing the drug from penetrating far enough within.[58] Another problem has been the side effects which result from tpzH's toxicity. Studies have found that the use of tpzH in clinical trials correlates with the increased occurrence of symptoms such as nausea, fever, low blood pressure and deafness.[59] There is therefore a large amount of ongoing research into analogues of tpzH which optimise its hypoxia selective cytotoxicity whilst improving its delivery and minimising

general toxicity. These include SN30000 ([**5**]) which is under clinical investigation,[60, 61] SN2971 (**[6]**) and 7-chloro-2-thienylcarbonyl-3-trifluoromethylquinoxaline-*N*1,*N*4-oxide (**[7]**) (**Figure 1.10**). [62, 63]

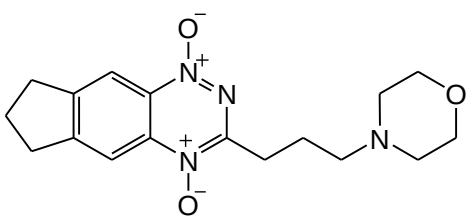

[**5**]

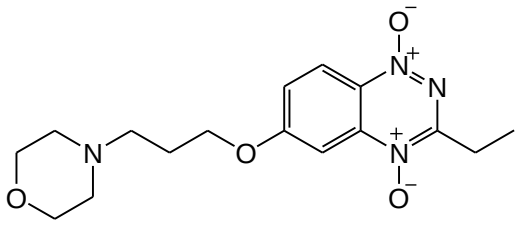

[**6**]

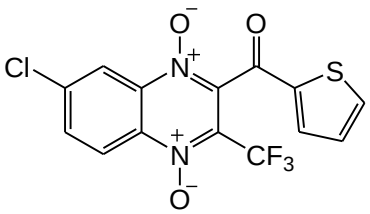

[**7**]

Figure 1.10: Examples of tpzH analogues investigated for their hypoxia-selective cytotoxicity.[60-63]

1.4. Transition metal anticancer agents

1.4.1. The platinum revolution

During the late 1960's experiments were being conducted into the effect of electrical current on cell growth in bacterial cultures. It was found that the *Escherichia coli* cells became abnormally elongated due to inhibition of cellular division.[64] It was found that this cell elongation was caused by the platinum(IV) complex $[NH_4]_2[PtCl_6]$. After the trialling of many platinum compounds against tumour cells, it was found that the anticancer activity required a neutral complex with two *cis* amine-type ligands. One of the compounds trialled was *cis*-diamminedichloroplatinum(II), and it was this compound which gained approval for clinical use in 1978 under the name of cisplatin (**Figure 1.11**).[64, 65]

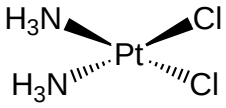

[8]

Figure 1.11: Structure of cisplatin

The mechanism of action of cisplatin has been intensively studied. The chloride concentration found within blood plasma (100 mM) is high enough that exchange of the chloride ligands of cisplatin for water is disfavoured.[66] Upon entering a cell (5-20 mM), one of the chloride ligands is exchanged for an aqua ligand.[67] This aquation process is vital to the complex's activity owing to the aqua ligand being a more reactive ligand than chloride when complexed to platinum(II).[68] The mono-aqua complex can then covalently bind to the cellular DNA, typically through the N7 atom of guanine (**Scheme 1.9**).[68, 69]

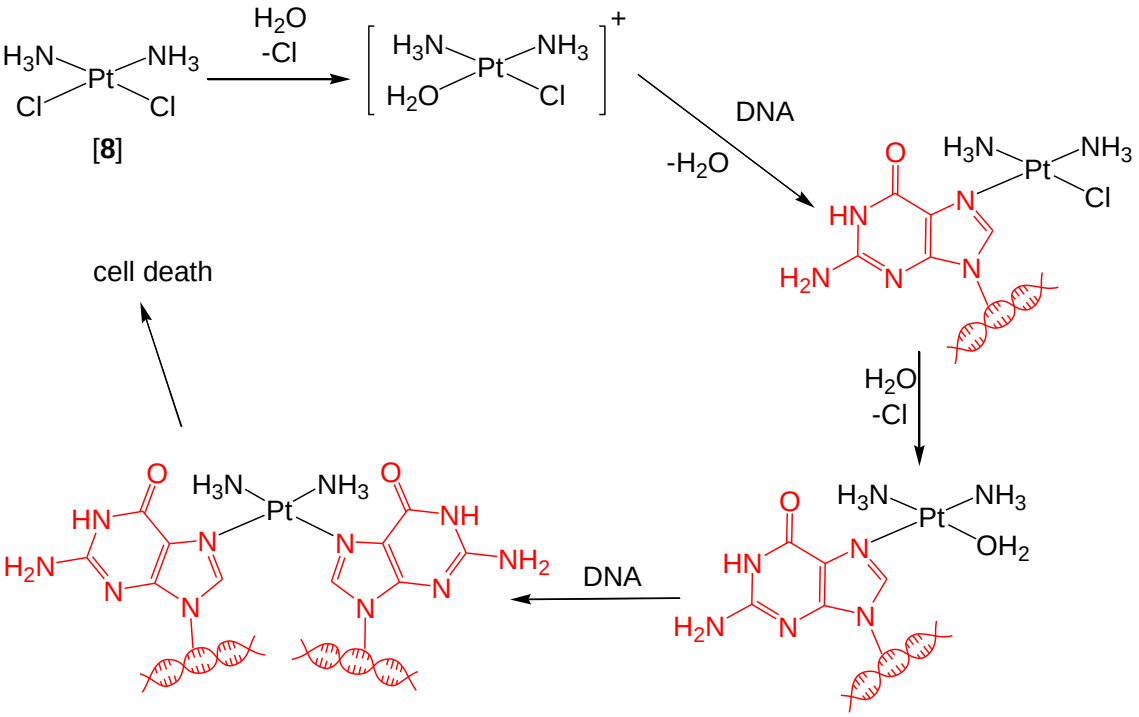

Scheme 1.9: Mechanism of how cisplatin is understood to bind to DNA within the cell nucleus

The binding of cisplatin to the DNA leads to the formation of a Pt-DNA adduct, causing structural distortion to the DNA (**Figure 1.12**).[69]

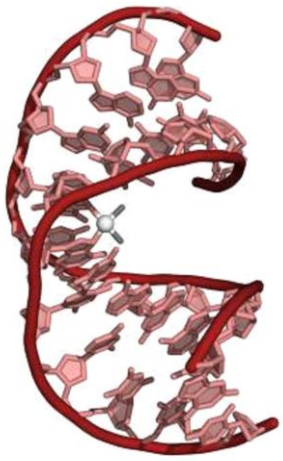

Figure 1.12: Crystal structure of cisplatin having formed a 1,2- guanine intrastrand crosslink, causing structural distortion to the DNA (image taken from reference 69).

Problems associated with cisplatin such as high renal toxicity are understood to be due to it reacting with proteins before reaching the cell.[70] Another problem with cisplatin is that it is ineffective against some cancers, whilst others are able to develop a resistance to it. These problems have led into many avenues of research, including the development of effective but less toxic platinum complexes such as carboplatin and or oxaliplatin (**Figure 1.13**),[71-73] or the use of alternative metals such as ruthenium.[30, 74] The platinum complexes [**9**] and [**10**] show reduced toxicity and therefore cause milder side effects in patients, but have lower cytotoxicities towards cancer cells, owing to the lower reactivity of the bidentate ligands which have replaced the two chloro ligands.[68]

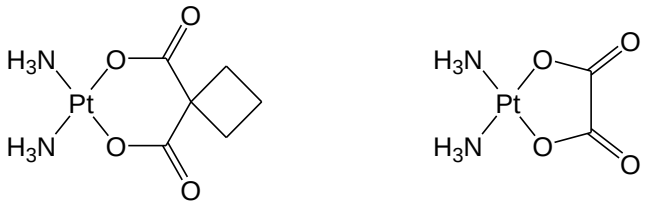

[**9**] [**10**]

Figure 1.13: Structures of the second generation cisplatin compounds carboplatin (*left*) and oxaliplatin (*right*)

1.4.2. Other examples of transition metal-based anticancer agents

The ability of a metal to alter the activity of a therapeutically active ligand has been demonstrated by examples including several relevant to anticancer treatments. Tamoxifen is a prodrug commonly used for the treatments of hormone dependant breast cancers and is converted within the body to its active hydroxytamoxifen form. Its activity derives from its ability to competitively bind to the estrogen ERα receptors but problems with this drug include its ineffectiveness against hormone-independent breast cancers, and the tendency of resistance amongst tumour cells which can increase over long periods of treatment.[75] There are numerous transition metal complexes reported in the literature which incorporate a hydroytamoxifen derivative as a ligand, stemming from the promising results with ferrocene derivatives (**Figure 1.14**).

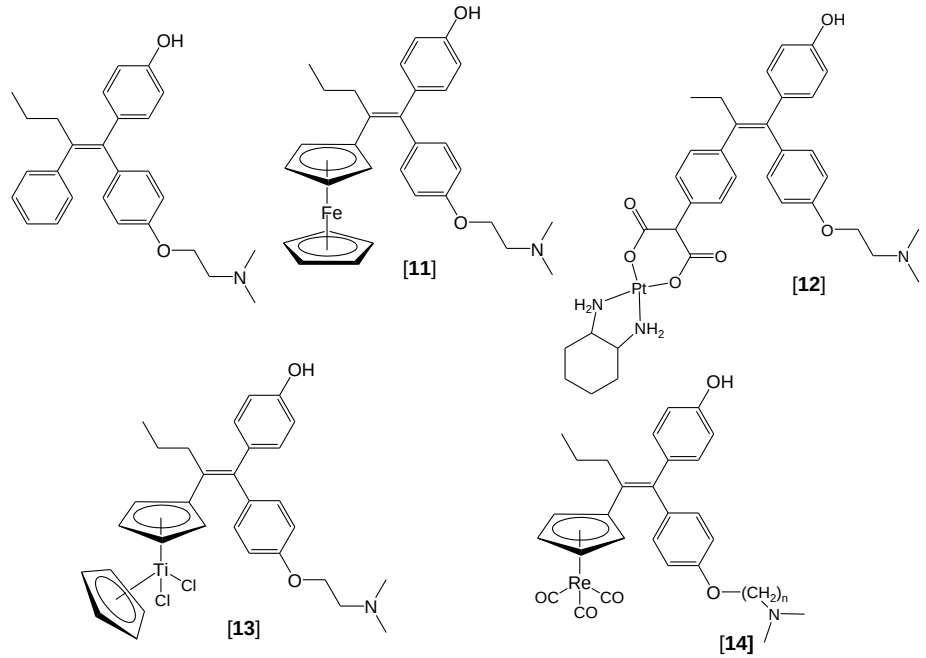

Figure 1.14: Structure of hydroxytamoxifen, the active form of the prodrug tamoxifen and its complexes of ferrocene [**11**],[76] oxaliplatin [**12**],[76, 77] titanocene dichloride [**13**],[78] and cyclopentadienyl rhenium tricarbonyl [**14**].[76, 79]

Ferrocene derivatives of hydroxytamoxifen, such as [**11**] were found to not only exhibit anti-proliferative activity against the hormone-dependent breast cancer cell line MCF7, but also against the hormone-independent cell line MDA-MB231,

against which tamoxifen shows poor activity.[80] It is believed that the activity against the hormone-dependent cell line is due to a similar mode of tamoxifen itself, in that it competitively binds to the estrogen receptors, demonstrated by several binding studies.[76, 80] Structure-activity relationship and electrochemical studies have supported the hypothesis that the cytotoxic species formed is a quinine methide (**Scheme 1.10**), where it was found that the activity of various analogues of [**11**] was dependent on the presence of at least one *para*-phenol moiety.[81] This mechanism is also supported by a study which involved a ruthenocene derivative, which showed similar activity against hormone-dependent MCF7 cells but no anti-proliferative activity against the hormone-independent MDA-MB231 cell line.[82]

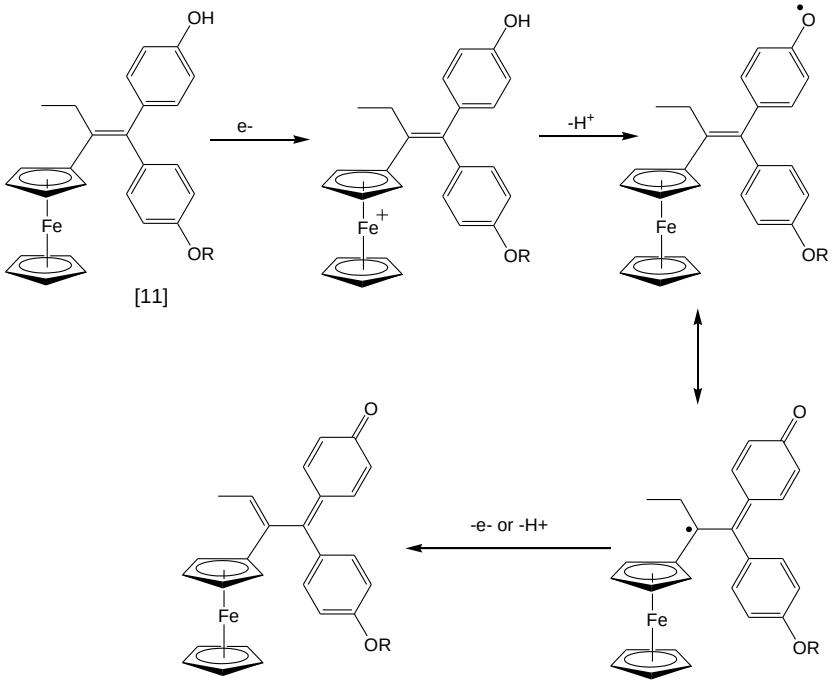

Scheme 1.10: Proposed mechanism for the generation of a putative cytotoxic quinine methide species from [**11**].[83, 84]

It was proposed that in preparing the oxaliplatin derivative [**12**], a system of selectively delivering platinum to breast tumours would result, but the results proved disappointing.[77] Complex [**13**] was tested against hormone-dependent breast cancer cell line MCF7 and compared with estradiol which provides the standard estrogenic effect so facilitates proliferation, and hydroytamoxifen which is the standard anti-

estrogenic effect and therefore has an anti-proliferative action. The results showed that rather than the anticipated increase in anti-proliferative activity brought about by the titanocene dichloride fragment, [**13**] increased cell proliferation almost to the extent of estradiol.[78] Therefore [**13**] does not appear to be a promising anti-tumour candidate compound. Two of the tested rhenium complexes, [**14**], exhibited anti-proliferative activity against MCF7 cells which was slightly higher than that obtained for the tamoxifen prodrug hydroxytamoxifen, suggesting this complex does show potential as an anticancer compound.[79]

Another biologically active ligand which has been incorporated into metal complexes which show anticancer properties is acetylsalicylic acid, more commonly known as the prodrug form as aspirin (**Figure 1.15**). There have been numerous variations of both ligand modifications and metal, some of which will now be discussed. It was found that [**15**] displayed anti-proliferative properties against breast cancer with a significantly lower IC_{50} than aspirin.[85] It was subsequently found that [**15**] showed equal inhibition of both COX-1 and COX-2 cyclooxygenase enzymes.[86] Aspirin, functions as an anti-inflammaory drug by inhibition of COX-1,[87] so it was thought that the anti-proliferative activity of [**15**] might be attributed to the inhibition of COX-2 which is over-expressed in certain tumour cells.

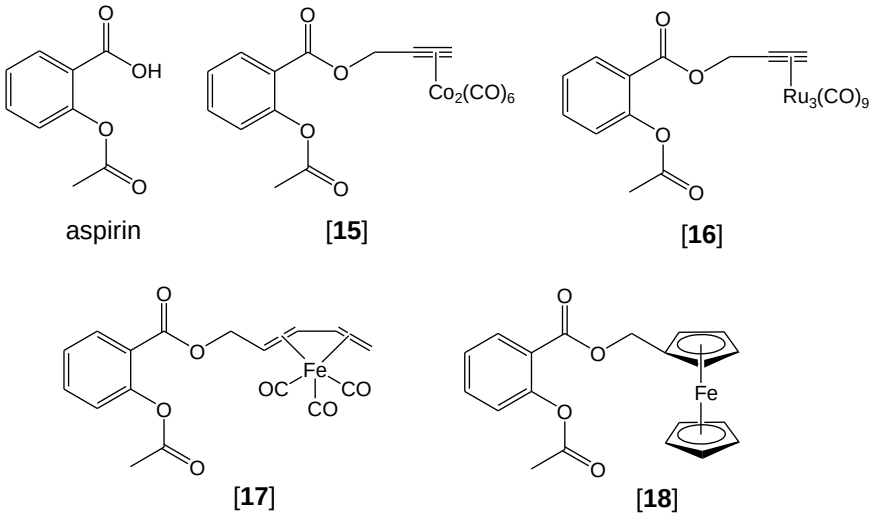

Figure 1.15: Structures of acetylsalicylic acid (aspirin) and examples of its complexes with fragments of cobalt [**15**], ruthenium [**16**], iron [**17**] and ferrocene [**18**]

The cobalt carbonyl complex [**15**] proved to be the most active complex, followed by the ruthenium complex [**16**], but unlike with the hydroxytamoxifen complexes, the ferrocene complex [**18**] and also iron complex [**17**] showed poor activity, suggesting the alkyne ligand is needed for activity.

The anti-proliferative activity of [**16**] against the cell lines has thrown doubt over the biological action of these complexes. COX inhibition studies of [**16**] showed it to be a poor inhibitor, but its anti-proliferative activity is almost equal to [**15**], suggesting it is either acting via a different biological target or COX inhibition is not the source of the anti-proliferative activity.

Table 1.4: IC_{50} data of selected complexes containing acetylsalicylic acid derivatized ligands.[88]

Compound	**IC_{50} / µM**		
	MCF7	**MDA-MB 231**	**HT-29**
Cisplatin [**8**]	2.0 ±0.3	3.3 ±0.5	2.4 ±0.4
Aspirin	>50	>50	>50
[**15**]	1.4 ± 0.3	1.0 ±0.3	9.8 ±3.0
[**16**]	1.4 ±0.2	2.4 ±0.0	2.2 ±0.0
[**17**]	>20	>20	>20
[**18**]	>20	>20	>20

1.4.3. The development of hypoxia selective transition metal complexes

1.4.3.1. Copper(II) complexes of *bis*-thiosemicarbazone ligands

The complex copper(II)-diacetyl-*bis*(N^4-methylthiosemicarbazone), [Cu(ATSM)] (**Figure 1.16**), has high selectivity for trapping ^{64}Cu within hypoxic tumour cells for the purpose of PET imaging.[89]

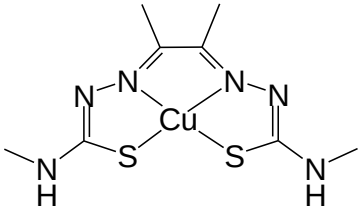

[**19**]

Figure 1.16: Structure of the PET imaging agent [Cu(ATSM)] (copper(II) diacetyl-*bis*-(*N*-methylthiosemicarbazone))

[Cu(ATSM)] reached the latter stages of clinical trials, but progress into full clinical use has been hindered by high liver accumulation of ^{64}Cu. Analogues similar to [**19**] (**Figure 1.17**) are retained within cells non-discriminatively, so these non-selective complexes and [Cu(ATSM)] have been widely studied to understand the hypoxia selectivity of the latter.

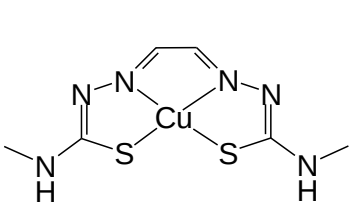

[Cu(GTSM)]

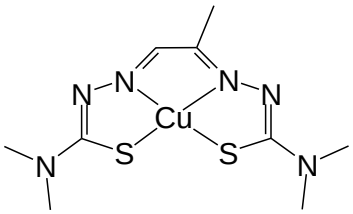

[Cu(PTSM)]

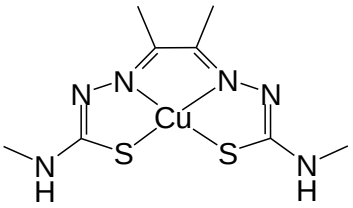

[**19**]

[CuATSM)]

Figure 1.17: Structures of [Cu(ATSM)] and some of its analogues show poorer hypoxia selectivity

Various chemical properties of this type of complex have been studied and correlated with their hypoxia selectivity, including redox potentials and partition coefficients. The results suggested that the more negative the one electron reduction potential of

the copper(II) complex, the greater the hypoxia selectivity and indicate that for a copper(II) complex to be hypoxia selective, it needs to have a reduction potential greater than -0.57 V *vs*. Ag/AgCl in DMSO, although it is important to note this is not the sole determining factor.[90, 91] It is thought that the selectivity of [Cu(ATSM)] arises from the complex undergoing reduction only in hypoxic cells. Upon reduction, the ligand dissociates, and the copper(I) isotope is then bound by 'copper-scavenging' proteins within the cell such as metallothionein (**Scheme 1.10**).[92] Experiments have shown that the copper(I) binding-proteins Ctr1 (a membrane copper transporter) and Atx1 (a copper chaperone protein) were not able to extract the copper(II) centre from [Cu(ATSM)]. Upon addition of a reducing agent, the proteins were observed to coordinate to the reduced copper(I) centre.[92]

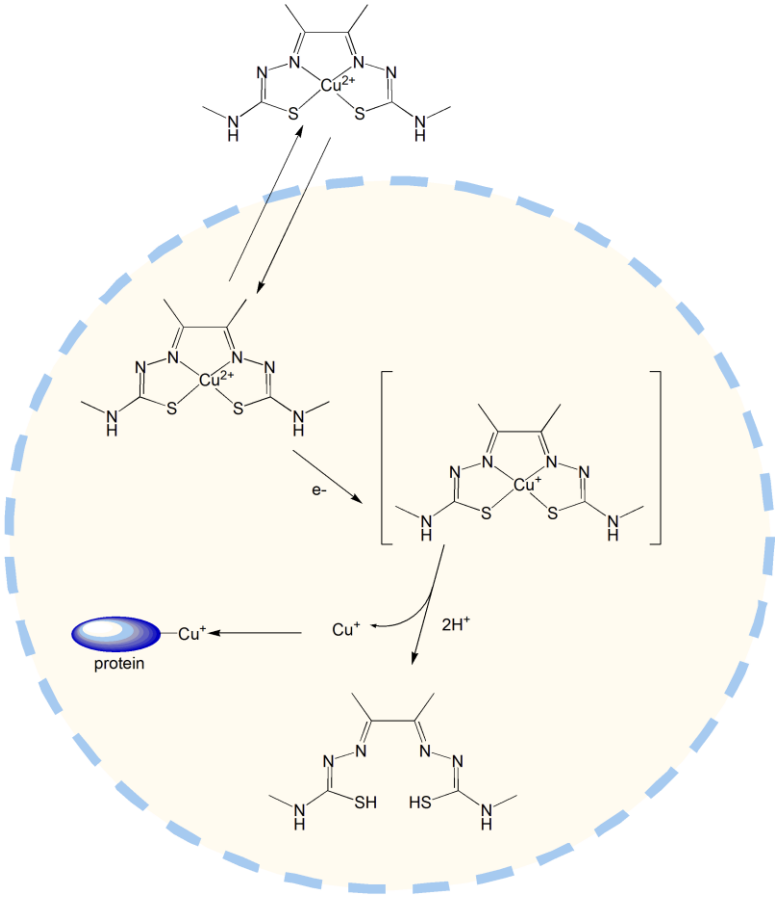

Scheme 1.11: Proposed mechanism for the selective trapping of ^{64}Cu from [^{64}Cu(ATSM)] in hypoxic cells

1.4.3.2. Cobalt(III) complexes of nitrogen mustard ligands

Nitrogen -mustards (**Figure 1.18**) are a group of potently cytotoxic compounds which take effect through DNA alkylation, acting upon both healthy and cancerous cells.[93, 94]

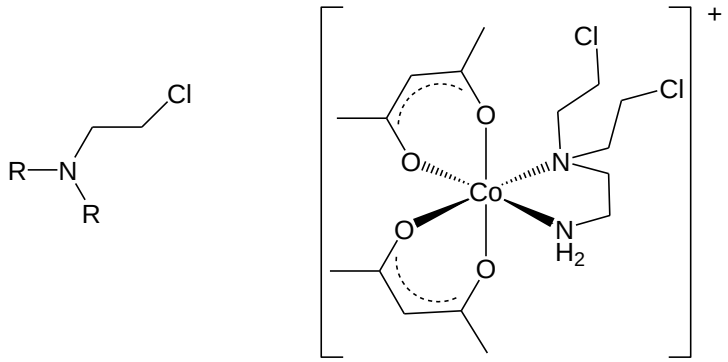

[**20**]

Figure 1.18: General structure of a *N*-mustard (*left*) and the cobalt(III) *N*-mustard complex [**20**] (*right*)

Denny *et al*. have explored how *N*-mustards might be developed into hypoxia selective agents by complexing mustard –type ligands to cobalt.[95, 96] Cobalt is one of the most suitable metals to be used for the purpose of hypoxia-selective ligand dissociation owing to the general coordination chemistry of its +3 and +2 oxidation states. In its +3 oxidation state, cobalt forms octahedral complexes and has a d^6 electron configuration. Cobalt(III) complexes are typically low spin, and owing to the electron configuration are kinetically inert. Upon undergoing a one-electron reduction to cobalt(II), a change to a high spin electron configuration occurs and so the e_g orbitals become partially filled (**Figure 1.19**). The e_g orbitals point directly at the ligand orbitals rather than in-between them, resulting in a weakening of the metal-ligand bonding interaction when they become occupied which corresponds to a lengthening bond length. The lability of cobalt(II) complexes is also contributed to by Jahn-Teller distortion which occurs upon there being an uneven distribution of electrons amongst degenerate d orbitals. The difference in lability of these two oxidation states is highlighted by the difference in the rate of aquation of their hexammine complexes.[97]

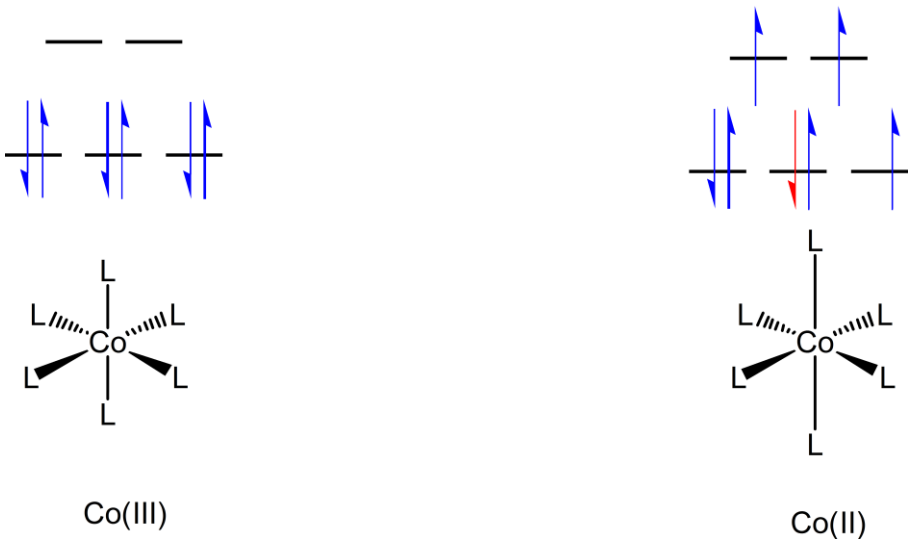

Figure 1.19: The electron configurations of a general cobalt(III) and cobalt(II) complex with octahedral geometry

With using cobalt(III) complexes as a prodrug, it is hoped that the complex will become selectively reduced in hypoxic cells to the equivalent but more reactive cobalt(II) complex. From the cobalt(II) complex, the ligands can easily dissociate and can then take effect on their biological targets. The reactivity of *N*-mustards is controlled by the electron density on the nitrogen atom, so by coordinating this to a metal centre reduces their reactivity. Complex [**20**] was found to show approximately 30-fold selective cytotoxicity towards EMT6 (mouse mammary tumour) cells under hypoxia compared to aerobic conditions.[98] This selectivity was assumed to be due to the complex undergoing selective reduction within hypoxic tumour cells (**Scheme 1.12**).

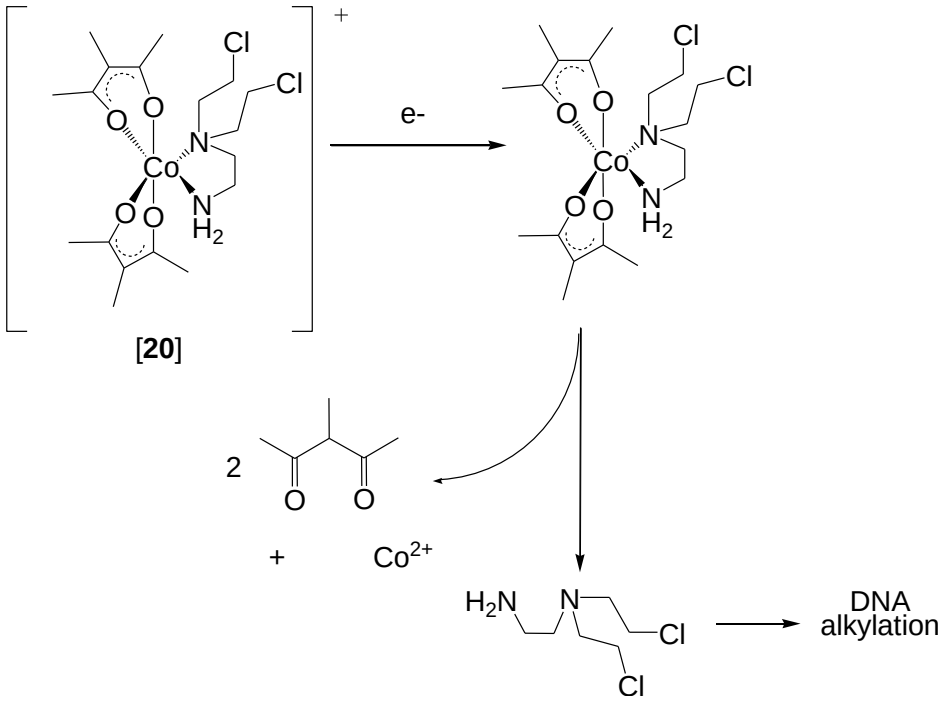

Scheme 1.12: Proposed mechanism of the selective release of the *N*-mustard ligand from the cobalt(III) complex [**20**].[99]

Similar complexes were prepared which in addition to the bidentate amine *N*-mustard contained carbonato or oxalato ligands. These complexes were found to reduce the toxicity of the *N*-mustard through being coordinated to the cobalt(III) centre (**Figure 1.20** and **Table 1.5**).[95]

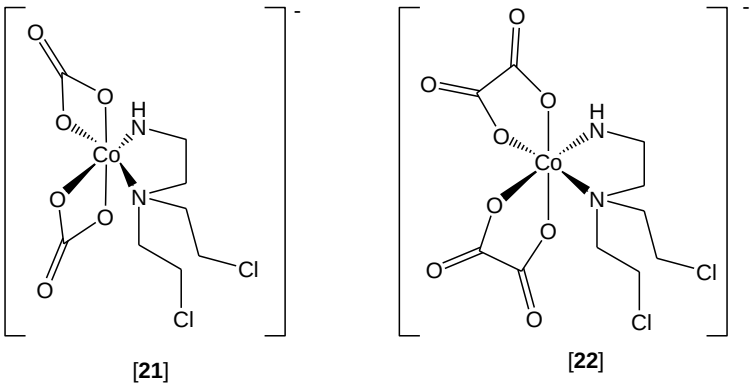

Figure 1.20: Structures of the cobalt(III) *N*-mustard *bis*-carbonato and oxalate complexes [**21**] and [**22**]

Table 1.5: IC_{50} values of the cobalt(III) *N*-mustard complexes [**21**] and [**22**] against AA8 and UV4 cells.[95]

	$1C_{50}$ / μM	
	AA8	UV4
Uncoordinated mustard	2.4	0.04
[**21**]	20	0.36
[**22**]	3.1	0.04

The difference in toxicity under hypoxic and aerobic conditions was also explored, with [**21**] found to be 20 times more potent under hypoxia and [**22**] over ten times more cytotoxic (**Table 1.6**).[95]

Table 1.6: CT_{10} values of the cobalt(III) *N*-mustard complexes [**21**] and [**22**] (CT_{10} = concentration × time (h) to give 10% survival).[95]

	CT_{10} / μM	
	air	**N_2**
Uncoordinated mustard	0.18	3.0
[**21**]	90	4.5
[**22**]	32	2.7

1.4.3.3. Cobalt(III) complexes of other ligands

Hambley has developed a cobalt(III) prodrug of marimastat (**Figure 1.21**), a drug which inhibits matrix metalloproteinase (MMP) enzymes which are thought to be involved in tumour metastasis.[100]

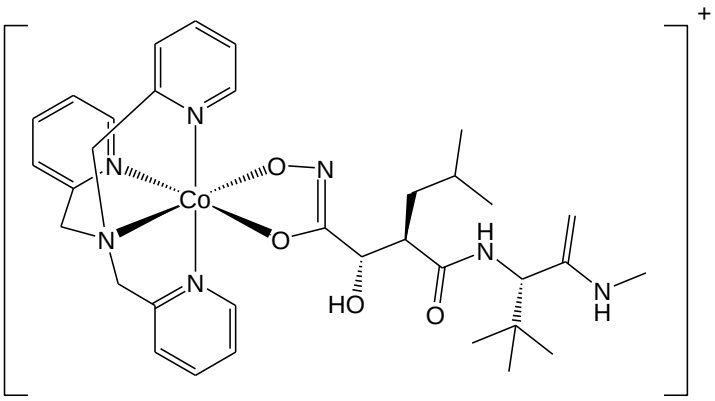

[**23**]

Figure 1.21: Structure of the cobalt(III) complex incorporating the MMP inhibitor marimastat [**23**].[101]

The prodrug complex was designed with the aim of selectively delivering the inhibitor to tumour cells. The reduced ability of marimastat to inhibit matrix metalloproteinase enzymes was demonstrated, showing an over 100-fold decrease in activity (**Table 1.7**).[101]

Table 1.7: IC_{50} values of marimastat and its cobalt(III) [**23**] determined by MMP inhibition assay under aerobic conditions

	IC_{50} / μM
Marimastat	7.0 ± 0.5
[**23**]	900 ± 100

It is widely reported that the fluorescence of certain fluorophores can be quenched upon coordination to a cobalt(III) centre.[102, 103] This provides a useful tool for being able to monitor the occurrence of bio-reduction within cells, but also to be able to observe where in the cell it occurs using techniques such as confocal microscopy. Hambley and co-workers have prepared a series of cobalt(III) complexes (**Figures 1.22** and **1.23**) and have examined their cytotoxicity and reduction chemistry.

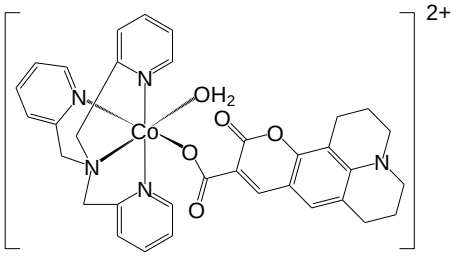

[**24**]

Figure 1.22: Structure of the cobalt(III) complex [**24**] containing a fluorescent ligand

The ability of [**24**] to be reduced by biologically relevant agents such as ascorbate and cysteine were investigated using fluorescence. The increase in emission brought about by the dissociation of the ligand upon reduction of the cobalt(III) centre was monitored as a function of time. Complex [**24**] was observed to have a significantly increased cytotoxicity against A2780 (human ovarian carcinoma) cells and to be over 40 times greater than that of the fluorophores or $[Co(Cl)_2(cyclam)]Cl$ (**Table 1.8**).[104] Complex [**24**] was observed to be reduced at the same rate by ascorbic acid under both aerobic and anaerobic conditions.[104]

Table 1.8: IC_{50} of the cobalt(III) complex [**24**] under aerobic conditions against A2780 cells.[104]

Compound	**IC_{50} / µM**
[**24**]	4.8 +/- 0.3
Ligand of [**24**]	>200
$[Co(Cl)_2(cyclam)]Cl$	>200

Another study investigated the cytotoxicity of complexes [**25**] and [**26**] (**Figure 1.22**) under both hypoxic and normoxic conditions, as well as fluorescence studies on tumour spheroids.[105]

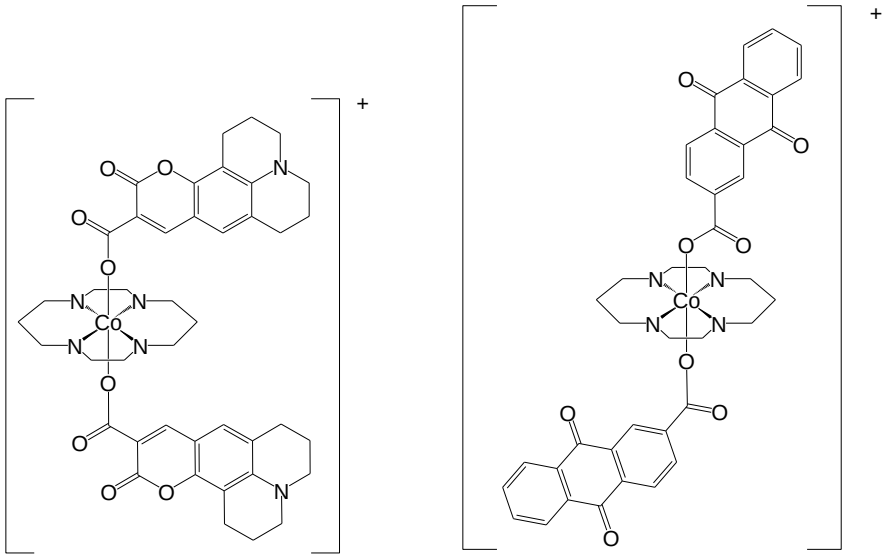

[**25**] [**26**]

Figure 1.23: Structures of the cobalt(III) complexes [**25**] and [**26**].[105]

The results of cytotoxicity assays against DLD-1 (human colon carcinoma) cells show that complexation of each of the two fluorophores to a cobalt(III) centre has dramatically increased their potency (**Table 1.9**).

Table 1.9: Activity of the cobalt(III) complexes [**25**] and [**26**] against DLD-1 cells.[105]

Compound	**IC_{50} under normoxia / µM**	**IC_{50} under hypoxia / µM**
[**25**]	1.3 +/- 0.7	1.9 +/- 0.2
Fluorophore of [**25**]	99 +/- 5	>200
[**26**]	35.6 +/- 0.9	20.04 +/- 0.1
Fluorophore of [**26**]	>200	177 +/- 0.2
$[Co(Cl)_2(cyclam)]^+$	>200	>200

The cytotoxicity of [**25**] did not change between hypoxic and normoxic conditions, whilst [**26**] showed a slight increase in cytotoxicity under hypoxia. Imaging results from spheroid experiments showed that complex [**26**] was able to penetrate deeper

into the spheroid than the ligand on its own. The deeper penetrating fluorescence observed with complex [**26**] showed that metal coordination was aiding the delivery of the ligand deeper into the mass but the ligand was then able to dissociate. The ligand of [**25**] was able to penetrate deeper into the tissue but complexation to cobalt(III) improved its delivery to the hypoxic regions. These findings from the spheroid experiments, however, do not explain the increased cytotoxicity values of [**25**] and [**26**] compared with their individual components.[105]

1.4.3.4. Copper(II) complexes of nitrogen mustard ligands

In addition to complexes of cobalt(III), *N*-mustard derivatives have been coordinated to copper(II) centres (**Figure 1.24**).[106]

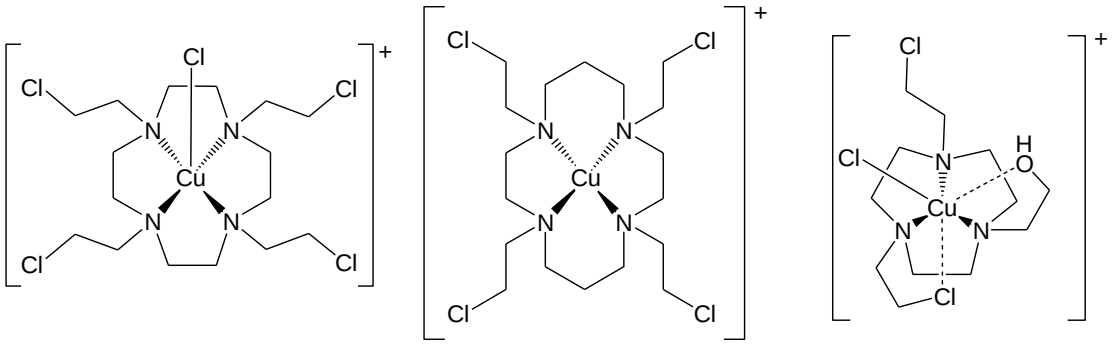

[**27**] [**28**] [**29**]

Figure 1.24: Structures of copper(II) *N*-mustard complexes [**27**], [**28**] and [**29**].[106]

Complex [**27**] was found to have the greatest aqueous stability out of the three complexes examined, and was shown to undergo a reversible one-electron reduction at -0.013 V. The other two complexes, [**28**] and [**29**], were shown to undergo reductions at more negative redox potentials, but showed no degree of reversibility (**Table 1.10**). The complexes were tested against K562 (human chronic myeloid leukaemia) cells under normoxic and hypoxic conditions, and compared to the cytotoxicity of their respective uncoordinated mustard ligands under normoxia (**Table 1.10**). Complexation of the ligand in [**27**] brought about the greatest reduction in aerobic cytotoxicity compared to the free ligand, whereas no significant

change was observed upon complexation to [**28**] and [**29**]. The toxicity of [**28**] and [**29**] slightly decreased under hypoxia, whereas the cytotoxicity of [**27**] increased over 20-fold, suggesting its promise as a hypoxia-selective cytotoxin.[106]

Table 1.10: IC_{50} values of the copper(II) complexes [**27**], [**28**] and [**29**] against K562 under normoxic and hypoxic conditions, and their reduction potentials in aqueous solution.[106]

Compound	**IC_{50}(air) / µM**	**IC_{50}(hypoxia) / µM**	**E_{red} / V *vs* Ag/AgCl**
[**27**]	53.4 ± 10	2.2 ±0.25	-0.212
Ligand of [**27**]	22	---	---
[**28**]	10.1 ±1	51.3 ±10	-0.339
Ligand of [**28**]	7.5	---	---
[**29**]	8.4 ±0.7	15.9 ±1	-0.439
Ligand of [**29**]	10.5	---	---

From studies with [Cu(ATSM)] ([**19**]), it appeared that a more negative reduction potential for the copper(II) centre aided hypoxia selectivity. This was demonstrated with [**19**] possessing a reversible reduction potential of -0.57 V *vs*. Ag/AgCl in DMSO, whilst its analogues were found to show a correlation between poorer hypoxia selectivity and a less negative reduction potential.[107, 108] On the basis of this, it would be expected that complex [**29**] would show the greatest hypoxia selectivity, owing to it having the most negative reduction potential of the complexes examined (0.439 V *vs*. Ag/AgCl in DMSO), but this complex showed no hypoxia selectivity. The selectivity of [**27**] demonstrates that the stability of the copper(II) complex and reversibility of the copper(II) reduction are important factors in obtaining hypoxia-selective ligand dissociation.

1.5. Conclusions

It has been established that owing to the nature of growth within tumours, regions of sub-normal oxygen levels occur. It has been found that in addition to the lack of oxygen in these hypoxic regions, which causes their environment to be more reducing, cellular adaptations cause the extracellular environment of these regions to become more acidic. It has been found that the occurrence of hypoxia renders many anticancer treatments less effective, but it also provides an opportunity for the development of prodrugs to selectively target these areas of tumours. One suitable area for the development of such prodrugs is transition metal chemistry where a metal can be used to deliver and control the activity of a cytotoxic ligand or contribute to the cytotoxicity itself. The requirements needed to achieve a hypoxia-selective prodrug that is both selective and effective *in vivo* are not yet fully understood and the pursuit of developing such a prodrug remains a challenge to medicinal chemists.

Metals can have a highly-varied role in medicinal chemistry; they can provide the cytotoxic activity, provide improved delivery of a therapeutically active ligand and can also modify a ligand's biological behaviour. The examples discussed highlight the unpredictable nature that designing inorganic medicinal compounds can involve, such as stability and reactivity. The accidental discovery of cisplatin is yet to be matched in success with other complexes. Trying to combine the second generation analogue of oxaliplatin with hydroxytamoxifen produced a complex with ineffective activity but the ferrohydroxytamoxifen complex [**11**] showed promising activity. With another family of metal complexes incorporating derivatives of aspirin, the ferrocene derivative [**18**] showed poor anti-proliferative activity compared with the cobalt complex [**15**] and ruthenium complex [**16**]. Studies of cobalt(III) complexes [**25**] and [**26**] have demonstrated that complexation can improve a drug's delivery throughout the tumour with the use of fluorescence studies. No cobalt(III) complexes have as yet emerged beyond laboratory use for as hypoxia-selective cytotoxic drugs, partly due to lack of cytotoxic selectivity. Complex [**19**] ([Cu(ATSM)] has failed to enter full clinical use over concerns of the isotopically-labelled copper accumulating in the liver and kidneys.[109, 110]

1.6. Project Aims

Although it has been demonstrated that hypoxia selectivity can be achieved, a hypoxia selective cytotoxic agent is yet to reach full clinical usage. This project aims to use ligand systems that are known to already demonstrate hypoxia selectivity, with the aim of improving their properties such as delivery, selectivity and stability. Ligands to be investigated in this way include those based upon 2,2'-dipyridylamine (dpHa) (**Figure 1.25**) which is a therapeutic fragment of several inhibitors designed to selectively act upon kinases essential for tumour cell growth and survival.

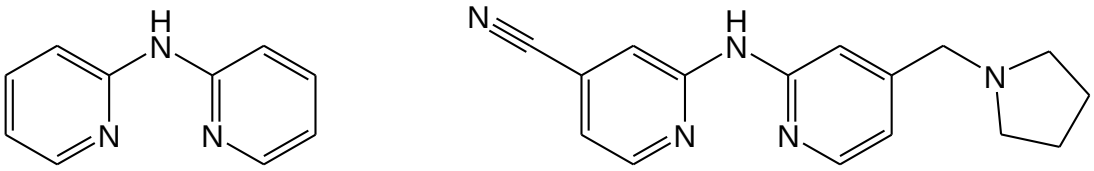

dpHa

Figure 1.25: Structure of dpHa (2,2'dipyridylamine) (*left*) and an example of a dpHa-based kinase inhibitor (*right*).[111]

Another ligand to be explored is tpzH (**Figure 1.26**). Despite its highly potent and selective cytotoxicity against hypoxic tumour cells *in vitro*, full clinical use has not been achieved owing to its apparent lack of effectiveness in clinical trials.[112]

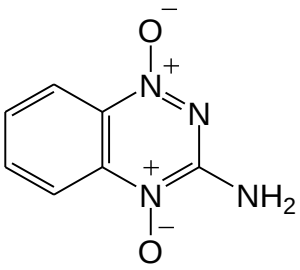

tpzH

Figure 1.26: Structure of tpzH (tirapazamine)

This project will focus on using copper(II) and cobalt(III) to form complexes that act as hypoxia-selective prodrug compounds. The aim is to develop compounds with a 'double trigger' action, where there is an additional activation step provided by the

metal before the active species is formed within the hypoxic tumour cellular environment (**Scheme 1.13**).

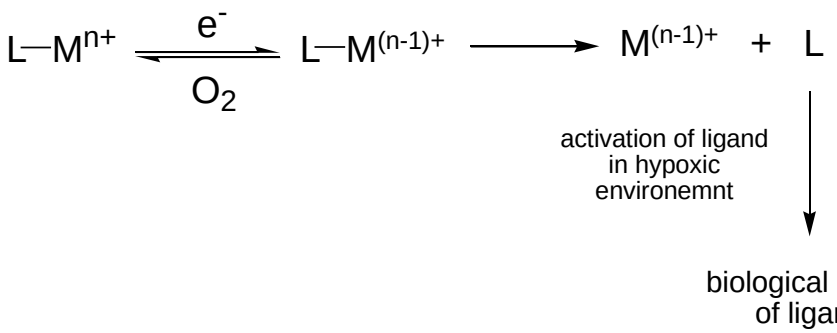

Scheme 1.13: Proposed 'double trigger' mechanism for the complexes to be prepared during this project

This strategy aims to produce transition-metal based prodrugs with improved biological properties and provide a method of improving upon compounds which already show a degree of hypoxia selectivity.

Most previous work on hypoxia selectivity has ignored the occurrence of sub-normal pH values within hypoxic regions of tumours. This project aims to study how this difference in pH may be used to aid the activation of hypoxia-selective prodrugs in conjunction with other properties such as reduction potentials. The use of more than one environmental factor to activate such prodrugs could result in improved hypoxia selectivity.

The target metal complexes will be fully characterised, including full chemical structure determination where possible. The various solution properties of the metal complexes and their ligands will studied, including their pH-dependant behaviour and redox chemistry because the anaerobic environment and acidified pH of hypoxic tumour cells are two features which differentiate them from normal cells. The cytotoxicity of the complexes will also be evaluated, and analysed in the context of the results obtained from the solution studies. This will allow for obtaining a better understanding of how their properties relate to activity and how they might be improved upon.

Chapter Two: Evaluation of 2, 2'-dipyridylamine complexes as kinase inhibitors

2.1. Introduction to kinase inhibitors

The majority of anti-cancer agents target cellular DNA, but there is an increase in the development of drugs that take effect on other biological targets. The human genome encodes for 518 known kinases and the past few decades have revealed the relationship between kinase gene mutations which alter their function, and many human diseases.[113, 114] Kinases are a class of enzymes which catalyse the phosphorylation of specific amino acids on proteins such tyrosine or threonine. Through the transfer of the phosphate group from ATP to the substrate, the electronic character of that region of the protein is altered which can result in a conformational change, and thus alter its function (**Scheme 2.1**). This conformational change can enable the protein to be 'switched' on and off, allowing kinases to play an integral role in the control of cellular processes such as replication, metabolism, apoptosis and signalling.[115]

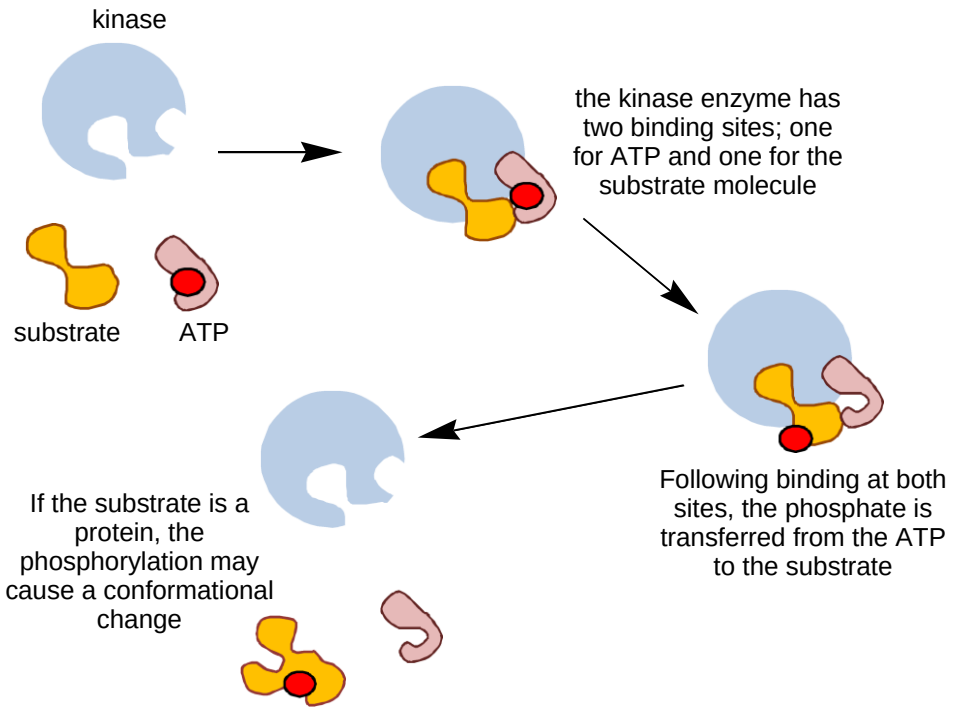

Scheme 2.1: Scheme showing the general biological activity of kinase enzymes

Due to their importance in cell regulation, and implications in disease, it is not surprising that in 2002, it was estimated that out of the biological targets used by

drugs, over a quarter of the targets were protein kinases.[116, 117] The specificity of kinases towards their particular substrate is usually due to altered structure and conformation about the active site. This feature can be exploited by medicinal chemists to develop inhibitors which can specifically target one particular kinase. An example of a kinase-selective inhibitor is Gefitinib which specifically inhibits epidermal growth factor receptors and thereby hinders cancer cell growth. However, broad spectrum inhibitors which act upon multiple pathways, such as Dasatinib which targets multiple tyrosine kinases, have also been proved clinically useful. In 2009, there were several clinically approved kinase inhibitors (**Figure 2.1**).

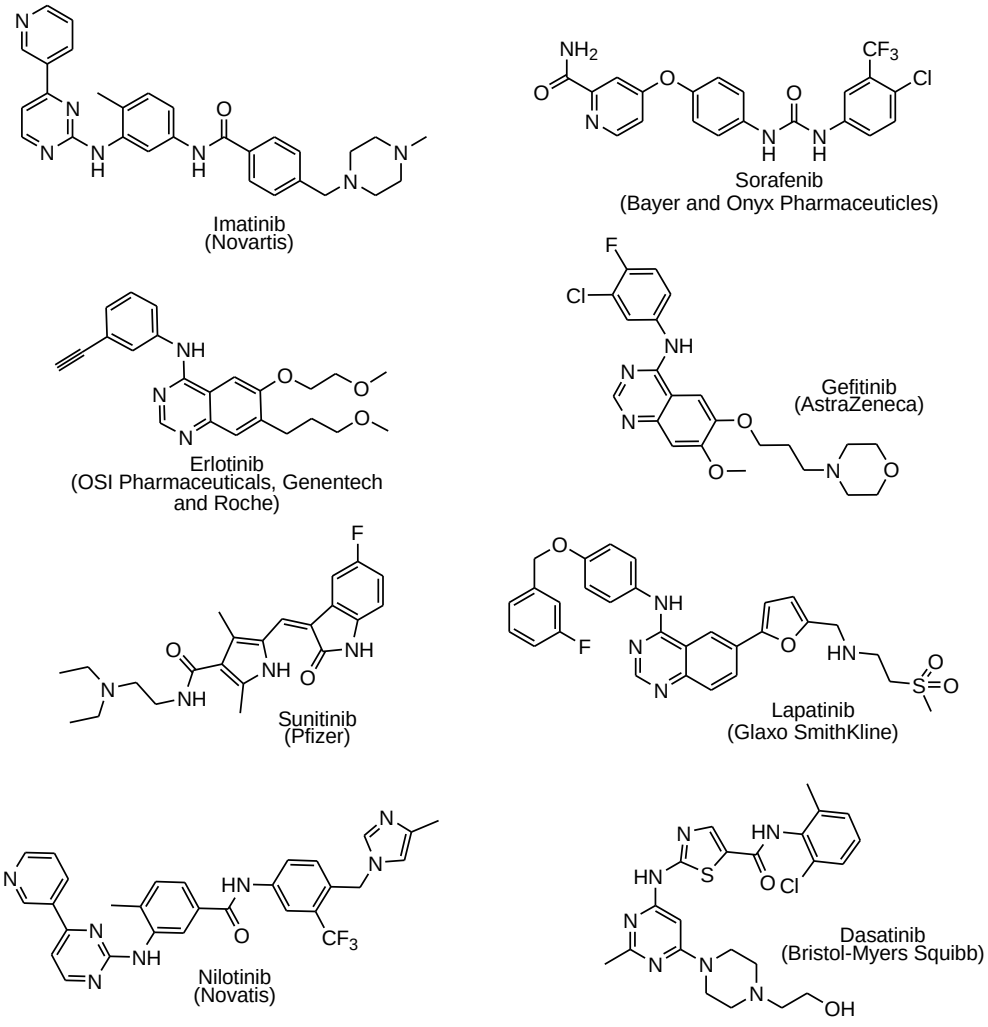

Figure 2.1: Kinase inhibitors which entered clinical use for the treatment of cancer by 2009 (and the companies who developed them).[118]

It can be seen that they all consist of a flexible chain of aromatic rings with groups capable of forming complimentary hydrogen-bonding interactions with the residues about the active site. The aromatic rings can be positioned into the hydrophobic regions within the kinase active site (**Figure 2.2**). The larger the number of interactions with the active site, the stronger the affinity of the inhibitor and the more effectively it can compete with the natural substrate.[119]

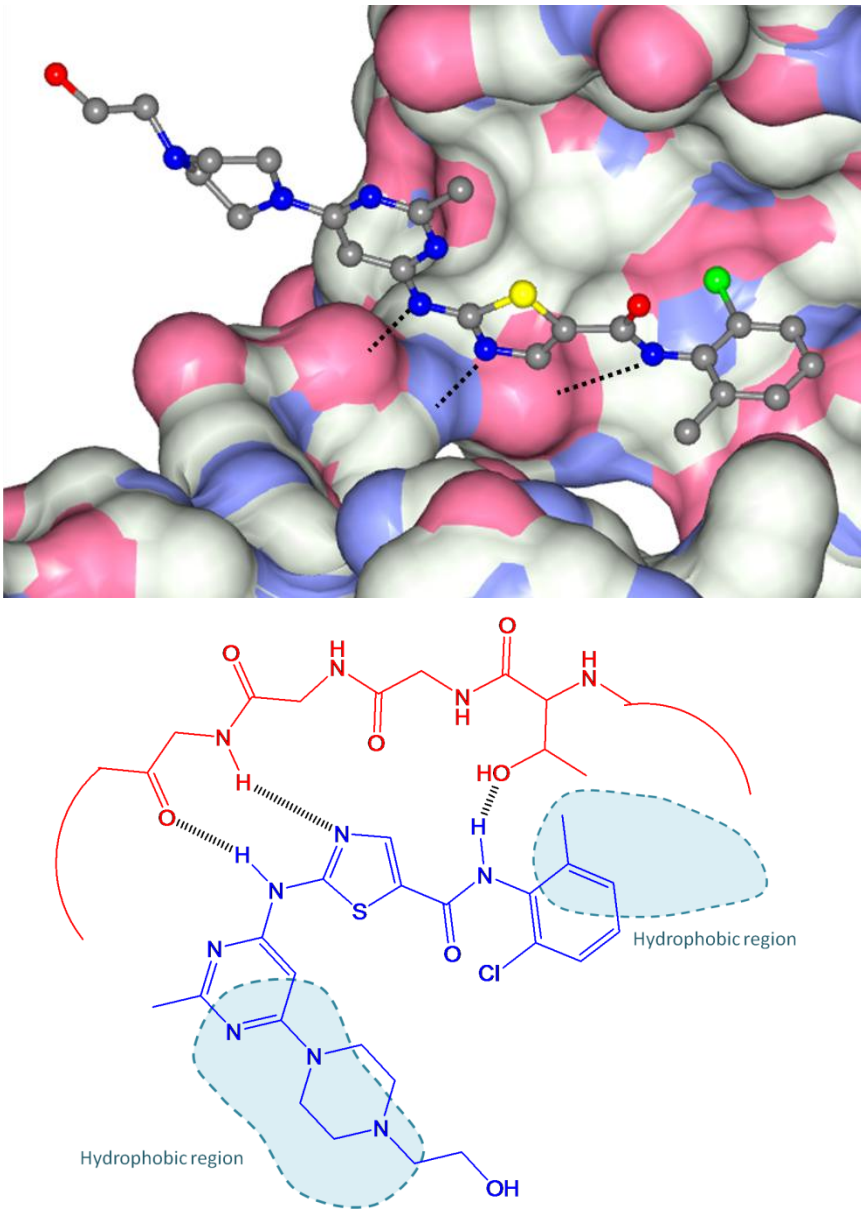

Figure 2.2: How the small molecule inhibitor dasatinib binds into the ATP cavity region of the active site of a protein kinase enzyme: Crystal structure (*above*) of dasatinib bound to Human p38 MAP Kinase (PDB code 3LFA),[120, 121] and scheme of interactions within the active site (*below*) showing hydrogen-bonds between protein and inhibitor (dashed lines) and hydrophobic regions.[118]

It can be seen how it may be possible to coordinate inhibitors such as dasatinib to a metal centre (**Figure 2.3**) due to it containing two nitrogen heterocycles which can give rise to a stable six-membered chelate ring.

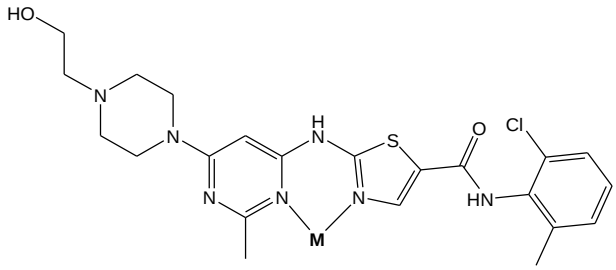

Figure 2.3: How the kinase inhibitor dasatinib could coordinate to a metal centre through its two pyridyl nitrogen atoms

There are now inhibitors emerging that can also be potentially coordinated to metal centres which contain a 2,2'-dipyridylamine fragment such as KI1 and KI2. [122, 123] These inhibitors feature phenyl or napthyl substituents on the pyridyl rings which are designed to fit within the hydrophobic pockets of the active site. The pyridyl nitrogen atoms can act as hydrogen-bond acceptors and the amine which can behave as a hydrogen-bond donor whilst in the active site (**Figure 2.4**).

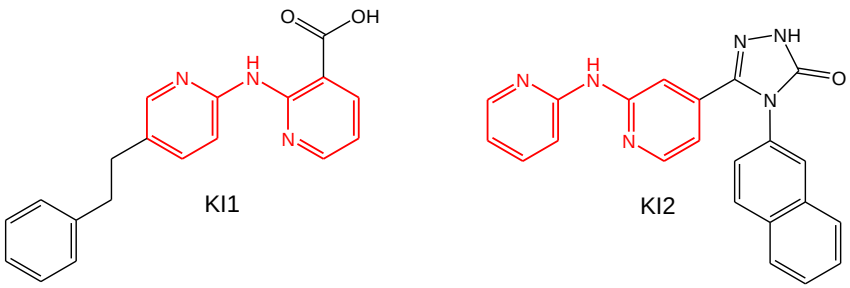

Figure 2.4: Structures of inhibitors containing the 2,2'-dipyridylamine fragment (shown in red) reported in the literature (KI1 and KI2).[122, 123]

Sentinel Oncology have developed a library of inhibitors based around the 2,2'-dipyridylamine fragment appended to a Lewis base group to act as a further hydrogen-bond acceptor (**Figure 2.5**).[111]

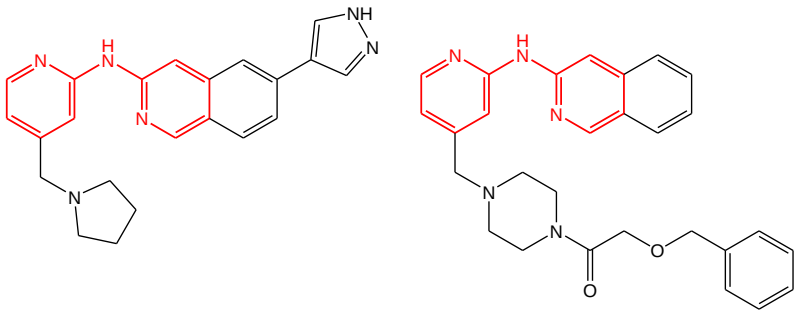

Figure 2.5: Examples of inhibitors developed by Sentinel Oncology which incorporate 2,2'-dipyridylamine.[111]

These inhibitors are designed so that they can bind to the kinase active site when in the *anti* conformation but is inactive when in the *syn* conformation (**Figure 2.6**). The aim of this study is to evaluate the therapeutic potential of coordinating a kinase inhibitor therapeutic fragment, 2,2'-dipyridyl amine (dpHa) to metals in order to provide a hypoxia selective kinase inhibitor. The pyridyl nitrogen atoms are well-positioned to be both coordinated to a metal centre, thus enforcing the inactive *syn* conformation of the dpHa ligand upon coordination.

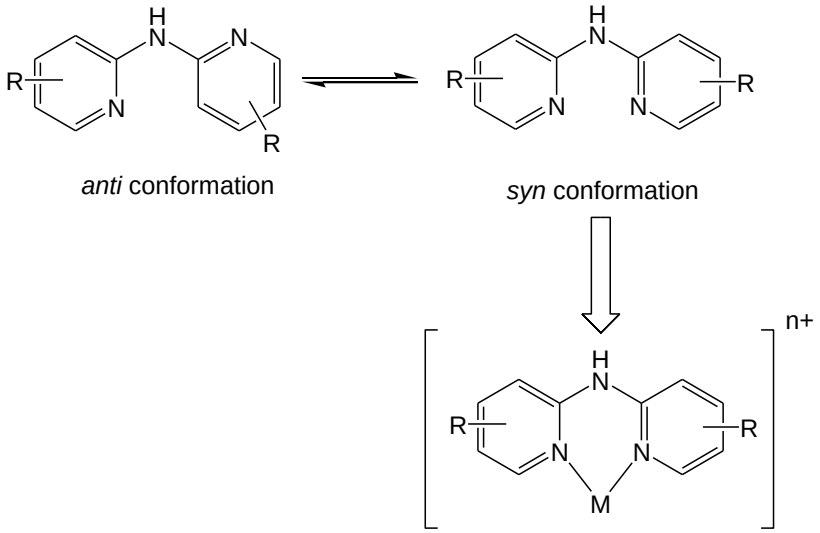

Figure 2.6: The *anti* and *syn* conformations of dpHa and the *syn* conformation that can be enforced upon coordination to a metal centre

2.2. Complexes of 2,2'-dipyridylamine as kinase inhibitors

This work starts off by preparing and studying complexes of 2,2'-dipyridylamine (dpHa). The coordination chemistry of dpHa has been widely reported including and includes various applications such as ruthenium complexes used for the reduction of aromatic ketones through transfer hydrogenation and lanthanide coordination chemistry (**Figure 2.7**) in addition to numerous examples of first row coordination chemistry.[124, 125]

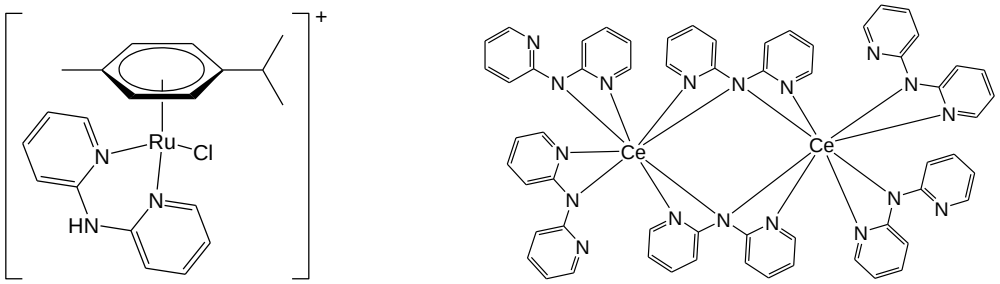

Figure 2.7: Examples of reported metal complexes of dpHa.[119, 120]

Complexes of $[M(Cl)_2(dpHa)]$ where M is copper(II),[126] cobalt(II),[127] and zinc(II) have previously been reported in the literature along with their structures, as has that for $[Zn(dpHa)_2]2BF_4$.[128, 129] The structures of $[Co(Cl)_2(dpHa)]$ and $[Zn(Cl)_2(dpHa)]$ were both reported as having a tetrahedral geometry whilst the $[Cu(Cl)_2(dpHa)]$ and $[Zn(dpHa)_2](BF_4)_2$ having distorted tetrahedral geometries. These complexes were all prepared and characterised, with diffraction quality crystals being obtained for $[Co(Cl)_2(dpHa)]$ and $[Zn(Cl)_2(dpHa)]$ by slow diffusion of Et_2O into a DMF solution. As the space group obtained for these crystals matched those of the reported structures in the literature, the identity of the complexes was confirmed.

2.2.1. Copper(II) and cobalt(II) *bis*-2,2'-dipyridylamine complexes

$[Cu(dpHa)_2]Cl_2$ was prepared according to the reported method by reacting a solution of two equivalents dpHa in acetone with an ethanolic solution containing one equivalent of $CuCl_2.2H_2O$ (**Scheme 2.2**).[130]

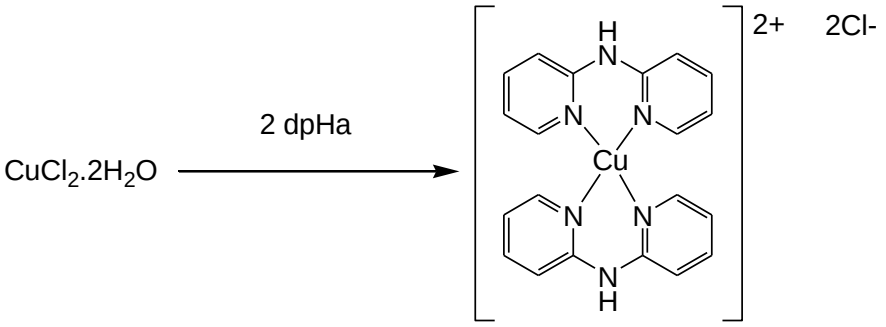

Scheme 2.2: Preparation of $[Cu(dpHa)_2]Cl_2$

The product formed as a green precipitate which could be isolated as a bright green powder in 87% yield. Filtering a methanolic suspension of the product removed any $[Cu(Cl)_2(dpHa)]$ which may have formed and which is insoluble in MeOH. The product could then be obtained by reducing the filtrate to dryness. Green diffraction quality crystals were obtained by slow evaporation from a solution of MeOH layered over ^{n}BuOH over the duration of a week at room temperature. The structure shows the two dpHa ligands coordinated to the copper(II) centre, with the N(1) and N(4) nitrogen atoms of the two pyridyl ligands being trans to each other (**Figure 2.8**). One of the chloride ligands is coordinated to the metal centre in the axial position.

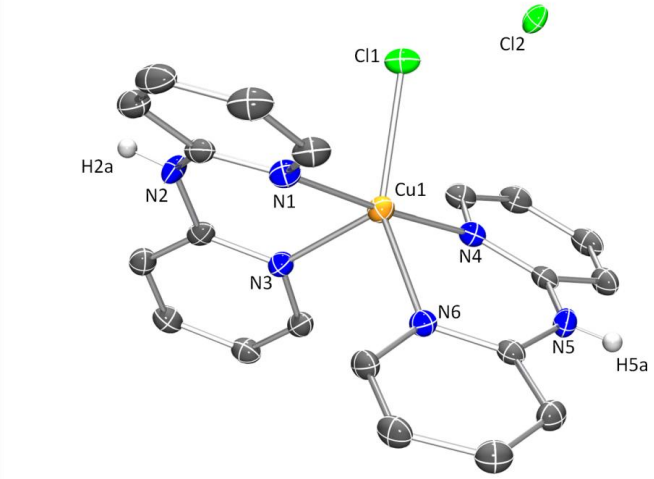

Figure 2.8: ORTEP diagram (50% probability ellipsoids) of $[Cu(Cl)(dpHa)_2]Cl$.[131] Hydrogen atoms (except H(2a), H(1b) and H(5)), omitted for clarity. Selected bond lengths / Å and angles / °: Cl(1)-Cu(1) 2.3013(8), Cu(1)-N(4) 1.989(2), Cu(1)-N(1) 2.007(2), Cu(1)-N(6) 2.075(2), Cu(1)-N(3) 2.139(2), N(1)-Cu(1)-N(3) 88.49(8), N(4)-Cu(1)-N(6) 88.72(8)

For five-coordinate metal complexes, a value, τ, can be calculated to qualitatively determine if the structure is square pyramidal, trigonal bipyramidal or distorted i.e. somewhere in between the two.[132]

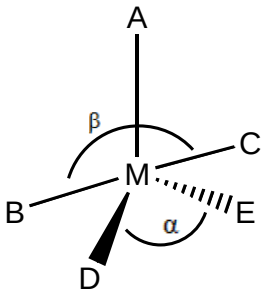

Figure 2.9: Relevant parameters of a five coordinated complex needed to calculate the τ value (A is the axial ligand, β is the greatest angle between the basal ligands and α is the angle *trans* to β).[132]

If a five coordinate complex such as that shown in **Figure 2.9** is of perfect square pyramidal geometry, then the angles α and β both equal 180º. If the complex adopts a perfect triganol-bipyramidal geometry, β is equal to 180º whilst α equals 120º. The τ value can be calculated according to the following equation:

$$\tau = \frac{(\beta - \alpha)}{60}$$

When τ is equal to 0 then the structure can be considered to be of a perfect square pyramidal geometry and 1 for a complex of trigonal-bipyramidal geometry. The calculated τ value for the copper complex is 0.024, indicating it has a near square pyramidal geometry.[132]

With cobalt(II), it is possible to form the *bis*-complex $[Co(Cl)_2(dpHa)_2]$ by reacting two equivalents of dpHa with one equivalent $CoCl_2.6H_2O$ in a methanolic solution.[133] The reaction mixture was filtered and the solvent of the filtrate allowed to partially evaporate at room temperature, leading to a precipitate, to allow for isolation of the product in 63% yield. This complex was converted to the mono dpHa complex $[Co(Cl)_2(dpHa)]$ upon the application of heat or addition of other solvents such as Et_2O, acetone or EtOH. Crystals of the *bis*-complex were obtained by slow evaporation from a concentrated methanolic solution. The x-ray structure (**Figure 2.10**) shows the two dpHa ligands in a *cis*-arrangement about the cobalt(II) centre along with two chlorides. One of the chloride ligands, Cl(2), has a 50% occupancy

due to it being exchanged for a neutral aqua ligand. When the aqua ligand is present, the charge of the complex is balanced by a non-coordinating chloride, Cl(3).

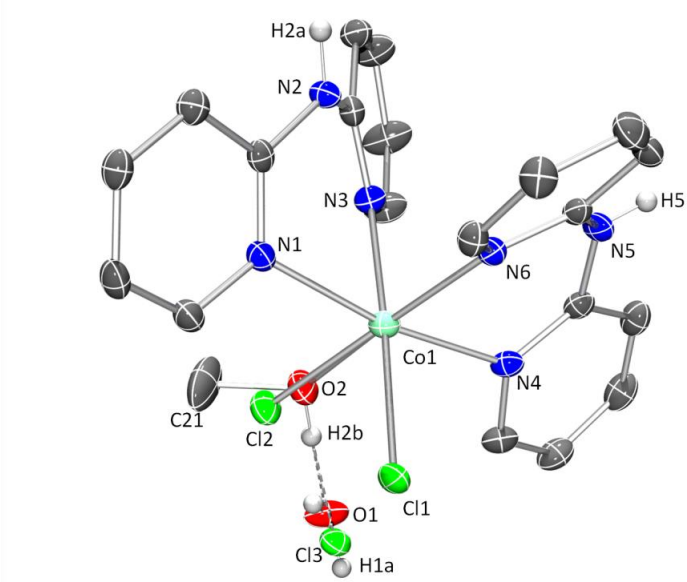

Figure 2.10: ORTEP diagram (50% probability ellipsoids) of $[Co(Cl)_2(dpHa)_2]$.[131] Hydrogen atoms (except H(1a), H(1b), H(2a), H(2b) and H(5)), omitted for clarity. Selected bond lengths /Å and angles /º : Co(1)-Cl(1) 2.4209(5), Co(1)-Cl(2) 2.5115(13), Co(1)-N(1) 2.1482(14), Co(1)-N(3) 2.1526(14), Co(1)-N(4) 2.1293(15) Co(1)-N(6) 2.1343(14), N(4)-Co(1)-N(6) 84.05(5), N(1)-Co(1)-N(3) 81.90(5). Hydrogen-bond distances / Å and angles /º: H(2b)···Cl(3) 2.34(5), O(2)···Cl(3) 3.159(4), O(2)- H(2b)···Cl(3) 166(4)

The chloride ligand with full occupancy forms a hydrogen-bond with the central amine of a pyridyl ligand of an adjacent complex. The presence of hydrogen-bonds can be determined crystallographically through the application of several criteria (**Table 2.1**). The traditional crystallographic method for hydrogen-bond determination is to compare the distance between the hydrogen-bond donor and acceptor atoms with the sum of their van der Waals radii. It is more reliable to use the distance between the donor and acceptor atoms rather than between the hydrogen and acceptor atoms owing to the position of hydrogen atoms not being as easily defined. The distance between Cl(1) and N(5) is 3.2295(16) Å which is less than the sum of their van der Waal radii of chlorine and nitrogen (1.75 and 1.55 Å respectively).

Table 2.1: Crystallographic criteria for hydrogen-bonds used by the PLATON programme.[134]

Parameter	Criteria for hydrogen-bond definition
$d_{D\cdots A}$	$< r_D + r_A + 0.5$
$d_{H\cdots A}$	$< r_H + r_A - 0.12$
$\phi_{D\text{-}H\cdots A}$	$> 100^o$

IUPAC have also recently stated a hydrogen-bond interaction needs to have a X–H···Y angle near to 180º and no less than 110º.[135] The measured angle of Cl(1)-H(5)-N(5) is 178(2)º which again provides evidence for the presence of a hydrogen-bonding interaction.

The second chloride ligand, Cl(2) is hydrogen-bonded to the H(1B) hydrogen of the uncoordinated water. This water also shows a hydrogen-bonding interaction between its oxygen O(1) and the amine proton H(2a) of the pyridyl ligand of an adjacent complex. When the coordination site of the second chloride is occupied by coordinated MeOH, this forms a hydrogen-bond with its alcohol proton, H(2b) to the uncoordinated chloride Cl(3) which in turn also acts as the hydrogen-bond donor with the amine proton on the adjacent complex. These combined interactions form infinite sheet structures throughout the crystal (**Figure 2.9**).

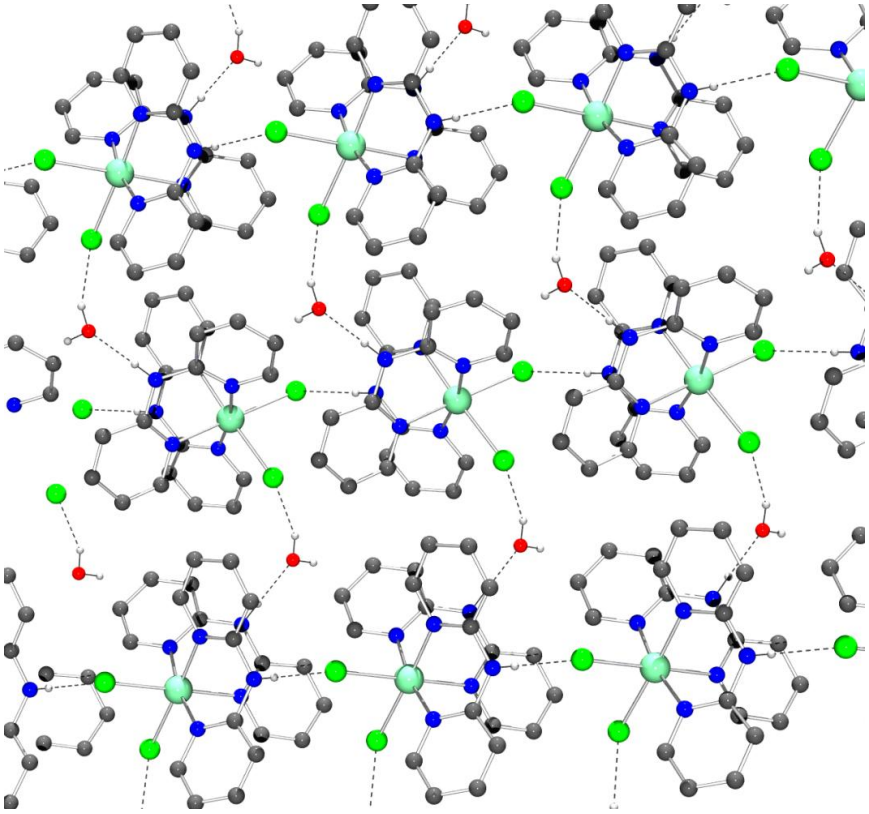

Figure 2.11: ORTEP representation of the infinite sheets formed by hydrogen-bonding interactions (dotted lines) between the complex and solvent.[131] Complex only shown as $[Co(Cl)_2(dpHa)_2].H_2O$ for clarity. Hydrogen-bond distances / Å and angles /°: H(2b)···Cl(3) 2.34(5), O(2)···Cl(3) 3.159(4), H(1b)···Cl(2) 2.36(6), O(1)···Cl(2) 3.123(5), H(5)···Cl(1) 2.43(2), N(5)···Cl(1) 3.2295(16), H(2a)···Cl(3) 2.39(2), N(2)···Cl(3) 3.265(2), H(2a)···O(1) 1.87(2), N(2)···O(1) 2.744(4), O(2)-H(2b)···Cl(3) 166(4), O(1)-H(1b)···Cl(2) 155(5), N(5)-H(5)···Cl(1) 178(2), N(2)-H(2a)···O(1) 178(2)

2.2.2. Cobalt(III) complex of 2,2'-dipyridylamine

A cobalt(III) complex was initially prepared by addition of H_2O_2 and one equivalent of NH_4PF_6 to a methanolic solution of $[Co(Cl)_2(dpHa)_2]$, with the resulting product expected to be $[Co(Cl)_2(dpHa)_2]PF_6$. Crystals were obtained upon the reaction mixture being left to stand overnight. The structure revealed a cobalt(III) centre coordinated to two dipyridylamine ligands as expected with the PF_6 counter-ion, but no chloride ligands. In their place was a four-atom triganol group, which was modelled as both nitrate and carbonate. It was found that modelling with a carbonate

ligand provided the best fit to the diffraction data. This was then confirmed experimentally by preparing the complex under nitrogen and in the presence of excess carbonate. Preparing the complex under inert conditions resulted in a reaction mixture that could not be characterised by NMR spectroscopy owing to the large proportion of cobalt(II) present. Carrying the reaction out with excess $NaHCO_3$ led to a far higher yield (41%) of red crystals was produced upon leaving the reaction mixture standing overnight. As PF_6 is not a biologically suitable anion, a more appropriate counter-ion was needed to be used in its place. The structure obtained for with the PF_6 counter-ion showed no evidence for the presence of chlorides from the original cobalt(II) salt being present in the complex, coordinating or non-coordinating. It was therefore decided to use nitrate, which could be provided by using a $Co(NO_3)_2.6H_2O$ in place off the chloride anion.

The cobalt(III) complex was therefore prepared directly by reacting $Co(NO_3)_2.6H_2O$ with two equivalents of dpHa, $NaHCO_3$ and H_2O_2 (**Scheme 2.3**) to form $[Co(CO_3)(dpHa)_2]NO_3$ in 79% yield.

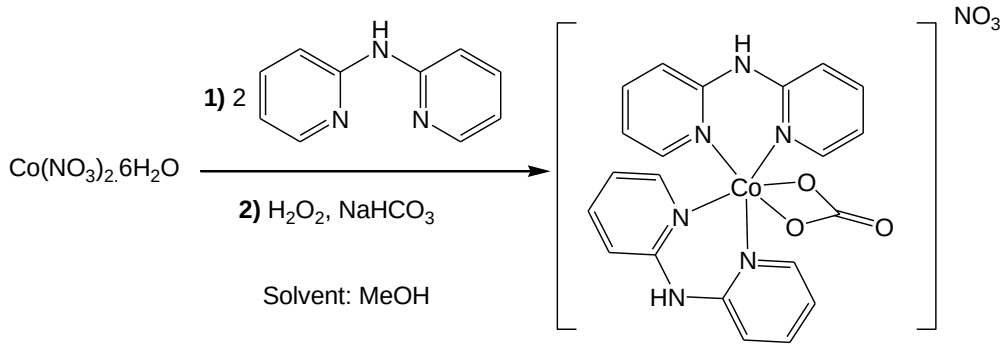

Scheme 2.3: Preparation of $[Co(CO_3)(dpHa)_2]NO_3$

Diffraction quality crystals of the resulting complex again were formed by leaving the filtered reaction mixture to stand. The data were fitted with two models; a coordinated carbonate and uncoordinated nitrate, and *vice versa*, to confirm that the carbonate was present as a ligand and nitrate as a counter-ion. Modelling the complex as $[Co(CO_3)(dpHa)_2]NO_3$ provided the best fit with the diffraction data (**Figure 2.12**).

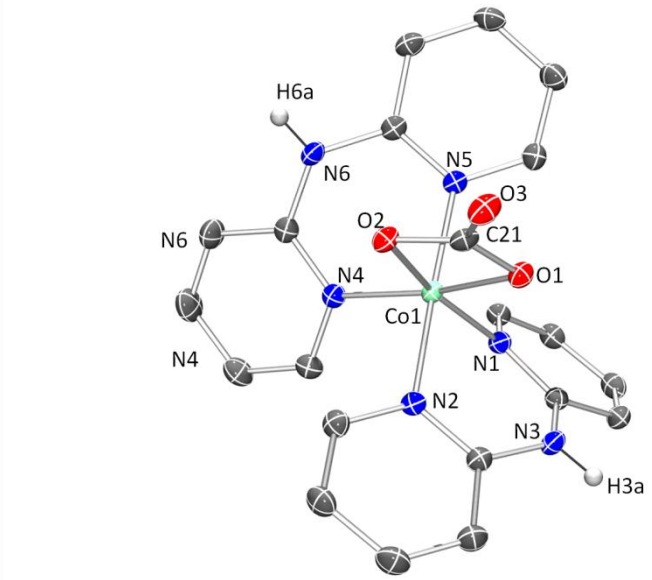

Figure 2.12: ORTEP diagram (50% probability ellipsoids) of $[Co(CO)_3(dpHa)_2]^+$.[131] NO_3 counter-ion and hydrogen atoms (except H(3a) and H(6a)) omitted for clarity. Selected bond lengths /Å and angles /º: Co(1)-O(1) 1.8981(10), Co(1)-O(2) 1.9117(10), Co(1)-N(1) 1.9250(12), Co(1)-N(2) 1.9261(12), Co(1)-N(5) 1.9342(12), Co(1)-N(4) 1.9437(13), O(1)-Co(1)-O(2) 69.23(4), N(1)-Co(1)-N(2) 88.94(5), N(5)-Co(1)-N(4) 89.57(5)

The structure shows a near-octahedral metal centre which appears to be slightly distorted by the carbonate having a bite angle of 69.23(4)º. The cobalt-ligand bond lengths are all under 2 Å which is characteristic for a cobalt(III) complex. The crystal structure reveals two complexes within the lattice are linked via two hydrogen-bonds formed between the amine proton H(3a) and the carbonate oxygen O(3) of the adjacent complex (**Figure 2.13**). The other amide proton of the complex, H(6a) forms a hydrogen-bond with the uncoordinated nitrate anion. These interactions have formed dimeric units throughout the lattice, with each consisting of two complexes and two nitrate counter-ions.

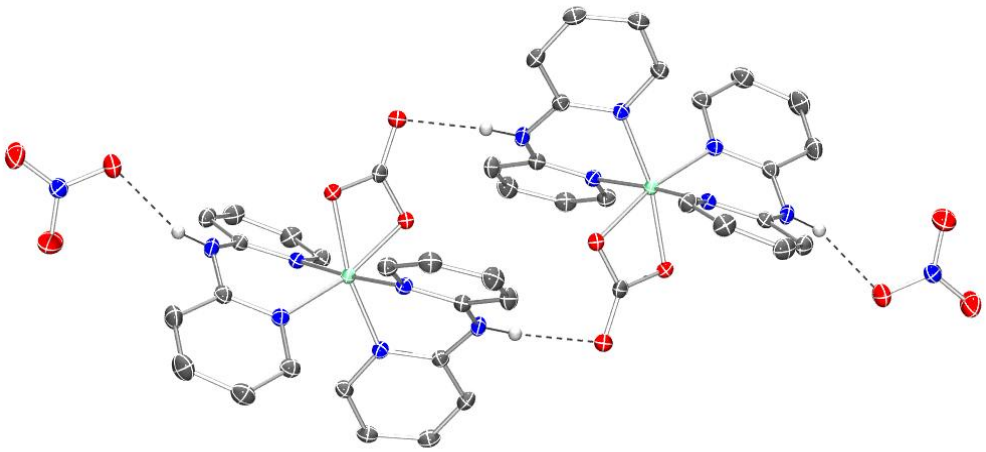

Figure 2.13: ORTEP representation of the hydrogen-bonding interactions evident within the crystal structure of $[Co(CO_3)(dpHa)_2]NO_3$.[131] Hydrogen-bond distances / Å and angles /°: H(6a)···O(6) 2.05(2), N(6)···O(6) 2.8175(18), H(3a)···O(3) 2.02(2), N(3)···O(3) 2.8553(17), N(6)-H(6a)···O(6) 159(2), N(3)-H(3a)···O(3) 173(2)

The ^{1}H NMR spectrum of the complex in D_2O (**Figure 2.14**) shows that there are eight signals for the sixteen aromatic protons, indicating that there are two equivalent sets of pyridyl rings. The NMR spectroscopic data fits with the two dpHa ligands being equivalent, each with two ring environments.

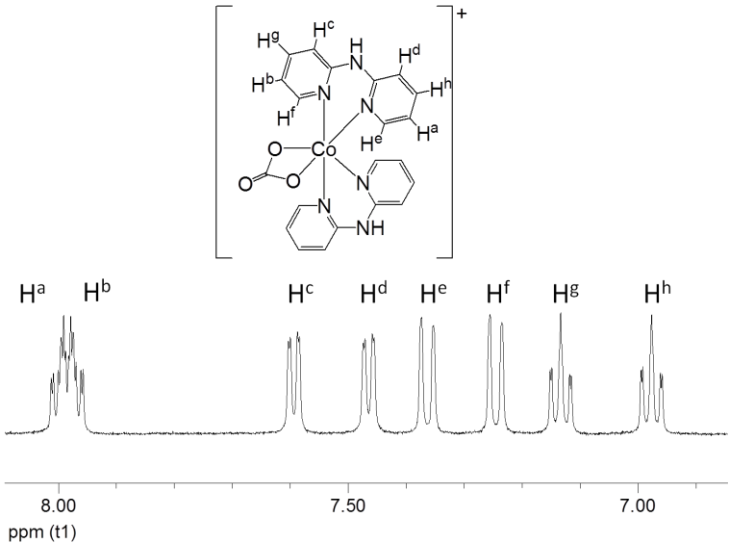

Figure 2.14: ^{1}H NMR (D_2O, 400 MHz) of $[Co(CO_3)(dpHa)_2]NO_3$. δ8.05 (td, 2H, J = 8.0, 1.0 Hz, H^a), δ7.99 (td, 2H, J = 8.0, 1.0 Hz, H^b), δ7.60 (dd, 1H, J = 6.0, 1.0 Hz, H^c), δ7.46 (dd, 1H, J = 6.0 Hz, 1.0 Hz, H^d), δ7.36 (d, 1H, J = 6.0 Hz, H^e), δ7.24 (d, 1H, J = 8.5 Hz, H^f), δ7.13 (ap.td, 2H, J = 7.0, 1.0 Hz, H^g), δ6.98 (td, 2H, J = 6.5, 1.0 Hz, H^h)

The ^{1}H-^{1}H COSY NMR spectrum (**Appendix 1**) shows correlation between H^{a} and the two protons H^{e} and H^{h}. The H^{h} peak is shown to also be coupled to H^{d}, indicating that these four signals correspond to protons on the same aromatic ring. Similar coupling is also seen for the proton signals H^{b}, H^{c}, H^{f} and H^{g}, indicating that these proton signals correspond to the second pyridyl ring environment.

2.3. Complexes of 2,2'-dipyriylmethylamine

To aid the solution studies which will be discussed in **Chapter 5,** which include pK_a determinations, it was decided that methylation of the central amine of dpHa would help ascertain whether observed processes were due to changes in the protonation state or not.

2.3.1. Preparation of *N*-methyl-2,2'-dipyriylamine

There is precedence in the literature for the preparation of *N*-methyl-2,2'-dipyridylamine (dpma) by methylation of dpaH after treatment with various bases. Boyer *et al.* used ^{n}BuLi as the base with the eventual product being a yellow oil, whereas Krebs *et al* had used NaH to produce a red oil.[136, 137] The latter paper described a series of dpHa derivatives where the central amine has been methylated, but for all other alkylations involving the addition of an ethyl or butyl group, hydroxide was used as the base instead. As no explanation was provided for the use of different bases, it was decided to attempt the preparation with hydroxide (**Scheme 2.4**).

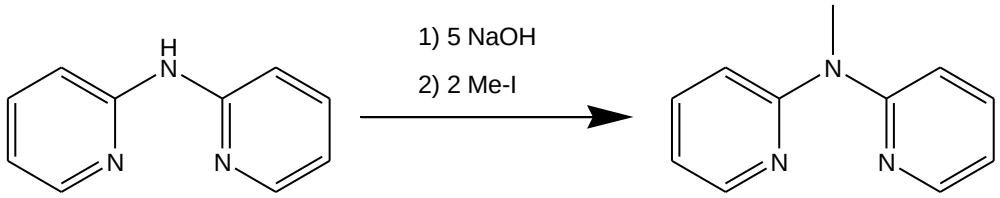

Scheme 2.4: Preparation of the dpma ligand from dpHa

The resulting product was isolated as a yellow oil and ^{1}H NMR spectroscopic analysis (**Figure 2.15**) indicated the addition of the methyl to the dpHa and that the two pyridyl rings had remained chemically equivalent, whilst ESI-MS confirmed the addition of the methyl group with the molecular ion increasing by 15 to *m/*z 186.

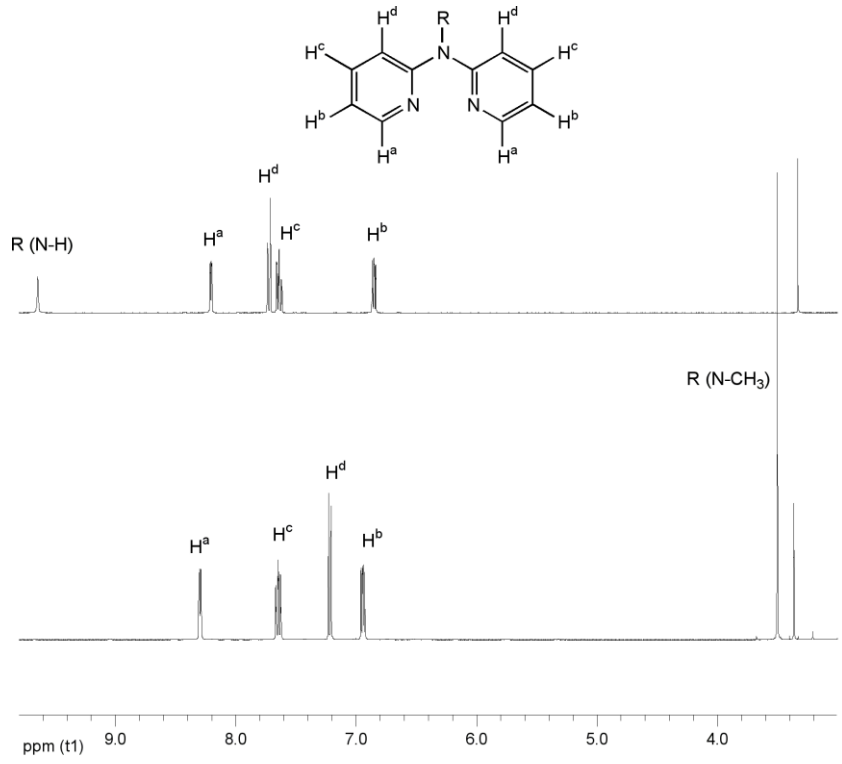

Figure 2.15: Assigned ^{1}H NMR spectra (400 MHz, d_6-DMSO) of dpHa (*above*) and dpma (*below*). ^{1}H NMR of dpHa: δ9.65 (br. s, 1H, NH), δ8.21 (ddd, 2H, J = 5.0, 2.0, 1.0 Hz, H^a), δ7.73 (dt, 2H, J = 8.5, 1.0 Hz, H^d), δ7.64 (ddd, 2H, J = 8.5, 7.0, 2.0 Hz, H^c), δ6.86 (ddd, 2H, J = 7.0, 5.0, 1.0 Hz, H^d). ^{1}H NMR of dpma: δ8.30 (ddd, 2H, J = 5.0, 2.0, 0.8 Hz, H^a), δ7.65 (ddd, 2H, J = 8.5, 7.0, 2.0 Hz, H^c), δ7.22 (dt, 2H, J = 8.0, 1.0 Hz, H^d), δ6.98 (dd, 2H, J = 7.0, 5.0, 1.0 Hz, H^b), δ3.51 (s, 3H, CH_3).

2.3.2. Preparation of metal(II) complexes of *N*-methyl-2,2'-dipyriylamine

The *N*-methyl-2,2'-dipyriylamine ligand (dpma) was complexed to metal(II) chloride salts in the same way as for dpHa. Complexation to copper(II) chloride was achieved by reacting equimolar amounts of the two together in methanolic solution where the product precipitated out as a green solid was then isolated by filtration in 69% yield. Diffraction quality crystals of the product were obtained through slow evaporation of the filtrate over a couple of days. The [$Cu(Cl)_2$(dpma)] complex crystallises as a dimer with two μ_2-chloride bridging ligands (**Figure 2.16**). The two copper centres are 3.6823(8) Å apart and are related by an inversion operation.

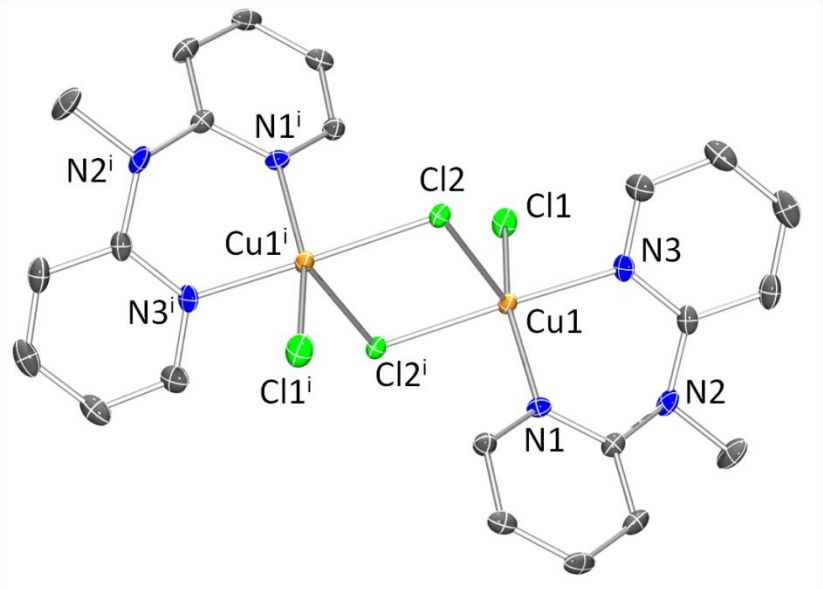

Figure 2.16: ORTEP diagram (50% probability ellipsoids) of [{$Cu(Cl)_2$(dpma)}$_2$].[131] Hydrogen atoms omitted for clarity. Selected bond lengths /Å and angles /º : Cl(1)-Cu(1) 2.2911(9), Cl(2)-Cu(1) 2.2838(9), Cl(2)-Cu(1) 2.6874(9), Cu(1)-N(3) 1.993(3), Cu(1)-N(1) 2.004(3), Cu(1)-Cl(2) 2.2838(9), N(3)-Cu(1)-N(1) 84.50(11)

The near-square pyramidal geometry of the complex is reflected in its τ value of 0.14.[127] The reported structure of [$Cu(Cl)_2$(dpHa)] shows the dpHa ligand to be almost planar with difference in angle between the planes of the two rings being 6.9º. In the [$Cu(Cl)_2$(dpma)] complex, the corresponding value is 49.6º. Possibly as a result of this increased bend through the central amine, the bite angle (N-Cu-N) of the dpma complex is, at 84.5º, smaller than that of the dpHa complex which is 94.6º.

The complex produced upon reacting equimolar amounts of dpma with $ZnCl_2$ in MeOH forms as a white precipitate which can be isolated by filtration in 71% yield. Diffraction quality crystals were obtained by slow diffusion of Et_2O into a solution of DMF. The resulting structure is analogous with that of the one previously reported for [$Zn(Cl)_2$(dpHa)], so allows a more direct comparison between the dpHa and dpma complexes than was possible for the copper(II) complexes. The complex has tetrahedral geometry (**Figure 2.17**) with similar metal-ligand bond lengths to the [$Zn(Cl)_2$(dpHa)].

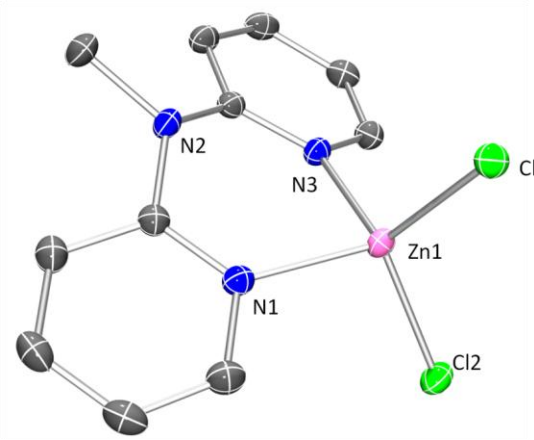

Figure 2.17: ORTEP diagram (50% probability ellipsoids) of $[Zn(Cl)_2(dpma)]$.[131] Hydrogen atoms omitted for clarity. Selected bond lengths /Å and angles /º : Cl(1)-Zn(1) 2.2100(4), Cl(2)-Zn(1) 2.2368(4), N(1)-Zn(1) 2.0275(13), N(3)-Zn(1) 2.0205(12), N(3)-Zn(1)-N(1) 90.71(5)

The differences arise in the bite angle for the dpRa ligand and the angle between the planes of the two pyridyl rings (**Table 2.2** and **Figure 2.18**).

Table 2.2: Comparison of dpRa bite angle in $[Zn(Cl)_2(dpHa)]$ and $[Zn(Cl)_2(dpma)]$

	N-Zn-N bite angle / º	**Angle between dpRa planes / º**
$[Zn(Cl)_2(dpHa)]$[128]	93.1(1)	5.5
$[Zn(Cl)_2(dpma)]$	90.71(5)	30.1

The comparison between these two structures suggests that the steric bulk of the forces the pyridyl ligand into a less planar conformation (**Figure 2.18**).

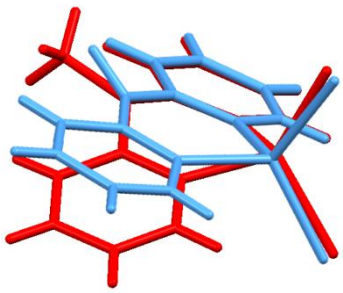

Figure 2.18: Overlay of $[Zn(Cl)_2(dpHa)]$ (blue) and $[Zn(Cl)_2(dpma)]$ (red) showing the increased bend between the two pyridyl rings upon methylation.[128, 171]

Diffraction quality crystals were obtained from the filtrate of the $[Zn(Cl)_2(dpma)]$ reaction mixture which produced an unexpected structure (**Figure 2.19**). It showed that one of the pyridyl nitrogen atoms had undergone methylation, leaving the central nitrogen as a secondary amine. The zinc(II) chloride then coordinated to the other pyridyl nitrogen, forming a tetrahedral *tris*-chloride species having obtained an additional chloride ion.

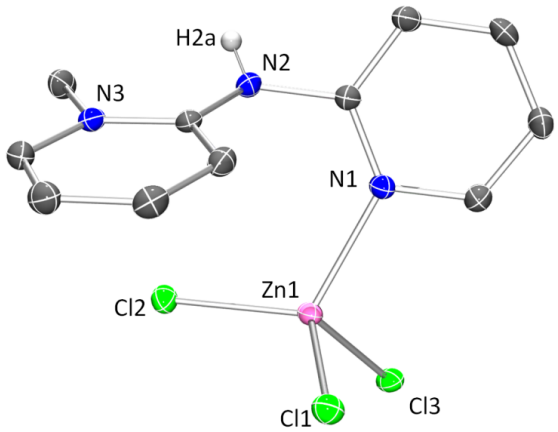

Figure 2.19: ORTEP diagram (50% probability ellipsoids) of $[Zn(Cl)_3(Me\text{-}dpHa)]$.[131] Hydrogen atoms except H(2a) omitted for clarity. Selected bond lengths /Å: Cl(1)-Zn(1) 2.2416(4), Cl(2)-Zn(1) 2.2406(4),Cl(3)-Zn(1) 2.2857(4), N(1)-Zn(1) 2.0883(12)

It is most probable that this pyridyl methylated ligand was formed as a very minor product in the methylation reaction rather than being a process occurring in the presence of the zinc(II) ion, but it has not been observed in ^{1}H NMR spectra or MS. Significantly, this structure shows the dpHa ligand in an *anti*-conformation when there is no interaction shared by the two pyridyl nitrogen atoms.

Crystallisation of reaction mixtures from reacting the dpma ligand with cobalt(II) chloride resulted in some diffraction quality crystals which revealed a *bis*-complex (**Figure 2.20**). The structures shows a cobalt(II) centre coordinated to two dpma ligands in an octahedral *cis*-geometry. The cobalt centre is also coordinated to a water molecule and a chloride. However, the chloride ligand is also coordinated to another cobalt(II) centre which has an additional three chloride ligands. One of the chloride ligands of the second cobalt centre, Cl(4) shares an intramolecular hydrogen-bonding interaction with H(1a) of the water ligand. The aqua ligand has

been identified as being water rather than hydroxide by locating two protons using the electron difference map. The other hydrogen of the water ligand, H(1b), forms an intermolecular hydrogen-bond with one of the chloride ligands of the second cobalt centre, Cl(2), of an adjacent complex, forming hydrogen-bonded chains within the crystal lattice (**Figure 2.21**).

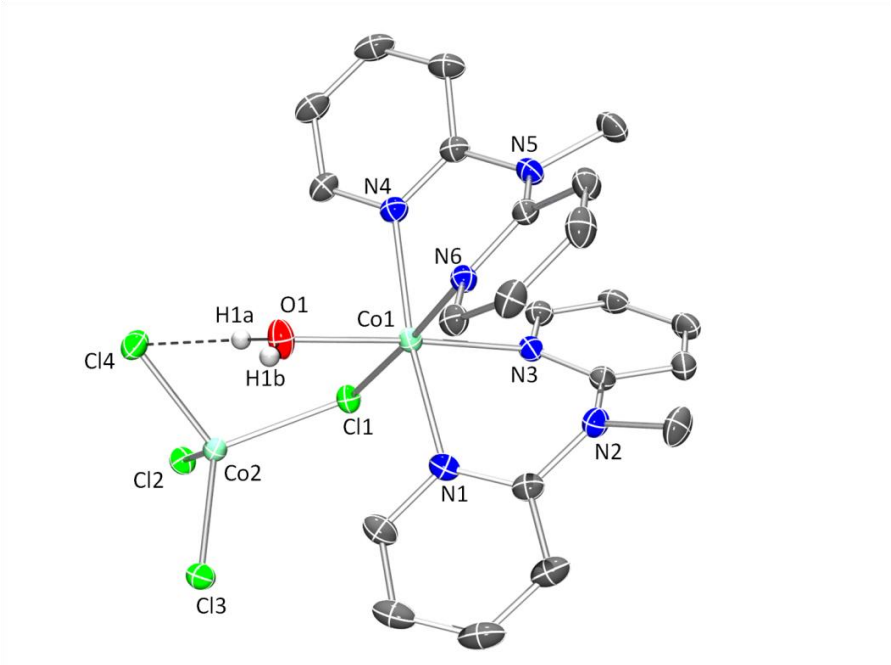

Figure 2.20: ORTEP diagram (50% probability ellipsoids) of [Co(μ_2-Cl)(dpma)$_2$(H_2O)($CoCl_3$)].[131] Hydrogen atoms (except H(1a) and H(1b)) omitted for clarity. Selected bond lengths /Å and angles /º: Cl(1)-Co(2) 2.3063(5), Cl(1)-Co(1) 2.5291(5), Cl(2)-Co(2) 2.2871(5), Cl(2)-Co(2) 2.2871(5), Cl(3)-Co(2) 2.2600(5), Cl(4)-Co(2) 2.2730(5), Co(1)-N(1) 2.1061(15), Co(1)-N(3) 2.1076(14), Co(1)-O(1) 2.1126(13), Co(1)-N(6) 2.1154(14), Co(1)-N(4) 2.1230(14), N(1)-Co(1)-N(3) 82.66(5), N(6)-Co(1)N(4) 82.66(6). Hydrogen-bond distances / Å and angles /º: H(1a)···Cl(4) 0.81(3), O(1)···Cl(4) 3.1531(15), O(1)-H(1a)···Cl(4) 177(2)

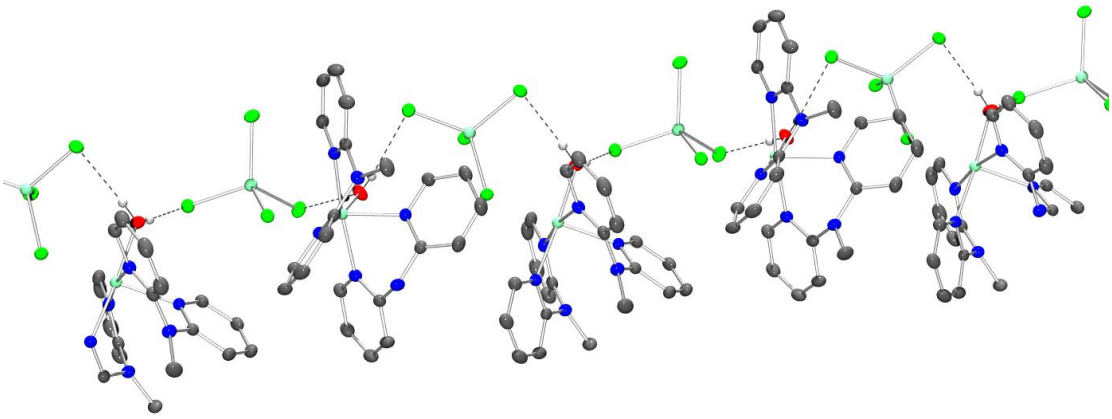

Figure 2.21: ORTEP representation of the supramolecular chains created through hydrogen-bonding interactions within the lattice of $[Co(Cl)(dpma)_2(H_2O)(CoCl_3)]$.[131] Hydrogen-bond distances / Å and angles /º: H(1b)···Cl(2) 2.52(3), O(1)···Cl(2) 3.1779(14), H(1a)···Cl(4) 2.35(3), O(1)···Cl(4) 3.1531(15), O(1)-H(1b)···Cl(2) 174(3), O(1)- H(1a)···Cl(4) 177(2)

2.3.3. Preparation of a cobalt(III) complex of *N*-methyl-2,2'-dipyriylamine (dpma)

To prepare and isolate the cobalt(III) complex, one equivalent cobalt(II) chloride was reacted with two equivalents of dpma in the presence of H_2O_2 and a triflate salt to provide a counter-ion which assisted the formation of diffraction-quality crystals. The reaction was originally carried out in the presence of excess $NaHCO_3$ in case of the carbonate complex being more favourable than the *bis*-chloride as with the dpHa complex. The product was obtained as diffraction quality crystals in low yield (2%) upon slow evaporation of the filtrate from the methanolic reaction mixture. The structure shows the octahedral cobalt(III) centre coordinated to two dpma ligands in a *cis*-geometry with two chloride ligands (**Figure 2.22**).

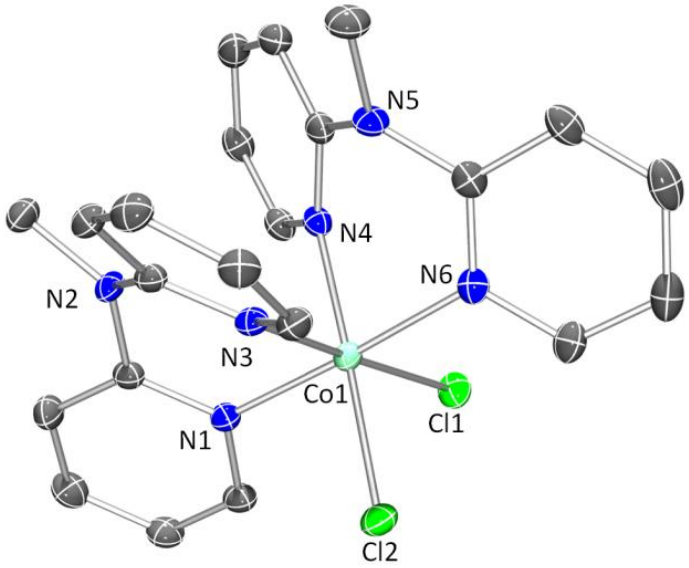

Figure 2.22: ORTEP diagram (50% probability ellipsoids) of $[Co(Cl)_2(dpma)_2]OTf$.[131] Hydrogen atoms and counter-ion omitted for clarity. Selected bond lengths /Å and angles /º : Cl(1)-Co(1) 2.2611(6), Cl(2)-Co(1) 2.2421(6), Co(1)-N(3) 1.9468(16), Co(1)-N(1) 1.9481(16), Co(1)-N(6) 1.9556(16), Co(1)-N(4) 1.9623(16), N(3)-Co(1)-N(1) 87.73(7), N(6)-Co(1)-N(4) 87.40(7), Cl(2)-Co(1)-Cl(1) 93.02(2)

As with the ^{1}H NMR spectrum of the cobalt(III) dpHa complex, each dpma ligand is split into two different ring environments but both the dpma ligands are equivalent (**Figure 2.23**).

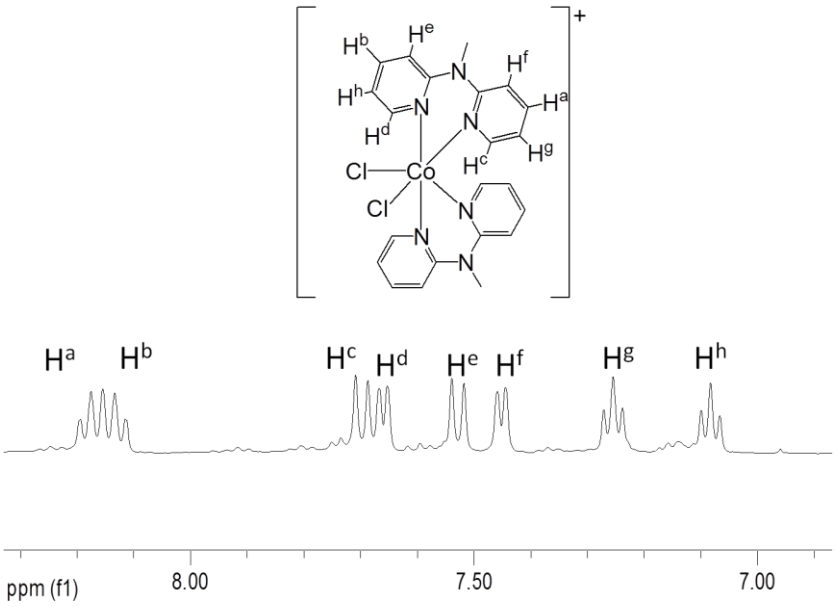

Figure 2.23: ^{1}HNMR spectrum of $[Co(Cl)_2(dpma)_2]OTf$ (400 MHz, d_6-DMSO): δ8.16 (ddd, 2H, J = 8.5, 7.0, 1.5 Hz, H^a), δ8.12 (ddd, 2H, J = 8.5, 7.0, 1.5 Hz, H^b) δ7.68 (d, 2H, J = 8.5 Hz, H^c), δ 7.65 (dd, 2H, J = 6.0, 1.5 Hz, H^d), δ7.51 (d, 2H, J = 8.5 Hz, H^e), δ7.44 (dd, 2H, J = 6.0, 1.5 Hz, H^f), δ7.24 (td, 2H, J = 6.5, 1.0 Hz, H^g), δ7.07 (td, 2H, J = 6.0, 1.0 Hz, H^h), δ3.82 (s, 6H, CH_3)

The greatest difference between the two molecular structures of the cobalt(III) complexes of dpHa and dpma is their altered preferences between a carbonate ligand or two chloride ligands. When the dpHa complex was first prepared from $[Co(Cl)_2(dpHa)_2]$, the chloride ions did not coordinate and it was with this reaction that carbonate coordination was first observed, affording $[Co(CO_3)(dpHa)_2]^+$. When preparing the equivalent dpma complex, the presence of a silver salt and excess carbonate did not bring about coordination of the latter, resulting in the formation of $[Co(Cl)_2(dpHa)_2]^+$. It seems that this difference is due to steric crowding about the metal centre brought about by the different orientation of the pyridyl rings about the cobalt(III) centre (**Figure 2.24**).

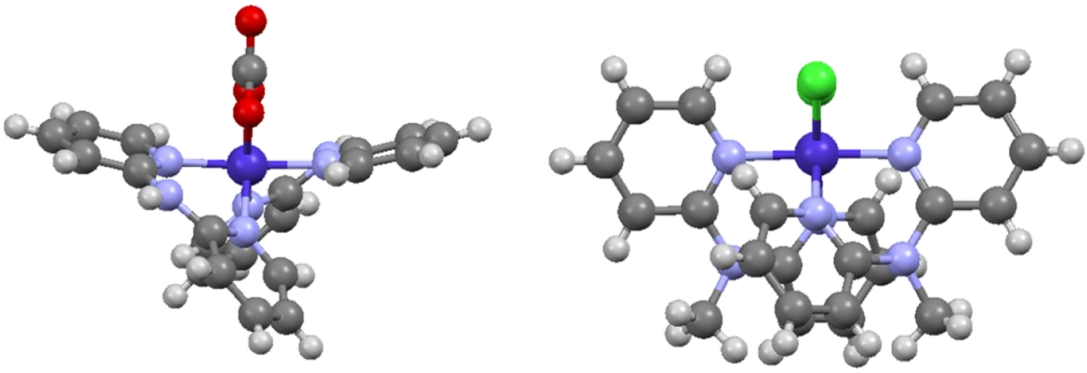

Figure 2.24: Ball and stick representation showing the different orientation about the cobalt(III) centres of dpHa and dpma (complexes shown perpendicular to the Co-CO_3 and Co-Cl_2 plane).[171]

2.4. Complexes of *N*-ethyl-2,2'-dipyriylamine (dpea)

In order to help ascertain whether differences between the dpHa and dpma complexes were predominantly steric or electronic, it was decided to use *N*-ethyl-2,2'-dipyridylamine (dpea), which was prepared using the same method as for dpma. The dpea ligand was complexed to both zinc(II) and copper(II) chloride, providing similar structures to those obtained for the analogous dpma complexes. $[Cu(Cl)_2(dpea)]$ again crystallised as a dimer with one chloride ligand from each metal Cl(2) bridging the two square pyramidal copper centres (**Figure 2.25**). The complex's square pyramidal geometry was confirmed by a τ value of 0.08.[132]

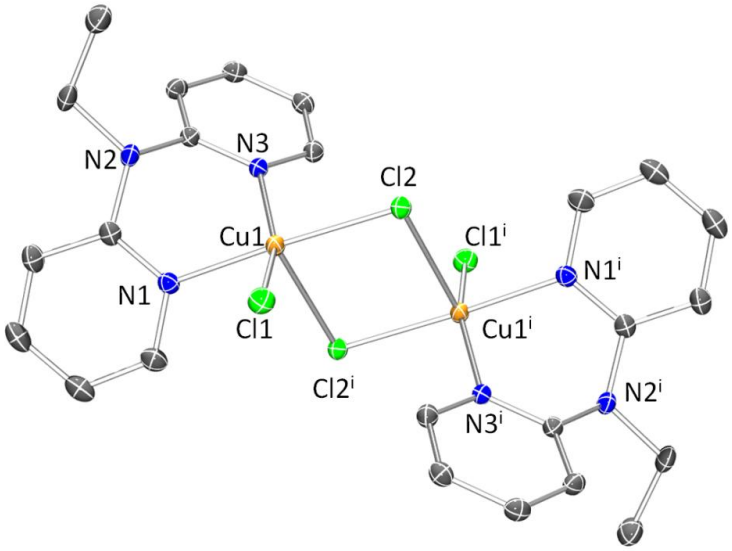

Figure 2.25: ORTEP diagram (50% probability ellipsoids) of $[\{Cu(Cl)_2(dpea)\}_2]$.[131] Hydrogen atoms omitted for clarity. Selected bond lengths /Å and angles /º : Cl(1)-Cu(1) 2.2830(4), Cl(2)-Cu(1) 2.2739(4), Cu(1)-N(1) 2.0114(14), Cu(1)-N(3) 2.0133(13), N(1)-Cu(1)-N(3) 85.74(5)

Similar structural derivatives have been recently reported in the literature where the ligands used include *N*-cyclohexylmethyl-2,2'-dipyridylamine and *N*-benzylmethyl-2,2'-dipyridylamine (**Figure 2.26**). Similar to the copper(II) complexes of dpma and dpea, these again crystalise as square-pyramidal dimers with similar structural parameter (**Table 2.23**).[138]

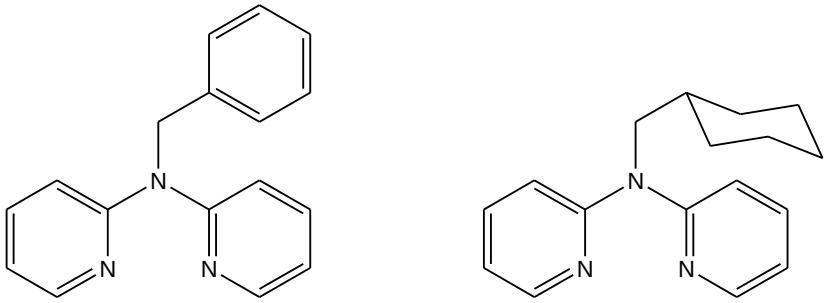

N-benzylmethyl-2,2'-dipyridylamine *N*-cyclohexylmethyl-2,2'-dipyridylamine

Figure 2.26: Ligands used by Lindoy *et al* to coordinate to copper(II) chloride.[138]

Table 2.3: Comparison of the structural parameters of $[\{Cu(Cl)_2(dpma)\}_2]$, $[\{Cu(Cl)_2(dpea)\}_2]$ and the structures of $[\{Cu(Cl)_2(dpPha)\}_2]$ and $[\{Cu(Cl)_2(dpcya)\}_2]$ reported previously in the literature.[138]

dpRa	Me	Et	CH_2Ph	CH_2Cy
Cu-Cl bond lengths / Å	2.2911(9) 2.2838(9) 2.6874(9)	2.2830(4) 2.2739(4)	2.2969(6) 2.6271(7) 2.6271(7)	2.2594(13) 2.2919(12) 2.7492(14)
Cu-N bond lengths/ Å	1.993(3) 2.004(3)	2.0114(14) 2.0133(13)	2.0010(18) 2.013(2)	2.004(4) 2.017(4)
N-Cu-N bond angle / °	84.50(11)	85.74(5)	85.16(8)	84.19(16)
Angle between rings / °	127.42	128.75	129.07	127.95
τ value	0.14	0.08	0.12	0.17
Cu1-Cu1^i / Å	3.682	3.729	3.605	3.732

These copper(II) complexes can all be considered to be of the form shown in **Figure 2.27** as the bulk of the atom directly attached to the amine nitrogen does not alter. The lack of significant change in the bond lengths and angles of these four structures suggests that the groups attached to the methylated central amine do not affect the coordination geometry of the metal centre.

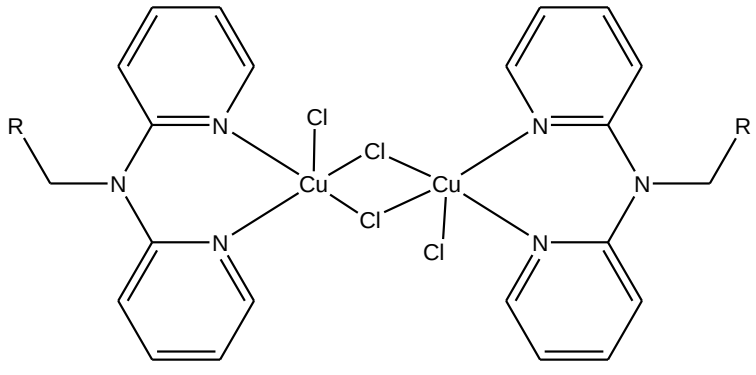

R = H, CH_3, Ph, cy

Figure 2.27: General structure of copper(II) chloride complexes of dpRa ligands

In order to alter the coordination geometry from this, dpRa ligands where R is an isopropyl or phenyl group (**Figure 2.28**) would be worth investigating as these bring increased steric bulk closer to the central amine and pyridyl rings.

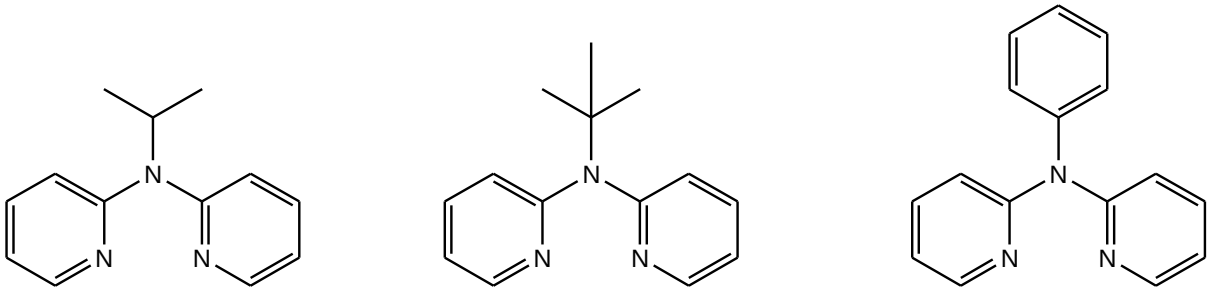

Figure 2.28: Potential dpRa ligands where there is increasing steric bulk closer to the central amine

The zinc(II) complex was prepared by reacting equimolar amounts of dpea and $ZnCl_2$ in methanolic solution. The product formed as a white precipitate which could then be isolated by filtration in 59% yield. Diffraction quality crystals were obtained by slow diffusion of Et_2O into a DMF solution. The obtained structure shows a tetrahedral geometry similar to that of the analogous zinc dpRa complexes (**Figure 2.29**).

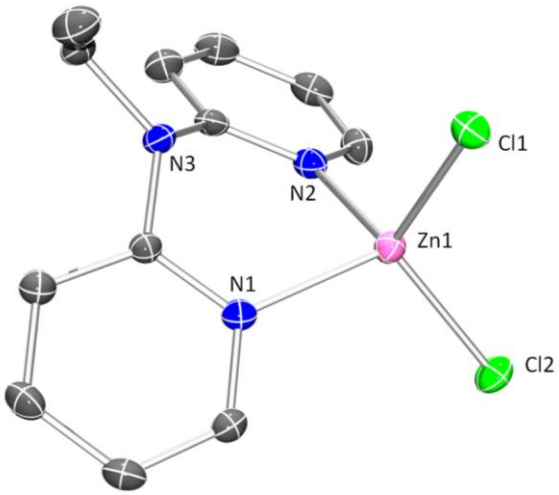

Figure 2.29: ORTEP diagram (50% probability ellipsoids) of $[Zn(Cl)_2(dpea)]$.[131] Hydrogen atoms omitted for clarity. Selected bond lengths / Å and angles / °: Cl(1)-Zn(1) 2.2274(7), Cl(2)-Zn(1) 2.2162(7), N(1)-Zn(1) 2.034(2), N(2)-Zn(1) 2.032(2), N(2)-Zn(1)-N(1) 89.95(8)

The complex shows similar metal-ligand bond lengths but a tighter bend between the two pyridyl rings of dpRa through the central amine (**Table 2.4**). The difference between the dpea and dpma zinc(II) complexes is less pronounced than between the dpma and dpHa complexes, suggesting that it is the steric bulk on the central amine which forces the dpRa ligand into a less planar conformation.

Table 2.4: Comparison of the structural parameters of $[Zn(Cl)_2(dpHa)]$, $[Zn(Cl)_2(dpma)]$ and $[Zn(Cl)_2(dpea)]$

	$[Zn(Cl)_2(dpHa)]$	**$[Zn(Cl)_2(dpma)]$**	**$[Zn(Cl)_2(dpea)]$**
Zn-Cl bond lengths / Å	2.203	2.2100(4)	2.2274(7)
	2.243	2.2368(4)	2.2162(7)
Zn-N bond lengths/ Å	2.024	2.0275(13)	2.034(2)
	2.023	2.0205(12)	2.032(2)
N-Zn-N bond angle / °	93.08	90.71(5)	89.95(8)
Angle between pyridyl rings / °	174.5	148.5	138.7

As with the copper complexes, the similarity between the dpma and dpea complexes suggests that it is the steric bulk directly attached to the central amine which alters the coordination properties of the ligand. Therefore, to investigate how the coordination geometries of dpRa ligands might further be influenced by the central amine, ligands such as those shown in **Figure 2.28** would be interesting to investigate. This work suggests that groups designed to increase the medicinal activity of dpRa type ligands could be attached to the central amine via a chain of one or more alkyl carbons, without compromising the ligand's ability to coordinate to a metal centre.

2.5. Complexations with a therapeutically active dpHa derivative

2.5.1. Ligand synthesis

Complexations with a therapeutically active kinase inhibitor, py-dpHa-CN, which contains the dpHa fragment were attempted. This derivative features a nitrile substituent on the 4-position on one pyridyl ring and a pyrrolidinylmethyl group in the same position on the other ring. These groups are designed to act as hydrogen-bond acceptors in the kinase active site. This ligand was synthesised by preparing 2-chloro-4-(1-pyrrolidinylmethyl)-pyridine from 2-chloro-4-pyridinecarboxaldehyde and coupling this with 2-amino-4-cyanopyridine through use of a Buchwald-Hartwig coupling reaction (**Scheme 2.5)**.[139]

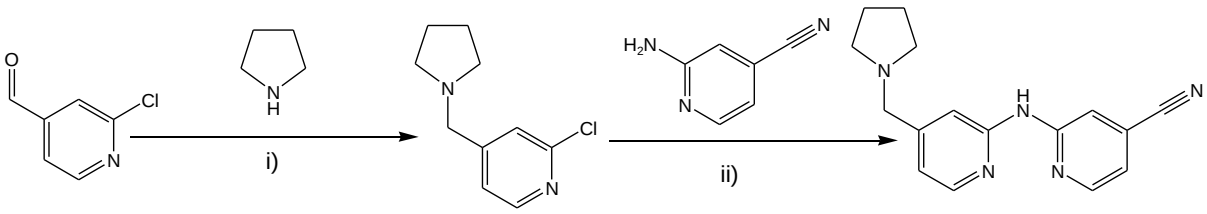

Scheme 2.5: Preparation of py-dpHa-CN. *Reagents*: i) 1.0 equiv. pyrrolidine, 2 mL acetic acid, 1.2 equiv. $NaBH(OAc)_3$, ii) 1.4 equiv. Cs_2CO_3, 0.1 equiv. $Pd(dba)_3$, 0.15 equiv. Xantphos, 1 equiv. 2-amino-4-nitrilepyridine

2.5.2. Attempt to prepare metal(II) complexes of py-dpHa-CN

It was attempted to complex this ligand to $M(II)Cl_2$ salts (where M is Co, Cu, Zn) in a manner similar to that used for the other dpRa ligands by reacting one equaivalent of the ligand with the required metal(II) chloride salt in methanolic solution (**Scheme 2.6**).

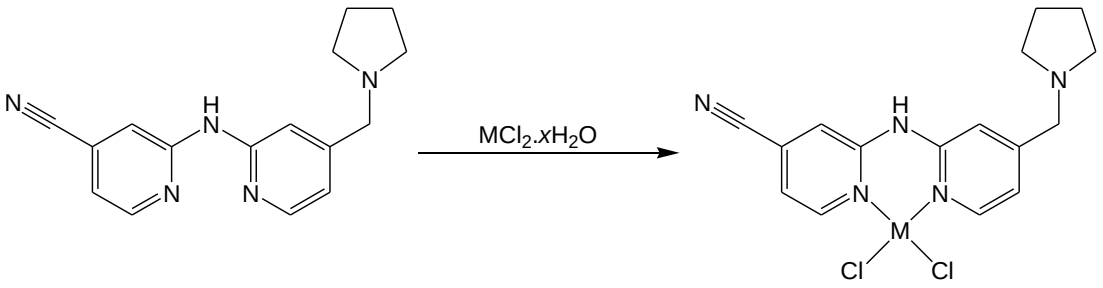

Scheme 2.6: Initial complexation reaction with py-dpHa-CN, where M = cobalt(II), copper(II) and zinc(II)

Crystals were obtained from the methanolic reaction mixture for the zinc(II) and cobalt(II) reactions but the structures obtained from these showed that complexation did not take place (**Figures 2.30** and **2.31**). Instead, both structures show the pyridyl nitrogen, N(3), with the pyrrolidine substituent is protonated and is hydrogen-bonded to the other pyridyl nitrogen, N(1). This interaction enforces the two pyridyl rings to be in a *syn*-conformation. The pyrrolidine nitrogen (N5) is also protonated, resulting in the ligand having an overall double cationic charge. This charge is balanced in both cases by a non-coordinating tetrachloride metal(II) anion.

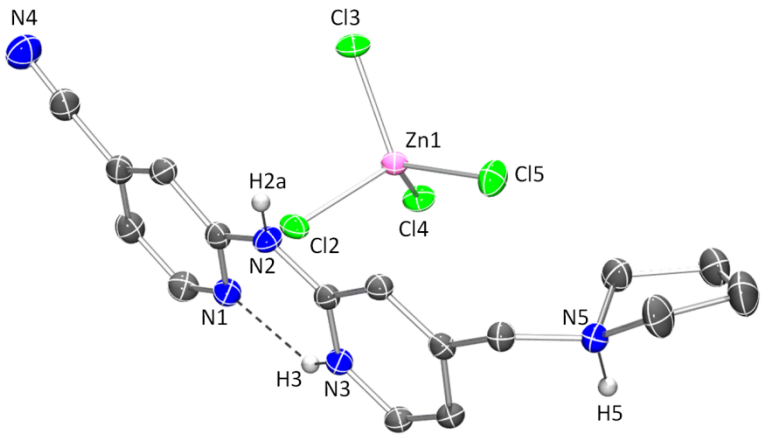

Figure 2.30: ORTEP diagram (50% probability ellipsoids) of [dp(CN)(pyH)Ha][Zn(Cl)$_4$].[131] Hydrogen atoms (except H(2a), H(3) and H(5)), and solvent molecules omitted for clarity.

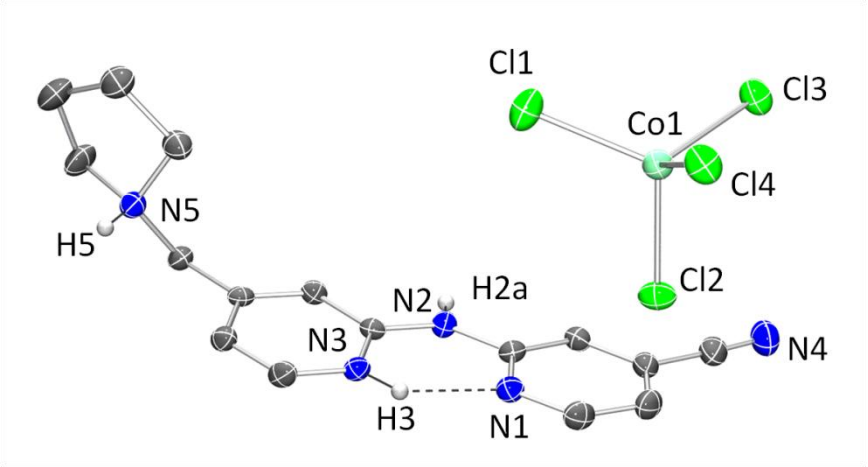

Figure 2.31: ORTEP diagram (50% probability ellipsoids) of [dp(CN)(pyH)Ha][Co(Cl)$_4$].[131] Hydrogen atoms (except H(2a), H(3) and H(5)) and solvent molecules omitted for clarity.

The product from the reaction with zinc(II) chloride has also been characterised by NMR (**Figure 2.32**). Analysis of the COSY spectra showed the H^a signal not to be coupled to any other signals, whilst H^b at δ9.94 was shown to be coupled to the protons corresponding to H^i, H^j and H^k, indicating it to be directly bonded to the pyrrolidine nitrogen. The peak corresponding to the protonated pyrrolidine was not observed in the spectrum of the free ligand (**Figure 2.33**).

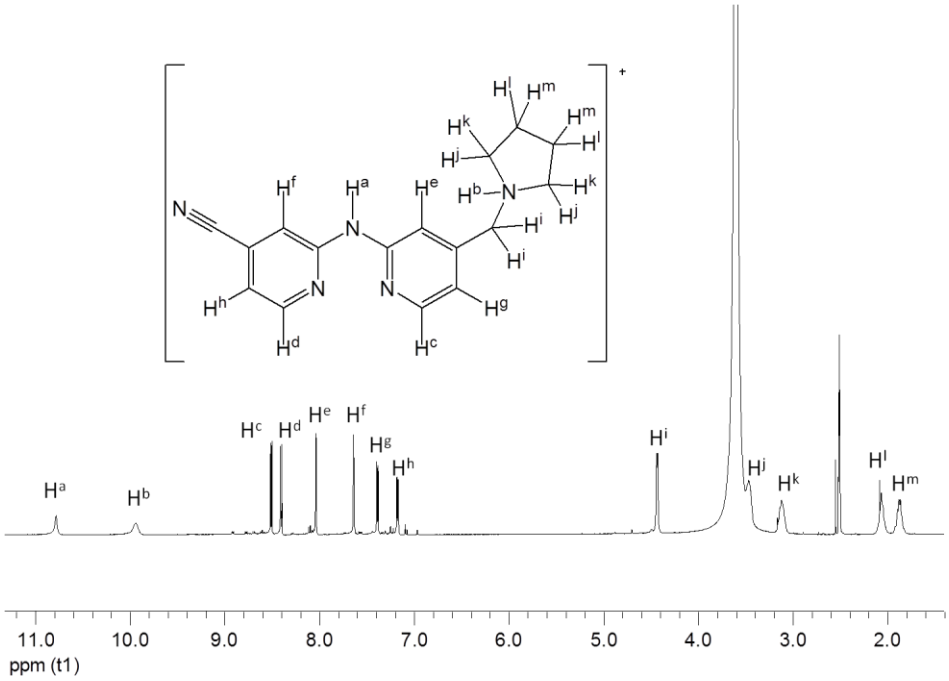

Figure 2.32: ^{1}H NMR (d_6-DMSO, 400 MHz) of [dp(CN)(pyH)Ha][$Zn(Cl)_4$]. δ10.80 (br. s, 1H, H^a), δ9.96 (br. s, 1H, H^b), δ8.52 (dd, 1H, J = 5.0, 1.0 Hz, H^c), δ8.41 (d, 1H, J = 5.5 Hz, H^d), δ8.04 (s, 1H, H^e), δ7.64 (s, 1H, H^f), δ7.38 (dd, 1H, J = 5.0, 1.0 Hz, H^g), δ7.18 (dd, 1H, J = 6.0, 1.5 Hz, H^h), δ4.43 (d, 2H, J = 4.5 Hz, H^i), δ3.45 (m, 2H, H^j), δ3.11, m, 2H, H^k) δ2.06 (m, 2H, H^l), δ1.86 (m, 2H, H^m)

The complexation was attempted in the presence of Et_3N which resulted in a different NMR spectrum (**Figure 2.30**), but the desired zinc complex was not successfully isolated or observed with MS.

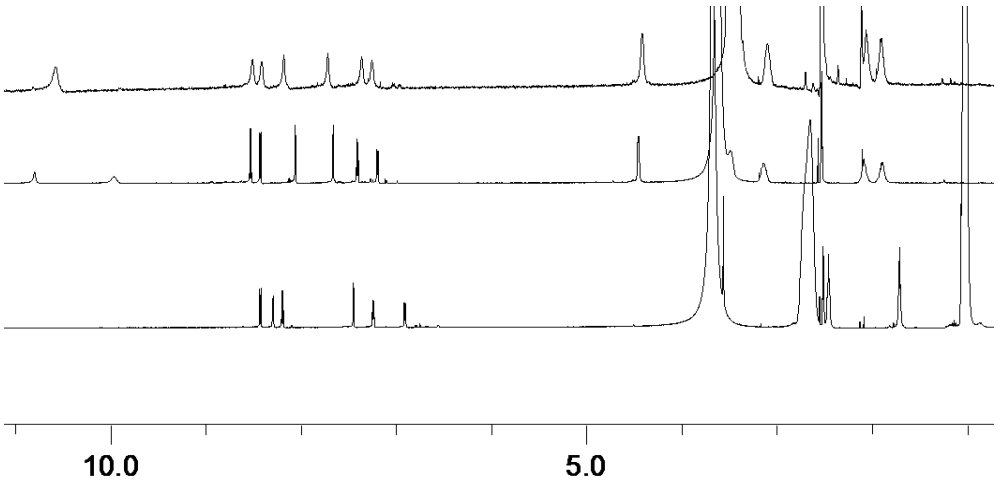

Figure 2.33: Overlay of ^{1}H NMR spectra in d_6-DMSO (400 MHz) of py-dpHa-CN (top), when reacted with $ZnCl_2$, and with $ZnCl_2$ and Et_3N (bottom)

The ^{1}H NMR spectrum of the product obtained by reacting py-dpHa-CN with $ZnCl_2$ in the presence of excess Et_3N (**Figure 2.34**) shows an absence of signals corresponding to protons attached to the amine or pyrrolidine. The latter not being protonated is also supported by the alkyl protons of the pyrrolidine ring being split into two sets of signals rather than the eight observed when reacted with $ZnCl_2$. Signals corresponding to the methylene linkage between the pyrrolidine and pyridyl ring have been tentatively assigned to the peak at δ3.55 which is partially obscured by a larger peak at δ3.66.

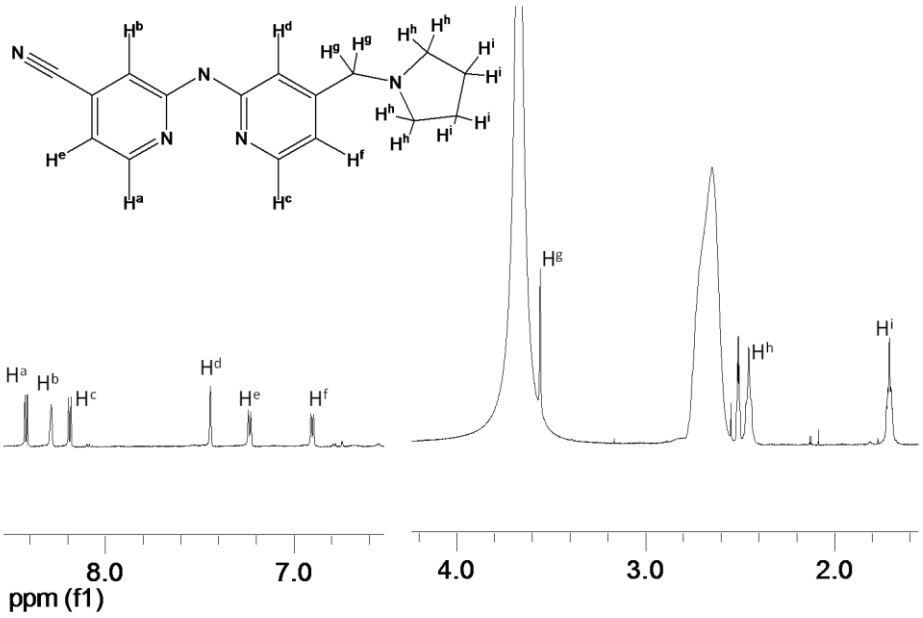

Figure 2.34: Assignment of the product obtained from the reaction of [dp(CN)(pyH)Ha][Zn(Cl)$_4$]with Et_3N. δ8.43 (d, 1H, J = 5.0 Hz, H^a), δ8.28 (m, 1H, H^b), δ8.20 (d, 1H, J = 5.0 Hz, H^c), δ7.44 (m, 1H, H^d), δ7.24 (dd, 1H, J = 5.0, 2.0 Hz, H^e), δ 6.92 (d, 1H, J = 5.0 Hz, H^f), δ3.56 (s, 2H, H^g), δ2.45 (m, 4H, H^h), δ1.70 (q, 4H, J = 3.0 Hz, H^i)

2.5.3. Attempt to prepare a cobalt(III) complex of py-dpHa-CN

It was thought that once the py-dpHa-CN ligand was coordinated to the cobalt(II) centre and then oxidised cobalt(III) then such a complex would be stable under physiological conditions until the metal centre underwent reduction at which point the therapeutically active ligand would rapidly dissociate. Several methods of achieving this were attempted without success, some of which are now described.

Firstly, it was tried using cobalt(II) chloride which was stirred with two equivalents of py-dpHa-CN in methanolic solution. After twenty minutes stirring, H_2O_2 was added to oxidise the cobalt (**Scheme 2.7**) which caused the reaction mixture to turn darker in colour. $NaPF_6$ was added to provide a counter-ion. After two hours stirring the reaction mixture was filtered and left to stand, leading to the gradual formation of a yellow-brown precipitate which gave rise to a mass spectrum which showed the peak corresponding to the free ligand, and a ^1H NMR spectrum which showed broad peaks corresponding to the presence of cobalt(II).

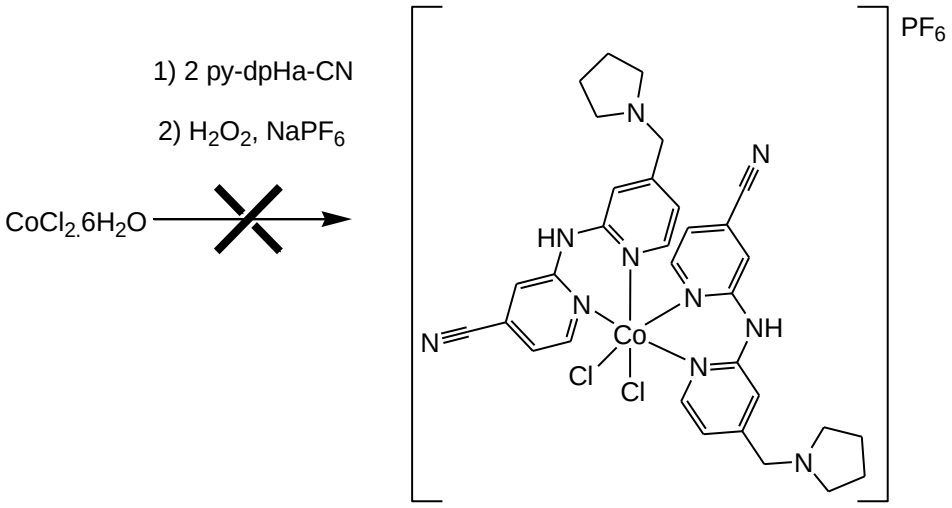

Scheme 2.7:Attempt to prepare a cobalt(III) py-dpHa-CN complex from cobalt(II) chloride using hydrogen peroxide

It was then attempted to prepare the complex by reacting $Co(NO_3)_2.6H_2O$ with two equivalents of py-dpHa-CN to remove the presence of chlorides from the reaction mixture, and to provide carbonate in case this was preferred as a ligand to nitrate as with $[Co(CO_3)(dpHa)_2]NO_3$ (**Scheme 2.8)**.

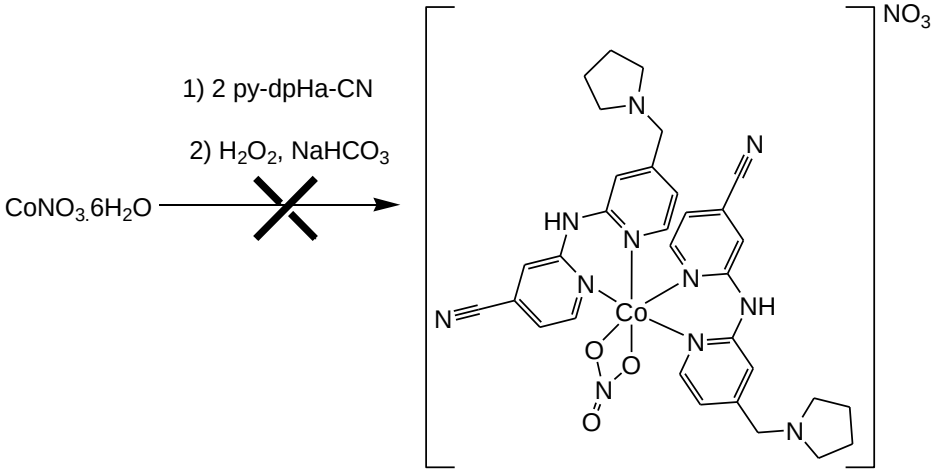

Scheme 2.8: Attempt to prepare a cobalt(III) py-dpHa-CN complex from cobalt(II) nitrate using hydrogen peroxide in the presence of excess carbonate

It was then tried to react two equivalents of py-dpHa-CN with $Co(NO_3)_2.6H_2O$ in the presence of Et_3N to try and ensure that the pyrrolidine nitrogen was not protonated, thereby aiding its coordination to the metal centre (**Scheme 2.9**). Addition of the Et_3N caused the reaction mixture to turn darker and after oxidation with H_2O_2, a fine brown precipitate was isolated which contained a paramagnetic mixture evident by ^1H NMR spectroscopic analysis.

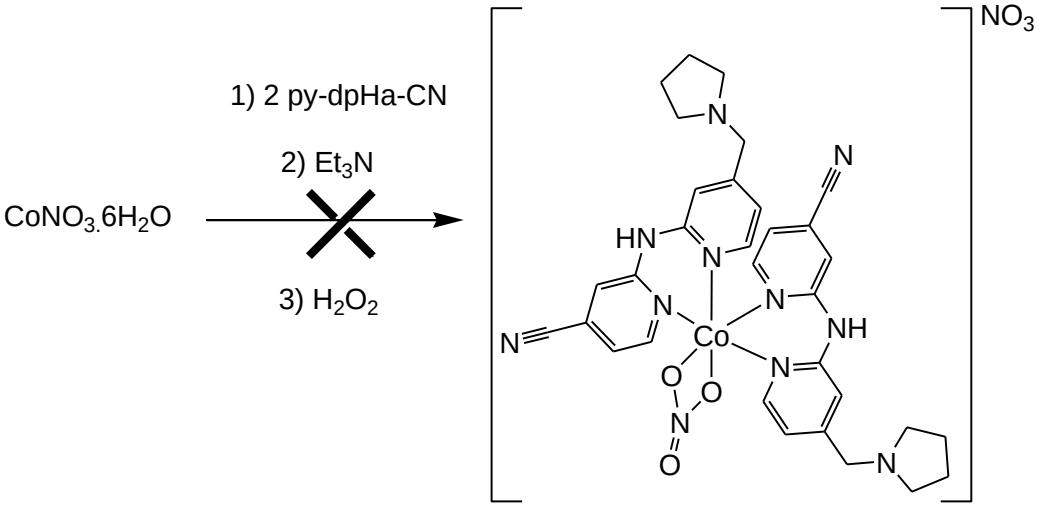

Scheme 2.9: Attempt to prepare a cobalt(III) py-dpHa-CN complex from cobalt(II) nitrate using Et_3N and H_2O_2

The results from this work suggest that ligands such as py-dpHa-CN are not suitable as ligands to coordinate to transition metal centres to create pro-drug complexes to act as kinase inhibitors. The previously described results suggest that the pyrrolidine

group is problematic due to its highly basic nature, resulting in it being protonated and therefore having a cationic charge. This decreases its ability to coordinate to a metal centre easily, even in the presence of bases intended to deprotonate the pyrrolidine nitrogen.

The doubly protonated py-dpHa-CN ligand observed in the crystal structures are shown in the *syn*-conformation with a hydrogen-bond formed between the two pyridyl nitrogens. This is significant in that the hypothesis behind the design of this ligand was that the ligand remains in its *anti*-conformation when not in the kinase active site or not coordinated to a metal at physiological pH.

2.6. Conclusions

The coordination chemistry of dipyridylamine-type ligands has been further expanded upon including with derivatives where the central amine has been alkylated. It has been observed that changing from dpHa to dpma causes a more noticeable difference than between dpma and dpea. This suggests that it is the steric bulk of the group directly coordinated to the central amine which directly alters how the two pyridyl rings arrange in relation to each other, and thus alter the coordination environment of the complex. For metal(II) complexes of cobalt, copper and zinc, the observed geometries include octahedral, tetrahedral and square pyramidal whilst the two cobalt(III) complexes have displayed octahedral geometries.

Structures of dpRa-type ligands have been obtained where the ligand is not coordinated through its two pyridyl nitrogen atoms. In one structure, the methyl group has added to the pyridyl nitrogen rather than the amide nitrogen and crystallised with a zinc trichloride species coordinated to the other pyridyl nitrogen atom. This structure showed the two pyridyl rings arranged in an *anti*-conformation where there are no hydrogen-bonds or coordinating metal species to hold the ligand into the *syn*-conformation. However, the structures obtained with py-dpHa-CN show that the presence of a hydrogen-bond between the two pyridyl nitrogen atoms can enforce the *syn*-conformation. The latter has highlighted that the presence of basic groups on dpHa ligand derivatives such as pyrrolidine can be problematic when trying to coordinate this type of a ligand to a metal centre. As the majority of the compounds in this library of kinase inhibitors feature a basic group designed to be

able to hydrogen-bond within the kinase active site, it would seem that this family of inhibitors are not the best candidates for use as transition metal-based prodrugs.

Chapter Three: The synthesis of *N*1,*N*4-oxide ligands and the preparation of their complexes

3.1. Introduction

As described in **Chapter 1**, much has already been done in attempting to understand the basis of the hypoxia selectivity of tirapazamine (tpzH) and to develop derivatives with improved biological activity.[46-63] In this context, derivatives of the structurally similar quinoxaline-*N*1,*N*4-oxides (**Figure 3.1**) have shown varied biological properties other than cancer cell cytotoxicity such as anti-parasitic activity against *Trypanosoma cruzi* and malarial parasites,[140-142] and the treatment of hypertension through the inhibition of angiotensin.[143]

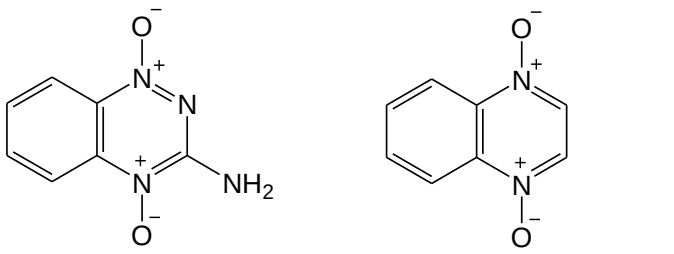

Figure 3.1: Structures of tpzH (*left*) and quinoxaline-*N*1,*N*4-oxide (*right*)

Both tpzH and quinoxaline-*N*1,*N*4-oxides have the potential to act as ligands in metal complexes. Gambino *et al*. have begun to exploit the coordination chemistry of *N*-oxide ligands to provide transition metal complexes with various biological properties.[140, 144-154] Aromatic *N*-oxides exist as stable species with the nitrogen-oxygen bond having dipolar character.[155] The electron-rich character of the oxygen makes *N*-oxides well-suited to being used as hard to medium-hard electron donor ligands to coordinate to metal centres which are hard or borderline in character including high oxidation state f-block ions such as uranyl or late first row transition metals such as copper(II).[156-158]

Coordination of pyridine-2-thiol-*N*-oxide to various metal centres has provided complexes with activity against *Trypanosoma cruzi* (**Figure 3.2**). This is the parasite responsible for diseases such as American trypanosomiasis (Chagas disease) which can lead to fatal cardiac damage, Leishmaniasis (a disease whose symptoms can range from skin ulcers to acute organ damage) and Human African trypanosomiasis (sleeping sickness) where the parasite eventually crosses the blood-brain barrier

leading to death. Coordination of pyridine-2-thiol-*N*-oxide to palladium(II) resulted in a three-fold increase in anti-parasitic activity compared to pyridine-2-thiol-*N*-oxide whilst coordination to platinum(II) achieved higher selectivity towards the parasite than the free ligand.[149] Coordination of pyridine-2-thiol-*N*-oxide to a gold(I) centre led to an enhancement of the ligand's anti-*T. cruzi* activity.[152]

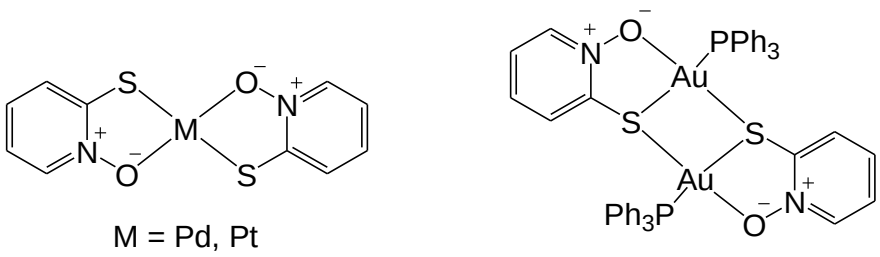

Figure 3.2: Hypothesised structures of Gambino's pyridine-2-thiol-*N*-oxide complexes which show activity against *T. Cruzi*.[149, 152]

The same research group have prepared and studied various transition metal complexes of quinoxaline-*N*1,*N*4-oxide ligands (**Figure 3.3**). Vanadyl complexes of this ligand were found to exhibit anti-parasitic activity against *T. Cruzi*,[146] as well as activity as having insulin mimicking properties for the treatment of diabetes.[145] Palladium(II) complexes have also shown anti-*T. cruzi* properties, whilst iron(III) complexes of this ligand were shown to have some activity against *M. tuberculosis*.[148, 153, 154] Several of these complexes have been examined for their anti-tumour activity, both against cells under normoxic and hypoxic conditions.[144]

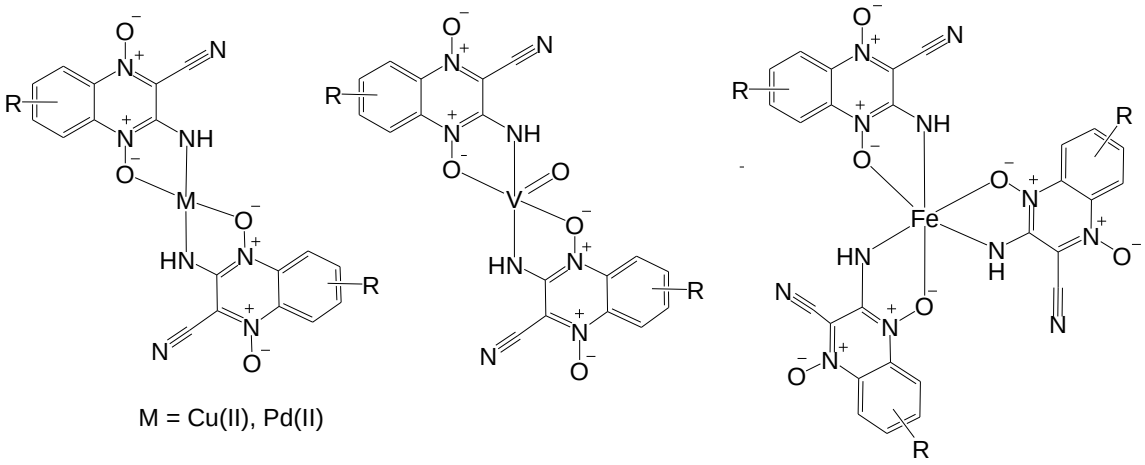

Figure 3.3: Examples quinoxaline-*N*1,*N*4-oxide complexes previously reported in the literature with biological applications.[140, 144-148, 151, 154, 159, 160]

Metal(II) complexes of palladium(II) and copper(II) were examined for their cytotoxic activity against V79 (Chinese hamster lung fibroblast) cancer cells under normoxic and hypoxic conditions (**Figure 3.4** and **Table 3.1**).

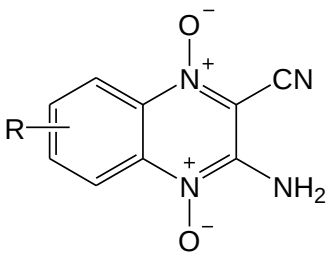

L1: R=H
L2: R = Cl
L3: R = Br
L4: R = Me

Figure 3.4: Ligands shown in **Table 3.1**

Table 3.1: Reported cytotoxicity against V79 cells under normoxic and hypoxic conditions of quinoxaline-*N*1,*N*4-oxide ligands and their complexes.[140, 144, 147, 151]

Compound	**Cell survival fraction with 20 μM compound / %**	
	normoxia	**hypoxia**
$[Cu(L1)_2]$	18	1
L2	100	0
$[Cu(L2)_2]$	100	1
$[VO(L2)_2]$	57	0
$[Pd(L2)_2]$	92	0
L3	90	0
$[Cu(L3)_2]$	91	5
$[VO(L3)_2]$	36	0
L4	82	22
$[Cu(L4)_2]$	100	10
$[VO(L4)_2]$	60	0
$[Pd(L4)_2]$	2	0

Complexation of the chloro-analogue (L2) to copper(II) or palladium(II) resulted in no significant change in cytotoxicity by remaining cytotoxic to hypoxic cells and non-cytotoxic normoxia.[144, 151] Complexation of L2 to a vanadyl centre increased the

survival fraction under normoxia from 100 to 57 whilst not reducing the potency under hypoxia.[147] The copper(II) complex of the bromo-derivative L3 again showed no significance in activity compared to the free ligand whereas the vanadyl complex showed increased activity under normoxic conditions, decreasing the survival fraction from 90 to 36.[144, 147] The copper(II) complex of the methylated-ligand L4 led to an increase in hypoxia cytotoxicity, increasing the survival fraction under normoxia from 82 to 100 and reducing the survival under hypoxia under hypoxia from 22 to 10.[144] Incorporation of this ligand into vanadyl complex led to a decrease in the survival fraction under normoxia to 60 and hypoxia to 0 whereas coordination to palladium(II) resulted in no cell survival under either conditions.[147, 151]

The solubility of these complexes was reported to be poor, with the palladium(II) complexes not being able to remain in DMSO solution long enough for ^{13}C NMR experiments whilst many of the compounds were not soluble enough for obtaining of IC_{50} values.[151] It was found that complexes of this type of ligand with a vanadyl centre led to complexes which not only showed higher potency and hypoxia selective cytotoxicity than tpzH, but showed improved solubility in solvents such as light alcohols than the ligands on their own.

Despite the number of reports of the work on these complexes, they are yet to be characterised by NMR spectroscopic analysis (owing to most of the metals used being paramagntic) or single crystal diffraction.

In this chapter, the work on *N*1,*N*4-oxide ligands is expanded upon using three ligands including the 3-aminoquinoxaline-2-carbonitrile-*N*1,*N*4-oxide (tpzH-CN) used by Gambino, but also 3-aminobenzo-1,2,4-triazine-*N*1,*N*4-oxide (tpzH) and 3-aminoquinoxaline-2-amido-*N*1,*N*4-oxide (tpzH-$CONH_2$) (**Figure 3.5**). The tpzH ligand is used for its hypoxia-selective cytotoxic properties whilst tpzH-$CONH_2$ is also used because it was initially thought the amide might aid solubility, but also the ligand has a group capable of donating and accepting additional hydrogen-bonds.

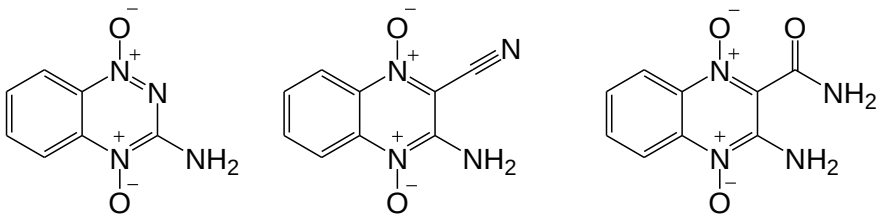

Figure 3.5: Structures of the *N*1,*N*4-oxide ligands used in this study

3.2. Preparation of *N*1,*N*4-oxide ligands

3.2.1. Preparation of 3-aminoquinoxaline-2-carbonitrile-*N*1,*N*4-oxide (tpzH-CN)

3-Aminoquinoxaline-2-carbonitrile-*N*1,*N*4-oxide **(**tpzH-CN**)** was prepared in a similar manner to that previously reported,[161] through the use of a Beirut reaction.[162] This involves the reaction of benzofuroxan and propanedinitrile in DMF solution in the presence of Et_3N (**Scheme 3.1**) to produce an orange precipitate which can then be isolated *in vacuo* (56% yield). The product was then washed with acetone, leaving a bright reddish orange fluorescent solid, which was then fully characterised by NMR and IR spectroscopy and MS spectrometry. After drying under vacuum, the ligand was used without further purification.

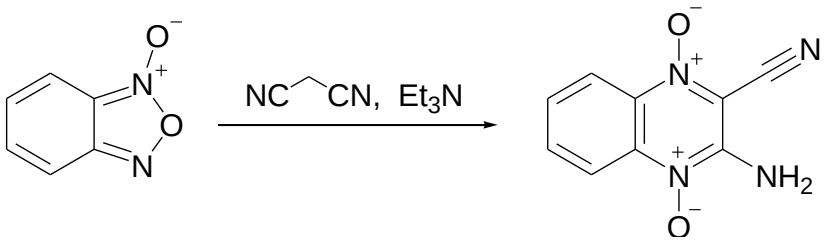

Scheme 3.1: Preparation of tpzH-CN using the Beirut reaction

The NMR spectra of the tpzH-CN ligand could not be fully assigned owing to the lack of proton-proton coupling throughout the whole molecule. It can be determined how the aromatic protons are arranged in relation to one another through the use of COSY, HSQC and HMBC NMR experiments, but not where they are in relation to the amine and nitrile groups (**Figure 3.6**).

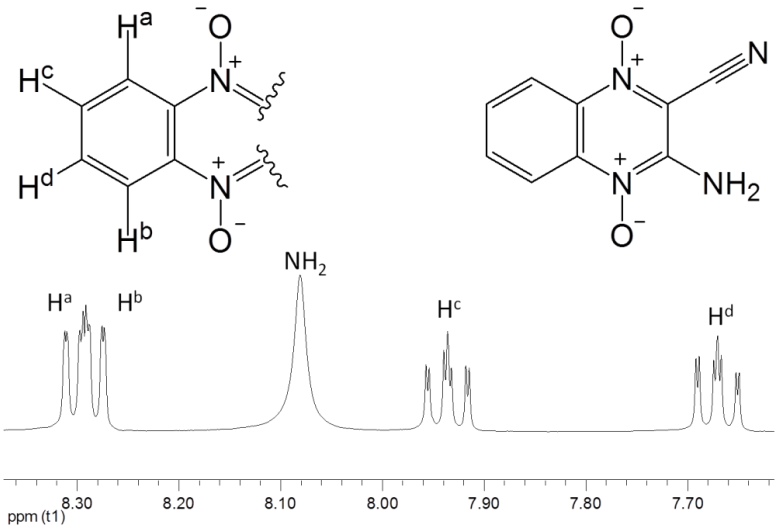

Figure 3.6: ^{1}H NMR spectrum of tpzH-CN (400 MHz, d_6-DMSO,). δ8.29 (dd, 1H, J = 5.5, 1.0 Hz, H^a), δ8.27 (dd, 1H, J = 5.5, 1.0 Hz, H^b), δ8.08 (br. s, 2H,NH_2), δ7.93 (ddd, 1H, J = 8.5, 7.5, 1.0 Hz, H^c), δ7.66 (ddd, 1H, J = 8.5, 7.5, 1.0 Hz, H^d)

3.2.2. Preparation of 3-aminoquinoxaline-2-amido-*N*1,*N*4-oxide (tpzH-$CONH_2$)

The ligand 3-aminoquinoxaline-2-amido-*N*1,*N*4-oxide (tpzH-$CONH_2$) was prepared by a method adapted from that reported in a patent.[163] The tpzH-$CONH_2$ was prepared by heating tpzH-CN in concentrated sulphuric acid which facilitates the hydrolysis of the nitrile group to a primary amide (**Scheme 3.2**).

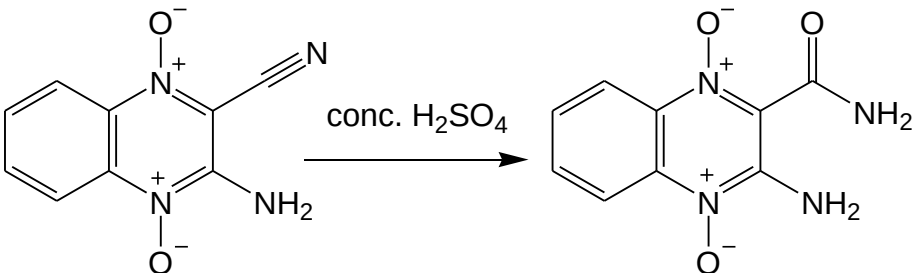

Scheme 3.2: Preparation of tpzH-$CONH_2$

The reaction mixture was then cooled before being neutralised with concentrated liquid NH_3 which caused the formation of an orange precipitate, isolatable by filtration.

The ^{1}H NMR spectrum of the crude product shows the presence of the ammonium salt through a characteristic set of three signals of equal intensity centred at δ7.10 with a ^{1}H-^{14}N coupling constant of 51 Hz (**Figure 3.5**).[164]

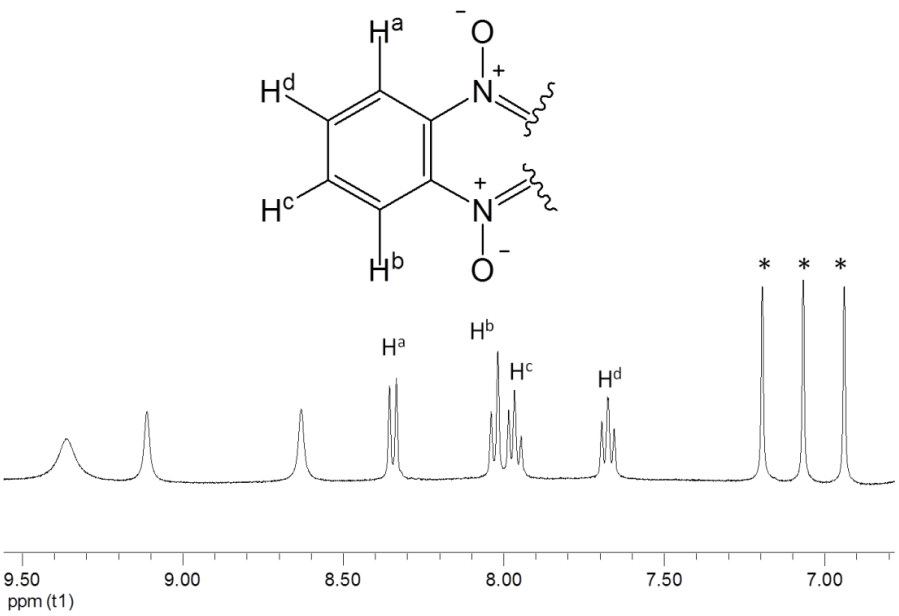

Figure 3.7: ^{1}H NMR assignment of crude tpzH-$CONH_2$ (400 MHz, d_6-DMSO) with peaks of NH_4^+ peaks at δ7.10 highlighted by *. δ9.41 (br. s, 2H), δ9.16 (br. s, 1H), δ8.67 (br. s, 1H), δ8.39 (d, 1H, J = 8.5 Hz, H^a), δ8.07 (d, 1H, J = 8.5 Hz, H^b), δ8.01 (dd, 1H, J = 8.5, 7.0 Hz, H^c), δ7.72 (dd, 1H, J = 8.5, 7.0 Hz, H^d), δ7.11 (t, 4H, J = 51.0 Hz, $[NH_4]^+$),

Dissolving the crude product in acetone and filtering the resulting solution removes the ammonium salt and any unreacted tpzH-CN, allowing the pure product to be isolated in 16% yield. Close analysis of the ^{1}H NMR spectrum of the pure product reveals that there are three broad singlets; one at δ9.85 and δ8.58 which both have an integration of one and a peak at δ8.19 which has an integration of two. It would be expected that there would be two broad singlets both with an integration of two which would correspond to the amide and amine NH_2 groups but it is apparent that one of these is split into two signals. With the other *N*-oxide ligands discussed in this chapter, the amine protons appear at *ca*. δ8.1, so logically the amine of the tpzH-$CONH_2$ would be at δ8.19.

^{1}H-^{1}H COSY NMR shows that the singlets at δ9.85 and δ8.58 are weakly coupled (**Figure 3.8**), indicating that these two protons are both bonded to the same heteroatom.

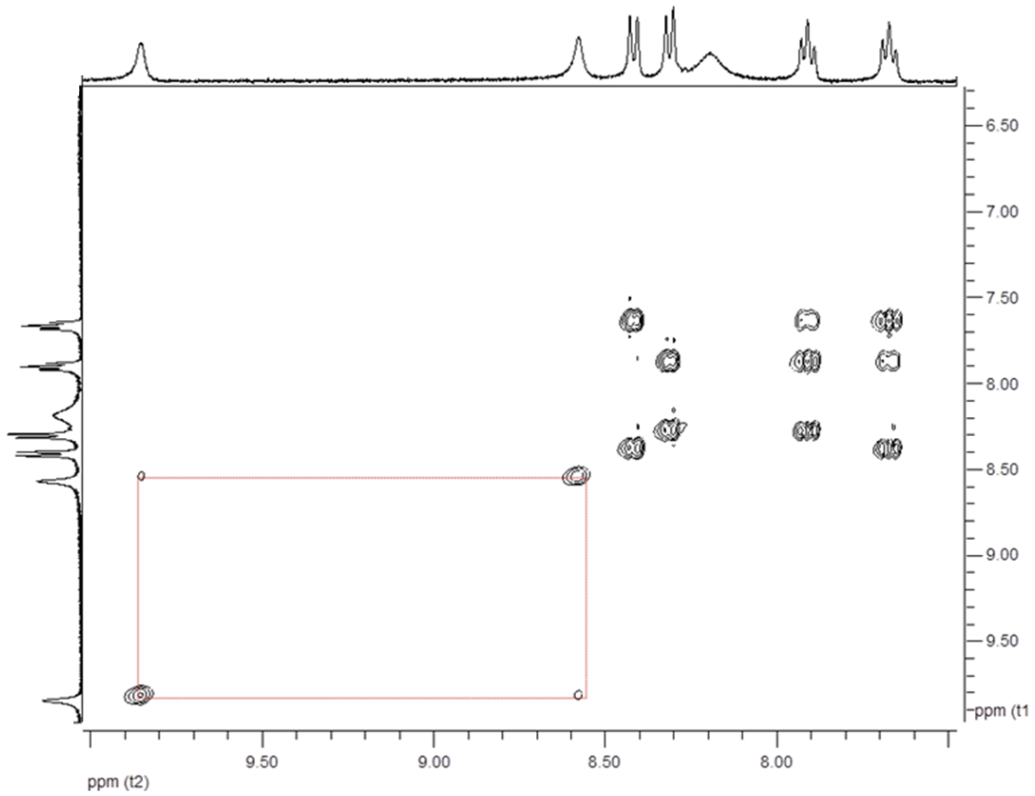

Figure 3.8: ^{1}H-^{1}H COSY NMR spectrum of tpzH-CONH$_2$ (400 MHz, d$_6$-DMSO) highlighting the coupling between the singlets at δ9.85 and δ8.58.

The fact that the two amide protons give two separate resonances suggests that they are not rotating fast enough for the two peaks to coalescence. Resonances of protons which form hydrogen-bonds typically move to a more downfield chemical shift, the extent of which depends on the interaction.[165] The downfield chemical shift of the amide proton suggests that the acceptor atom of the hydrogen-bond is very electron rich character, such as an oxygen atom of an *N*-oxide group. The broad singlet with an integration of two at δ8.20 is at a chemical shift similar to the amine protons observed in the other *N*-oxide ligands.

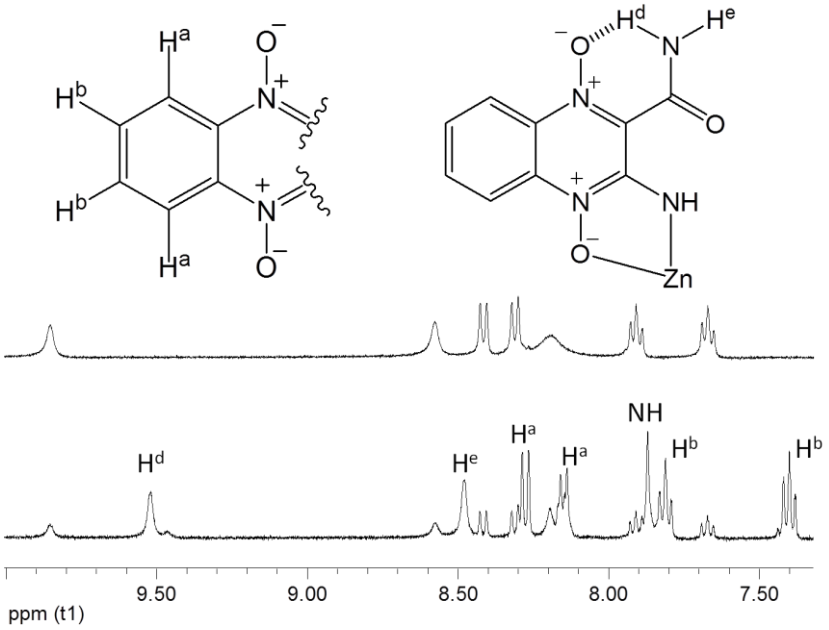

Figure 3.9: ^{1}H NMR (400 MHz, d_6-DMSO) spectrum of tpzH-CONH$_2$ δ9.85 (br. s, 1H, H^{e}), δ8.58 (br. s, 1H, H^{f}), δ8.41 (d, 1H, J = 8.0 Hz, H^{a}), δ8.31 (d, 1H, J = 8.0 Hz, H^{b}), δ8.19 (br. s, 2H, NH$_2$), δ7.91 (ap. t, 1H, J = 8. 0 Hz, H^{c}), δ7.67 (ap. t, 1H, J = 7.5 Hz, H^{d})

The distinct two environments shown by the resonances for H^{e} and H^{f} implies there is a lack of rotation about the amide N-C bond, which is not uncommon for amides, owing to the distribution of electrons throughout the group (**Scheme 3.3**). The interaction between the C=O and N lone pairs results in a decrease of electron density on the C=O bond and increase on the C-N bond results in partial N=C character, hindering rotation about this bond.[155, 166]

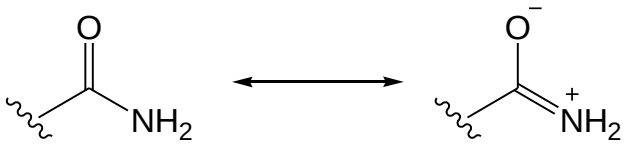

Scheme 3.3: Resonance structures of a primary amide functional group

Single red coloured crystals suitable for diffraction were obtained from a reaction of [Co(tpz-CN)$_2$] with H_2O_2 in MeOH. The structure shows that the amide is arranged so N(4)-H(4b) is able to act as a hydrogen-bond donor to the *N*-oxide oxygen O(1). A hydrogen-bond is also evident between the carbonyl oxygen O(3) of the amide and the amine N(3)-H(3b) (**Figure 3.10**).

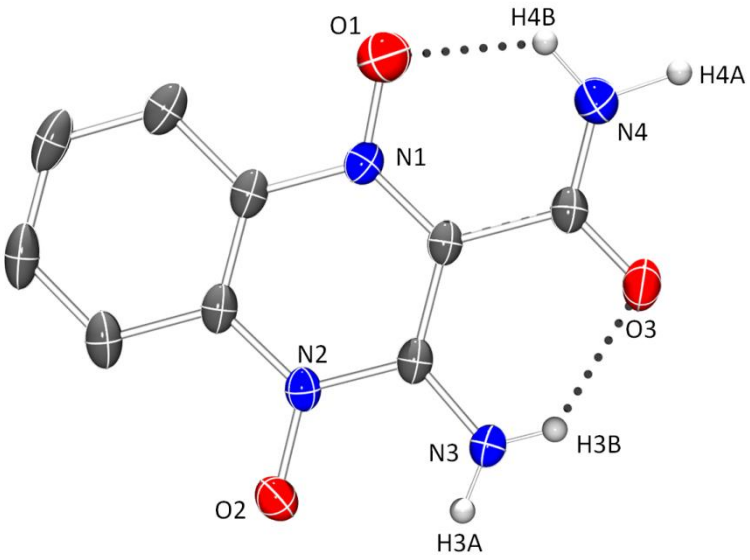

Figure 3.10: ORTEP diagram (50 % probability ellipsoids) of tpzH-$CONH_2$.[131] Hydrogen atoms (except H(3a), H(3b), H(4a) and H(4b)) and solvent removed for clarity. Selected bond lengths /Å and angles /º: N(1)-O(1) 1.274(2), N(2)-O(2) 1.327(2), C(7)-N(3) 1.326(2), C(9)-O(3) 1.228(2), C(9)-N(4) 1.329(2). Hydrogen-bond distances / Å and angles /º: N(4)-O(1)···2.557(2), H(4B)···O(1) 1.90(3), N(3)···O(3) 2.622(2), H(3B)···O(3) 1.98(3), N(4)-H(4B)···O1 126(3), N(3)-H(3B)···O3 (136(2),

Analyses of the C-N bond lengths the C=O bond lengths within the amine do not indicate a reduction of C=O bond double bond character or any resulting change in the N-C bond (**Table 3.2**).

Table 3.2: Comparison of selected bond lengths of tpzH-$CONH_2$ with standard literature values.[167]

Bond	**Bond length from structure / Å**	**Standard literature value / Å**
C(9)-O(3)	1.228(2)	1.234 (for amide C=O)
C(9)-N(4)	1.329(2)	1.325 (for amide C-N)

3.2.3. Preparation of 3-amino-1,2,4-benzotriazine-*N*1,*N*4-oxide (tpzH)

3-amino-1,2,4-benzotriazine-*N*1,*N*4-oxide (tpzH) was prepared accordingly to a previously reported method from 2-nitroaniline via a *N*4-oxide intermediate (**Scheme 3.4**).[168]

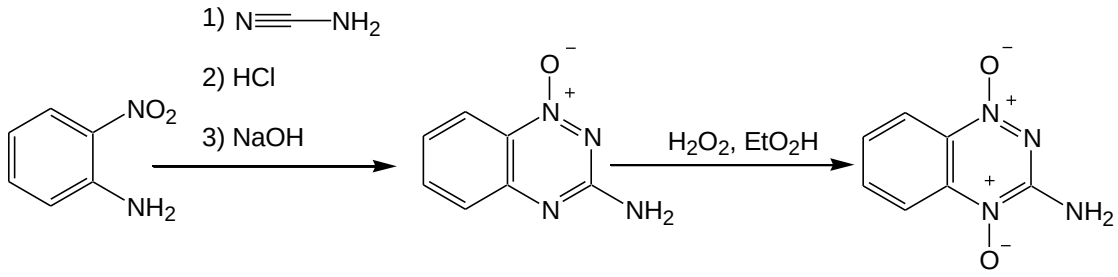

Scheme 3.4: Preparation of tpzH from 2-nitroaniline and cyanamide

As 2-nitroaniline can be formed upon the reduction of benzofuroxan (**Scheme 3.5**), the preparation used for the synthesis of tpzH is not unrelated to that used to prepare tpzH-CN. Both involve the reaction of a nitrile amine with benzofuroxan or 2-nitroaniline.

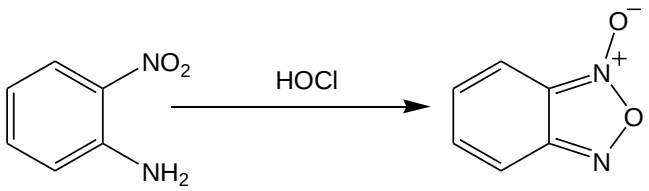

Scheme 3.5: Preparation of benzofuroxan from 2-nitroaniline

As the reduced form of the starting material is used, an additional oxidation step is needed to form the *N*1,*N*4-oxide product. This latter method has the advantage that if substituents are desired on the phenyl ring in the 5, 6, 7 or 8-positions then greater control is provided to ensure that only the desired isomer is obtained (**Scheme 3.6**).

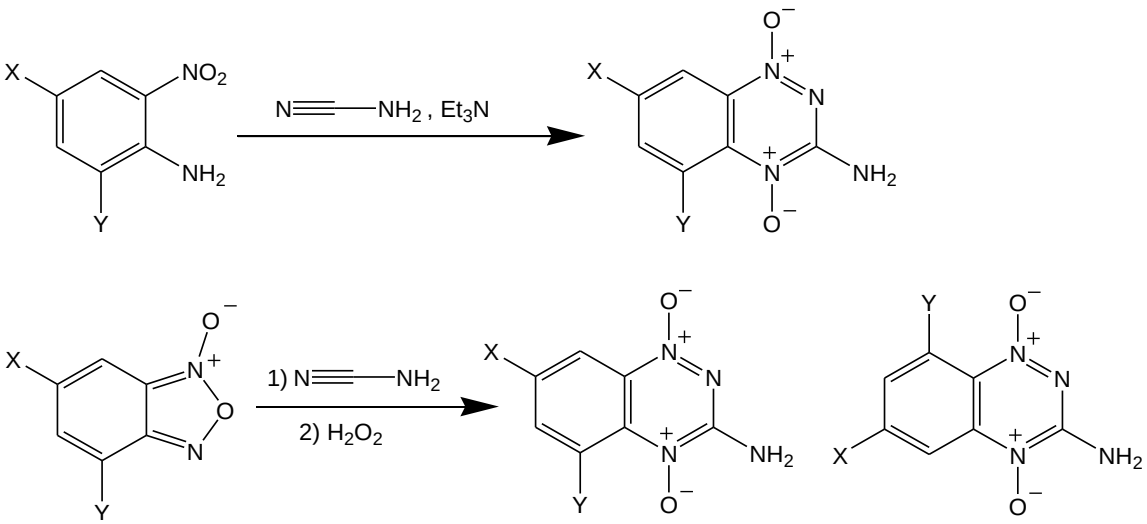

Scheme 3.6: Possible isomers that can be produced from the two different methods of preparing tpzH-R type *N*1,*N*4-oxide ligands

The product, once extracted with $CHCl_3$, was recrystallised and then used without further purification. The intermediate and product were characterised, including by NMR spectroscopic analysis (**Figure 3.11**).

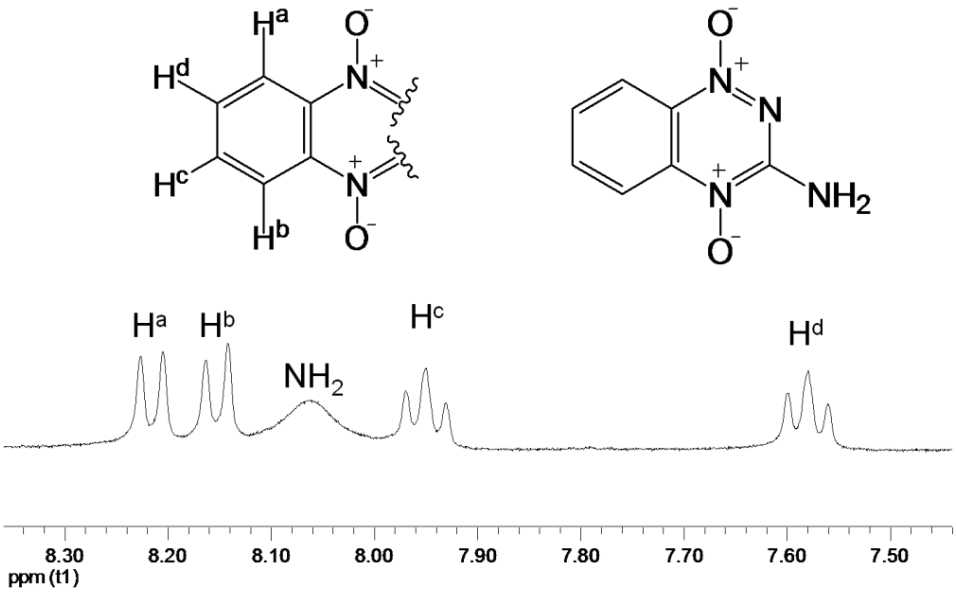

Figure 3.11: ^{1}H NMR (400 MHz, d_6-DMSO) spectrum of tpzH. δ8.21 (ddd, 1H, J = 9.0, 1.5, 1.0 Hz, H^a), δ8.15 (dd, 1H, J = 9.0, 1.0 Hz, H^b), δ8.06 (br. s, 2H, NH_2), δ7.95 (ddd, 1H, J = 9.0, 7.2, 1.0 Hz, H^c), δ7.57 (ddd, 1H, J = 9.0, 7.2, 1.0 Hz, H^d)

Hay reported on the full NMR characterisation of tpzH, for which ^{15}N NMR spectroscopy was employed in addition to ^{1}H and ^{13}C (**Figure 3.11** and **Table 3.3**).[169]

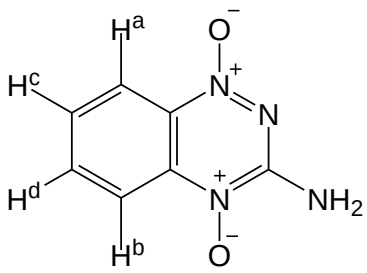

Figure 3.12: Assignment of protons reported for the ^{1}H NMR data of tpzH shown in **Table 3.3**.[169]

The ^{1}H NMR spectrum and assignment shown in **Figure 3.10** agrees with that reported by Hay, so this assignment for the free tpzH ligand can be used.

Table 3.3: ^{1}H NMR assignment of tpzH reported by Hay.[169]

Proton environment	**^{1}H chemical shift (splitting, J value / Hz)**
H^a	8.14 (d, J = 8.7 Hz)
H^b	8.21 (d, J = 8.8 Hz)
H^c	7.95 (d, J = 8.8 Hz)
H^d	7.58 (ddd, J = 8.8, 7.1, 1.4 Hz)
NH_2	8.04 (br. s)

Crystals suitable for study by x-ray diffraction were obtained through evaporation from a methanolic solution (**Figure 3.13)**.

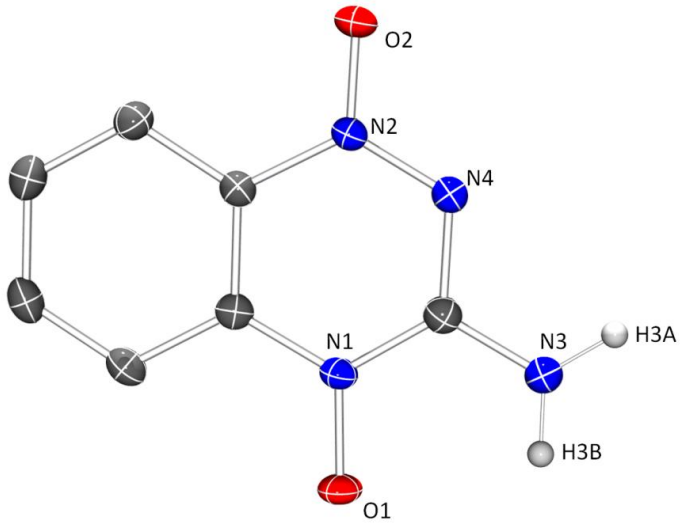

Figure 3.13: ORTEP diagram (50 % probability ellipsoids) of tpzH.[131] Hydrogen atoms (except H(3a) and H(3b)) and solvent removed for clarity. Selected bond lengths /Å: N(1)-O(1) 1.3330(15), N(2)-O(2) 1.2574(15).

The crystal structure shows the O1 oxygen atom to form a hydrogen-bond with the proton H(3c) from the OH of a methanol molecule as well as to H(3b) of an adjacent tpzH molecule (**Figure 3.14**).

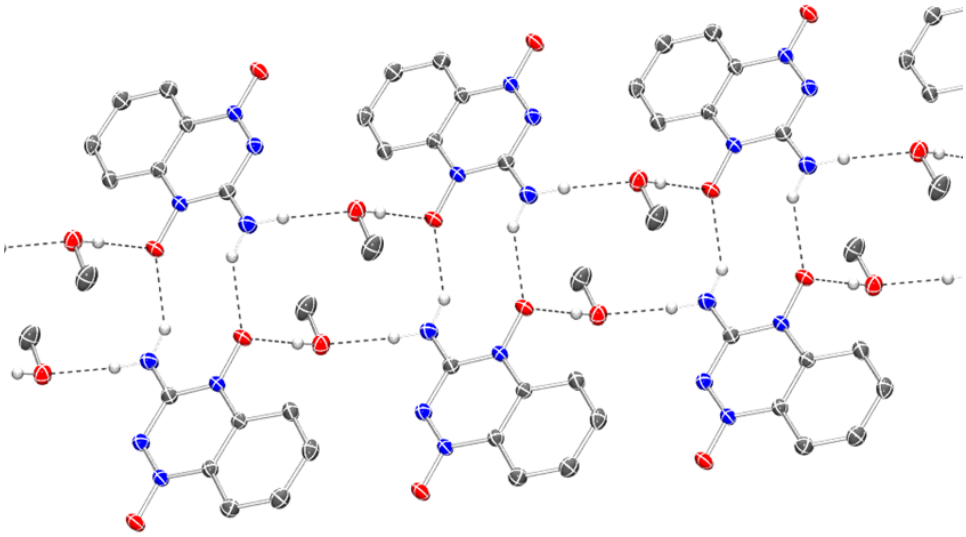

Figure 3.14: ORTEP diagram of the hydrogen-bonding interactions evident in the crystal structure of tpzH.[131] Hydrogen-bond distances /Å and angles /º: H(3C) ··O(1) 1.83(2), O(3)···O(1) 2.6962(16), H(3B)··· O(1) 2.04(2), N(3)···O(1) 2.8347(17), H(3A)···O(3) 1.89(2), N(3)···O(3) 2.8137(18), O(3)-H(3C)···O(1) 174(2), N(3)-H(3B)···O(1) 147.5(19), N(3)-H(3A)···O(3) 174.5(17)

*N*1,*N*4-oxide ligands have been produced using two synthetic routes. These three ligands have been fully characterised, including assignment by NMR spectroscopic analysis as far as possible (**Table 3.4** and **Figure 3.15**).

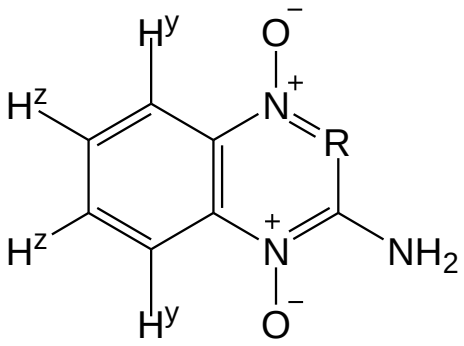

Figure 3.15: Proton environments used in **Table 3.4**

Comparing the ^{1}H NMR spectroscopic data of the three *N*-oxide ligands that the amine protons of tpzH-$CONH_2$ are in the more deshielded environment with the amine protons having a chemical shift of δ8.91 whilst tpzH and tpzH-CN have their corresponding peaks appearing at δ8.05, and δ8.05 respectively. However, it should be noted that the more downfield shift of the amine of tpzH-$CONH_2$ could be predominantly due to the hydrogen-bonds this group forms.

Table 3.4: Summary of the ^{1}H resonances of the prepared *N*1,*N*4-oxide ligands tpzH, tpzH-CN and tpzH-$CONH_2$ (400 MHz, d_6-DMSO)

Ligand	**tpzH**	**tpzH-CN**	**tpzH-$CONH_2$**
H^y	δ8.20 (dd, 1H)	δ8.29 (dd, 1H)	δ8.41 (d, 1H)
	δ8.14 (dd, 1H)	δ8.27 (dd, 1H)	δ8.31 (d, 1H)
H^z	δ7.93 (ddd, 1H)	δ7.93(ddd, 1H)	δ 7.91 (ap. t, 1H)
	δ7.57 (ddd, 1H)	δ7.66(ddd, 1H)	δ7.67 (ap. t, 1H)
NH_2	δ8.05 (br. s, 2H)	δ8.05 (br. s, 2H)	δ8.91 (br. s, 2H)
$CONH_2$			δ9.85 (s, 1H)
			δ8.58 (s, 1H)

It can be seen that the protons in the H^y environment on the different ligands all have similar chemical shifts, with one ranging from δ7.93 to 7.1, and the second from δ7.67 to 7.57, as these are too far away from the substituents in the 2-position to be affected. The chemical shifts of the protons in the H^y environments increases to a

more downfield value going from tpzH to tpzH-CN to tpzH-$CONH_2$. This indicates that the different substituents on the ligands are most likely to affect the electronic nature of the *N*-oxide groups, as any electronic difference would have to go through the *N*-oxide nitrogen to affect the H^y protons. Therefore, the two groups through which the *N*1,*N*4-oxide ligands coordinate to metals are affected by altering the substituent in the 2-position, so a noticeable difference might be observed in their coordination chemistry such as the strength of bonding interaction to the metal centre.

3.3. Preparation of metal(II) complexes

The metal(II) complexes were prepared by a method adapted from that used by Gambino *et al.* where they typically used metal(II) sulfate salts reacting with two equivalents of tpzH-CN in the presence of Et_3N to deprotonate the amine of the ligand The complexes reported here were prepared from metal(II) acetate salts as it was found that this removed the need to use Et_3N. The cobalt(II), copper(II) and zinc(II) acetate salts were reacted with two equivalents of the *N*-oxide ligand in methanolic solution (**Scheme 3.6**) to afford the relevant *bis*-*N*-oxide metal (II) complex.

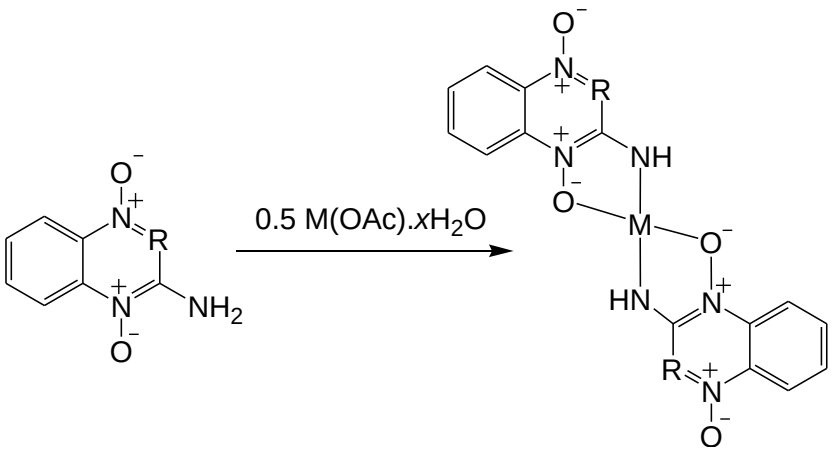

Scheme 3.7: Preparation of *bis*-*N*1,*N*4-oxide metal(II) complexes (R = N, C-CN and C-CO-NH_2, M = Co, Cu, Zn)

Characterisation of these in solution has been hindered by their lack of solubility in solvents other the DMSO and DMF. Therefore the only solution phase characterisation carried out has been NMR spectroscopic analysis but this could only

be done for the zinc(II) complexes owing to cobalt(II) and copper(II) being paramagnetic.

3.3.1. Preparation of metal(II) complexes with 3-aminoquinoxaline-2-carbonitrile-*N*1,*N*4-oxide

As some previous complexes of tpzH-CN with various metals had been previously reported, it was decided to start with this ligand and prepare complexes of zinc(II), cobalt(II) and copper(II). Mixing two equivalents of tpzH-CN with $M(OAc)_2.xH_2O$ (M = Co, Cu, Zn) in methanolic solution caused the formation of a dark red precipitate which was then isolated by filtration in yields greater than 75%. Formation of the zinc(II) complex could be confirmed by ^{1}H NMR spectroscopy (**Figure 3.16**), where the peak corresponding to NH_2 of the free ligand undergoes a downfield shift from δ8.05 to δ6.56, as well as integration change from two to one. The NMR spectrum indicates that the two tpz-CN ligands of the zinc(II) complex are equivalent on the NMR time scale.

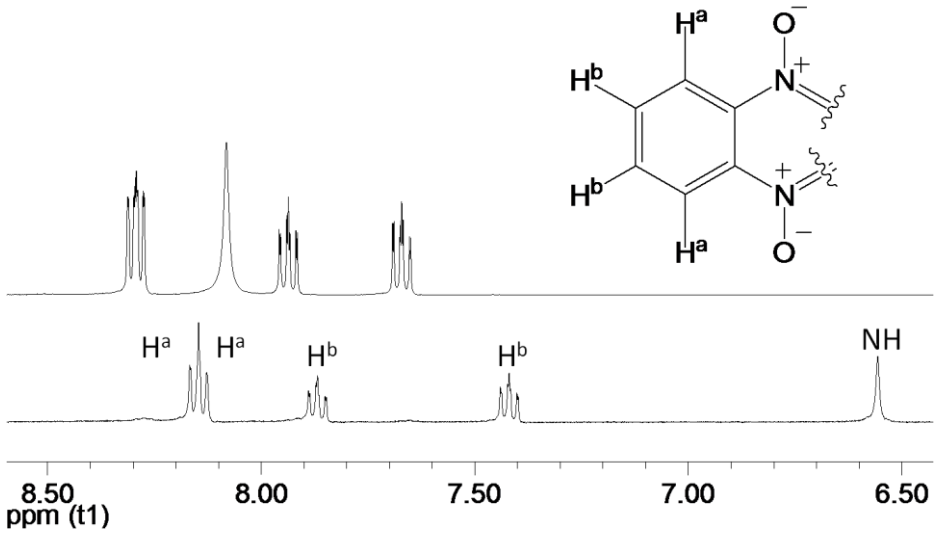

Figure 3.16: ^{1}H NMR) (400 MHz, d_6-DMSO) spectra of tpzH-CN (*above*) and $[Zn(tpz\text{-}CN)_2]$ (*below* δ8.16 (d, 1H, J = 8.0 Hz, H^a), δ8.14 (d, 1H, J = 7.5 Hz, H^a), δ7.87 (ddd, 1H, J = 8.5, 7.0, 1.0 Hz, H^b), δ7.42 (ddd, 1H, J = 8.5, 7.0, 1.0 Hz, H^b), δ6.55 (br. s, 1H, NH)

For all of the metal(II) tpzH-CN complexes, complexation was easily confirmed through IR spectroscopic analysis (**Figure 3.17**). The amine NH stretch absorbance frequency changes from two bands at 3347 and 3310 cm^{-1} (ν_{sym} and ν_{asym}) in the free

ligand to one vibration at *ca*. 3380 cm^{-1} in the metal(II) complexes. Such a change is characteristic of the symmetry change in a primary amine occurring upon coordination to a metal centre.

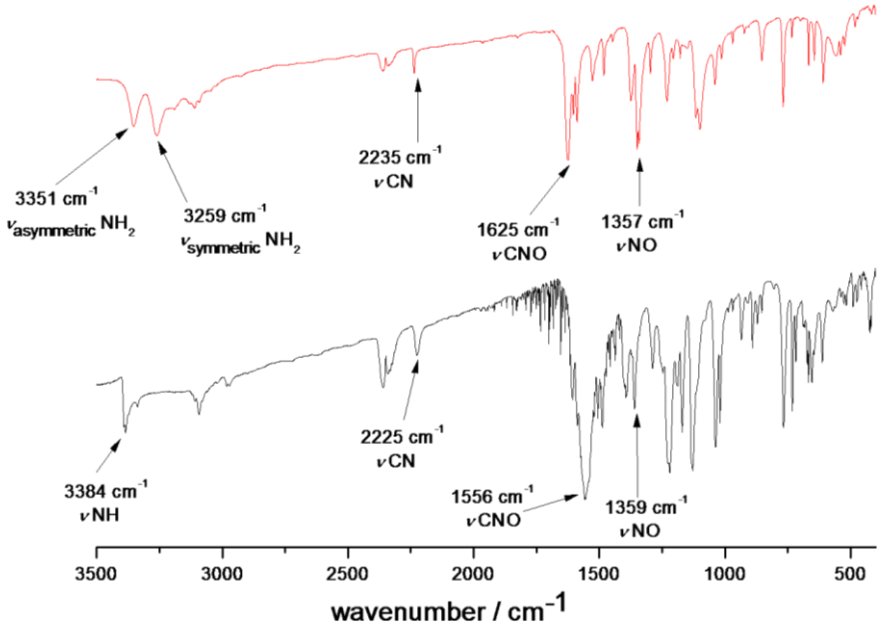

Figure 3.17: IR (KBr disc) of tpzH (*above*) and [Co(tpz-CN)$_2$] (*below*).

Obtaining crystals of these complexes proved challenging but small deep purple crystals of diffraction quality were obtained by slow diffusion of Et_2O into a solution of DMF. One of the limitations in growing crystals of these complexes was their poor solubility, being only soluble in DMF and DMSO, and partially soluble in pyridine. It was attempted to carry out crystallisations in the presence of compounds such as indole, in the hope that by providing a hydrogen-bond donor to interact with the *N*-oxide groups, crystallinity might be encouraged but this was without success. Therefore, the complex of [Zn(tpz-CN)$_2$] is currently the only structurally characterised metal(II) *bis*-*N*1,*N*4-oxide complex.

The zinc(II) centre is coordinated to two tpz-CN ligands and a DMF solvent molecule (**Figure 3.18**). The five-coordinate metal centre has a distorted square-pyramidal geometry (τ = 0.15).[132] There was a high level of disordered solvent present in the unit cell so both the solved structure including the disorder and that using the SQUEEZE logarithm are presented in the appendix of crystallography data. However, the former is used for quoting bond lengths and other structural parameters

owing to the whole unit cell having been modelled, providing a better model of the structure.

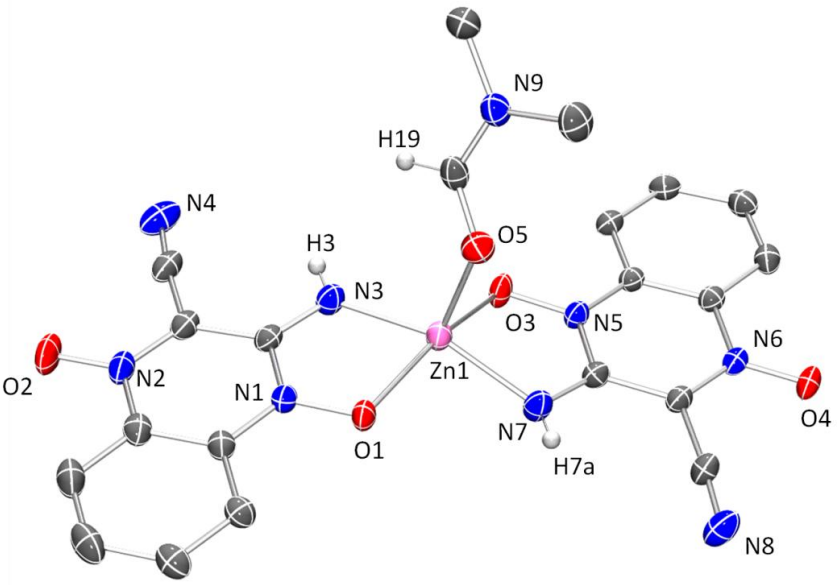

Figure 3.18: ORTEP (50 % probability) of [Zn(tpz-CN)$_2$(DMF)].[131] Hydrogen atoms (except H(3), H(7a) and H(19) and H(3b)) and solvent molecules removed for clarity. Selected bond lengths /Å and angles /º:N(1)-O(1) 1.340(3), N(2)-O(2) 1.282(3), N(3)-Zn(1) 1.990(2), N(5)-O(3) 1.348(3), N(6)-O(4) 1.280(3), N(7)-Zn(1) 1.989(2), O(1)-Zn(1) 2.0838(18), O(3)-Zn(1) 2.1196(19), O(5)-Zn(1) 2.078(2), N(3)-Zn(1)-O(1) 79.60(8), N(7)-Zn(1)-O(3) 79.01(8)

The effect of coordination of this type of ligand to a metal centre has upon the *N*-oxide bond can be examined by comparing the N-O bond lengths of *N*1,*N*4-oxide ligands described previously with those from the [Zn(tpz-CN)$_2$(DMF)] complex (**Table 3.4**).

Table 3.5: N-O bond lengths of tpzH, tpzH-CONH$_2$ and [Zn(tpz-CN)$_2$(DMF)]

Structure	**N-O bond distance /Å**	
	1-position	**4-position**
tpzH	1.3330(15)	1.2574(15).
tpzH-CONH$_2$	1.327(2),	1.274(2)
[Zn(tpz-CN)$_2$(DMF)]	1.340(3)	1.282(3)
	1.348(3)	1.280(3)

The structures of tpzH and tpzH-$CONH_2$ show that out of the two *N*-oxide moieties, the one adjacent to the amino group in the 1-position (1.333(5) and 1.327(2) Å respectively) is longer than the one in the 4-position (1.257(5) and 1.274(2) Å). Upon coordination to the zinc(II) centre, the N-O bond lengths, both N-O bond lengths appear to increase in length. The two coordinated ligands have bond lengths of 1.340(3) and 1.348(3) Å in the 1-position whilst those in the 4-position are 1.282(3) and 1.280(3) Å. This concurs with the conclusions reported by Murthy and Patel who investigated the effect of coordinating *N*-oxide ligands to different metal centres using IR spectroscopy.[170] They observed that the vibrational frequency of the N-O stretch decreased upon coordination which was attributed to the decreasing π character of the *N*-oxide bond. They also demonstrated that the stretch of the N-O bond when coordinated to a metal centre decreased going from a zirconyl complex (1222 cm^{-1}), to thorium (1218 cm^{-1}) then to a uranyl complex (1207 cm^{-1}). This was correlated with a decrease in π-character of the *N*-oxide, resulting in a weakening of the N-O bond whilst the strength of the M-O bond increased. The lengthening of the *N*-oxide bonds observed in the complex can be attributed to the same effect, although it is interesting that the *N*-oxides in the 4-position have also lengthened even though they are not coordinated to the metal centre.[170]

It can be seen from the crystal structure that the coordination of the two tpzH-CN ligands with the metal centre appear to be different, with one (ligand A) remaining linear whilst the other (ligand B) is distorted (**Figure 3.19**). However, it cannot be concluded that this difference results from different bonding interactions or is an effect of crystal packing. The zinc(II) centre lies within the plane of one of the tpz-CN ligands (ligand A) but above the plane of the second (ligand B).

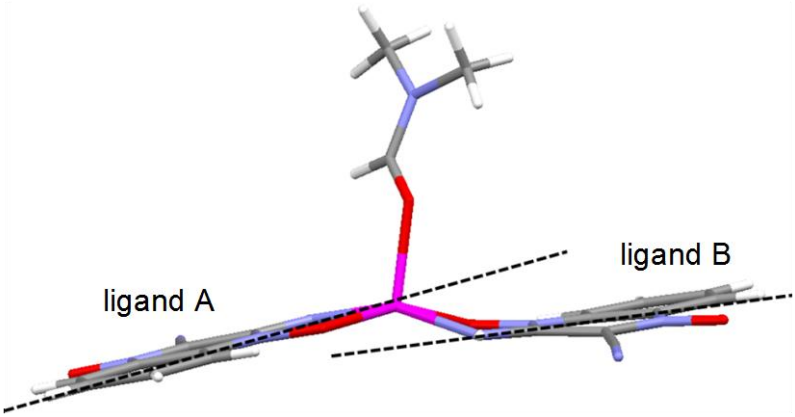

Figure 3.19: Mercury Stick representation of [Zn(tpz-CN)$_2$(DMF)]to highlight the distortion in ligand B.[171]

The degree to which ligand B is bent can be represented by an interplanar angle, which measures the angle between the plane through which the metal coordinates to the ligand (plane one) and the plane that the ligand lies on (plane two) (**Figure 3.18**). The crystal structure of [Zn(tpz-CN)$_2$(DMF)] shows an interplanar angle within ligand B of 23.16°.

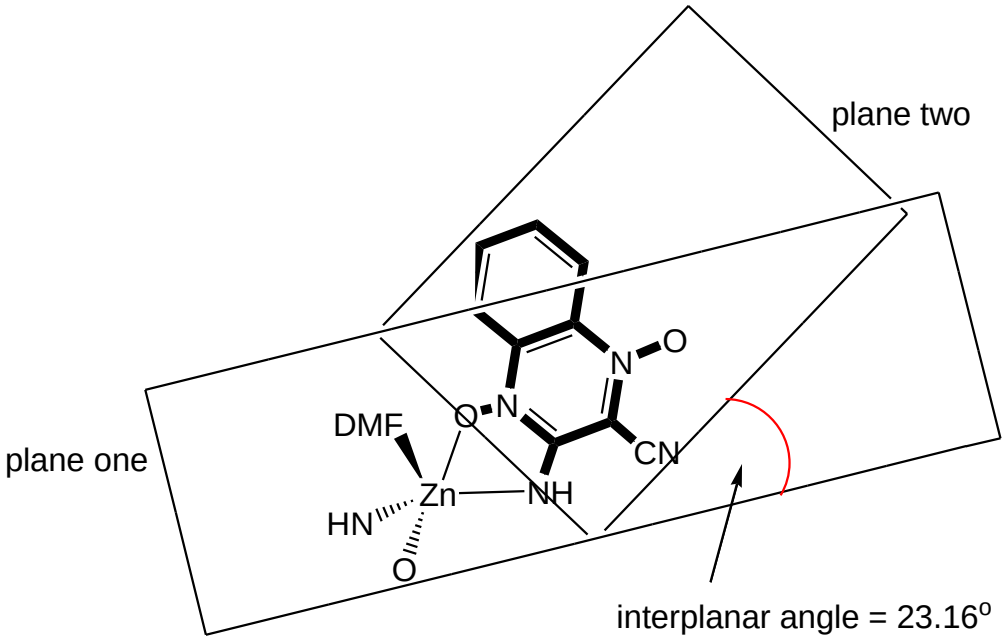

Figure 3.20: Diagram to represent the interplanar angle between the metal-donor atoms and ligand

This interplanar angle distortion could be a result of the decrease in π-character of the N-O bond coordinated to the metal centre resulting in a general slight decrease in

π-density throughout the whole ligand and thus the effect is observed also in the uncoordinated *N*-oxide in the 4-position.

From the structure, it is also evident that the two aromatic rings of the ligand, which would be expected to be planar, bend with respect to each other (**Figure 3.21**) which would further decrease the aromaticity of the system. For ligand A, this bend is 1.3° and for ligand B, 4.3°.

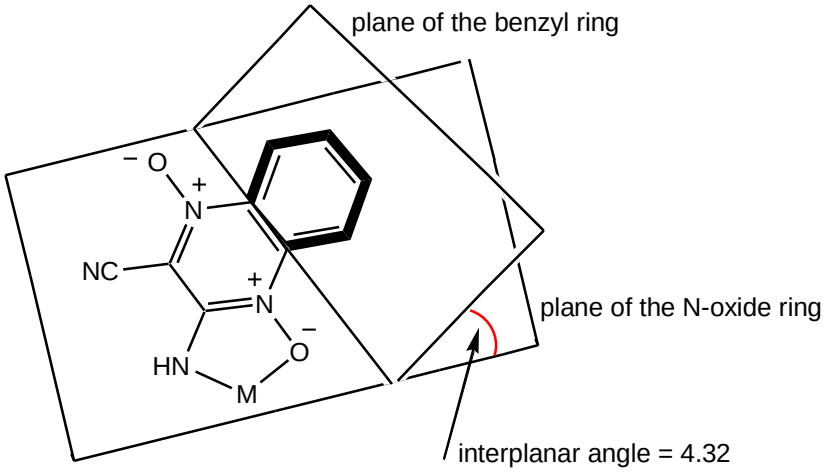

Figure 3.21: Diagram to represent the bend between the two rings of coordinated tpzH-CN (ligand B)

This structure contrasts with Torre's reported EPR spectroscopic data which suggested that complexes of this nature exist as dimers in the solid state with the copper coordinating to an uncoordinated *N*-oxide in the axial position (**Figure 3.22**).[140, 144]

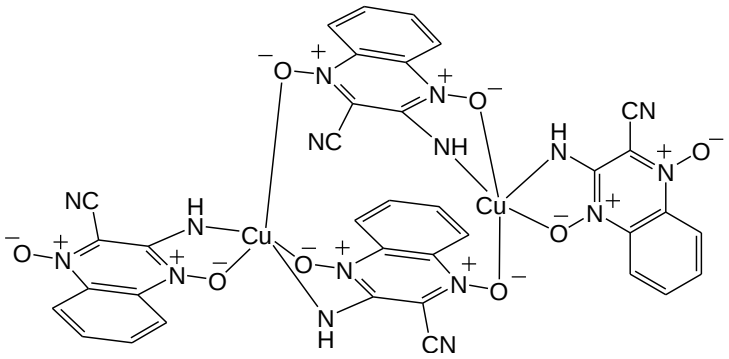

Figure 3.22: Representation of the structure of copper *bis*-tpz-CN ligand complexes proposed as a result of theoretical calculations.[140, 144]

Several strategies were attempted in obtaining crystals, such as use of a solvent that was capable of π-stacking interactions which could facilitate crystal growth (e.g. pyridine), and adding an aromatic hydrogen-bond donor to the crystallisation such as indole. However, no further suitable crystals have yet been obtained for the zinc complex or any of diffraction quality for the cobalt(II) or copper(II) complexes of this ligand or for *bis*-complexes any of the other *N*1,*N*4-oxide ligands discussed in this chapter.

3.3.2. Preparation of metal(II) complexes with an 3-aminoquinoxaline-2-amido-*N*1,*N*4-oxide

With tpzH-$CONH_2$, there are three possible coordination sites through which it may coordinate to a metal centre. It can coordinate to a metal centre through the amine and adjacent *N*-oxide to form a 5-membered chelate ring as with tpzH-CN and tpzH, or through the amide. If coordination occurs through the amide, it would be most likely for the metal to bond to the carbonyl and *N*-oxide NH_2 and its adjacent *N*-oxide to form a 6-membered chelate ring (**Figure 3.23**).

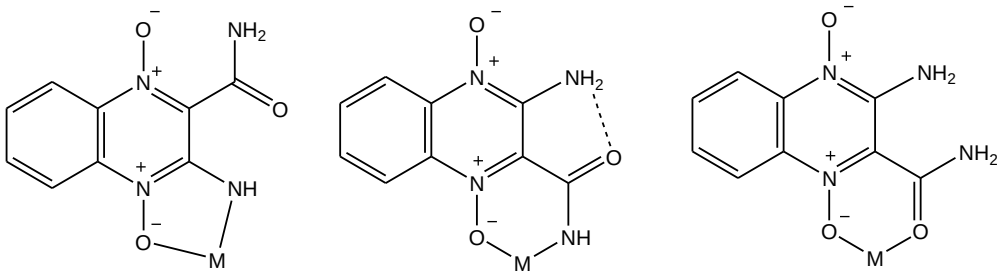

Figure 3.23: The possible two possible coordination sites of tpzH-$CONH_2$; through the amine (A), through the amide NH and *N*-oxide (B) or through the amide carbonyl and *N*-oxide (*C*).

Coordination through the amide nitrogen (B) is unlikely due to delocalisation of nitrogen atom's electron density as described previously.[155, 166] However, the rotation of the amide group so that coordination mode C can occur would have to overcome the hydrogen-bond between the carbonyl and *N*-oxide. Coordination through the *N*-oxide and amine (A) would therefore seem most likely.

Upon the reaction of two equivalents of tpzH-$CONH_2$ with copper(II) and zinc(II) acetate, a dark precipitate formed which could then be isolated in 88% and 78% yields, respectively. ^{1}H NMR spectroscopic analysis of the zinc complex showed that some free ligand was present in the product. Comparison of the ^{1}H NMR spectra of the free ligand and zinc(II) complex shows a general decrease in chemical shift of all the proton resonances shows that the protons have become more shielded. This indicates the ligand has become less electron rich upon coordination. There are still three broad singlets, two of which are shown to be coupled by ^{1}H-^{1}H COSY NMR (**Figure 3.24**). The coupling between these two singlets indicates that the two amide protons are in two different chemical environments, with the one at the higher chemical shift (δ9.52) remaining hydrogen-bonded to the highly electronegative *N*-oxide oxygen atom.

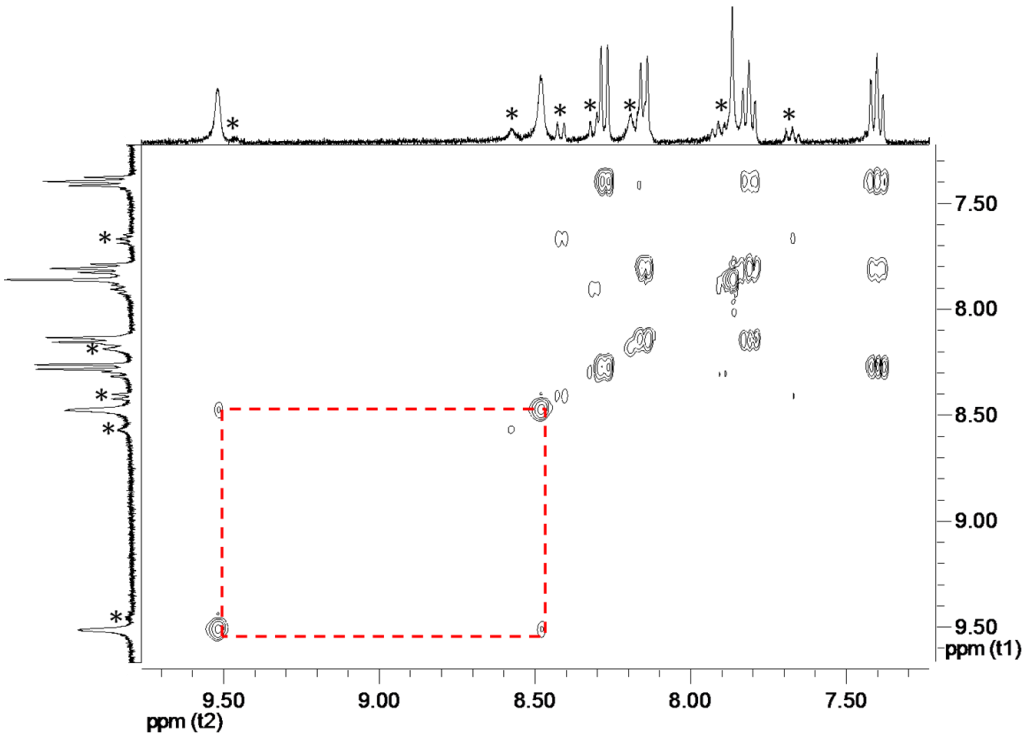

Figure 3.24: ^{1}H-^{1}H COSY spectrum (400 MHz, d_6-DMSO) of [Zn(tpz-$CONH_2$)$_2$] highlighting the coupling between the two amide proton peaks at δ9.52 and δ8.48 (peaks corresponding to unreacted ligand denoted by *)

With the zinc(II) complex, the signal for the amine remains at a relatively high chemical shift (δ7.87) compared with those from the complexes of tpzH-CN and tpzH (δ6.55 and δ6.98, respectively). This is indicative of the amine proton of the

tpzH-$CONH_2$ ligand retaining the hydrogen-bond it forms with the amide carbonyl upon coordination to zinc(II) (**Figure 3.25**).

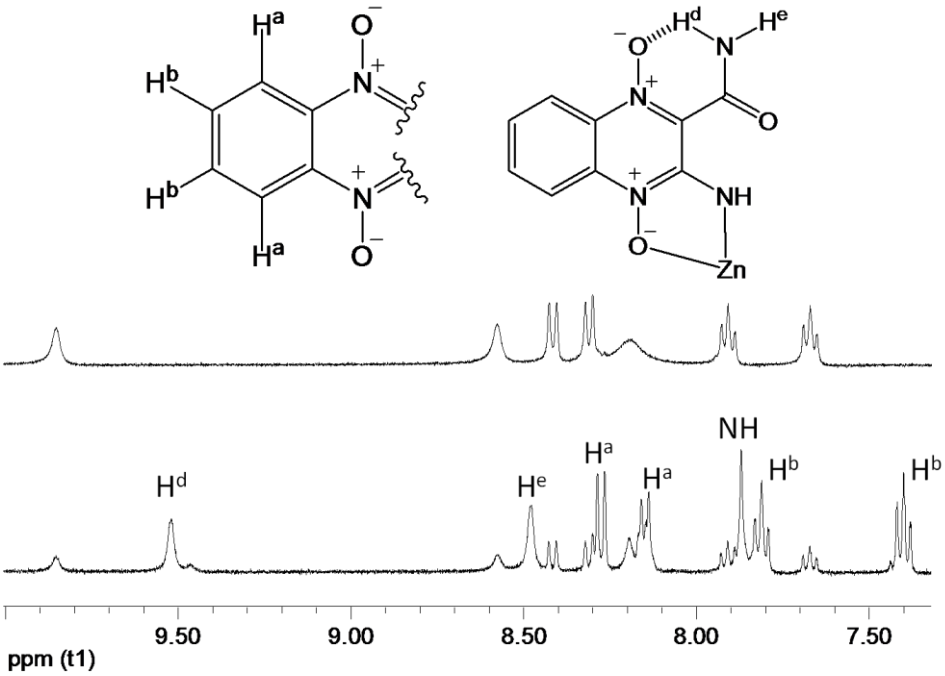

Figure 3.25: ^{1}H NMR (400 MHz, d_6-DMSO) of tpzH-$CONH_2$ (*above*) and [Zn(tpz-$CONH_2)_2$] (*below*). δ9.52 (br. s, 1H, H^d), δ8.48 (br. s, 1H, H^e), δ8.27 (d, 1H, J = 8.0 Hz, H^a), δ8.14 (d, 1H, J = 8.0 Hz, H^a), δ7.87 (s, 1H, NH), δ7.81 (ap. t, 1H, J = 8.0 Hz, H^b), δ7.40 (ap. t, J = 8.0 Hz, 1H, H^b)

3.3.3. Preparation of metal(II) complexes with tpzH

There are no previous reports describing the coordination of tpzH to metal centres but it was found that the ligand could be coordinated to metal(II) centres using the same method as for the previous two *N*-oxide ligands. The tpzH ligand is more readily soluble in solvents such as H_2O, MeOH and EtOH than tpzH-CN and tpzH-$CONH_2$, but it was found that the prepared [$M(tpz)_2$] complexes still had poor solubility. Metal(II) complexes of cobalt, copper and zinc were prepared and isolated in yields of around 60%.

^{1}H NMR spectroscopic analysis of zinc(II) complex shows the similar upfield shift which occurs upon complexation of tpzH with the other ligands (**Figure 3.26**), indicating the decrease in electron density of the ligand. The amine signal of tpzH shifts from δ8.06 to δ7.03 upon coordination, an upfield shift less significant in size

than that experienced by the amine of tpzH-CN (δ8.08 to δ6.55). This implies that the tpzH-CN ligand donates more electron density to the metal centre than tpzH.

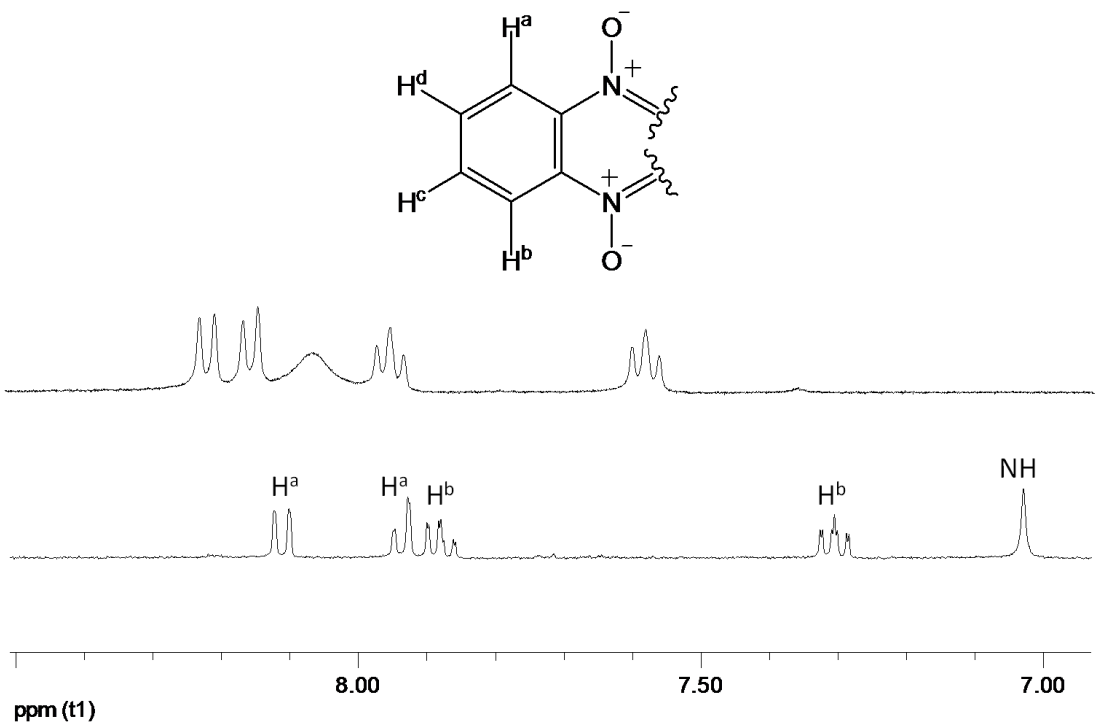

Figure 3.26: ^{1}H NMR (400 MHz, d_6-DMSO) of tpzH (*above*) and [Zn(tpz)$_2$] (*below*). δ8.10 (d, 1H, J = 8.0 Hz, H^{a}), δ7.93 (d, 1H, J = 8.0 Hz, H^{a}), δ7.87 (ap. t, 1H, J = 7.5 Hz, H^{b}), δ7.29 (ap. t, 1H, J = 7.5 Hz, H^{b}), δ7.03 (br. s, 1H, NH)

3.4. Attempts to prepare cobalt(III) complexes

Attempts to prepare cobalt(III) complexes of tpzH and tpzH-CN (**Figure 3.27**) proved unsuccessful. Some of the methods used to try to prepare these complexes are now discussed.

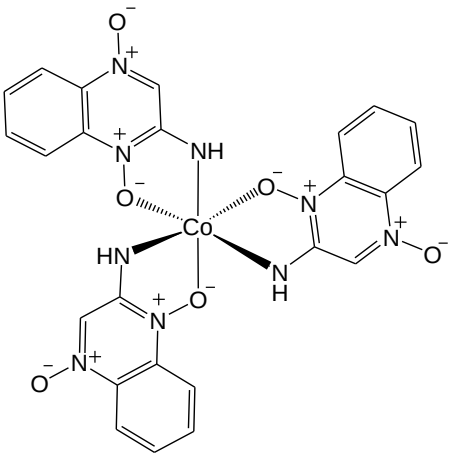

Figure 3.27: The desired form of cobalt(III) *N*1,*N*4-oxide complexes

It was first attempted to prepare a cobalt(III) tpz-R complex by reacting three equivalents of tpzH-R with $Co(OAc)_2.4H_2O$ in MeOH with H_2O_2 (**Scheme 3.8**). Before the addition of the H_2O_2, the formation of a purple suspension indicated that the cobalt(II) *bis*-complex had been made, but upon addition of H_2O_2, the reaction mixture started to turn orange with a purple precipitate. The solid was isolated by filtration, and then shown by ^{1}H NMR spectroscopy to be a paramagnetic species which was probably cobalt(II). This purple solid had the same IR spectrum as the [Co(tpz-R)$_2$]. The solvent was dried off from the filtrate, and this was shown by ^{1}H NMR and MS to contain the free tpzH-R ligand.

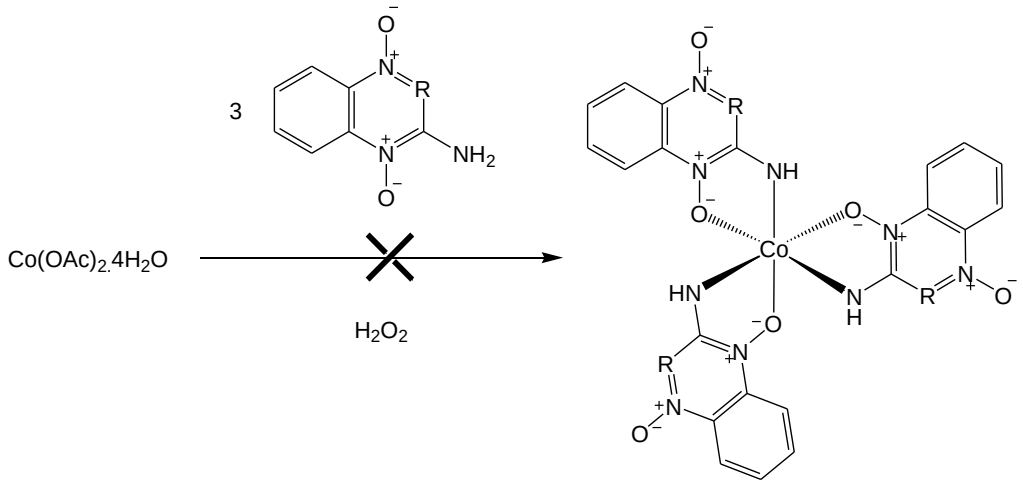

Scheme 3.8: Attempted preparation of a cobalt(III) tpzH-R complex using H_2O_2

As it had previously been observed that the cobalt(II) complex dissociated in aqueous solution (discussed in **Chapter 5**), it was thought that the addition of H_2O_2 was causing the cobalt complex to dissociate and therefore prevent the cobalt(III)

complex forming. It was therefore decided to attempt the same reaction in the presence of an alternative oxidising agent, $K_2S_2O_8$ (**Scheme 3.9**). Attempting this reaction at room temperature gave [Co(tpz-R)$_2$] and free ligand. It seems that the cobalt(II) complex forming then precipitated out of solution, which was hindering the formation of the cobalt(III) complex, so the reaction mixture was heated at reflux for 24 hours in an attempt to keep the cobalt(II) complex in solution so it could be oxidised. It was from the attempts at this reaction which produced that diffraction quality single crystals of tpzH-CONH$_2$ (**Figure 3.9**).

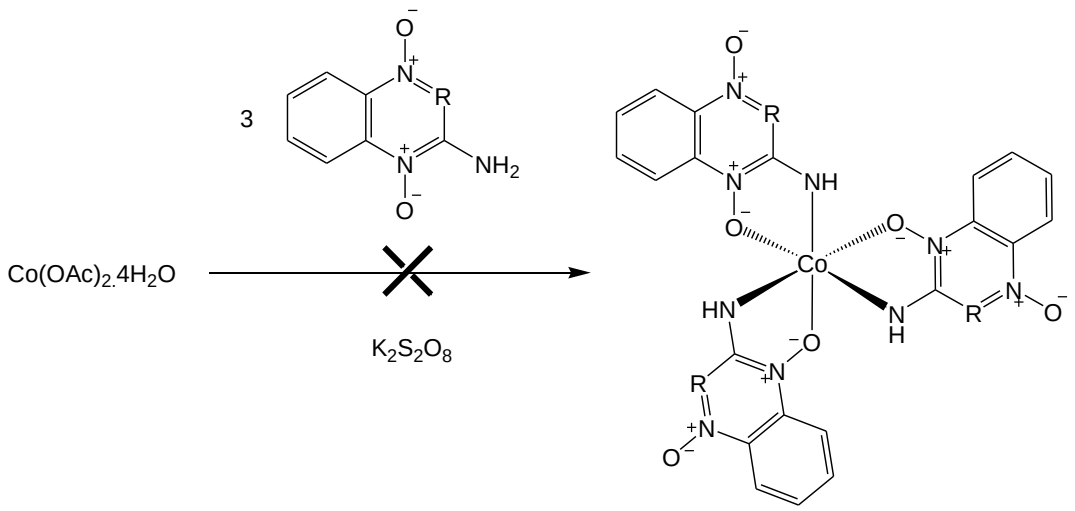

Scheme 3.9: Attempted preparation of a cobalt(III) tpzH-R complex using $K_2S_2O_8$

These reactions were also tried in solvents in which the [Co(tpz-R)$_2$] complexes were more soluble; namely DMSO and DMF. Both of these failed to yield the desired cobalt(III) complex. It is likely that had the desired cobalt(III) complexes been successfully prepared, they would have suffered from the same poor solubility problems that the metal(II) complexes suffered by the metal(II) complexes, as they would also be electronically neutral

3.5. Conclusions

Three medicinally relevant *N*1,*N*4-oxide ligands have been prepared and fully characterised. It was observed that tpzH-CONH$_2$ has an intramolecular bond between its amide NH and *N*-oxide which has been observed by both crystallography and ^{1}H NMR spectroscopy. Metal(II) complexes (cobalt, copper, zinc) of tpzH, tpzH-CN and tpzH-CONH$_2$ have been prepared and studied. Cobalt(II), copper(II)

and zinc(II) complexes of these ligands have been prepared and it was observed, through NMR, that the intramolecular hydrogen-bond of tpzH-$CONH_2$ remains upon coordination. The first crystal structure of a *bis*-quinoxaline-*N*1,*N*4-oxide complex has been successfully obtained, providing valuable information such as the decrease in the *N*-oxide N-O bond lengths upon coordination, indicating that this bond becomes weaker.

Chapter 4: Heteroleptic complexes of *N*1,*N*4-oxide ligands

4.1. Introduction

As described in **Chapter 3**, a significant limitation of the prepared complexes of *N*1,*N*4-oxide ligands tpzH, tpzH-CN and tpzH was their poor solubility. There was also the problem of not being able to prepare the desired cobalt(III) complexes. It was therefore attempted to incorporate the *N*-oxide ligands into metal complexes in a different manner to see if these limitations could be overcome.

A strategy was found which enabled the preparation of a series of heteroleptic complexes containing *N*1,*N*4-oxide ligands. Whilst commonplace amongst 2nd and 3rd row transition metals, heteroleptic complexes do not as regularly occur with 1st row metals. As an example, there is a reported series of heteroleptic complexes designed to act as antimycobacterial agents, featuring substituted tpzH-CN ligands coordinated to a copper(II) centre, also coordinated to an alanine ligand (**Figure 4.1**).[172]

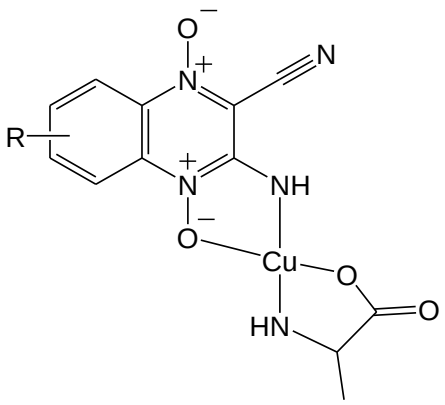

Figure 4.1: Structure of a previously reported heteroleptic copper(II) complex containing a *N*1,*N*4-oxide ligand.[172]

From the work described in **Chapter 2**, it was found that a cobalt(III) complex containing two dpHa ligands could be easily prepared in the presence of carbonate anion, a bidentate ligand with two hard negatively charged oxygen donor atoms (**Figure 4.2**). Comparably, the *N*1,*N*4-oxide ligands also coordinate via two hard donor atoms; a deprotonated amine and the oxygen of an *N*-oxide bond.

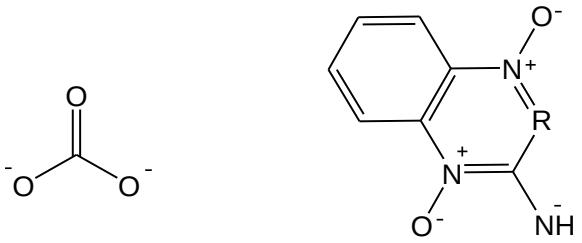

Figure 4.2: The Lewis structures of the coordinating species of CO_3^{2-} and tpz-R

The first reaction was with one equivalent of tpzH-CN added to a stirred methanolic solution of $Co(BF_4)_2.6H_2O$, in the presence of two equivalents of dpHa. This reaction was monitored with UV-vis spectroscopy which showed the λ_{max} peak of the $[Co(dpHa)_2](BF_4)_2$ reaction mixture at 482 nm decreases in intensity upon addition of tpzH-CN, with a new λ_{max} peak emerging at 512 nm (**Figure 4.3**).

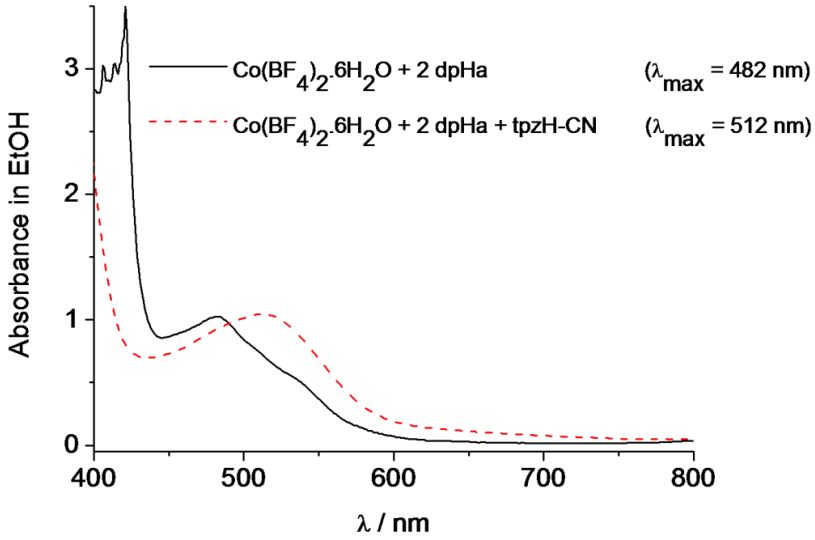

Figure 4.3: UV-vis spectra overlay of the ethanolic reaction mixture of $Co(BF_4)_2.6H_2O$ with two equivalents dpHa before and after addition of one equivalent tpzH-CN

This reaction caused the solution to turn gradually from orange to a dark purple, with the significant observation being that the dark purple product had remained in solution. As this was in stark contrast to the previous complexation reactions involving the 1 *N*1,*N*4-oxide ligands, the oxidising agent was not added in order to identify this cobalt(II) species. After being left to stir overnight, the solvent was dried off from the reaction mixture *in vacuo* and the resulting dark purple solid analysed by MS-ESI. The product produced a peak at *m/z* 601.1 which fitted for a cobalt(II) ion containing one tpzH-CN and two dpHa ligands (**Scheme 4.1**).

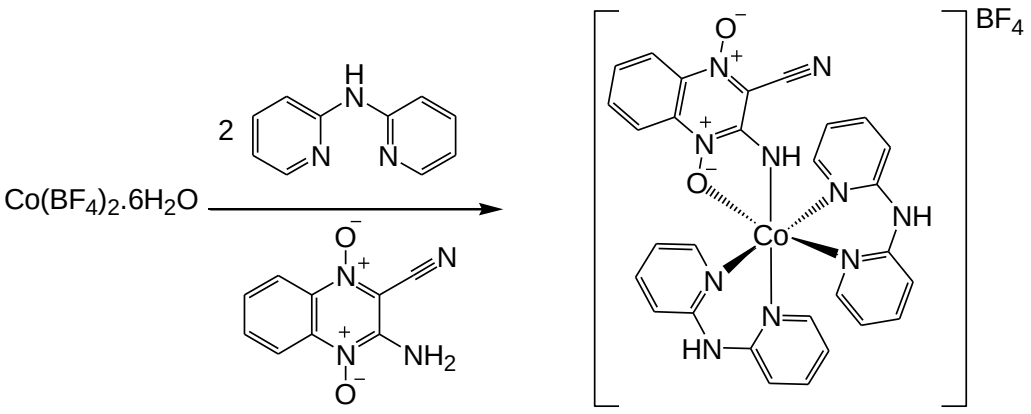

Scheme 4.1: Reaction which provided the first evidence for the formation of a heteroleptic complex containing dpHa and tpzH-CN

This chapter presents the studies which have built upon this initial experimental observation.

4.2. Preparation of heteroleptic metal(II) complexes

4.2.1. Preparation of metal(II) complexes containing 2,2'-dipyridylamine and aminoquinoxaline-2-carbonitrile-*N*1,*N*4-oxide

After it was found that cobalt heteroleptic complexes containing dpHa and tpzH-CN could be prepared, a synthetic strategy was needed that would allow complexes of other metals to be synthesised and isolated. This was first attempted by adding one equivalent of $[Cu(Cl)_2(dpHa)]$ or $[Zn(Cl)_2(dpHa)]$ to a stirred solution of tpzH-CN (**Scheme 4.2**).

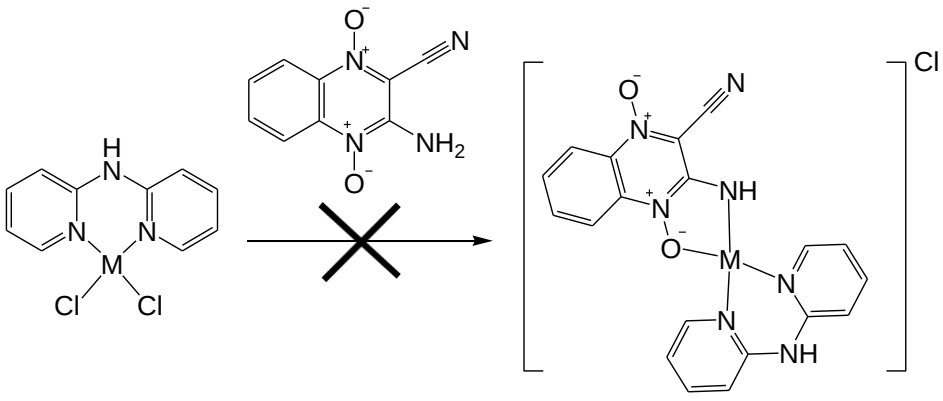

Scheme 4.2: Unsuccessful attempt to prepare [M(tpz-CN)(dpHa)]Cl (where M is copper or zinc) from $[M(Cl)_2(dpHa)]$

It was found that no reaction occurred so Et_3N was added to the reaction mixture, but this resulted in the formation of the *bis*-homoleptic tpzH-CN complex (**Scheme 4.3**).

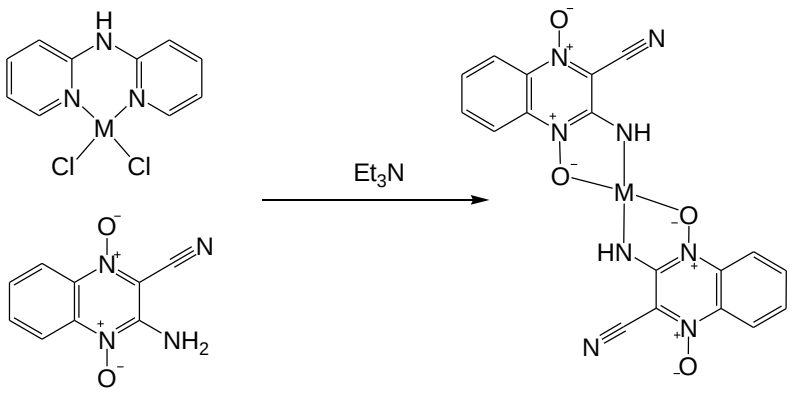

Scheme 4.3: Unsuccessful attempt to prepare [M(tpz-CN)(dpHa)]Cl (where M is copper or zinc) from $[M(Cl)_2(dpHa)]$ using Et_3N

It was then decided to switch to precursor complexes which were more readily soluble in light alcohols so that the reactants could be in solution to help facilitate the reaction. It was also decided to use precursor complexes which had weakly coordinating anions in place of coordinating ones, as the preliminary result of this study used BF_4^- as a counter-ion. There were already reported preparations in the literature for $[Cu(dpHa)_2]Cl_2$ and $[Zn(dpHa)_2](BF_4)_2$ so it was decided to explore if these would be suitable precursor complexes. One equivalent of tpzH-CN was added to a green methanolic solution of $[Cu(dpHa)_2]Cl_2$, causing it to change colour to brown, and then dark red. This reaction was monitored with UV-vis spectroscopy, which indicated a new species had been formed as the absorbance of the mixture changed upon addition of the tpzH-CN (**Figure 4.4**). On comparing the UV-vis spectra it can be seen that the peaks at 433 and 695 nm present in the $[Cu(dpHa)_2]Cl_2$ were replaced with a peak at 490 nm upon reaction with tpzH-CN. The reaction mixture was allowed to stir for an hour before being filtered to isolate the product as a dark red solid which was isolated in 68% yield. This was also confirmed with MS, which showed a peak at *m/z* 435.1 corresponding to a copper cation species coordinated to both dpHa and tpzH-CN moieties. Therefore, a synthetic route for forming [Cu(tpz-CN)(dpHa)]Cl had been established (**Scheme 4.4**).

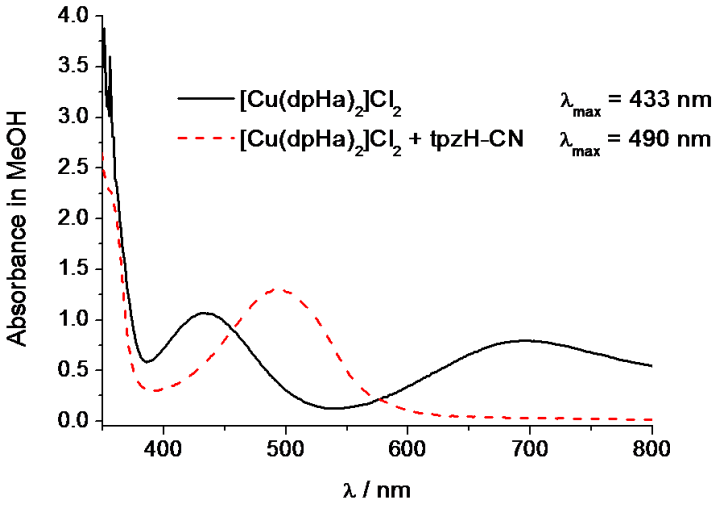

Figure 4.4: UV-vis of $[Cu(dpHa)_2]Cl_2$ in MeOH before and after the addition of one equivalent tpzH-CN

To confirm that $[Cu(dpHa)_2]Cl_2$ and tpzH-CN were reacting in a 1:1 ratio, $[Cu(dpHa)_2]Cl_2$ was titrated into a solution of tpzH-CN (**Figure 4.5**). The reaction was monitored at 478 nm, the λ_{max} of uncoordinated tpzH-CN in methanolic solution. Upon sequential addition of $[Cu(dpHa)_2]Cl_2$, the absorbance of tpzH-CN at 478 nm decreased until approximately one molar equivalent of $[Cu(dpHa)_2]Cl_2$ had been added, supporting a 1:1 reaction ratio.

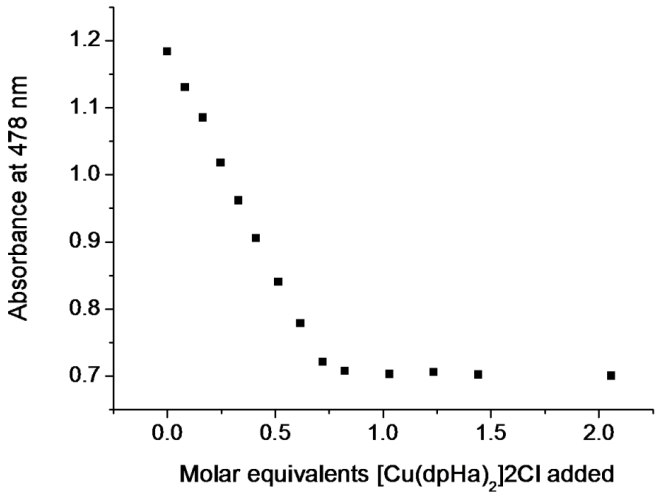

Figure 4.5: Absorbance at 478 nm during the titration of $[Cu(dpHa)_2]Cl_2$ into a methanolic solution of tpzH-CN

Dark red diffraction quality crystals were obtained after several days of slow evaporation of the ethanolic filtrate under ambient conditions, and the resulting structure confirmed the formation of a heteroleptic complex.

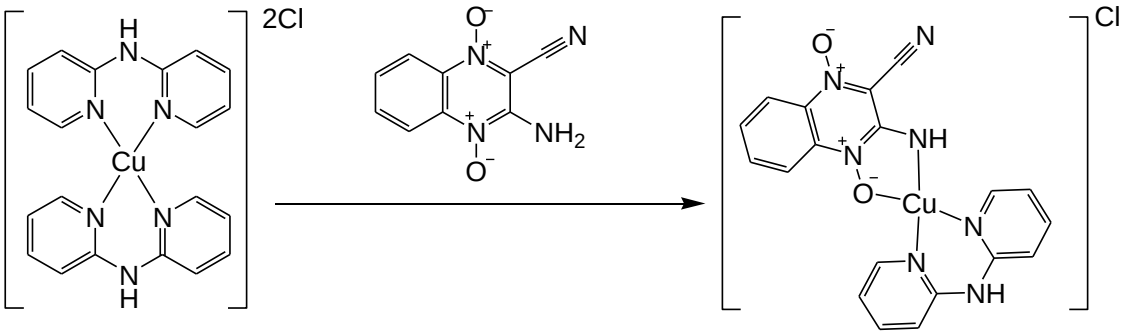

Scheme 4.4: Successful preparation of [Cu(tpz-CN)(dpHa)]Cl from $[Cu(dpHa)_2]Cl_2$

The structure showed a near square-pyramidal copper(II) centre (τ = 0.19) coordinated to one of each ligand, and an aqua ligand coordinated in the axial position (**Figure 4.6**).[132]

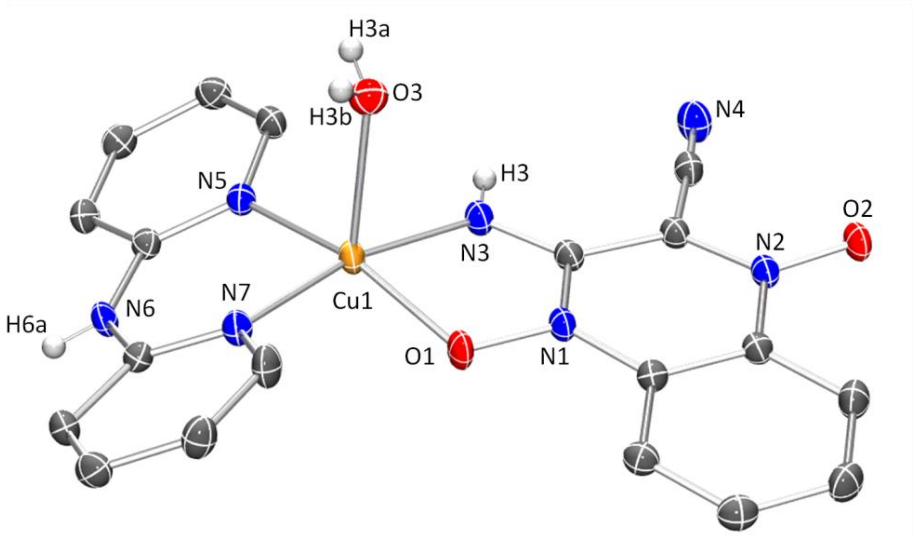

Figure 4.6: ORTEP diagram (50% probability) of $[Cu(tpz\text{-}CN)(dpHa)(H_2O)]Cl$.[131] Hydrogen atoms (except H(3), H(3a), H(3b) and H(6a)) and chloride counter-ion removed for clarity. Selected bond lengths / Å and angles /º: Cu(1)-O(1) 1.9614(13), Cu(1)-N(3) 1.9764(16), Cu(1)-N(7) 1.9828(15), Cu(1)-N(5) 1.9928(15), Cu(1)-O(3) 2.3772(15), N(1)-O(1) 1.3508(18), N(2)-O(2) 1.2814(18), O(1)-Cu(1)-N(3) 81.21(6), N(7)-Cu(1)-N(5) 90.99(6)

The N-O bond length of the *N*-oxide coordinated to the metal centre is 1.3508(18) Å and is therefore longer than the uncoordinated *N*-oxide bond which is 1.2814(18) Å. This agrees with the loss of π-character in the N-O bond that was said to occur upon coordination to a metal centre, with a greater loss of π-character correlating with a

stronger metal-oxygen bond. The lengthening of the uncoordinated *N*-oxide bond implies that the whole tpzH-CN ligand has decreased in π-character.

Both hydrogen atoms of the aqua ligand were found using the electron difference map. The aqua ligand forms a hydrogen-bond from one of its protons, H(3a) to an uncoordinated chloride, which forms a hydrogen-bond with the H(6a) proton of the dpHa amine of an adjacent complex. The overall effect of this is the formation of linear chains throughout the crystal lattice (**Figure 4.7**).

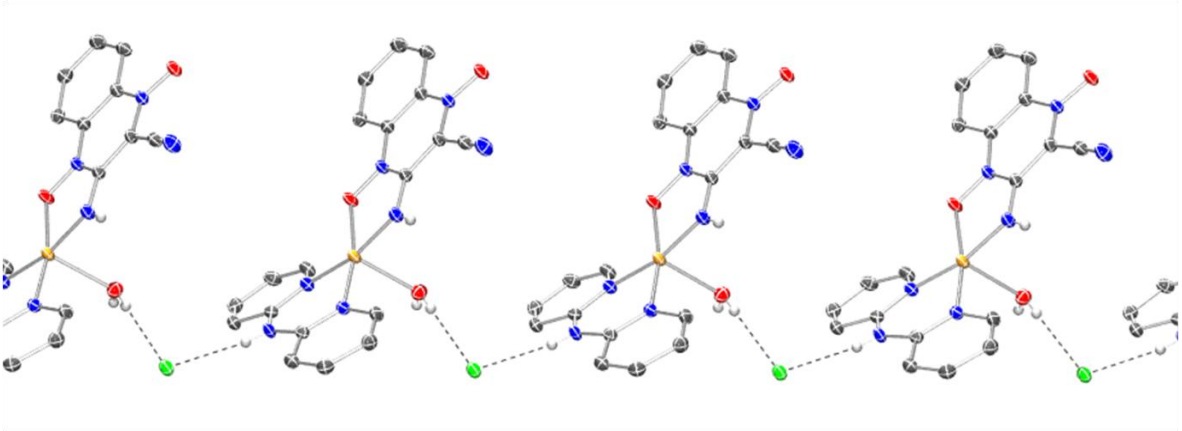

Figure 4.7: ORTEP diagram showing the intermolecular hydrogen-bonds present within the crystal structure of [Cu(tpz-CN)(dpHa)(H_2O)]Cl.[131] Hydrogen-bond distances / Å and angles /º: H(3a)···Cl(1) 2.59(3), O(3) ··Cl(1) 3.3250(17), H(6a)···Cl(1) 2.39(3), N(6)···Cl(1) 3.1487(16)O(3)-H(3a)···Cl(1) 166(3), N(6)-H(6a)···Cl(1) 172(2)

The preparation of the analogous *bis*-dpHa zinc(II) chloride precursor complex, [Zn(dpHa)$_2$]Cl_2, was not available in the literature. Therefore the previously reported [Zn(dpHa)$_2$](BF_4)$_2$ complex was used instead, as it seemed that any anions present needed to be weakly coordinating to allow the formation of these complexes. This complex was reacted with one equivalent of tpzH-CN in ethonolic solution to afford [Zn(tpz-CN)(dpHa)]BF_4 as a crimson solid in 50% yield. The formation of this compound was first confirmed by MS which showed a peak at *m/z* 436.05, and then by NMR spectroscopy. Comparing the ^{1}H NMR spectra of the crimson solid with that of tpzH-CN, dpHa, [Zn(dpHa)$_2$](BF_4)$_2$ and [Zn(tpz-CN)$_2$], which highlighted the formation of a new species which was soluble in methanol (**Figure 4.8**).

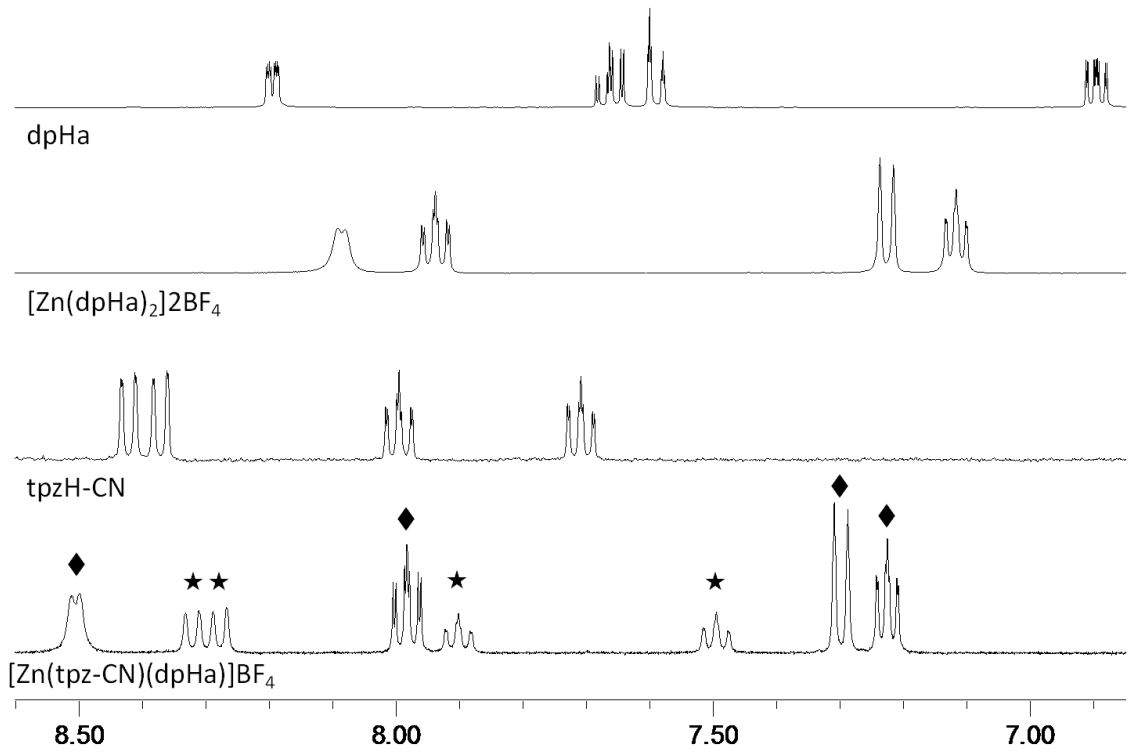

Figure 4.8: Overlay of ^{1}H NMR spectra (MeOD, 400 MHz) of dpHa, $[Zn(dpHa)_2](BF_4)_2$, tpzH-CN and $[Zn(tpz\text{-}CN)(dpHa)]BF_4$. Peaks of $[Zn(tpz\text{-}CN)(dpHa)]BF_4$ corresponding to tpzH-CN indicated by ★ and dpHa indicated by ♦

The comparison of the ^{1}H NMR spectra shows that the resonances corresponding to tpzH-CN ligand have experienced an upfield shift upon incorporation into this heteroleptic complex, whilst the resonances corresponding to the dpHa ligand have experienced a general downfield shift. This indicates that effect of incorporating dpHa into this complex has caused its protons to become more deshielded with respect to the chemical shifts observed in the free ligand and other zinc(II) dpHa complexes, whilst the protons of tpzH-CN have become more shielded.

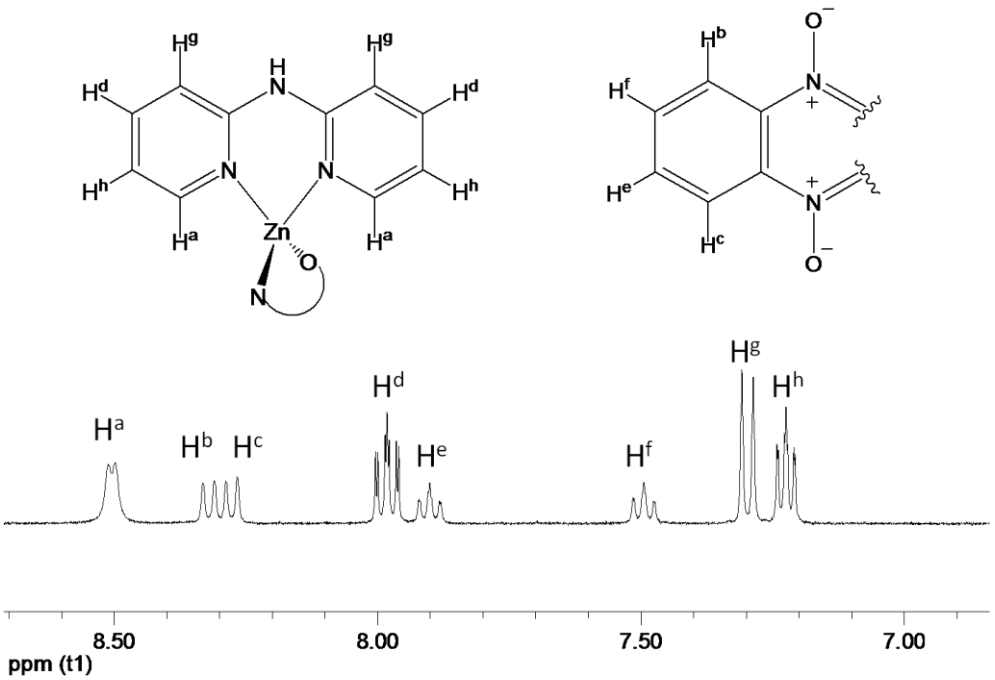

Figure 4.9: ^{1}H NMR (MeOD, 400 MHz) of [Zn(tpz-CN)(dpHa)]BF_4: δ8.50 (d, 2H, J = 5.0 Hz, H^a), δ8.32 (d, 1H, J = 8.5 Hz, H^b), δ8.27 (d, 1H, J = 8.5 Hz, H^c), δ7.99 (ddd, 2H, J = 8.5, 7.0, 2.0 Hz, H^d), δ7.90 (ddd, 1H, J = 8.5, 7.5, 1.0 Hz, H^e), δ7.49 (ddd, 1H, J = 8.5, 7.5, 1.0 Hz, H^f), δ7.30 (d, 2H, J = 8.4 Hz, H^g), δ7.22 (ddd, 2H, J = 7.0, 5.5 , 1.0 Hz, H^h)

The dpHa protons becoming more deshielded within the heteroleptic complex concurs with the donation of electron density from this ligand to the metal centre upon coordination. This is supported by the increase in shielding of the tpzH-CN ligand's protons experience upon inclusion in the heteroleptic complex with respect to the free ligand, suggesting it has become more electron-rich upon coordination.

Dark red diffraction-quality crystals of [Zn(tpz-CN)(dpHa)]BF_4 were obtained by layering a methanolic solution over ^{n}BuOH then allowing this to slowly evaporate over the course of a several days at room temperature. The structure shows the zinc(II) centre coordinated to one tpzH-CN and one dpHa ligand with one coordinated molecule of methanol (**Figure 4.10**). The metal centre has a near square pyramidal geometry (τ = 0.20).[132]

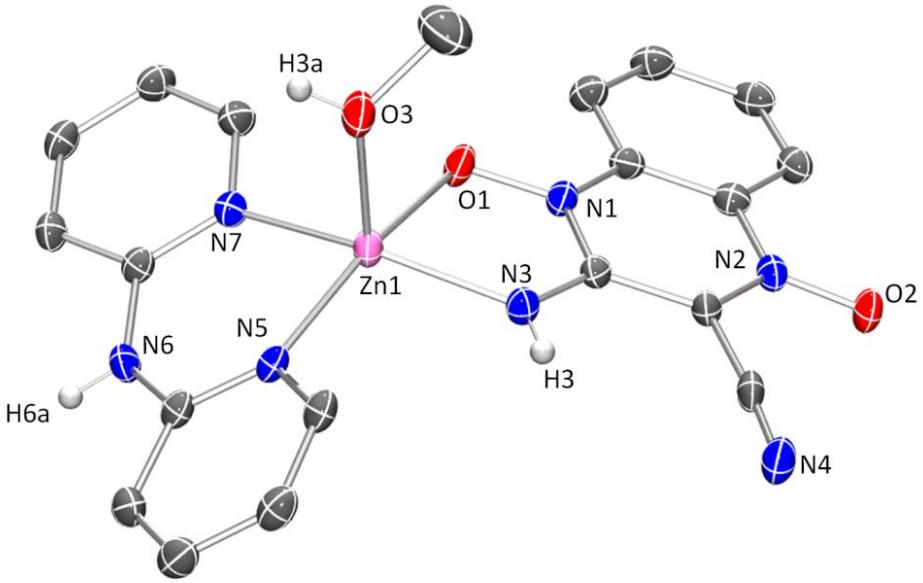

Figure 4.10: ORTEP diagram (50% probability) of [Zn(tpzH-CN)(dpHa)(MeOH)]BF_4.[131] Hydrogen atoms except H(3), H(3a) and H(6a) and BF_4^- counter-ion removed for clarity. Selected bond lengths / Å and angles /º: N(1)-O(1) 1.339(3), N(2)-O(2) 1.288(3), N(3)-Zn(1) 2.024(2), N(5)-Zn(1), 2.088(2), N(7)-Zn(1) 2.080(2), O(1)-Zn(1) 2.0891(19), O(3)-Zn(1) 2.097(2), N(7)-Zn(1)-N(5) 89.01(8), N(3)-Zn(1)-O(1) 78.32(8)

The *N*-oxide bond coordinated to the metal centre has a N(1)-O(1) bond length of 1.339(3), which is longer than that of the uncoordinated *N*-oxide which is 1.288(3). **Table 4.1** compares some of the bond lengths found in [Zn(tpz-CN)(dpHa)]BF_4 with those found for [Zn(tpz-$CN)_2$(DMF)]. It can be seen the homoleptic complex has shorter bond lengths between the *N*-oxide amine and metal centre (1.990(2) and 1.989(2) Å) as opposed to the heteroleptic complex where the equivalent bond length is 2.024(2) Å.

Table 4.1: Comparison of selected bond lengths of $[Zn(tpz\text{-}CN)_2(DMF)]$ and $[Zn(tpz\text{-}CN)(dpHa)(MeOH)]BF_4$ / Å

	$[Zn(tpz\text{-}CN)_2(DMF)]$	**$[Zn(tpz\text{-}CN)(dpHa)(MeOH)]BF_4$**
O(1)-Zn(1)	2.082(2)	2.089 (192)
	2.112(2)	
N(3)-Zn(1)	1.990(2)	2.024(2)
	1.989(2)	
N(1)-O(1)	1.340(3)	1.339(3)
	1.348(3),	
N(2)-O(2)	1.282(3)	1.288(3)
	1.280(3),	

Table 4.2 lists the zinc(II)-pyridyl bond lengths of $[Zn(tpz\text{-}CN)(dpHa)(MeOH)]BF_4$, $[Zn(dpHa)_2](BF_4)_2$ and $[Zn(Cl)_2(dpHa)]$. The data shows that the metal-pyridyl bond lengths are also longest in the heteroleptic complex. This, combined with the NMR data, implies that there may be exchange of electron density between the two ligands through the metal centre.

Table 4.2: Comparison of zinc(II)-pyridyl bond lengths of $[Zn(tpz\text{-}CN)(dpHa)(MeOH)]BF_4$, $[Zn(dpHa)_2]2BF_4$ and $[Zn(Cl)_2(dpHa)]$ / Å.[128, 129]

$[Zn(tpz\text{-}CN)(dpHa)(MeOH)]BF_4$	**$[Zn(dpHa)_2]2BF_4$**	**$[Zn(Cl)_2(dpHa)]$**
2.088(2)	2.024	1.989(3)
2.080(2)	2.023	1.990(2)

The $[Zn(tpz\text{-}CN)(dpHa)(MeOH)]BF_4$ complex forms two intermolecular hydrogen-bonds using its tpzH-CN ligand; one from the amine proton H(3) to the nitrile N(4) of the adjacent complex, and the same interaction repeated *vice versa* (**Figure 4.11**). These two interactions lead to the formation of hydrogen-bonded dimers within the crystal.

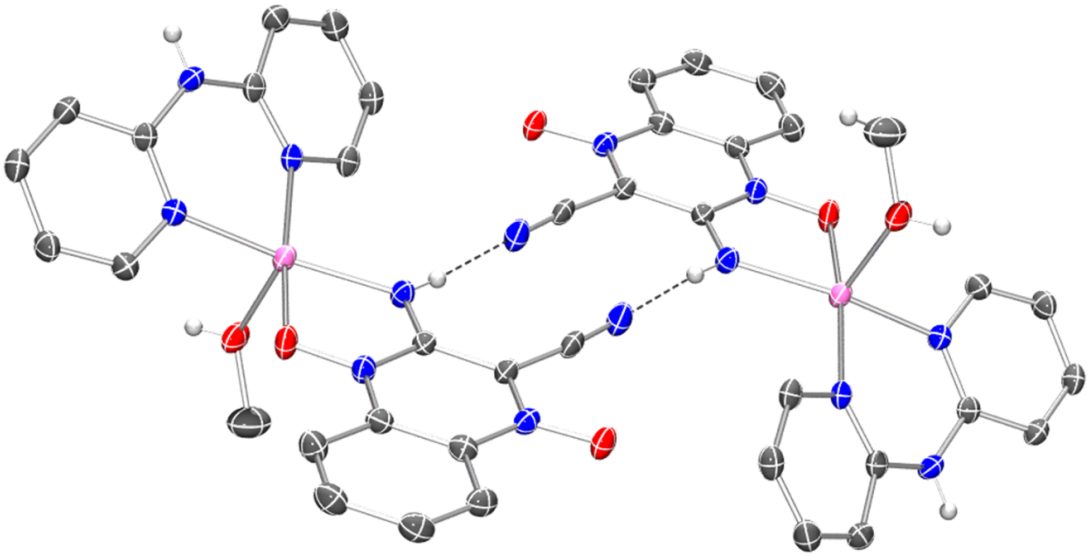

Figure 4.11: ORTEP diagram showing the hydrogen-bonds formed within the crystal of [Zn(tpz-CN)(dpHa)(MeOH)]BF_4.[131] Hydrogen-bond distances / Å and angles /°: H(3)···N(4) ··2.39(3), N(3) ··N(4) 3.182(3), N(3) H(3)···N(4) 169(3)]

4.2.2. Preparation of metal(II) complexes containing 2,2'-dipyridylamine and aminoquinoxaline-2-amido-*N*1,*N*4-oxide

[Cu(tpz-$CONH_2$)(dpHa)]Cl was prepared by adding a methanolic solution of [Cu(dpHa)$_2$](Cl)$_2$ to an ethanolic solution of tpzH-$CONH_2$. The dark red product was isolated as a dark red powder in 48% yield and was found to give a M^+ peak at *m/z* 453.1, corresponding to a copper species bound to one dpHa and one tpzH-$CONH_2$ ligand ([Cu(tpz-$CONH_2$)(dpHa)]$^+$). Diffraction-quality dark red crystals were obtained by allowing a methanolic solution layered over ^{n}BuOH to slowly evaporate over the course of a few days at room temperature.

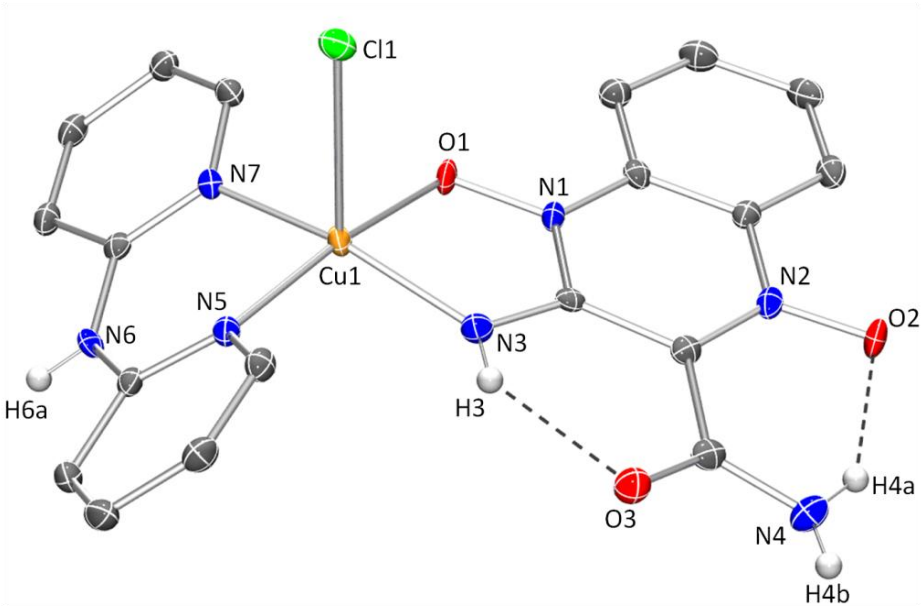

Figure 4.12: ORTEP diagram (50% probability) of [Cu(Cl)(tpz-$CONH_2$)(dpHa)].[131] Hydrogen atoms (except H3, H4a, H4b and H6a) and solvent molecules removed for clarity. Selected bond lengths / Å and angles / º: Cl(1)-Cu(1) 2.7263(6), Cu(1)-N(3) 1.9334(19), Cu(1)-N(5) 1.9804(17), Cu(1)-N(7) 1.9839(18), Cu(1)-O(1) 1.9495(14), N(1)-O(1) 1.357(2), N(2)-O(2) 1.294(2), N(3)-Cu(1)-(O1) 81.88(7), N(5)-Cu(1)-N(7) 89.75(7). Hydrogen-bond distances / Å and angles /º: H(3)···O(3) 2.06(3), N(3) ··O(3) 2.709(2), N(3)-H(3) ··O(3) 140(2), H(4a)···O(2) 1.85(3), N(4) ··O(2) 2.580(3), N(4)-H(2) ··O(3) 140(3)

The near square pyramidal copper(II) centre (τ = 0.08) is coordinated to one dpHa and one tpz-$CONH_2$ ligand, with one axially coordinated chloride (**Figure 4.12**).[132] The intramolecular hydrogen-bonds within the tpz-$CONH_2$ ligand which occur between the amide NH and *N*-oxide oxygen, and amine NH with the carbonyl oxygen are still present upon coordination. Upon comparing the hydrogen-bond lengths of the free and coordinated ligand (**Table 4.3**), it can be seen that both of these intramolecular hydrogen-bonds have become longer upon coordination. It can also be seen that both of the *N*-oxide bonds become longer upon coordination, where as the carbon amine C(1)-N(3) bond decreases in length.

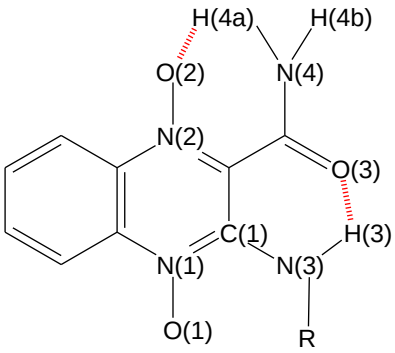

Figure 4.13: Atom numbering used in **Table 4.2**

Table 4.3: Comparison of selected bond lengths / Å and angles / º of uncoordinated tpzH-$CONH_2$ and [Cu(Cl)(tpz-$CONH_2$)(dpHa)]

Bond	**tpzH-$CONH_2$**	**[Cu(Cl)(tpz-$CONH_2$)(dpHa)]**
N(1)-O(1)	1.327(2)	1.357(2)
N(2)-O(2)	1.274(2)	1.294(2)
C(1)-N(3)	1.326(2)	1.308(3)
H(3)···O(3)	1.98(3)	2.06(3)
N(3) ··O(3)	2.622(2)	2.709(2)
N(3)-H(3) ··O(3)	136(2)	140(2)
H(4a) ··O(2)	1.90(3)	1.85(3)
N(4) ··O(2)	2.557(2)	2.580(3)
N(4)-H(2) ··O(2)	126(3)	140(3)

In addition to the two intramolecular hydrogen-bonds, there is also an intermolecular hydrogen-bond network present within the crystal structure. A molecule of water present within the crystal structure forms two hydrogen-bonds with H(4c) and H(4d) to the axially coordinated chloride Cl(1) from two separate complexes. The O(3) oxygen of the water forms a hydrogen-bond to the N(6)-H(6a) amine of a third complex. The overall effect is the formation of 'ladder' type structures within the crystal (**Figure 4.14**) with the tpz-$CONH_2$ moieties on the exterior.

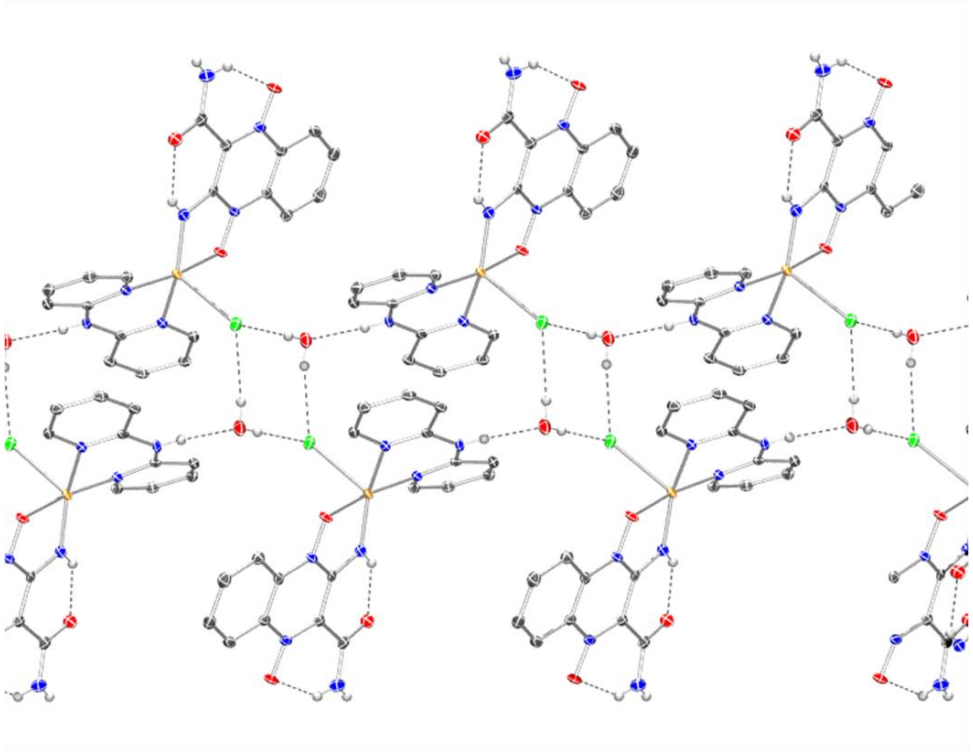

Figure 4.14: ORTEP diagram showing the hydrogen-bonds present in the structure of [Cu(Cl)(tpz-$CONH_2$)(dpHa)].[131] Hydrogen-bond distances / Å and angles /°: H(3)···O(3) 2.06(3), N(3) ··O(3) 2.709(2), N(3)-H(3) ··O(3) 140(2), N(4)-H(4a) ··O(2) 140(3), N(6)-H(6a) ··O(4) 173(3), H(4c)···Cl(1) 2.42(3), O(4) ··Cl(1) 3.154 (2), H(4d)-Cl(1) 2.41 (3),O(4) ··Cl(1) 3.215 (2), O(4)-H(4c) ··Cl(1) 174 (3), O(4)-H(4d) ··Cl(1) 172 (3)

The [Zn(tpz-$CONH_2$)(dpHa)]BF_4 complex was prepared by adding a methanolic solution of [Zn(dpHa)$_2$](BF_4)$_2$ to a stirred ethanolic orange suspension of tpzH-$CONH_2$, causing it to turn from orange to red. A reddish-pink precipitate was isolated by filtration which was found by ^{1}H NMR spectroscopic analysis to contain the product in a 1:12 ratio with another species (**Figure 4.15**). This second compound does not have the same proton signals as any of the starting materials or free dpHa and is as yet unidentified but is most likely to be a zinc dpHa species.

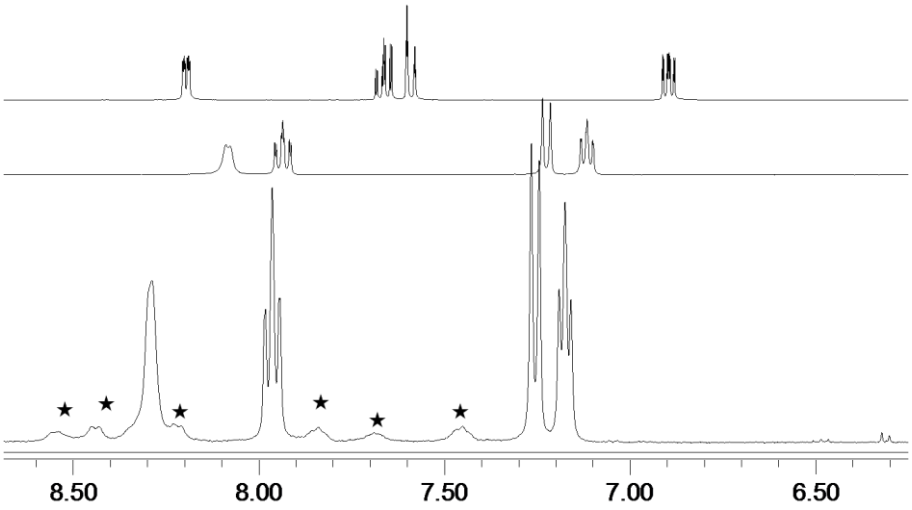

Figure 4.15: Overlay of the ^{1}H NMR spectra (MeOD, 400 MHz) of dpHa, $[Zn(dpHa)_2](BF_4)_2$ and $[Zn(tpz\text{-}CONH_2)(dpHa)]BF_4$ (peaks of product denoted by ★). δ8.53 (m, 1H), δ8.44 (d, 2H, J = 8.5 Hz), δ8.32 (m, 1H), δ8.21 (m, 2H), δ8.16 (ap. br. s, 20H), δ 7.95 (t, 20H, J = 7.5 Hz), δ7.83 (ap. t, 1H, J = 6.5 Hz), δ7.68 (m, 1H), δ7.44 (t, 2H, J = 7.5 Hz), δ7.23 (d, 20H, J = 8.5 Hz), δ7.14 (t, 20H, J = 6.5 Hz)

4.2.3. Preparation of metal(II) complexes containing 3-amino-1,2,4-benzotriazine- *N*1,*N*4-oxide

$[Cu(tpz)(dpHa)]Cl$ was prepared by reacting one equivalent of $[Cu(dpHa)_2]Cl_2$ with an equimolar amount of tpzH in ethanolic solution and was isolated in 45% yield. The product has a MS peak at *m/z* 411.1, corresponding to a copper cation species containing one dpHa and one tpz ligand i.e. $[Cu(tpz)(dpHa)]^+$. Diffraction-quality dark red crystals of the complex were obtained by allowing a concentrated methanolic solution to slowly evaporate over a few days at room temperature. The structure shows two independent complexes within the unit cell (**Figure 4.16**), each of which show a five-coordinate copper(II) centre bound to one tpzH and one dpHa ligand with one coordinated MeOH molecule and one non-coordinating chloride.

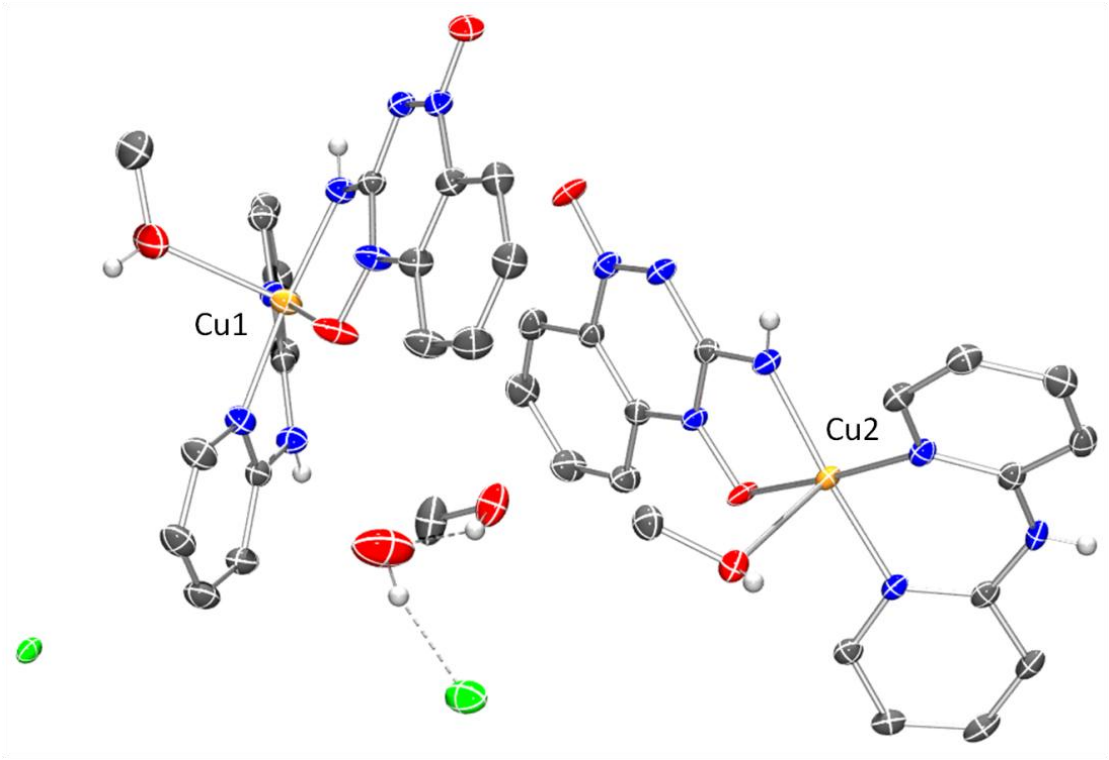

Figure 4.16: ORTEP diagram showing the two [Cu(tpz)(dpHa)(MeOH)]Cl complexes present in the unit cell.[131]

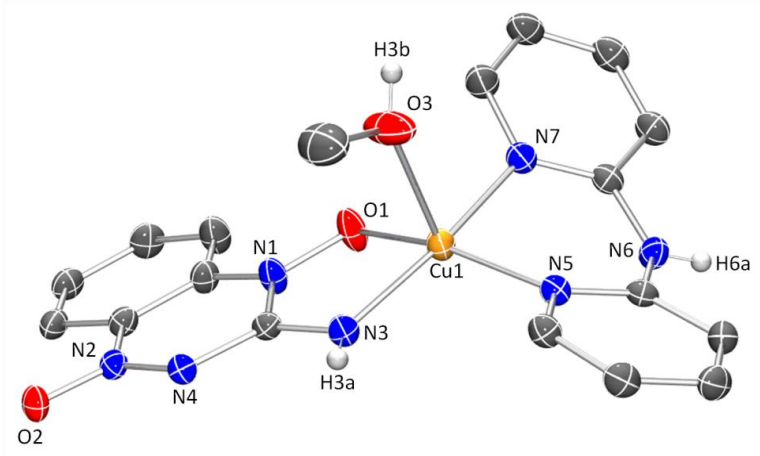

Figure 4.17: ORTEP diagram (50% probability) of (the Cu(1) complex) [Cu(tpz)(dpHa)(MeOH)]Cl.[131] Hydrogen atoms (except H3, H3a and H6a) and BF_4^- counter-ion removed for clarity. Selected bond lengths / Å and angles /º: Cu(1)-N(3) 1.9429(18), Cu(1)-O(1) 1.9509(15), Cu(1)-N(7) 1.9714(18), Cu(1)-N(5) 1.9881(17), Cu(1)-O(3) 2.3323(19), N(1)-O(1) 1.355(2), N(2)-O(2) 1.261(2), N(3)-Cu(1)-O(1) 83.02(7), N(7)-Cu(1)-N(5) 89.48(7)

The complex containing the Cu(1) centre has near-square pyramidal geometry (τ = 0.21) (**Figure 4.17**) and is the most distorted out of the two complexes with the tpz

ligand forced to twist out of its non-planar conformation.[132] The plane of the C(1), N(1), N(3) and N(4) atoms is twisted by 7.8° away from the plane of the rest of the aromatic molecule (**Figure 4.18**).

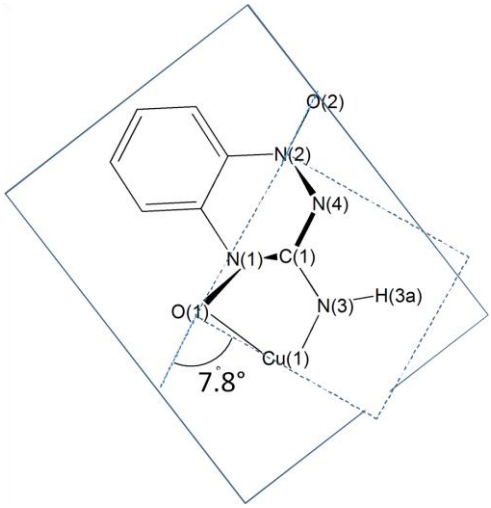

Figure 4.18: Diagram to illustrate the distortion within the tpzH ligand of the Cu(1) complex found in the crystal structure of [Cu(tpz)(dpHa)(MeOH)]Cl

The second complex which contains the Cu(2) centre has a less distorted square pyramidal geometry ($\tau = 0.09$), coordinated to one tpzH, one dpHa and one MeOH ligand (**Figure 4.19**).[132]

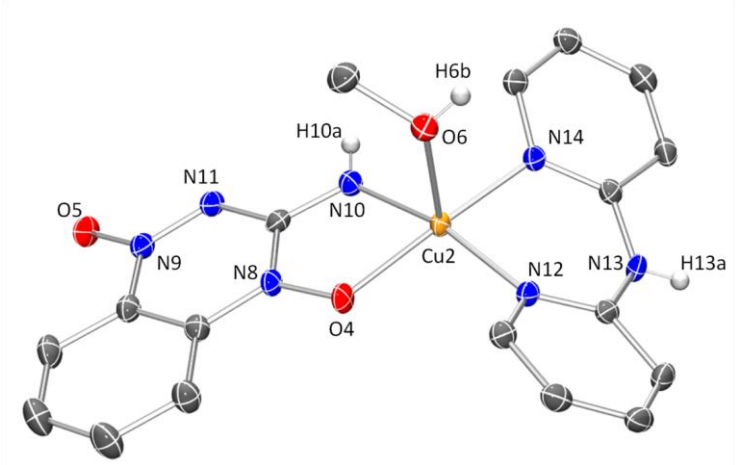

Figure 4.19: ORTEP diagram (50% probability) of (the Cu(2) complex) [Cu(tpz)(dpHa)(MeOH)]Cl.[131] Hydrogen atoms (except H(3), H(3a) and H(6a)) and BF_4^- counter-ion removed for clarity. Selected bond lengths / Å and angles /º: Cu(2)-N(10) 1.9437(16), Cu(2)-N(12) 1.9736(16), Cu(2)-N(14) 1.9981(17), Cu(2)-O(4) 2.0005(14), Cu(2)-O(6) 2.3215(15), N(8)-O(4) 1.3548(19), N(9)-O(5) 1.259(2), N(12)-Cu(2)-N(14) 90.20(7), N(10)-Cu(2)-O(4) 81.50(6)

Table 4.4 shows that upon coordination the N(1)-O(1) bond lengthens, an effect which has been previously attributed to the loss of π-character in the N-O bond.[170] The data shows that the uncoordinated N(2)-O(2) bond lengthens, whereas the C(1)-N(3) bond shortens upon incorporation into this complex.

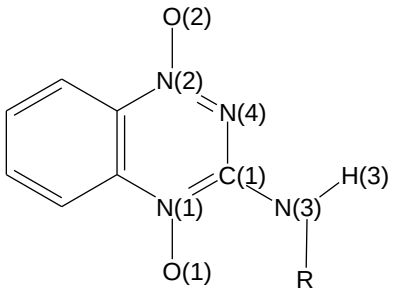

Figure 4.20: Atom assignments for used in **Table 4.2**

Table 4.4: Comparison of selected bond lengths of uncoordinated and coordinated tpzH

	tpzH	**[Cu(tpz)(dpHa)(MeOH)]Cl**	
		Cu(1) centre	**Cu(2) centre**
N(1)-O(1)	1.3330(15)	1.355(2)	1.3548(19)
N(2)-O(2)	1.2574(15)	1.261(2)	1.259(2)
C(1)-N(3)	1.3241(19)	1.301(3)	1.305(2)

The analogous zinc(II) complex was prepared by reacting equimolar amounts of $[Zn(dpHa)_2](BF_4)_2$ and tpzH in methanol, and subsequently observed with MS (*m/z* 412.2) and ^{1}H NMR spectroscopy (**Figure 4.21**).

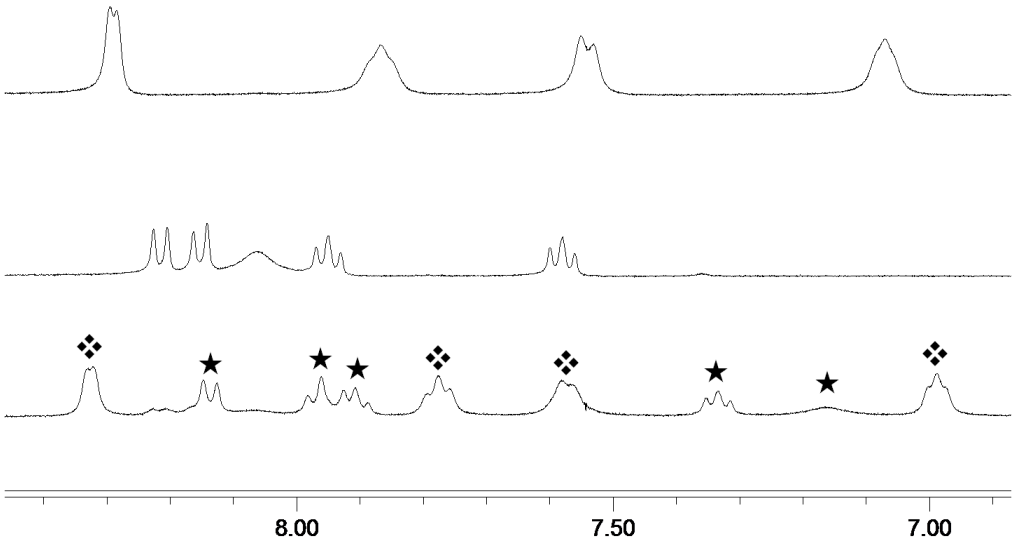

Figure 4.21: Overlay of the ^{1}H NMR spectra (400 MHz, d_6-DMSO) of $[Zn(dpHa)_2](BF_4)_2$ (*above*), tpzH (*middle*) and $[Zn(tpz)(dpHa)]BF_4$ (*bottom*). Data for $[Zn(tpz)(dpHa)]BF_4$: δ8.32 (br. d, 2H, J = 3.0 Hz), δ8.14 (d, 1H, J = 8.5 Hz), δ7.97 (ap. d, 1H, J = 8.5 Hz), δ7.91 (t, 1H, 7.5 Hz), δ7.77 (t, 2H, J = 6.0 Hz), δ7.57 (d, 2H, J = 6.0 Hz), δ7.33 (t, 1H, J = 7.5 Hz), δ7.16 (br. s, 1H), δ6.99 (t, 2H, J = 6.0 Hz). In the spectrum of $[Zn(tpz)(dpHa)]BF_4$, the coordinated tpz ligand is denoted by ★ and dpHa denoted by ❖

4.3. Preparation of heteroleptic cobalt(III) complexes

$[Co(tpz\text{-}CN)(dpHa)_2](BF_4)_2$ was prepared in 19% yield by adding one equivalent tpzH-CN to a stirred mixture of $Co(BF_4)_2.6H_2O$ and two equivalents dpHa. Upon addition of the tpzH-CN, the reaction mixture turned a dark red-purple colour, and after stirring, $K_2S_2O_8$ was added to act as an oxidising agent (**Scheme 4.5**).

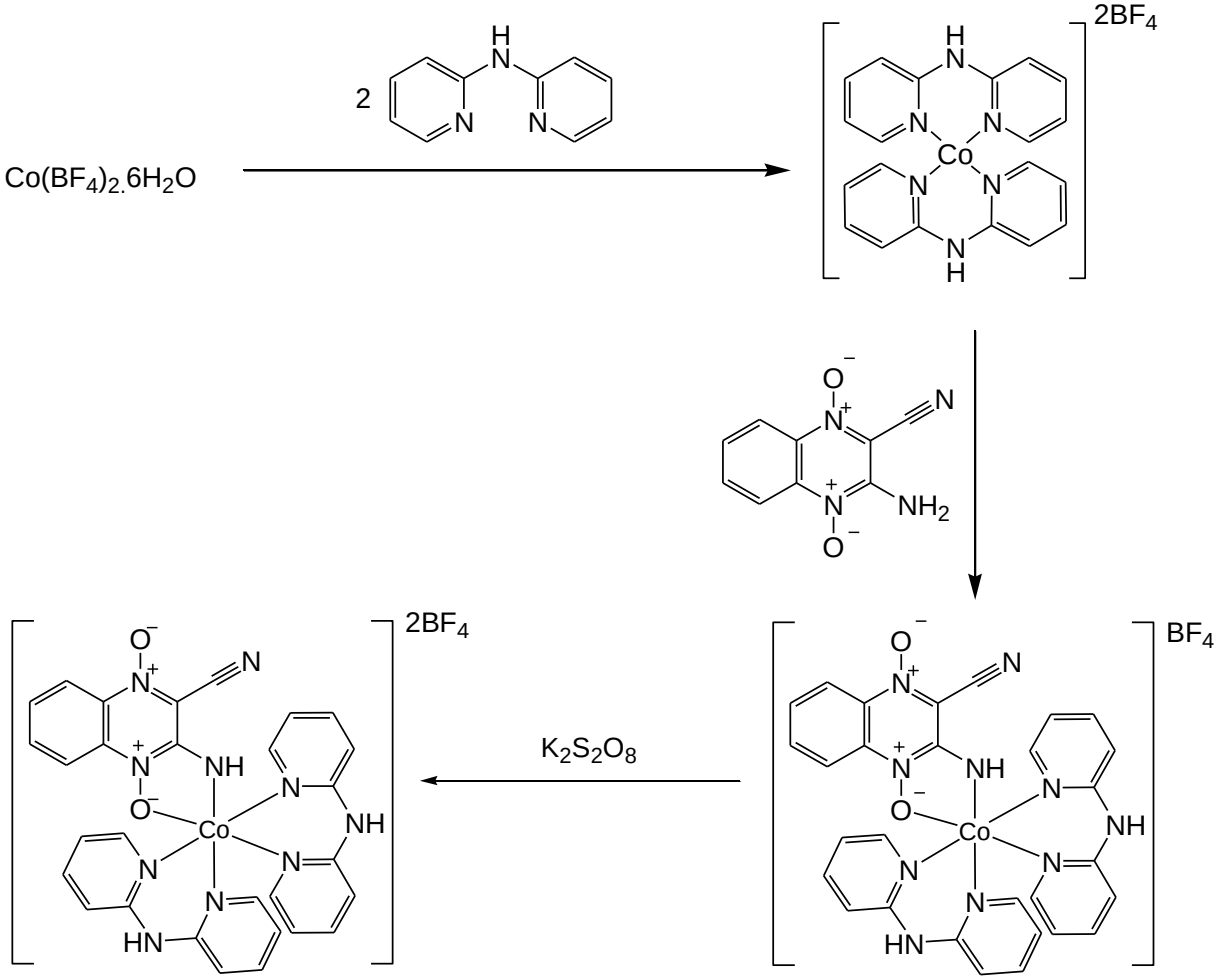

Scheme 4.5: Preparation of $[Co(tpz\text{-}CN)(dpHa)_2](BF_4)_2$

Formation of $[Co(tpz\text{-}CN)(dpHa)_2]$ was confirmed through MS where a peak at *m/z* 601.13 and a +2 peak at *m/z* 301.07 corresponding to $[Co(tpz\text{-}CN)(dpa)(dpHa)]^+$ and $[Co(tpz\text{-}CN)(dpHa)_2]$, respectively, were observed. ^1H NMR spectroscopic analysis confirmed the formation of a new species containing several different aromatic rings. However, it was not possible to fully assign the NMR spectra owing to the similarity in chemical environment be of the different aromatic rings. From the combined results of 700 MHz COSY, HSCQ and HMBC NMR experiments, it was possible to assign the proton signals to one of five different ring environments, and to assign one as belonging to the tpzH-CN ligand (**Figure 4.22**). Even though four separate pyridyl rings had been identified, the lack of coupling through the central amine of dpHa and lack of any correlation between the different rings prevented the full assignment of these signals.

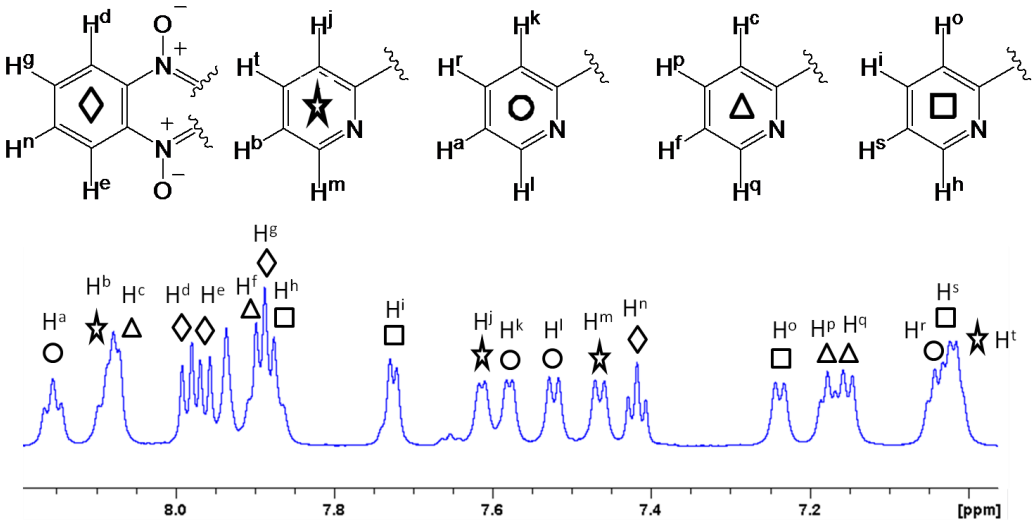

Figure 4.22: ^{1}H NMR (d_6-DMSO, 700 MHz) of $[Co(tpz\text{-}CN)(dpHa)_2](BF_4)_2$. δ8.16 (t, 1H, J = 7.3 Hz, H^b), δ8.10 (m, 1H, H^c), δ8.07 (d, 1H, J = 4.8 Hz, H^d), δ7.99 (d, 1H, J = 8.5, H^e), δ9.96 (d, 1H, J = 8.6 Hz, H^f), δ7.94 (s, 1H, H^g), δ7.90 (t, 1H, H^h), δ7.89 (t, 1H, H^i), δ 7.88 (t, 1H, H^j), δ7.73 (d, 1H, J = 5.7 Hz, H^k), δ7.61 (d, 1H, J = 5.0 Hz, H^l), δ 7.58 (d, 1H, J = 5.0 Hz, H^m), δ 7.52 (d, 1H, J = 8.3 Hz, H^n), δ7.46 (d, 1H, J = 8.0, H^m), δ7.42 (t, 1H, J = 7.7 Hz, H^n), δ7.24 (d, 1H, J = 7.8, H^o), δ7.18 (t, 1H, J = 6.1, H^p), δ7.15 (d, 1H, J = 8.4 Hz, H^q), δ7.04 (t, 1H, H^r), δ7.03 (t, 1H. H^s), δ7.02 (t, 1H, H^t)

Dark red diffraction-quality crystals were obtained through allowing an ethanolic solution to slowly evaporate at room temperature over the course of several days. The structure shows one tpzH-CN ligand and two dpHa ligands coordinated to an octahedral cobalt(III) centre (**Figure 4.23**) with two non-coordinating BF_4^- counter-ions.

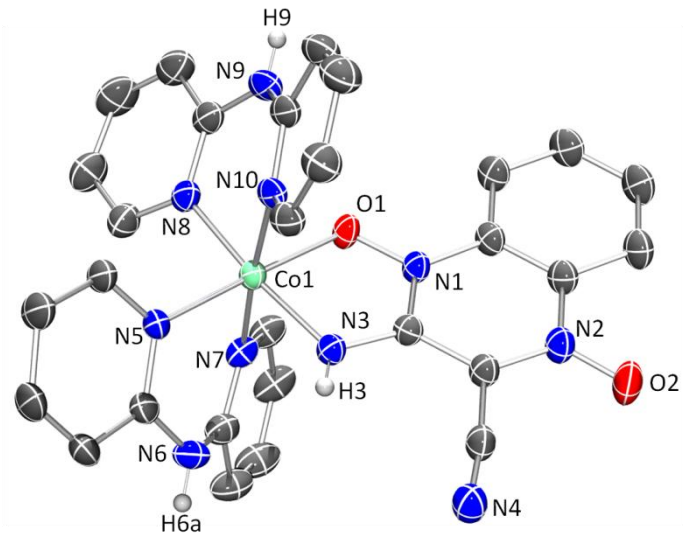

Figure 4.23: ORTEP diagram (50% probability) of $[Co(tpz\text{-}CN)(dpHa)_2]^{2+}$.[131] Hydrogen atoms (except H(3), H(3a) and H(6a)) and BF_4^- counter-ions removed for clarity. Selected bond lengths / Å and angles /º: Co(1)-N(3) 1.9022(13), Co(1)-O(1) 1.9059(11), Co(1)-N(5) 1.9337(13), Co(1)-N(8) 1.9422(14), Co(1)-N(7) 1.9484(14), Co(1)-N(10) 1.9484(13), N(1)-O(1) 1.3745(16), N(2)-O(2) 1.2645(18), N(3)-Co(1)-O(1) 84.07(5), N(5)-Co(1)-N(7) 89.88(6), N(8)-Co(1)-N(10) 89.62(6)

Within the crystal, the individual complexes are linked as dimeric units by two intermolecular hydrogen-bonds formed between the nitrile group from one complex and the amine of the tpz-CN of the other complex (**Figure 4.24**).

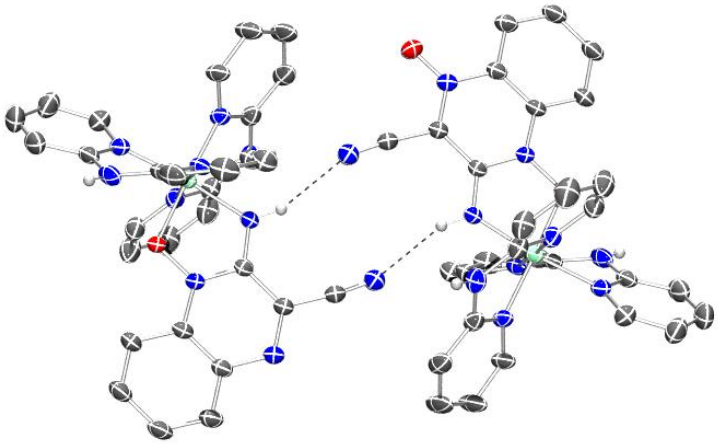

Figure 4.24: ORTEP diagram showing the intermolecular hydrogen-bonding present within the crystal structure of $[Co(tpz\text{-}CN)(dpHa)_2](BF_4)_2$.[131] Hydrogen-bond distances / Å and angles /º: H(3)···N(4) 2.23(2), N(3)···N(4) 3.048(2), N(3)-H(3)···N(4) 156.8(19)

In order to be able to use the complex in biological assays, it was needed to be able to prepare the complex with an alternative counter-ion which is more biologically compatible. It was first tried to prepare $[Co(tpz\text{-}CN)(dpHa)_2]Cl_2$ by reacting one equivalent $CoCl_2.6H_2O$ with two equivalents of dpHa in MeOH to form $[Co(Cl)_2(dpHa)_2]$ *in situ*, then react this with one equivalent tpzH-CN. The resulting complex was then oxidised with $K_2S_2O_8$ to form the cobalt(III) complex. It was necessary to discourage the formation of the *bis*-dpHa cobalt(III) complex so the reaction mixture was heated at reflux, as the stability of the *bis*-cobalt(II) octahedral complex becomes entropically less favourable upon heating compared with the tetrahedral $[Co(Cl)_2(dpHa)]$.[133] It was subsequently found that using cobalt(II) nitrate in place of cobalt(II) chloride resulted in $[Co(tpz\text{-}CN)(dpHa)_2]^{2+}$ being obtained in greater purity (**Scheme 4.6**) and as a more crystalline product.

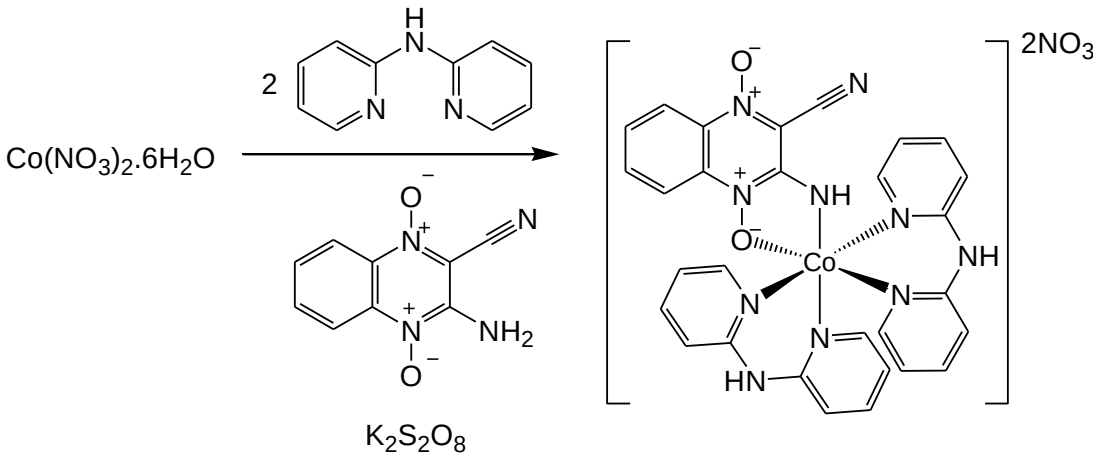

Scheme 4.6: Preparation of $[Co(tpz\text{-}CN)(dpHa)_2](NO_3)_2$

With the tpzH-$CONH_2$ ligand, it was initially thought that the *bis*-N-oxide cobalt(III) complex $[Co(tpz\text{-}CONH_2)_2(dpHa)]^+$ complex was being formed. A peak at *m/z* 668.1 was observed with MS-ESI, corresponding to $[Co(tpz\text{-}CONH_2)_2(dpHa)]^+$. ^{1}H NMR spectroscopy indicated the presence of eight different proton environments and therefore two chemically different aromatic rings each containing four protons (**Figure 4.25**). The two separate ring environments only fits for the complex having two N-oxide ligands and one dpHa ligand (**Figure 4.26**).

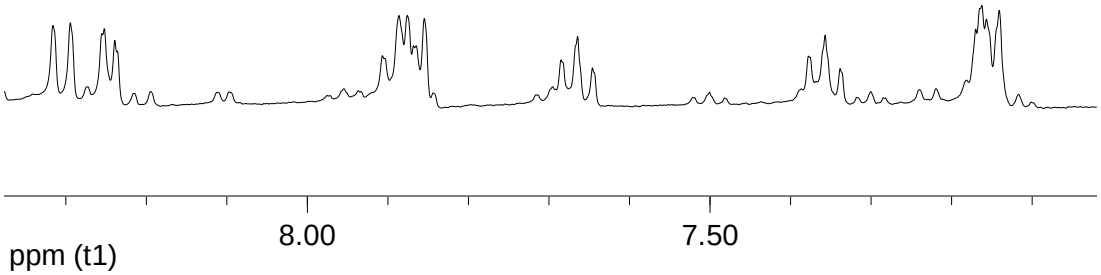

Figure 4.25: ^{1}H NMR (400 MHz, MeOD) of $[Co(tpz\text{-}CONH_2)_2(dpHa)]^+$: δ8.30 (d, 1H, J = 8.5 Hz), δ8.24 (dd, 1H, J = 6.5 , 1.5 Hz), δ7.87 (m, 4H), δ7.67 (ddd, 2H, J =7.5, 7.0, 1.0 Hz), δ7.36 (ddd, 2H, J = 8.5, 7.0, 1.0 Hz), δ7.16 (m, 4H)

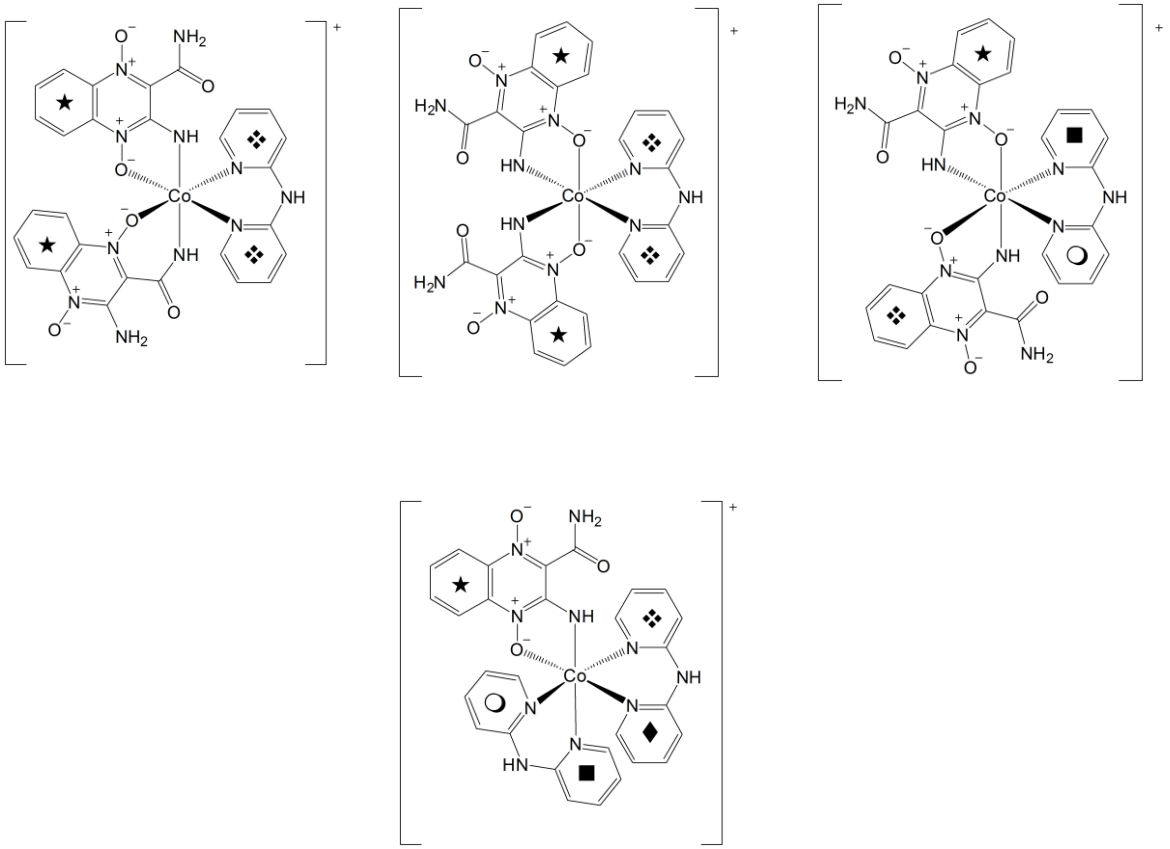

Figure 4.26: The three isomers of $[Co(tpz\text{-}CONH_2)_2(dpHa)]^+$ (above) and the single isomer of $[Co(tpz\text{-}CONH_2)\ (dpHa)_2]^{2+}$ with their chemically equivalent ring environments denoted by ★, ♦, ■, ❍ and ❖

It was therefore attempted to prepare the complex using two equivalents of the tpzH-$CONH_2$ ligand and one of the dpHa ligand (**Scheme 4.7**).

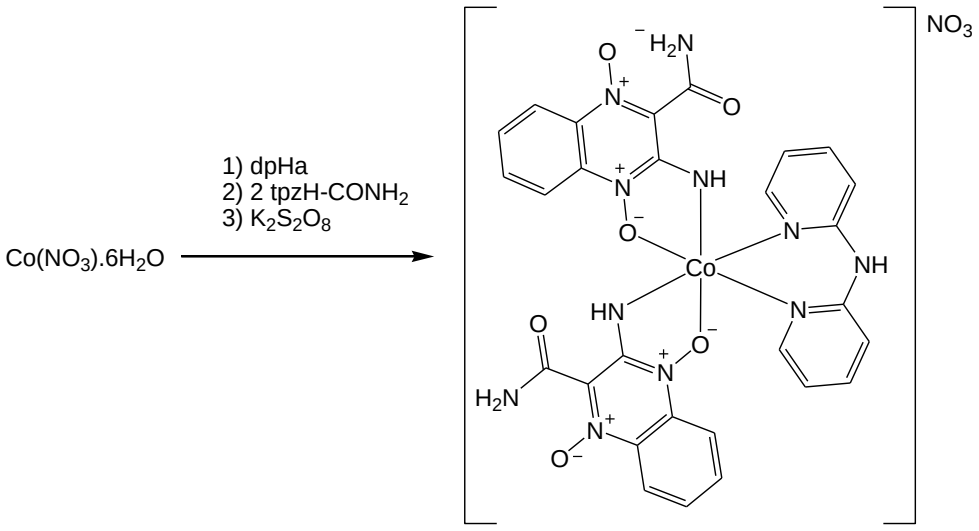

Scheme 4.7: Attempt to prepare $[Co(tpz\text{-}CONH_2)_2(dpHa)]NO_3$ from equimolar amounts of $Co(NO_3).6H_2O$ and dpHa with two equivalents tpzH-$CONH_2$

Dark red diffraction quality-crystals from this reaction were obtained by allowing a methanolic solution layered over ^{n}BuOH to slowly evaporate under ambient conditions over several days. The structure did not show the expected *bis*-N-oxide cobalt(III) structure, but that of $[Co(tpz\text{-}CONH_2)(dpHa)_2](NO_3)_2$. The structure shows an octahedral cobalt(III) centre coordinated to one tpzH-$CONH_2$ ligand and two dpHa ligands (**Figure 4.27**), with two non-coordinating nitrate counter-ions. The structure shows that the two intramolecular hydrogen-bonds within tpzH-$CONH_2$ remain upon incorporation into this complex.

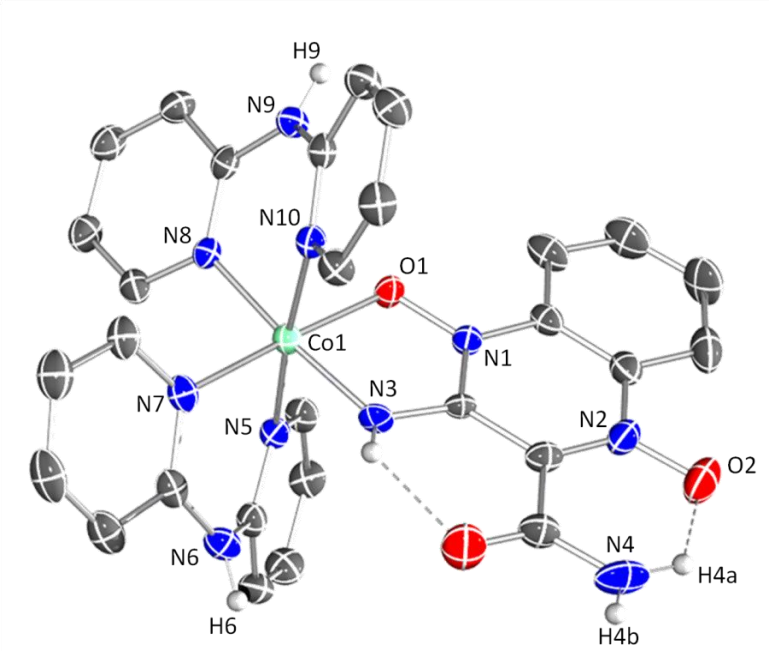

Figure 4.27: ORTEP diagram (50% probability) of $[Co(tpz\text{-}CONH_2)(dpHa)_2]^{2+}$.[131] Hydrogen atoms (except H(3), H(3a) and H(6a)) and BF_4^- counter-ion removed for clarity. Selected bond lengths / Å and angles /º: Co(1)-N(3) 1.882(3), Co(1)-N(5) 1.941(3), Co(1)-N(7) 1.941(3), Co(1)-N(8) 1.948(3), Co(1)-N(10) 1.953(3), Co(1)-O(1) 1.883(2), N(1)-O(1) 1.373(3), N(2)-O(2) 1.292(4), N(3)-Co(1)-O(1) 84.32(11), N(5)-Co(1)-N(7) 90.59(11), N(8)-Co(1)-N(10) 89.41(11). Hydrogen-bond distances / Å and angles /º: H(4a)···O(2) 1.79 (5), N(4)···O(2) 2.552(6), H(3a)···O(3) 2.13 (4), N(3)···O(3) 2.638(4), N(4)-H(4a)···O(2) 129(4), N(3)-H(3a)···O(3) 138(4)

By comparing the bond lengths of the free and coordinated tpzH-$CONH_2$ ligand, it can be seen that both of the *N*-oxide bonds lengthen upon coordination (**Table 4.5**) whereas its carbon-amine C(1)-N(3) bond length shortens.

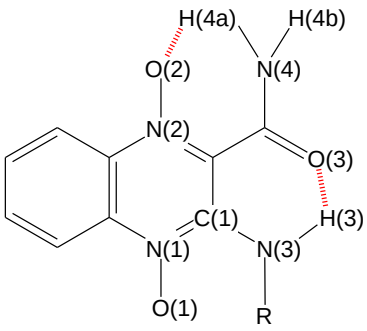

Figure 4.28: Atom numbering used in **Table 4.5**

Table 4.5: Comparison of selected bond lengths / Å and angles / º of tpzH-$CONH_2$ bond lengths in the free ligand and $[Co(tpz\text{-}CONH_2)(dpHa)_2]2NO_3$ complex

	tpzH-$CONH_2$	**$[Co(tpz\text{-}CONH_2)(dpHa)_2]2NO_3$**
N(1)-O(1)	1.327(2)	1.373(3)
N(2)-O(2)	1.274(2)	1.292(4)
C(1)-N(3)	1.326(2)	1.307(4)
H(3)···O(3)	1.98(3)	2.13 (4)
N(3) ··O(3)	2.622(2)	2.638(4)
N(3)-H(3) ··O(3)	136(2)	138(4)
H(4a) ··O(2)	1.90(3)	1.79 (5)
N(4) ··O(2)	2.557(2)	2.552(6)
N(4)-H(2) ··O(2)	126(3)	129(4)

Within the crystal, the central amine of one dpHa ligand, N(9)-H(9) forms a hydrogen-bond to the O(5) atom of a nitrate. The amide of the *N*-oxide ligand, N(4)-H(4b), forms a hydrogen-bond with O(8) of another nitrate. This same oxygen atom forms a hydrogen-bond with a second complex, to the N(6)-H(6) amine of a dpHa ligand. These interactions combine to form a hydrogen-bonded dimeric type structure comprising of two complexes and four non-coordinated nitrate anions, two of which are bridging (**Figure 4.29**).

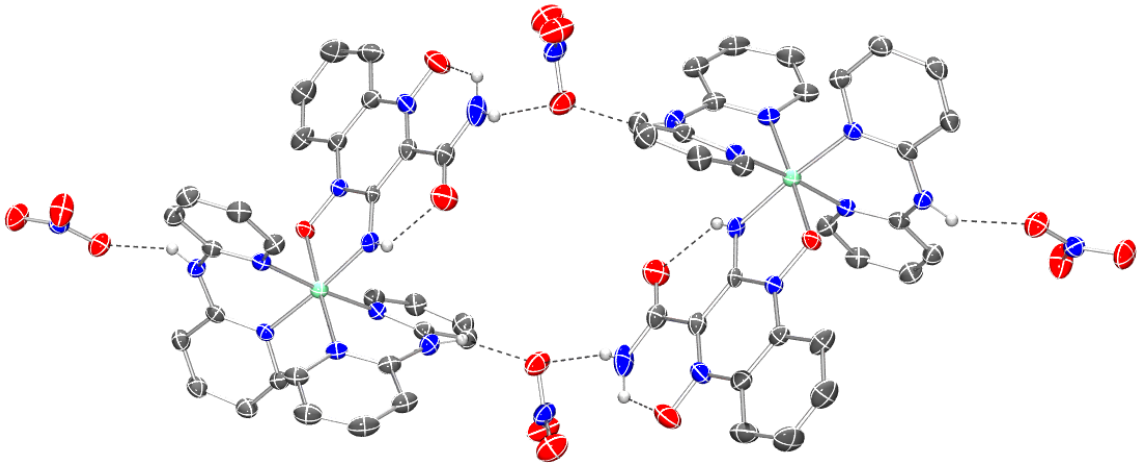

Figure 4.29: ORTEP diagram showing the intermolecular hydrogen-bonding present within the crystal structure of $[Co(tpz\text{-}CONH_2)(dpHa)_2]2NO_3$.[131] Hydrogen-bond distances / Å and angles /º: H(4b)···O(8) 2.413, N(4) ··O(8) 3.062, H(6) ··O(8) 1.97, N(6)···O(8) 2.784(4), H(9)···O(5) 2.08, N(9)···O(5) 2.872 (4), N(4)- H(4b)···O(8) 161.56, N(6)- H(6)···O(8) 153.5, N(9)-H(9)···O(5) 149.8

The presence of $[Co(tpz\text{-}CONH_2)(dpHa)_2]^{2+}$ had not been observed with MS-ESI prior to the setting up of the crystallisations, despite complexes of this type being observed previously. It was therefore thought that the obtained crystals were of the minor product formed from the reaction, with the bulk product being $[Co(tpz\text{-}CONH_2)_2(dpHa)]^{+}$. It was subsequently tried to prepare the former as the main product. Reacting two equivalents of dpHa and one equivalent of tpzH-$CONH_2$ produced a ^1H NMR spectra in D_2O which resembled that of the $[Co(tpz\text{-}R)(dpHa)_2]^{2+}$ complexes (**Figure 4.30**) with the number of different proton environments. MS peaks were observed at *m/z* 619.14 and 668.12, corresponding to $[Co(tpz\text{-}CONH_2)_2(dpHa)_2]^{+}$ and the $[M\text{-}H]^{+}$ ion of $[Co(tpz\text{-}CONH_2)(dpHa)_2]^{2+}$. Using the cobalt(II) chloride in place of the nitrate salt also yielded a mixture. It was found that the difference in aqueous solubility between the two complexes provides a means of separating them, as $Co(tpz\text{-}CONH_2)(dpHa)_2]^{2+}$ is the more soluble in water. As the reaction is low yielding and the amount of $Co(tpz\text{-}CONH_2)(dpHa)_2]^{2+}$ isolated in this way is sufficient only for a ^1H NMR spectrum, a more efficient means of preparing $Co(tpz\text{-}CONH_2)(dpHa)_2]^{2+}$ still needs to be found.

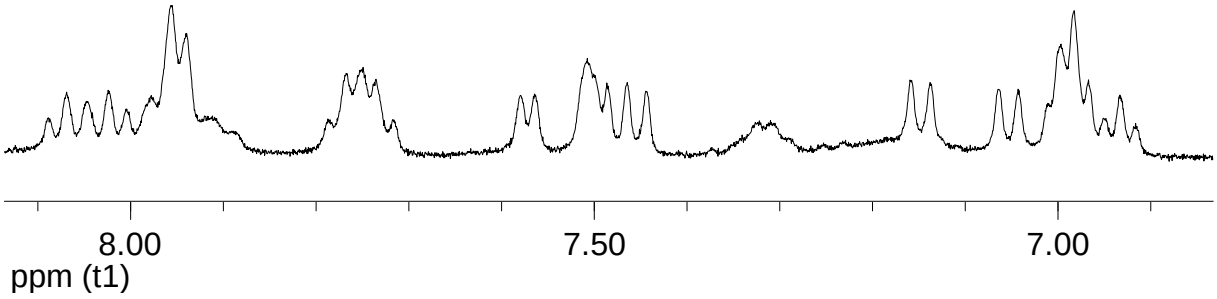

Figure 4.30:[1]H NMR (400 MHz, D_2O) of $[Co(tpz\text{-}CONH_2)(dpHa)_2]^{2+}$: δ8.05 (m, 2H), δ7.94 (m, 4H), δ7.75 (m, 3H), δ7.57 (d, 1H, J = 6.0 Hz), δ7.50 (m, 2H), δ7.45 (d, 1H, J = 8.0 Hz), δ7.32 (d, br. d, 1H, J = 8.0 Hz), δ7.15 (d, 1H, J = 8.0 Hz), δ7.05 (d, 1H, J = 8.0 Hz), δ6.98 (m, 3H), δ6.93 (t, 1H, J = 6.0 Hz)

The cobalt(III) tpzH complex was similarly obtained to $[Co(tpz\text{-}CN)(dpHa)_2]^{2+}$, by reacting two equivalents of dpHa and one of tpzH with the appropriate cobalt salt, with $[Co(tpz)(dpHa)_2]Cl_2$ prepared in 23% yield (**Scheme 4.8**).

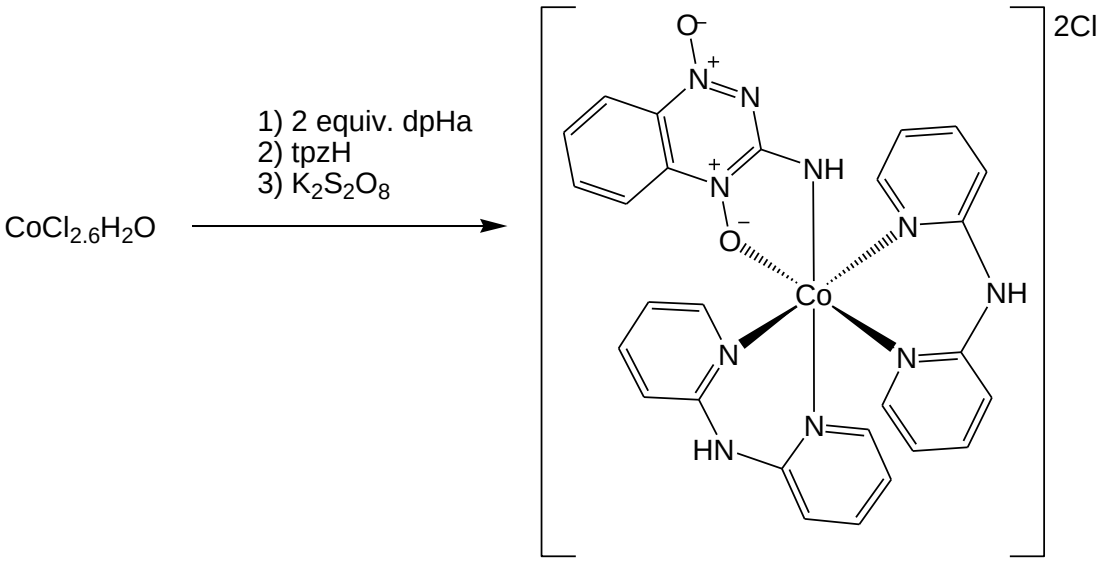

Scheme 4.8: Preparation of $[Co(tpz)(dpHa)_2]Cl_2$

MS-ESI showed peaks at *m/z* 577.13 and 289.07 corresponding to $[Co(tpz)(dpHa)_2]^{2+}$, whilst ^{1}HNMR spectroscopic analysis showed a similar spectrum to that observed for the $[Co(tpz\text{-}CN)(dpHa)_2]^{2+}$ complexes (**Figure 4.31**).

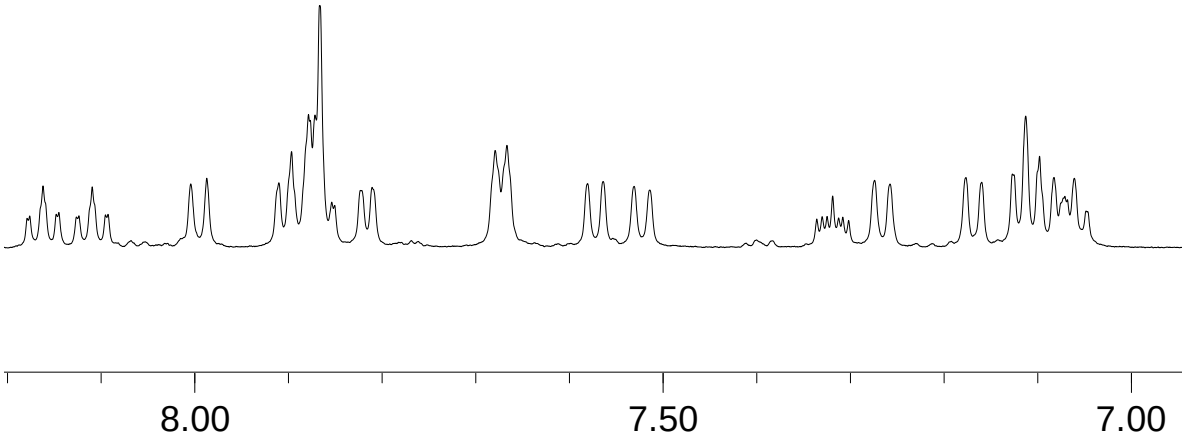

Figure 4.31: ^{1}H NMR (500 MHz, MeOD) of $[Co(tpz)(dpHa)_2]^{2+}$: δ8.16 (ddd, 1H, J = 7.5, 7.0, 1.0 Hz), δ8.11 (ddd, 1H, J = 8.0, 7.0, 1.5 Hz), δ7.99 (d, 1H, J = 8.5 Hz), δ7.87 (m, 5H), δ7.82 (dd, 1H, J = 5.5, 1.0 Hz), δ7.67 (d, 2H, J = 6.5 Hz), δ7.57 (d, 1H, J = 8.0 Hz), δ7.52 (d, 1H, J = 8.0 Hz), δ7.32 (ddd, 1H, J = 8.5, 5.5, 3 Hz), δ7.26 (d, 1H, J = 8.0 Hz), δ7.17 (d, 1H, J = 8.5 Hz), δ7.10 (m, 4H)

Crystals of $[Co(tpz)(dpHa)_2](BF_4)_2$ were obtained by allowing a methanolic solution layered over ^{n}BuOH to slowly evaporate over the course of a few days at room temperature. The structure is similar to that of the other two cobalt(III) structures, having an octahedral centre coordinated to one tpzH ligand and two dpHa ligands, with two non-coordinating $BF4^{-}$ counter-ions (**Figure 4.32**).

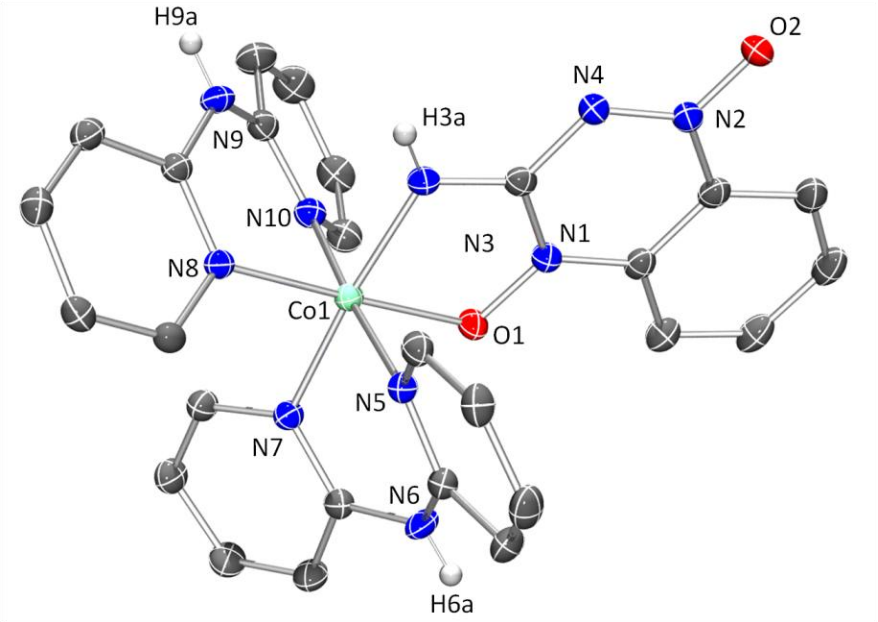

Figure 4.32: ORTEP (50% probability) of $[Co(tpz)(dpHa)_2]^{2+}$.[131] Hydrogen atoms (except H(3a), H(6a) and H(9a)) and BF_4^- counter-ions and solvent molecules removed for clarity. Selected bond lengths / Å and angles /º: Co(1)-O(1) 1.9059(12), Co(1)-N(3) 1.9077(14), Co(1)-N(8) 1.9314(14), Co(1)-N(7) 1.9361(14), Co(1)-N(10) 1.9385(14), Co(1)-N(5) 1.9494(14), N(1)-O(1) 1.3650(17), N(2)-O(2) 1.2668(18), O(1)-Co(1)-N(3) 84.49(5), N(7)-Co(1)-N(5) 89.37(6), N(8)-Co(1)-N(10) 90.65(6)

Comparing the bond lengths of the tpzH ligand when free and when coordinated to the cobalt(III) centre again shows that the *N*-oxide bond lengths lengthen upon coordination and that the carbon amine C(1)-N(3) bond lengths shorten (**Table 4.6**).[171]

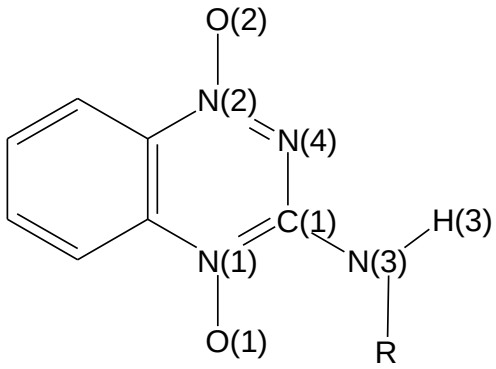

Figure 4.33: Atom numbering scheme used in **Table 4.6**

Table 4.6: Comparison of *N*-oxide bond lengths in tpzH and $[Co(tpz)(dpHa)_2](BF_4)_2$

	tpzH	**$[Co(tpz)(dpHa)_2]2BF_4$**
N(1)-O(1)	1.3330(15)	1.3650(17)
N(2)-O(2)	1.2574(15)	1.2668(18)
C(1)-N(3)	1.3241(19)	1.300(2)

Within the crystal, dimer structures are formed by a two-fold hydrogen-bond between the uncoordinated *N*-oxide O(2) and the dpHa amine N(9)-H(9a) of the second complex (**Figure 4.34**).

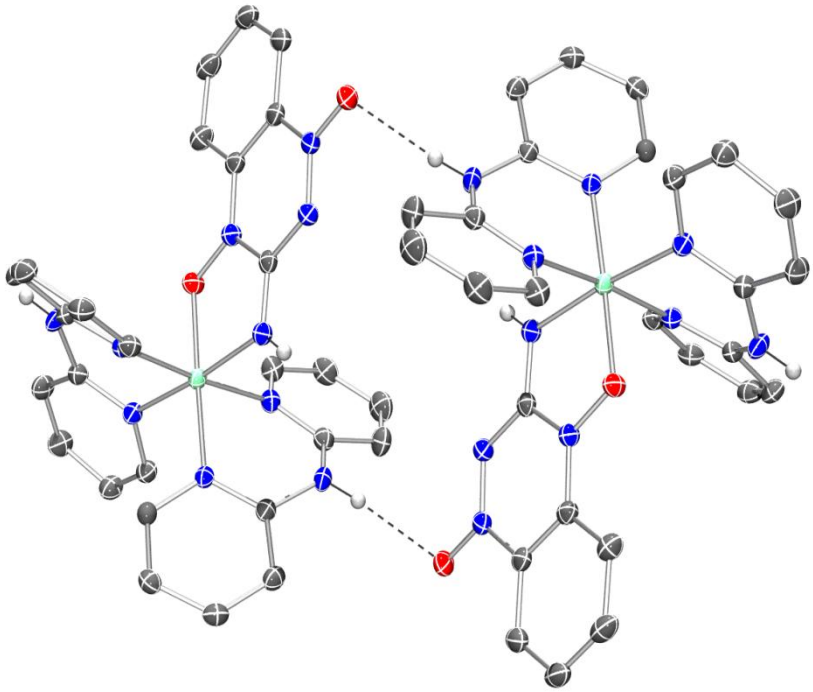

Figure 4.34: ORTEP diagram showing the intermolecular hydrogen-bonding present within the crystal structure of $[Co(tpz)(dpHa)_2](BF_4)_2$.[131] Hydrogen-bond distances / Å and angles /º: H(9a)···O(2) 2.06(2), N(9)···O(2) 2.8639(19), N(9)-H(9a) H(9a)···O(2) 174(2)

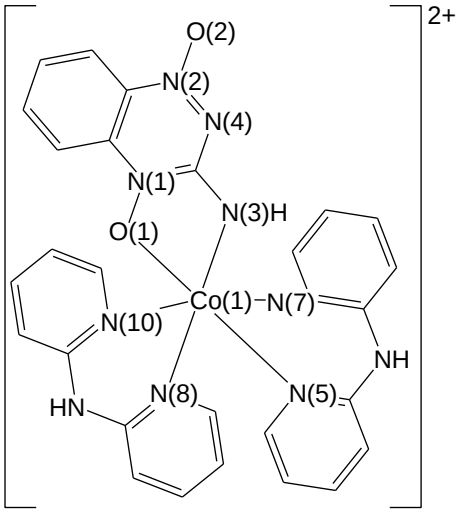

Figure 4.35: Atom labelling used in **Table 4.7** for the comparison of crystallographically determined $[Co(tpz\text{-}R)(dpHa)_2]^{2+}$ complexes

Upon comparing the bond lengths of the three cobalt(III) complexes (**Table 4.7**), it can be seen that the tpzH-$CONH_2$ complex has the shortest metal-*N*-oxide bond lengths but longest metal-dpHa bond lengths.

Table 4.7: Comparison of the crystallographically determined bond lengths of the cobalt(III) heteroleptic *N*-oxide complexes

Bond	**tpzH-CN**	**tpzH**	**tpzH-$CONH_2$**
Co(1)-O(1)	1.9059(11)	1.9059(12)	1.883(2)
Co(1)-N(3)	1.9022(13)	1.9077(14)	1.882(3)
Co(1)-N(5)	1.9337(13)	1.9314(14)	1.941(3)
Co(1)-N(7)	1.9484(14)	1.9385(14)	1.941(3)
Co(1)-N(8)	1.9422(14),	1.9361(14)	1.948(3)
Co(1)-N(10)	1.9484(13)	1.9494(14)	1.953(3)
N(1)-O(1)	1.3745(16)	1.3650(17)	1.373(3)
N(2)-O(2)	1.2645(18),	1.2668(18)	1.292(4)

A notable difference when preparing the heteroleptic cobalt(III) complexes was observed between using tpzH-CN and tpzH compared to tpzH-$CONH_2$. With the former two ligands, the colour change from that of the precursor species to the purple colour of the heteroleptic complex was observed upon addition of the *N*-oxide ligand. With the tpzH-$CONH_2$ ligand, this colour change did not take place until the

addition of the oxidising agent, and took place a lot more gradually. This difference in the readiness of formation might help explain the difference in distribution of products obtained for the cobalt(III) complexes of tpzH-CN and tpzH compared to tpzH-$CONH_2$.

4.4. Extending the range of heteroleptic complexes

The work described in **Chapter 2** demonstrated that the methyl substituent of 2,2-dipyridylmethylamine (dpma) affected the interplanar angle between the ligand's two pyridyl rings. The copper(II) complex $[Cu(tpz\text{-}CN)(dpma)]^+$ was prepared according to **Scheme 4.9** and obtained in 68% yield as the crude product. A peak at *m/z* 449.07 was observed by MS, corresponding to the $[Cu(tpz\text{-}CN)(dpma)]^+$ complex.

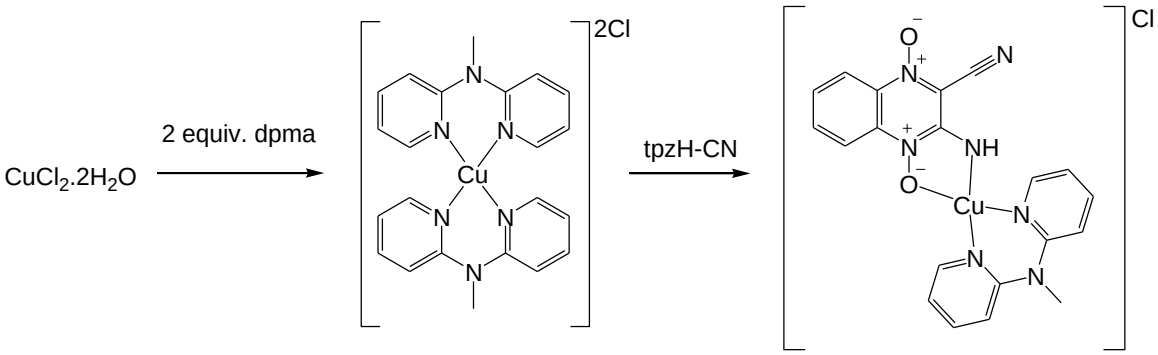

Scheme 4.9: Preparation of [Cu(tpz-CN)(dpma)]Cl

The cobalt(III) complex $[Co(tpz\text{-}CN)(dpma)_2]^{2+}$ was prepared according to **Scheme 4.10** in 23% yield.

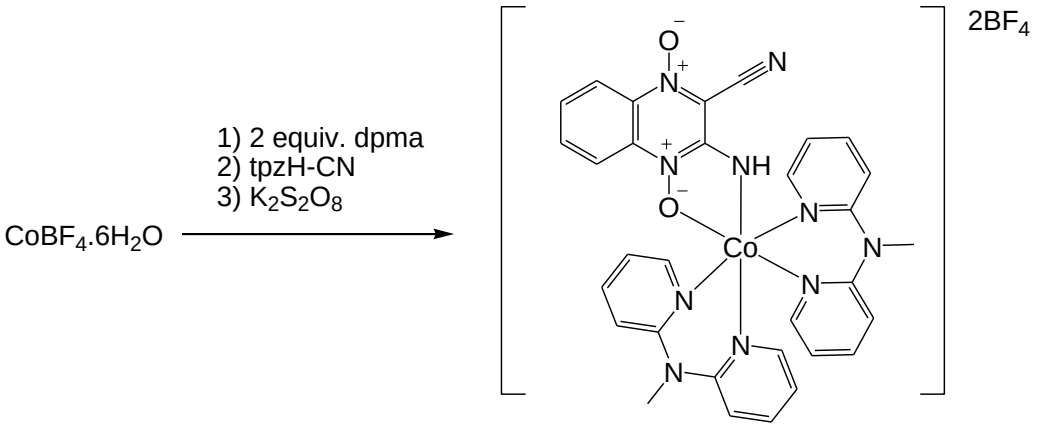

Scheme 4.10: Preparation of $Co(tpz\text{-}CN)(dpma)_2](BF_4)_2$

Analysis of the product by MS showed a peak at *m/z* 629.15 which corresponds to the $[Co(tpz\text{-}CN)(dpma)_2]^{2+}$ complex. ^1H NMR spectroscopic analysis showed that the complex was cobalt(III) owing to the peaks being sharp as opposed to broad which would be the case for cobalt(II). The spectrum (**Figure 4.36**) shows numerous peaks focused within the aromatic make proton region, making it difficult to assign but the presence of three signals rather than two in the region where the methyl group of dpma appears implies the product is not pure.

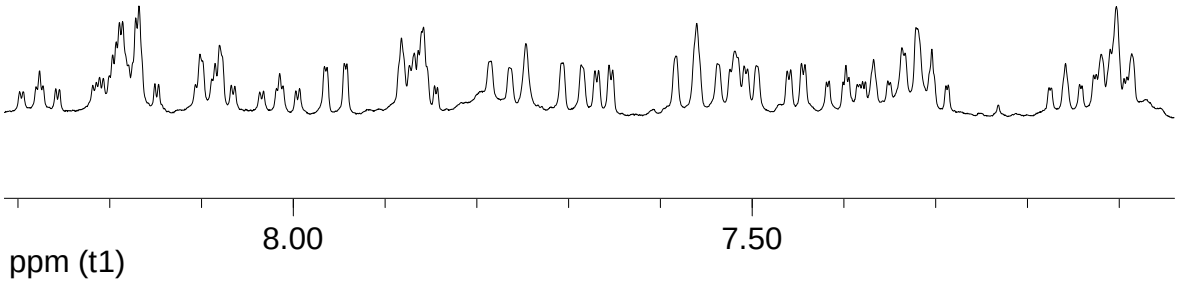

Figure 4.36:^1H NMR (400 MHz, d_6-DMSO) of the crude reaction mixture from the formation of $[Co(tpz\text{-}CN)(dpma)_2](BF_4)_2$

1,10-Phenanthroline (phen), like many other planar aromatic compounds, has been long accepted for its ability to chealte DNA.[173] It has been incorporated into cisplatin analogues such as $[Pt(phen)(en)]Cl_2$ and lanthanide complexes such as $[La(SCN)_3(phen)_3]$ (**Figure 4.37**) which have been examined for their anticancer activity.[174, 175]

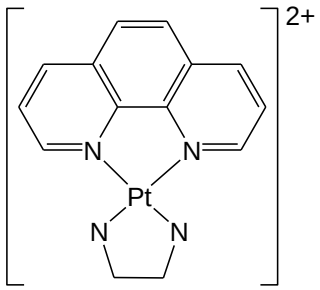

[Pt(phen)(en)]

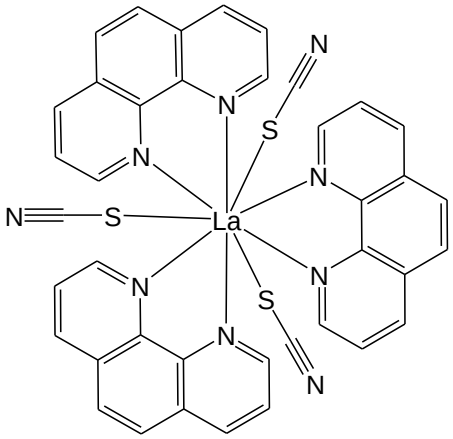

$[La(SCN)_3(phen)_3]$

Figure 4.37: Examples of phen containing complexes which have been examined for their anti-cancer activities.[174, 175]

Phen is a planar has two nitrogen donor atoms which coordinate to a metal centre to form a 5-membered metallocycle. It was thought that this more structurally ligand would provide an interesting comparison to the more structurally flexible dpHa ligand, which forms 6-membererd metallocycles. The complex was prepared by reacting two equivalents of the phen ligand with $Co(BF_4)_2.6H_2O$, and then adding one equivalent tpzH-CN. It was found to be necessary to add one equivalent Et_3N to the reaction mixture prior to the addition of the $K_2S_2O_8$ oxidising agent in order to ensure coordination of the *N*-oxide ligand (**Scheme 4.11**).

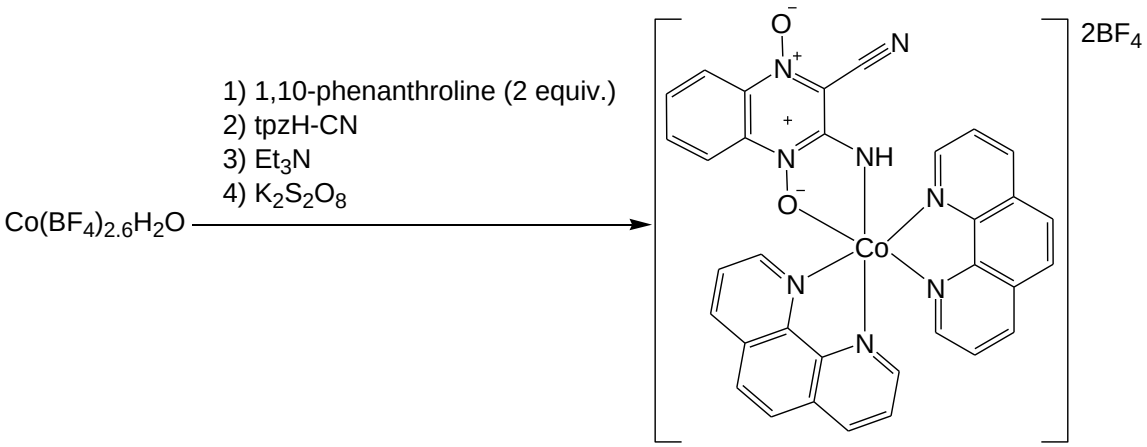

Scheme 4.11: Preparation of $[Co(tpz\text{-}CN)(phen)_2](BF_4)_2$

Crystals were obtained by layering a DMF solution with Et_2O, but these proved too small to provide sufficient X-ray diffraction. MS analysis of the product showed multiple peaks including one at 620.11 *m/z*, which corresponds to $[Co(tpz\text{-}CN)(phen)_2]^+$. ^1H NMR spectroscopic analysis showed a vast array of sharp signals within the aromatic proton region (**Figure 4.38**) which differs to those of the free ligands.

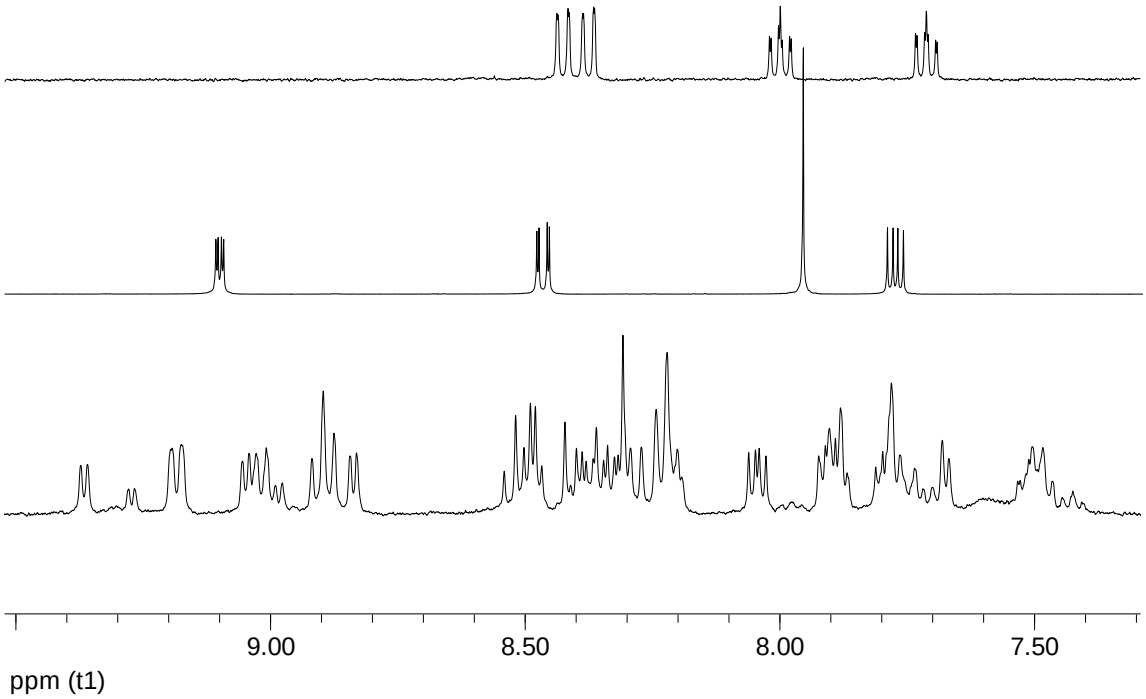

Figure 4.38: ^{1}H NMR (400 MHz, MeOD) overlay of tpzH-CN (*above*), phen and the crude $[Co(tpz\text{-}CN)(phen)_2]^{2+}$ product (*bottom*). Data for $[Co(tpz\text{-}CN)(phen)_2]^{2+}$: δ9.36 (d, 1H, J = 5.0 Hz), δ9.27 (d, 1H, J = 5.0 Hz), δ9.18 (dd, 2H, J = 8.0, 1.0 Hz), δ9.03 (m, 3H), δ8.90 (ap. t, 3H, J = 8.0 Hz), δ8.83 (d, 1H, J = 5.0 Hz), δ8.50 (m, 4H), δ8. 4-8.3 (m, 14H), δ8.04 (dd, 2H, J = 8.0, 5.0 Hz), δ7.9 (m, 4H), δ7.8-7.6 (m, 7H), δ7.50 (m, 3H)

4.5. Conclusions

A novel series of heteroleptic metal(II) and cobalt(III) complexes incorporating 2,2-dipyridyl amine (dpHa) and one *N*1,*N*4-oxide ligand (tpzH, tpzH-CN or tpzH-$CONH_2$) has been prepared and characterised including several crystal structures. The metal(II) complexes were shown to contain a 1:1 ratio of dpHa to *N*-oxide through NMR, titrations and crystallography. The cobalt(III) complexes of tpzH and tpzH-CN form in a 1:2 ratio of *N*-oxide to dpHa. The cobalt(III) complex of tpzH-$CONH_2$ seems to be able to form in a 1:2 or 2:1 ratio, with the former structurally determined crystallographically along with $[Co(tpz)(dpHa)_2]^{2+}$ and $[Co(tpz\text{-}CN)(dpHa)_2]^{2+}$. These complexes display vastly improved solubility in solvents such as EtOH and MeOH, with several which will dissolve into aqueous solution.

The potential to extend this range of complexes has been demonstrated with the observation of complexes where the dpHa ligand has been substituted for other bidentate neutral nitrogen donor ligands. The inclusion of phenanthroline into these complexes could provide an interesting direction for further work.

Chapter Five: Evaluation of solution phase properties

As drug compounds take effect on their biological targets in solution, it is important to assess various solution properties such as aqueous stability. The objective of this part of the project was therefore was to examine the pH-dependent stability and redox chemistry of the complexes and ligands discussed in **Chapters 2**, **3** and **4**.

5.1. Examining the aqueous and pH-dependent solution stability

5.1.1. Ligand stability and pK_a determination

Before considering the stability of the complexes, it is important to examine the ligands. It was found that the titrations of the ligands could be followed spectrophotometrically, focusing on wavelengths between 200 and 300 nm for the dpRa ligands, where electronic transitions of aromatic species typically occur.[165] For the *N*-oxide ligands, changes in absorbance in the visible region between 400 and 600 nm were monitored.

5.1.1.1. pK_a Determination of 2,2'-dipyridylamine type ligands

The overlaid UV-vis spectra of dpHa at different pH values (**Figure 5.1**) show that as the pH increases, the absorbance at 319 nm decreases whilst the absorbance at 262 and 308 nm increases. The absorbance at these wavelengths can be plotted as a function of pH. A sigmoidal curve can then be fitted to the data points which after fitting, allows for the calculation of the pK_a value of that particular deprotonation process. The single curve fitted to the absorbance at 262 nm against pH for dpHa gives a pK_a value of 6.9(0).

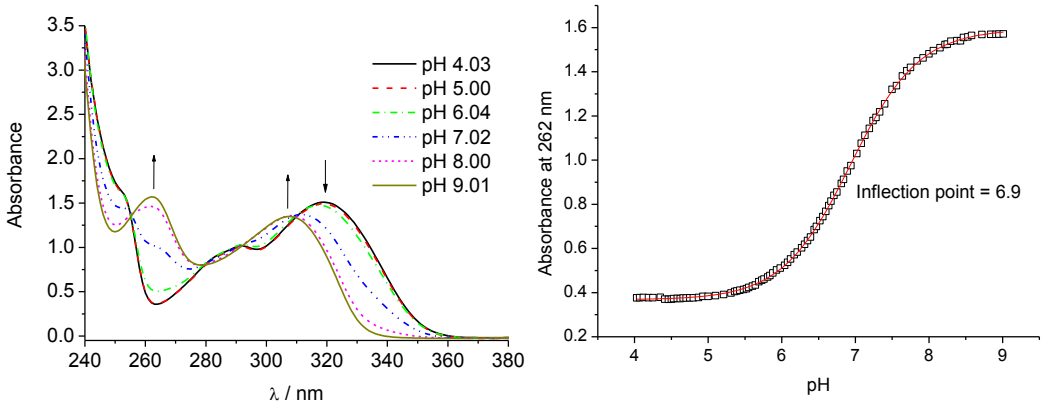

Figure 5.1: UV-vis spectra at varying pH of dpHa (*left*) and a plot of absorbance of dpHa at 262 nm against pH (*right*) in water

There are two possible deprotonation processes which could give rise to this pK_a value; the deprotonation of a pyridinium ion or the deprotonation of the central amine (**Scheme 5.1**). Either of these processes feasibly could have a pK_a of 6.9 given that pyridinium deprotonating to give pyridine has a pK_a of 5.23 whilst the deprotonation of 2-amino-pyridine has a pK_a of 6.86.[176-178]

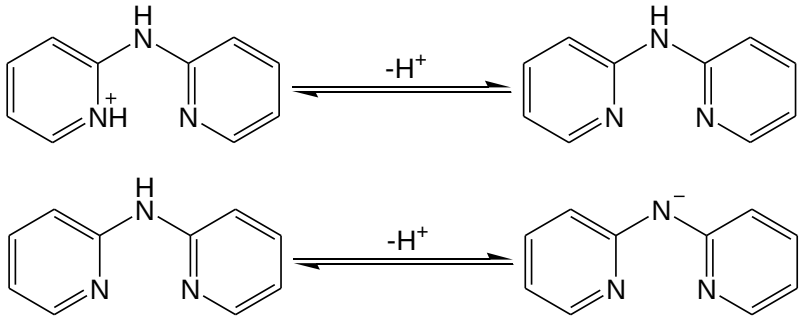

Scheme 5.1: Possible processes that could occur in dpHa to give a pK_a of 6.9; deprotonation of the pyridinium ion (*above*) or deprotonation of the central amine (*below*)

The number of protons involved in this deprotonation process can be determined through use of the relationship stated by the Henderson-Hasselbalch equation:

$$pH = pK_a + log\frac{[A^-]}{[HA]}$$

This equation can be expressed in the form of the gradient for a straight line where *y* is the *y* axis value, *m* is the slope of the line, *x* is the *x* axis value and *c* is the intercept of the *y* axis.

$$y = mx + c$$

In terms of the Henderson-Hasselbalch equation, this makes the y axis value equal to pH, the x axis value equal to log([A-]/[HA]), the y intercept equal to the pK_a and the gradient equal to the number of protons exchanged.

The relative concentrations of [HA] (the species prior to deprotonation) and [A^-] (the species after deprotonation) were obtained using the absorbances at 262 and 319 nm. These values were then used to plot log([A^-]/[HA]) against pH (**Figure 5.2**).

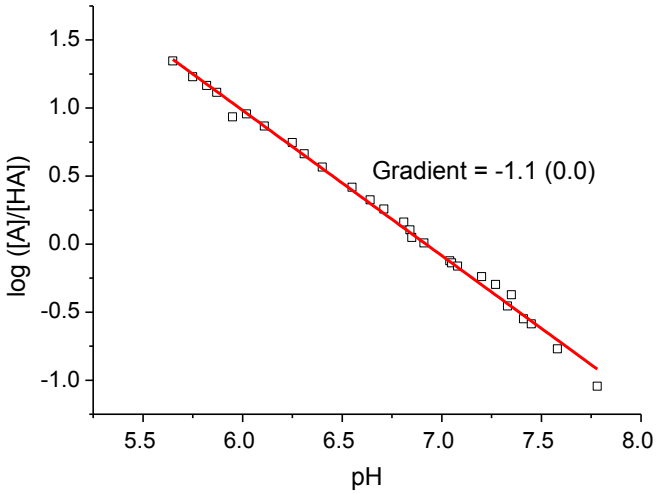

Figure 5.2: Plot of log([A^-]/[HA] against pH for dpHa

The line fitted to the data has a gradient of -1.1, indicating that one proton per dpHa molecule is involved in the observed deprotonation process. In order to help elucidate whether the amine or pyridinium ion is being deprotonated during this process, a derivative of dpHa was employed where the central amine had been methylated. The methyl group on the central amine of 2,2'-dipyridylamine (dpma) rules out deprotonation of the central amine occurring, but should still allow formation of a pyridinium ion species. Addition of $NaOH_{(aq)}$ to an acidified solution of dpma caused the absorbance at 272 and 308 nm to increase, and the absorbance at

253 and 321 nm to decrease. Plotting of the change in absorbance at 272 nm against the change in pH provides a pK_a value of 5.3(0) (**Figure 5.3**).

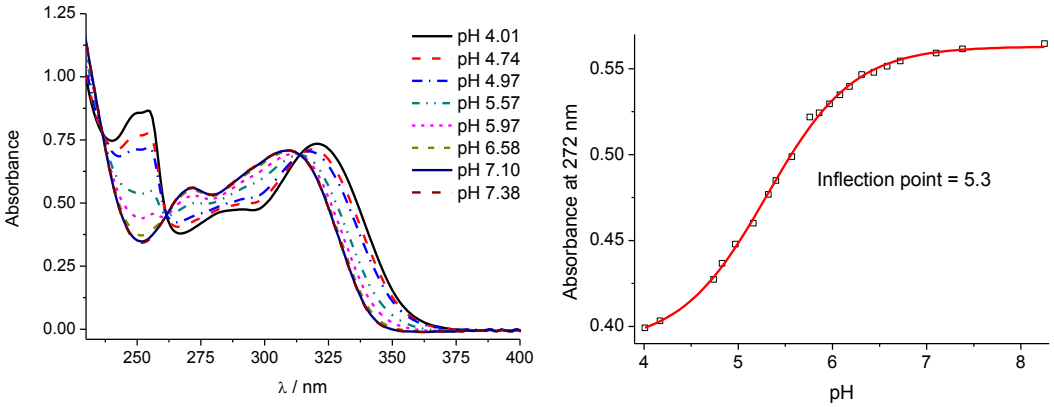

Figure 5.3: UV-vis spectra at varying pH of dpma (*left*) and absorbance of dpma at 272 nm against pH (*right*) in water

This one-proton process can be attributed to the deprotonation of the pyridinium ion (**Scheme 5.2**). This pK_a value is close to that reported in the literature for the analogous process in pyridine (5.23), suggesting that the pyridinium ion is no more stabilised than in pyridine.[179]

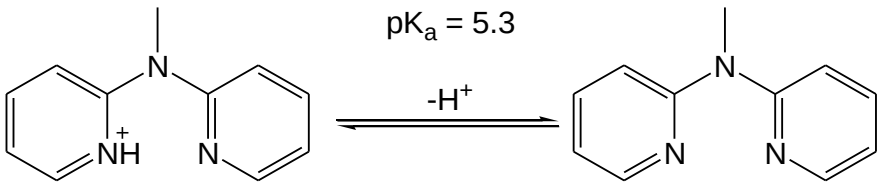

Scheme 5.2: The process which gives rise to dpma's pK_a value of 5.3

Analysis of the crystal structures of $[Zn(Cl)_2(dpHa)]$ and $[Zn(Cl)_2(dpma)]$ described in **Chapter 2** provides one possible explanation as to why the dpma pyridinium species has a similar pK_a value to that of pyridine, whilst the dpHa pyridinium ion has a pK_a of 6.9. The crystal structure of the $[Zn(Cl)_2(dpHa)]$ complex shows that the ligand adopted an almost planar conformation with the interplanar angle between the two pyridyl rings being 174.5°. In the $[Zn(Cl)_2(dpma)]$ complex, the ligand is less linear with the interplanar angle between the two pyridyl rings being 148.5° (**Figure 5.4**).

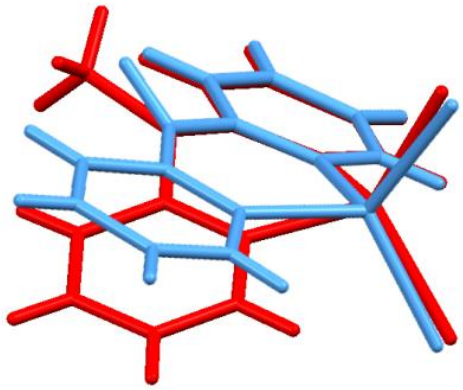

Figure 5.4: Overlay of the crystal structures of [Zn(Cl)$_2$(dpHa)] (*blue*) and [Zn(Cl)$_2$(dpma)] (*red*) showing the increased bend between the two pyridyl rings brought about by methylation of the central amine. [128, 171]

As the two rings in the dpHa complex are more planar with respect to one another, the protonated pyridyl nitrogen forming a N-H···N hydrogen bond to the other pyridyl nitrogen would be shorter and stronger than the hydrogen bond in dpma as the pyridinium N-H lies in same plane as its pyridyl ring so points towards the lone electron pair containing p orbital of the unprotonated nitrogen (**Figure 5.5**).

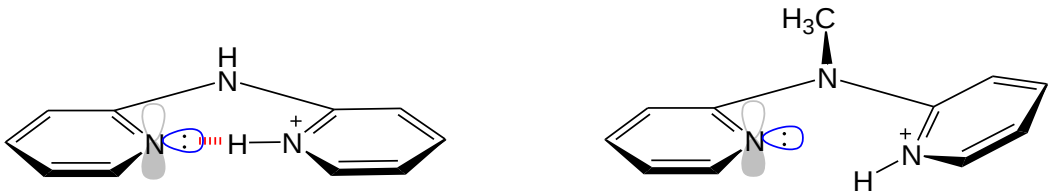

Figure 5.5: How the interplanar angle of dpHa favours and of dpma disfavours the formation of a N-H···N hydrogen bond

To test this hypothesis, the dpea ligand where the central amine had been ethylated was employed. It was predicted that as the ethyl group would provide degree of steric bulk to the central amine

With increasing pH, the absorbance increases at 276 and 308 nm and decreases at 254 and 318 nm (**Figure 5.5**). Plotting the absorbance at 276 nm against pH produces a sigmoidal curve which gives a pK_a value of 5.3(0.0).

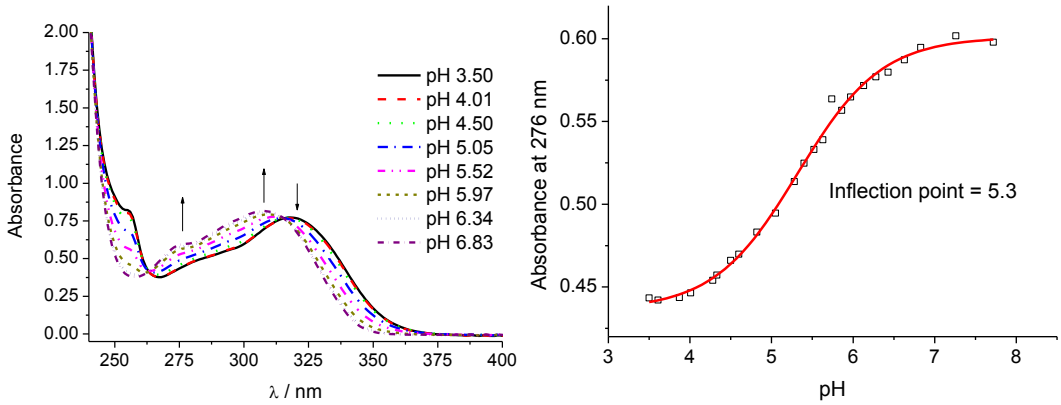

Figure 5.6: UV-vis spectra at varying pH of dpea (*left*) and absorbance of dpea at 276 nm as a function of pH (*right*) in water

Both the dpea and dpma ligands were found to have a pK_a value of 5.3, similar to that of free pyridine. This similarity indicates that there is no additional stabilisation of the protonated species contributed by the amine substituent or the second pyridyl ring. The methyl and ethyl substituents provide a similar amount of steric bulk adjacent to the central amine. The crystal structures of $[Zn(Cl)_2(dpea)]$ and $[Zn(Cl)_2(dpma)]$ discussed in **Chapter 2** showed that these two ligands have similar interplanar angles between their two pyridyl rings, and this would seem to correlate with their pK_a values (**Table 5.1**).

Table 5.1: Experimentally found pK_a values and interplanar angles for dpHa, dpma and dpea

Ligand	**pk_a**	**Interplanar angle in Zn complex / °**
dpHa	6.9(0.0)	174.5
dpma	5.3(0.0)	148.5
dpea	5.3(0.0)	138.7

With the py-dpHa-CN ligand, there are several sites which potentially can be protonated or deprotonated including the central amine, the two pyridyl nitrogen atoms and the pyrrolidine nitrogen (**Figure 5.6**).

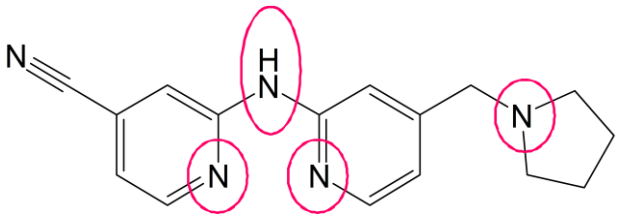

Figure 5.7: Sites of py-dpHa-CN that could be protonated or deprotonated

Comparison of the UV-vis spectra at varied pH values show that at the pH increases from 3 to 6, the absorbance at 336 nm decreases whilst undergoing a bathochromic shift to 338 nm. Above pH 6, the absorbance at 338 nm continues to decrease and the λ_{max} shifts to 342 nm whilst the absorbance at 295 nm increases (**Figure 5.7**).

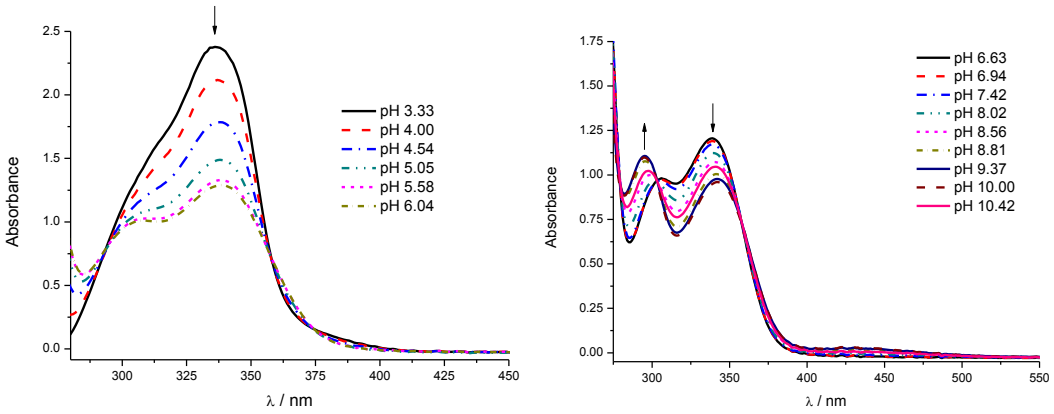

Figure 5.8: UV-vis spectra at varying pH of the py-dpHa-CN between pH 3 and 6 (*left*) and pH 6.5 and 10.5 (*right*) in water

Plotting the absorbance at 295 and 338 nm against pH shows that the pK_a values for these two processes are 4.4(1) and 8.5(0) (**Figure 5.8**).

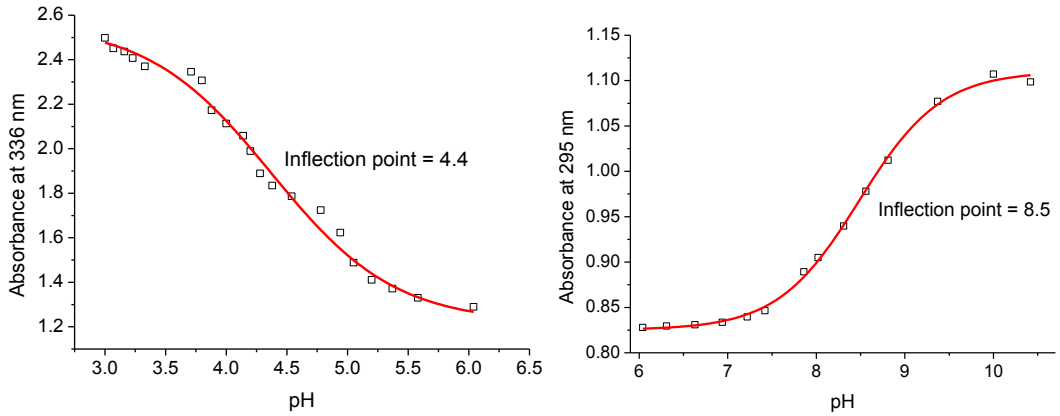

Figure 5.9: Sigmoidal fits for the py-dpHa-CN ligand for the absorbance at 336 nm between pH 3 and 6.5 (*left*) and absorbance at 295 nm between pH 6 and 10.5 (*right*) in water

These two processes most likely to correspond to the deprotonation of the pyridyl nitrogens or central amine, as pyrrolidines are characteristically highly basic in nature (**Scheme 5.3**).[155] Therefore the pK_a of the pyrrolidinium appears to high to measure, which would go some way to explain the lack of success in the attempts to complex this ligand.

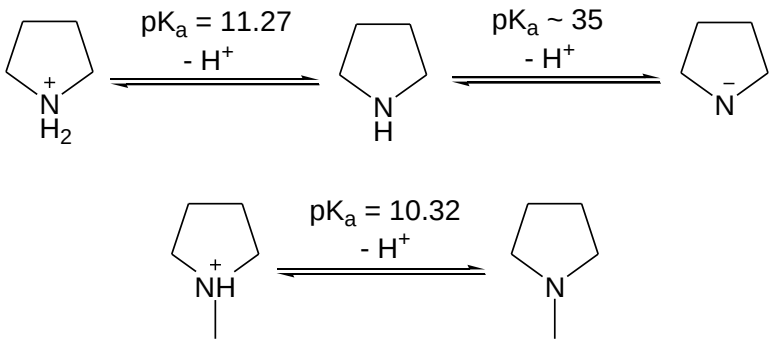

Scheme 5.3: The pK_a values of pyrrolidine and *N*-methyl pyrrolidine.[167]

5.1.1.2. pK_a determination of 1,4-*N*-oxide ligands

The 1,4-*N*-oxide ligands tpzH, tpzH-CN and tpzH-$CONH_2$ all absorb strongly in the UV region and in the visible region between 430 and 475 nm due to a π- π* transition.[180] This band in the visible region was used to monitor the titrations as its corresponding absorption band decreases in intensity upon deprotonation, whilst a

band between 500 and 560 nm increases. In the case of tpzH and tpzH-CN this corresponds to a colour change from yellow to purple (**Figure 5.6**).

Figure 5.10: The colour change which occurs upon deprotonation of tpzH and tpzH-CN (tpzH-CN shown) in water

When titrating OH^- into a solution of tpzH, no change is observed in the absorbance of the UV-vis spectrum until pH 10. Above this pH, the absorbance at 461 nm decreases whilst the absorbance at 535 nm increases (**Figure 5.7**). The absorbance at 535 nm increases beyond the pH that can be measured accurately (pH 12), but the obtained data affords an approximate pK_a value of 12.6(0). This pK_a value is most likely to correspond to the deprotonation of the amine (**Scheme 5.4**).

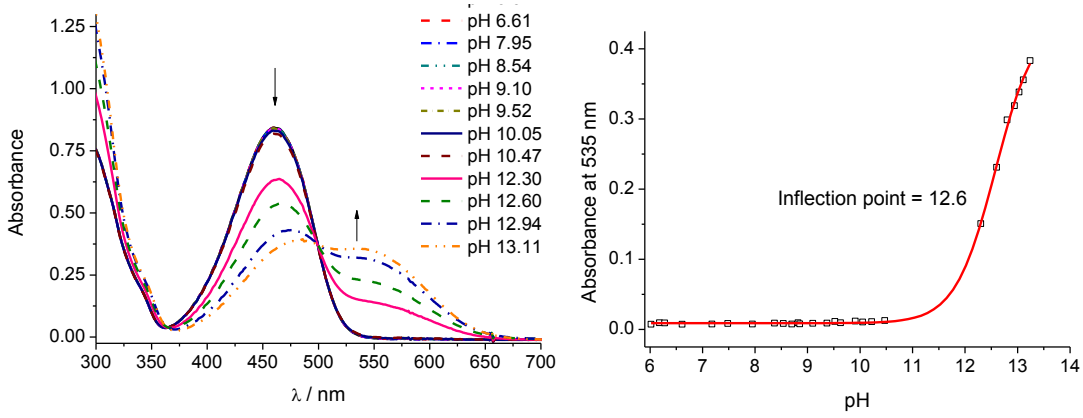

Figure 5.11: UV-vis spectra at varying pH of tpzH (*left*) and absorbance of tpzH at 535 nm against pH (*right*) in water

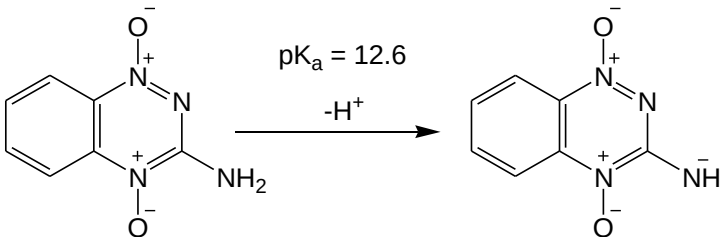

Scheme 5.4: Deprotonation of tpzH

The tpzH-CN ligand displays similar pH-dependent behaviour, showing no change in absorbance until above pH 9. Above this pH, the colour of the solution changes from orange to purple corresponding to a decrease in absorbance at 470 nm and an increase at 560 nm (**Figure 5.8**). Plotting the change in absorbance at 560 nm against pH gives a pK$_a$ value of 10.6(0).

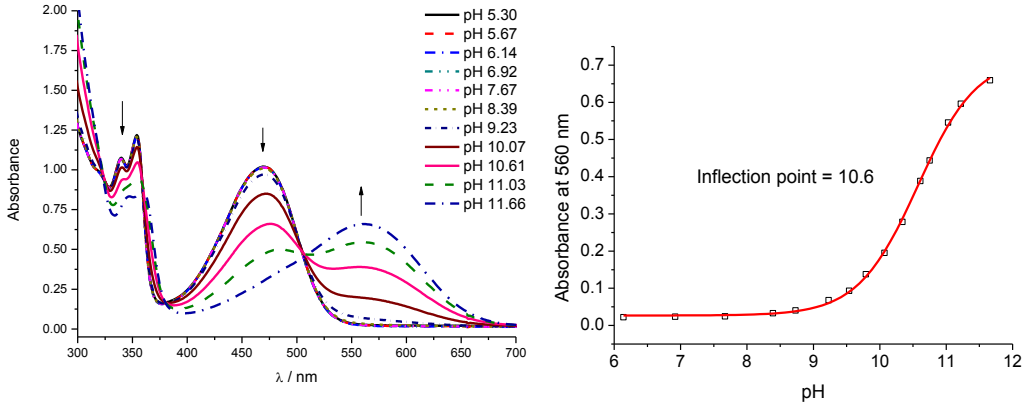

Figure 5.12: UV-vis spectra at varying pH of tpzH-CN (*left*) and absorbance of tpzH-CN at 560 nm against pH (*right*) in water.

Similarly, the absorbance of tpzH-CONH$_2$ remained unaltered until *ca.* pH 10.5, when the absorbance at 430 nm decreases and increases at 490 nm (**Figure 5.9**). However, the change in absorbance is not as pronounced with this ligand as for tpzH and tpzH-CN, with the colour becoming slightly darker rather than turning purple. The increase in absorbance at 490 nm provides a pK$_a$ value of 11.9(1).

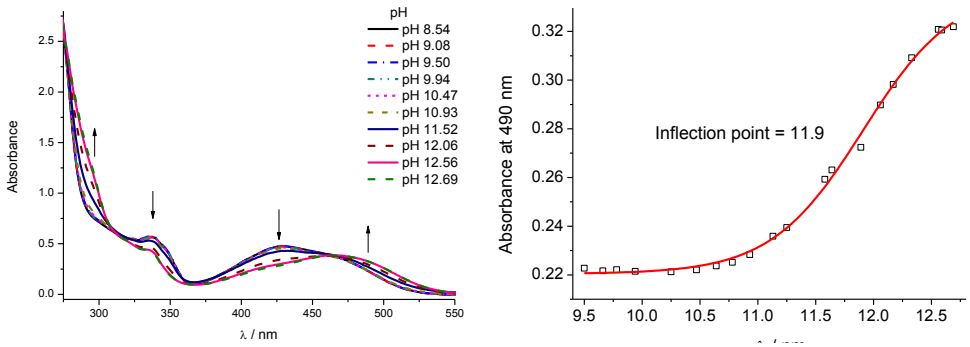

Figure 5.13: UV-vis spectra at varying pH of tpzH-$CONH_2$ (*left*) and its absorbance at 490 nm against pH (*right*) in water

The pK_a values of the *N*-oxide ligands are summarised in **Table 5.2.**

Table 5.2: Summary of pK_a values of the studied *N*-oxide ligands

Ligand	**pk_a**
tpzH	12.6(0.0)
tpzH-CN	10.6(0.0)
tpzH-$CONH_2$	11.9(1)

5.1.2. Determining the pH stability of dipyridylamine complexes

5.1.2.1. Cobalt(II) and zinc(II) complexes of dpHa

With complexes of labile metal centres intended for use in biological systems, it is important to examine their stability in aqueous solution in addition to understanding the protonated state of the ligand. If a complex dissociates in aqueous solution to give an aqua species then it is not suitable to put into biological media where, in addition to water, there are many chelating agents.

Upon addition of OH^- to an acidified solution of [$Co(Cl)_2$(dpHa)] the absorbance at 250, 285 and 320 nm decreases whilst an increase occurs at 262 and 300 nm (**Figure 5.10**). Plotting the change in absorbance at 262 nm against pH produces a single sigmoidal curve with a pK_a value of 6.7, similar to that obtained for dpHa which gave a pK_a value of 6.9.

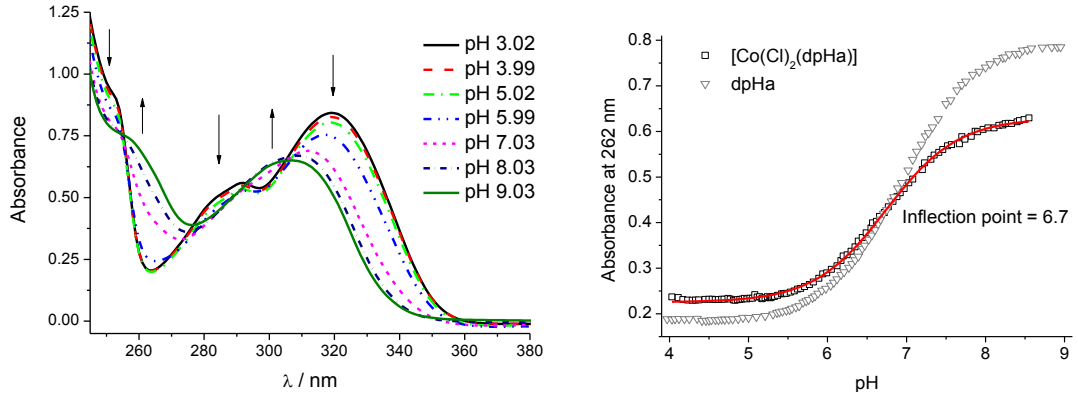

Figure 5.14: UV-vis spectra at varying pH of $[Co(Cl)_2(dpHa)]$ (*left*) and absorbance at 262 nm against pH overlaid with the absorbance of dpHa (*right*) in water

The UV-vis spectra obtained during the titration of $[Zn(Cl)_2(dpHa)]$ show similar behaviour to the cobalt(II) complex (**Figure 5.11**). At pH 3, the solution absorbs at 250, 285 and 320 nm. As the pH increases, the absorbance at these wavelengths decreases whilst the absorbance at 262 and 310 nm increases. Plotting the absorbance of the solution at 262 nm against pH affords a single sigmoidal curve which gives a pK_a value of 6.7(0).

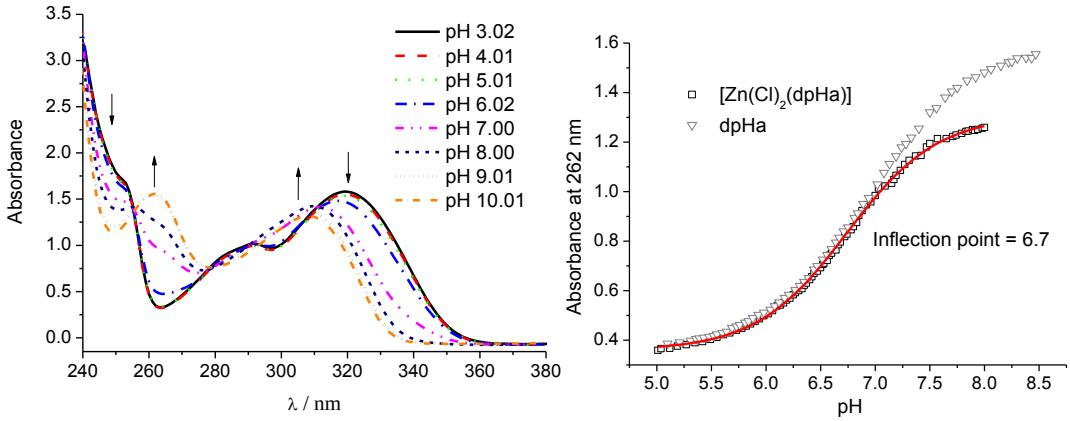

Figure 5.15: UV-vis spectra at varying pH of $[Zn(Cl)_2(dpHa)]$ (*left*) and absorbance at 262 nm against pH overlaid with the absorbance of dpHa (*right*) in water

When titrating $[Co(Cl)_2(dpHa)]$ it was observed that above pH 8.5, a brown precipitate formed and when titrating $[Zn(Cl)_2(dpHa)]$ a white precipitate formed above pH 7.5. It was suspected that these precipitates were the result of the formation of metal hydroxo species so to try and confirm this, the respective metal chloride results were titrated and compared to that of the complexes (**Figure 5.12**).

The curves produced from the metal chloride salts have similar inflection points to those obtained from the second pK_a process of the complexes, supporting the hypothesis that the deprotonation of aqua ligands is being observed.

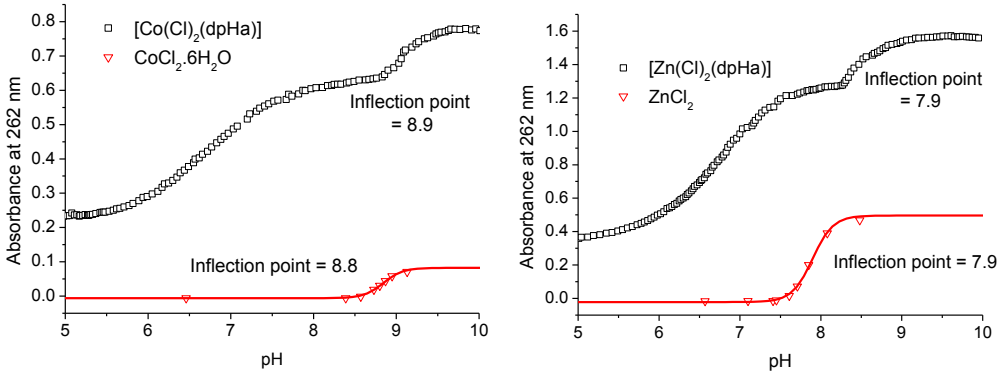

Figure 5.16: Overlay of $[Co(Cl)_2(dpHa)]$ and $CoCl_2.6H_2O$ (*left*) and overlay of $[Zn(Cl)_2(dpHa)]$ and $ZnCl_2$ (*right*) in water

5.1.2.2. Copper(II) complexes of dpHa

The UV-vis spectra of $[Cu(Cl)_2(dpHa)]$ shows that as the pH is increased from 2.5 to 6.3, there is an increase in absorbance at 300 nm and a decrease at 318 nm (**Figure 5.13**). Above pH 6, the absorbance at 300 and 313 nm increases.

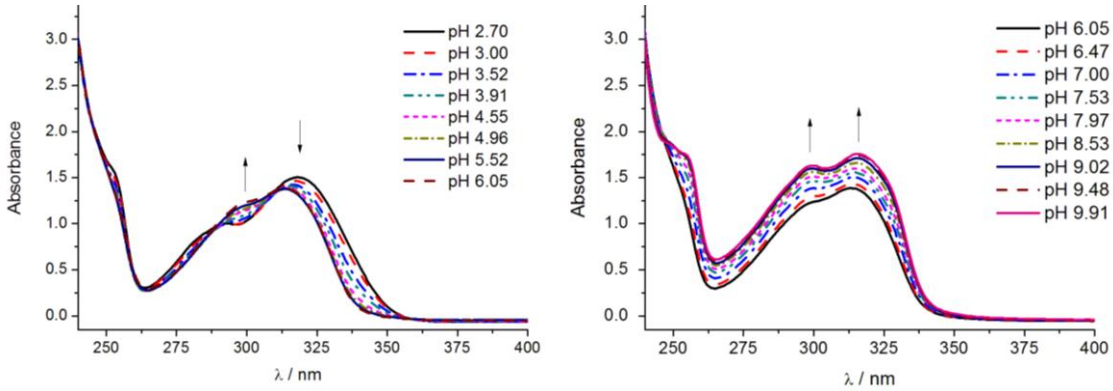

Figure 5.17: UV-vis spectra at varying pH of $[Cu(Cl)_2(dpHa)]$ between pH 2.5 and pH 6.0 (*left*) and between pH 6.0 and pH 10.0 (*right*) in water

Plotting the absorbance at 300 nm against pH for the first process between *ca.* pH 2.5 and 6.0 provides a single sigmoidal curve which gives a pK_a value of 4.0(0)

(**Figure 5.14**). The absorbance between pH 5.5 and 10 gives a second sigmoidal curve with a pK_a of 7.4(0).

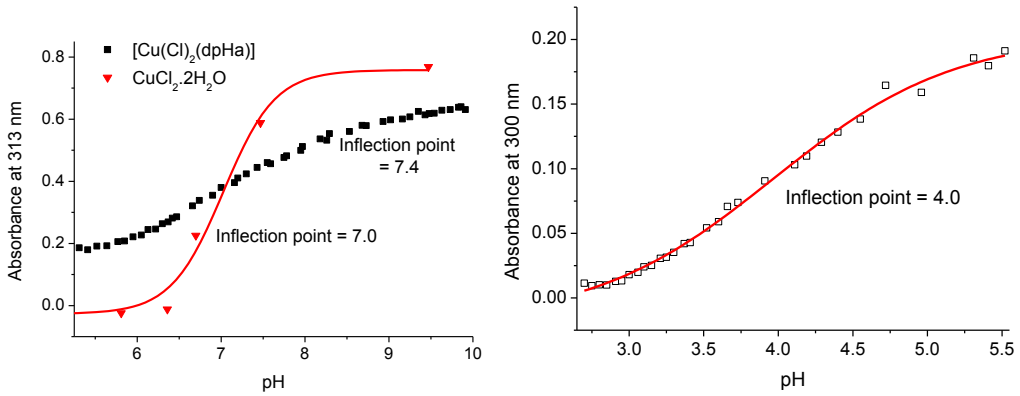

Figure 5.18: Absorbance of $[Cu(Cl)_2(dpHa)]$ at 300 nm against pH between pH 2.5 and 6 (*left*) and between pH 5.5 and 10 (*right*) in water

As the second process, which occurs above pH 5.5, appears to have no isosbestic point, there was concern that the change in absorbance was due to a form of ligand exchange such as an alteration in the number of coordinated chlorides rather than a deprotonation. To rule out this possibility, $[Cu(NO_3)_2(dpHa)]$ was titrated, using HNO_3 as the acid to acidify the solution rather than HCl. In the absence of chloride, a similar change in absorbance is observed. As the pH is increased from pH 3, the absorbance at 317 nm decreases, whilst an increase is observed at 299 nm.

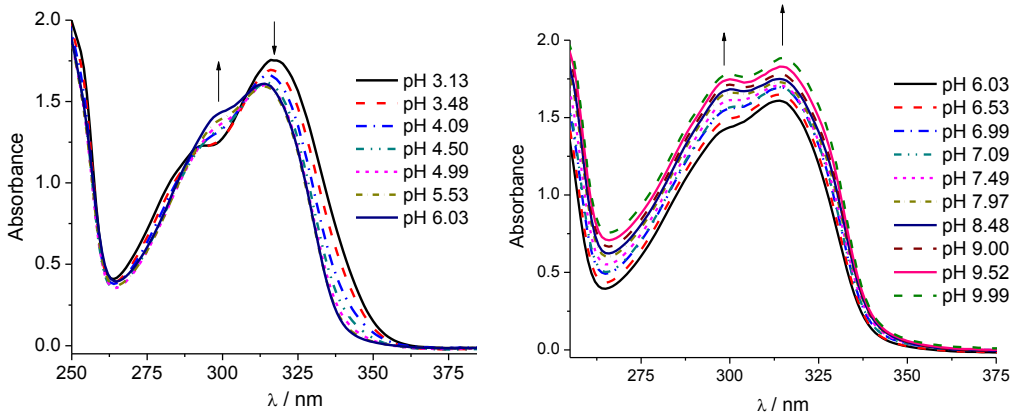

Figure 5.19: UV-vis spectra at varying pH of $[Cu(NO_3)_2(dpHa)]$ between pH 3 and 6 (*left*) and between pH 6 and 10 (*right*) in water

The absorbance at 300 nm between pH 3 and 5 affords a sigmoidal curve which gives a pK_a value of 3.7(0).

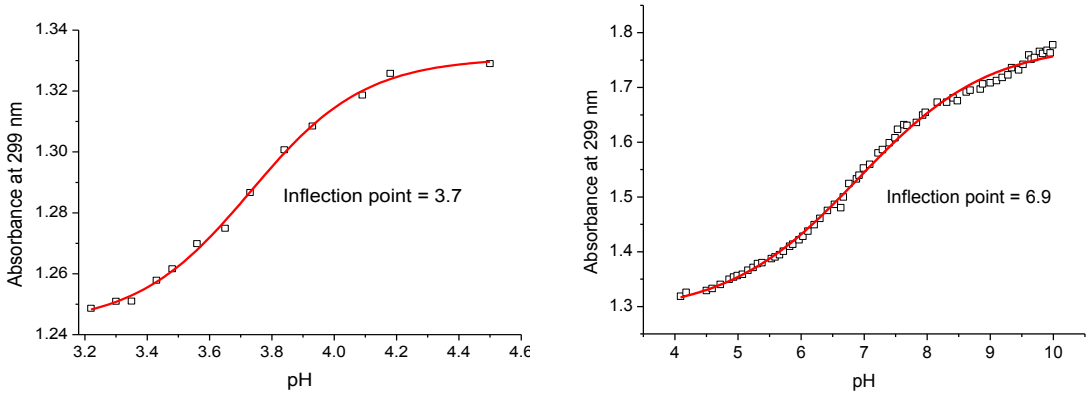

Figure 5.20: Absorbance of $[Cu(NO_3)_2(dpHa)]$ at 299 nm between pH 3 and 5 (*left*) and between pH 4 and 10 (*right*) in water

Both of the copper(II) complexes display the increased absorbance above pH 6 which corresponds to a process which has no isosbestic point. As this was found to occur in the absence of chloride ions, it is not a process which can be attributed to a change in the number of chlorides coordinated to the copper(II) centres.

The similarity between the spectra of all three of the metal(II) complexes with that of dpHa at pH 3 suggests that at this pH, the dpHa ligand has dissociated (**Figure 5.20**). At pH 7 and 9, the complexes of cobalt(II) and zinc(II) still have UV-vis spectra which match that of the free ligand, which along with having similar pK_a values to free dpHa implies that these metal(II) complexes dissociate in aqueous solution.

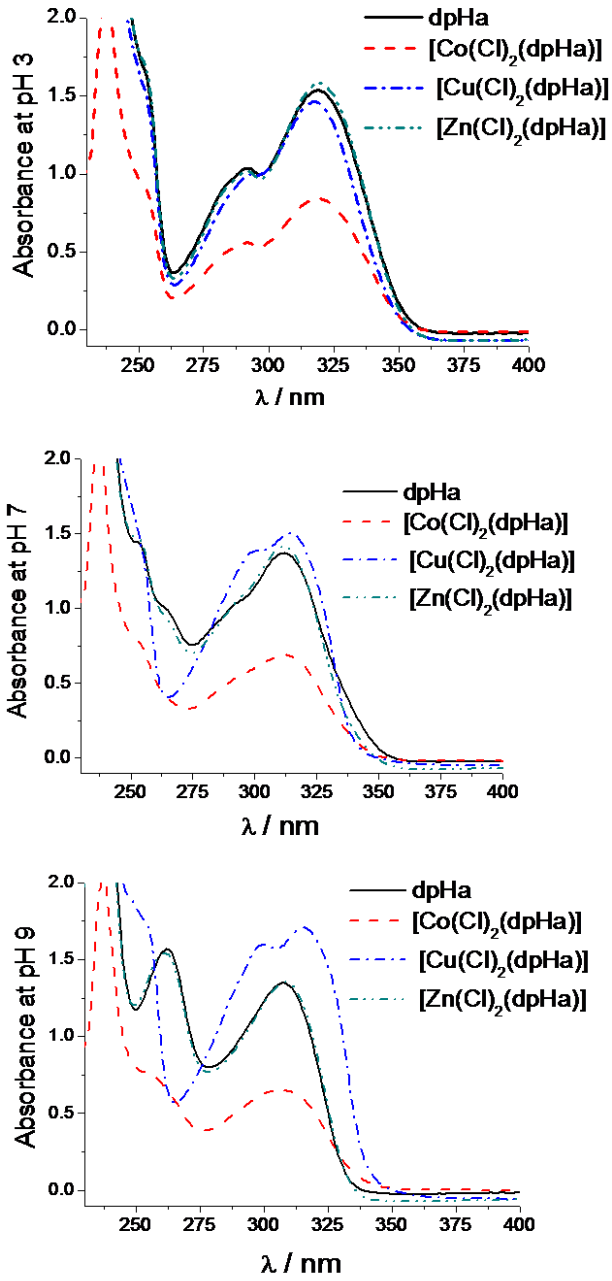

Figure 5.21: Overlay of the aqueous UV-vis spectra of dpHa, $[Co(Cl)_2(dpHa)]$, $[Cu(Cl)_2(dpHa)]$ and $[Zn(Cl)_2(dpHa)]$ at pH 3, 7 and 9

As the two copper(II) complexes both have UV-vis spectra which, above pH 5, differ to that of the free ligand, it suggests that the dpHa remains coordinated in aqueous solution. This trend in stability of the copper(II) complexes over those of the cobalt (II) and zinc(II) is described by the Irving Williams series, which shows that the formation constants of metal(II) complexes is in aqueous solution increases across

the first row of d-block with copper(II) having the greatest formation constant owing to additional stability arising from Jahn-Teller distortion.[181]

5.1.2.3. Copper(II) complexes of dpRa

The alkylated copper(II) complexes were titrated in order to help identify the protonation process observed with the copper(II) dpHa complexes, as the alkylation removes the possibility of deprotonation at the central amine.

When the pH of a solution of $[Cu(Cl)_2(dpma)$ was increased from pH 3, it was observed that the absorbance at 310 nm blue-shifted to 302 nm at pH 5.5 (**Figure 5.25**). Above pH 5, the absorbance at 302 nm increased in a manner similar to that observed for the copper(II) dpHa complexes.

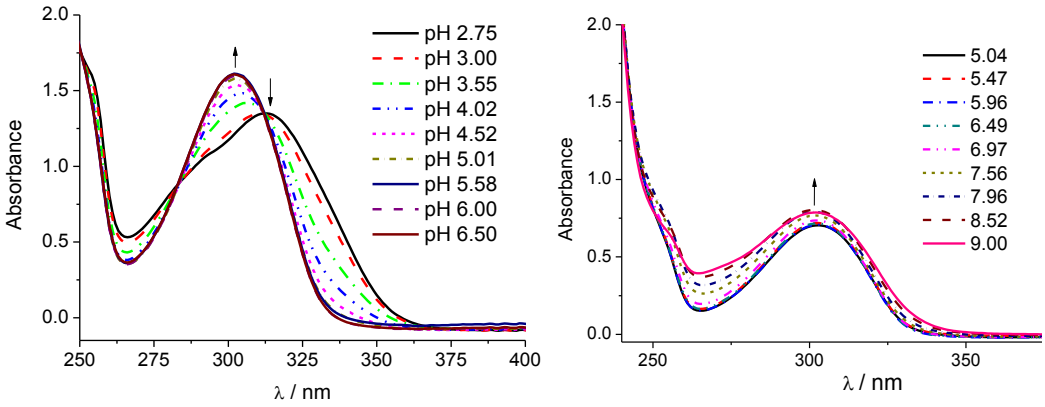

Figure 5.22: UV-vis spectra at varying pH of $[Cu(Cl)_2(dpma)]$ between pH 2.5 and pH 5.5 (*left*) and between pH 5 and pH 9 (*right*) in water

Both of these processes can be fitted to a single sigmoidal curve to afford pK_a values of 3.5(0.0) and 7.4(0.0) (**Figure 5.26**).

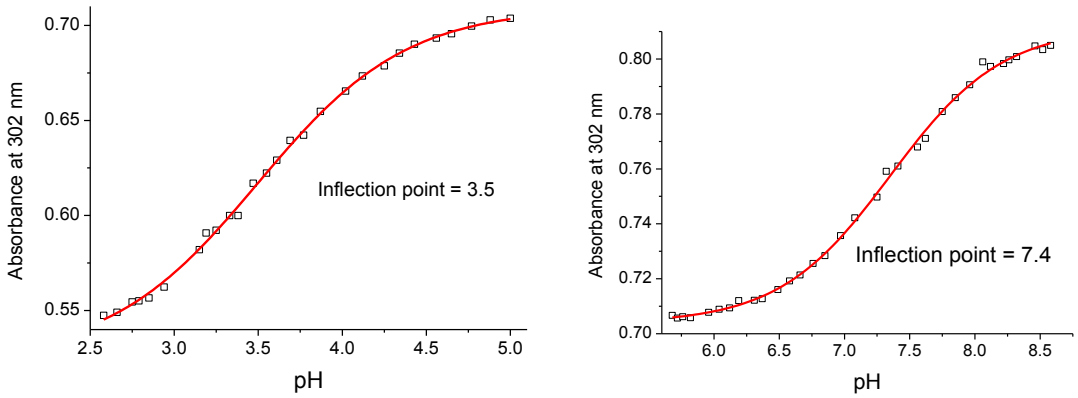

Figure 5.23: Absorbance of $[Cu(Cl)_2(dpma)]$ at 302 nm against pH between pH 2.5 and 5.5 (*left*) and between pH 5.5 and 9 (*right*) in water

As the pH of a solution of $[Cu(Cl)_2(dpea)]$ is increased from pH 3, the absorbance at 316 nm decreases as the absorbance at 302 nm increases (**Figure 5.27**). Beyond pH 5, the absorbance increases but no isosbestic point is found upon overlaying the spectra.

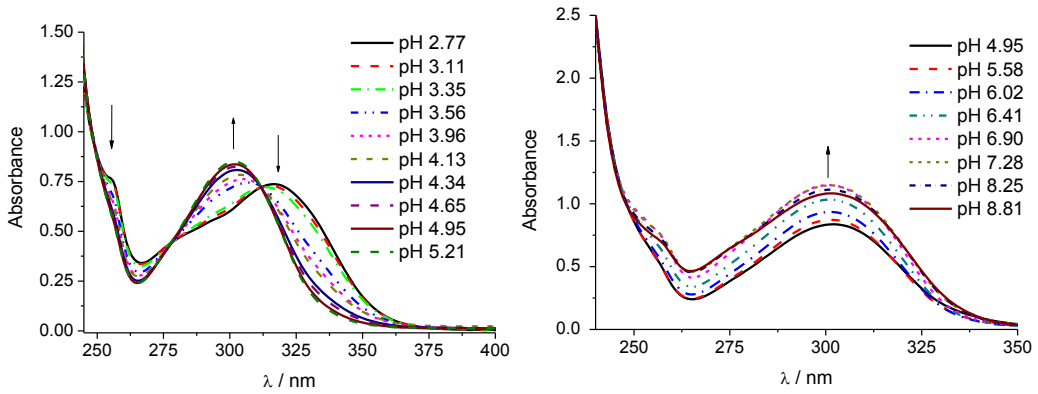

Figure 5.24: Absorbance of $[Cu(Cl)_2(dpea)]$ between pH 3 and 5 (*left*) and pH 5 and 9 (*right*) in water

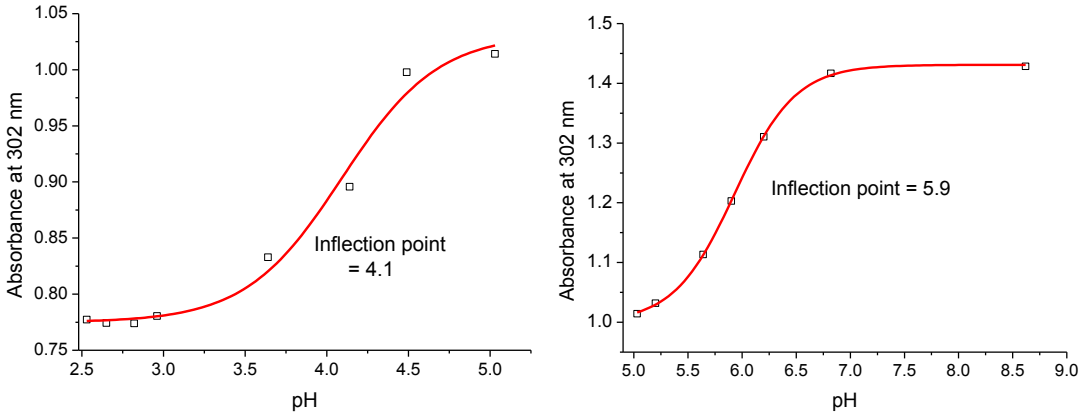

Figure 5.25: Absorbance of $[Cu(Cl)_2(dpea)]$ at 302 nm against pH between n pH 2.5 and 5 (*left*) and pH 5 and 9 (*right*) in water

A sigmoidal curve can be fitted to a curve from both processes obtained by plotting the absorbance at 302 nm against pH, affording pK_a values of 4.1(1) and 5.9(0) (**Figure 5.28**).

Table 5.3: Summary of pK_a values obtained by titrating Cu(II) complexes of dpRa ligands.[182]

Complex	**pK_a (1)**	**pK_a (2)**
$CuCl_2.2H_2O$		7.0(1)
$[Cu(dpHa)(H_2O)_2]^{2+}$		6.74
$[Cu(Cl)_2(dpHa)]$	4.0(0.0)	7.4(0.0)
$[Cu(NO_3)_2(dpHa)]$	3.7(0.0)	6.9(0.0)
$[Cu(Cl)_2(dpma)]$	3.5(0.0)	7.4(0.0)
$[Cu(Cl)_2(dpea)]$	4.1(1)	5.9(0.0)

All the copper(II) dipyridylamine type complexes were observed to undergo two processes; one between pH 3 and 4 and the other between pH 6 and 7.5. The second process has a similar pK_a to that previously reported for the deprotonation of an aqua ligand in $[Cu(dpHa)(H_2O)_2]^{2+}$.[182] This, along with copper(II) chloride being observed

to under a deprotonation process at 7.0(1) suggests that the complexes all undergo a certain degree of aquation when in aqueous solution. The similarity of the UV-vis spectra at lower pH values of the complexes when compared to their respective free ligand suggests that at this pH, the complex is dissociated.

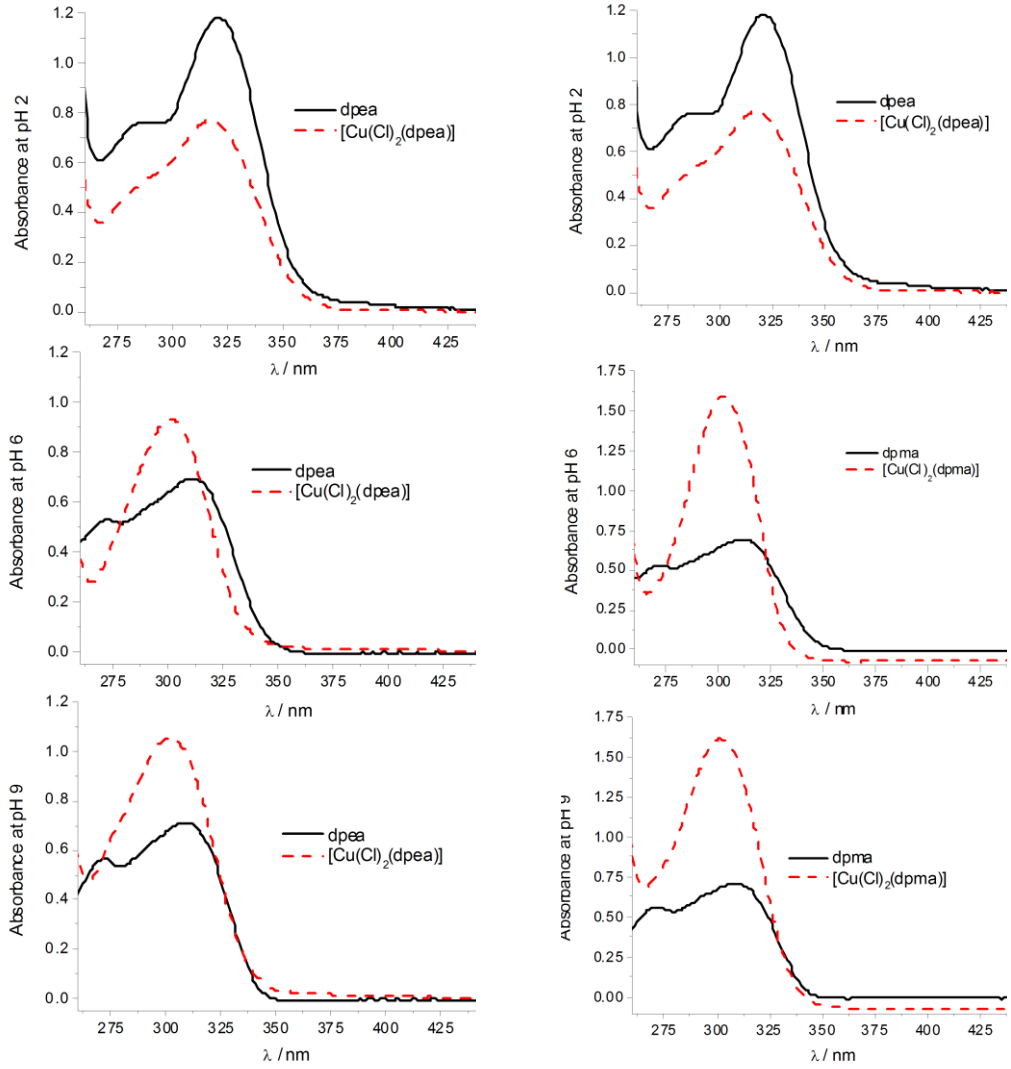

Figure 5.26: Overlay of the aqueous UV-vis spectra of the dpea (*left*) and dpma (*right*) with their copper(II) complexes at pH 3 (*from top*), pH 6 and pH 9

5.1.2.4. Cobalt(III) complexes of dpRa ligands

As complexes of cobalt(III) are considered to be kinetically inert, it was expected that the complexes would be stable to ligand exchange.

As the pH is increased from 2.5 to 5, the absorbance of $[Co(CO_3)(dpHa)_2]^+$ at 300 nm increases (**Figure 5.29**). Above pH 8, the solution becomes darker in colour as the absorbance at 300 nm decreases whilst the absorbance at 377 nm increases.

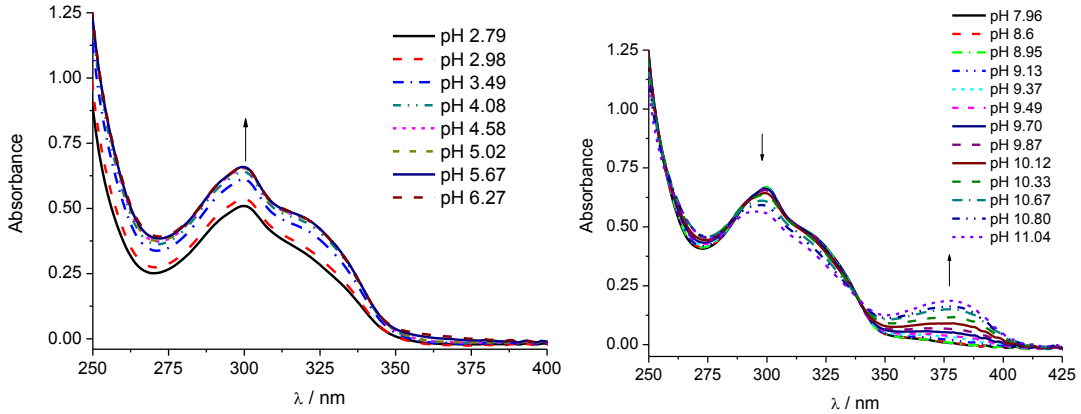

Figure 5.27: pH dependence of the absorption spectra of $[Co(CO_3)(dpHa)_2]^+$ between pH 2.5 and pH 6.5 (*left*) and between pH 8 and pH 11 (*right*) in water

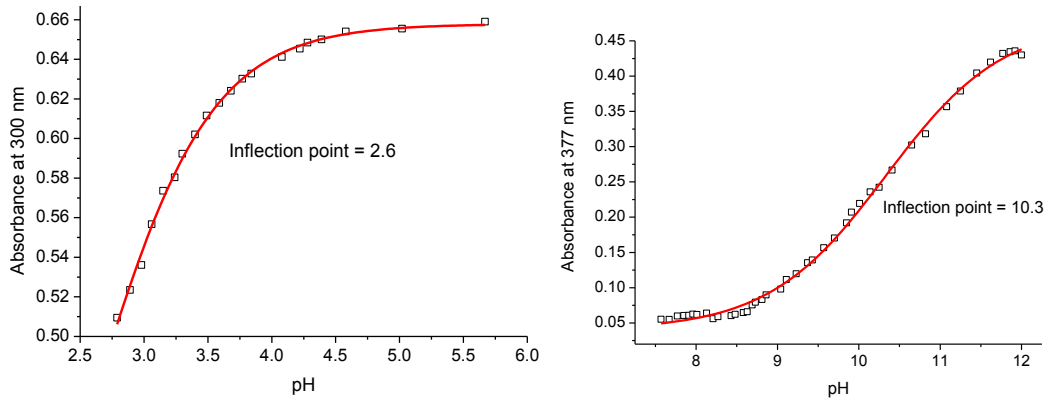

Figure 5.28: Absorbance of $[Co(CO_3)(dpHa)_2]^+$ against pH between pH 2.5 and pH 6 (*left*) and between pH 7.5 and pH 12 (*right*) in water

With the *N*-methylated complex $[Co(Cl)_2(dpma)_2]^+$, no change in absorbance is observed between pH 2 and 10 (**Figure 5.31**).

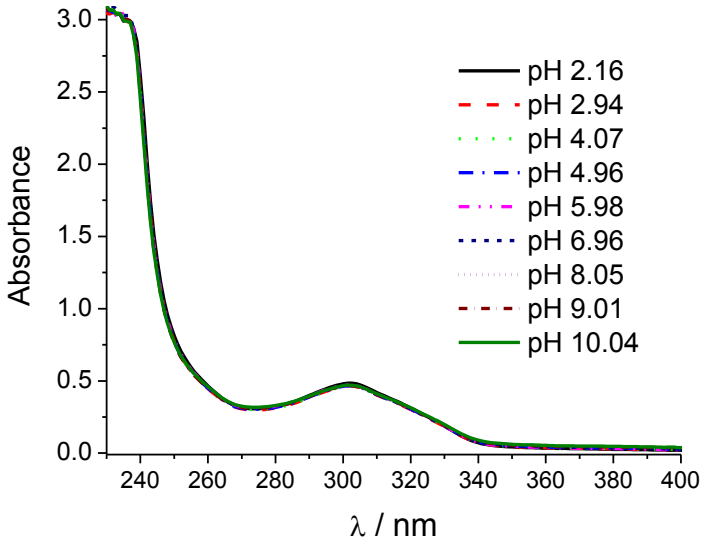

Figure 5.29: UV-vis spectra at varying pH of $[Co(Cl)_2(dpma)_2]^+$ in water

The cobalt(III) dpHa complex has, in addition to the two secondary amine ligands which can undergo deprotonation, a carbonato ligand which can be protonated to form bicarbonate. There are known examples of cobalt(III) bicarbonate complexes where the other ligands are pyridyl in character which were found to be kinetically stable under acidic conditions.[183, 184] Although spectral evidence was not obtained to confirm the formation of a bicarbonate complex, the stability the complex showed in acidic solution as monitored by ^{1}H NMR spectroscopy is similar to that of reported cobalt(III) bicarbonate complexes which have pyridyl ligands (**Figure 5.30**). It can be seen that after 48 hours, the peaks start to broaden, and by 72 hours, the sample contains a mixture of species. Although spectral evidence was not obtained to confirm the formation of a bicarbonate complex, the stability the complex showed in acidic solution as monitored by ^{1}H NMR spectroscopy is similar to that of reported cobalt(III) bicarbonate complexes which have pyridyl ligands (**Figure 5.30**). It can be seen that after 48 hours, the peaks start to broaden, and by 72 hours, the sample contains a mixture of species.

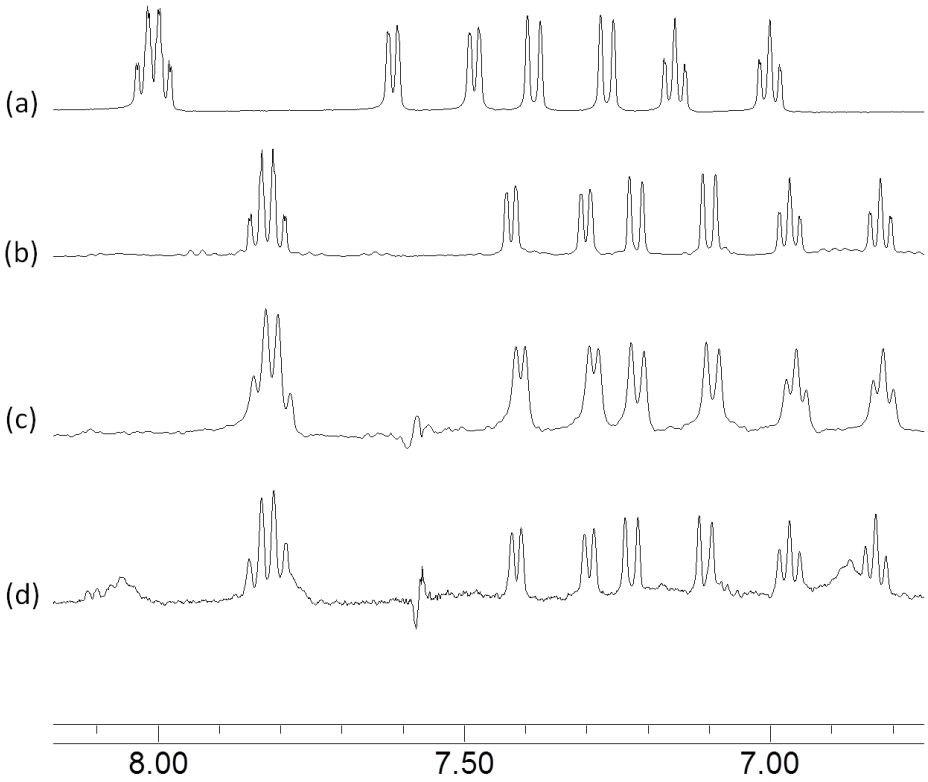

Figure 5.30: ^{1}H NMR (400 MHz, D_2O) of $[Co(CO_3)(dpHa)_2]^+$ before addition of HCl (*spectrum a*), then at time intervals after acidification; 24 hours (*spectrum b*), 48 hours (*spectrum c*) and 72 hours (*spectrum d*).

5.1.3. Titrations of metal(II) homoleptic *N*-oxide complexes

The *bis*-*N*-oxide complexes were found to be insoluble in water. Due to the poor solubility of these complexes, it was not possible to have the solutions concentrated enough to enable accurate absorbance measurements of the band at *ca.* 520 nm of the coordinated ligand. The homoleptic complexes of all three *N*-oxide ligands had to be pre-dissolved in DMSO in-order to prepare their aqueous solutions. It was found that if starting at an acidic pH, only the free ligand was present but as the pH was increased, the *bis*-*N*-oxide complex formed and precipitated out of solution. The titrations of these complexes were subsequently carried out starting with a higher pH value titrating downwards to a more acidic pH. It was also found that the complexes of cobalt(II) and zinc(II) dissociated in aqueous solution of any pH value, evident by only the absorbance of the uncoordinated *N*-oxide ligand being observed. Consequently only titrations of $[Cu(tpz\text{-}R)_2]$ complexes are discussed.

Addition of acid to a neutral solution of $[Cu(tpz)_2]$ causes the absorbance at 534 nm to decrease whilst the absorbance at 274, 354 and 460 nm increases (**Figure 5.31**). A single sigmoidal curve can be fitted to the absorbance at 460 nm when it is plotted against pH, providing a pK_a value of 2.6(0).

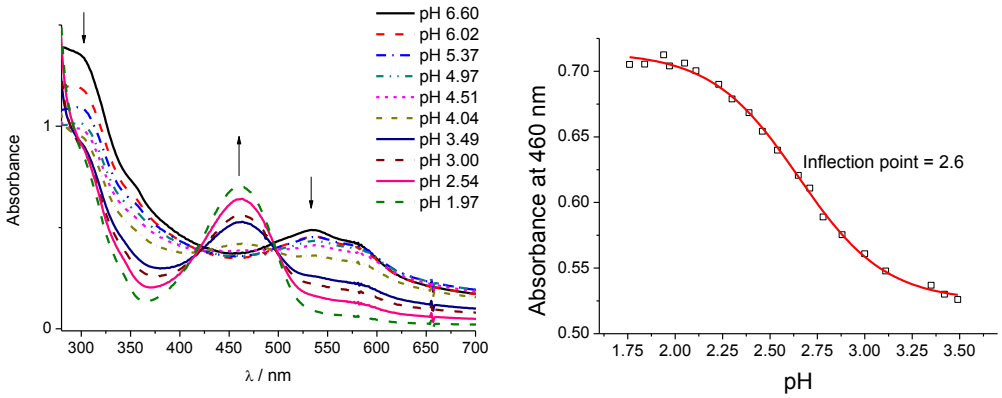

Figure 5.31: UV-vis spectra at varying pH of $[Cu(tpz)_2]$ (*left*) and absorbance at 460 nm plotted against pH (*right*) in water

When the pH of a solution of [Cu(tpz-CN)(dpHa)]Cl is decreased from pH 7, the absorbance at 275 and 470 increases whilst decreasing at 550 nm. A single sigmoidal curve can be fitted to the absorbance at 275 nm when it is plotted against pH, providing a pK_a value of 2.4(0) (**Figure 5.32**).

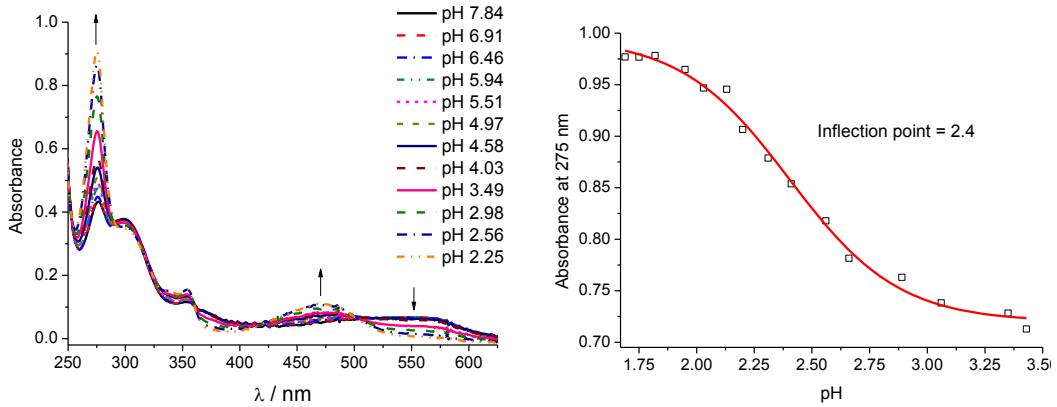

Figure 5.32: UV-vis spectra at varying pH of $[Cu(tpz\text{-}CN)_2]$ (*left*) and absorbance at 470 nm plotted against pH (*right*) in water

$[Cu(tpz\text{-}CONH_2)_2]$ shows similar behaviour to the other complexes when the pH of the solution is altered. As the pH is decreased, the absorbance at 296 and 530 nm decreases as the absorbance at 265 and 426 nm increases (**Figure 5.33**). A single

sigmoidal curve can be fitted to the absorbance at 265 nm when it is plotted against pH, providing a pK_a value of 2.2(1).

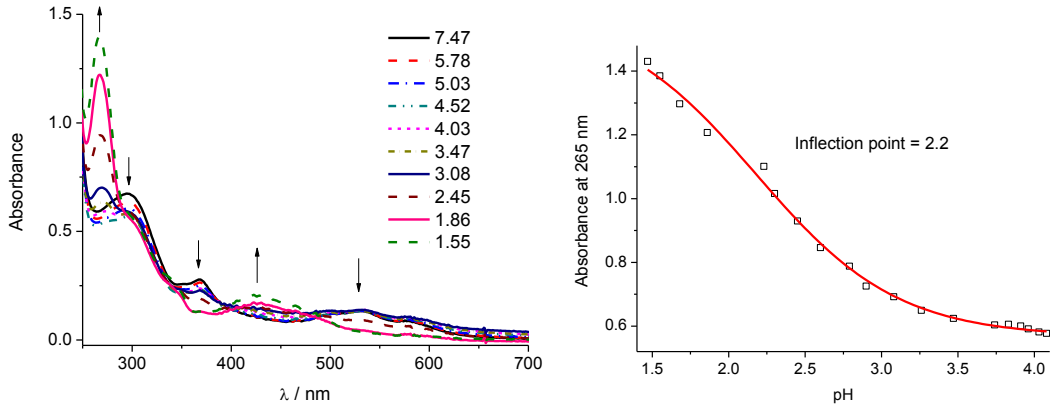

Figure 5.33: UV-vis spectra at varying pH of [Cu(tpz-$CONH_2$)$_2$] (*left*) and absorbance at 265 nm plotted against pH (*right*) in water

It can be seen from **Table 5.4**, it can be seen that copper(II) *bis*-*N*-oxide complexes of this type dissociate when the pH is lowered to *ca*. 2.4. This dissociation is presumably caused by the amine of the *N*-oxide ligand becoming reprotonated, causing formation of the aqua copper(II) complex to become more favourable (**Scheme 5.5**).

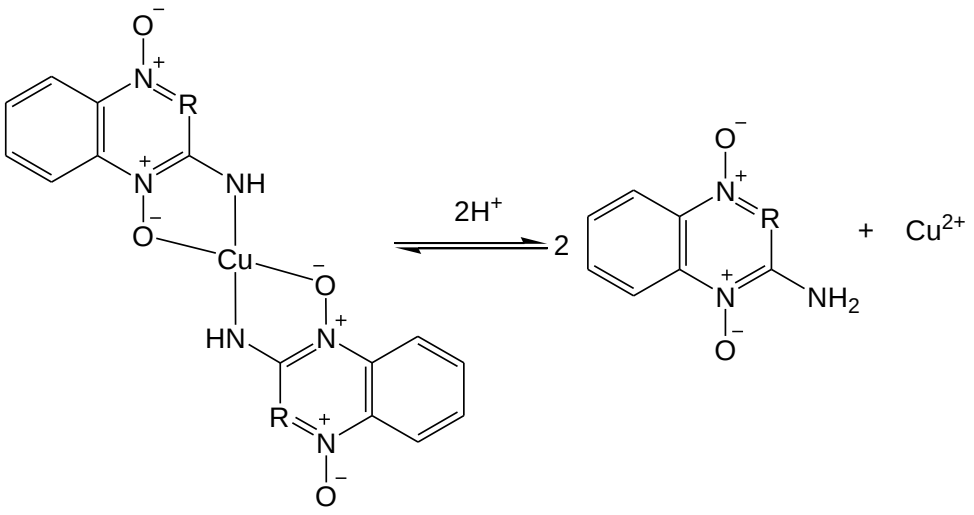

Scheme 5.5: Dissociation of the *N*-oxide ligand which occurs at *ca*. pH 2 – 2.5

Table 5.4: pH values at which the [Cu(tpz-R)$_2$] complexes dissociate

Complex	Dissociation pH
[Cu(tpz)$_2$]	2.6(0.0)
[Cu(tpz-CN)$_2$]	2.4(0.0)
[Cu(tpz-CONH$_2$)$_2$]	2.2(1)

5.1.4. Titrations of heteroleptic metal *N*-oxide complexes

5.1.4.1. Titrations of heteroleptic metal(II) *N*-oxide complexes

Out of the metal(II) heteroleptic complexes, only those of tpzH were found to be readily water soluble. However, these complexes were all found to be readily soluble in MeOH so were pre-dissolved in this solvent before being added to the aqueous solution, enabling their aqueous chemistry to be studied It was again found that only the copper(II) complexes remained associated in aqueous solution. It was found that the copper(II) complexes formed red coloured solutions until the required amount of acid was added for the complex to dissociate, where upon the solution turned yellow due to the absorbance of the free ligand (**Figure 5.34**).

Figure 5.34: Aqueous solution of [Cu(tpz-CN)(dpHa)]Cl (*left*) and after addition of acid which causes the *N*-oxide ligand to dissociate (*right*).

When the pH of a neutral aqueous solution of [Cu(tpz)(dpHa)]Cl is decreased, the absorbance at 463 nm increases whilst the absorbance at 520 nm decreases (**Figure 5.35**). Plotting the absorbance at 463 nm against pH affords a pK_a value of 5.4.

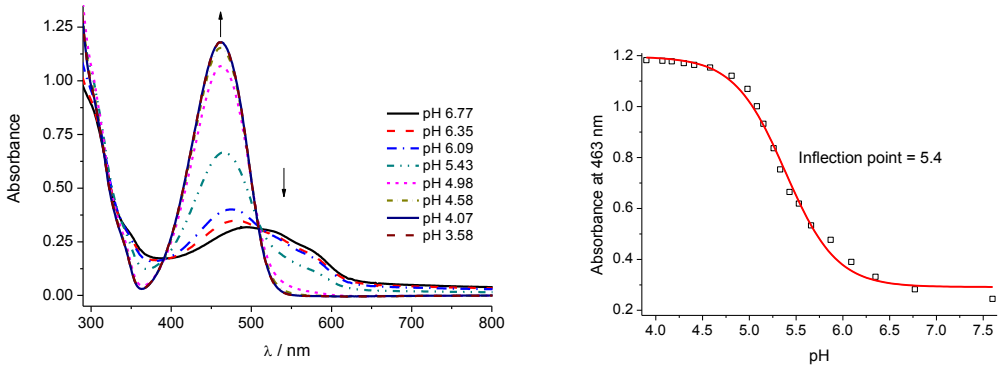

Figure 5.35: UV-vis spectra at varying pH of [Cu(tpz)(dpHa)]Cl (*left*) absorbance at 463 nm plotted against pH (*right*) in water

With [Cu(tpz-CN)(dpHa)]Cl, the absorbance at 470 nm increases and decreases at 505 nm when the pH of a neutral solution is lowered (**Figure 5.36**). Fitting a sigmoidal curve to the absorbance at 470 nm plotted against pH affords a pK_a value of 5.0(0).

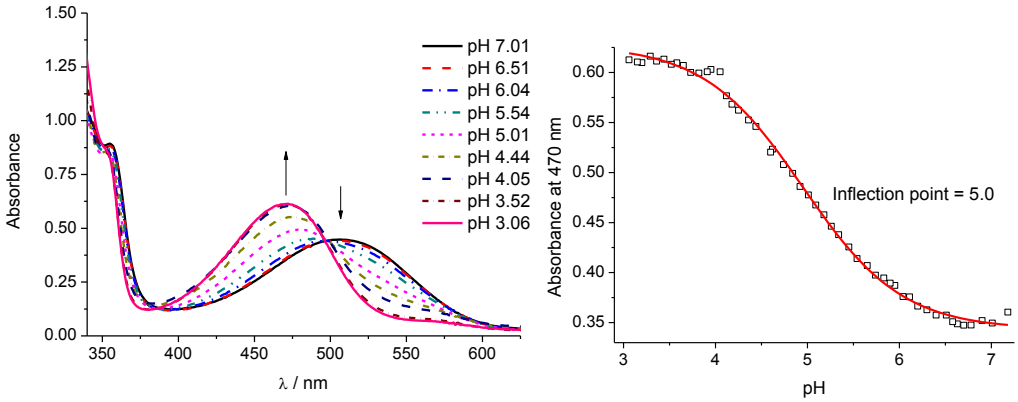

Figure 5.36: UV-vis spectra at varying pH of [Cu(tpz-CN)(dpHa)]Cl (*left*) and absorbance at 470 nm against pH (*right*) in water

At neutral pH, [Cu(tpz-$CONH_2$)(dpHa)]Cl absorbs at 467 nm with a shoulder at 533 nm. As the pH is decreased, the absorbance at these wavelengths decreases as the absorbance at 430 nm increases (**Figure 5.37**). Fitting a sigmoidal curve to the absorbance at 430 nm plotted against pH affords a pK_a value of 5.8(0).

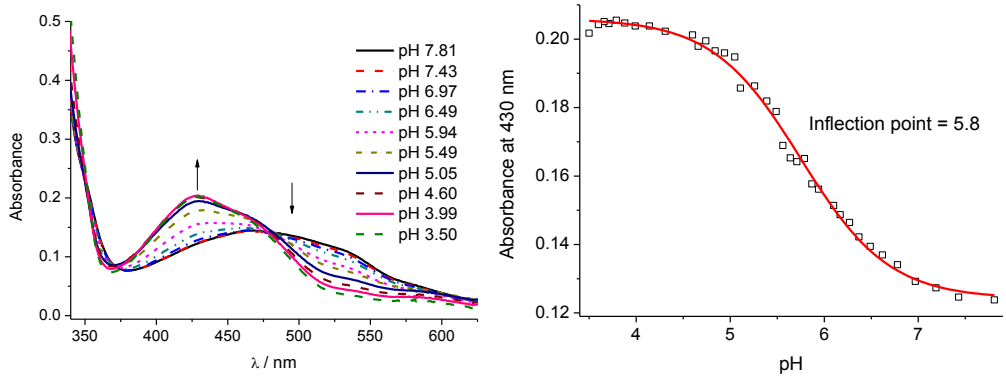

Figure 5.37: UV-vis spectra at varying pH of [Cu(tpz-$CONH_2$)(dpHa)]Cl (*left*) and absorbance at 430 nm plotted against pH (*right*) in water

Table 5.5 shows that the *N*-oxide ligand dissociates from complexes of the type $[Cu(tpzR)(dpHa)]^+$ between pH 5 and 6. Less acidic conditions are therefore required to facilitate dissociation of the *N*-oxide ligand from the heteroleptic complex than from the homoleptic complex which dissociated between pH 2 and 3.

Table 5.5: pH values at which the [Cu(tpz-R)(dpHa)]Cl complexes dissociate

Complex	**Dissociation pH of the *N*-oxide ligand**
[Cu(tpz)(dpHa)]Cl	5.4(0)
[Cu(tpz-CN)(dpHa)]Cl	5.0(0)
[Cu(tpz-$CONH_2$)(dpHa)]Cl	5.8(0)

5.1.4.2. Titrations heteroleptic cobalt(III) *N*-oxide complexes

The cobalt(III) heteroleptic complexes would be expected to be kinetically stable against ligand dissociation upon acidification. No change in absorption was noticed with any of the three cobalt(III) complexes until above *ca.* pH 9.5. Above this pH, a shoulder on the band at *ca*. 500 nm would form at 600 nm (**Figure 5.38**). This process was found to be non-reversible as the addition of acid did not result in a return to the UV-vis spectrum of the complex below pH 9.

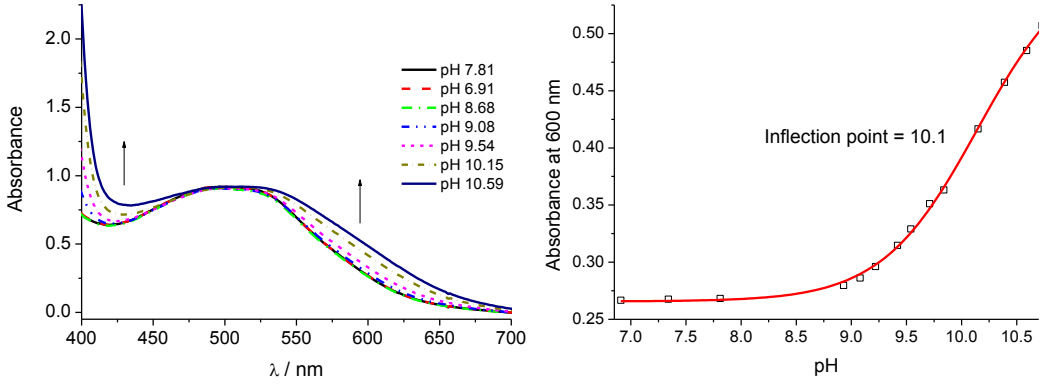

Figure 5.43: UV-vis spectra at varying pH of $[Co(tpz)(dpHa)_2]^{2+}$ (*left*) and absorbance at 600 nm plotted against pH (*right*) in water

5.1.5. Conclusions

In terms of solution stability, all of the cobalt(II) and zinc(II) complexes of both dpRa and tpzH-R ligands were found to dissociate in aqueous solution. All of the copper(II) complexes investigated were found not to dissociate in aqueous solution. This increase in stability agrees with the trend in stability of metal(II) complexes described by the Irving-Williams series, which shows a general increase in ligand affinity moving across M^{2+} first row d-block ions from left to right.[8] The cobalt(III) complexes were found to be stable in aqueous solution due to the characteristic kinetic and thermodynamic stability of this ion's +3 oxidation state.

A deprotonation process was observed to occur in uncoordinated dpHa with a pK_a of 6.9, which was found to involve the loss of one proton. It is still unclear if this process corresponds to the deprotonation of the amine or the pyridinium ion. Alkylation of the central amine with a methyl or ethyl substituent resulted provided dpRa type ligands which were observed to undergo a deprotonation process with a pK_a of 5.3. With the dpRa type ligands, it was observed that altering the substituent on the central amine affected the pK_a of the ligand's pyridinium ion. It was found that the altered pK_a might be attributed to the influence exerted by the steric bulk of the amine's substituent on the interplanar angle between the two pyridyl rings. As the steric bulk of the substituent is increased, the planar angle between the two pyridyl rings is increased, resulting in poorer stabilisation of the pyridinium proton by hydrogen-bonding to the non-protonated pyridyl nitrogen.

The amine groups of the *N*-oxide ligands were found to have pK_a values above pH 10. The deprotonation of tpzH and tpzH-CN resulted in dramatic changes to their UV-vis absorbance spectra correlating with a colour change from orange-yellow to deep purple. The purple coloured species was found to form an orange-yellow coloured species which had different UV-vis spectra to the original ligands. With the tpzH-CN ligand, the new species has a similar UV-vis spectrum to that of tpzH-$CONH_2$, indicating that the nitrile group may have undergone hydrolysis under the basic conditions.

The copper(II) dpRa complexes were found to each undergo two proton-dependent processes; one at *ca*. pH 3.5 and the second between pH 6 and 7.5. $[Cu(dpHa)(H_2O)_2]^{2+}$ has been previously reported to undergo a process with a pK_a at 6.7 which was attributed to the deprotonation an aqua ligand.[9] As $CuCl_2$ was observed to undergo a process with a pK_a value of 7, the second process observed with these complexes seems likely to be the deprotonation of an aqua ligand coordinated to the copper(II) centre through the displacement of a chloride ligand.

The homoleptic tpzH-R copper(II) complexes were found to be more stable towards acidic conditions than the heteroleptic complexes. The *N*-oxide ligands were observed to dissociate from the homoleptic complexes at *ca.* pH 2.5, whereas dissociation from the heteroleptic complexes occurred at *ca.* pH 5.5. The latter is a more biologically relevant pH, being near to that which can occur in the extracellular environment of hypoxic tumour cells. The difference between the acid stability of the homoleptic and heteroleptic complexes suggests that the interaction between the metal centre and *N*-oxide ligand differs upon incorporation of the dpHa ligand.

5.2. Cyclic Voltammetry

The technique of cyclic voltammetry allows for the measurement of reduction and oxidation potentials of a compound, but also a means of exploring their reversibility. The experiment uses a cell which contains three electrodes; a reference electrode which carries out the measurement, a working electrode to vary potential and an auxiliary electrode which completes the electrical circuit. The potential at the working electrode is swept from the starting potential, E_0, at which no process takes place, to a second potential, E_1, which is beyond the potential of the reaction occurring at the electrode. Upon reaching E_1, the potential is then returned to the E_0

starting potential. The current across the working electrode is measured as a function of the potential. There are several forms of electron transfer reactions which can take place at the electrode, which may be reversible, quasi-reversible or irreversible (**Figure 5.39**).

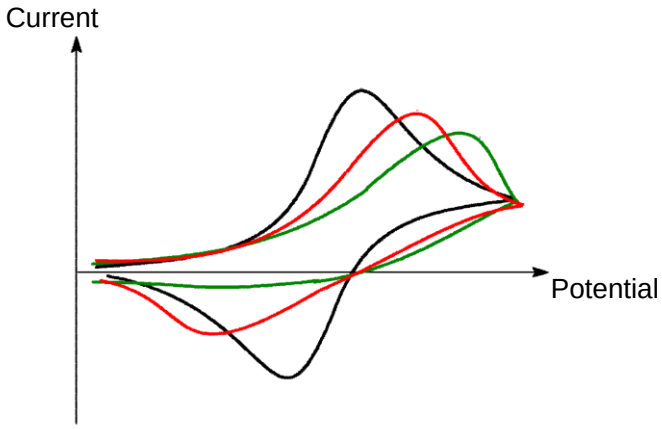

Figure 5.39: Representative cyclic voltammograms of a reversible process (*black*), a quasi-reversible process (*red*) and an irreversible process (*green*)

For a reversible reaction, the electron transfer product is at the electrode on the reverse scan, so is able to undergo the reverse process and a change of current equal to that of the forward scan is observed. A true reversible system is rarely observed, and the current on the reverse wave is less than that on the forward scan so is said to be a quasi-reversible process. The two main factors which govern the reversibility of an electron transfer process are the kinetics of the transfer reaction and the rate of diffusion of the electroactive species between the bulk solution and the layer of solution surrounding the electrode. Reversible processes have a rate of electron transfer which is fast with respect to the scan rate. An irreversible process is when no corresponding peak is observed on the reverse scan. A process may be irreversible for several reasons. It may be that the product of the electron transfer is highly reactive so has all been consumed by another reaction before the reverse reaction may occur. The criteria used to assign electrode processes as reversible, irreversible or quasi-reversible are shown in **Table 5.6**.[185-187]

Table 5.6: Criteria for reversible, irreversible and *quasi*-reversible electron transfer processes

Parameter	**Reversible**	**Quasi-reversible**	**Irreversible**
E_{ox} and E_{red}	Independant of v	Varies with v	E_{ox} or E_{red} observed, varies with v
Δ E	59/n Independant of v	Increases with v	No return wave
I_{ox} / I_{red}	I_{ox} / I_{red} = 1	I_{ox} / $I_{red} \neq 1$	No return wave
Plot of I_{ox} *vs.* $v^{1/2}$	linear	Non-linear	Linear

All experiments were carried out under a N_2 atmosphere, with the cell and electrodes being thoroughly cleaned with a suitable solvent and concentrated HNO_3 between samples. Experiments in DMSO were carried out using 0.1 M $^{n}Bu_4NPF_6$ as the supporting electrolyte with the potentials measured between -1.75 0.75 V. Before analysis of each of the compounds, a blank sample was run and after analysis of the compound, the internal standard was added. For experiments in DMSO, the internal standard used was ferrocene (**Figure 5.40**). Using ferrocene not only acts as an internal standard, but provides a means of judging how effectively the cell is measuring the redox processes, as indicated by how close the peak separation of the E_{ox} and E_{red} potentials are to the theoretical value of 0.059 V / *n* (where *n* is equal to the number of electrons transferred). Experimentally, a peak separation which is below 0.09 V is usually considered sufficient.

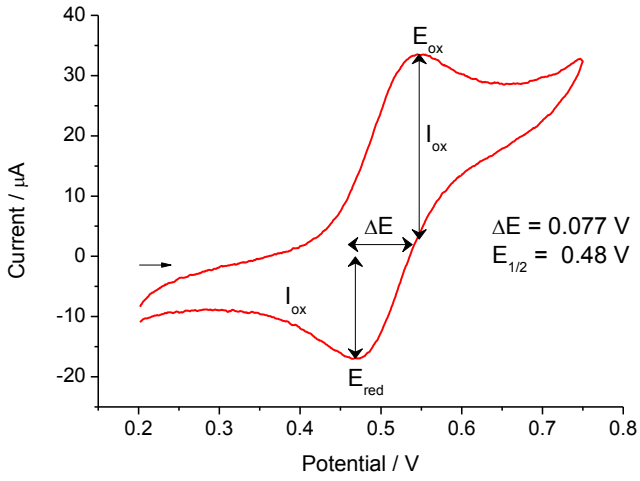

Figure 5.40: Cyclic voltammogram of ferrocene in DMSO (0.001M with 0.1 M $^{n}Bu_4NPF_6$ supporting electrolyte) at 100 mV s^{-1}

Aqueous experiments were carried out using KCl as the supporting electrolyte and $K_3[Fe(CN)_6]$ as the internal standard. The literature values for the internal standards used are provided in **Table 5.7**.

Table 5.7: Literature electrode potentials for internal standards.[188]

Redox process	**$E_{1/2}$ / V**
Fc^+ / Fc	0.48
$[Fe(CN)_6]^{3-}$ / $[Fe(CN)_6]^{4-}$	0.24

Electrode potentials are reported *vs.* Ag/AgCl, but are converted to *vs.* NHE when required for the purposes of comparison with potentials reported in the literature (**Table 5.8**). Electrode potentials are quoted at 100 mV s^{-1}.

Table 5.8: Values used to convert potentials between different reference electrodes.[185]

Reference electrode	E° *vs* NHE / V	E° *vs* SCE / V
NHE	0	-0.2412
SCE	0.2412	0
Ag/AgCl	0.197	-0.0450

5.2.1. Electrochemical properties of the ligands

All the ligands were examined in DMSO solution. It was found that the dpRa ligands had no observable redox processes occurring in the potential range used. There has been much in the literature on the redox chemistry of tpzH and derivatives of its similar analogue tpzH-CN (**Figure 5.41** and **Table 5.9**), with many studies attempting to interpret their complex electrochemistry.

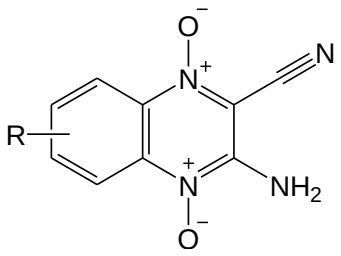

Figure 5.41: Structures of tpzH-CN derivatives discussed in **Table 5.9**

The cyclic voltammograms of these two ligands were obtained and found to be comparable to those reported previously.

Table 5.9: Comparison of E_{red} values of tpzH-CN and its derivatives *vs.* NHE at 100 mV s^{-1}

R	Reduction potential / V vs NHE		
	$E_{red}(1)$	$E_{red}(2)$	$E_{red}(2)-E_{red}(1)$
H	-0.65	-0.785	
Cl	-0.82	-0.97	0.15
Br	-0.76	-0.89	0.13
Me	-0.84	-0.97	0.13

The tpzH ligand has peaks associated with reductive processes at -0.977, -1.181 and -1.300 V. On the return sweep, some poorly defined oxidative processes are observed at -1.427 and -1.109 with two more clearly defined processes at 0.326 and 0.514 V (**Figure 5.42**).

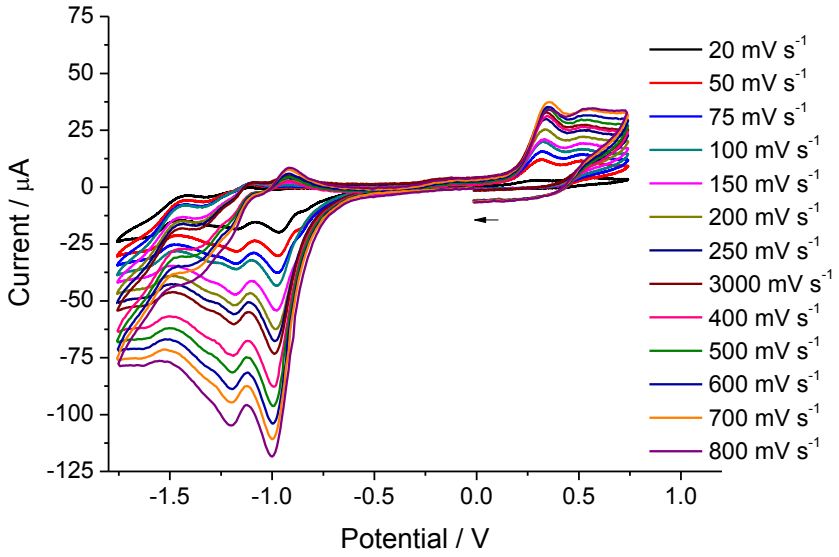

Figure 5.42: Cyclic voltammogram of tpzH in DMSO (0.001M with 0.1 M $^{n}Bu_4NPF_6$ supporting electrolyte at varied scan rates (from 20 to 800 mV s^{-1})

For tpzH-CN, reductive processes are observed at -0.855 and -0.990 V, whilst oxidative processes are observed at -1.547, -1.269, 0.894 and 0.401 V (**Figure 5.43**).

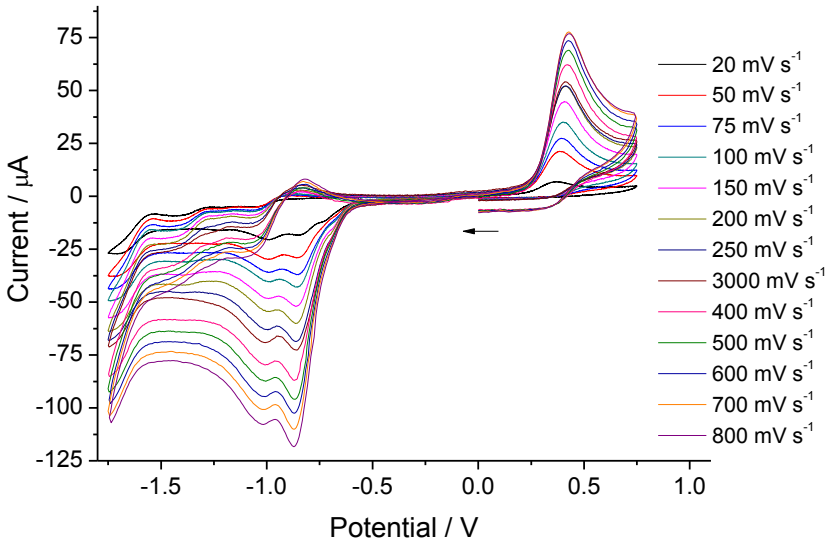

Figure 5.43: Cyclic voltammogram of tpzH-CN in DMSO (0.001M with 0.1 M $^{n}Bu_4NPF_6$ supporting electrolyte at varied scan rates

It has been hypothesised that the first reductive process is due to the reduction of one of the *N*-oxide groups at -0.855 V, quickly followed by it reacting with the DMSO solvent at -0.990 V.[147]

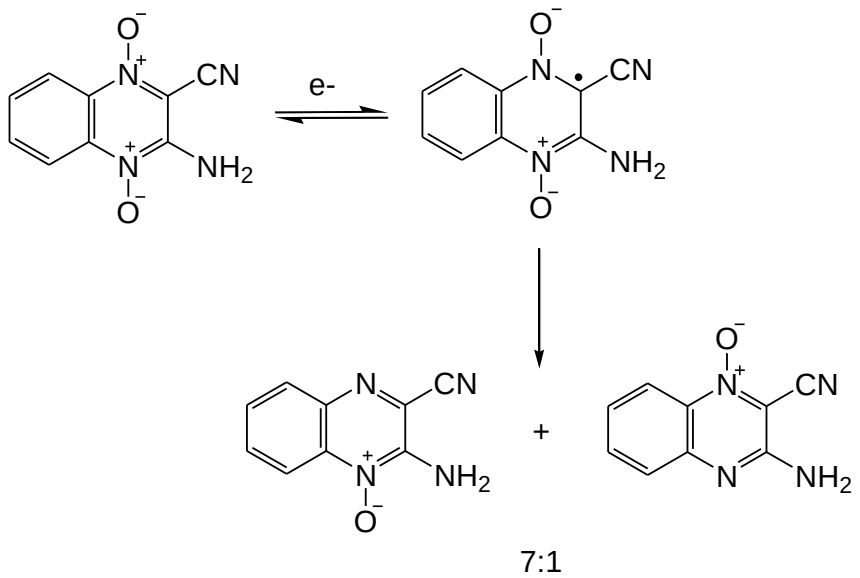

Scheme 5.6: Distribution of products upon reduction of tpzH-CN by NADPH cytochrome P450 reductase

Gates and co-workers reported that when reduced by NADPH cytochrome P450 reductase, the most likely species to be formed has the radical at the 2 position (**Scheme 5.6**) rather than the 4-position.[189] This is due to the nitrile group being better at stabilising the radical species than the amine because of the conjugation between the unpaired electron and the nitrile's π-orbitals (**Scheme 5.7**).[190]

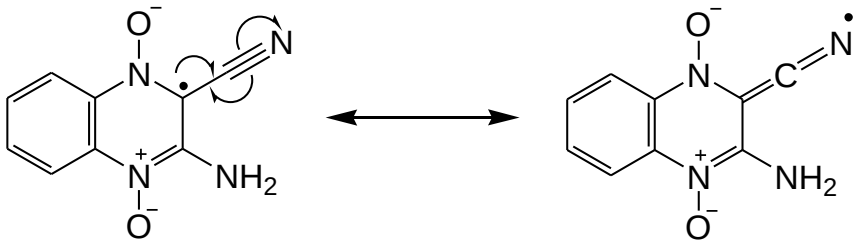

Scheme 5.7: Resonance stabilisation of the radical tpzH-CN species provided by the nitrile group

The redox chemistry of tpzH-$CONH_2$ is yet to be reported. The ligand undergoes reductive processes at -0.831 V, -0.977 V and -1.246 V. On the reverse scan, oxidation processes are observed at -0.907 V and 0.252 V. Running the potential sweep between -0.6 and -1.1 V does not provide evidence for the oxidation at -0.907 V to be the reverse process for the reduction at -0.977 V.

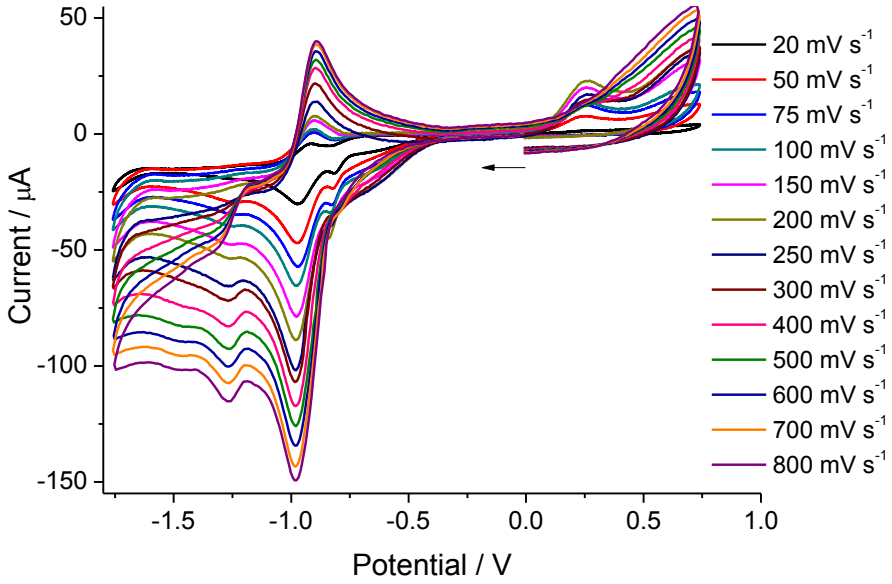

Figure 5.44: CV of tpzH-$CONH_2$ in DMSO (0.001M with 0.1 M $^{n}Bu_4NPF_6$ supporting electrolyte at varied scan rates.

Like the tpzH-CN ligand, the *N*-oxide most likely to be reduced first is the one in 2-position, adjacent to the amide group. **Table 5.10** summarises the reduction potential of these ligands. It can be seen that tpzH-CN and tpzH-$CONH_2$ were both found to undergo a reduction between -0.84 and -0.86 V with all three ligands undergoing a process at *ca.* -0.98 V.

Table 5.10: Comparison of reduction potentials in dmso (values quoted as *vs.* Ag/AgCl at 100 mV s^{-1} with ferrocene as internal standard)

	E_{red} (1) / V	**E_{red} (2) / V**	**E_{red}(3) / V**
tpzH		-0.976	-1.177
tpzH-CN	-0.855	-0.988	
tpzH-$CONH_2$	-0.835	-0.978	

5.2.2. Electrochemical properties of dpRa complexes

As this project is concerned with investigating the use of transition metal complexes as bioreductive prodrugs, it is important to obtain an understanding of their reductive chemistry so that it can be hypothesised which reducing agents may act upon them in biological systems. It is also beneficial if their reductions are found to be reversible, as this is believed to aid selectivity for hypoxic cells if the reduced species can be oxidised back to the prodrug species in the presence of oxygen. $[Cu(dpHa)_2]Cl_2$ displays a reduction at -0.08 V and an oxidation at 0.05 V in aqueous solution (**Figure 5.45**).

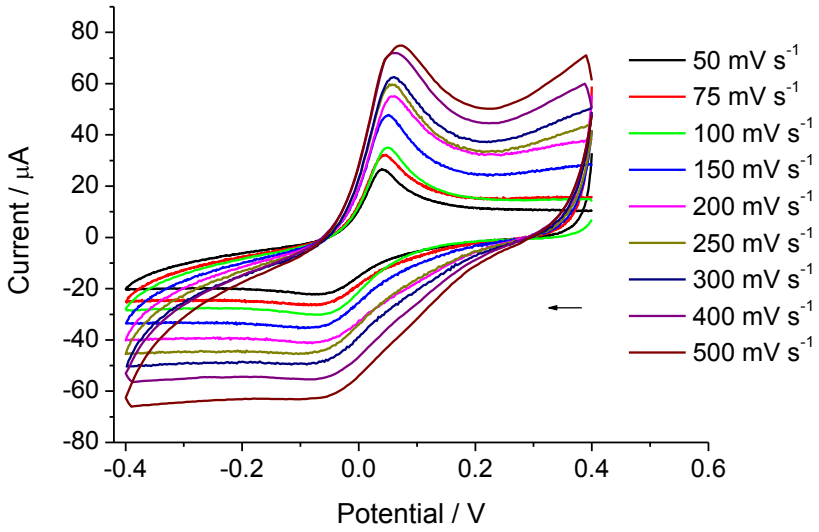

Figure 5.45: Cyclic voltammogram of $[Cu(dpHa)_2]2Cl$ in H_2O (0.001M with 0.1 M KCl supporting electrolyte) at varied scan rates

By looking at the parameters of these electron transfer processes, it can be seen that the reduction is *quasi*-reversible, shown by I_{ox} / I_{red} having a value of 1, and ΔE having a separation of 110 to 170 mV (**see appendix 5**.) This process is probably due to the reduction and subsequent oxidation of the copper centre, and the quasi-reversible nature of the process indicates that the complex does not undergo immediate dissociation upon reduction.

No clear cyclic voltammograms of the neutral copper(II) dpHa complexes could be obtained so these were studied in DMSO solution. $[Cu(NO_3)_2(dpHa)]$ shows reductive processes at 0.010 and -0.226V, the former of which is not clearly defined and becomes less distinct with increasing scan rate (**Figure 5.46**). An oxidative process is observed at 0.238 V and the shape of it implies a species which has adsorbed onto the electron is being stripped off upon oxidation.

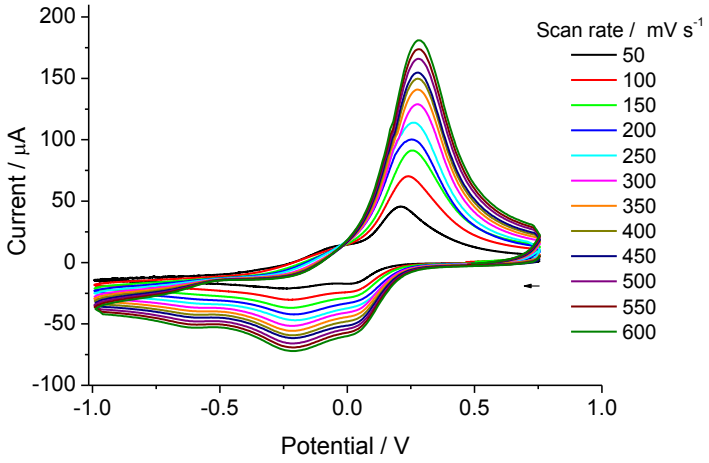

Figure 5.46: Cyclic voltammogram of $[Cu(Cl)_2(dpHa)]$ in DMSO (0.001M with 0.1 M $^{n}Bu_4NPF_6$ supporting electrolyte) at varied scan rates.

$[Cu(Cl)_2(dpma)]$ in DMSO undergoes reductive processes at -0.11 and -0.48 V and oxidative processes at -0.0754, 0.2034 and 0.4184 V (**Figure 5.47**).

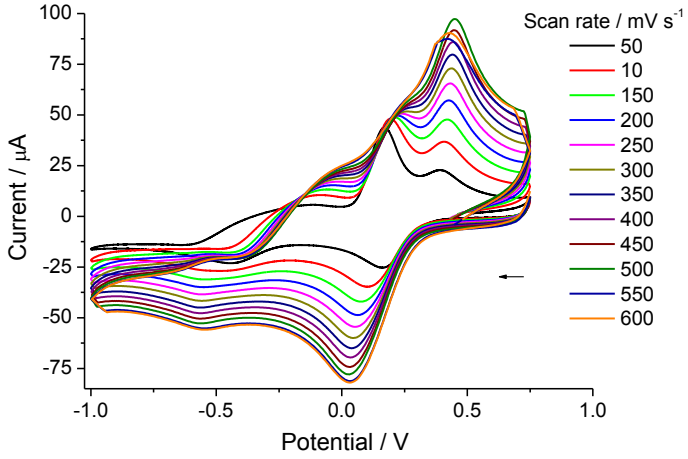

Figure 5.47: Cyclic voltammogram of $[Cu(Cl)_2(dpma)]$ in DMSO (0.001M with 0.1 M $^{n}Bu_4NPF_6$ supporting electrolyte at varied scan rates

The $[Co(CO_3)(dpHa)_2]^{+}$ complex undergoes a reduction at -0.185 V, with no oxidative processes observed on the return scan (**Figure 5.48**). This most likely corresponds to the one electron reduction of cobalt(III) to cobalt(II). Reasons for the lack of the reversibility of this reduction can be partially explained using the observations described in **Chapter Two**, where it was found that in solvents other than MeOH, one of the dpHa ligands dissociated from the cobalt(II) centre. This

concurs with the many reported cobalt(III) reductions in the literature being irreversible owing to the chemical changes which characteristically occur upon reduction to the more labile cobalt(II).[191]

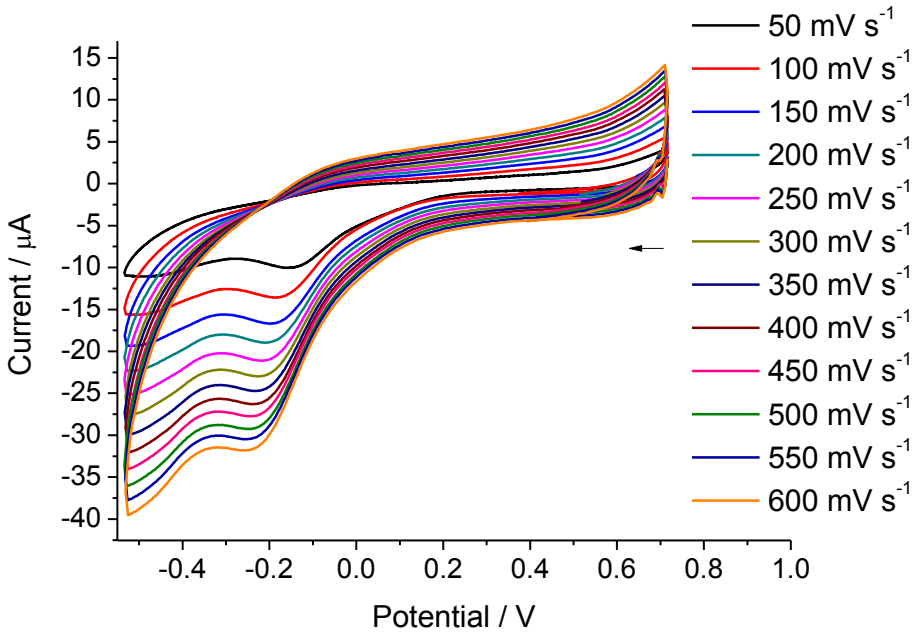

Figure 5.48: Cyclic voltammogram of $[Co(CO_3)(dpHa)_2]^{2+}$ in DMSO (0.001M with 0.1 M $^{n}Bu_4NPF_6$ supporting electrolyte) at 100 mV s^{-1}

Table 5.11 summarises the reduction potentials obtained for the dpRa complexes. Copper(II) complexes of this ligand undergo a reduction at *ca.* -1.0 V. These values, when compared to those of the hypoxia selective complex [Cu(ATSM)] and its non-selective analogue [Cu(PTSM)] (-0.59 and -0.51 V, respectively),[87] would appear not to be negative enough in value to bring about hypoxia selective reduction.

Table 5.11: Summary of dpRa complex reduction potentials

Complex	**Solvent**	**E_{red} / V *vs.* Ag / AgCl**
$[Cu(dpHa)_2]^{2+}$	H_2O	-0.08 V
$[Cu(NO_3)_2(dpHa)]$	DMSO	0.010
$[Cu(Cl)_2(dpHa)]$	DMSO	-0.11
$[Co(CO_3)(dpHa)_2]^{2+}$	DMSO	-0.185

5.2.3. Electrochemical properties of *N*-oxide complexes

5.2.3.1. Electrochemical properties of homoleptic *N*-oxide complexes

All the copper(II) complexes analysed show several reductive processes, many of which can be attributed to the redox-rich chemistry of the ligands. $[Cu(tpz)_2]$ undergoes reductive processes at -0.75, -0.93 and -1.18 V and then several poorly defined oxidative peaks are *ca*. -1.0, 0.25 and 0.48 V (**Figure 5.49**). None of the reductive processes show any degree of reversibility.

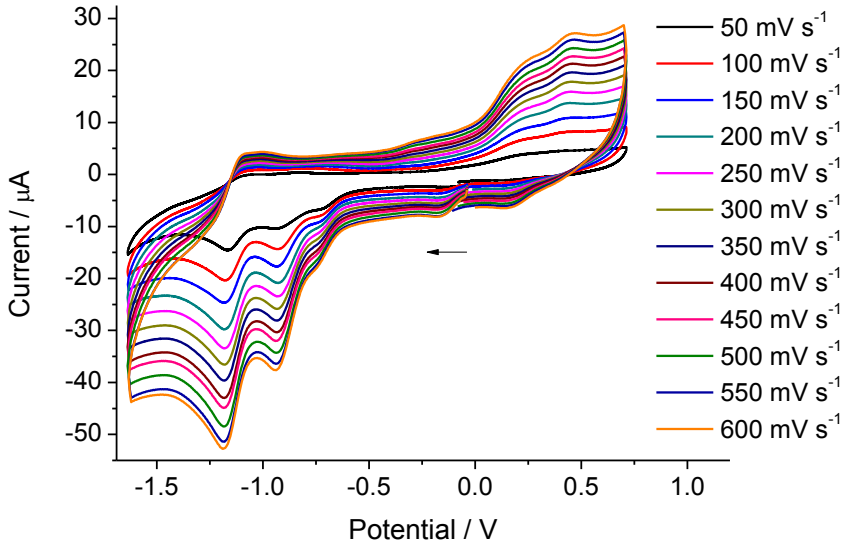

Figure 5.49: Cyclic voltammogram of $[Cu(tpz)_2]$ in DMSO (0.001M with 0.1 M $^{n}Bu_4NPF_6$ supporting electrolyte at varied scan rates

The $[Cu(tpz\text{-}CN)_2]$ complex undergoes three irreversible reductions at -0.35, -0.69, -0.85 and -1.06 V. On the reverse scan, it undergoes three oxidative processes at -0.91, 0.31 and 0.54 V followed by a reduction at 0.12 V.

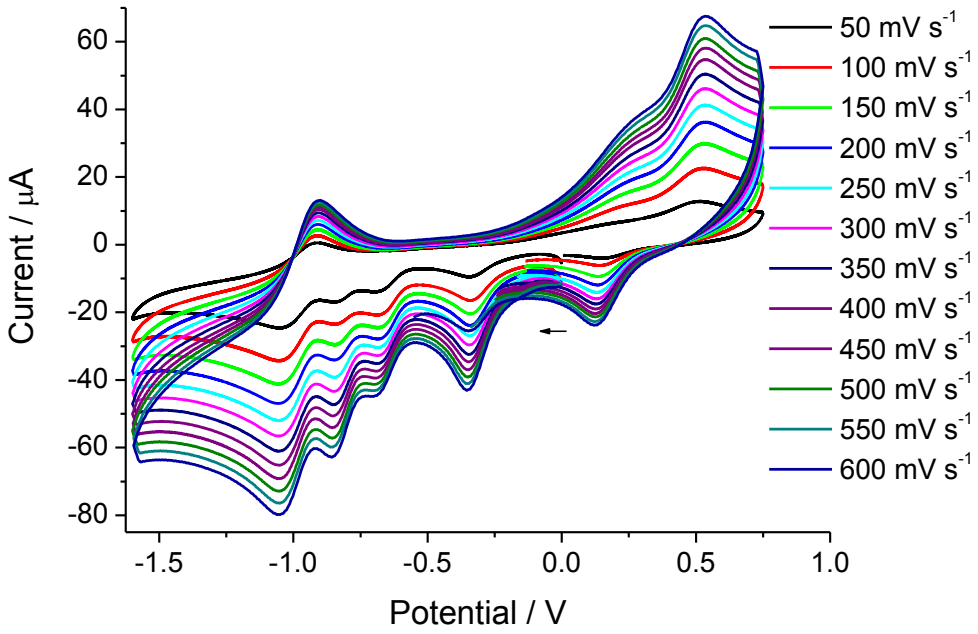

Figure 5.50: CV of $[Cu(tpz\text{-}CN)_2]$ in DMSO (0.001M with 0.1 M $^{n}Bu_4NPF_6$ supporting electrolyte at varied scan rates

The solubility of the $[Cu(tpz\text{-}CONH_2)_2]$ complex was too poor to allow for CV experiments to be carried out. When pre-dissolved in DMSO, it precipitated out of the electrolyte solution over too short a time interval to allow measurements to be made. The two copper(II) complexes were observed to undergo a number of reductive processes, none of which were found to be reversible.

5.2.3.2. Electrochemical properties of heteroleptic *N*-oxide complexes

The [Cu(tpz)(dpHa)]Cl complex undergoes four irreversible reductions at -0.40, -0.79, -0.985 and -1.24 V, and then oxidative processes at -1.077, 0.194 and 0.517 V on the return sweep.

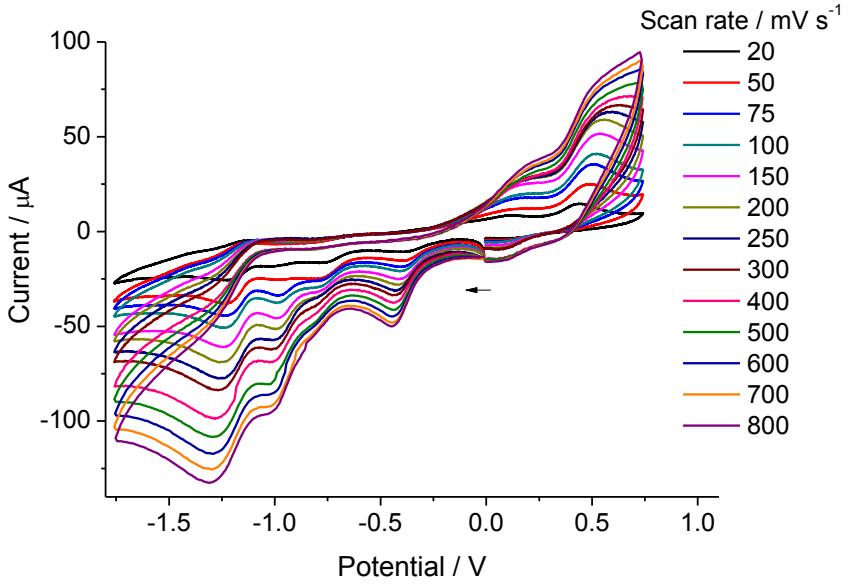

Figure 5.51: CV of [Cu(tpz)(dpHa)]Cl in DMSO (0.001M with 0.1 M $^{n}Bu_4NPF_6$ supporting electrolyte at varied scan rates

Table 5.12 compares the reduction potentials found for tpzH, [Cu(tpz)$_2$] and [Cu(tpz)(dpHa)]Cl. It can be seen that both the homo- and heteroleptic complexes undergo a reduction at *ca.* -0.77 V, but only the heteroleptic complex undergoes a reduction at a less negative potential than this at -0.4 V. Both complexes and the free ligand undergo reduction at *ca.* -0.95 and -1.2 V, implying these are both processes based on the ligand with little effect from the metal.

Table 5.12: Reduction potentials of tpzH, [Cu(tpz)$_2$] and [Cu(tpz)(dpHa)]Cl

Compound	**E_{red} / V**			
tpzH			-0.98	-1.18
[Cu(tpz)$_2$]		-0.75	-0.93	-1.18
[Cu(tpz)(dpHa)]Cl	-0.40	-0.79	-0.99	-1.24

The cyclic voltammogram of [Cu(tpz-CN)(dpHa)]Cl shows reductive processes occurring at -0.31, -0.66, -0.84 V, -1.04 and-1.35 V and oxidations at -1.24, -0.99 and 0.44 V on the reverse scan (**Figure 5.52**).

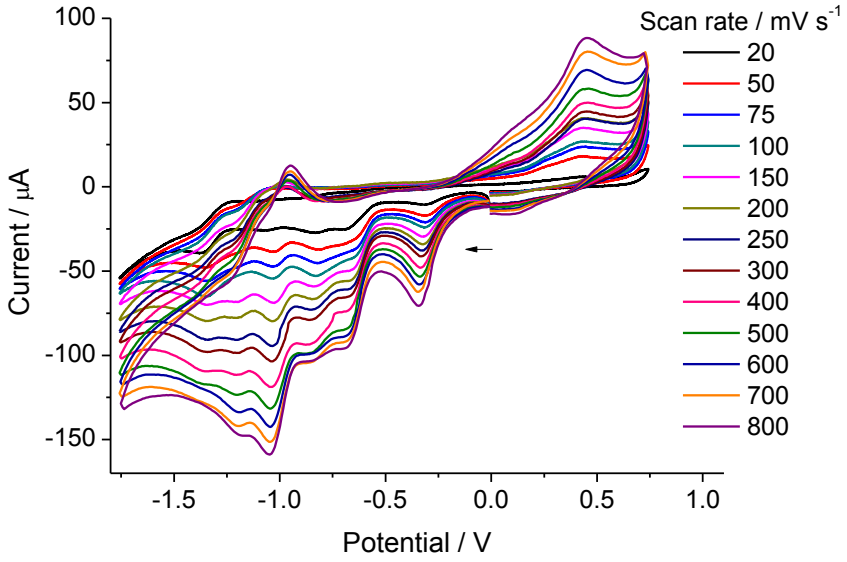

Figure 5.52: CV of [Cu(tpz-CN)(dpHa)]Cl in DMSO (0.001M with 0.1 M $^{n}Bu_4NPF_6$ supporting electrolyte at varied scan rates

Table 5.13 shows the reduction potentials found for the tpzH-CN complexes and free ligand. The two complexes and free ligand again show similarity in their behaviour above -0.8V by undergoing two reductive processes at comparable potentials, implying these are ligand based processes. Both the homo- and heteroleptic complexes undergo reduction at *ca.* -0.33 and -0.67 V, suggesting that these are a result of coordination.

Table 5.13: Reduction potentials of tpzH, [Cu(tpz-CN)$_2$] and [Cu(tpz-CN)(dpHa)]Cl

Compound	**E_{red} / V**			
tpzH-CN			-0.86	-0.99
[Cu(tpz-CN)$_2$]	-0.35	-0.69	-0.85	-1.06
[Cu(tpz-CN)(dpHa)]Cl	-0.31	-0.66	-0.84	-1.04

The [Cu(tpz-$CONH_2$)(dpHa)]Cl complex undergoes reductions at -0.397, -0.781, -0.959, -1.180 and, -1.154 V, with oxidations at -1.361, -0.174 V and 0.436 V on the reverse scan followed by a reduction at 0.107 V (**Figure 5.53**).

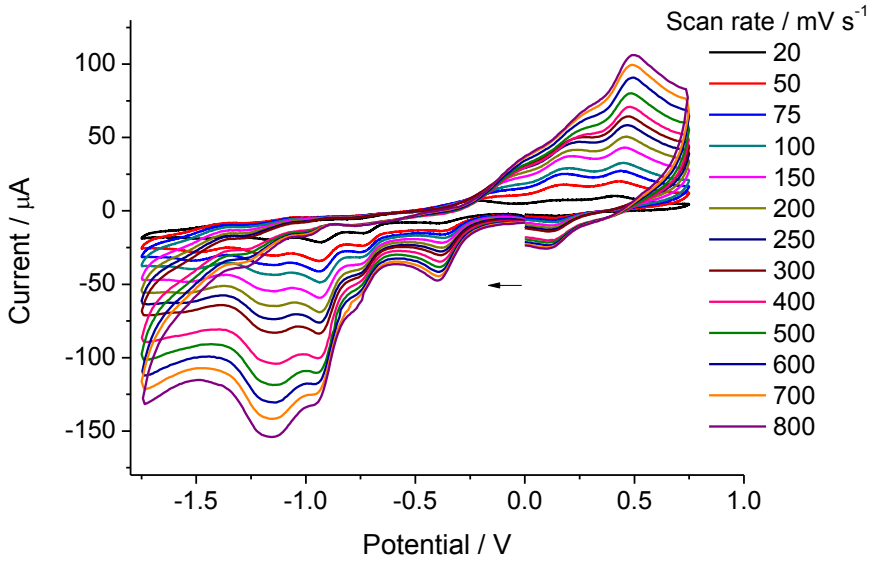

Figure 5.53: CV of [Cu(tpz-$CONH_2$)(dpHa)]Cl in DMSO (0.001M with 0.1 M $^{n}Bu_4NPF_6$ supporting electrolyte at varied scan rates

The three heteroleptic copper(II) complexes all display similar redox behaviour in DMSO (**Table 5.14**), with three reductive processes centred around -0.35, -0.70 and -0.9 V. The latter two appear to be due to reductions occurring on the ligand, whilst the processes at *ca.* -0.35 V can tentatively be assigned as the reduction of the copper(II) centre. If this assignment is correct, then this is a reduction potential which is more suited to hypoxia selectivity than those found for the copper(II) dpHa complexes.

Table 5.14: Summary of reduction potentials for [Cu(tpz-R)(dpHa)]Cl complexes in DMSO

	E_{red}(1) / V	**E_{red}(2) / V**	**Er_{ed}(3) / V**
[Cu(tpz)(dpHa)]Cl	-0.404	-0.792	-0.985
[Cu(tpz-CN)(dpHa)]Cl	-0.314	-0.655	-0.828
[Cu(tpz-$CONH_2$)(dpHa)]Cl	-0.397	-0.781	-0.959

The three cobalt(III) heteroleptic complexes were all found to undergo irreversible reduction. $[Co(tpz)(dpHa)_2]Cl_2$ undergoes reduction at -0.056 and -0.946 V (**Figure 5.54**).

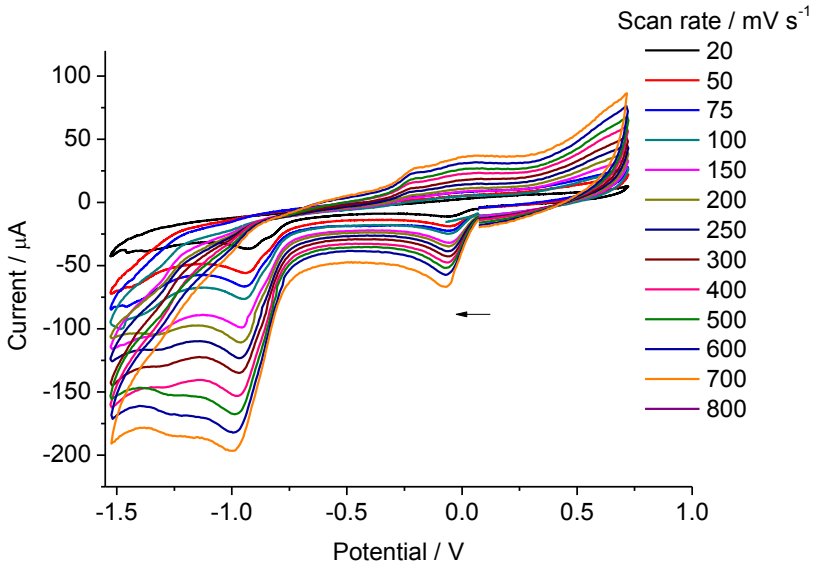

Figure 5.54: CV of $[Co(tpz)(dpHa)_2]Cl_2$ in DMSO (0.001M with 0.1 M $^{n}Bu_4NPF_6$ supporting electrolyte at varied scan rates.

$[Co(tpz\text{-}CN)(dpHa)_2]Cl_2$ undergoes reduction at -0.002 and -0.876 V, with a shoulder on the peak of the latter at -0.712 V (**Figure 5.55**).

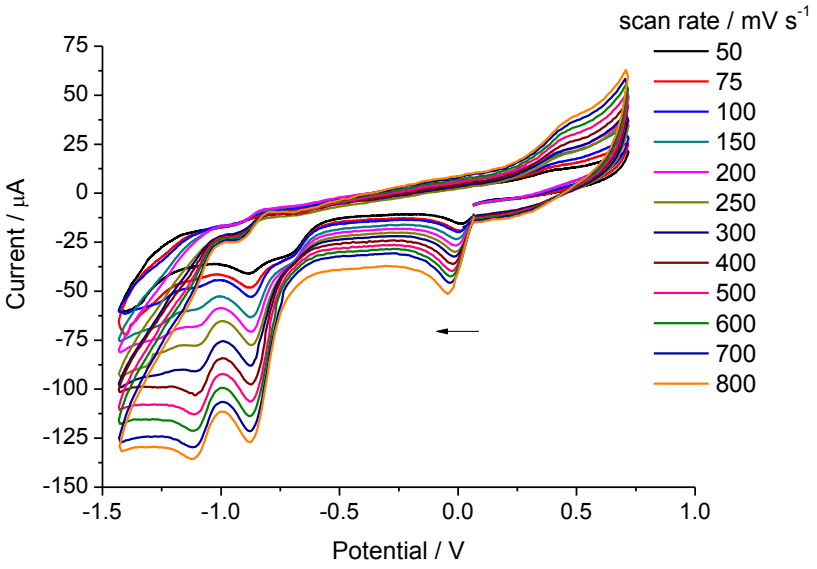

Figure 5.55: CV of $[Co(tpz\text{-}CN)(dpHa)]Cl_2$ in DMSO (0.001M with 0.1 M $^{n}Bu_4NPF_6$ supporting electrolyte at varied scan rates.

$[Co(tpz\text{-}CONH_2)(dpHa)_2]Cl_2$ undergoes reduction at -0.447, -0.963 and -1.273 V (**Figure 5.56**).

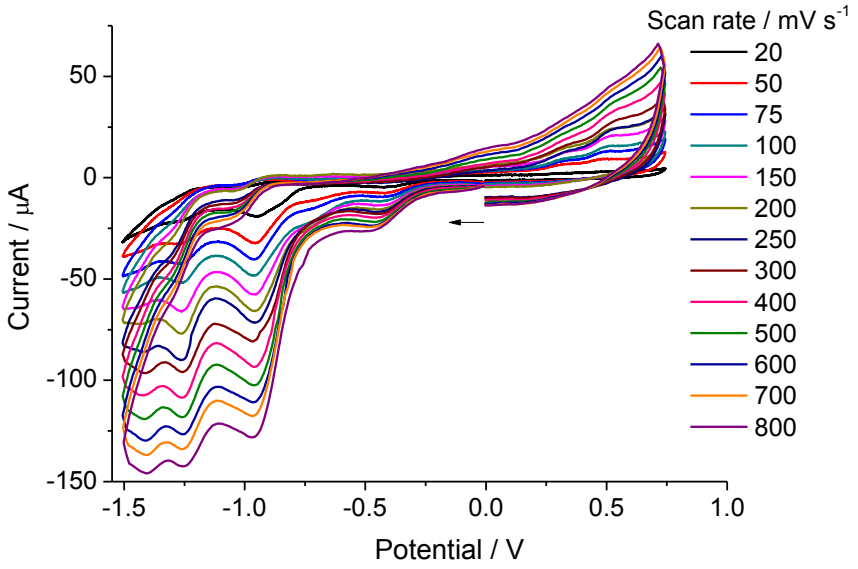

Figure 5.56: CV of $[Co(tpz\text{-}CONH_2)(dpHa)]Cl_2$ in DMSO (0.001M with 0.1 M $^{n}Bu_4NPF_6$ supporting electrolyte at varied scan rates.

All three of the cobalt(III) complexes share a reductive process centred around -0.9 V which were found to be irreversible in nature. These reduction potentials are more negative than the range suggested by Reisner (-0.30 to -0.70 V *vs.* Ag/AgCl) for hypoxia-selective cobalt(III) complexes.[192] A reduction potential that is too negative could place the complex beyond the capability of biological reagents within the cell whereas a complex has a reduction potential less negative than this range may undergo reduction too easily for any degree of hypoxia-selective cytotoxicity to be obtained.

For copper(II) complexes, the results from [Cu(atsm)] studies have shown that its superior selectivity for hypoxic cells over its analogues is a result of its more reduction potential (-0.57 V *vs*. Ag/AgCl). $[Cu(tpz)_2]$ was observed to undergo its first reductive process at -0.75 V *vs*. Ag/AgCl whilst $[Cu(tpz\text{-}CN)_2]$ was found to undergo a reduction at -0.35 then a second process at -0.69 V *vs* Ag/AgCl. On the basis of these results, the homoleptic copper(II) tpzH complex should show the greatest selectivity for reduction within a hypoxic environment.

The heteroleptic copper(II) complexes all undergo a reductive process within the range of -0.314 to -0.404 V *vs.* Ag/AgCl, with [Cu(tpz)(dpHa)]Cl having the most negative reduction potential. This suggests that [Cu(tpz)(dpHa)]Cl should be the most resistant to reduction under normoxic conditions out of the three complexes. However, the study by Robins showed that a copper(II) *N*-mustard with a reversible reduction potential of -0.212 V *vs.* Ag/AgCl exhibited a degree of hypoxia selectivity whereas related copper(II) complexes with more negative but irreversible reduction potentials did not demonstrate any selectivity.[102]

The copper(II) complex which appears most promising in terms of hypoxia selectivity, compared to Robins' *N*-mustard complex is $[Cu(dpHa)_2]Cl_2$, which was found to have a quasi-reversible reduction at -0.08 V *vs.* Ag/AgCl in aqueous solution.[102] Although its reduction potential is unlikely to be negative enough to prevent reduction outside of hypoxia, the reversible nature of this process indicates a desired stability in the reduced copper(I) complex.

5.3. Effect of biological reducing agents

Reductive enzymes hypothesised to have roles in bioreduction of drug molecules include cytochrome P450 and DT-diaphorase In addition to these, there are also several small molecule reducing agents present such as ascorbic acid, sulphur-containing amino acids such as cysteine, and other species including glutathione and NADPH. From the work described thus far, it has been established that the cobalt(III) heteroleptic complexes are stable in aqueous solution, and the cobalt(II) complexes undergo ligand dissociation. It has also been demonstrated that the coordinated and uncoordinated *N*-oxide ligands can be distinguished using UV-vis spectroscopy. The work discussed presently utilises UV-vis spectroscopy to study the effect of biological small molecule reducing agents on $[Co(tpz\text{-}CN)(dpHa)_2]^{2+}$.

A 10-fold excess of ascorbic acid was added into a UV-vis cuvette containing an aqueous solution of $[Co(tpz\text{-}CN)(dpHa)_2]^{2+}$. The subsequent series of recorded spectra show a decrease in absorbance at 525 nm, corresponding to the cobalt(III) complex, and an increase in absorbance at 471 nm, caused by the uncoordinated ligand (**Figure 5.57**).

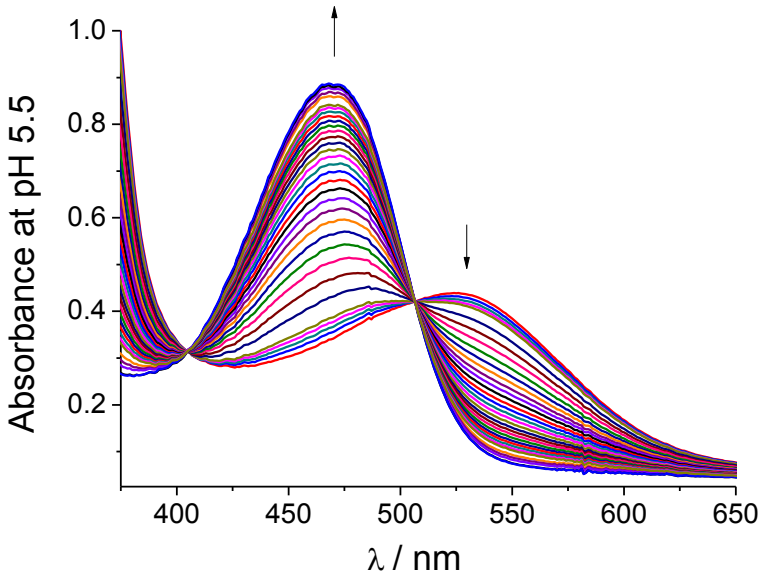

Figure 5.57: UV-vis spectra monitoring the reaction of excess ascorbic acid with $[Co(tpz\text{-}CN)(dpHa)_2]^{2+}$ in aqueous solution

By plotting the absorbance at 471 nm as a function of time, it can be seen that the ligand dissociation proceeds rapidly on the second time scale, but closer inspection of the start of the reaction shows that there is a delay before ligand dissociation occurs (**Figure 5.58**).

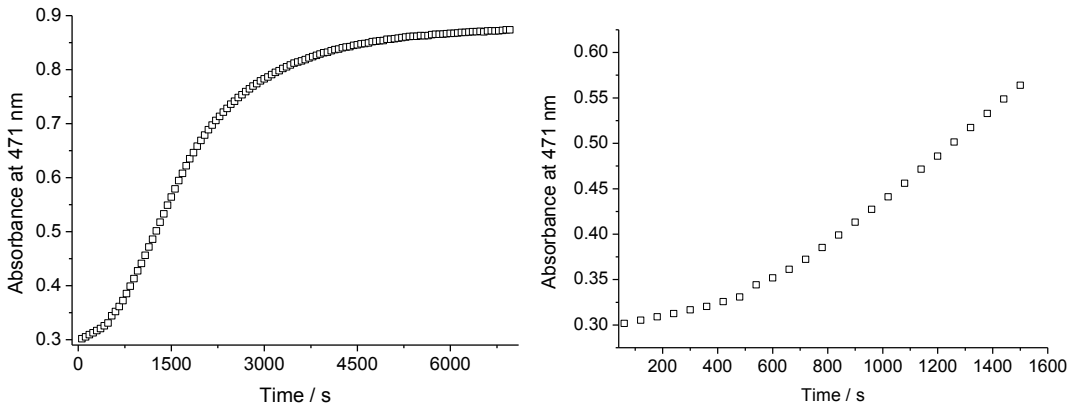

Figure 5.58: Plot of absorbance at 471 nm against time following the reaction between $[Co(tpz\text{-}CN)(dpHa)_2]Cl_2$ and ascorbic acid to completion (*left*) and focusing on the start of the reaction (*right*)

This induction period at the start of the reaction is attributed to the presence of oxygen in the solutions, as neither that of the complex or reducing agent were purged

with nitrogen before use. The rate of dissociation increases after *ca.* 600 s once the oxygen present in the solution has been consumed. To prove this hypothesis, the same reaction was carried out under nitrogen (**Figure 5.59**) where no induction period for the reaction is observed.

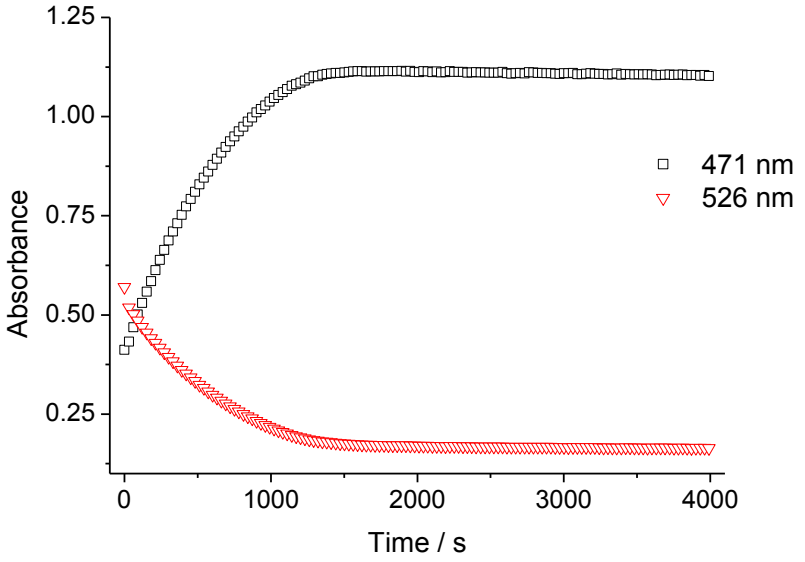

Figure 5.59: Plot of absorbance at 471 and 565nm against time following the reaction between $[Co(tpz\text{-}CN)(dpHa)_2]^{2+}$ and ascorbic acid under anaerobic conditions

As hypoxic regions in tumours have a sub-normal extracellular pH, it was decided to investigate if the rate of reduction differed between neutral pH and that found in the extracellular hypoxic environment (pH 5.5). The reduction of $[Co(tpz\text{-}CN)(dpHa)_2]^{2+}$ by ascorbate is noticeably faster at neutral pH than at pH 5.5 (**Figure 5.60**) but this is likely to be due to the rate of ascorbate oxidation being greater at more neutral pH values.[193]

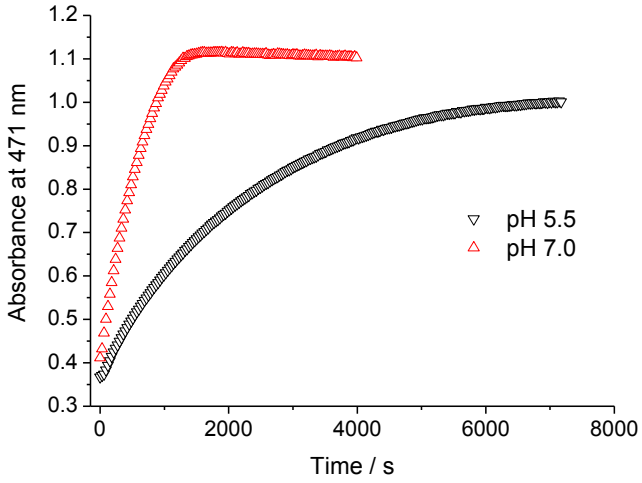

Figure 5.60: Absorbance at 471 nm during the ascorabte mediated reduction of $[Co(tpz\text{-}CN)(dpHa)_2]^{2+}$ at pH 5.5 and pH 7

Reduction by cysteine under anaerobic conditions is also observed to be more rapid at neutral pH than at pH 5.5 (**Figure 5.61**). When the reaction is carried out at pH 5.5, the absorbance corresponding to free tpzH-CN starts to decrease after the reaction has gone to completion, indicating that the free ligand is being consumed by a further reaction.

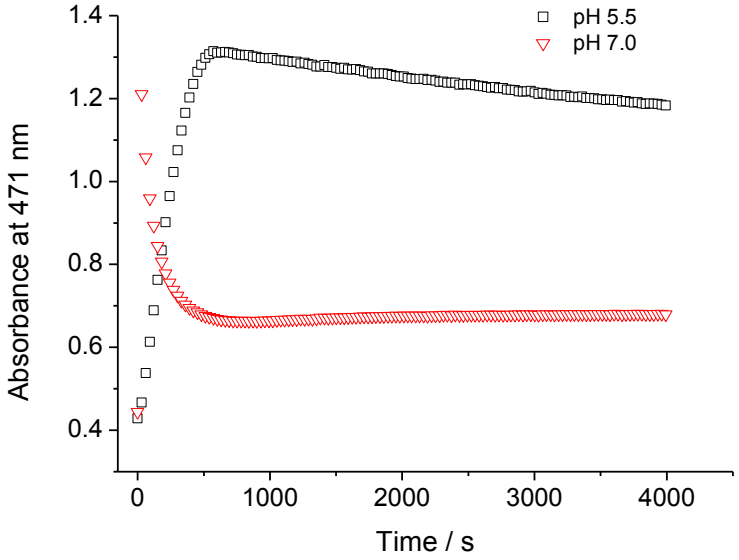

Figure 5.61: Absorbance at 471 nm during the cysteine mediated reduction of $[Co(tpz\text{-}CN)(dpHa)_2]^{2+}$ at pH 5.5 and pH 7

The UV-vis spectra obtained when this reduction is carried out at pH 7 are similar to those of obtained for when ascorbate is the reducing agent. When the reduction is carried out at pH 5.5, it can be seen that a species forms with a λ_{max} value at *ca*. 420 nm (**Figure 5.62**).

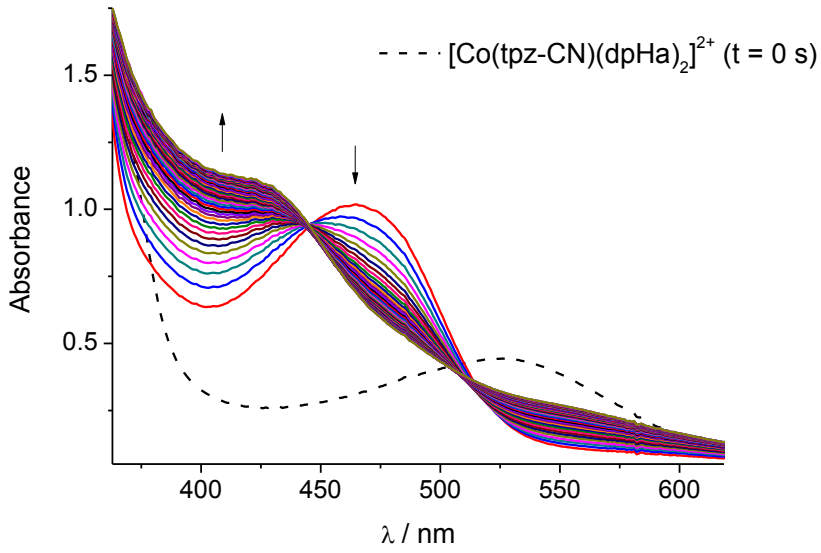

Figure 5.62: UV-vis spectra of the cysteine mediated reduction of $[Co(tpz\text{-}CN)(dpHa)_2]^{2+}$ at pH 5.5

It has been reported that the reduction product of tpzH-CN can undergo hydrolysis (**Scheme 5.8**) in the presence of 2-sulfanylethan-1-ol.[189] It is probable that a similar reaction is being observed in the presence of cysteine, supported by the newly formed species having an absorbance centred at 420 nm which is similar to that observed for tpzH-$CONH_2$.

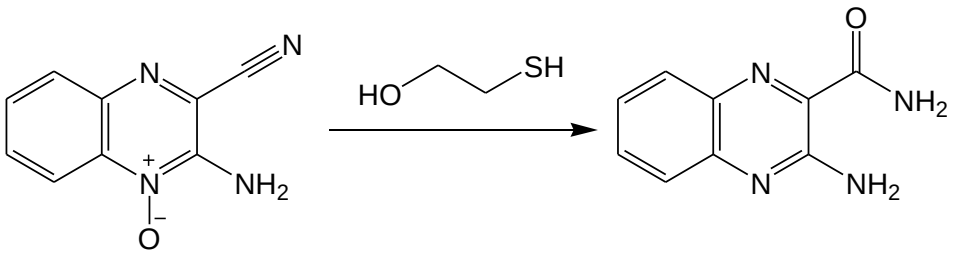

Scheme 5.8: Hydrolysis of the reduction product of tpzH-CN

The depletion of the uncoordinated ligand is also observed with glutathione (**Figure 5.63**).

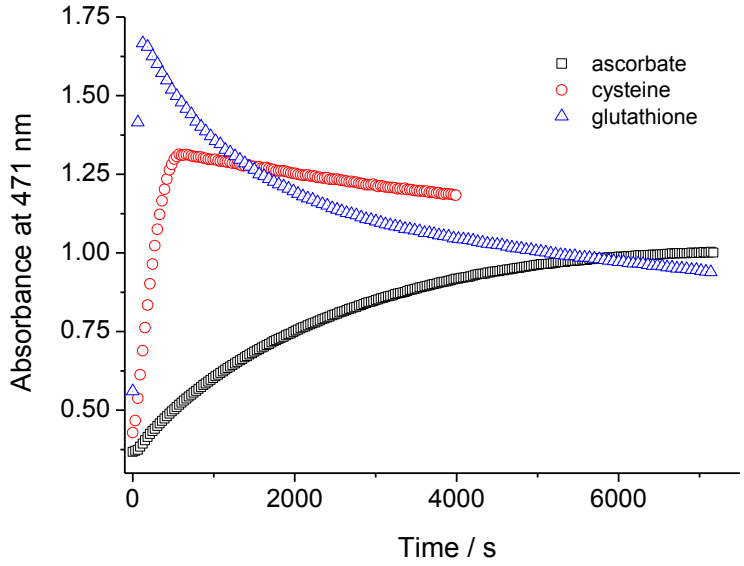

Figure 5.63: Absorbance at 471 nm when $[Co(tpz\text{-}CN)(dpHa)_2]^{2+}$ is reduced by ascorbate, cysteine and glutathione at pH 5.5

Comparison of the rate of reduction by the three reducing agents under anaerobic conditions show that reduction by glutathione and cysteine are similar, and are more rapid than the reduction by cysteine. This reflects the reduction potentials of the reducing agents (**Table 5.15**) and demonstrates that the reduction of the cobalt(III) complex occurs at a greater rate when in a more biologically reducing environment.

Table 5.15: Reduction potentials of ascorbic acid, cysteine and glutathione

Biological reducing agent	**E°' / V**
Ascorbic acid	0.06
Cysteine	-0.34
Glutathione	-0.23

The reduction by ascorbate can also be followed by monitoring the fluorescence of the uncoordinated tpzH-CN ligand (**Figure 5.64**) which provides the basis for possible future studies using confocal microspopy to see if the distribution of free tpzH-CN differs between the free ligand and $[Co(tpz\text{-}CN)(dpHa)_2]^{2+}$.

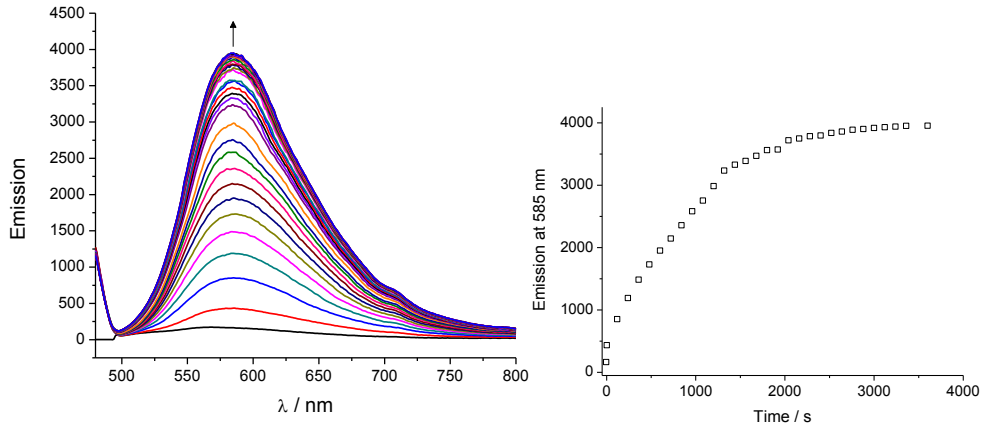

Figure 5.64: Emission spectra following the reduction of $[Co(tpz\text{-}CN)(dpHa)_2]^{2+}$ by ascorbate at pH 5.5 under anaerobic conditions ($\lambda_{excitation}$ = 470 nm)

The cobalt(III) heteroleptic system has been shown to undergo reduction with biologically relevant reducing agents with the *N*-oxide ligand rapidly dissociating upon reduction to cobalt(II) in aqueous solution (**Scheme 5.9**). The fate of the dpHa ligand from the heteroleptic complexes has not been specifically investigated, but the results described in this chapter relating to their homoleptic complexes indicate that they have dissociated from the cobalt centre upon reduction.

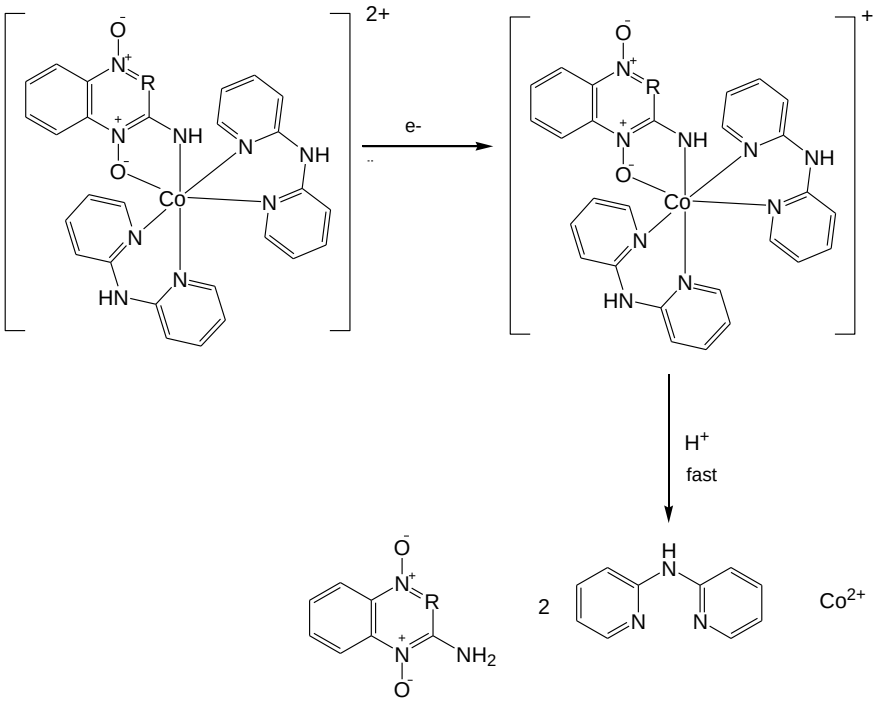

Scheme 5.9: Reduction of $[Co(tpz\text{-}R)(dpHa)_2]^{2+}$ resulting in the dissociation of tpzH-R

The reduction was shown to be hindered in the presence of oxygen, taking place at a reduced rate, but the results suggest that in order to achieve selective reduction under hypoxic conditions, the reduction potential needs to be made more negative.

5.4. Conclusions

Studies on the pH-dependent properties of the complexes provided information on the solubility and stability of the complexes in aqueous solution. With both dpRa and tpzH-R ligands, complexes of cobalt(II) and zinc(II) were found to dissociate in aqueous solution. This order of stability is expected from that given by the Irving-Williams series which shows an increase in ligand affinity going from left to right across the first row of d-block M^{2+} ions.[181] The copper(II) complexes were found to be the most stable owing to the additional stabilisation of these complexes from Jahn-Teller distortion. The cobalt(III) complexes were all found to be stable in aqueous solution owing to the kinetic and thermodynamic stability of this element's oxidation state which makes it ideal to be exploited in the development of hypoxic prodrugs.

A method of altering the stability of dpRa-type complexes has been found by introducing steric bulk onto the central amine. Introduction of a methyl or ethyl group at this position resulted in the ligand's dissociation from copper(II) at pH 5.3, a value near to that found within the extracelluar environment of hypoxic tumour cells. The homoleptic *bis*-tpzH-R copper(II) complexes were all found to be insoluble in water, and had to be dissolved in DMSO prior to aqueous studies. These complexes were found to dissociate between pH 2.2 and 2.6, a value much more acidic that that found in the extracellular hypoxic tumour environment.[21] All of the copper(II) complexes were found to undergo irreversible reductions at various potentials, with $[Cu(dpHa)_2]Cl_2$ being the exception by having a *quasi*-reversible reduction. The copper(II) complexes containing tpzH were found to show the most negative reduction potentials compared to their analogous complexes. The cobalt(III) complexes were found to be stable apart from at extreme pH values, highlighting their characteristic stability. The heteroleptic complexes were all found to undergo an irreversible reduction at *ca*. at -0.9 V with $[Co(tpz\text{-}CN)(dpHa)_2]Cl_2$ at -0.002 V. It has been demonstrated that $[Co(tpz\text{-}CN)(dpHa)_2]Cl_2$ can be reduced by biological

reducing agents such as ascorbate, cysteine and glutathione. Significantly for the purposes of hypoxia selectivity, it appears that this reduction proceeds at a slower rate in the presence of oxygen.

The dissociation of tpzH-CN from its cobalt(III) complex was followed by using UV-vis and fluorescence techniques, which will provide a useful method for monitoring the behaviour of this complex in biological systems.

Chapter Six: Biological studies, conclusions and future work

This chapter discusses the results of biological studies and reviews them in the context of the conclusions from the previous chapters.

6.1. Procedure for cell assays

This chapter describes the results obtained from biological experiments using A549 cells. A549 is a cell line originating from human lung adenocarcinoma. The cells were grown in DMEM. Upon reaching *ca*. 75% confluence, the medium was removed and the cells washed twice with 5 mL PBS. To remove the cells from the flask, they were then incubated with 1 mL 0.25% EDTA trypsin for 10 minutes at 37 °C. 9 mL of medium was then added to the cells to form a single suspension. 0.5 and 1.0 mL of the resulting supernatant were added to two new culture flasks, each containing 10 mL of fresh medium.

Cell viability was measured using the MTT assay.[194] MTT (3-(4,5-Dimethylthiazol-2-yl)-2,5-diphenyltetrazolium bromide) is a yellow compound which undergoes reduction catalysed by mitochondrial dehydrogenase enzymes within living cells to form a purple formazan compound (**Scheme 6.1**).

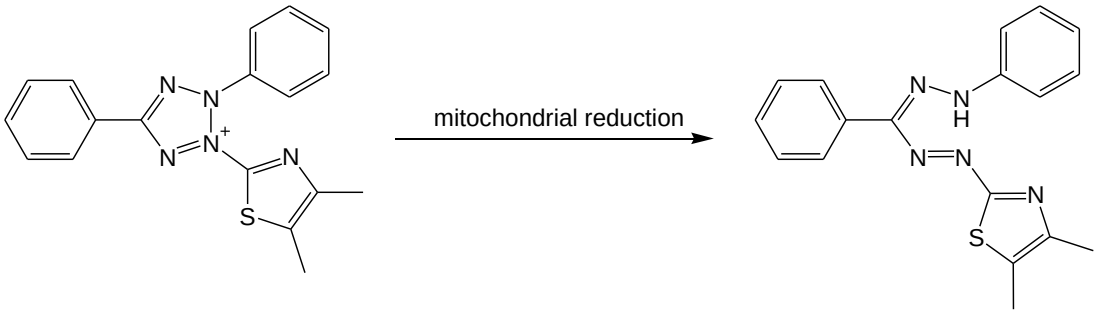

Scheme 6.1: Mitochondrial reduction of 3-(4,5-Dimethylthiazol-2-yl)-2,5-diphenyltetrazolium bromide to MTT formazan

Cells were plated in 100 μL medium at the seeding density of 1000 cells per well into 11 of the 12 columns of a 96-well microtitre plate. The first column was left to contain just media so to act as negative control. The plate was incubated for 20 hours to allow the cells to adhere to the plate. The compounds were dissolved in medium to form solutions of the required concentrations, which were sterilised before addition to the plate. 100μL of the drug solutions were added to the cells, with one

concentration per column of the plate. To one column, 100 µL medium was added which contained no drug, so as to provide the positive control.

Following 3 days incubation, 50 µL of a solution containing 0.0125 g MTT in 6.25 mL of PBS was added to each well then the plates incubated for two hours. The plates were centrifuged for 10 minutes then 220 µL of the supernatant removed from each well. DMSO (150 µL) was added to each well to solubilise the MTT formazan crystals, which become fully dissolved during 5 minutes agitation on a plate shaker.[195] The absorbance at 540 nm of each well was measured using an automated plate reader. The absorbance at 540 nm for the positive and negative controls was used to calculate the absorbance for 100% and 0% cell viability, and from this, the percentage cell viability for each of the drug concentrations was calculated. The percentage cell viability was plotted as a function of drug concentration, and to this a logistic sigmoidal curve was fitted. From the curve, a value for the IC_{50} (concentration at which 50% of the cells are no longer viable) could be obtained.

6.2. Cytotoxicity studies of the uncoordinated ligands

The dpHa ligand was not able to be tested owing to its insolubility in the biological medium. **Figure 6.1** shows an example IC_{50} curve obtained for tpzH and tpzH-CN.

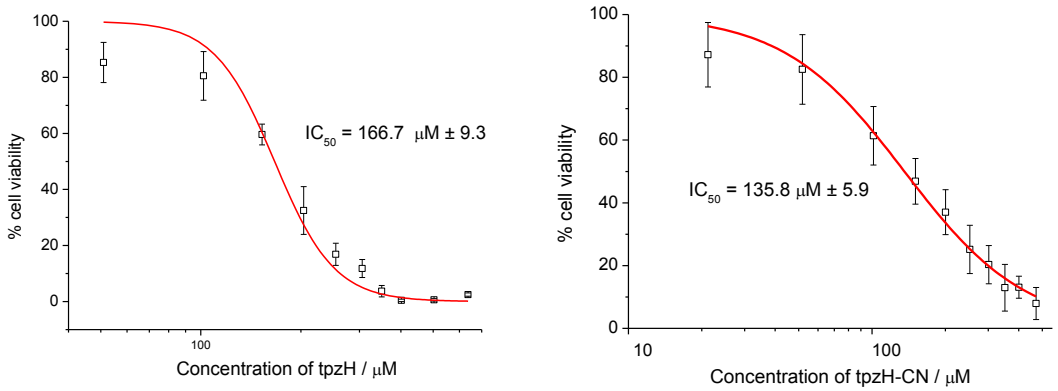

Fig 6.1: Example IC_{50} curves of tpzH (*left*) and tpzH-CN (*right*) against A549 cells

The tpzH-$CONH_2$ does not have high enough solubility to enable all the concentrations needed to obtain a full IC_{50} curve and therefore a meaningful value.

The partial IC_{50} curve (**Figure 6.2**) shows that tpzH-$CONH_2$ has an IC_{50} above 450 μM.

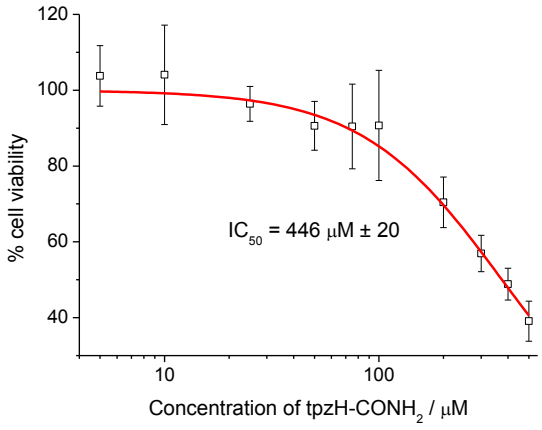

Figure 6.2: Partial IC_{50} curve of tpzH-$CONH_2$ against A549 cells

The results from three separate plates were used to obtain a weighted average (a_{all}), calculated by the following equation (a_n is the experimental result, δ_n = error for the experimental result):[196]

$$a_{all} = \frac{\sum \frac{a_n}{\delta_n^2}}{\sum \frac{1}{\delta_n^2}}$$

The error for the weighted average can then be calculated by:

$$\delta_{all} = \sqrt{\frac{1}{\sum \frac{1}{\delta_n^2}}}$$

The weighted average IC_{50} values are presented in **Table 6.1**.

Table 6.1: IC_{50} values (weighted mean) of tpzH, tpzH-CN and tpzH-$CONH_2$ against A549

Ligand	**IC_{50} / μMol**	**E_{red} / V *vs.* Ag/AgCl**
tpzH	170.3 ± 6.2	-0.98
tpzH-CN	143.0 ± 4.5	-0.86
tpzH-$CONH_2$	> 450	-0.835

Comparing the reduction potentials of these two ligands with their IC_{50} values suggests that a lower reduction potential correlates with a lower IC_{50} value and therefore greater cytotoxicity under aerobic conditions. The reduction potential of tpzH-$CONH_2$ is the least negative but the cytotoxic capability of this ligand under hypoxia is not yet known. Therefore, conclusions cannot yet be drawn as to if the lack of activity shown under normoxia is a result of tpzH-$CONH_2$ good hypoxia selectivity or a lack of cytoxicity.

The decreased activity of tpzH-$CONH_2$ compared with tpzH and tpzH-CN may be a result of the chemical differences described in **Chapter Five**. When tpzH and tpzH-CN underwent deprotonation, the UV-vis spectrum of the spectrum drastically altered as the solutions turned from orange to purple. When repeated with the tpzH-$CONH_2$ ligand, the solution was observed to become slightly darker rather than undergo a drastic colour change. There was also a noted difference in the reactivity of tpzH-$CONH_2$ compared to the other two N-oxide ligands described in **Chapter Four**. Whilst tpzH and tpzH-CN were found to rapidly coordinate to the cobalt(II) centre of $[Co(dpHa)_2]^{2+}$ upon mixing, the tpzH-$CONH_2$ ligand did not coordinate until the reaction mixture was heated at reflux with the oxidising agent. These observations suggest the tpzH-$CONH_2$ ligand has greater kinetic stability than the other two N-oxide ligands, which may possibly arise from its intramolecular hydrogen bonds which were observed in both solution and the solid state. Future studies would need to examine the cytotoxicity of this ligand under hypoxic conditions to examine the potential of this ligand as a hypoxia selective agent.

6.3. Cytotoxicity studies of copper(II) and cobalt(III) complexes

The copper(II) and cobalt(III) complexes prepared in this thesis were tested but it was found that the solubility of some of the compounds prevented this. For those which would not dissolve directly into the biological medium, it was tried to pre-dissolve them into a concentrated stock solution of water or DMSO from which to prepare the solution in medium. Unfortunately $[Cu(Cl)_2(dpHa)]$, [Cu(tpz-CN)(dpHa)]Cl and [Cu(tpz-$CONH_2$)(dpHa)]Cl precipitated out of solution when added to the medium, so could not be assayed.

The two copper(II) complexes assayed were $[Cu(dpHa)_2]$ Cl_2 and [Cu(tpz)(dpHa)]Cl. An example IC_{50} curve obtained for each is shown in **Figure 6.3**.

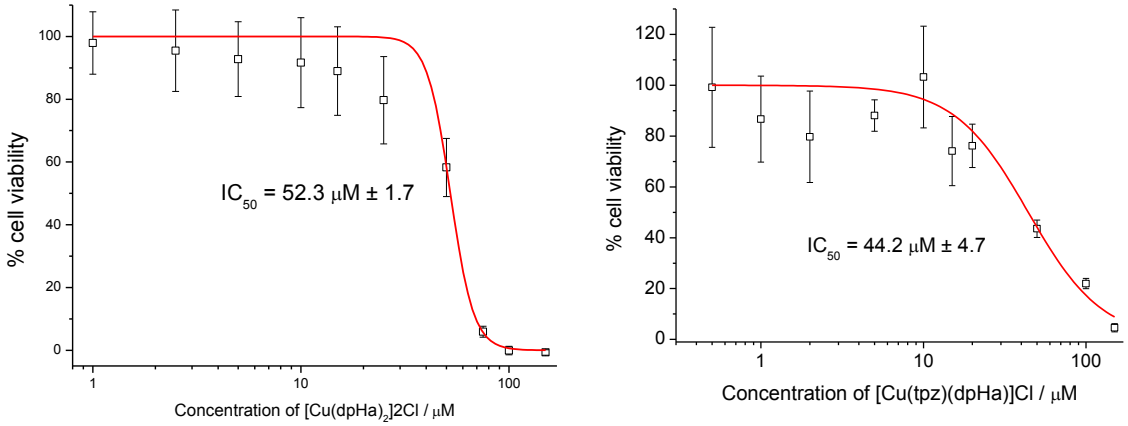

Figure 6.3: Example IC_{50} curves of $[Cu(dpHa)_2]Cl_2$ (*left*) and [Cu(tpz)(dpHa)]Cl (*right*) against A549 cells

Table 6.2 summarises the mean weighted IC_{50} values for these complexes.

Table 6.2: IC_{50} data for $[Cu(dpHa)_2]Cl_2$ and [Cu(tpz)(dpHa)]Cl against A549 cells

Complex	**IC_{50} / μM**
$[Cu(dpHa)_2]Cl_2$	53.5 ± 0.8
[Cu(tpz)(dpHa)]Cl	44.8 ± 2.1

Firstly, it can be seen that the [Cu(tpz)(dpHa)]Cl complex is more potent than tpzH which was found to have an IC_{50} value of 170.3 ± 6.2 μM. This result is perhaps not surprising when compared to the IC_{50} value of $[Cu(dpHa)_2]Cl_2$ which is slightly less active. The cytotoxicity of these complexes is most likely to arise from rapid dissociation of the complex due to the copper centre undergoing substitution more rapidly than desired for a hypoxia prodrug.

Figure 6.4 shows example IC_{50} curves obtained for $[Co(tpz)(dpHa)_2]Cl_2$ and $[Co(tpz\text{-}CN)(dpHa)_2](NO_3)_2$.

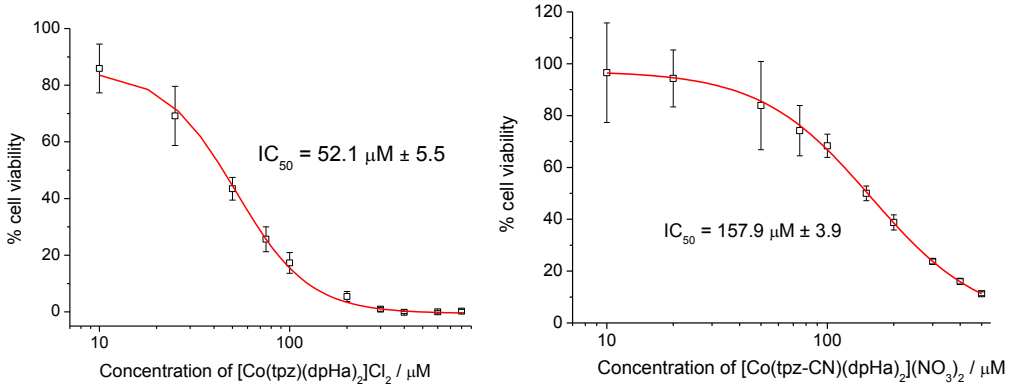

Figure 6.4: Example IC_{50} curves of $[Co(tpz)(dpHa)_2]2Cl$ (*left*) and $[Co(tpz\text{-}CN)(dpHa)_2](NO_3)_2$(*right*) against A549 cells

It can be seen that there is a marked difference between the obtained IC_{50} values for the heteroleptic cobalt(III) complexes of tpzH and tpzH-CN (**Figure 6.4** and **Table 6.3**).

Table 6.3: IC_{50} values (weighted mean) of tpzH, tpzH-CN, and the cobalt(III) complexes

Compound	**IC_{50} / µM**
tpzH	170.3 ± 6.2
tpzH-CN	143.0 ± 4.5
$[Co(tpz)(dpHa)_2]Cl_2$	60.7 ± 2.1
$[Co(tpz\text{-}CN)(dpHa)_2](NO_3)_2$	158.3 ± 3.7
$[Co(CO_3)(dpHa)_2]NO_3$	> 466

The $Co(tpz\text{-}CN)(dpHa)_2](NO_3)_2$ complex has an IC_{50} value close to that of the uncoordinated tpzH-CN ligand, implying that no additional activity is brought about by the dpHa ligand or cobalt centre. This is further supported by the cytotoxic activity of $[Co(CO_3)(dpHa)_2]NO_3$ being found to be beyond the tested range, being near to 500 µM (**Figure 6.5**).

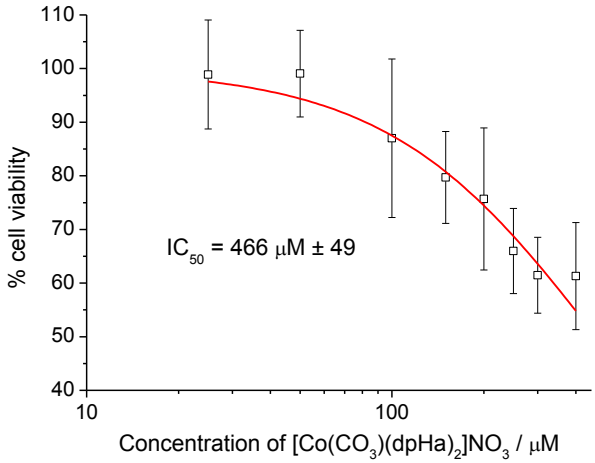

Figure 6.5: Example IC_{50} curve of $[Co(CO_3)(dpHa)_2]NO_3$ against A549 cells

The results obtained with $[Co(tpz)(dpHa)_2]Cl_2$ afford an IC_{50} value which is in juxtaposition to this, with the cobalt(III) complex having an almost three-fold greater activity than uncoordinated tpzH (**Table 6.4**). Significantly, this increase in activity brought about upon complexation is supported by the increased cytotoxic activity observed with the copper(II) heteroleptic complex.

The results suggest that complexation of tpzH-CN to a cobalt(III) centre does increase its cytotoxic activity. One immediate advantage of the cobalt(III) complex over the free tpzH-CN ligand was its greater solubility; the complex was easily dissolved directly into the biological medium whereas the tpzH-CN ligand required being dissolved within a sonic bath. Complexation of tpzH to a metal centre would seem to bring about an increase in activity compared to the free ligand and future work would need to investigate this further. However, this dramatic increase in cytotoxicity compared to the active ligand and control complex not containing the active ligand is not unprecedented.

A similar trend has been reported for the cobalt(III) complexes [**21**], [**22**] and [**23**] (**Figure 6.6** and **Tables 6.4** and **6.5**), where the cytotoxicity of the cobalt(III) complex was greater than that of the uncoordinated ligand and the $[Co(Cl)_2(cyclam)]Cl$ control complex combined.

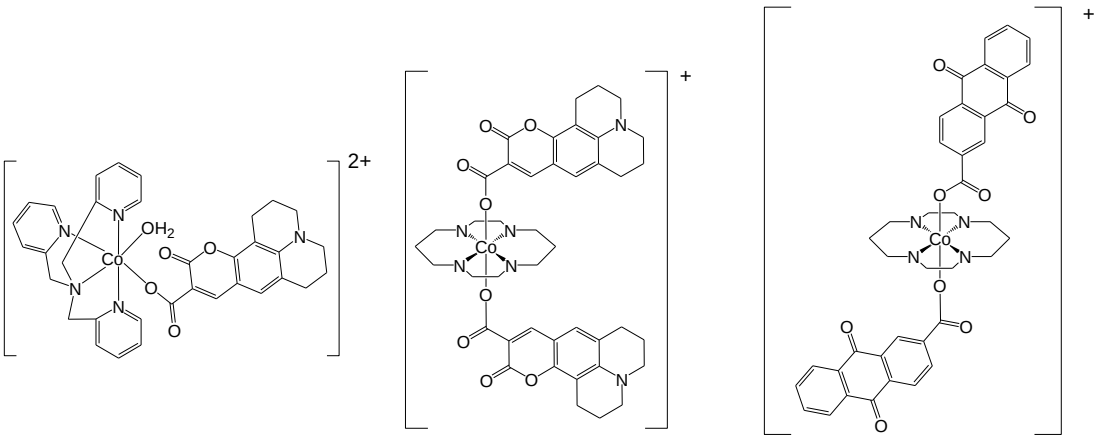

[**24**] [**25**] [**26**]

Figure 6.6: Structures of the cobalt(III) complexes [**24**], [**25**] and [**26**].[104, 105]

Table 6.4: IC_{50} under aerobic conditions of complex [**24**] against A2780.[104]

Compound	**IC_{50} against A2780 under / µM**
[**24**]	4.8 +/- 0.3
Active ligand of [**24**]	>200
$[Co(Cl)_2(cyclam)]Cl$	>200

Table 6.5: Activity of complexes [**25**] and [**26**] against DLD-1 cells.[105]

Compound	**IC_{50} under normoxia/ µM**	**IC_{50} under hypoxia / µM**
[**25**]	1.3 +/- 0.7	1.9 +/- 0.2
Active ligand of [**25**]	99 +/- 5	>200
[**26**]	35.6 +/- 0.9	20.04 +/- 0.1
Active ligand of [**26**]	>200	177 +/- 0.2
$[Co(Cl)_2(cyclam)]^+$	>200	>200

6.4. Reduction in cells

Owing to the similarity of the IC_{50} values of $[Co(tpz\text{-}CN)(dpHa)_2](NO_3)_2$ and tpzH-CN, it was thought that the N-oxide ligand was dissociating from the cobalt centre and taking effect upon the cell. To test this hypothesis, the complex was incubated with the cells at several concentrations, and its absorbance at 540 nm was monitored over 72 hours.

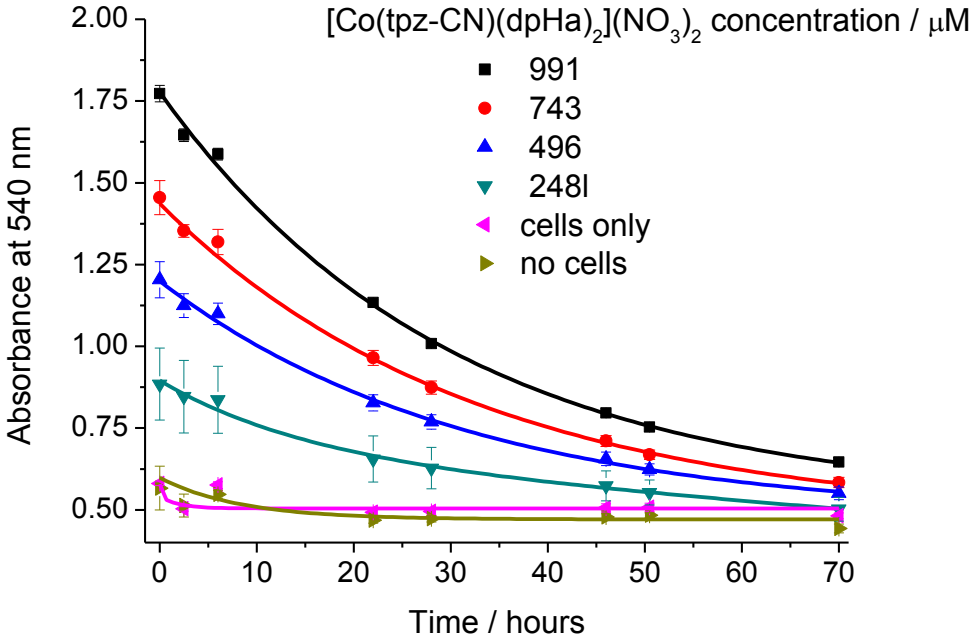

Figure 6.7: Absorbance at 540 nm of $[Co(tpz\text{-}CN)(dpHa)_2](NO_3)_2$ during incubation with A549 cells

Figure 6.7 clearly shows the gradual decrease in amount of the coordinated N-oxide ligand as it dissociated upon reduction of the cobalt(III) centre (**Scheme 6.2**).

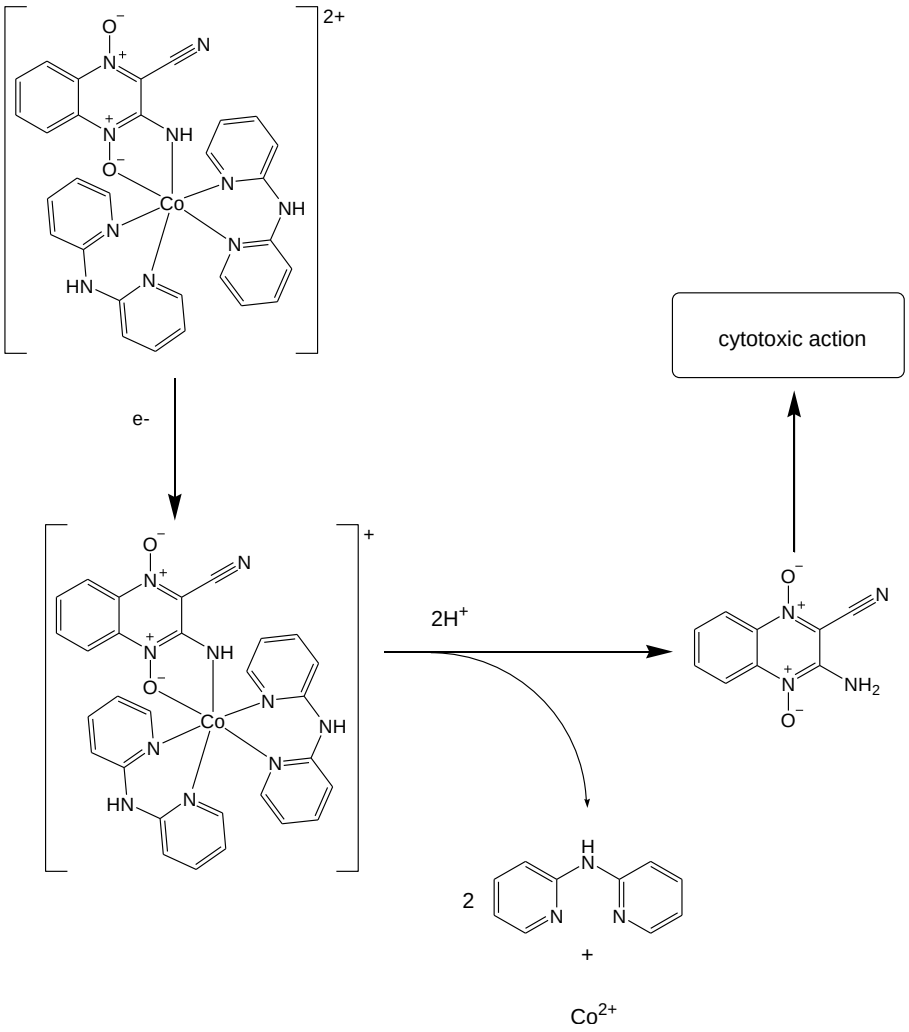

Scheme 6.2: Dissociation of tpzH-CN from its cobalt(III) complex found to occur upon incubation with A549 cells

The controls carried out with this experiment included monitoring the absorbance of the medium on its own, and the absorbance of medium containing cells but no complex. The absorbances of both controls were very similar and remained at a constant absorbance throughout, providing a measurement of no coordinated tpzH-CN being present. The absorbance of the two controls at 540 nm is due to the strong colour of the DMEM medium. After 70 hours, the complex, when at 248 μM concentration, is observed to have almost undergone complete dissociation. This concentration is greater than the IC_{50} complex (158.3 ± 3.7 μM), which does not have a large enough absorbance at 540 nm to provide clear absorbance data for this experiment. If the tpzH-CN ligand was not dissociating, then this would have made $[Co(tpz\text{-}CN)(dpHa)_2](NO_3)_2$ an unsuccessful candidate as a prodrug for tpzH-CN as it would have showed that complexation had not reduced its activity. The gradual

release observed of the tpzH-CN ligand from the cobalt(III) centre needs further investigation so that the difference in cytotoxicty profiles between the complex and free ligand after different incubation times can be explored.

To investigate if the reduction was due to cellular activity or the components of the medium, the experiment was repeated; one plate containing cells and one without. The absorbance of the equivalent concentrations between the plates remain the same over time (**Figure 6.8**), showing the reduction of the cobalt(III) complex is occurring independently of the cells.

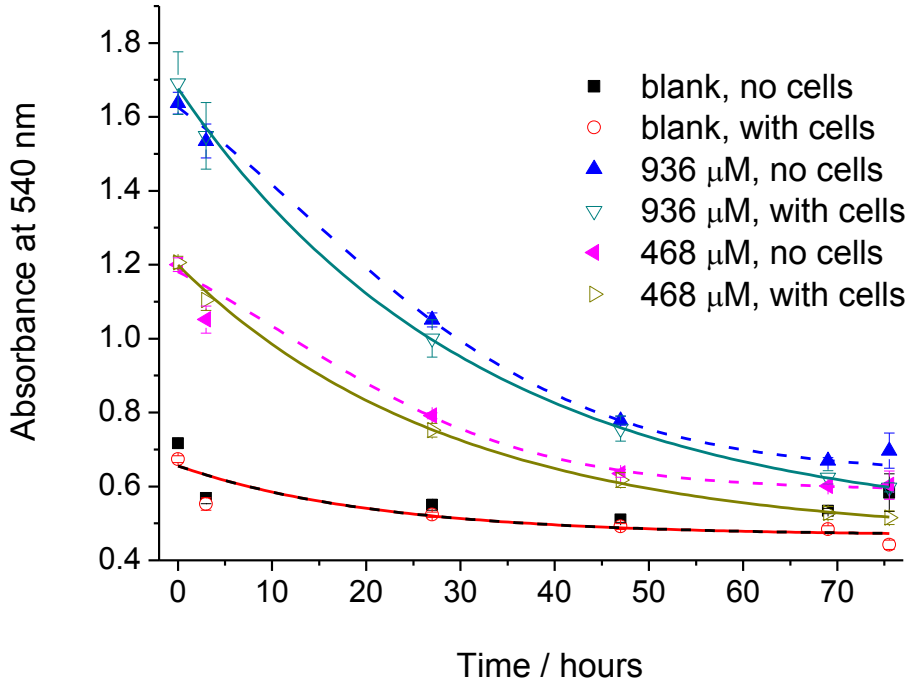

Figure 6.8: Absorbance at 540 nm of $[Co(tpz\text{-}CN)(dpHa)_2](NO_3)_2$ during incubation with A549 cells and incubation with DMEM medium

The DMEM medium contains several compounds which can be reducing in nature (**Table 6.6**), including cysteine which was shown to be able to reduce $[Co(tpz\text{-}CN)(dpHa)_2]^{2+}$ as described in **Chapter Five**. With or without the presence of cells, the reduction of the complex, and therefore dissociation of the tpzH-CN ligand, occurred over several days under aerobic conditions. This is significantly slower than the rate of reduction observed when the complex was mixed in solution with various reducing agents, suggesting the reduction of the complex dissociation of the tpzH-CN ligand increases under anaerobic conditions. This will hopefully result in more

rapid release of the tpzH-CN ligand in the hypoxic tumour environment than under normoxic conditions.

6.5. Overall Conclusions

The general aim of this project was to explore further the development of transition metal-based hypoxia prodrugs. It was observed that there were several organic compounds reported in the literature which had been shown to have high hypoxia-selective cytotoxicity, but were failing to meet their full therapeutic potential in vivo owing to factors such as poor delivery or chemical instability. Therefore, it was decided to see if therapeutically active species could be improved upon through incorporation into a transition metal complex. The reasoning behind this was to add the reduction of the metal centre as an additional 'barrier' to the generation of the cytotoxic species of the drug, which should help improve selectivity.

A series of complexes incorporating varied ligands have been prepared and characterised including a new class of heteroleptic complexes which incorporate two dpHa ligands and a therapeutically active 1, 4-*N*-oxide ligand such as tpzH. The metal centres used include copper(II) and cobalt(III) which are two of the most suitable metals to be used in the development of hypoxia-selective complexes. These complexes have been fully characterised and most have been structurally characterised using single crystal x-ray diffraction. One of the obtained structures was the first quinoxaline-1,4-*N*-oxide (tpz-H-R) transition metal complex (**Figure 6.9**), despite there being many reports into the coordination chemistry of these quinoxaline di-*N*-oxide ligands.

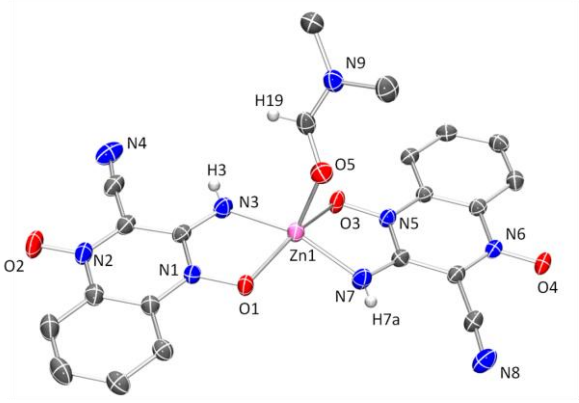

Figure 6.9: ORTEP plot of $[Zn(tpz\text{-}CN)_2(DMF)]$.[131]

It became increasingly apparent that the poor solubility of this family of complexes would greatly hinder their biological applications but also their ease to study in solution. To overcome this, we were able to develop a novel range of heteroleptic complexes incorporating both a tpzH-R ligand and a dipyridylamine ligand (dpHa). Structural characterisation has shown that in metal(II) complexes of copper and zinc, these ligands are in a 1:1 ratio (**Figure 6.10**).

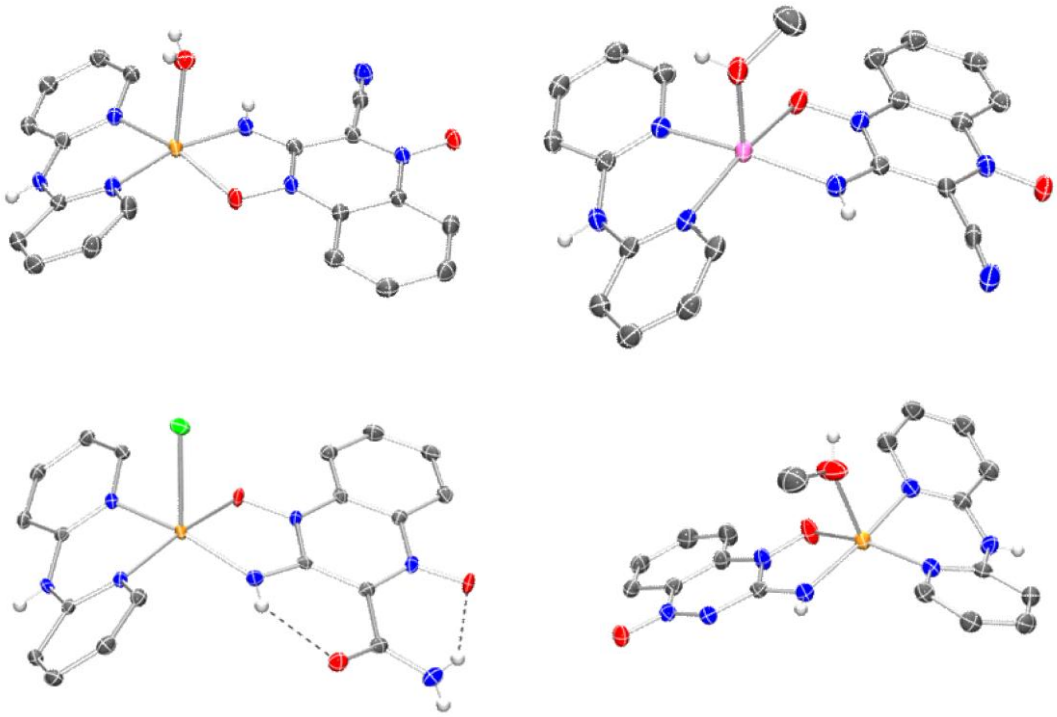

Figure 6.10: Obtained structures of metal(II) heteroleptic complexes which incorporate a dipyridylamine and N-oxide ligand in a 1:1 ratio.[131] *Clockwise from top left*: [Cu(tpz-CN)(dpHa)]Cl, [Zn(tpz-CN)(dpHa)]Cl, [Cu(tpz)(dpHa)]Cl and [Cu(Cl)(tpz-$CONH_2$)(dpHa)].

These heteroleptic complexes were immediately observed to have better solubility in various solvents which meant that their behaviour in solution could be studied. 2,2'-dipyridylamine happened to be a ligand already studied in this project, allowing the chemistry of the heteroleptic complexes to be compared with the equivalent homoleptic complexes of each ligand.

It was found that the difficulty of preparing cobalt(III) complexes of the tpzH-R ligands was overcome by using this heteroleptic system with the resulting products structurally characterised(**Figure 6.11**).

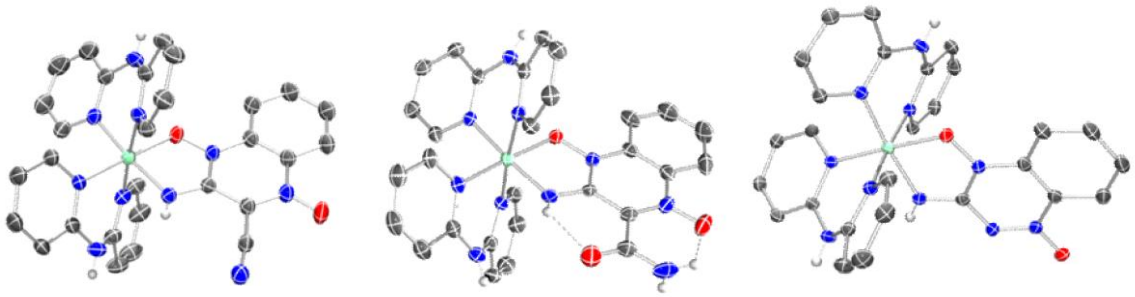

Figure 6.11: Structurally characterised heteroleptic cobalt(III) complexes (from left): $[Co(tpz\text{-}CN)(dpHa)_2]^{2+}$, $[Co(tpz\text{-}CNH_2)(dpHa)_2]^{2+}$and $[Co(tpz)(dpHa)_2]^{2+}$.[131]

One of the tpzH-R ligands successfully utilised was tirapazamine (tpzH), a compound which shows very high hypoxia selective toxicity *in vivo*. The successful synthesis of tpzH complexes provides a basis for one tactic of improving its biological properties.

The solution properties of these complexes have been studied and compared to their homoleptic analogues where possible. For the copper(II) complexes, both the hetero- and homoleptic complexes of dpHa and the tpzH-R ligands were found to not undergo dissociation upon being in aqueous solution. The heteroleptic complexes were found to undergo dissociation at pH values similar to those believed to occur in the extracellular environments of solid tumours. They were found to undergo a reductive process using cyclic voltammetry in DMSO at potentials more negative that -0.3 V *vs.* Ag/AgCl which was shown to be irreversible. These reductions occur at a potential less negative than that found to be required for hypoxia selectivity in copper(II) complexes (-0.57 V *vs*. Ag/AgCl in DMSO) by studies of [Cu(ATSM)] analogues.[90, 91] The heteroleptic copper(II) complex which had high enough solubility in biological medium for cytotoxicity assays against A549 cells was found to have an IC_{50} value of 44.8 ± 2.1 μM. This value is lower than that obtained for tpzH (170.3 ± 6.2 μM) and $[Cu(dpHa)_2]Cl_2$ (53.5 ± 0.8 μM), implying that the coordination of tpzH into this complex has not reduced the toxicity of tpzH under aerobic conditions. This agrees with the reduction potential not being negative enough according to the findings of the studies on [Cu(ATSM)].

The cobalt(III) heteroleptic complexes were found to contain one 1,4-N-oxide and two dpHa ligands. These were found to be stable in aqueous solution below pH 10. The reduction potential of cobalt(III) thought to be needed to facilitate hypoxia selectivity is of -0.305 to -0.705 V *vs*. Ag/AgCl.[193] The heteroleptic cobalt(III) complexes of tpzH and tpzH-CN both showed a reduction process at -0.06 and 0.00 V respectively.

The $[Co(tpz\text{-}CN)(dpHa)_2](NO_3)_2$ complex was found to have an IC_{50} value of 158.3 ± 3.7 μM against a549 cells under aerobic conditions, a value similar to that of uncoordinated tpzH-CN (143.0 ± 4.5 μM). This result along with the $[Co(CO_3)(dpHa)_2](NO_3)_2$ complex having an IC_{50} value greater than > 466 μM implies that the dpHa ligands and cobalt centre do not provide significant additional toxicity. The similarity of the IC_{50} values for the complex and tpzH-CN ligand indicates that the ligand is dissociating upon reduction of the metal centre. This was supported with spectroscopic studies monitoring absorbance of the complex incubated with A549 cells over several days. This, along with the reduction potentials for these complexes being less negative than that suggested to be needed for hypoxia selectivity by previous studies implies that the reduction potential of these cobalt(III) complexes needs to be made more negative. The monitoring of the reduction of $[Co(tpz\text{-}CN)(dpHa)_2](NO_3)_2$ in cells was found to occur due to reducing agents within the biological medium, but encouragingly the reduction occurred over several days, implying that complexation of tpzH-CN to cobalt(III) brings about a decreased rate of release of the 1,4-*N*-oxide ligand, even under aerobic conditions. UV-vis spectroscopy experiments measuring the reduction by various biological reducing agents over time also support that the reduction of these cobalt(III) complexes is inhibited under aerobic conditions, so the ligands therefore dissociate at a slower rate.

Cytotoxicity results of the $[Co(tpz)(dpHa)_2]Cl_2$ complex followed a trend observed with previously reported cobalt(III) complexes, in that the complex was more cytotoxic than its individual components. It is not clear how the complex affects the activity of the tpzH ligand, so studies are needed to confirm that the cytotoxic action of tpzH are inhibited upon complexation or if there is a cooperative mechanism between the different components. If the ligand is inactive when coordinated to the cobalt(III) centre, then this provides a promising basis for a hypoxia-selective

prodrug as long as its reduction potential can be tuned to a more negative value. If successful, this could result in a tpzH based hypoxia-selective prodrug with increased potency.

6.6. Future Work

Studies are needed to enable a fuller understanding of the results from the cytotoxicity assays. Time dependant IC_{50} studies would provide a useful indicator of how the activity of the 1,4-*N*-oxide ligands is altered through complexation. Confocal microscopy studies could provide beneficial information on if the distribution of the 1,4-*N*-oxide ligands within the cell differs when delivered as a complex or as an uncoordinated ligand. The cytotoxicity of these complexes under hypoxia needs to be investigated, including an investigation into whether the tpzH-$CONH_2$ ligand displays cytotoxicity in the absence of oxygen.

The dpHa ligand for these complexes does not seem to induce significant cytotoxicity on its own, so perhaps provides an opportunity for this to be modified in an attempt to make the reduction potentials of the cobalt(III) complexes more negative. The potential to expand upon the library of these heteroleptic complexes has already been briefly illustrated with the incorporation of dpma and phen in place of the dpHa ligand. Exchanging the dpHa ligand for ones with three or four amine donors (**Figure 6.12**), to see what effect this has on the complex's properties such as if it induces greater stability for the reduced cobalt(II) species.

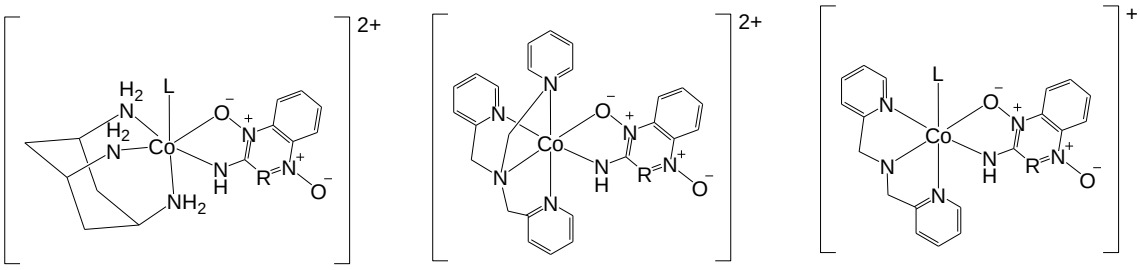

Figure 6.12: Possible alternative ligands to use for the 1,4-*N*-oxide cobalt(III) heteroleptic complexes

7. Experimental

All experiments were carried out using chemicals obtained from Sigma Aldrich, Fluka, Lancaster Chemicals or Alfa Aesar and used without further purification. The compound CN-dpHa-py was provided by Sentinel Oncology, who also prepared its precursor 2-chloro-4-(1-pyrrolidin-1-ylmethyl)pyridine. Mass spectrometry and elemental analyses were performed by the mass spectrometry and microanalytical services at the University of York. All data analysis was carried out using Origin v8.5.

7.1. Instrumentation

Elemental analyses were carried out on an Exeter Analytical Analyser calibrated against acetanilide and with S-Benzylthiuronium chloride as the internal standard. UV-vis spectra were collected on an Agilent 8453 instrument and IR data collected on an Avatar 370 FT-IR Thermo Nicolet Instrument. Fluorescence spectra were recorded on a Hitachi F-4500 fluorescence spectrophotometer. Mass spectrometry was carried out on a Bruker microTOF electrospray mass spectrometer. Measurements of pH were made with a standard glass electrode.

X-ray diffraction data was collected on a single-crystal Bruker Smart Apex CCD diffractometer with a Mo-K(alpha) radiation source (λ = 0.71073 Å). Diffractometer control, data collection and initial unit cell determination were performed using SAINT^{+}.[197] Data collection was carried out by the crystallography service at the University of York. Absorption corrections were applied by SADABS.[198] Structures were solved by either Patterson or direct methods using SHELXS-97 and refined by full-matrix, least squares using SHELXL-97.[199, 200] All non-hydrogen atoms and hydrogen atoms of heteroatoms were refined anisotropically. Hydrogen atoms were placed using a "riding model" and included in the refinement at the calculated positions.

7.2. Chapter Two proceedures

7.2.1. Synthesis of dpRa ligands

Synthesis of 2,2'-dipyridylmethylamine (dpma)

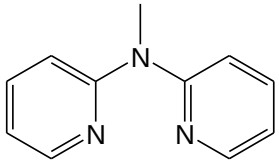

Five equivalents NaOH (0.24 g, 6.00 mmol) dissolved in 1 mL H_2O was added to a stirred solution of dpHa (0.21 g, 1.24 mmol) in 6 mL DMSO, causing it to turn pale yellow. After 20 minutes stirring, two equivalents MeI (0.2 mL, 3.21 mmol) were added and the re action mixture was left to stir overnight. 20 mL H_2O was added to the reaction mixture before the product was extracted with Et_2O and dried over $MgSO_4$. The product was obtained as yellow oil.

Yield: 0.53 g, 0.0029 mmol, 66%

^{1}H NMR (400 MHz, d_6-DMSO): δ8.30 (ddd, 2H, J = 5.0, 2.0, 0.8 Hz, pyridyl-H), δ7.65 (ddd, 2H, J = 8.5, 7.0, 2.0 Hz, pyridyl-H), δ7.22 (dt, 2H, J = 8.0, 1.0 Hz, pyridyl-H), δ6.98 (dd, 2H, J = 7.0, 5.0, 1.0 Hz, pyridyl-H), δ3.51 (s, 3H, CH_3).

^{13}C{^{1}H} NMR (400 MHz, d_6-DMSO): δ154.3, δ147.3, δ137.4, δ115.7, δ111.6

MS ESI (+ve ion) / *mz*: 186.10 (M^+)

IR (NaCl cell) / cm^{-1}: 3053, 3004.5, 2913, 1734, 1700, 1653, 1583, 1472, 1430, 1355, 1326, 1278, 1139

Synthesis of 2,2'-dipyridylethylamine (dpea)

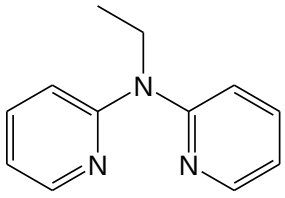

Five equivalents NaOH (0.15 g, 3.75 mmol) dissolved in 1 mL H_2O was added to a stirred solution of dpHa (0.10 g, 0.58 mmol) in 6 mL DMSO, causing it to turn pale yellow. After 20 minutes stirring, two equivalents EtI (0.1 mL, 1.2 mmol) were added and the re action mixture was left to stir overnight. 20 mL H_2O was added to the reaction mixture before the product was extracted with Et_2O and dried over $MgSO_4$. The product was obtained as a yellow oil.

Yield: 0.08 g, 0.40 mmol, 69%

MS ESI (+ve ion) / *mz*: 200.12 (M^+)

^{1}H NMR (400 MHz, d_6-DMSO): δ8.29 (ddd, 2H, J = 5.0, 1.0, 0.5 Hz, pyridyl-H), δ7.60 (ddd, 2H, J = 7.5, 2.0, 1.0 Hz, pyridyl-H), δ7.12 (dt, 2H, J = 8.5, 1.0 Hz, pyridyl-H), δ6.92 (ddd, 2H, J = 7.4, 5.0, 1.0 Hz, pyridyl-H), δ4.15 (q, 2H, J = 7.0 Hz, CH_2), δ1.14 (t, 2H, J = 7.0 Hz, CH_3)

^{13}C{^{1}H} NMR (400 MHz, d_6-DMSO): δ156.4, δ148.0, δ137.4, δ117.0, δ114.4, δ42.2 (CH_2) , δ13.3 (CH_3)

IR (NaCl cell) / cm^{-1}:2974, 2929, 1583, 1468, 1422, 1321, 1267, 1140, 1090, 985, 772

Synthesis of 2-chloro-4-(1-pyrrolidin-1-ylmethyl)pyridine

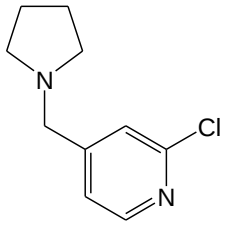

2-chloro-4-pyridinecarboxaldehyde (1.42 g, 10 mmol) was stirred with 1 equivalent pyrrolidine (0.8 mL, 10 mmol) in 50 mL DCM and 2 mL acetic acid was then added. To the stirred solution 1.2 equivalents $NaBH(OAc)_3$ (2.54 g, 12.0 mmol)was added then the reaction mixture was left to stir overnight. The reaction mixture was then filtered through celite and washed with DCM. The filtrate was concentrated and purified by column chromatography to afford the product as a brown oil.

Yield: 1.5 g, 7.63 mmol, 74%

Synthesis of CN-dpHa-py

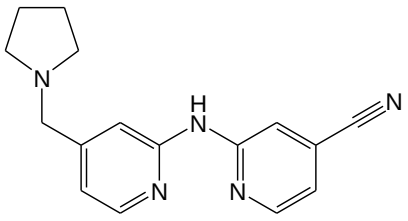

$Pd_2(dba)_3$ (0.09 g, 0.1 mmol), Xantphos ligand (0.09 g, 0.15 mmol), 2-amino-isonicotinonitrile (0.12 g, 1.0 mmol) finely ground Cs_2CO_3 (0.46 g, 1.4 mmol), 2-chloro-4-(1-pyrrolidin-1-ylmethyl)pyridine (0.20g, 1.0 mmol) in 4 mL toluene were placed in a re-sealable microwave tube. The tube was then sealed and underwent

three cycles of being placed under vacuum and then filled with N_2. The mixture was heated at 100ºC overnight and then allowed to cool. The reaction mixture was diluted with THF and then filtered and concentrated. The product was purified on a SiO_2 flash column using 0-100% gradient DCM then 10% saturated NH_3 / MeOH in DCM to afford the product as an off-white powder.

^{1}H NMR (400 MHz, d_6-DMSO): δ10.51 (br. s, 1H, NH), δ8.48 (br. s, 1H, pyridyl-H), δ8.39 (br. s, 1H, pyridyl-H), δ8.16 (br. s, 1H, pyridyl-H), δ7.70 (br. s, 1H, pyridyl-H), δ7.33 (br. s, 1H), δ7.22 (br. s, 1H), δ4.38 (br. s, 2H, alkyl-H), δ3.32 (br. s, 2H, py-H), δ3.08 (br. s, 2H, py-H), δ2.04 (br. s, 2H, py-H), δ1.88 (br. s, 2H, py-H)

7.2.2. Preparation of dpRa complexes

Preparation of $[Co(Cl)_2(dpHa)]$.[127, 133]

One equivalent dpHa (0.98 g, 5.6 mmol) was added to a stirred solution of $CoCl_2.6H_2O$ (1.32 g, 5.5 mmol), causing the formation of a dark blue precipitate. After stirring for 10 minutes, the precipitate was isolated by filtration *in vacuo* as a royal blue powder and washed with EtOH then Et_2O. Dark blue single crystals suitable for diffraction were obtained by slow diffusion of Et_2O into a DMF solution.

Yield: 1.39 g, 4.6 mmol, 84%

CHN; found: %C 39.03, %H 2.84, %N 13.54; calculated ($CoC_{10}H_9N_3Cl_2$): %C 39.90, %H 2.95, %N 13.67

Preparation of $[Co(Cl)_2(dpHa)_2]$.[133]

Two equivalents dpHa (0.27 g, 1.6 mmol) were added to a stirred solution of $CoCl_2.6H_2O$ (0.91 g, 0.8 mmol) in 10 mL MeOH. After 0.5 hours stirring, the solution was left to stand and over the course of a week, deep pink crystals suitable for diffraction formed.

Yield: 0.24 g, 0.51 mmol, 64%

Preparation of $[Co(CO_3)(dpHa)_2]NO_3$

One equivalent $Co(NO_3)_2.6H_2O$ (0.20 g, 0.69 mmol) was stirred in 10 mL MeOH and to this, two equivalents dpHa (0.24 g, 1.40 mmol) were added causing a colour change from pink to orange. After 0.5 hours, two equivalents $NaHCO_3$ (0.1282 g,

1.53 mmol) were added followed by 5 mL H_2O_2 which caused the reaction mixture to turn dark red. After two hours stirring, the reaction mixture was filtered and then the filtrate left to stand. After a couple of days, red crystals had formed which were isolated by filtration and washed with Et_2O.

Yield: 0.14 g, 0.28 mmol, 41%

^{1}H NMR (400 MHz, D_2O): δ8.05 (td, 2H, J = 8.0, 1.0 Hz, pyridyl-H), δ7.99 (td, 2H, J = 8.0, 1.0 Hz, pyridyl-H), δ7.66 (dd, 2H, J = 6.0, 1.0 Hz, pyridyl-H), δ7.47 (ap. t, 2H, J = 6.0 Hz, pyridyl-H), δ7.40 (dd, 2H, J = 6.0, 1.0 Hz, pyridyl-H), δ7.30 (br. d, 2H, J = 8.5 Hz, pyridyl-H) δ7.15 (ap. td, 2H, J = 7.0, 1.0 Hz, pyridyl-H), δ6.98 (td, 2H, J = 6.5, 1.0 Hz, pyridyl-H)

^{13}C{^{1}H} NMR (400 MHz, d_6-DMSO): δ157.7, δ154.8, δ153.5, δ151.9, δ141.7, δ141.3, δ120.4, δ119.7, δ114.2, δ113.6

IR (KBr disc) / cm-1: 3193, 3076, 2980, 1646, 1569, 1506, 1419, 1384, 1322, 776

MS ESI (+ve) / *m/z*: 461.1 $[Co(CO_3)(dpHa)_2]^+$

CHN Analysis; found: %C 47.69, %H 3.48, %N 18.53; calculated (for $CoC_{21}H_{18}N_7O_6$): %C 48.19, %H 3.47, %N 18.73

Preparation of $[Cu(dpHa)_2]Cl_2$.[130]

Two equivalents dpHa (0.74 g, 4.34 mmol) dissolved in 20 mL acetone were added to 1 equivalent $CuCl_2.6H_2O$ (0.37 g, 2.17 mmol) stirred in 30 mL EtOH, causing the formation of a bright green suspension. After 45 minutes stirring the product was isolated by filtration *in vacuo* and washed with acetone. Green diffraction quality single crystals were obtained by slow evaporation from a solution of MeOH layered over ^{n}BuOH over the duration of a week at room temperature

Yield = 0.90 g, 1.88 mmol, 87%

MS ESI (+ve ion) / *m/z*: = 405.1 $[Cu(dpHa)_2]^{2+}$

CHN Analysis; found: %C 48.78, %H 3.86, %N 17.00; calculated (for $CuC_{20}H_{18}N_6Cl_2$): %C 50.38, %H 3.80, % N 17.62

Preparation of $[Cu(Cl)_2(dpHa)]$.[130]

Two equivalents dpHa (0.88 g, 5.10 mmol) were added to a stirred solution of $CuCl_2.2H_2O$ (0.87 g, 5.00 mmol) in 10 mL MeOH, resulting in the formation of a dark green precipitate. After 20 minutes stirring, the precipitate was collected *in vacuo* and washed with EtOH.

Yield: 1.43 g, 4.60 mmol, 90%

MS FD (M+): 306 *m/z*

Preparation of $[Cu(NO_3)_2(dpHa)]$.[201]

One equivalent dpHa (0.27 g, 1.6 mmol) was added to $Cu(NO_3)_2.3H_2O$ (0.39 g, 1.6 mmol) stirred in 10 mL EtOH, causing the formation of a green precipitate. After 15 minutes stirring, the precipitate was isolated as a green solid by filtration *in vacuo* and washed with EtOH then Et_2O.

Yield: 0.39 g, 1.1 mmol, 69%

CHN Analysis; found: %C 33.33, %H 2.54, %N 18.97; calculated (for $CuC_{10}H_9N_5O_6$): %C 33.48, %H 2.53, %N 19.52

Preparation of $[Zn(Cl)_2(dpHa)]$.[128]

One equivalent dpHa (1.13 g, 6.6 mmol) was added to a stirred solution of ZnCl2 (0.90 g, 6.7 mmol) in 10 mL hot MeOH, causing the formation of a white precipitate. This was stirred for 10 minutes before the white precipitate was isolated by filtration *in vacuo* and washed with EtOH then Et_2O. Colourless single crystals suitable for x-ray diffraction were obtained by slow diffusion of Et_2O into a DMF solution.

^1H NMR (400 MHz, d_6-DMSO): δ10.01 (br. s, 1H, NH), δ8.25 (br. s, 2H, pyridyl-H), δ 7.80 (br. s, 2H, pyridyl-H), δ7.44 (br. s, 2H, pyridyl-H), δ7.00 (br. s, 2H, pyridyl-H)

$^{13}C\{^1H\}$ NMR (400 MHz, d_6-DMSO): δ153.8, δ146.7, δ140.8, δ117.8, δ114.3

CHN Analysis; found: %C 39.03, %H 2.84, %N 13.54; calculated (for $ZnC_{10}H_9N_3Cl_2$): %C 39.06, %H 2.95, %N 13.67

Preparation of $[Zn(dpHa)_2](BF_4)_2$.[129]

Two equivalents dpHa (0.71 g, 4.16 mmol) was added to solution of $Zn(BF_4)_2$ (0.49 g, 2.05 mmol) in 30 mL MeOH which was heated at reflux. The reaction was left to heat at reflux overnight and allowed to cool before Et2O was added, causing the formation of a white precipitate. The white solid was isolated by filtration and washed with EtOH then Et_2O.

Yield: 0.47g, 0.81 mmol, 39%

^{1}H NMR (400 MHz, MeOD): δ8.05 (br. d, 4H, J = 4.0 Hz, pyridyl-H), δ7.94 (ddd, 4H, J = 8.0, 7.5, 1.5 Hz, pyridyl-H), δ7.20 (d, 4H, J = 8.0 Hz, pyridyl-H), δ7.10 (t, 4H, J = 6.0 Hz, pyridyl-H)
MS ESI (+ve ion) / *mz*: 406.1

Preparation of [Co(Cl)$_2$(dpma)$_2$]OTf

$CoCl_2.6H_2O$ (0.42 g, 1.77 mmol) was added to a stirred solution of two equivalents dpma (0.66 g, 3.57 mmol) in 10 mL EtOH. After 10 minutes stirring, one equivalent KOTf (0.34 g, 1.8 mmol) was added followed by 2 mL H_2O_2 which immediately caused the solution to turn dark red. This was stirred for one hour then the reaction mixture was filtered. Dark red single crystals suitable for diffraction were obtained upon leaving the filtrate to stand over the course of a week.
Yield (of crystals): 0.03g, 0.04 mmol, 2%
^{1}H NMR (400 MHz, d_6-DMSO): δ8.16 (ddd, 2H, J = 8.5, 7.0, 1.5 Hz, pyridyl-H), δ8.12 (ddd, 2H, J = 8.5, 7.0, 1.5 Hz, pyridyl-H), δ7.68 (d, 2H, J = 8.5 Hz, pyridyl-H), δ 7.65 (dd, 2H,J = 6.0, 1.5 Hz, pyridyl-H), δ7.51 (d, 2H, J = 8.5 Hz, pyridyl-H), δ7.44 (dd, 2H, J = 6.0, 1.5 Hz, pyridyl-H), δ7.24 (td, 2H, J = 6.5, 1.0 Hz, pyridyl-H), δ7.07 (td, 2H, J = 6.0, 1.0 Hz, pyridyl-H), δ3.82 (s, 6H, CH_3)
MS (ESI) / *mz*: 499.1 $[Co(Cl)_2(dpma)_2]^+$

Preparation of [Cu(Cl)$_2$(dpma)]

One equivalent dpma (1.01 g, 5.5 mmol) was added to a stirred solution of $CuCl_2.2H_2O$ (0.98 g, 5.7 mmol) in 10 mL MeOH, causing a green precipitate to form. After 20 minutes stirring, the product was isolated by filtration *in vacuo* as a green solid and washed with MeOH then Et_2O. Green diffraction quality single crystals were obtained by leaving the filtrate to stand for two days at room temperature.
Yield: 0.84 g, 2.6 mmol, 47%
CHN Analysis; found: %C 41.00, %H 3.45, %N 12.89; calculated (for $CuC_{11}H_{11}N_3Cl_2$): %C 41.33, %H 3.47, %N 13.14

Preparation of [Zn(Cl)$_2$(dpma)]

One equivalent dpma (0.34 g, 1.8 mmol) was added to a stirred solution of $ZnCl_2$ (0.26 g, 1.9 mmol) in 6 mL hot MeOH, causing the formation of a white precipitate. After 10 minutes stirring, the reaction mixture was filtered *in vacuo* to isolate the product as a white powder. The product was washed with MeOH then Et_2O. Colourless single crystals suitable for x-ray diffraction were obtained by slowly diffusing Et_2O into a DMF solution.

Yield: 0.34 g, 1.1 mmol, 61%

^{1}H NMR (400 MHz, d_6-DMSO): δ8.25 (2H, ddd, J = 5.0, 2.0, 1.0 Hz, pyridyl-H), δ7.61 (ddd, 2H, J = 9.0, 7.0, 2.0 Hz, pyridyl-H), δ7.18 (dt, 2H, J = 9.0, 1.0 Hz, pyridyl-H), δ6.91 (ddd, 2H, J = 7.0, 5.0, 1.0 Hz, pyridyl-H), δ3.46 (s, 3H, CH_3)

^{13}C{^{1}H} NMR (400 MHz, d_6-DMSO): δ157.51, δ148.2, δ137.8, δ117.3, δ114.4, δ35.5

Preparation of [Cu(Cl)$_2$(dpea)]

One equivalent dpea (0.05 g, 0.26 mmol) was added to a solution of $CuCl_2.2H_2O$ (0.05g, 0.27 mmol) in 5 mL MeOH, causing the formation of a green precipitate. After 10 minutes stirring, the green solid was isolated by filtration *in vacuo* and washed with MeOH then Et_2O. Green single crystals of diffraction quality were obtained by allowing the filtrate from the reaction to stand for several days at room temperature.

Yield: 0.02g, 0.06 mmol, 23%

Preparation of [Zn(Cl)$_2$(dpea)]

One equivalent dpea (0.05 g, 0.25 mmol) was added to a stirred solution of $ZnCl_2$ (0.04 g, 0.29 mmol) in 5 mL MeOH, causing the formation of a white precipitate. After 10 minutes stirring, the white solid was isolated by filtration *in vacuo* and washed with MeOH then Et_2O. Colourless single crystals of diffraction quality were obtained by allowing Et_2O to slowly diffuse into a DMF solution.

Yield: 0.04 g, 0.12 mmol, 49%

^{1}H NMR (400 MHz, d_6-DMSO): δ8.31 (br. d, 2H, J = 4.0 Hz, pyridyl-H), δ7.64 (ap. t, 2H, J = 7.5 Hz, pyridyl-H), δ7.14 (d, 2H, J = 8.0 Hz, pyridyl-H), δ6.98 (ap. t, 2H, J = 5.0 Hz, pyridyl-H), δ4.16 (q, 2H, J = 7.0 Hz, CH_2), δ1.15 (t, 3H, J = 7.0 Hz, CH_3)

7.3. Chapter Three procedures

7.3.1. Synthesis of *N*1,*N*4-oxide ligands

Synthesis of 3-amino-1,2,4-benzotriazine-*N*1-oxide.[168]

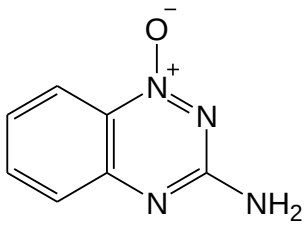

2-nitroaniline (2.40 g, 17.4 mmol) was stirred at 100ºC with cyanamide (1.29 g, 30.7 mmol) until a molten red liquid formed. This was then allowed to cool to room temperature before the slow drop-wise addition of ice cold conc. HCl (37%). The mixture was then stirred at 100 ºC for 30 minutes and was then allowed to cool to room temperature. 4 mL 16 M NaOH(aq) was added drop-wise before the reaction was stirred at 100 ºC for 2 hours. 50 mL H2O was added to the reaction mixture after it had been allowed to cool. A bright yellow precipitate was isolated by filtration and washed with cold MeOH.

Yield: 1.81 g, 11.2 mmol, 65%

MS ESI (+ve ion): 163.06

^{1}H NMR (400 MHz, d_6-DMSO): δ8.12 (ddd, 1H, J = 8.0, 1.2, 1.0 Hz, phenyl-H), δ7.77 (ddd, 1H, J = 8.5, 8.0, 1.5 Hz, phenyl-H), δ5.52 (ddd, 1H, J = 8.5, 1.5, 1.0 Hz, phenyl-H), δ7.3 (m, 3H, phenyl-H and NH_2)

Synthesis of 3-amino-1,2,4-benzotriazine-*N*1,*N*4-oxide (tpzH).[168]

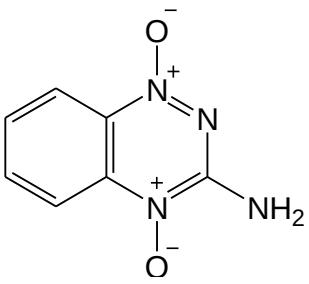

3-amino-1,2,4-benzotriazine-1-oxide (0.54 g, 3.33 mmol) was stirred in a mixture of 50 mL glacial acetic acid and 50 mL H_2O_2 at 70°C overnight. The bright orange reaction mixture was then slowly neutralised with $NaHCO_3$ and filtered, before the product was extracted from the filtrated with $CHCl_3$. The dark bright orange product was recrystallised from hot EtOH.

Yield: 0.12g, 0.65 mmol, 20% yield

^{1}H NMR (400 MHz, MeOD): δ8.34 (dt, 1H, J = 8.0, 1.0 Hz, phenyl-H), δ8.21 (ddd, 1H, J = 8.5, 1.0, 0.5 Hz, phenyl-H), δ8.02 (ddd, 1H, J = 8.5, 7.0, 1.5 Hz, phenyl-H), δ7.62 (ddd, J = 9.0, 7.0, 1.5 Hz, phenyl-H)

^{1}H NMR (400 MHz, d_6-DMSO): δ8.20 (d, 1H, J = 8.0 Hz, phenyl-H), δ8.13 (d, 1H, J = 8.0 Hz, phenyl-H), δ8,05 (br. s, 2H, NH_2), δ7.94 (dt, 1H, J = 8.5, 7.0, 1.0 Hz, phenyl-H), δ7.57 (td, 1H, J = 8.5, 8.0, 1.0 Hz, phenyl-H).

^{13}C{^{1}H} NMR (400 MHz, d_6-DMSO): δ151.9, δ138.8, δ135.8, 131.0, 127.0, 121.4, 117.3

IR (KBr disc) / cm-1: 3411, 3290, 3095, 1646, 1592, 1490, 1422, 1364, 1173, 1101

MS ESI (+ve ion) / *mz*: 179.06 (M+)

CHN Analysis; found: %C 47.24, %H 3.50, %N 30.94; calculated (for $C_7H_6N_4O_2$): %C 47.19, %H 3.39, %N 31.45

Synthesis of 3-aminoquinoxaline-2-carbonitrile-*N*1,*N*4-oxide (tpzH-CN).[161]

Benzofuroxan (3.06 g, 22.5 mmol) was stirred with two equivalents propanedinitrile (2.6 mL, 45.4 mmol) in 5 mL DMF and cooled with an ice bath. Upon addition of Et_3N (0.05 mL, 0.36 mmol) the reaction mixture became more red in colour and was stirred at 0ºC for 2 hours. The reaction mixture was then filtered to isolate the product as a fluorescent orange suspension which was then washed with acetone until the washings were no longer brown. The product was then dried *in vacuo*.

Yield: 2.56g, 12.7 mmol, 56%

MS ESI (+ve ion) / *mz*: 203.01 (M+)

^{1}H NMR (400 MHz, MeOD): δ8.42 (ddd, 1H, J = 9.0, 1.5, 0.5 Hz), δ8.37 (ddd, 1H, J = 8.5, 1.2, 0.5 Hz), δ8.00 (td, 1H, J = 7.0, 1.5 Hz), δ7.10 (ddd, 1H, J = 9.0, 7.0, 1.2 Hz)

^{1}H NMR (400 MHz, d_6-DMSO): δ8.29 (dd, 1H, J = 5.5, 1.0 Hz, phenyl-H), δ8.27 (dd, 1H, J = 5.5, 1.0 Hz, phenyl-H), δ8.08 (br. s, 2H, NH_2), δ7.93 (ddd, 1H, J = 8.5, 7.5, 1.0 Hz, phenyl-H), δ7.66 (ddd, 1H, J = 8.5, 8.0, 1.0 Hz, phenyl-H)

^{13}C{^{1}H} NMR (400 MHz, d_6-DMSO): δ146.4, 137.3, 134.6, 132.1, 127.9, 120.1, δ118.3, δ110.9, δ109.0

IR (KBr) / cm^{-1}: 3352 (NH_2), 3259 (NH_2), 2234 (CN), 1625, 1348, 1235, 1101, 857, 767, 609

CHN Analysis; found: %C 53.26, %H 3.03, %N 27.43; calculated (for $C_9H_6N_4O_2$): %C 53.47, %H 2.99, %N 27.71

Synthesis of 3-aminoquinoxaline-2-amido-*N*1,*N*4-oxide (tpzH-CONH$_2$).[163]

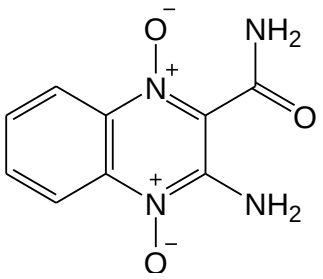

3-aminoquinoxaline-2-carbonitrile-N1,N4-oxide **(**tpzH-CN) (0.99 g 4.9 mmol) was stirred in 100 mL >95% H_2SO_4 to afford a yellow solution. This was stirred overnight at 90ºC then allowed to cool to room temperature. This was then poured onto *ca*. 800 cm^3 crushed ice and stirred in an ice bath whilst the reaction mixture was neutralised with concentrated NH_3, bringing about a colour change from yellow to a bright reddish orange. About 100 cm^3 more crushed ice was added to the mixture which was left to stir for an hour, during which time a bright orange precipitate formed. This was collected by filtration *in vacuo* and the resulting orange solid dissolved in acetone. The orange solution was filtered and then the solvent dried off from the filtrate to afford the product as an orange solid. Single red coloured crystals suitable for diffraction were obtained from a reaction of [Co(tpz-CN)$_2$] with H_2O_2 in MeOH.

Yield: 0.17g, 0.76 mmol, 6%

MS ESI (+ve ion) / *mz*: 221.06 (M+1)

IR (KBr disc) / cm^{-1}: 3371 (NH), 3251 (NH_2), 1671 (C=O), 1581, 1459, 1397, 1343, 1283, 1277, 1101, 1039, 767, 657

^{1}H NMR (d$_6$-DMSO, 400 MHz): δ9.85 (br. s, 1H, amide NH), δ 8.58 (br. s, 1H, amide NH), δ8.41 (d, 1H, J = 8.5 Hz, phenyl-H), δ8.30 (d, 1H, J = 8.5 Hz, phenyl-H), δ8.19 (br. s, 1H, NH_2), δ7.91 (ap. t, 1H, J = 7.5 Hz, phenyl-H), δ7.67 (ap. t, 1H, J = 7.5 Hz, phenyl-H).

^{13}C{^{1}H} NMR d$_6$-DMSO, 400 MHz): δ162.2, δ145.3, δ135.2, δ133.2, δ131.1, δ127.4, δ123.9, δ120.2, δ117.4.

CHN Analysis; found: %C 48.79, %H 3.75, %N 24.90; calculated (for $C_9H_8N_4O_3$): %C 49.09, %H 3.66, %N 25.45

7.3.2. Preparation of homoleptic complexes of *N*1,*N*4-oxide ligands

Preparation of [Cu(tpz)$_2$]

Two equivalents tpzH (0.05 g, 0.30 mmol) were added to a stirred solution of $Cu(OAc)_2.2H_2O$ (0.03 g, 0.15 mmol) in 10 mL MeOH, causing the formation of a deep red precipitate. After 0.5 hours, the dark red solid was isolated by filtration *in vacuo* and washed with MeOH.

Yield: 0.04 g, 0.09 mmol, 59%

IR (KBr disc) / cm^{-1}: 3360, 3310, 3110, 1570, 1500, 1410, 1360, 1260, 1210, 1160, 1110, 1030

Preparation of [Zn(tpz)$_2$]

Two equivalents tpzH (0.02 g, 0.09 mmol) were added to a stirred solution of $Zn(OAc)_2$ (0.01 g, 0.05 mmol) in 10 mL MeOH, causing the formation of a deep red precipitate. After 0.5 hours, the dark red solid was isolated by filtration *in vacuo* and washed with MeOH.

Yield: 0.02 g, 0.04 mmol, 84%

^{1}H NMR (d_6-DMSO, 400 MHz): δ8.10 (d, 1H, J = 8.5 Hz, phenyl-H), δ7.93 (d, 1H, J = 8.08 Hz, phenyl-H), δ7.87 (t, 1H, J = 7.68 Hz, phenyl-H), δ7.29 (t, 1H, J = 7.86 Hz, phenyl-H), δ6.98 (s, 1H, NH).

^{13}C{^{1}H} NMR (d_6-DMSO, 400 MHz): δ149.5, δ134.8, δ129.2, δ124.0, δ119.6, δ116.0, δ111.2

IR (KBr disc) / cm^{-1}: 3380, 3310, 1580, 1500, 1410, 1360, 1220, 1160, 1110, 1030

Preparation of [Co(tpz-CN)$_2$]

Two equivalents tpzH-CN (0.08 g, 0.39 mmol) were added to a stirred solution of $Co(OAc)_2.4H_2O$ (0.05 g, 0.20 mmol) in 10 mL MeOH, causing the formation of a dark purple precipitate. After 0.5 hours, the purple solid was isolated by filtration *in vacuo* and washed with MeOH.

Yield: 0.08 g, 0.16 mmol, 83%

IR (KBr disc) / cm^{-1}: 3380 (N-H), 3090, 2980, 2230 (C≡N), 1560, 1490, 1400, 1360, 1290, 1220, 1130, 1040

Preparation of [Cu(tpz-CN)$_2$]

Two equivalents tpzH-CN (0.16 g, 0.79 mmol) were added to a stirred solution of $Cu(OAc)_2.2H_2O$ (0.07 g, 0.39 mmol) in 10 mL MeOH, causing the formation of a deep red precipitate. After 0.5 hours, the dark red solid was isolated by filtration *in vacuo* and washed with MeOH.

Yield: 0.14 g, 0.30, 76%

IR (KBr disc) / cm^{-1} 3380 (N-H), 3350, 2990, 2230 (C≡N), 1640, 1560, 1470, 1380, 1290, 1230, 1150, 1050

Preparation of [Zn(tpz-CN)$_2$]

Two equivalents tpzH-CN (0.20 g, 0.99 mmol) were added to a stirred solution of $Zn(OAc)_2$ (0.10 g, 0.54 mmol) in 10 mL MeOH, causing the formation of a deep red precipitate. After 0.5 hours, the dark red solid was isolated by filtration *in vacuo* and washed with MeOH. Small deep –purple coloured single crystals suitable for single x-ray diffraction were obtained upon slow diffusion of Et_2O into a DMF solution.

Yield: 0.14 g, 0.30 mmol, 56%

^{1}H NMR (400 MHz, d_6-DMSO): δ8.15 (br. s, 2H, phenyl-H), δ7.87 (br. s, 1H, phenyl-H), δ7.41 (br. s, 1H, phenyl-H), δ6.56 (br. s, 1H, NH).

$^{13}C\{^1H\}$ NMR (400 MHz, d_6-DMSO z): δ149.5, δ134.8, δ129.2, δ124.0, δ124.0, δ119.6, δ116.0, δ111.1

IR (KBr disc) / cm^{-1}: 3360 (N-H), 3100, 2230 (C≡N), 1580, 1490, 1360, 1220, 1130, 1050

Preparation of [Cu(tpz-CONH$_2$)$_2$]

$Cu(OAc)_2.H_2O$ (0.017 g, 0.08 mmol) was added to a stirred suspension of tpzH-$CONH_2$ (0.033 g, 0.15 mmol) in 20 mL MeOH, causing it to turn from orange to dark red / purple. The reaction mixture was stirred or 1 hour before the precipitate was isolated by filtration *in vacuo* as a dark red-purple solid which was then washed with methanol then acetone.

Yield: 0.07 g, 0.13 mmol, 89%

IR (KBr disc) / cm^{-1}: 3330, 3290, 1675, 1539, 1400, 1240, 1196, 1134, 1039, 889, 668, 588, 520

Preparation of [Zn(tpz-$CONH_2$)$_2$]

$Zn(OAc)_2$.(0.01 g, 0.06 mmol) was dissolved in 5 mL MeOH and added to a stirred orange suspension of tpzH-$CONH_2$ (0.02 g, 0.11 mmol) in 15 mL MeOH, causing the formation of a purple-red precipitate. This was stirred for 1 hour then the solid isolated by filtration *in vacuo* and washed with methanol then acetone.

Yield: 0.0236 g, 0.047 mmol, 78%

^{1}H NMR (d_6-DMSO, 400 MHz): δ9.52 (br. s, 1H, CONH), δ8.48 (br. s, 1H, CONH), δ8.27 (d, 1H, J = 8.0 Hz, phenyl-H), δ8.14 (d, 1H, J = 8.0, phenyl-H), δ7.87 (s, 1H, NH), δ7.81 (ap. t, 1H, J = 8.0 Hz, phenyl-H), δ7.40 (ap. t, J = 8.0 Hz, 1H, phenyl-H)

Solubility was too poor to allow for ^{13}C NMR

IR (KBr disc): 3283, 3268, 3101, 1679, 1560, 1500, 1439, 1403, 1322, 1274, 1202, 1118, 1042, 1020, 768, 665, 598, 504, 450

7.4. Chapter Four procedures

7.4.1. Preparation of heteroleptic complexes containing tpzH

Preparation of [Co(tpz)(dpHa)$_2$](BF$_4$)$_2$

Two equivalents dpHa (0.65 g, 3.80 mmol) and one equivalent $Co(BF_4)_2.6H_2O$ (0.65 g, 1.90 mmol) were stirred together in 20 mL EtOH to afford an orange solution. One equivalent tpzH-CN (0.37 g, 1.82 mmol) was added, causing the reaction mixture to turn dark red. After 20 minutes stirring, one equivalent $K_2S_2O_8$ (0.55 g, 2.03 mmol) was added and this was stirred for 2 hours. The reaction mixture was filtered then Et_2O added to the filtrate to cause the formation of a dark red-purple precipitate. The precipitate was isolated by filtration, washed with Et2O and dried *in vacuo* to afford the product as a dark red-purple solid. Dark red diffraction quality crystals were obtained by allowing a methanolic solution layered over ^{n}BuOH to slowly evaporate at room temperature.

Yield: 0.57 g, 0.76 mmol, 42%

MS ESI / *mz*: 577.12 [M-*H*]$^+$, 289.07 [Co(tpz)(dpHa)$_2$]$^{2+}$

^{1}H NMR (400 MHz, MeOD): δ8.15 (ddd, 1H, J = 8.5, 7.0, 1.5 Hz), δ8.09, 1H, (ddd, J = 8.5, 7.0, 1.5 Hz), δ8.00 (d, 1H, J = 8.5 Hz), δ7.90 (dd, 1H, J = 6.5, 1.0 Hz), δ7.89 (m, 5H), δ7.80 (dd, 1H, J = 7.0, 1.0 Hz), δ7.68 (d, 2H, J = 6.5 Hz), δ7.54 (d, 1H, J =

8.5 Hz), δ7.47 (d,1H, J = 8.0 Hz), δ7.31 (ddd, 1H, J = 8.5, 5.0, 3.0 Hz), δ7.22 (d, 1H, J = 8.5 Hz), δ7.22 (d,1H, J = 8.5 Hz), δ7.15 (m, 4H)

$^{13}C\{^{1}H\}$ NMR (400 MHz, MeOD): δ154.7, δ153.6, δ152.3, δ152.1, δ150.2, δ147.3, δ142.0, δ141.6, δ141.0, δ137.3, δ135.1, δ129.4, δ124.6, δ121.2, δ120.3, δ120.2, δ120.0, δ114.4, δ113.8, δ113.6, δ112.5

IR (KBr disc) / cm^{-1}:3427, 3323, 3183, 3043, 1658, 1561, 1471, 1391, 1379, 1301, 1277, 1155, 1033, 1016, 821, 675

Preparation of $[Co(tpz)(dpHa)_2]Cl_2$

Two equivalents dpHa (0.16 g, 0.96 mmol) and one equivalent $CoCl_2.6H_2O$ (0.11 g, 0.47 mmol) were stirred together in 20 mL EtOH to afford a blue suspension. One equivalent tpzH (0.09 g, 0.48 mmol) was added, causing the reaction mixture to turn dark red. After 20 minutes stirring, one equivalent $K_2S_2O_8$ (0.22 g, 0.81 mmol) was added and this was stirred for 2 hours. The reaction mixture was filtered then Et_2O added to the filtrate to cause the formation of a dark red-purple precipitate. The precipitate was isolated by filtration, washed with Et_2O and dried *in vacuo* to afford the product as a dark red-purple solid. Yield: 0.064 g, 0.098 mmol, 21%

MS ESI / *mz*: 577.12 $[M\text{-}H]^+$, 289.07 $[Co(tpz)(dpHa)_2]^{2+}$

^{1}H NMR (400 MHz, MeOD): δ8.14 (ddd, 1H, J = 8.5, 7.0, 1.5 Hz), δ8.09, 1H, (ddd, J = 8.5, 7.0, 1.5 Hz), δ8.00 (d, 1H, J = 8.5 Hz), δ7.90 (dd, 1H, J = 6.5, 1.0 Hz), δ 7.89 (m, 5H), δ7.80 (dd, 1H, J = 7.0, 1.0 Hz), δ7.67 (d, 2H, J = 6.5 Hz), δ7.54 (d, 1H, J = 8.0 Hz), δ7.47 (d,1H, J = 8.0 Hz), δ7.31 (ddd, 1H, J = 8.5, 5.0, 3.0 Hz), δ7.22 (d, 1H, J = 8.5 Hz), δ7.21 (d,1H, J = 8.5 Hz), δ7.15 (m, 4H)

Preparation of [Cu(tpz)(dpHa)]Cl

$[Cu(dpHa)_2]Cl_2$ (0.23g, 0.49 mmol) was added to a stirred suspension of one equivalent tpzH (0.09 g, 0.49 mmol) in 15 mL EtOH, causing the reaction mixture to gradually turn dark red. After 1 hour of stirring the reaction mixture was filtered, before the solvent was dried off from the filtrate to give the crude product as a dark red powder which was then recrystallised from hot EtOH.

Yield: 0.09 g, 0.21 mmol, 46%

MS ESI (+ve ion) / *mz*: 411.05

CHN Analysis; found: %C 45.88, %H 4.86, %N 19.21; calculated (for $CuC_{17}H_{14}N_7O_2Cl$): %C 45.64, %H 3.15, %N 21.92

7.4.2. Preparation of heteroleptic complexes containing tpzH-CN

Preparation of [Co(tpz-CN)(dpHa)]Cl

One equivalent tpzH-CN (0.038 g, 0.19 mmol) was added to a stirred suspension of $[Co(Cl)_2(dpHa)]$ (0.05 g, 0.17 mmol) in 10 mL EtOH, causing it to turn from blue to purple. After 1 hour of stirring, the solid was isolated by filtration and washed with EtOH then Et_2O. The solid was dissolved in the minimum amount MeOH. The solvent was dried off from the filtrate to afford the product as a purple solid.

Yield: 0.045g, 0.01 mmol, 57%

MS ESI (+ve) / *m/z*: 431.05

Preparation of $[Co(tpz\text{-}CN)(dpHa)_2]BF_4$

Two equivalents dpHa (0.65 g, 3.80 mmol) was added to a stirred solution of $Co(BF_4)_2.6H_2O$ (0.65 g, 1.90 mmol) in 15 mL EtOH, causing the reaction mixture to turn orange. To this, one equivalent tpzH-CN (0.37 g, 1.83 mmol) was added, causing the solution to gradually turn dark red. This was stirred for 0.5 hours before $K_2S_2O_8$ (0.55 g, 2.03 mmol) was added. The reaction mixture was heated at reflux overnight. The reaction mixture was allowed to cool then filtered. Et_2O was added to the filtrate, and the resulting precipitate was isolated by filtration *in vacuo*.

Yield: 0.57 g, 0.74 mmol, 40%

MS ESI (+ve ion): 601.13 $[M\text{-}H]^+$, 301.067 $[Co(tpz\text{-}CN)(dpHa)_2]^{2+}$

^{1}H NMR (d_6-DMSO, 700 MHz) of $[Co(tpz\text{-}CN)(dpHa)_2](BF4)_2$. δ8.16 (t, 1H, J = 7.3 Hz), δ8.10 (m, 1H), δ8.07 (d, 1H, J = 4.8 Hz,), δ7.99 (d, 1H, J = 8.5), δ9.96 (d, 1H, J = 8.6 Hz), δ7.94 (s, 1H), δ7.90 (t, 1H), δ7.89 (t, 1H), δ 7.88 (t, 1H), δ7.73 (d, 1H, J = 5.7 Hz), δ7.61 (d, 1H, J = 5.0 Hz), δ 7.58 (d, 1H, J = 5.0 Hz), δ 7.52 (d, 1H, J = 8.3 Hz), δ7.46 (d, 1H, J = 8.0 Hz), δ7.42 (t, 1H, J = 7.7 Hz), δ7.24 (d, 1H, J = 7.8 Hz), δ7.18 (t, 1H, J = 6.1 Hz), δ7.15 (d, 1H, J = 8.4 Hz), δ7.04 (t, 1H), δ7.03 (t, 1H), δ7.02 (t, 1H)

^{1}H (400 MHz, MeOD): δ8.12 (m, 2H), δ8.07 (dd, 1H, J = 8.5, 1.0 Hz), δ8.01 (dd, 1H, J = 8.5, 1.0 Hz), δ7.88 (m, 5H), δ7.70 (dd, 1H, J = 6.0, 1.5 Hz), δ7.60 (dd, 3H, J = 7.5, 1.0 Hz), δ7.41 (ddd, 1H, J = 8.5, 7.5, 1.0 Hz), δ7.33 (dd, 1H, J = 7.5, 1.0 Hz), δ7.20 (dd, 1H, J = 8.0, 1.0 Hz), δ7.10 (m, 3H), δ7.03 (ddd, 1H, J = 7.0, 6.5, 1.0 Hz)

$^{13}C\{^{1}H\}$ NMR (400 MHz, d_6-DMSO): δ155.48, δ154.27, δ152.81, δ151.78, δ151,32, δ149.72, δ147.67, δ142.09, δ141.55, δ136.13, δ133.15, δ130.74, δ125.75, δ120.78, δ120.74, δ120.06, δ116.02, δ114.79, δ114.35, δ113.92, δ112.13, δ110.82

IR (KBr disc) / cm^{-1}: 3351 (NH), 3257 (NH), 2241 (C≡N), 1641, 1588, 1576, 1532, 1488 1389, 1375, 1230, 1159, 1109, 1046, 1018, 851, 775, 609, 5306

CHN Analysis; found: %C 42.86, %H 3.20, %N 16.94; calculated (for $CoC_{29}H_{23}N_{10}O_2B_2F_8$): %C 44.88, %H 2.99, %N 18.05

Preparation of $[Co(tpz\text{-}CN)(dpma)_2](BF_4)_2$

$Co(BF_4)_2.6H_2O$ (0.12 g, 0.36 mmol) was added to a stirred solution of two equivalents dpma (0.15 g, 0.81 mmol) in 10 mL EtOH, causing it to change from yellow to orange. After 10 minutes stirring, one equivalent tpzH-CN (0.08 g, 0.37 mmol) was added and then, after an additional 0.5 hours stirring, two equivalents $K_2S_2O_8$ (0.12g, 0.44 mmol) were added. The reaction mixture was heated at reflux overnight then allowed to cool. The reaction mixture was filtered then Et_2O added to the dark purple filtrate to cause a purple solid to form. This was then isolated by filtration *in vacuo* then the solid dissolved in EtOH and filtered. The solvent was dried off from the filtrate to yield the product as a dark purple solid.

Yield: 0.067 g, 0.083 mmol, 23%

MS ESI (+ve) / *m/z*: 629.15 $[M\text{-}H]^+$, 315.08 $[Co(tpz\text{-}CN(dpma)_2]^{2+}$

Preparation of [Cu(tpz-CN)(dpHa)]Cl

$[Cu(dpHa)_2]Cl_2$ (0.29g, 0. 58 mmol) was added to a stirred suspension of one equivalent tpzH-CN (0.12 g, 0.59 mmol) in 10 mL EtOH, causing the reaction mixture to gradually turn dark red. After 2 hours of stirring the reaction mixture was filtered to isolate a dark red solid. This was then dissolved in MeOH and filtered. The solvent was dried off from filtrate to give the product as a dark red powder. Diffraction quality dark red crystals were obtained after several days of slow evaporation of the ethanolic filtrate under ambient conditions.

Yield: 0.1853 g, 0.39 mmol, 68%

MS ESI (+ve) / *m/z*: 435.05

IR (KBr disc) / cm^{-1}: 3353 (NH), 3256 (NH), 2237 (C≡N), 1636, 1588, 1526, 1476, 1351, 1230, 1159, 1109, 1046, 1018, 851, 775, 609, 530

CHN Analysis; found: %C 46.58, %H 3.54, %N 19.48; calculated (for $CuC_{19}H_{14}N_7O_2Cl$): %C 48.41, %H 2.99, %N 20.80; calculated (for $CuC_{19}H_{16}N_7O_3Cl$): %C 46.63, %H 3.30, %N 20.04

Preparation of $[Zn(tpz\text{-}CN)(dpHa)]BF_4$

Two equivalents dpHa (0.035 g, 0.16 mmol) were stirred in EtOH with 0.024 g $Zn(BF_4)_2$ (0.16 mmol) for 10 minutes. To this, 0.032 g tpzH-CN (0.16 mmol) was added, gradually forming a crimson precipitate during 30 minutes stirring. The precipitate was isolated by filtration and washed with EtOH and Et_2O. Dark red crystals suitable for x-ray diffraction were obtained by slow evaporation from a solution of MeOH and ^{n}BuOH.

Yield: 0.028 g, 0.054 mmol, 85%

MS (ESI) / *mz*: 436 (M^+)

^{1}H NMR (MeOD, 400 MHz): δ8.43 (d, 2H, J = 4.3 Hz, pyridyl-H), δ8.21 (d, 1H, J = 8 Hz, phenyl-H), δ8.17 (d, 1H, J = 8.8 Hz, phenyl-H), δ7.88 (t, 2H, J = 7.8 Hz, pyridyl-H), δ7.80 (t, 1H, J = 7.9 Hz, phenyl-H), δ7.39 (t, 1H, J = 7.9 Hz, phenyl-H), δ7.20 (d, 2H, J = 7.13 Hz, pyridyl-H), δ7.13 (t, 2H, J = 6 Hz, pyridyl-H)

^{1}H NMR (d_6-DMSO, 400 MHz): δ 10.24 (br. s, 1H, pyridyl-NH), δ8.38 (d, 2H, J = 4.0 Hz, pyridyl-H), δ8.18 (ap. t, 2H, J = 9.5 Hz, phenyl-H), δ7.91 (ddd, 1H, J = 8.0, 7.0, 1.0 Hz, phenyl-H), δ7.85 (ap. t, 2H, J = 7.0 Hz, pyridyl-H), δ7.46 (m, 3H, pyridyl-H and phenyl-H), δ7.07 (ap. t, 2H, J = 6.0 Hz, pyridyl-H), δ6.90 (br. s, 1H, phenyl-NH)

^{13}C{^{1}H} NMR (d_6-DMSO, 400 MHz): δ152.25, 150.20, δ147.37, δ139.94, δ135.56, δ135.47, δ124.59, δ119.97, δ117.08, δ116.22, δ113.66, δ111.82

IR (KBr disc) / cm^{-1}: 3525, 3337, 3086, 2238 (CN), 1641, 1590, 1564, 1530, 1479.3, 1438, 1421, 1377, 1269, 1226, 1193, 1164, 1137, 1057, 1012, 770

CHN Analysis; found: %C 43.76, %H 3.46, %N 16.97; calculated (for $ZnC_{19}H_{14}N_7O_2BF_4$): %C 43.22, %H 2.88, %N 18.66

7.4.3. Preparation of heteroleptic complexes containing tpzH-$CONH_2$

Preparation of [Co(tpz-$CONH_2$)(dpHa)$_2$]2NO_3:

Two equivalents tpzH-$CONH_2$ (0.059 g, 0.27 mmol) were added to a stirred solution of $Co(NO_3)_2.6H_2O$ (0.051 g, 0.18 mmol) and dpHa (0.033 g, 0.19 mmol) in 10 mL EtOH. After two hours stirring, two equivalents $K_2S_2O_8$ (0.11 g, 0.40 mmol) were added then the reaction mixture was left to heat at reflux overnight.

Red-pink crystals suitable for diffraction were obtained through slow evaporation from a solution of MeOH layered over ^{n}BuOH.

Yield: 0.026 g, 0.035 mmol, 19%

MS ESI (+ve ion) (*m/z*): 668 (M^+)

^{1}H NMR (400 MHz, D_2O): δ8.05 (m, 2H), δ7.94 (m, 4H), δ7.75 (m, 3H), δ7.57 (d, 1H, J = 6.0 Hz), δ7.50 (m, 2H), δ7.45 (d, 1H, J = 8.0 Hz), δ7.32 (d, br.d, 1H, J = 8.0 Hz), δ7.15 (d, 1H, J = 8.0 Hz), δ7.05 (d, 1H, J = 8.0 Hz), δ6.98 (m, 3H), δ6.93 (t, 1H, J = 6.0 Hz)

Preparation of [Cu(tpz-$CONH_2$)(dpHa)]Cl

One equivalent [Cu(dpHa)$_2$]2Cl (0.05 g, 0.09 mmol) dissolved in 5 mL EtOH was added to a stirred suspension of tpzH-$CONH_2$ (0.02 g, 0.10 mmol) in 10 mL EtOH, causing it to gradually change from orange to brown to red. After 2.5 hours stirring, the dark red solid was isolated by filtration in vacuo before being washed with cold EtOH then Et_2O. Diffraction quality dark red crystals were obtained by allowing a methanolic solution layered over ^{n}BuOH to slowly evaporate over the course of a few days at room temperature.

Yield: 0.02 g, 0.05 mmol, 48%

CHN Analysis; found: %C 46.28, %H 3.37, %N 19.47; calculated (for $CuC_{19}H_{16}N_7O_3Cl$): %C 46.63, %H 3.30, %N 20.04

7.5. Chapter Five Experimental Procedures

Spectrophotometric pH titrations

Titrations were carried out using 100 mL solution to minimise alterations in concentration and maintained at 0.1 M ionic strength with KNO_3 with the analyte at an appropriate concentration for the monitoring of its absorbance. Solutions of the complexes were adjusted to a basic pH with $NaOH_{(aq)}$ and titrated with $HCl_{(aq)}$ and where needed, the complexes were dissolved in the minimum amount DMSO before being added to the aqueous solution. Solutions of the uncoordinated ligands were adjusted to an acidic pH with HCl(aq) and then titrated with NaOH(aq).

Cyclic Voltammetry

Electrochemical solutions were carried out either in DMSO or H_2O. With DMSO, the solutions contained 0.1 M Bu_4NPF_6 as the supporting electrolyte and referenced against the ferrocene redox couple for this system (0.48 V). The potential was swept from 0 V to -1.75 V then to 0.6 V. For aqueous measurements, 0.1 M KCl was used as the supporting electrolyte and referenced against the $[Fe(CN)_6]^{3-}$ / $[Fe(CN)_6]^{4-}$ redox couple. The potential was swept from 0.4 V to -0.4 V then to 0.4 V. The solutions were purged with N_2 for 10 minutes prior to measurements being taken and samples were used at $1*10^{-3}$ M concentration.

Experiments following reduction by biological agents

All solutions were buffered using an appropriate buffer for the pH range (HEPES, MES, acetic acid). For anaerobic experiments the solutions were purged with N_2 and injected into a quartz cuvette sealed with a suba-seal. 10-fold excesses of the reducing agents were used, and injected into the cuvette in 0.5 mL solution.

7.6. Chapter Six Experimental Procedures

A549 (human lung adenocarcinoma epithelial) cells were kindly provided by the Department of Biology at the University of York. The cells were maintained in Dulbeco's modified Eagle medium (DMEM) supplemented with 1% 2 mmol dm^{-3} L-glutamine, 10% foetal bovine serum and 50 mmol dm^{-3} sodium pyruvate. The cells were kept in a humidified incubator maintained with 5% CO_2 at 37°C. All manipulations were carried out in a class II laminar flow hood under a filtered laminar air flow. Upon reaching *ca*. 75% confluence, the medium was removed and the cells washed twice with 5 mL PBS. To remove the cells from the flask, they were then incubated with 1 mL 0.25% EDTA trypsin for 10 minutes at 37 °C. 9 mL medium added to the cells to form a single suspension. 0.5 and 1.0 mL of the resulting supernatant were added to two new culture flasks, each containing 10 mL of fresh medium.

Cells were plated in 100 μL medium at the seeding density of 1000 cells per well into 11 of the 12 columns of a 96-well microtitre plate with the first column containing just media so to act as negative control. The plate was incubated for 20 hours to allow them to adhere to the plate. The compounds were dissolved in medium to form solutions of the required concentrations, which were sterilised before addition to the plate.

Following 3 days incubation, 100 μg MTT (150 μL of 2 mg mL^{-1}) were added to each well then the plates incubated for two hours. The plates were centrifuged at 450 g for 10 minutes then 220 μL of the supernatant removed from each well. 150 μL DMSO was added to each well to solubilise the MTT formazan crystals, which become fully dissolved during 5 minutes agitation on a plate shaker.[195] The absorbance at 540 nm of each well was measured using an automated plate reader. The absorbance at 540 nm for positive and negative controls was used to calculate the absorbance for 100% and 0% cell viability, and from this, the percentage cell viability for each of the drug concentrations was calculated. The percentage cell viability was plotted as a function of drug concentration, and to this a logistic sigmoidal curve was fitted. From the curve, a value for the IC_{50} (concentration at which the cell viability has been halved) could be obtained graphically.

8. References

1. V. Speechley, M. Rosenfield, *Cancer at your fingertips*, Class Publishing, 2001.
2. Cancer Research UK, http://info.cancerresearchuk.org/cancerstats (accessed 15/12/11)
3. Data collected by SEER (The Surveillance, Epidemiology and End Results Program of the National Cancer Institute, www.cancer.gov (accessed 15/12/11)
4. D. Hanahan, R. A. Weinberg, *Cell*, 2000, 57-70.
5. J. M. Berg, J. L. Tymoczko, L. Stryer, *Biochemistry*, W.H. Freeman and Company, 2002.
6. R. J. Epstein, *Human Molecular Biology*, Cambridge University Press, 2002.
7. M. J. Brown, A. J. Giaccia, *Cancer Res.*, 1998, **58**, 1408-1416.
8. T. W. Grunt, A. Lametschwandtner, O. Staindl, *Microvascular Res.*, 1985, **29**, 371-386.
9. I. J. Hoogsten, H. A. M. Marres, A. J. van der Kogel, J. H. A. M. Kanders, *Clin. Oncology*,, 2007, **19**, 385-396.
10. M. J. Brown, W. R. Wilson, *Nature Rev. Cancer*, 2004, **4**, 437-447.
11. M. Hockel, P. Vaupel, *J. Natl. Cancer Inst.*, 2001, **93**, 266-276.
12. G. L. Semenza, *J. Clin. Invest.*, 2008, **118**, 3835–3837.
13. K. Lee, R. A. Roth, J. J. LaPres, *Pharmacology & Therapeutics*, 2007, **113**, 229-246.
14. C. N. Coleman, J. B. Mitchell, K. Camphausen, *J. Clin. Oncol.*, 2002, **20**, 610-615.
15. G. L. Semenza, P. H. Roth, H. M. Fang, G. L. Wang, *J. Biol. Chem.*, 1994, **269**, 23757-23763.
16. S. M. Wigfield, S. C. Winter, A. Giatromanolaki, J. Taylor, M. L. Koukourakis, A. L. Harris, *Br. J. Cancer*, 2008, **98**, 1975-1984.
17. K. L. Bennewith, R. E. Durand, *Cancer Res.*, 2004, **64**, 6183-6189.
18. J. M. Heddleston, Z. Li, J. D. Lathia, S. Bao, A. B. Hjelmeland, J. N. Rich, *Br. J. Cancer*, 2010, **102**, 789-795.
19. P. Vaupel, *Oncologist*, 2008, **13**, 21-26.
20. P. Vaupel, F. Kallinowski, P. Okunieff, *Cancer Res.*, 1989, **49**, 6449-6465.

21. P. Swietach, R. D. Vaughan-Jones, A. L. Harris, *Cancer and Metastasis Rev.*, 2007, **26**, 299-310.
22. J. R. Griffiths, *Br. J. Cancer*, 1991, **64**, 425-427.
23. J. S. Fang, R. D. Gillies, R. A. Gatenby, *Seminars in Cancer Biology*, 2008, **18**, 330-337.
24. M. J. Boyer, I. F. Tannock, *Cancer Res.*, 1992, **52**, 4441-4447.
25. A. L. Harris, *Nature Rev. Cancer*, 2002, **2**, 38-47.
26. L. P. Liu, T. P. Cash, R. G. Jones, B. Keith, C. B. Thompson, M. C. Simon, *Molecular Cell*, 2006, **21**, 521-531.
27. L. B. Gardner, Q. Li, M. S. Park, W. M. Flanagan, G. L. Semenza, C. V. Dang, *J. Biol. Chem.*, 2001, **276**, 7919-7926.
28. P. Vaupel, O. Thews, M. Hoeckel, *Medical Oncology*, 2001, **18**, 243-259.
29. B. D. Palmer, W. R. Wilson, S. M. Pullen, W. A. Denny, *J. Med. Chem.*, 1990, **33**, 112-121.
30. S. P. Fricker, *Dalton Trans.*, 2007, 4903-4917.
31. M. Vieites, P. Noblia, M. H. Torre, H. Cerecetto, M. L. Lavaggi, A. J. Costa-Filho, A. Azqueta, A. L. de Cerain, A. Monge, B. Parajon-Costa, M. Gonzalez, D. Gambino, *J. Inorg. Biochem.*, 2006, **100**, 1358-1367.
32. D. Cerretani, F. Roviello, M. Pieraccini, L. Civeli, P. Correale, G. Francini, D. Marrelli, G. De Manzoni, E. Pinto, G. Giorgi, *Vascular Pharmacology*, 2002, **39**, 1-6.
33. A. M. Rauth, J. K. Mohindra, I. F. Tannock, *Cancer Res.*, 1983, **43**, 4154-4158.
34. M. F. Belcourt, W. F. Hodnick, S. Rockwel, A. C. Sartorelli, *Adv. Enz. Regul.*, 1998, **38**, 111-133.
35. W. A. Denny, *Lancet Oncology*, 2000, **1**, 25-29.
36. M. F. Belcourt, P. G. Penketh, W. F. Hodnick, D. A. Johnson, D. H. Sherman, S. Rockwell, A. C. Sartorelli, *Proc. Natl. Acad. Sci.*, 1999, **96**, 10489-10494.
37. I. Sanchez, R. Reches, D. H. Caignard, P. Renard, M. D. Pujol, *Eur. J. Med. Chem.*, 2006, **41**, 340-352.
38. M. Tomasz, A. K. Chawla, R. Lipman, *Biochemistry*, 1988, **27**, 3182-3187.
39. W. R. Wilson, W. A. Denny, S. J. Twigden, B. C. Baguley, J. C. Probert, *Br. J. Cancer*, 1984, **49**, 215-223.

40. W. M. Cholody, M. F. Lhomme, J. Lhomme, *Tetrahedron Lett.*, 1987, **28**, 5029-5032.
41. K. Gorlewska, Z. Mazerska, P. Sowinski, J. Konopa, *Chem. Res. Toxicol.*, 2001, **14**, 1-10.
42. W. A. Denny, *Eur. J. Med. Chem.*, 2001, **36**, 577-595.
43. J.-X. Duan, H. Jiao, J. Kaizerman, T. Stanton, J. W. Evans, L. Lan, G. Lorente, M. Banica, D. Jung, J. Wang, H. Ma, X. Li, Z. Yang, R. M. Hoffman, W. S. Ammons, C. P. Hart, M. Matteucci, *J. Med. Chem.*, 2008, **51**, 2412-2420.
44. A. R. Padhani, K. A. Krohn, J. S. Lewis, M. Alber, *Eur. Radiol.*, 2007, **17**, 861-872.
45. M. Piert, H. J. Machulla, M. Picchio, G. Reischl, S. Ziegler, P. Kumar, H. J. Wester, R. Beck, A. J. B. McEwan, L. I. Wiebe, M. Schwaiger, *J. Nucl. Med.*, 2005, **46**, 106-113.
46. J. von Pawel, R. von Roemeling, U. Gatzemeier, M. Boyer, L. O. Elisson, P. Clark, D. Talbot, A. Rey, T. W. Butler, V. Hirsh, I. Olver, B. Bergman, J. Ayoub, G. Richrdson, D. Dunlop, A. Arcenas, R. Vescio, J. Viallet, J. Treat, *J. Clin. Oncol.*, 2000, **18**, 1351-1359.
47. J. Treat, E. Johnson, C. Langer, C. Belani, B. Haynes, R. Greenberg, R. Rodriquez, P. Drobins, W. Miller, L. Meehan, A. McKeon, J. Devin, R. von Roemeling, J. Viallet, *J. Clin. Oncol.*, 1998, **16**, 3524-3527.
48. S. R. McKeown, O. P. Friery, I. A. McIntyre, M. V. Hejmadi, L. H. Patterson, D. G. Hirst, *Br. J. Cancer*, 1996, **74**, S39-S42.
49. E. C. Chinje, A. V. Patterson, M. P. Saunders, S. D. Lockyer, A. L. Harris, I. J. Stratford, *Br. J. Cancer*, 1999, **81**, 1127-1133.
50. J. M. Brown, *Br. J. Cancer*, 1993, **67**, 1163-1170.
51. M. P. Saunders, A. V. Patterson, E. C. Chinje, A. L. Harris, I. J. Stratford, *Br. J. Cancer*, 2000, **82**, 651-656.
52. S. A. Fitzsimmons, A. D. Lewis, R. J. Riley, P. Workman, *Carcinogenesis*, 1994, **15**, 1503-1510.
53. G. D. D. Jones, M. Weinfeld, *Cancer Res.*, 1996, **56**, 1584-1590.
54. G. Chowdhury, V. Junnotula, J. S. Daniels, M. M. Greenberg, K. S. Gates, *J. Am. Chem. Soc.*, 2007, **129**, 12870-12877.

55. R. F. Anderson, S. S. Shinde, M. P. Hay, S. A. Gamage, W. A. Denny, *J. Am. Chem. Soc.*, 2003, **125**, 748-756.

56. S. S. Shinde, M. P. Hay, A. V. Patterson, W. A. Denny, R. F. Anderson, *J. Am. Chem. Soc.*, 2009, **131**, 14220-14221.

57. F. B. Pruijn, J. R. Sturman, H. D. S. Liyanage, K. O. Hicks, M. P. Hay, W. R. Wilson, *J. Med. Chem.* 2005, **48**, 1079-1087.

58. K. O. Hicks, F. B. Pruijn, J. R. Sturman, W. A. Denny, W. R. Wilson, *Cancer Res.*, 2003, **63**, 5970-5977.

59. S. K. Williamson, J. J. Crowley, P. N. Lara, J. McCoy, D. H. M. Lau, R. W. Tucker, G. M. Mills, D. R. Gandara, *J. Clin. Oncol.*, 2005, **23**, 9097-9104.

60. K. O. Hicks, B. G. Siim, J. K. Jaiswal, F. B. Pruijn, A. M. Fraser, R. Patel, A. Hogg, H. D. S. Liyanage, M. J. Dorie, J. M. Brown, W. A. Denny, M. P. Hay, W. R. Wilson, *Clin. Cancer Res.*, 2010, **16**, 4946-4957.

61. M. P. Hay, K. O. Hicks, K. Pchalek, H. H. Lee, A. Blaser, F. B. Pruijn, R. F. Anderson, S. S. Shinde, W. R. Wilson, W. A. Denny, *J. Med. Chem.*, 2008, **51**, 6853-6865.

62. V. Junnotula, A. Rajapakse, L. Arbillaga, A. Lopez de Cerain, B. Solano, R. Villar, A. Monge, K. S. Gates, *Bioorg. Med. Chem.*, 2010, **18**, 3125-3132.

63. K. Pchalek, M. P. Hay, *J. Org. Chem.*, 2006, **71**, 6530-6535.

64. W. Sneader, *Drug discovery: a history*, Wiley, 2005.

65. *Cisplatin : chemistry and biochemistry of a leading anticancer drug*, Verlag Helvetica Chimica Acta, Zürich, 1999.

66. R. A. Alderden, M. D. Hall, T. W. Hambley, *J. Chem. Ed.*, 2006, **83**, 728-734.

67. S. E. Miller, D. A. House, *Inorg. Chim. Acta*, 1989, **166**, 189-197.

68. L. Kelland, *Nature Rev. Cancer*, 2007, **7**, 573-584.

69. R. C. Todd, S. J. Lippard, *Metallomics*, 2009, **1**, 280-291.

70. A. I. Ivanov, J. Christodoulou, J. A. Parkinson, K. J. Barnham, A. Tucker, J. Woodrow, P. J. Sadler, *J. Biol. Chem.*, 1998, **273**, 14721-14730.

71. A. H. Calvert, S. J. Harland, D. R. Newell, Z. H. Siddik, K. R. Harrap, *Cancer Treatment Rev.*, 1985, **12**, 51-57.

72. K. R. Harrap, *Cancer Treatment Rev.*, 1985, **12**, 21-33.

73. S. Giacchetti, B. Perpoint, R. Zidani, N. Le Bail, R. Faggiuolo, C. Focan, P. Chollet, J. F. Llory, Y. Letourneau, B. Coudert, F. Bertheaut-Cvitkovic, D.

Larregain-Fournier, A. Le Rol, S. Walter, R. Adam, J. L. Misset, F. Levi, *J. Clin. Oncol.*, 2000, **18**, 136-147.

74. A. Bergamo, G. Sava, *Dalton Trans.*, 2011, **40**, 7817-7823.
75. G. Gasser, I. Ott, N. Metzler-Nolte, *J. Med. Chem.*, 2011, **54**, 3-25.
76. A. Vessières, S. Top, W. Beck, E. Hillard, G. Jaouen, *Dalton Trans.*, 2006, 529-541.
77. S. Top, E. B. Kaloun, A. Vessières, G. Leclercq, I. Laïos, M. Ourevitch, C. Deuschel, M. J. McGlinchey, G. Jaouen, *ChemBioChem*, 2003, **4**, 754-761.
78. S. Top, E. B. Kaloun, A. Vessieres, I. Laios, G. Leclercq, G. Jaouen, *J. Organomet. Chem.*, 2002, **643**, 350-356.
79. S. Top, A. Vessieres, P. Pigeon, M. N. Rager, M. Huche, E. Salomon, C. Cabestaing, J. Vaissermann, G. Jaouen, *ChemBioChem*, 2004, **5**, 1104-1113.
80. Q. Michard, G. Jaouen, A. Vessieres, B. A. Bernard, *J. Inorg. Biochem.*, 2008, **102**, 1980-1985.
81. E. A. Hillard, P. Pigeon, A. Vessieres, C. Amatore, G. Jaouen, *Dalton Trans.*, 2007, 5073-5081.
82. P. Pigeon, S. Top, A. Vessières, Huché, Michel, E. A. Hillard, E. Salomon, G. Jaouen, *J. Med. Chem.*, 2005, **48**, 2814-2821.
83. E. Hillard, A. Vessières, L. Thouin, G. Jaouen, C. Amatore, *Angew. Chem. Int. Ed.*, 2006, **45**, 285-290.
84. Didier Hamels, E. A. H. Patrick M. Dansette, Siden Top, Anne Vessières,, G. J. Patrick Herson, D. Mansuy, *Angew. Chem.*, 2009, **121**, 9288–9290.
85. I. Ott, B. Kircher, R. Gust, *J. Inorg. Biochem.*, 2004, **98**, 485-489.
86. I. Ott, B. Kircher, C. P. Bagowski, D. H. W. Vlecken, E. B. Ott, J. Will, K. Bensdorf, W. S. Sheldrick, R. Gust, *Angew. Chem. Int. Ed.*, 2009, **48**, 1160-1163.
87. I. Ott, A. Abraham, P. Schumacher, H. Shorafa, G. Gastl, R. Gust, B. Kircher, *J. Inorg. Biochem.*, 2006, **100**, 1903-1906.
88. G. Rubner, K. Bensdorf, A. Wellner, B. Kircher, S. Bergemann, I. Ott, R. Gust, *J. Med. Chem.*, 2010, **53**, 6889-6898.
89. F. Dehdashti, P. W. Grigsby, J. S. Lewis, R. Laforest, B. A. Siegel, M. J. Welch, *J. Nucl. Med.*, 2008, **49**, 201-205.
90. P. J. Blower, M. J. Went, K. E. Martin, G. E. Smith, *Journal of Labelled Compounds & Radiopharmaceuticals*, 2007, **50**, 354-359.

91. J. L. J. Dearling, J. S. Lewis, D. W. McCarthy, M. J. Welch, P. J. Blower, *Chem. Comm.*, 1998, 2531-2532.
92. Z. Xiao, P. S. Donnelly, M. Zimmermann, A. G. Wedd, *Inorg. Chem.*, 2008, **47**, 4338-4347.
93. G. L. Patrick, *An introduction to medicinal chemistry*, Oxford University Press, 2001.
94. B. Wang, T. Siahaan, R. Soltero, *Drug delivery: principles and applications*, Wiley (USA), 2005.
95. P. R. Craig, P. J. Brothers, G. R. Clark, W. R. Wilson, W. A. Denny, D. C. Ware, *Dalton Trans.*, 2004, 611-618.
96. D. C. Ware, B. D. Palmer, W. R. Wilson, W. A. Denny, *J. Med. Chem.*, 1993, **36**, 1839-1846.
97. M. Simic, J. Lilie, *J. Am. Chem. Soc.*, 1974, **96**, 291-292.
98. B. A. Teicher, M. J. Abrams, K. W. Rosbe, T. S. Herman, *Cancer Res.*, 1990, **50**, 6971-6975.
99. R. F. Anderson, W. A. Denny, D. C. Ware, W. R. Wilson, *Brit. J. Cancer Supplement*, 1996, **27**, S48-51.
100. T. W. Failes, T. W. Hambley, *Dalton Trans.*, 2006, 1895-1901.
101. T. W. Failes, C. Cullinane, C. I. Diakos, N. Yamamoto, J. G. Lyons, T. W. Hambley, *Chem. Eur. J.*, 2007, **13**, 2974-2982.
102. T. Salthammer, H. Dreeskamp, *J. Photochem. Photobiol.*, 1990, **55**, 53-62.
103. J. A. Kemlo, T. M. Shepherd, *Chem. Phys. Lett.*, 1977, **47**, 158-162.
104. N. Yamamoto, S. Danos, P. D. Bonnitcha, T. W. Failes, E. J. New, T. W. Hambley, *J. Biol. Inorg. Chem.*, 2008, **13**, 861-871.
105. B. J. Kim, T. W. Hambley, N. S. Bryce, *Chem. Sci.*, 2011, **2**, 2135-2142.
106. L. L. Parker, S. M. Lacy, L. J. Farrugia, C. Evans, D. J. Robins, C. C. O'Hare, J. A. Hartley, M. Jaffar, I. J. Stratford, *J. Med. Chem.*, 2004, **47**, 5683-5689.
107. J. L. J. Dearling, J. S. Lewis, G. E. D. Muller, M. J. Welch, P. J. Blower, *J. Biol. Inorg. Chem.*, 2002, **7**, 249-259.
108. P. J. Blower, M. J. Went, K. E. Martin, G. E. Smith, *J. Label Compd. Radiopharm.*, 2007, **50**, 354-359.
109. A. L. Vavere, J. S. Lewis, *Dalton Trans.*, 2007, 4893-4902.
110. A. R. Jalilian, H. Yousefnia, M. Kamali-Dehghan, S. Moradkhani, F. Bolourinovin, K. Shafaii, G. Aslani, *Iran. J. Nucl Med.*, 2010, **18**, 14-21.

111. *Preparation of pyridylaminoisoquinoline compounds as kinase inhibitors for treatment of proliferative disorders*, R. G. Boyle, D. W. Walker, GB Pat. WO 2010007374, 2010.

112. K. O. Hicks, F. B. Pruijn, J. R. Sturman, W. A. Denny, W. R. Wilson, *Cancer Res.*, 2003, **63**, 5970-5977.

113. G. Manning, D. B. Whyte, R. Martinez, T. Hunter, S. Sudarsanam, *Science*, 2002, **298**, 1912-+.

114. P. Lahiry, A. Torkamani, N. J. Schork, R. A. Hegele, *Nature Rev. Genetics*, 2010, **11**, 60-74.

115. H. Kubinyi, G. Müller, *Chemogenomics in drug discovery: a medicinal perspective*, Wiley, 2004.

116. P. Cohen, *Nature Rev. Drug Discov.*, 2002, **1**, 309-315.

117. Y. Liu, N. S. Gray, *Nature Chem. Biol.*, 2006, **2**, 358-364.

118. P. A. Jaenne, N. Gray, J. Settleman, *Nature Rev. Drug Discov.*, 2009, **8**, 709-723.

119. P. D. Beer, P. A. Gale, D. K. Smith, *Supramolecular Chemistry*, Oxford Chemistry Primers, 1999.

120. M. Getlik, C. Gruetter, J. R. Simard, W. Van Otterlo, A. Robubi, B. Aust, D. Rauh, unpublished crystal structure, 2010, PDB 3LFA.

121. L. Potterton, S. McNicholas, E. Krissinel, J. Gruber, K. Cowtan, P. Emsley, G. N. Murshudov, S. Cohen, A. Perrakis, M. Noble, *Acta Cryst.*, 2004, **60**, 2288-2294.

122. A. Afantitis, G. Melagraki, P. A. Koutentis, H. Sarimveis, G. Kollias, *Eur. J. Med. Chem.*, 2011, **46**, 497-508.

123. G. D. Probst, S. Bowers, J. M. Sealy, A. P. Truong, R. K. Hom, R. A. Galemmo, Jr., A. W. Konradi, H. L. Sham, D. A. Quincy, H. Pan, N. Yao, M. Lin, G. Toth, D. R. Artis, W. Zmolek, K. Wong, A. Qin, C. Lorentzen, D. F. Nakamura, K. P. Quinn, J.-M. Sauer, K. Powell, L. Ruslim, S. Wright, D. Chereau, Z. Ren, J. P. Anderson, F. Bard, T. A. Yednock, I. Griswold-Prenner, *Bioorg. Med. Chem. Lett.*, 2011, **21**, 315-319.

124. C. Romain, S. Gaillard, M. K. Elmkaddem, L. Toupet, C. Fischmeister, C. M. Thomas, J.-L. Renaud, *Organometallics*, 2010, **29**, 1992-1995.

125. K. Muller-Buschbaum, C. C. Quitmann, *Inorg. Chem.*, 2006, **45**, 2678-2687.

126. E. Spodine, A. M. Atria, R. Baggio, M. T. Garland, *Acta Cryst.*, 1996, **52**, 1407-1410.

127. F. A. Cotton, L. M. Daniels, G. T. Jordan, C. A. Murillo, *Polyhedron*, 1998, **17**, 589-597.

128. K. Y. Ho, W. Y. Yu, K. K. Cheung, C. M. Che, *J. Chem. Soc. Dalton Trans.*, 1999, 1581-1586.

129. Y. Gultneh, A. R. Khan, D. Blaise, S. Chaudhry, B. Ahvazi, B. B. Marvey, R. J. Butcher, *J. Inorg. Biochem.*, 1999, **75**, 7–18.

130. S. Kirshner, *Inorg. Syn.*, 1957, **5**, 14-16.

131. C. L. Barnes, *J. Appl. Cryst.*, 1997, **30**, 568-568.

132. A. W. Addison, T. N. Rao, J. Reedijk, J. Vanrijn, G. C. Verschoor, *J. Chem. Soc. Dalton Trans.*, 1984, 1349-1356.

133. M. P. Suh, Y. H. Oh, *Bull. Kor. Chem. Soc.*, 1982, **3**, 5-9.

134. A. L. Spek, *Acta Cryst.*, 2009, **65**, 148-155.

135. E. Arunan, G. R. Desiraju, R. A. Klein, J. Sadlej, S. Scheiner, I. Alkorta, D. C. Clary, R. H. Crabtree, J. J. Dannenberg, P. Hobza, H. G. Kjaergaard, A. C. Legon, B. Mennucci, D. J. Nesbitt, *Pure Appl. Chem., 2011,* **83**, 1619-1636.

136. G. Sathyamoorthi, M. L. Soong, T. W. Ross, J. H. Boyer, *Heteroatom. Chem.*, 1993, **4**, 603-608.

137. M. J. Rauterkus, S. Fakih, C. Mock, I. Puscasu, B. Krebs, *Inorg. Chim. Acta*, 2003, **350**, 355-365.

138. B. Antonioli, D. J. Bray, J. K. Clegg, K. Gloe, K. Gloe, A. Jaeger, K. A. Jolliffe, O. Kataeva, L. F. Lindoy, P. J. Steel, C. J. Sumby, M. Wenzel, *Polyhedron*, 2008, **27**, 2889-2898.

139. .Synthesis developed by D. W. Winter, Sentinel Oncology Limited

140. C. Urquiola, D. Gambino, M. Cabrera, M. L. Lavaggi, H. Cerecetto, M. Gonzalez, A. L. de Cerain, A. Monge, A. J. Costa-Filho, M. H. Torre, *J. Inorg. Biochem.*, 2008, **102**, 119-126.

141. M. L. Lavaggi, G. Aguirre, L. Boiani, L. Orelli, B. Garcia, H. Cerecetto, M. Gonzalez, *Eur. J. Med. Chem.*, 2008, **43**, 1737-1741.

142. E. Vicente, L. M. Lima, E. Bongard, S. Charnaud, R. Villar, B. Solano, A. Burguete, S. Perez-Silanes, I. Aldana, L. Vivas, A. Monge, *Eur. J. Med. Chem.*, 2008, **43**, 1903-1910.

143. K. S. Kim, L. Qian, K. E. J. Dickinson, C. L. Delaney, J. E. Bird, T. L. Waldron, S. Moreland, *Bioorg. Med. Chem. Lett.*, 1993, **3**, 2667-2670.

144. M. H. Torre, D. Gambino, J. Araujo, H. Cerecetto, B. Gonzalez, M. L. Lavaggi, A. Azqueta, A. L. de Cerain, A. M. Vega, U. Abram, A. J. Costa, *Eur. J. Med. Chem.*, 2005, **40**, 473-480.

145. P. Noblia, M. Vieites, M. H. Torre, A. J. Costa, H. Cercetto, M. Gonzalez, M. L. Lavaggi, Y. Adachi, H. Sakurai, D. Gambino, *J. Inorg. Biochem.*, 2006, **100**, 281-287.

146. C. Urquiola, M. Vieites, G. Aguirre, A. Marin, B. Solano, G. Arrambide, P. Noblia, M. L. Lavaggi, M. H. Torre, M. Gonzalez, A. Monge, D. Gambino, H. Cerecetto, *Bioorg. Med. Chem.*, 2006, **14**, 5503-5509.

147. M. Vieites, P. Noblia, M. H. Torre, H. Cerecetto, M. L. Lavaggi, A. J. Costa-Filho, A. Azqueta, A. L. de Cerain, A. Monge, B. Parajon-Costa, M. Gonzalez, D. Gambino, *J. Inorg. Biochem.*, 2006, **100**, 1358-1367.

148. M. B. Tarallo, C. Urquiola, A. Monge, F. R. Pavan, C. Q. Leite, M. H. Torre, D. Gambino, *Met. Ions Biol. Med.*, 2008, **10**, 867-872.

149. M. Vieites, P. Smircich, B. Parajon-Costa, J. Rodriguez, V. Galaz, C. Olea-Azar, L. Otero, G. Aguirre, H. Cerecetto, M. Gonzalez, A. Gomez-Barrio, B. Garat, D. Gambino, *J. Biol. Inorg. Chem.*, 2008, **13**, 723-735.

150. M. B. Tarallo, A. J. Costa-Filho, E. D. Vieira, A. Monge, C. Q. Leite, F. R. Pavan, G. Borthagaray, D. Gambino, M. H. Torre, *J. Argent. Chem. Soc.*, 2009, **97**, 80-89.

151. C. Urquiola, M. Vieites, M. H. Torre, M. Cabrera, M. Laura Lavaggi, H. Cerecetto, M. Gonzalez, A. Lopez de Cerain, A. Monge, P. Smircich, B. Garat, D. Gambino, *Bioorg. Med. Chem.*, 2009, **17**, 1623-1629.

152. M. Vieites, P. Smircich, L. Guggeri, E. Marchan, A. Gomez-Barrio, M. Navarro, B. Garat, D. Gambino, *J. Inorg. Biochem.*, 2009, **103**, 1300-1306.

153. M. Belen Tarallo, C. Urquiola, A. Monge, B. Parajon Costa, R. R. Ribeiro, A. J. Costa-Filho, R. C. Mercader, F. R. Pavan, C. Q. F. Leite, M. H. Torre, D. Gambino, *J. Inorg. Biochem.*, 2010, **104**, 1164-1170.

154. D. Benítez, M. L. Lavaggi, D. Gambino, M. H. Torre, H. Cerecetto, M. González, *Med. Chem. Res.*, 2011, **20**, 1-6.

155. P. D. Worthers, N. Greeves, S. Warren, J. P. Clayden, *Organic Chemistry*, Oxford University Press.

156. R. G. Pearson, *J. Am. Chem. Soc.*, 1963, **85**, 3533-3539.

157. G. Szigethy, K. N. Raymond, *J. Am. Chem. Soc.*, 2011, **133**, 7942-7956.

158. E. Peyroux, W. Ghattas, R. Hardre, M. Giorgi, B. Faure, A. J. Simaan, C. Belle, M. Reglier, *Inorganic Chemistry*, 2009, **48**, 10874-10876.

159. B. Antonioli, D. J. Bray, J. K. Clegg, K. Gloe, K. Gloe, A. Jaeger, K. A. Jolliffe, O. Kataeva, L. F. Lindoy, P. J. Steel, C. J. Sumby, M. Wenzel, *Polyhedron*, 2008, **27**, 2889-2898.

160. M. B. Tarallo, C. Urquiola, A. Monge, B. Parajon Costa, R. R. Ribeiro, A. J. Costa-Filho, R. C. Mercader, F. R. Pavan, C. Q. F. Leite, M. H. Torre, D. Gambino, *J. Inorg. Biochem.*, 2010, **104**, 1164-1170.

161. A. Monge, J. A. Palop, A. Pinol, F. J. Martinezcrespo, S. Narro, M. Gonzalez, Y. Sainz, A. L. Decerain, E. Hamilton, A. J. Barker, *J. Heterocyclic Chem.*, 1994, **31**, 1135-1139.

162. J.-J. Li, E. J. Corey, *Named reactions in heterocyclic chemistry*, John Wiley and Sons, 2005.

163. *Quinoxaline di-N-oxides as bactericides*, F. Seng, K. Ley, K. G. Metzger, D. Fritsche, 1969, patent application no. GB 1968-35747

164. S. A. Richards, J. C. Hollerton, *Essential Practical NMR for Organic Chemistry*, J. Wiley & Sons, 2011.

165. D. H. Williams, I. Flemming, McGraw Hill Publishing Group, 5th Ed., 1996.

166. J. R. Hanson, *Functional Group Chemistry*, RSC Publishing, 2001.

167. D. R. Lide, *CRC Handbook of Chemistry and Physics*, CRC Press, 1992.

168. T. Fuchs, G. Chowdhury, C. L. Barnes, K. S. Gates, *J. Org. Chem.*, 2001, **66**, 107–114.

169. M. Boyd, M. P. Hay, P. D. W. Boyd, *Magn. Reson. Chem.*, 2006, **44**, 948-954.

170. P. R. Murthy, C. C. Patel, *Can. J. Chem.*, 1964, **42**, 856-860.

171. Mercury v2.4, CCDC 1994. Vista - A Program for the Analysis and Display of Data, retrieved from the CSD. Cambridge Crystallographic Data Centre

172. M. B. Tarallo, A. J. Costa-Filho, E. D. Vieira, A. Monge, C. Q. Leite, F. R. Pavan, G. Borthagaray, D. Gambino, M. H. Torre, *J. Argent. Chem. Soc.*, 2009, **97**, 80-89.

173. L. S. Lerman, *J. Mol. Biol.*, 1961, **3**, 18-30.

174. K. W. Jennette, S. J. Lippard, Vassilia.Ga, W. R. Bauer, *Proc. Natl. Acad. Sci.*, 1974, **71**, 3839-3843.

175. F. Biba, M. Groessl, A. Egger, A. Roller, C. G. Hartinger, B. K. Keppler, *Eur. J. Inorg. Chem.*, 2009, 4282-4287.

176. D. R. Lide, *CRC Handbook of Chemistry and Physics*, CRC Press, 2009.

177. S. J. Angyal, C. L. Angyal, *J. Chem. Soc.*, 1952, 1461-1466.

178. L. W. Deady, W. L. Finlayson, *Aust. J. Chem.*, 1980, **33**, 2441-2446.

179. D. R. Lide, *CRC Handbook of Chemistry and Physics*, CRC Press, 1992.

180. J. S. Poole, C. M. Hadad, M. S. Platz, Z. P. Fredin, L. Pickard, E. L. Guerrero, M. Kessler, G. Chowdhury, D. Kotandeniya, K. S. Gates, *Photochem. Photobiol.*, 2002, **75**, 339-345.

181. D. F. Shriver, P. W. Atkins, *Inorganic Chemistry*, Oxford University Press, 1999.

182. R. W. Hay, Y. Q. Chen, *Polyhedron*, 1995, **14**, 869-872.

183. K. E. Baxter, L. R. Hanton, J. Simpson, B. R. Vincent, A. G. Blackman, *Inorg. Chem.*, 1995, **34**, 2795-2796.

184. P. M. Jaffray, L. F. McClintock, K. E. Baxter, A. G. Blackman, *Inorg. Chem.*, 2005, **44**, 4215-4225.

185. D. Astruc, *Electron Transfer And Radical Processes in Transition-Metal Chemistry*, Wiley-VCH, 1995.

186. R. G. Compton, G. H. W. Sanders, *Electrode Potentials*, Oxford Science Publications, 1996.

187. A. C. Fisher, *Electrode Dynamics*, Oxford Science Publishing, 1996.

188. N. G. Connelly, W. E. Geiger, *Chem. Rev.*, 1996, **96**, 877-910.

189. G. Chowdhury, D. Kotandeniya, J. S. Daniels, C. L. Barnes, K. S. Gates, *Chem. Res. Toxicol.*, 2004, **17**, 1399-1405.

190. A. F. Parsons, *An Introduction To Free Radical Chemistry*, Blackwell Science, 2000.

191. C. Schieber, J. Howitt, U. Putz, J. M. White, C. L. Parish, P. S. Donnelly, S.-S. Tan, *J. Biol. Chem.*, 2011, **286**, 8555-8564.

192. E. Reisner, V. B. Arion, B. K. Keppler, A. J. L. Pombeiro, *Inorg. Chim. Acta*, 2008, **361**, 1569-1583.

193. S. Lakshmi, D. Saravanan, R. Renganathan, M. Velusamy, *J. Inorg. Biochem.*, 1996, **61**, 155-163.

194. T. Mosmann, *J. Immunol. Methods*, 1983, **65**, 55-63.

195. J. Carmichael, J. B. Mitchell, W. G. Degraff, J. Gamson, A. F. Gazdar, B. E. Johnson, E. Glatstein, J. D. Minna, *Br. J. Cancer*, 1988, **57**, 540-547.

196. L. Lyons, *A practical guide to data analysis for physical science students*, University Press, Cambridge, 1991.

197. .SAINT+ (v6.22), Bruker AXS, Bruker AXS GmbH, Karlshrue, Germany

198. .SADABS, v2.03, Sheldrick

199. .SHELXS-97 Programme for the solution of crystal structures, G.M. Sheldrick, Universität Göttingen, 2007

200. .SHELXL-97 Programme for the solution of crystal structures, G.M. Sheldrick, Universität Göttingen, 2007

201. T. D. Coombs, B. J. Brisdon, C. P. Curtis, M. F. Mahon, S. A. Brewer, C. R. Willis, *Polyhedron*, 2001, **20**, 2935-2943.

Abbreviations

Å	Amstrong
A	Amps
A2780	Human ovarian carcinoma cells
A549	Human Caucasian lung carcinoma cells
AA8	Chinese Hamster ovarian cells
ARNT	Aryl hydrocarbon receptor nuclear translocator
ATP	Adenosine triphosphate
ap.	apparent
Atx	Copper chaperone protein
br.	Broad
Bu	Butyl
CA	Carbonic anhydrase
conc.	Concentrated
COSY	Correlation spectroscopy
COX	Cyclooxygenase enzyme
Ctr1	Membrane copper transporter
CV	Cyclic voltammetry
cyclam	1,4,8,11-tetraazacyclotetradecane
d (NMR)	Doublet
DCM	Dichloromethane
DLD-1	Human colon adenocarcinoma cells
δ	Chemical shift
ΔE	Peak separation
DMEM	Dulbecco's modified Eagle's medium
DMF	Dimethylformamide
DMSO	Dimethylsulfoxide
DNA	Deoxyribonucleic acid
dpea	2,2’-dipyridylethylamine
dpHa	2,2’-dipyridylamine
dpma	2,2’-dipyridylmethylamine
e-	Electron
$E_{1/2}$	Half wave potential

EDTA	Ethylenediaminetetraacetic acid
EMT6	Mouse mammary carcinoma cells
EPR	Electron paramagnetic spectroscopy
E_{ox}	Oxidation potential
equiv.	Equivalents
E_{red}	Reduction potential
ESI	Electrospray ionisation
Et	Ethyl
FBS	Foetal bovine serum
FMISO	Fluoromisonidazole
g	Relative centrifugal force
GLUT	Glucose transporter protein
GSH	Glutathione
HIF-1	Hypoxia inducible factor 1
HMBC	Heteronuclear Multiple Bond Correlation
HSQC	Heteronuclear Single Quantum Coherence
H226	Human lung squamous carcinoma cells
HT29	Human Caucasian colon adenocarcinoma cells
H460	Human Non-small lung cancer cells
i(prefix)	Iso
in vacuo	Under reduced pressure
I_{ox}	Oxidation current
I_{ox}	Oxidation current
IR	Infra red
I_{red}	Reduction current
K562	Human Caucasian chronic myelogenous leukaemia cells
λ	Wavelength
m	Milli
M	Metal
m/z	Mass to charge ratio
MCF7	Human Caucasian breast adenocarcinoma cells
MCT	monocarboxylate transporter protein
Me	Methyl

MDA-MB 231	Human Caucasian breast adenocarcinoma cells
μ	Micro
MMP	Matrix metalloproteinase
MS	Mass spectrometry
MTT	3-(4,5-Dimethylthiazol-2-yl)-2,5-diphenyltetrazolium bromide
mV	Milli volts
n (prefix)	Normal
NBC	Na^+-HCO_3 co-transporter protein
NHE	Normal hydrogen electrode
NHE (protein)	Na^+-H^+ membrane transporter protein
NMR	Nuclear magnetic resonance
OAc	Acetate
ORTEP	Oak Ridge Thermal Ellipsoid Programme
OTf	trifluoromethanesulfonate
PBS	Phosphate buffer solution
PHD	Prolyl hydroxylase enzyme
phen	1,10-phenanthroline
py	Pyrrolidine
q (NMR)	Quintet
s (NMR)	Singlet
t (NMR)	Triplet
tpzH	3-amino-1,2,4 –benzotriazine-*N*1,*N*4-oxide
tpzH-CN	3-aminoquinoxaline-2-carbonitrile-*N*1,*N*4-oxide
tpzH-$CONH_1$	3-aminoquinoxaline-2-amido- *N*1,*N*4-oxide
UV	Ultraviolet
UV4	Mutant Chinese Hamster ovarian cells
V	Volts
VEGF	Vascular endothelial growth factor
vis	Visible
V79	Chinese Hamster lung fibroblast cells
xantphos	4,5-bis(diphenylphosphino)-9,9-dimethylxanthene
XRD	X-ray diffraction

Appendices

Appendix 1: ^{1}H-^{1}H COSY NMR (D_2O, 400 MHz) of $[Co(CO_3)(dpHa)_2]NO_3$

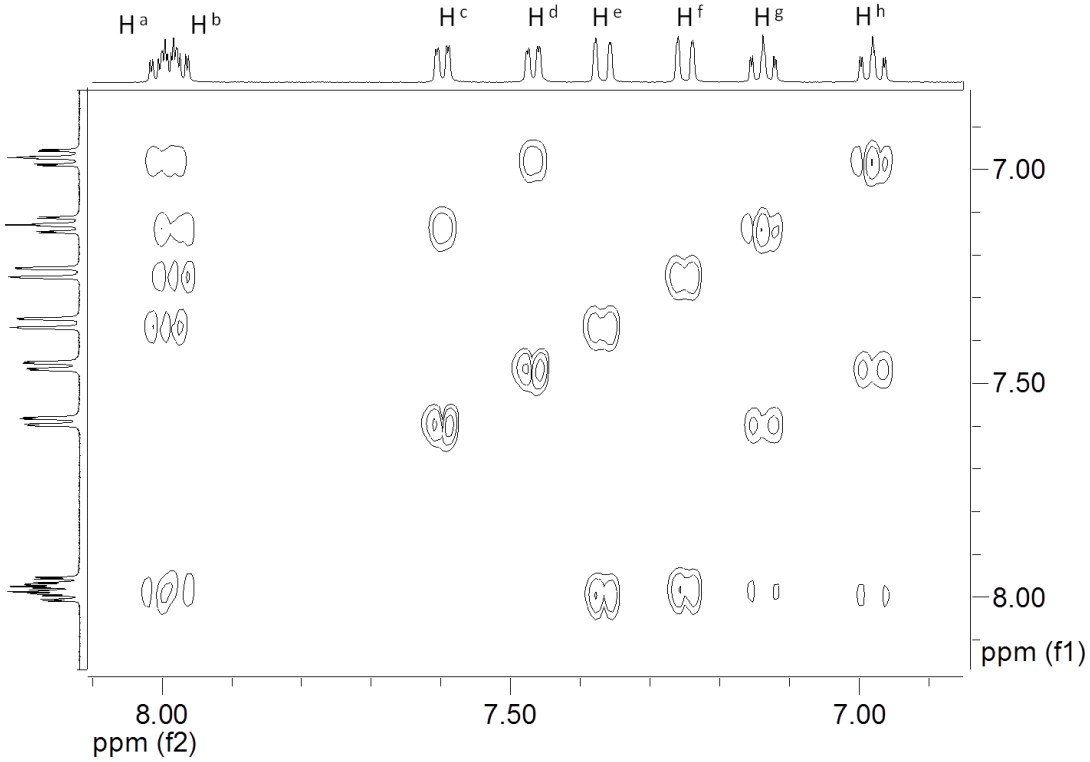

Appendix 2: ^{1}H-^{1}H COSY NMR (d_6-DMSO, 400 MHz) of dp(CN)(py)Ha (whole spectrum)

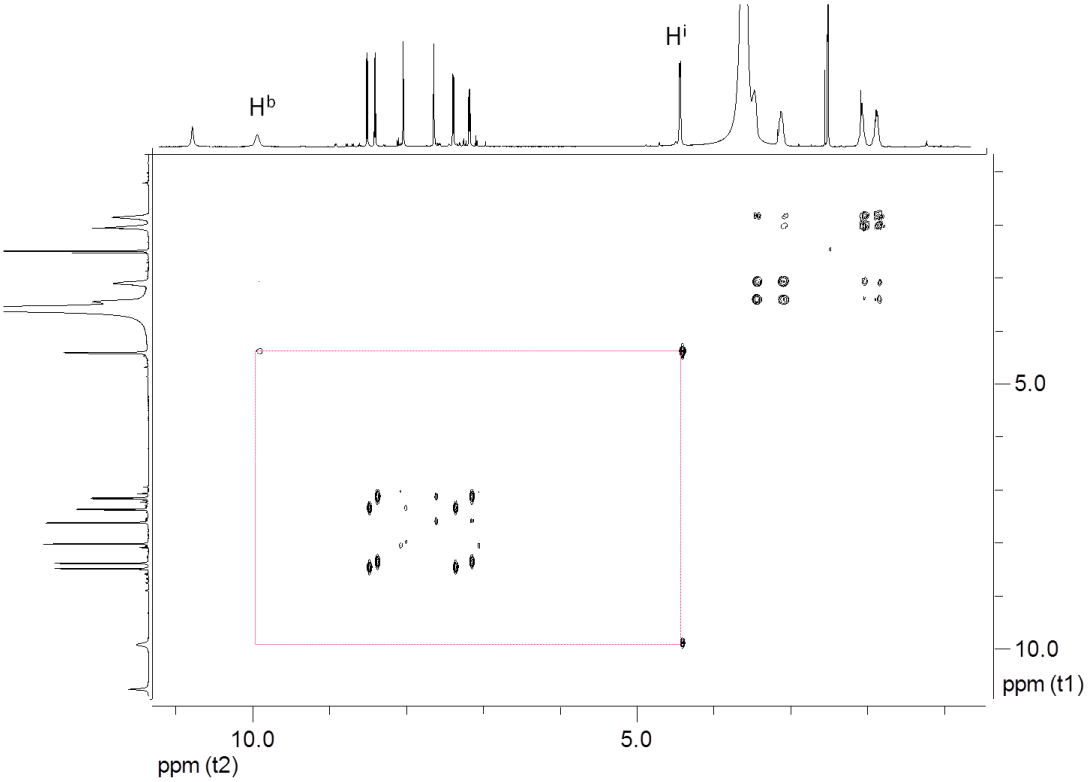

^{1}H-^{1}H COSY NMR (d_6-DMSO, 400 MHz) of dp(CN)(py)Ha (aromatic region)

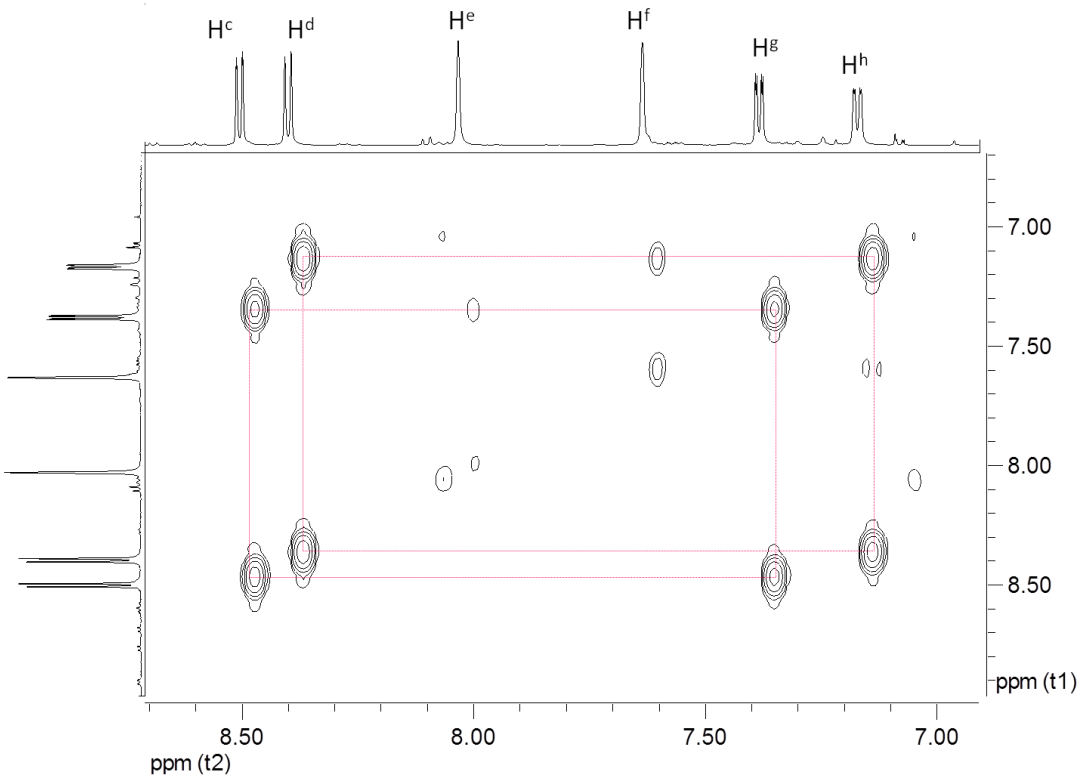

^{1}H-^{1}H COSY NMR (d_6-DMSO, 400 MHz) of dp(CN)(py)Ha (alkyl region)

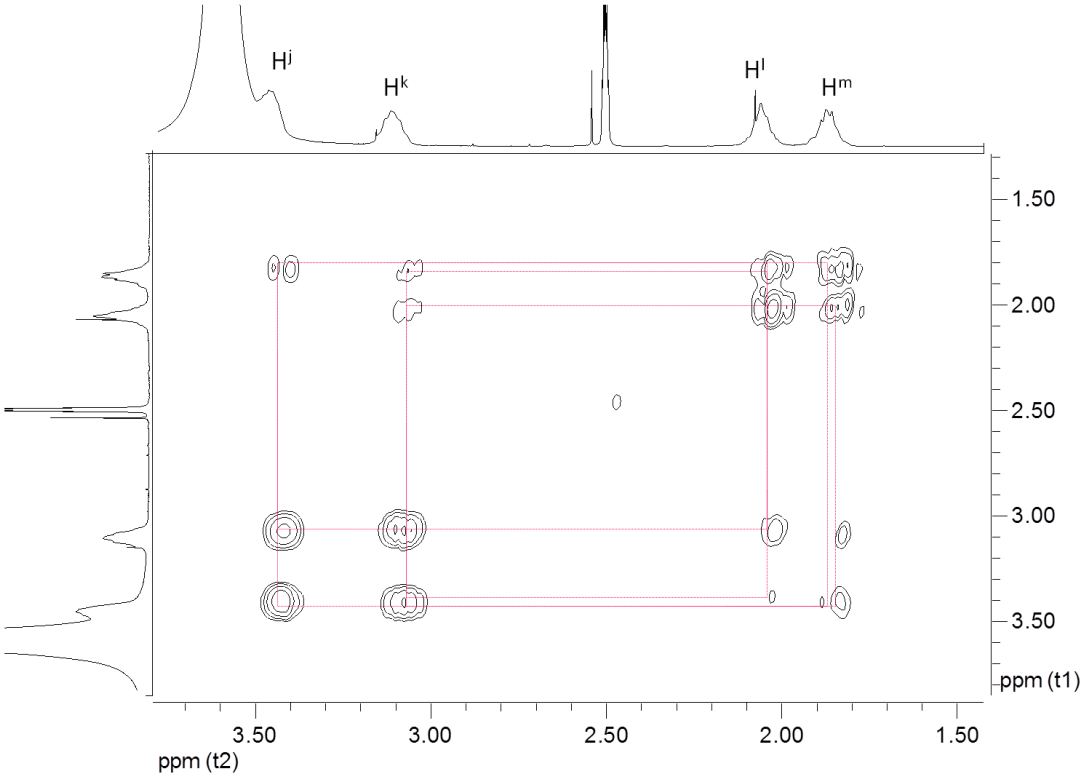

Appendix 3: ^{1}H-^{1}H COSY NMR (d_6-DMSO, 700 MHz) of [Co(tpz-CN)(dpHa)$_2$](BF$_4$)$_2$

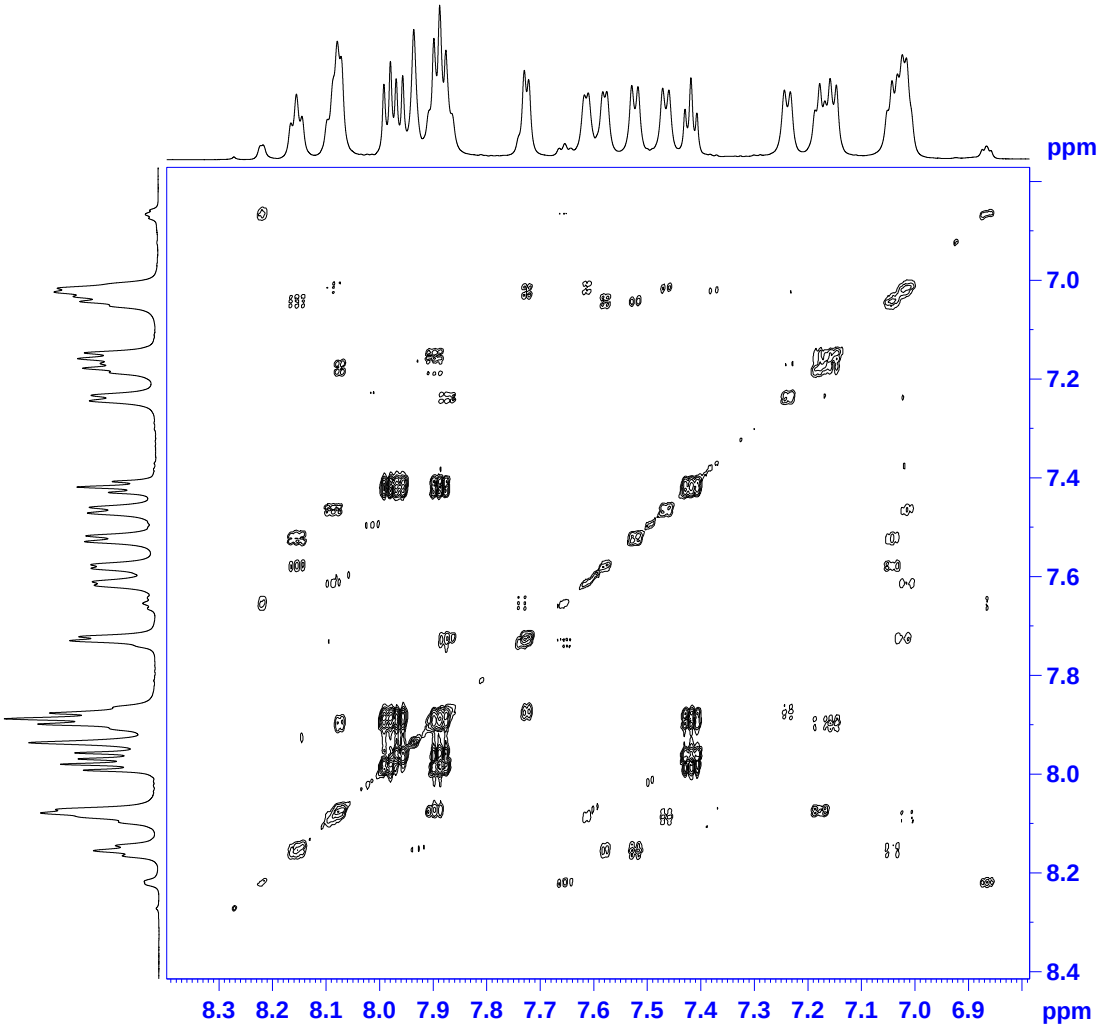

Appendix 4: NOESY NMR (d_6-DMSO, 700 MHz) of $[Co(tpz\text{-}CN)(dpHa)_2](BF_4)_2$

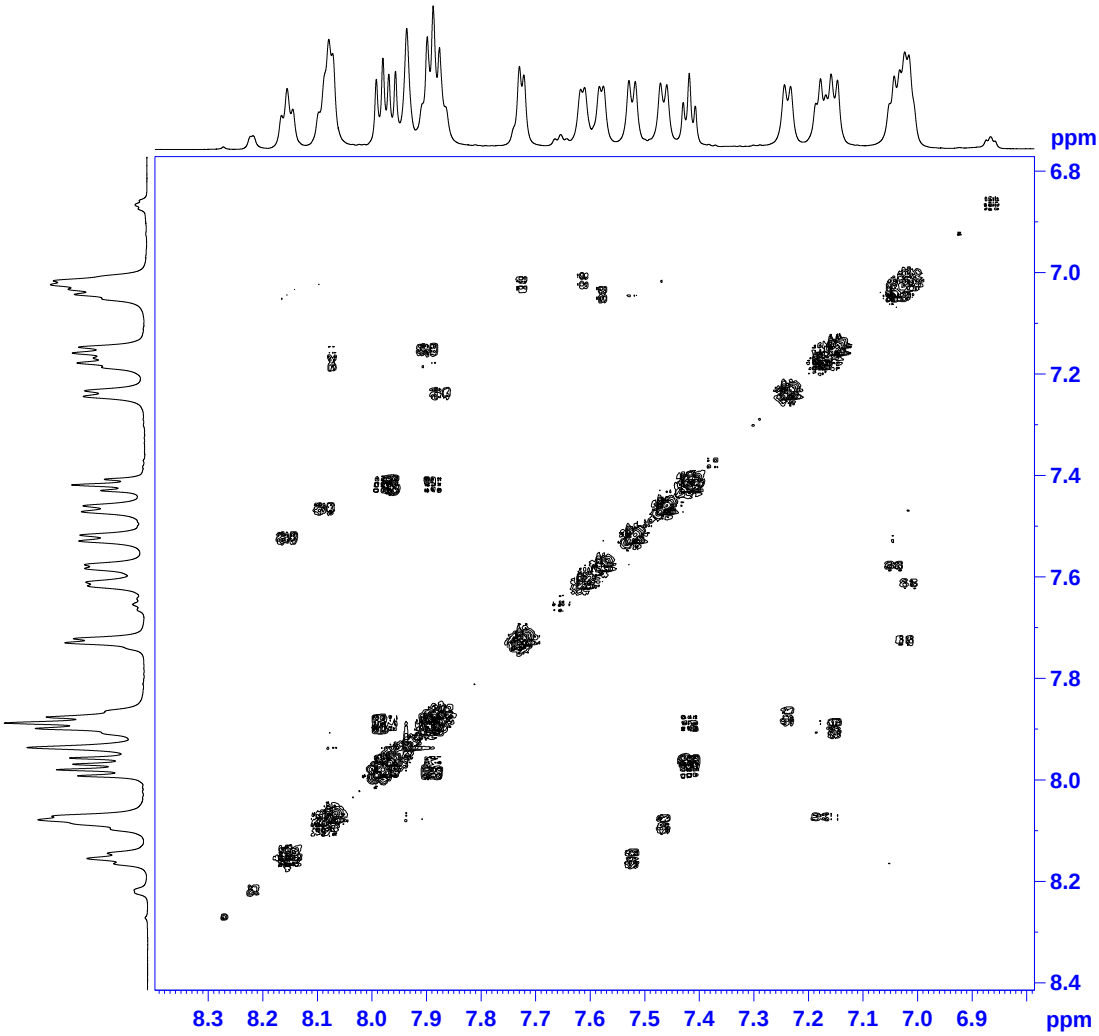

Appendix 5: Electrochemical data for $[Cu(dpHa)_2]Cl_2$ at varied scan rates in H_2O

$\nu^{1/2}$ / mV s^{-1}	E_{red} / V	I_{red} / µA	E_{ox} / V	I_{ox} / µA	ΔE / V	I_{ox}/I_{red}
7.1	-0.074	-22.0	0.040	26.50	0.11	-1.2
8.7	-0.080	-26.3	0.045	32.00	0.13	-1.2
10.0	-0.077	-30.1	0.050	35.00	0.13	-1.2
12.2	-0.091	-35.3	0.050	47.60	0.14	-1.4
14.1	-0.092	-41.1	0.059	55.00	0.15	-1.3
15.8	-0.109	-45.2	0.057	62.40	0.17	-1.4
17.3	-0.107	-49.3	0.060	62.40	0.17	-1.3
20.0	-0.086	-55.5	0.062	72.10	0.15	-1.3
22.4	-0.092	-63.0	0.071	75.00	0.16	-1.2

Appendix 6: IC_{50} data for the compounds reported within this thesis

IC_{50} data for tpzH and tpzH-CN against A549 cells

	tpzH	**tpzH-CN**
plate 1 IC_{50} / µM	166.7198	165.5346
plate 1 errors	9.28159	10.257
plate 2 IC_{50} / µM	167.9529	135.766
plate 2 errors	9.80719	5.89943
plate 3 IC_{50} / µM	185.4239	142.48
plate 3 errors	15.1865	9.6964
Mean/ IC_{50} µM	170.285377	143.0166726
error	6.2	4.5

IC_{50} data for $[Cu(dpHa)_2]Cl_2$ and [Cu(tpz)(dpHa)]Cl against A549 cells

	$[Cu(dpHa)_2]Cl_2$	**[Cu(tpz)(dpHa)]Cl**
plate 1 IC_{50} / µM	52.3054	44.1623
plate 1 errors	1.72019	4.71266
plate 2 IC_{50} / µM	52.9496	45.137
plate 2 errors	1.62683	3.48761
plate 3 IC_{50} / µM	54.3705	44.8474
plate 3 errors	1.17799	3.24293
Mean/ IC_{50} µM	53.51087956	44.81574974
error	0.8	2.1

IC_{50} data for $[Cu(dpHa)_2]Cl_2$ and [Cu(tpz)(dpHa)]Cl against A549 cells

	$[Co(tpz)(dpHa)_2]Cl_2$	**$[Co(tpz\text{-}CN)(dpHa)_2]Cl_2$**
plate 1 IC_{50} / µM	52.113	164.115
plate 1 errors	5.5061	13.9674
plate 2 IC_{50} / µM	61.09	157.852
plate 2 errors	7.6159	3.88064
plate 3 IC_{50} / µM	62.1932	138.9426
plate 3 errors	2.35108	74.02022
Mean/ IC_{50} µM	60.67240249	158.2515222
error	2.1	3.7

Appendix 7: Crystallographic data

Crystallographic data for $[Cu(Cl)(dpHa)_2]Cl$

Table 1. Crystal data and structure refinement for phw1009m.

Identification code	phw1009m	
Empirical formula	C20 H18 Cl2 Cu N6	
Formula weight	476.84	
Temperature	110(2) K	
Wavelength	0.71073 Å	
Crystal system	Monoclinic	
Space group	P2(1)/n	
Unit cell dimensions	a = 9.7191(19) Å	α= 90°.
	b = 14.334(3) Å	β= 98.896(5)°.
	c = 14.571(3) Å	γ = 90°.
Volume	2005.4(7) $Å^3$	
Z	4	
Density (calculated)	1.579 Mg/m^3	
Absorption coefficient	1.375 mm^{-1}	
F(000)	972	
Crystal size	0.36 x 0.24 x 0.16 mm^3	
Theta range for data collection	2.00 to 28.34°.	
Index ranges	-12<=h<=12, -19<=k<=19, -19<=l<=19	
Reflections collected	20466	
Independent reflections	4988 [R(int) = 0.0579]	
Completeness to theta = 28.34°	99.9 %	
Absorption correction	Semi-empirical from equivalents	
Max. and min. transmission	0.803 and 0.575	
Refinement method	Full-matrix least-squares on F^2	
Data / restraints / parameters	4988 / 0 / 270	
Goodness-of-fit on F^2	1.037	
Final R indices [I>2sigma(I)]	R1 = 0.0406, wR2 = 0.0909	
R indices (all data)	R1 = 0.0591, wR2 = 0.0998	
Largest diff. peak and hole	0.651 and -0.388 $e.Å^{-3}$	

Table 2. Atomic coordinates (x 10^4) and equivalent isotropic displacement parameters ($Å^2$x 10^3) for phw1009m. U(eq) is defined as one third of the trace of the orthogonalized U^{ij} tensor.

	x	y	z	U(eq)
C(1)	9572(3)	-465(2)	1665(2)	23(1)
C(2)	10554(3)	-760(2)	1144(2)	27(1)
C(3)	11422(3)	-94(2)	836(2)	28(1)
C(4)	11269(3)	824(2)	1064(2)	24(1)
C(5)	10247(3)	1078(2)	1604(2)	19(1)
C(6)	8289(3)	2453(2)	3715(2)	19(1)
C(7)	8802(3)	3301(2)	4037(2)	22(1)
C(8)	9804(3)	3738(2)	3600(2)	22(1)
C(9)	10259(3)	3296(2)	2861(2)	21(1)
C(10)	9670(3)	2434(2)	2561(2)	17(1)
C(11)	5215(3)	1877(2)	2472(2)	22(1)
C(12)	3910(3)	2135(2)	2613(2)	24(1)
C(13)	3212(3)	1561(2)	3160(2)	24(1)
C(14)	3830(3)	759(2)	3528(2)	21(1)
C(15)	5181(3)	539(2)	3354(2)	17(1)
C(16)	9453(3)	-405(2)	3802(2)	20(1)
C(17)	9817(3)	-1165(2)	4357(2)	22(1)
C(18)	8764(3)	-1681(2)	4661(2)	23(1)
C(19)	7407(3)	-1384(2)	4441(2)	20(1)
C(20)	7119(3)	-577(2)	3897(2)	16(1)
Cl(1)	6590(1)	904(1)	890(1)	24(1)
Cl(2)	1465(1)	3415(1)	536(1)	24(1)
Cu(1)	7663(1)	779(1)	2407(1)	17(1)
N(1)	9402(2)	440(2)	1899(1)	19(1)
N(2)	10141(2)	2007(2)	1815(2)	19(1)
N(3)	8689(2)	2020(1)	2969(1)	17(1)
N(4)	5867(2)	1082(1)	2833(1)	18(1)
N(5)	5764(2)	-267(2)	3744(2)	18(1)
N(6)	8115(2)	-117(1)	3533(1)	17(1)

Table 3. Bond lengths [Å] and angles [°] for phw1009m.

C(1)-N(1)	1.357(3)
C(1)-C(2)	1.375(4)
C(1)-H(1)	0.9500
C(2)-C(3)	1.393(4)
C(2)-H(2)	0.9500
C(3)-C(4)	1.371(4)
C(3)-H(3)	0.9500
C(4)-C(5)	1.406(3)
C(4)-H(4)	0.9500
C(5)-N(1)	1.343(3)
C(5)-N(2)	1.375(3)
C(6)-N(3)	1.360(3)
C(6)-C(7)	1.369(4)
C(6)-H(6)	0.9500
C(7)-C(8)	1.392(4)
C(7)-H(7)	0.9500
C(8)-C(9)	1.380(4)
C(8)-H(8)	0.9500
C(9)-C(10)	1.402(3)
C(9)-H(9)	0.9500
C(10)-N(3)	1.338(3)
C(10)-N(2)	1.384(3)
C(11)-C(12)	1.366(4)
C(11)-N(4)	1.369(3)
C(11)-H(11)	0.9500
C(12)-C(13)	1.394(4)
C(12)-H(12)	0.9500
C(13)-C(14)	1.367(4)
C(13)-H(13)	0.9500
C(14)-C(15)	1.411(3)
C(14)-H(14)	0.9500
C(15)-N(4)	1.335(3)
C(15)-N(5)	1.371(3)
C(16)-N(6)	1.363(3)
C(16)-C(17)	1.370(4)
C(16)-H(16)	0.9500
C(17)-C(18)	1.390(4)
C(17)-H(17)	0.9500

C(18)-C(19)	1.376(4)
C(18)-H(18)	0.9500
C(19)-C(20)	1.407(3)
C(19)-H(19)	0.9500
C(20)-N(6)	1.347(3)
C(20)-N(5)	1.375(3)
Cl(1)-Cu(1)	2.3013(8)
Cu(1)-N(4)	1.989(2)
Cu(1)-N(1)	2.007(2)
Cu(1)-N(6)	2.075(2)
Cu(1)-N(3)	2.139(2)
N(2)-H(2A)	0.81(3)
N(5)-H(5)	0.76(2)

N(1)-C(1)-C(2)	123.7(3)
N(1)-C(1)-H(1)	118.2
C(2)-C(1)-H(1)	118.2
C(1)-C(2)-C(3)	118.2(3)
C(1)-C(2)-H(2)	120.9
C(3)-C(2)-H(2)	120.9
C(4)-C(3)-C(2)	119.1(3)
C(4)-C(3)-H(3)	120.5
C(2)-C(3)-H(3)	120.5
C(3)-C(4)-C(5)	119.7(3)
C(3)-C(4)-H(4)	120.1
C(5)-C(4)-H(4)	120.1
N(1)-C(5)-N(2)	121.2(2)
N(1)-C(5)-C(4)	121.5(2)
N(2)-C(5)-C(4)	117.3(2)
N(3)-C(6)-C(7)	123.1(2)
N(3)-C(6)-H(6)	118.5
C(7)-C(6)-H(6)	118.5
C(6)-C(7)-C(8)	119.0(2)
C(6)-C(7)-H(7)	120.5
C(8)-C(7)-H(7)	120.5
C(9)-C(8)-C(7)	118.8(2)
C(9)-C(8)-H(8)	120.6
C(7)-C(8)-H(8)	120.6
C(8)-C(9)-C(10)	118.9(2)
C(8)-C(9)-H(9)	120.5

C(10)-C(9)-H(9)	120.5
N(3)-C(10)-N(2)	119.8(2)
N(3)-C(10)-C(9)	122.4(2)
N(2)-C(10)-C(9)	117.8(2)
C(12)-C(11)-N(4)	123.6(2)
C(12)-C(11)-H(11)	118.2
N(4)-C(11)-H(11)	118.2
C(11)-C(12)-C(13)	118.1(2)
C(11)-C(12)-H(12)	120.9
C(13)-C(12)-H(12)	120.9
C(14)-C(13)-C(12)	119.8(2)
C(14)-C(13)-H(13)	120.1
C(12)-C(13)-H(13)	120.1
C(13)-C(14)-C(15)	118.9(2)
C(13)-C(14)-H(14)	120.6
C(15)-C(14)-H(14)	120.6
N(4)-C(15)-N(5)	121.1(2)
N(4)-C(15)-C(14)	122.2(2)
N(5)-C(15)-C(14)	116.8(2)
N(6)-C(16)-C(17)	124.0(2)
N(6)-C(16)-H(16)	118.0
C(17)-C(16)-H(16)	118.0
C(16)-C(17)-C(18)	118.4(2)
C(16)-C(17)-H(17)	120.8
C(18)-C(17)-H(17)	120.8
C(19)-C(18)-C(17)	119.2(2)
C(19)-C(18)-H(18)	120.4
C(17)-C(18)-H(18)	120.4
C(18)-C(19)-C(20)	119.1(2)
C(18)-C(19)-H(19)	120.5
C(20)-C(19)-H(19)	120.5
N(6)-C(20)-N(5)	120.5(2)
N(6)-C(20)-C(19)	122.2(2)
N(5)-C(20)-C(19)	117.3(2)
N(4)-Cu(1)-N(1)	176.12(8)
N(4)-Cu(1)-N(6)	88.72(8)
N(1)-Cu(1)-N(6)	93.11(8)
N(4)-Cu(1)-N(3)	94.54(8)
N(1)-Cu(1)-N(3)	88.49(8)
N(6)-Cu(1)-N(3)	100.56(8)

N(4)-Cu(1)-Cl(1)	89.59(6)
N(1)-Cu(1)-Cl(1)	86.94(6)
N(6)-Cu(1)-Cl(1)	144.73(6)
N(3)-Cu(1)-Cl(1)	114.69(6)
C(5)-N(1)-C(1)	117.8(2)
C(5)-N(1)-Cu(1)	122.96(17)
C(1)-N(1)-Cu(1)	117.79(18)
C(5)-N(2)-C(10)	130.5(2)
C(5)-N(2)-H(2A)	116(2)
C(10)-N(2)-H(2A)	111(2)
C(10)-N(3)-C(6)	117.7(2)
C(10)-N(3)-Cu(1)	121.38(16)
C(6)-N(3)-Cu(1)	120.74(16)
C(15)-N(4)-C(11)	117.4(2)
C(15)-N(4)-Cu(1)	126.16(17)
C(11)-N(4)-Cu(1)	116.05(17)
C(15)-N(5)-C(20)	131.6(2)
C(15)-N(5)-H(5)	114.5(19)
C(20)-N(5)-H(5)	113.4(19)
C(20)-N(6)-C(16)	116.7(2)
C(20)-N(6)-Cu(1)	122.48(16)
C(16)-N(6)-Cu(1)	119.41(16)

Symmetry transformations used to generate equivalent atoms:

Table 4. Anisotropic displacement parameters ($Å^2 x\ 10^3$) for phw1009m. The anisotropic displacement factor exponent takes the form: $-2\pi^2[\ h^2\ a^{*2}U^{11} + ...\ + 2\ h\ k\ a^*\ b^*\ U^{12}\ ]$

	U^{11}	U^{22}	U^{33}	U^{23}	U^{13}	U^{12}
C(1)	29(2)	22(1)	18(1)	0(1)	3(1)	4(1)
C(2)	34(2)	27(1)	21(1)	-1(1)	3(1)	11(1)
C(3)	24(2)	42(2)	17(1)	-2(1)	5(1)	10(1)
C(4)	22(1)	32(2)	17(1)	-1(1)	4(1)	1(1)
C(5)	17(1)	27(1)	13(1)	0(1)	1(1)	3(1)
C(6)	16(1)	25(1)	18(1)	3(1)	3(1)	2(1)

C(7)	20(1)	25(1)	20(1)	-4(1)	1(1)	4(1)
C(8)	23(2)	18(1)	24(1)	-1(1)	-2(1)	2(1)
C(9)	20(1)	21(1)	21(1)	5(1)	2(1)	1(1)
C(10)	17(1)	19(1)	16(1)	6(1)	1(1)	5(1)
C(11)	25(1)	20(1)	20(1)	-2(1)	0(1)	2(1)
C(12)	22(1)	23(1)	25(1)	-1(1)	-2(1)	8(1)
C(13)	16(1)	31(2)	25(1)	-7(1)	-1(1)	7(1)
C(14)	15(1)	26(1)	21(1)	-3(1)	2(1)	1(1)
C(15)	14(1)	21(1)	15(1)	-4(1)	-1(1)	1(1)
C(16)	14(1)	27(1)	19(1)	0(1)	2(1)	1(1)
C(17)	17(1)	26(1)	22(1)	-1(1)	0(1)	6(1)
C(18)	26(2)	20(1)	23(1)	1(1)	2(1)	5(1)
C(19)	22(1)	17(1)	20(1)	1(1)	4(1)	-1(1)
C(20)	15(1)	19(1)	14(1)	-4(1)	1(1)	2(1)
Cl(1)	27(1)	26(1)	17(1)	0(1)	1(1)	5(1)
Cl(2)	20(1)	27(1)	26(1)	5(1)	11(1)	4(1)
Cu(1)	17(1)	18(1)	17(1)	1(1)	4(1)	2(1)
N(1)	21(1)	19(1)	18(1)	0(1)	4(1)	2(1)
N(2)	21(1)	20(1)	19(1)	2(1)	10(1)	-2(1)
N(3)	17(1)	19(1)	16(1)	1(1)	4(1)	1(1)
N(4)	19(1)	17(1)	17(1)	-1(1)	0(1)	1(1)
N(5)	16(1)	19(1)	20(1)	2(1)	5(1)	-2(1)
N(6)	17(1)	19(1)	16(1)	0(1)	3(1)	0(1)

Table 5. Hydrogen coordinates (x 10^4) and isotropic displacement parameters ($Å^2$x 10^3) for phw1009m.

	x	y	z	U(eq)
H(1)	8978	-919	1872	28
H(2)	10639	-1401	998	33
H(3)	12110	-273	473	33
H(4)	11851	1288	859	28
H(6)	7622	2153	4027	23
H(7)	8478	3587	4552	26
H(8)	10168	4329	3807	27
H(9)	10959	3570	2561	25

H(11)	5696	2271	2105	26
H(12)	3491	2690	2344	29
H(13)	2309	1726	3278	29
H(14)	3359	358	3894	25
H(16)	10177	-58	3591	24
H(17)	10767	-1335	4529	27
H(18)	8979	-2232	5017	28
H(19)	6675	-1720	4654	23
H(2A)	10600(30)	2370(20)	1550(20)	24(8)
H(5)	5270(30)	-568(17)	3978(17)	6(6)

Table 6. Torsion angles [°] for phw1009m.

N(1)-C(1)-C(2)-C(3)	-0.2(4)
C(1)-C(2)-C(3)-C(4)	0.2(4)
C(2)-C(3)-C(4)-C(5)	0.1(4)
C(3)-C(4)-C(5)-N(1)	-0.5(4)
C(3)-C(4)-C(5)-N(2)	179.8(2)
N(3)-C(6)-C(7)-C(8)	-1.5(4)
C(6)-C(7)-C(8)-C(9)	-0.7(4)
C(7)-C(8)-C(9)-C(10)	1.6(4)
C(8)-C(9)-C(10)-N(3)	-0.5(4)
C(8)-C(9)-C(10)-N(2)	179.7(2)
N(4)-C(11)-C(12)-C(13)	0.7(4)
C(11)-C(12)-C(13)-C(14)	-0.9(4)
C(12)-C(13)-C(14)-C(15)	1.0(4)
C(13)-C(14)-C(15)-N(4)	-0.9(4)
C(13)-C(14)-C(15)-N(5)	179.4(2)
N(6)-C(16)-C(17)-C(18)	0.5(4)
C(16)-C(17)-C(18)-C(19)	-3.7(4)
C(17)-C(18)-C(19)-C(20)	1.4(4)
C(18)-C(19)-C(20)-N(6)	4.3(4)
C(18)-C(19)-C(20)-N(5)	-175.7(2)
N(2)-C(5)-N(1)-C(1)	-179.8(2)
C(4)-C(5)-N(1)-C(1)	0.5(4)
N(2)-C(5)-N(1)-Cu(1)	14.3(3)
C(4)-C(5)-N(1)-Cu(1)	-165.42(19)
C(2)-C(1)-N(1)-C(5)	-0.1(4)

C(2)-C(1)-N(1)-Cu(1)	166.5(2)
N(4)-Cu(1)-N(1)-C(5)	108.2(12)
N(6)-Cu(1)-N(1)-C(5)	-133.7(2)
N(3)-Cu(1)-N(1)-C(5)	-33.2(2)
Cl(1)-Cu(1)-N(1)-C(5)	81.58(19)
N(4)-Cu(1)-N(1)-C(1)	-57.7(13)
N(6)-Cu(1)-N(1)-C(1)	60.36(19)
N(3)-Cu(1)-N(1)-C(1)	160.86(19)
Cl(1)-Cu(1)-N(1)-C(1)	-84.31(18)
N(1)-C(5)-N(2)-C(10)	27.3(4)
C(4)-C(5)-N(2)-C(10)	-153.0(3)
N(3)-C(10)-N(2)-C(5)	-30.3(4)
C(9)-C(10)-N(2)-C(5)	149.5(3)
N(2)-C(10)-N(3)-C(6)	178.1(2)
C(9)-C(10)-N(3)-C(6)	-1.6(3)
N(2)-C(10)-N(3)-Cu(1)	-6.7(3)
C(9)-C(10)-N(3)-Cu(1)	173.58(18)
C(7)-C(6)-N(3)-C(10)	2.7(4)
C(7)-C(6)-N(3)-Cu(1)	-172.55(19)
N(4)-Cu(1)-N(3)-C(10)	-147.90(19)
N(1)-Cu(1)-N(3)-C(10)	29.68(19)
N(6)-Cu(1)-N(3)-C(10)	122.56(18)
Cl(1)-Cu(1)-N(3)-C(10)	-56.26(19)
N(4)-Cu(1)-N(3)-C(6)	27.13(19)
N(1)-Cu(1)-N(3)-C(6)	-155.29(19)
N(6)-Cu(1)-N(3)-C(6)	-62.41(19)
Cl(1)-Cu(1)-N(3)-C(6)	118.77(17)
N(5)-C(15)-N(4)-C(11)	-179.7(2)
C(14)-C(15)-N(4)-C(11)	0.7(3)
N(5)-C(15)-N(4)-Cu(1)	7.6(3)
C(14)-C(15)-N(4)-Cu(1)	-172.02(18)
C(12)-C(11)-N(4)-C(15)	-0.6(4)
C(12)-C(11)-N(4)-Cu(1)	172.9(2)
N(1)-Cu(1)-N(4)-C(15)	93.5(12)
N(6)-Cu(1)-N(4)-C(15)	-24.7(2)
N(3)-Cu(1)-N(4)-C(15)	-125.2(2)
Cl(1)-Cu(1)-N(4)-C(15)	120.1(2)
N(1)-Cu(1)-N(4)-C(11)	-79.3(13)
N(6)-Cu(1)-N(4)-C(11)	162.52(18)
N(3)-Cu(1)-N(4)-C(11)	62.03(18)

Cl(1)-Cu(1)-N(4)-C(11)	-52.71(17)
N(4)-C(15)-N(5)-C(20)	17.3(4)
C(14)-C(15)-N(5)-C(20)	-163.0(2)
N(6)-C(20)-N(5)-C(15)	-9.3(4)
C(19)-C(20)-N(5)-C(15)	170.7(2)
N(5)-C(20)-N(6)-C(16)	172.8(2)
C(19)-C(20)-N(6)-C(16)	-7.3(3)
N(5)-C(20)-N(6)-Cu(1)	-20.6(3)
C(19)-C(20)-N(6)-Cu(1)	159.33(18)
C(17)-C(16)-N(6)-C(20)	4.9(4)
C(17)-C(16)-N(6)-Cu(1)	-162.1(2)
N(4)-Cu(1)-N(6)-C(20)	30.93(19)
N(1)-Cu(1)-N(6)-C(20)	-145.65(19)
N(3)-Cu(1)-N(6)-C(20)	125.31(18)
Cl(1)-Cu(1)-N(6)-C(20)	-56.5(2)
N(4)-Cu(1)-N(6)-C(16)	-162.81(19)
N(1)-Cu(1)-N(6)-C(16)	20.61(19)
N(3)-Cu(1)-N(6)-C(16)	-68.43(19)
Cl(1)-Cu(1)-N(6)-C(16)	109.72(18)

Symmetry transformations used to generate equivalent atoms:

Table 7. Hydrogen bonds for phw1009m [Å and °].

D-H...A	d(D-H)	d(H...A)	d(D...A)	<(DHA)
N(5)-H(5)...Cl(2)#1	0.76(2)	2.42(3)	3.173(2)	171(2)
N(2)-H(2A)...Cl(2)#2	0.81(3)	2.35(3)	3.152(2)	168(3)

Symmetry transformations used to generate equivalent atoms:

#1 -x+1/2,y-1/2,-z+1/2 #2 x+1,y,z

Crystallographic data for $[Co(Cl)_2(dpHa)_2]$

Table 1. Crystal data and structure refinement for phw0805m.

Identification code	phw0805m	
Empirical formula	C20.50 H21 Cl2 Co N6 O	
Formula weight	497.26	
Temperature	110(2) K	
Wavelength	0.71073 Å	
Crystal system	Monoclinic	
Space group	P2(1)/n	
Unit cell dimensions	a = 7.8029(5) Å	α= 90°.
	b = 16.0834(9) Å	β= 95.5590(10)°.
	c = 16.7459(10) Å	γ = 90°.
Volume	2091.7(2) $Å^3$	
Z	4	
Density (calculated)	1.579 Mg/m^3	
Absorption coefficient	1.102 mm^{-1}	
F(000)	1020	
Crystal size	0.20 x 0.10 x 0.04 mm^3	
Theta range for data collection	1.76 to 28.29°.	
Index ranges	-10<=h<=10, -21<=k<=21, -22<=l<=22	
Reflections collected	21119	
Independent reflections	5195 [R(int) = 0.0319]	
Completeness to theta = 28.29°	100.0 %	
Absorption correction	Semi-empirical from equivalents	
Max. and min. transmission	0.957 and 0.821	
Refinement method	Full-matrix least-squares on F^2	
Data / restraints / parameters	5195 / 0 / 319	
Goodness-of-fit on F^2	1.043	
Final R indices [I>2sigma(I)]	R1 = 0.0306, wR2 = 0.0742	
R indices (all data)	R1 = 0.0431, wR2 = 0.0790	
Largest diff. peak and hole	0.461 and -0.245 $e.Å^{-3}$	

Table 2. Atomic coordinates (x 10^4) and equivalent isotropic displacement parameters ($Å^2$x 10^3) for phw0805m. U(eq) is defined as one third of the trace of the orthogonalized U^{ij} tensor.

	x	y	z	U(eq)
Co(1)	7965(1)	8302(1)	1441(1)	17(1)
C(1)	11088(2)	9150(1)	2339(1)	20(1)
C(2)	11982(2)	9762(1)	2770(1)	22(1)
C(3)	11108(2)	10253(1)	3284(1)	20(1)
C(4)	9393(2)	10093(1)	3357(1)	20(1)
C(5)	8581(2)	9445(1)	2905(1)	16(1)
C(6)	6096(2)	8497(1)	2974(1)	17(1)
C(7)	4937(2)	8304(1)	3537(1)	21(1)
C(8)	4240(3)	7524(1)	3536(1)	29(1)
C(9)	4695(3)	6945(1)	2974(1)	35(1)
C(10)	5794(3)	7186(1)	2430(1)	27(1)
N(1)	9387(2)	8997(1)	2380(1)	18(1)
N(2)	6875(2)	9276(1)	3017(1)	17(1)
N(3)	6483(2)	7958(1)	2409(1)	19(1)
C(11)	6736(2)	6987(1)	235(1)	23(1)
C(12)	5652(3)	6404(1)	-136(1)	27(1)
C(13)	3885(3)	6516(1)	-119(1)	28(1)
C(14)	3283(2)	7222(1)	220(1)	24(1)
C(15)	4481(2)	7805(1)	565(1)	18(1)
C(16)	4644(2)	9302(1)	961(1)	16(1)
C(17)	3595(2)	10011(1)	851(1)	21(1)
C(18)	4347(2)	10781(1)	929(1)	24(1)
C(19)	6135(2)	10843(1)	1099(1)	23(1)
C(20)	7065(2)	10120(1)	1194(1)	19(1)
N(4)	6187(2)	7670(1)	607(1)	19(1)
N(5)	3845(2)	8530(1)	866(1)	20(1)
N(6)	6351(2)	9352(1)	1153(1)	16(1)
Cl(1)	9745(1)	8682(1)	392(1)	25(1)
Cl(2)	9979(2)	7103(1)	1761(1)	24(1)
O(1)	9444(6)	5366(3)	942(3)	32(1)
C(21)	10575(7)	7012(3)	2283(3)	48(1)
O(2)	9198(5)	7124(2)	1682(2)	28(1)
Cl(3)	9703(2)	5495(1)	678(1)	22(1)

Table 3. Bond lengths [Å] and angles [°] for phw0805m.

Co(1)-N(4)	2.1293(15)
Co(1)-N(6)	2.1343(14)
Co(1)-O(2)	2.145(4)
Co(1)-N(1)	2.1482(14)
Co(1)-N(3)	2.1526(14)
Co(1)-Cl(1)	2.4209(5)
Co(1)-Cl(2)	2.5115(13)
C(1)-N(1)	1.359(2)
C(1)-C(2)	1.371(2)
C(1)-H(1)	0.9500
C(2)-C(3)	1.393(3)
C(2)-H(2)	0.9500
C(3)-C(4)	1.379(2)
C(3)-H(3)	0.9500
C(4)-C(5)	1.403(2)
C(4)-H(4)	0.9500
C(5)-N(1)	1.339(2)
C(5)-N(2)	1.390(2)
C(6)-N(3)	1.338(2)
C(6)-N(2)	1.391(2)
C(6)-C(7)	1.404(2)
C(7)-C(8)	1.368(3)
C(7)-H(7)	0.9500
C(8)-C(9)	1.394(3)
C(8)-H(8)	0.9500
C(9)-C(10)	1.366(3)
C(9)-H(9)	0.9500
C(10)-N(3)	1.355(2)
C(10)-H(10)	0.9500
N(2)-H(2A)	0.88(2)
C(11)-N(4)	1.353(2)
C(11)-C(12)	1.370(3)
C(11)-H(11)	0.9500
C(12)-C(13)	1.393(3)
C(12)-H(12)	0.9500
C(13)-C(14)	1.372(3)

C(13)-H(13)	0.9500
C(14)-C(15)	1.408(2)
C(14)-H(14)	0.9500
C(15)-N(4)	1.343(2)
C(15)-N(5)	1.382(2)
C(16)-N(6)	1.342(2)
C(16)-N(5)	1.391(2)
C(16)-C(17)	1.406(2)
C(17)-C(18)	1.371(3)
C(17)-H(17)	0.9500
C(18)-C(19)	1.400(2)
C(18)-H(18)	0.9500
C(19)-C(20)	1.372(2)
C(19)-H(19)	0.9500
C(20)-N(6)	1.354(2)
C(20)-H(20)	0.9500
N(5)-H(5)	0.80(2)
Cl(2)-H(2B)	0.94(5)
O(1)-H(1A)	0.86(5)
O(1)-H(1B)	0.82(5)
C(21)-O(2)	1.410(5)
C(21)-H(21A)	0.9800
C(21)-H(21B)	0.9800
C(21)-H(21C)	0.9800
O(2)-H(2B)	0.83(5)
Cl(3)-H(1A)	0.54(6)
Cl(3)-H(1B)	0.82(6)

N(4)-Co(1)-N(6)	84.05(5)
N(4)-Co(1)-O(2)	87.36(12)
N(6)-Co(1)-O(2)	170.24(12)
N(4)-Co(1)-N(1)	170.41(5)
N(6)-Co(1)-N(1)	90.31(5)
O(2)-Co(1)-N(1)	97.55(12)
N(4)-Co(1)-N(3)	90.46(5)
N(6)-Co(1)-N(3)	91.44(5)
O(2)-Co(1)-N(3)	83.98(11)
N(1)-Co(1)-N(3)	81.90(5)
N(4)-Co(1)-Cl(1)	91.58(4)
N(6)-Co(1)-Cl(1)	90.22(4)

O(2)-Co(1)-Cl(1)	94.65(10)
N(1)-Co(1)-Cl(1)	96.21(4)
N(3)-Co(1)-Cl(1)	177.49(4)
N(4)-Co(1)-Cl(2)	97.36(5)
N(6)-Co(1)-Cl(2)	177.39(5)
O(2)-Co(1)-Cl(2)	12.12(11)
N(1)-Co(1)-Cl(2)	88.58(5)
N(3)-Co(1)-Cl(2)	90.75(5)
Cl(1)-Co(1)-Cl(2)	87.55(3)
N(1)-C(1)-C(2)	123.57(16)
N(1)-C(1)-H(1)	118.2
C(2)-C(1)-H(1)	118.2
C(1)-C(2)-C(3)	118.52(16)
C(1)-C(2)-H(2)	120.7
C(3)-C(2)-H(2)	120.7
C(4)-C(3)-C(2)	119.14(16)
C(4)-C(3)-H(3)	120.4
C(2)-C(3)-H(3)	120.4
C(3)-C(4)-C(5)	118.76(16)
C(3)-C(4)-H(4)	120.6
C(5)-C(4)-H(4)	120.6
N(1)-C(5)-N(2)	119.98(15)
N(1)-C(5)-C(4)	122.53(15)
N(2)-C(5)-C(4)	117.49(15)
N(3)-C(6)-N(2)	119.51(15)
N(3)-C(6)-C(7)	122.42(15)
N(2)-C(6)-C(7)	118.06(15)
C(8)-C(7)-C(6)	118.91(16)
C(8)-C(7)-H(7)	120.5
C(6)-C(7)-H(7)	120.5
C(7)-C(8)-C(9)	119.12(17)
C(7)-C(8)-H(8)	120.4
C(9)-C(8)-H(8)	120.4
C(10)-C(9)-C(8)	118.56(17)
C(10)-C(9)-H(9)	120.7
C(8)-C(9)-H(9)	120.7
N(3)-C(10)-C(9)	123.59(17)
N(3)-C(10)-H(10)	118.2
C(9)-C(10)-H(10)	118.2
C(5)-N(1)-C(1)	117.31(14)

C(5)-N(1)-Co(1)	121.21(11)
C(1)-N(1)-Co(1)	119.66(11)
C(5)-N(2)-C(6)	126.11(14)
C(5)-N(2)-H(2A)	111.3(13)
C(6)-N(2)-H(2A)	115.6(13)
C(6)-N(3)-C(10)	117.27(15)
C(6)-N(3)-Co(1)	122.69(11)
C(10)-N(3)-Co(1)	119.87(12)
N(4)-C(11)-C(12)	123.72(17)
N(4)-C(11)-H(11)	118.1
C(12)-C(11)-H(11)	118.1
C(11)-C(12)-C(13)	118.10(17)
C(11)-C(12)-H(12)	121.0
C(13)-C(12)-H(12)	121.0
C(14)-C(13)-C(12)	119.64(17)
C(14)-C(13)-H(13)	120.2
C(12)-C(13)-H(13)	120.2
C(13)-C(14)-C(15)	118.68(17)
C(13)-C(14)-H(14)	120.7
C(15)-C(14)-H(14)	120.7
N(4)-C(15)-N(5)	120.41(15)
N(4)-C(15)-C(14)	121.94(16)
N(5)-C(15)-C(14)	117.65(16)
N(6)-C(16)-N(5)	120.30(15)
N(6)-C(16)-C(17)	122.30(15)
N(5)-C(16)-C(17)	117.40(15)
C(18)-C(17)-C(16)	118.80(16)
C(18)-C(17)-H(17)	120.6
C(16)-C(17)-H(17)	120.6
C(17)-C(18)-C(19)	119.52(16)
C(17)-C(18)-H(18)	120.2
C(19)-C(18)-H(18)	120.2
C(20)-C(19)-C(18)	117.95(16)
C(20)-C(19)-H(19)	121.0
C(18)-C(19)-H(19)	121.0
N(6)-C(20)-C(19)	123.83(16)
N(6)-C(20)-H(20)	118.1
C(19)-C(20)-H(20)	118.1
C(15)-N(4)-C(11)	117.59(15)
C(15)-N(4)-Co(1)	122.47(11)

C(11)-N(4)-Co(1)	118.30(12)
C(15)-N(5)-C(16)	128.44(14)
C(15)-N(5)-H(5)	110.8(16)
C(16)-N(5)-H(5)	113.3(16)
C(16)-N(6)-C(20)	117.47(14)
C(16)-N(6)-Co(1)	123.85(11)
C(20)-N(6)-Co(1)	118.64(11)
Co(1)-Cl(2)-H(2B)	95(3)
H(1A)-O(1)-H(1B)	107(6)
O(2)-C(21)-H(21A)	109.5
O(2)-C(21)-H(21B)	109.5
H(21A)-C(21)-H(21B)	109.5
O(2)-C(21)-H(21C)	109.5
H(21A)-C(21)-H(21C)	109.5
H(21B)-C(21)-H(21C)	109.5
C(21)-O(2)-Co(1)	122.9(3)
C(21)-O(2)-H(2B)	99(4)
Co(1)-O(2)-H(2B)	130(3)
H(1A)-Cl(3)-H(1B)	166(7)

Symmetry transformations used to generate equivalent atoms:

Table 4. Anisotropic displacement parameters ($Å^2 x\ 10^3$) for phw0805m. The anisotropic displacement factor exponent takes the form: $-2\pi^2[\ h^2\ a^{*2}U^{11} + ... + 2\ h\ k\ a^*\ b^*\ U^{12}\ ]$

	U^{11}	U^{22}	U^{33}	U^{23}	U^{13}	U^{12}
Co(1)	18(1)	17(1)	18(1)	-2(1)	4(1)	-1(1)
C(1)	16(1)	25(1)	20(1)	2(1)	2(1)	2(1)
C(2)	14(1)	27(1)	23(1)	5(1)	-1(1)	-2(1)
C(3)	21(1)	19(1)	20(1)	2(1)	-3(1)	-4(1)
C(4)	21(1)	18(1)	20(1)	2(1)	0(1)	0(1)
C(5)	15(1)	17(1)	17(1)	4(1)	0(1)	0(1)
C(6)	14(1)	18(1)	18(1)	1(1)	-1(1)	0(1)
C(7)	20(1)	24(1)	19(1)	-3(1)	4(1)	-2(1)
C(8)	34(1)	30(1)	26(1)	-2(1)	13(1)	-11(1)
C(9)	52(1)	23(1)	32(1)	-4(1)	18(1)	-16(1)
C(10)	39(1)	17(1)	27(1)	-4(1)	11(1)	-5(1)
N(1)	14(1)	20(1)	18(1)	1(1)	2(1)	0(1)
N(2)	15(1)	17(1)	20(1)	-3(1)	4(1)	-1(1)

N(3)	21(1)	17(1)	18(1)	0(1)	4(1)	-2(1)
C(11)	27(1)	22(1)	20(1)	-2(1)	8(1)	-1(1)
C(12)	39(1)	22(1)	21(1)	-6(1)	3(1)	-1(1)
C(13)	36(1)	24(1)	23(1)	-3(1)	-4(1)	-10(1)
C(14)	23(1)	27(1)	21(1)	0(1)	-2(1)	-7(1)
C(15)	21(1)	20(1)	15(1)	0(1)	4(1)	-4(1)
C(16)	16(1)	20(1)	14(1)	-1(1)	3(1)	-1(1)
C(17)	14(1)	28(1)	21(1)	2(1)	3(1)	3(1)
C(18)	23(1)	22(1)	28(1)	2(1)	2(1)	6(1)
C(19)	25(1)	19(1)	25(1)	2(1)	0(1)	-3(1)
C(20)	18(1)	20(1)	19(1)	1(1)	0(1)	-2(1)
N(4)	20(1)	19(1)	18(1)	-2(1)	6(1)	-3(1)
N(5)	12(1)	25(1)	23(1)	-3(1)	4(1)	-3(1)
N(6)	14(1)	18(1)	16(1)	-1(1)	2(1)	-1(1)
Cl(1)	12(1)	42(1)	22(1)	-5(1)	3(1)	-3(1)
Cl(2)	22(1)	22(1)	27(1)	-1(1)	-1(1)	4(1)
O(1)	45(2)	28(2)	27(2)	1(2)	18(2)	3(2)
C(21)	63(3)	38(3)	37(3)	-2(2)	-24(3)	20(2)
O(2)	23(2)	31(2)	30(2)	-5(1)	-3(2)	8(2)
Cl(3)	21(1)	23(1)	23(1)	4(1)	6(1)	4(1)

Table 5. Hydrogen coordinates (x 10^4) and isotropic displacement parameters (Å^{2}x 10^3) for phw0805m.

	x	y	z	U(eq)
H(1)	11692	8814	1993	24
H(2)	13170	9850	2720	26
H(3)	11685	10691	3580	24
H(4)	8774	10416	3707	24
H(7)	4642	8709	3914	25
H(8)	3456	7378	3913	35
H(9)	4251	6395	2969	42
H(10)	6092	6791	2045	33
H(2A)	6480(30)	9625(13)	3357(12)	22(5)
H(11)	7941	6906	231	27
H(12)	6093	5937	-396	32
H(13)	3102	6107	-342	34

H(14)	2081	7315	222	29
H(17)	2386	9958	726	25
H(18)	3661	11269	868	29
H(19)	6687	11370	1148	28
H(20)	8281	10160	1294	23
H(5)	2830(30)	8561(14)	759(13)	30(6)
H(1A)	9790(70)	5230(40)	490(30)	39
H(1B)	9760(60)	5850(30)	1030(30)	39
H(21A)	11645	7209	2085	72
H(21B)	10685	6421	2420	72
H(21C)	10351	7330	2761	72
H(2B)	9440(70)	6750(30)	1370(30)	37(14)

Table 6. Torsion angles [°] for phw0805m.

N(1)-C(1)-C(2)-C(3)	0.5(3)
C(1)-C(2)-C(3)-C(4)	1.6(3)
C(2)-C(3)-C(4)-C(5)	-0.6(2)
C(3)-C(4)-C(5)-N(1)	-2.7(2)
C(3)-C(4)-C(5)-N(2)	177.24(15)
N(3)-C(6)-C(7)-C(8)	3.3(3)
N(2)-C(6)-C(7)-C(8)	-176.01(17)
C(6)-C(7)-C(8)-C(9)	-0.2(3)
C(7)-C(8)-C(9)-C(10)	-1.6(3)
C(8)-C(9)-C(10)-N(3)	0.6(3)
N(2)-C(5)-N(1)-C(1)	-175.27(15)
C(4)-C(5)-N(1)-C(1)	4.7(2)
N(2)-C(5)-N(1)-Co(1)	20.1(2)
C(4)-C(5)-N(1)-Co(1)	-159.92(12)
C(2)-C(1)-N(1)-C(5)	-3.6(2)
C(2)-C(1)-N(1)-Co(1)	161.27(14)
N(4)-Co(1)-N(1)-C(5)	-7.0(4)
N(6)-Co(1)-N(1)-C(5)	46.81(13)
O(2)-Co(1)-N(1)-C(5)	-127.38(16)
N(3)-Co(1)-N(1)-C(5)	-44.60(12)
Cl(1)-Co(1)-N(1)-C(5)	137.07(12)
Cl(2)-Co(1)-N(1)-C(5)	-135.56(13)

N(4)-Co(1)-N(1)-C(1)	-171.3(3)
N(6)-Co(1)-N(1)-C(1)	-117.45(13)
O(2)-Co(1)-N(1)-C(1)	68.36(16)
N(3)-Co(1)-N(1)-C(1)	151.14(13)
Cl(1)-Co(1)-N(1)-C(1)	-27.19(13)
Cl(2)-Co(1)-N(1)-C(1)	60.18(12)
N(1)-C(5)-N(2)-C(6)	33.5(2)
C(4)-C(5)-N(2)-C(6)	-146.43(16)
N(3)-C(6)-N(2)-C(5)	-39.4(2)
C(7)-C(6)-N(2)-C(5)	139.89(17)
N(2)-C(6)-N(3)-C(10)	175.05(16)
C(7)-C(6)-N(3)-C(10)	-4.2(3)
N(2)-C(6)-N(3)-Co(1)	-9.8(2)
C(7)-C(6)-N(3)-Co(1)	170.99(12)
C(9)-C(10)-N(3)-C(6)	2.3(3)
C(9)-C(10)-N(3)-Co(1)	-173.04(17)
N(4)-Co(1)-N(3)-C(6)	-134.57(13)
N(6)-Co(1)-N(3)-C(6)	-50.52(13)
O(2)-Co(1)-N(3)-C(6)	138.13(17)
N(1)-Co(1)-N(3)-C(6)	39.59(13)
Cl(1)-Co(1)-N(3)-C(6)	80.9(9)
Cl(2)-Co(1)-N(3)-C(6)	128.05(13)
N(4)-Co(1)-N(3)-C(10)	40.50(14)
N(6)-Co(1)-N(3)-C(10)	124.56(14)
O(2)-Co(1)-N(3)-C(10)	-46.80(18)
N(1)-Co(1)-N(3)-C(10)	-145.33(15)
Cl(1)-Co(1)-N(3)-C(10)	-104.0(9)
Cl(2)-Co(1)-N(3)-C(10)	-56.87(14)
N(4)-C(11)-C(12)-C(13)	-0.9(3)
C(11)-C(12)-C(13)-C(14)	3.9(3)
C(12)-C(13)-C(14)-C(15)	-1.8(3)
C(13)-C(14)-C(15)-N(4)	-3.5(3)
C(13)-C(14)-C(15)-N(5)	176.76(16)
N(6)-C(16)-C(17)-C(18)	1.3(3)
N(5)-C(16)-C(17)-C(18)	-179.06(16)
C(16)-C(17)-C(18)-C(19)	1.2(3)
C(17)-C(18)-C(19)-C(20)	-1.0(3)
C(18)-C(19)-C(20)-N(6)	-1.8(3)
N(5)-C(15)-N(4)-C(11)	-173.91(16)
C(14)-C(15)-N(4)-C(11)	6.3(2)

N(5)-C(15)-N(4)-Co(1)	21.0(2)
C(14)-C(15)-N(4)-Co(1)	-158.80(13)
C(12)-C(11)-N(4)-C(15)	-4.1(3)
C(12)-C(11)-N(4)-Co(1)	161.61(15)
N(6)-Co(1)-N(4)-C(15)	-39.89(13)
O(2)-Co(1)-N(4)-C(15)	135.47(17)
N(1)-Co(1)-N(4)-C(15)	14.4(4)
N(3)-Co(1)-N(4)-C(15)	51.51(13)
Cl(1)-Co(1)-N(4)-C(15)	-129.95(13)
Cl(2)-Co(1)-N(4)-C(15)	142.32(13)
N(6)-Co(1)-N(4)-C(11)	155.11(13)
O(2)-Co(1)-N(4)-C(11)	-29.53(16)
N(1)-Co(1)-N(4)-C(11)	-150.6(3)
N(3)-Co(1)-N(4)-C(11)	-113.49(13)
Cl(1)-Co(1)-N(4)-C(11)	65.05(12)
Cl(2)-Co(1)-N(4)-C(11)	-22.68(13)
N(4)-C(15)-N(5)-C(16)	25.9(3)
C(14)-C(15)-N(5)-C(16)	-154.27(17)
N(6)-C(16)-N(5)-C(15)	-34.3(3)
C(17)-C(16)-N(5)-C(15)	146.02(17)
N(5)-C(16)-N(6)-C(20)	176.51(15)
C(17)-C(16)-N(6)-C(20)	-3.8(2)
N(5)-C(16)-N(6)-Co(1)	-6.1(2)
C(17)-C(16)-N(6)-Co(1)	173.58(12)
C(19)-C(20)-N(6)-C(16)	4.1(2)
C(19)-C(20)-N(6)-Co(1)	-173.42(14)
N(4)-Co(1)-N(6)-C(16)	32.46(13)
O(2)-Co(1)-N(6)-C(16)	4.0(7)
N(1)-Co(1)-N(6)-C(16)	-139.76(13)
N(3)-Co(1)-N(6)-C(16)	-57.85(13)
Cl(1)-Co(1)-N(6)-C(16)	124.03(12)
Cl(2)-Co(1)-N(6)-C(16)	155.3(10)
N(4)-Co(1)-N(6)-C(20)	-150.15(13)
O(2)-Co(1)-N(6)-C(20)	-178.6(7)
N(1)-Co(1)-N(6)-C(20)	37.62(12)
N(3)-Co(1)-N(6)-C(20)	119.53(12)
Cl(1)-Co(1)-N(6)-C(20)	-58.58(12)
Cl(2)-Co(1)-N(6)-C(20)	-27.3(11)
N(4)-Co(1)-O(2)-C(21)	-174.9(4)
N(6)-Co(1)-O(2)-C(21)	-146.5(6)

N(1)-Co(1)-O(2)-C(21)	-3.2(4)
N(3)-Co(1)-O(2)-C(21)	-84.1(4)
Cl(1)-Co(1)-O(2)-C(21)	93.7(4)
Cl(2)-Co(1)-O(2)-C(21)	39.4(5)

Symmetry transformations used to generate equivalent atoms:

Table 7. Hydrogen bonds for phw0805m [Å and °].

D-H...A	d(D-H)	d(H...A)	d(D...A)	<(DHA)
O(2)-H(2B)...Cl(3)	0.83(5)	2.34(5)	3.159(4)	166(4)
O(1)-H(1B)...Cl(2)	0.82(5)	2.36(6)	3.123(5)	155(5)
N(5)-H(5)...Cl(1)#1	0.80(2)	2.43(2)	3.2295(16)	178(2)
N(2)-H(2A)...Cl(3)#2	0.88(2)	2.39(2)	3.265(2)	175.9(18)
N(2)-H(2A)...O(1)#2	0.88(2)	1.87(2)	2.744(4)	178(2)

Symmetry transformations used to generate equivalent atoms:

#1 x-1,y,z #2 -x+3/2,y+1/2,-z+1/2

Crystallographic data for $[Co(CO)_3(dpHa)_2]NO_3$

Table 1. Crystal data and structure refinement for phw0906m.

Identification code	phw0906m	
Empirical formula	C21 H18 Co N7 O6	
Formula weight	523.35	
Temperature	110(2) K	
Wavelength	0.71073 Å	
Crystal system	Monoclinic	
Space group	P2(1)/n	
Unit cell dimensions	a = 10.7832(7) Å	α= 90°.
	b = 13.1835(9) Å	β= 93.4550(10)°.
	c = 15.4280(10) Å	γ = 90°.
Volume	2189.3(3) $Å^3$	
Z	4	
Density (calculated)	1.588 Mg/m^3	
Absorption coefficient	0.840 mm^{-1}	
F(000)	1072	
Crystal size	0.35 x 0.10 x 0.07 mm^3	
Theta range for data collection	2.03 to 28.31°.	
Index ranges	-14<=h<=14, -17<=k<=17, -20<=l<=20	
Reflections collected	22341	
Independent reflections	5450 [R(int) = 0.0198]	
Completeness to theta = 28.31°	99.9 %	
Absorption correction	Semi-empirical from equivalents	
Max. and min. transmission	0.944 and 0.826	
Refinement method	Full-matrix least-squares on F^2	
Data / restraints / parameters	5450 / 0 / 324	
Goodness-of-fit on F^2	1.055	
Final R indices [I>2sigma(I)]	R1 = 0.0314, wR2 = 0.0788	
R indices (all data)	R1 = 0.0347, wR2 = 0.0811	
Largest diff. peak and hole	0.791 and -0.300 $e.Å^{-3}$	

Table 2. Atomic coordinates (x 10^4) and equivalent isotropic displacement parameters ($Å^2$x 10^3) for phw0906m. U(eq) is defined as one third of the trace of the orthogonalized U^{ij} tensor.

	x	y	z	U(eq)
C(1)	3835(1)	1868(1)	1575(1)	17(1)
C(2)	4788(1)	1526(1)	2129(1)	19(1)
C(3)	5799(1)	2168(1)	2324(1)	20(1)
C(4)	5786(1)	3137(1)	1997(1)	19(1)
C(5)	4731(1)	3469(1)	1496(1)	15(1)
C(6)	1437(1)	5035(1)	711(1)	19(1)
C(7)	1335(2)	6040(1)	929(1)	22(1)
C(8)	2405(2)	6555(1)	1242(1)	24(1)
C(9)	3510(2)	6040(1)	1340(1)	21(1)
C(10)	3544(1)	5004(1)	1133(1)	16(1)
C(11)	955(2)	2949(1)	1643(1)	19(1)
C(12)	-147(2)	2695(1)	1992(1)	25(1)
C(13)	-1016(2)	2121(1)	1494(1)	29(1)
C(14)	-746(2)	1806(1)	681(1)	23(1)
C(15)	406(1)	2069(1)	369(1)	17(1)
C(16)	4016(1)	1582(1)	-471(1)	19(1)
C(17)	4205(2)	786(1)	-1024(1)	23(1)
C(18)	3158(2)	319(1)	-1438(1)	23(1)
C(19)	1992(2)	629(1)	-1243(1)	20(1)
C(20)	1869(1)	1421(1)	-647(1)	16(1)
C(21)	2960(1)	3992(1)	-1027(1)	17(1)
Co(1)	2670(1)	3196(1)	287(1)	13(1)
N(1)	3815(1)	2824(1)	1240(1)	15(1)
N(2)	2527(1)	4520(1)	800(1)	15(1)
N(3)	4637(1)	4480(1)	1288(1)	17(1)
N(4)	1222(1)	2661(1)	825(1)	16(1)
N(5)	2864(1)	1912(1)	-295(1)	15(1)
N(6)	697(1)	1698(1)	-429(1)	17(1)
O(1)	3851(1)	3761(1)	-439(1)	17(1)
O(2)	1872(1)	3701(1)	-766(1)	17(1)
O(3)	3137(1)	4413(1)	-1725(1)	22(1)
N(7)	8024(1)	503(1)	8506(1)	20(1)
O(4)	7035(1)	418(1)	8062(1)	36(1)
O(5)	8272(2)	-56(1)	9139(1)	53(1)
O(6)	8797(1)	1170(1)	8318(1)	29(1)

Table 3. Bond lengths [Å] and angles [°] for phw0906m.

C(1)-N(1)	1.3625(18)
C(1)-C(2)	1.373(2)
C(1)-H(1)	0.9500
C(2)-C(3)	1.399(2)
C(2)-H(2)	0.9500
C(3)-C(4)	1.373(2)
C(3)-H(3)	0.9500
C(4)-C(5)	1.405(2)
C(4)-H(4)	0.9500
C(5)-N(1)	1.3451(19)
C(5)-N(3)	1.3734(19)
C(6)-N(2)	1.3572(19)
C(6)-C(7)	1.373(2)
C(6)-H(6)	0.9500
C(7)-C(8)	1.399(2)
C(7)-H(7)	0.9500
C(8)-C(9)	1.372(2)
C(8)-H(8)	0.9500
C(9)-C(10)	1.405(2)
C(9)-H(9)	0.9500
C(10)-N(2)	1.3430(19)
C(10)-N(3)	1.3745(19)
C(11)-N(4)	1.3653(19)
C(11)-C(12)	1.375(2)
C(11)-H(11)	0.9500
C(12)-C(13)	1.399(3)
C(12)-H(12)	0.9500
C(13)-C(14)	1.369(2)
C(13)-H(13)	0.9500
C(14)-C(15)	1.402(2)
C(14)-H(14)	0.9500
C(15)-N(4)	1.3437(19)
C(15)-N(6)	1.379(2)
C(16)-N(5)	1.3587(19)

C(16)-C(17)	1.375(2)
C(16)-H(16)	0.9500
C(17)-C(18)	1.406(2)
C(17)-H(17)	0.9500
C(18)-C(19)	1.373(2)
C(18)-H(18)	0.9500
C(19)-C(20)	1.403(2)
C(19)-H(19)	0.9500
C(20)-N(5)	1.3398(19)
C(20)-N(6)	1.3758(19)
C(21)-O(3)	1.2365(18)
C(21)-O(1)	1.3169(18)
C(21)-O(2)	1.3202(18)
C(21)-Co(1)	2.3212(15)
Co(1)-O(1)	1.8981(10)
Co(1)-O(2)	1.9117(10)
Co(1)-N(1)	1.9250(12)
Co(1)-N(2)	1.9261(12)
Co(1)-N(5)	1.9342(12)
Co(1)-N(4)	1.9437(13)
N(3)-H(3A)	0.84(2)
N(6)-H(6A)	0.81(2)
N(7)-O(4)	1.2379(18)
N(7)-O(5)	1.2389(19)
N(7)-O(6)	1.2574(17)

N(1)-C(1)-C(2)	122.29(14)
N(1)-C(1)-H(1)	118.9
C(2)-C(1)-H(1)	118.9
C(1)-C(2)-C(3)	118.67(14)
C(1)-C(2)-H(2)	120.7
C(3)-C(2)-H(2)	120.7
C(4)-C(3)-C(2)	119.56(14)
C(4)-C(3)-H(3)	120.2
C(2)-C(3)-H(3)	120.2
C(3)-C(4)-C(5)	118.84(14)
C(3)-C(4)-H(4)	120.6
C(5)-C(4)-H(4)	120.6
N(1)-C(5)-N(3)	120.16(13)
N(1)-C(5)-C(4)	121.31(14)

N(3)-C(5)-C(4)	118.51(13)
N(2)-C(6)-C(7)	122.63(14)
N(2)-C(6)-H(6)	118.7
C(7)-C(6)-H(6)	118.7
C(6)-C(7)-C(8)	118.49(15)
C(6)-C(7)-H(7)	120.8
C(8)-C(7)-H(7)	120.8
C(9)-C(8)-C(7)	119.36(15)
C(9)-C(8)-H(8)	120.3
C(7)-C(8)-H(8)	120.3
C(8)-C(9)-C(10)	119.37(15)
C(8)-C(9)-H(9)	120.3
C(10)-C(9)-H(9)	120.3
N(2)-C(10)-N(3)	120.01(13)
N(2)-C(10)-C(9)	121.13(14)
N(3)-C(10)-C(9)	118.86(14)
N(4)-C(11)-C(12)	122.06(15)
N(4)-C(11)-H(11)	119.0
C(12)-C(11)-H(11)	119.0
C(11)-C(12)-C(13)	118.80(15)
C(11)-C(12)-H(12)	120.6
C(13)-C(12)-H(12)	120.6
C(14)-C(13)-C(12)	119.71(15)
C(14)-C(13)-H(13)	120.1
C(12)-C(13)-H(13)	120.1
C(13)-C(14)-C(15)	118.76(15)
C(13)-C(14)-H(14)	120.6
C(15)-C(14)-H(14)	120.6
N(4)-C(15)-N(6)	119.74(13)
N(4)-C(15)-C(14)	122.02(14)
N(6)-C(15)-C(14)	118.24(14)
N(5)-C(16)-C(17)	122.68(14)
N(5)-C(16)-H(16)	118.7
C(17)-C(16)-H(16)	118.7
C(16)-C(17)-C(18)	118.11(15)
C(16)-C(17)-H(17)	120.9
C(18)-C(17)-H(17)	120.9
C(19)-C(18)-C(17)	119.39(14)
C(19)-C(18)-H(18)	120.3
C(17)-C(18)-H(18)	120.3

C(18)-C(19)-C(20)	119.35(14)
C(18)-C(19)-H(19)	120.3
C(20)-C(19)-H(19)	120.3
N(5)-C(20)-N(6)	119.86(13)
N(5)-C(20)-C(19)	121.32(14)
N(6)-C(20)-C(19)	118.82(13)
O(3)-C(21)-O(1)	124.05(14)
O(3)-C(21)-O(2)	125.65(14)
O(1)-C(21)-O(2)	110.30(12)
O(3)-C(21)-Co(1)	178.89(12)
O(1)-C(21)-Co(1)	54.85(7)
O(2)-C(21)-Co(1)	55.45(7)
O(1)-Co(1)-O(2)	69.23(4)
O(1)-Co(1)-N(1)	97.39(5)
O(2)-Co(1)-N(1)	166.57(5)
O(1)-Co(1)-N(2)	87.67(5)
O(2)-Co(1)-N(2)	89.44(5)
N(1)-Co(1)-N(2)	88.93(5)
O(1)-Co(1)-N(5)	88.55(5)
O(2)-Co(1)-N(5)	88.03(5)
N(1)-Co(1)-N(5)	92.82(5)
N(2)-Co(1)-N(5)	176.01(5)
O(1)-Co(1)-N(4)	168.15(5)
O(2)-Co(1)-N(4)	99.02(5)
N(1)-Co(1)-N(4)	94.39(5)
N(2)-Co(1)-N(4)	93.88(5)
N(5)-Co(1)-N(4)	89.57(5)
O(1)-Co(1)-C(21)	34.56(5)
O(2)-Co(1)-C(21)	34.66(5)
N(1)-Co(1)-C(21)	131.94(5)
N(2)-Co(1)-C(21)	88.13(5)
N(5)-Co(1)-C(21)	88.04(5)
N(4)-Co(1)-C(21)	133.67(5)
C(5)-N(1)-C(1)	118.64(13)
C(5)-N(1)-Co(1)	119.28(10)
C(1)-N(1)-Co(1)	121.35(10)
C(10)-N(2)-C(6)	118.91(13)
C(10)-N(2)-Co(1)	120.23(10)
C(6)-N(2)-Co(1)	120.12(10)
C(5)-N(3)-C(10)	125.33(13)

C(5)-N(3)-H(3A)	112.9(15)
C(10)-N(3)-H(3A)	117.4(15)
C(15)-N(4)-C(11)	118.48(13)
C(15)-N(4)-Co(1)	120.38(10)
C(11)-N(4)-Co(1)	120.89(10)
C(20)-N(5)-C(16)	118.94(13)
C(20)-N(5)-Co(1)	120.32(10)
C(16)-N(5)-Co(1)	119.91(10)
C(20)-N(6)-C(15)	125.04(13)
C(20)-N(6)-H(6A)	114.6(14)
C(15)-N(6)-H(6A)	115.8(14)
C(21)-O(1)-Co(1)	90.58(8)
C(21)-O(2)-Co(1)	89.89(8)
O(4)-N(7)-O(5)	121.31(15)
O(4)-N(7)-O(6)	119.79(13)
O(5)-N(7)-O(6)	118.90(14)

Symmetry transformations used to generate equivalent atoms:

Table 4. Anisotropic displacement parameters ($Å^2 x\ 10^3$) for phw0906m. The anisotropic displacement factor exponent takes the form: $-2\pi^2[\ h^2\ a^{*2}U^{11} + ... + 2\ h\ k\ a^*\ b^*\ U^{12}\ ]$

	U^{11}	U^{22}	U^{33}	U^{23}	U^{13}	U^{12}
C(1)	18(1)	15(1)	17(1)	1(1)	2(1)	0(1)
C(2)	22(1)	18(1)	17(1)	3(1)	2(1)	4(1)
C(3)	19(1)	25(1)	17(1)	1(1)	-1(1)	7(1)
C(4)	16(1)	22(1)	18(1)	-3(1)	-2(1)	0(1)
C(5)	16(1)	17(1)	14(1)	-1(1)	1(1)	1(1)
C(6)	18(1)	19(1)	19(1)	2(1)	-1(1)	2(1)
C(7)	23(1)	19(1)	23(1)	1(1)	2(1)	7(1)
C(8)	30(1)	16(1)	27(1)	-2(1)	3(1)	2(1)
C(9)	23(1)	16(1)	25(1)	-3(1)	1(1)	-3(1)
C(10)	17(1)	16(1)	15(1)	1(1)	1(1)	-1(1)
C(11)	22(1)	18(1)	18(1)	1(1)	2(1)	1(1)
C(12)	28(1)	26(1)	22(1)	1(1)	9(1)	2(1)
C(13)	22(1)	32(1)	33(1)	1(1)	10(1)	-3(1)

C(14)	18(1)	24(1)	28(1)	1(1)	2(1)	-5(1)
C(15)	17(1)	15(1)	19(1)	3(1)	0(1)	0(1)
C(16)	17(1)	20(1)	20(1)	1(1)	0(1)	0(1)
C(17)	22(1)	22(1)	24(1)	-2(1)	2(1)	4(1)
C(18)	29(1)	18(1)	21(1)	-4(1)	0(1)	4(1)
C(19)	24(1)	15(1)	20(1)	-1(1)	-4(1)	-2(1)
C(20)	18(1)	13(1)	16(1)	3(1)	-1(1)	-1(1)
C(21)	20(1)	14(1)	17(1)	-2(1)	-1(1)	-3(1)
Co(1)	13(1)	12(1)	13(1)	0(1)	-1(1)	-1(1)
N(1)	15(1)	14(1)	15(1)	0(1)	0(1)	1(1)
N(2)	17(1)	14(1)	15(1)	0(1)	-1(1)	0(1)
N(3)	15(1)	15(1)	20(1)	-1(1)	-3(1)	-2(1)
N(4)	16(1)	15(1)	17(1)	1(1)	0(1)	1(1)
N(5)	16(1)	14(1)	14(1)	1(1)	0(1)	-1(1)
N(6)	15(1)	17(1)	19(1)	-2(1)	-2(1)	-3(1)
O(1)	16(1)	18(1)	16(1)	1(1)	0(1)	-3(1)
O(2)	17(1)	18(1)	16(1)	1(1)	-2(1)	-2(1)
O(3)	25(1)	23(1)	18(1)	4(1)	-2(1)	-7(1)
N(7)	23(1)	16(1)	21(1)	1(1)	-1(1)	-1(1)
O(4)	25(1)	36(1)	45(1)	12(1)	-14(1)	-9(1)
O(5)	71(1)	41(1)	43(1)	24(1)	-27(1)	-23(1)
O(6)	25(1)	31(1)	31(1)	5(1)	0(1)	-11(1)

Table 5. Hydrogen coordinates (x 10^4) and isotropic displacement parameters ($Å^2$x 10^3) for phw0906m.

	x	y	z	U(eq)
H(1)	3166	1422	1420	20
H(2)	4761	866	2375	23
H(3)	6490	1936	2681	24
H(4)	6477	3575	2107	23
H(6)	716	4686	488	23
H(7)	556	6377	869	26
H(8)	2366	7255	1385	29
H(9)	4245	6382	1546	26

H(11)	1548	3336	1981	23
H(12)	-314	2906	2562	30
H(13)	-1790	1951	1718	34
H(14)	-1328	1417	334	28
H(16)	4719	1915	-202	23
H(17)	5021	559	-1123	27
H(18)	3256	-208	-1849	27
H(19)	1276	310	-1508	24
H(3A)	5260(20)	4814(16)	1458(14)	28(5)
H(6A)	139(19)	1420(16)	-709(13)	21(5)

Table 6. Torsion angles [°] for phw0906m.

N(1)-C(1)-C(2)-C(3)	-2.9(2)
C(1)-C(2)-C(3)-C(4)	3.4(2)
C(2)-C(3)-C(4)-C(5)	2.2(2)
C(3)-C(4)-C(5)-N(1)	-8.7(2)
C(3)-C(4)-C(5)-N(3)	169.73(14)
N(2)-C(6)-C(7)-C(8)	1.1(2)
C(6)-C(7)-C(8)-C(9)	-1.5(2)
C(7)-C(8)-C(9)-C(10)	-0.6(2)
C(8)-C(9)-C(10)-N(2)	3.4(2)
C(8)-C(9)-C(10)-N(3)	-175.76(15)
N(4)-C(11)-C(12)-C(13)	0.2(2)
C(11)-C(12)-C(13)-C(14)	1.4(3)
C(12)-C(13)-C(14)-C(15)	0.1(3)
C(13)-C(14)-C(15)-N(4)	-3.5(2)
C(13)-C(14)-C(15)-N(6)	176.28(15)
N(5)-C(16)-C(17)-C(18)	1.8(2)
C(16)-C(17)-C(18)-C(19)	-3.6(2)
C(17)-C(18)-C(19)-C(20)	1.3(2)
C(18)-C(19)-C(20)-N(5)	3.1(2)
C(18)-C(19)-C(20)-N(6)	-177.35(14)
O(2)-C(21)-Co(1)-O(1)	179.67(13)
O(1)-C(21)-Co(1)-O(2)	-179.67(13)
O(1)-C(21)-Co(1)-N(1)	1.74(11)
O(2)-C(21)-Co(1)-N(1)	-178.59(8)
O(1)-C(21)-Co(1)-N(2)	88.61(9)
O(2)-C(21)-Co(1)-N(2)	-91.72(8)
O(1)-C(21)-Co(1)-N(5)	-90.29(9)
O(2)-C(21)-Co(1)-N(5)	89.38(8)
O(1)-C(21)-Co(1)-N(4)	-177.81(8)
O(2)-C(21)-Co(1)-N(4)	1.86(11)
N(3)-C(5)-N(1)-C(1)	-169.20(13)
C(4)-C(5)-N(1)-C(1)	9.2(2)
N(3)-C(5)-N(1)-Co(1)	20.43(18)
C(4)-C(5)-N(1)-Co(1)	-161.13(11)
C(2)-C(1)-N(1)-C(5)	-3.4(2)
C(2)-C(1)-N(1)-Co(1)	166.80(11)
O(1)-Co(1)-N(1)-C(5)	41.81(11)
O(2)-Co(1)-N(1)-C(5)	37.4(3)

N(2)-Co(1)-N(1)-C(5)	-45.70(11)
N(5)-Co(1)-N(1)-C(5)	130.71(11)
N(4)-Co(1)-N(1)-C(5)	-139.51(11)
C(21)-Co(1)-N(1)-C(5)	40.82(14)
O(1)-Co(1)-N(1)-C(1)	-128.28(11)
O(2)-Co(1)-N(1)-C(1)	-132.7(2)
N(2)-Co(1)-N(1)-C(1)	144.21(12)
N(5)-Co(1)-N(1)-C(1)	-39.39(12)
N(4)-Co(1)-N(1)-C(1)	50.39(12)
C(21)-Co(1)-N(1)-C(1)	-129.28(11)
N(3)-C(10)-N(2)-C(6)	175.33(13)
C(9)-C(10)-N(2)-C(6)	-3.8(2)
N(3)-C(10)-N(2)-Co(1)	-14.50(18)
C(9)-C(10)-N(2)-Co(1)	166.35(11)
C(7)-C(6)-N(2)-C(10)	1.5(2)
C(7)-C(6)-N(2)-Co(1)	-168.63(12)
O(1)-Co(1)-N(2)-C(10)	-54.55(11)
O(2)-Co(1)-N(2)-C(10)	-123.78(11)
N(1)-Co(1)-N(2)-C(10)	42.89(11)
N(4)-Co(1)-N(2)-C(10)	137.22(11)
C(21)-Co(1)-N(2)-C(10)	-89.14(11)
O(1)-Co(1)-N(2)-C(6)	115.50(11)
O(2)-Co(1)-N(2)-C(6)	46.26(11)
N(1)-Co(1)-N(2)-C(6)	-147.07(12)
N(4)-Co(1)-N(2)-C(6)	-52.74(12)
C(21)-Co(1)-N(2)-C(6)	80.91(11)
N(1)-C(5)-N(3)-C(10)	26.5(2)
C(4)-C(5)-N(3)-C(10)	-152.00(14)
N(2)-C(10)-N(3)-C(5)	-29.8(2)
C(9)-C(10)-N(3)-C(5)	149.33(15)
N(6)-C(15)-N(4)-C(11)	-174.67(13)
C(14)-C(15)-N(4)-C(11)	5.1(2)
N(6)-C(15)-N(4)-Co(1)	10.99(19)
C(14)-C(15)-N(4)-Co(1)	-169.26(12)
C(12)-C(11)-N(4)-C(15)	-3.4(2)
C(12)-C(11)-N(4)-Co(1)	170.86(12)
O(1)-Co(1)-N(4)-C(15)	41.0(3)
O(2)-Co(1)-N(4)-C(15)	48.12(12)
N(1)-Co(1)-N(4)-C(15)	-132.62(11)
N(2)-Co(1)-N(4)-C(15)	138.16(11)

N(5)-Co(1)-N(4)-C(15)	-39.82(12)
C(21)-Co(1)-N(4)-C(15)	47.05(14)
O(1)-Co(1)-N(4)-C(11)	-133.2(2)
O(2)-Co(1)-N(4)-C(11)	-126.08(11)
N(1)-Co(1)-N(4)-C(11)	53.18(12)
N(2)-Co(1)-N(4)-C(11)	-36.04(12)
N(5)-Co(1)-N(4)-C(11)	145.98(12)
C(21)-Co(1)-N(4)-C(11)	-127.15(11)
N(6)-C(20)-N(5)-C(16)	175.50(13)
C(19)-C(20)-N(5)-C(16)	-5.0(2)
N(6)-C(20)-N(5)-Co(1)	-14.98(18)
C(19)-C(20)-N(5)-Co(1)	164.57(11)
C(17)-C(16)-N(5)-C(20)	2.5(2)
C(17)-C(16)-N(5)-Co(1)	-167.07(12)
O(1)-Co(1)-N(5)-C(20)	-126.42(11)
O(2)-Co(1)-N(5)-C(20)	-57.16(11)
N(1)-Co(1)-N(5)-C(20)	136.25(11)
N(4)-Co(1)-N(5)-C(20)	41.88(11)
C(21)-Co(1)-N(5)-C(20)	-91.85(11)
O(1)-Co(1)-N(5)-C(16)	43.01(11)
O(2)-Co(1)-N(5)-C(16)	112.27(11)
N(1)-Co(1)-N(5)-C(16)	-54.32(12)
N(4)-Co(1)-N(5)-C(16)	-148.69(12)
C(21)-Co(1)-N(5)-C(16)	77.58(12)
N(5)-C(20)-N(6)-C(15)	-32.5(2)
C(19)-C(20)-N(6)-C(15)	147.97(15)
N(4)-C(15)-N(6)-C(20)	34.6(2)
C(14)-C(15)-N(6)-C(20)	-145.17(15)
O(3)-C(21)-O(1)-Co(1)	-179.75(14)
O(2)-C(21)-O(1)-Co(1)	-0.29(11)
O(2)-Co(1)-O(1)-C(21)	0.20(8)
N(1)-Co(1)-O(1)-C(21)	-178.69(8)
N(2)-Co(1)-O(1)-C(21)	-90.08(9)
N(5)-Co(1)-O(1)-C(21)	88.65(9)
N(4)-Co(1)-O(1)-C(21)	7.7(3)
O(3)-C(21)-O(2)-Co(1)	179.74(15)
O(1)-C(21)-O(2)-Co(1)	0.29(11)
O(1)-Co(1)-O(2)-C(21)	-0.20(8)
N(1)-Co(1)-O(2)-C(21)	4.5(2)
N(2)-Co(1)-O(2)-C(21)	87.52(9)

N(5)-Co(1)-O(2)-C(21)	-89.39(9)
N(4)-Co(1)-O(2)-C(21)	-178.64(8)

Symmetry transformations used to generate equivalent atoms:

Table 7. Hydrogen bonds for phw0906m [Å and °].

D-H...A	d(D-H)	d(H...A)	d(D...A)	<(DHA)
N(6)-H(6A)...O(6)#1	0.81(2)	2.05(2)	2.8175(18)	159(2)
N(3)-H(3A)...O(3)#2	0.84(2)	2.02(2)	2.8553(17)	173(2)

Symmetry transformations used to generate equivalent atoms:

#1 x-1,y,z-1 #2 -x+1,-y+1,-z

Crystallographic data for [{Cu(Cl)$_2$(dpma)}$_2$]

Table 1. Crystal data and structure refinement for phw0814m.

Identification code	phw0814m	
Empirical formula	C22 H22 Cl4 Cu2 N6	
Formula weight	639.34	
Temperature	110(2) K	
Wavelength	0.71073 Å	
Crystal system	Triclinic	
Space group	P-1	
Unit cell dimensions	a = 7.0435(11) Å	α= 101.376(3)°.
	b = 8.6428(13) Å	β= 105.068(3)°.
	c = 11.4144(17) Å	γ = 107.467(3)°.
Volume	610.78(16) Å^3	
Z	1	
Density (calculated)	1.738 Mg/m^3	
Absorption coefficient	2.203 mm^{-1}	
F(000)	322	
Crystal size	0.18 x 0.13 x 0.04 mm^3	
Theta range for data collection	1.94 to 28.32°.	
Index ranges	-9<=h<=9, -11<=k<=11, -15<=l<=15	
Reflections collected	6294	
Independent reflections	3013 [R(int) = 0.0377]	
Completeness to theta = 28.32°	98.9 %	
Absorption correction	Semi-empirical from equivalents	
Max. and min. transmission	0.916 and 0.666	
Refinement method	Full-matrix least-squares on F^2	
Data / restraints / parameters	3013 / 0 / 155	
Goodness-of-fit on F^2	1.036	
Final R indices [I>2sigma(I)]	R1 = 0.0439, wR2 = 0.0992	
R indices (all data)	R1 = 0.0594, wR2 = 0.1048	
Largest diff. peak and hole	0.726 and -0.895 e.Å^{-3}	

Table 2. Atomic coordinates (x 10^4) and equivalent isotropic displacement parameters ($Å^2$x 10^3) for phw0814m. U(eq) is defined as one third of the trace of the orthogonalized U^{ij} tensor.

	x	y	z	U(eq)
C(1)	7085(5)	8692(4)	10261(3)	15(1)
C(2)	8279(5)	10399(4)	10687(3)	16(1)
C(3)	8201(5)	11340(4)	9848(4)	18(1)
C(4)	6875(6)	10545(4)	8597(3)	18(1)
C(5)	5707(5)	8810(4)	8216(3)	14(1)
C(6)	2178(5)	6973(4)	6781(3)	15(1)
C(7)	460(6)	7133(5)	5947(3)	22(1)
C(8)	-1565(6)	6213(5)	5872(3)	25(1)
C(9)	-1856(6)	5178(5)	6648(3)	23(1)
C(10)	-99(6)	5023(5)	7417(3)	19(1)
C(11)	4631(6)	8815(5)	6000(3)	25(1)
Cl(1)	2932(2)	2704(1)	7000(1)	22(1)
Cl(2)	2889(1)	5109(1)	10389(1)	14(1)
Cu(1)	4295(1)	5361(1)	8434(1)	12(1)
N(1)	5841(4)	7886(3)	9036(3)	13(1)
N(2)	4282(5)	7940(4)	6956(3)	17(1)
N(3)	1889(4)	5888(4)	7477(3)	15(1)

Table 3. Bond lengths [Å] and angles [°] for phw0814m.

C(1)-N(1)	1.350(4)
C(1)-C(2)	1.372(4)
C(1)-H(1)	0.9500
C(2)-C(3)	1.374(5)
C(2)-H(2)	0.9500
C(3)-C(4)	1.385(5)
C(3)-H(3)	0.9500
C(4)-C(5)	1.389(4)
C(4)-H(4)	0.9500
C(5)-N(1)	1.347(4)
C(5)-N(2)	1.418(4)
C(6)-N(3)	1.347(4)
C(6)-C(7)	1.394(5)

C(6)-N(2)	1.404(4)
C(7)-C(8)	1.379(5)
C(7)-H(7)	0.9500
C(8)-C(9)	1.387(6)
C(8)-H(8)	0.9500
C(9)-C(10)	1.379(5)
C(9)-H(9)	0.9500
C(10)-N(3)	1.351(4)
C(10)-H(10)	0.9500
C(11)-N(2)	1.475(4)
C(11)-H(11A)	0.9800
C(11)-H(11B)	0.9800
C(11)-H(11C)	0.9800
Cl(1)-Cu(1)	2.2911(9)
Cl(2)-Cu(1)#1	2.2838(9)
Cl(2)-Cu(1)	2.6874(9)
Cu(1)-N(3)	1.993(3)
Cu(1)-N(1)	2.004(3)
Cu(1)-Cl(2)#1	2.2838(9)

N(1)-C(1)-C(2)	122.3(3)
N(1)-C(1)-H(1)	118.8
C(2)-C(1)-H(1)	118.8
C(1)-C(2)-C(3)	119.4(3)
C(1)-C(2)-H(2)	120.3
C(3)-C(2)-H(2)	120.3
C(2)-C(3)-C(4)	119.0(3)
C(2)-C(3)-H(3)	120.5
C(4)-C(3)-H(3)	120.5
C(3)-C(4)-C(5)	119.1(3)
C(3)-C(4)-H(4)	120.4
C(5)-C(4)-H(4)	120.4
N(1)-C(5)-C(4)	121.5(3)
N(1)-C(5)-N(2)	117.0(3)
C(4)-C(5)-N(2)	121.5(3)
N(3)-C(6)-C(7)	121.1(3)
N(3)-C(6)-N(2)	116.6(3)
C(7)-C(6)-N(2)	122.2(3)
C(8)-C(7)-C(6)	119.3(3)
C(8)-C(7)-H(7)	120.4

C(6)-C(7)-H(7)	120.4
C(7)-C(8)-C(9)	119.6(3)
C(7)-C(8)-H(8)	120.2
C(9)-C(8)-H(8)	120.2
C(10)-C(9)-C(8)	118.3(3)
C(10)-C(9)-H(9)	120.8
C(8)-C(9)-H(9)	120.8
N(3)-C(10)-C(9)	122.5(3)
N(3)-C(10)-H(10)	118.7
C(9)-C(10)-H(10)	118.7
N(2)-C(11)-H(11A)	109.5
N(2)-C(11)-H(11B)	109.5
H(11A)-C(11)-H(11B)	109.5
N(2)-C(11)-H(11C)	109.5
H(11A)-C(11)-H(11C)	109.5
H(11B)-C(11)-H(11C)	109.5
Cu(1)#1-Cl(2)-Cu(1)	95.25(3)
N(3)-Cu(1)-N(1)	84.50(11)
N(3)-Cu(1)-Cl(2)#1	176.95(8)
N(1)-Cu(1)-Cl(2)#1	92.87(8)
N(3)-Cu(1)-Cl(1)	90.14(8)
N(1)-Cu(1)-Cl(1)	154.73(8)
Cl(2)#1-Cu(1)-Cl(1)	92.89(3)
N(3)-Cu(1)-Cl(2)	94.05(8)
N(1)-Cu(1)-Cl(2)	97.33(8)
Cl(2)#1-Cu(1)-Cl(2)	84.75(3)
Cl(1)-Cu(1)-Cl(2)	107.69(3)
C(5)-N(1)-C(1)	118.6(3)
C(5)-N(1)-Cu(1)	120.6(2)
C(1)-N(1)-Cu(1)	120.8(2)
C(6)-N(2)-C(5)	118.3(3)
C(6)-N(2)-C(11)	116.9(3)
C(5)-N(2)-C(11)	115.4(3)
C(6)-N(3)-C(10)	119.0(3)
C(6)-N(3)-Cu(1)	120.9(2)
C(10)-N(3)-Cu(1)	119.7(2)

Symmetry transformations used to generate equivalent atoms:

#1 -x+1,-y+1,-z+2

Table 4. Anisotropic displacement parameters ($Å^2 x\ 10^3$) for phw0814m. The anisotropic displacement factor exponent takes the form: $-2\pi^2[\ h^2\ a^{*2}U^{11} + ... + 2\ h\ k\ a^*\ b^*\ U^{12}\ ]$

	U^{11}	U^{22}	U^{33}	U^{23}	U^{13}	U^{12}
C(1)	16(2)	12(2)	14(2)	3(1)	4(1)	4(1)
C(2)	14(2)	13(2)	19(2)	0(1)	6(1)	4(1)
C(3)	16(2)	8(2)	29(2)	2(1)	9(2)	4(1)
C(4)	24(2)	13(2)	22(2)	9(1)	12(2)	8(1)
C(5)	18(2)	14(2)	13(2)	4(1)	9(1)	8(1)
C(6)	21(2)	17(2)	9(2)	1(1)	4(1)	11(1)
C(7)	32(2)	23(2)	13(2)	5(1)	5(2)	17(2)
C(8)	26(2)	33(2)	11(2)	-2(2)	1(2)	17(2)
C(9)	17(2)	32(2)	15(2)	-1(2)	5(2)	8(2)
C(10)	20(2)	21(2)	11(2)	0(1)	5(1)	5(2)
C(11)	40(2)	21(2)	16(2)	11(2)	14(2)	9(2)
Cl(1)	32(1)	16(1)	14(1)	1(1)	2(1)	8(1)
Cl(2)	17(1)	13(1)	14(1)	6(1)	6(1)	6(1)
Cu(1)	15(1)	9(1)	9(1)	2(1)	1(1)	2(1)
N(1)	14(1)	10(1)	12(1)	2(1)	6(1)	2(1)
N(2)	25(2)	17(2)	11(1)	8(1)	6(1)	7(1)
N(3)	19(2)	18(1)	6(1)	3(1)	2(1)	7(1)

Table 5. Hydrogen coordinates ($x\ 10^4$) and isotropic displacement parameters ($Å^2 x\ 10^{\ 3}$) for phw0814m.

	x	y	z	U(eq)
H(1)	7136	8053	10849	17
H(2)	9151	10927	11554	20
H(3)	9045	12519	10122	22
H(4)	6765	11177	8006	21
H(7)	682	7868	5436	26

H(8)	-2752	6287	5293	29
H(9)	-3232	4591	6650	27
H(10)	-294	4279	7925	23
H(11A)	3821	8019	5146	37
H(11B)	6142	9230	6109	37
H(11C)	4164	9777	6110	37

Table 6. Torsion angles [°] for phw0814m.

N(1)-C(1)-C(2)-C(3)	0.7(5)
C(1)-C(2)-C(3)-C(4)	1.6(5)
C(2)-C(3)-C(4)-C(5)	-1.8(5)
C(3)-C(4)-C(5)-N(1)	-0.1(5)
C(3)-C(4)-C(5)-N(2)	178.3(3)
N(3)-C(6)-C(7)-C(8)	2.6(5)
N(2)-C(6)-C(7)-C(8)	-176.5(3)
C(6)-C(7)-C(8)-C(9)	1.6(5)
C(7)-C(8)-C(9)-C(10)	-4.1(5)
C(8)-C(9)-C(10)-N(3)	2.6(5)
Cu(1)#1-Cl(2)-Cu(1)-N(3)	-177.19(9)
Cu(1)#1-Cl(2)-Cu(1)-N(1)	-92.23(8)
Cu(1)#1-Cl(2)-Cu(1)-Cl(2)#1	0.0
Cu(1)#1-Cl(2)-Cu(1)-Cl(1)	91.37(4)
C(4)-C(5)-N(1)-C(1)	2.4(5)
N(2)-C(5)-N(1)-C(1)	-176.1(3)
C(4)-C(5)-N(1)-Cu(1)	-175.7(2)
N(2)-C(5)-N(1)-Cu(1)	5.8(4)
C(2)-C(1)-N(1)-C(5)	-2.7(5)
C(2)-C(1)-N(1)-Cu(1)	175.4(2)
N(3)-Cu(1)-N(1)-C(5)	-44.1(2)
Cl(2)#1-Cu(1)-N(1)-C(5)	137.4(2)
Cl(1)-Cu(1)-N(1)-C(5)	34.4(4)
Cl(2)-Cu(1)-N(1)-C(5)	-137.5(2)
N(3)-Cu(1)-N(1)-C(1)	137.8(3)
Cl(2)#1-Cu(1)-N(1)-C(1)	-40.7(2)
Cl(1)-Cu(1)-N(1)-C(1)	-143.6(2)
Cl(2)-Cu(1)-N(1)-C(1)	44.4(2)
N(3)-C(6)-N(2)-C(5)	-49.1(4)

C(7)-C(6)-N(2)-C(5)	130.0(3)
N(3)-C(6)-N(2)-C(11)	165.8(3)
C(7)-C(6)-N(2)-C(11)	-15.1(5)
N(1)-C(5)-N(2)-C(6)	52.4(4)
C(4)-C(5)-N(2)-C(6)	-126.0(3)
N(1)-C(5)-N(2)-C(11)	-161.9(3)
C(4)-C(5)-N(2)-C(11)	19.6(5)
C(7)-C(6)-N(3)-C(10)	-4.0(5)
N(2)-C(6)-N(3)-C(10)	175.0(3)
C(7)-C(6)-N(3)-Cu(1)	169.2(2)
N(2)-C(6)-N(3)-Cu(1)	-11.7(4)
C(9)-C(10)-N(3)-C(6)	1.4(5)
C(9)-C(10)-N(3)-Cu(1)	-171.9(3)
N(1)-Cu(1)-N(3)-C(6)	47.6(2)
Cl(1)-Cu(1)-N(3)-C(6)	-107.7(2)
Cl(2)-Cu(1)-N(3)-C(6)	144.6(2)
N(1)-Cu(1)-N(3)-C(10)	-139.2(3)
Cl(1)-Cu(1)-N(3)-C(10)	65.6(2)
Cl(2)-Cu(1)-N(3)-C(10)	-42.2(2)

Symmetry transformations used to generate equivalent atoms:

#1 -x+1,-y+1,-z+2

Crystallographic data for $[Zn(Cl)_2(dpma)]$

Table 1. Crystal data and structure refinement for phw0816m.

Identification code	phw0816m	
Empirical formula	C11 H11 Cl2 N3 Zn	
Formula weight	321.50	
Temperature	110(2) K	
Wavelength	0.71073 Å	
Crystal system	Triclinic	
Space group	P-1	
Unit cell dimensions	a = 7.5744(5) Å	α= 98.9620(10)°.
	b = 8.3068(6) Å	β= 98.0740(10)°.
	c = 11.2830(8) Å	γ = 114.5630(10)°.
Volume	620.93(8) $Å^3$	
Z	2	
Density (calculated)	1.720 Mg/m^3	
Absorption coefficient	2.386 mm^{-1}	
F(000)	324	
Crystal size	0.24 x 0.12 x 0.03 mm^3	
Theta range for data collection	1.88 to 28.31°.	
Index ranges	-10<=h<=10, -11<=k<=11, -15<=l<=15	
Reflections collected	6367	
Independent reflections	3047 [R(int) = 0.0125]	
Completeness to theta = 28.31°	98.9 %	
Absorption correction	Semi-empirical from equivalents	
Max. and min. transmission	0.931 and 0.741	
Refinement method	Full-matrix least-squares on F^2	
Data / restraints / parameters	3047 / 0 / 155	
Goodness-of-fit on F^2	1.050	
Final R indices [I>2sigma(I)]	R1 = 0.0206, wR2 = 0.0513	
R indices (all data)	R1 = 0.0231, wR2 = 0.0527	
Largest diff. peak and hole	0.368 and -0.365 $e.Å^{-3}$	

Table 2. Atomic coordinates (x 10^4) and equivalent isotropic displacement parameters ($Å^2$x 10^3) for phw0816m. U(eq) is defined as one third of the trace of the orthogonalized U^{ij} tensor.

	x	y	z	U(eq)
C(1)	7191(2)	8439(2)	9969(1)	22(1)
C(2)	8096(2)	9674(2)	11090(1)	24(1)
C(3)	8407(2)	11455(2)	11152(1)	24(1)
C(4)	7837(2)	11937(2)	10100(1)	21(1)
C(5)	7010(2)	10637(2)	8972(1)	17(1)
C(6)	4902(2)	10176(2)	6907(1)	16(1)
C(7)	4095(2)	11095(2)	6230(1)	19(1)
C(8)	2431(2)	10100(2)	5282(1)	22(1)
C(9)	1534(2)	8200(2)	5011(1)	21(1)
C(10)	2416(2)	7392(2)	5699(1)	19(1)
C(11)	7674(2)	13138(2)	7955(2)	24(1)
Cl(1)	7381(1)	6362(1)	6340(1)	21(1)
Cl(2)	2983(1)	4533(1)	7862(1)	23(1)
N(1)	6681(2)	8901(2)	8920(1)	17(1)
N(2)	6594(2)	11171(2)	7882(1)	18(1)
N(3)	4076(2)	8340(2)	6614(1)	16(1)
Zn(1)	5310(1)	6883(1)	7359(1)	17(1)

Table 3. Bond lengths [Å] and angles [°] for phw0816m.

C(1)-N(1)	1.3542(18)
C(1)-C(2)	1.375(2)
C(1)-H(1)	0.9500
C(2)-C(3)	1.386(2)
C(2)-H(2)	0.9500
C(3)-C(4)	1.379(2)
C(3)-H(3)	0.9500
C(4)-C(5)	1.402(2)
C(4)-H(4)	0.9500
C(5)-N(1)	1.3471(18)
C(5)-N(2)	1.4097(18)
C(6)-N(3)	1.3486(18)
C(6)-N(2)	1.4054(19)

C(6)-C(7)	1.4060(19)
C(7)-C(8)	1.376(2)
C(7)-H(7)	0.9500
C(8)-C(9)	1.395(2)
C(8)-H(8)	0.9500
C(9)-C(10)	1.375(2)
C(9)-H(9)	0.9500
C(10)-N(3)	1.3513(19)
C(10)-H(10)	0.9500
C(11)-N(2)	1.4739(18)
C(11)-H(11A)	0.9800
C(11)-H(11B)	0.9800
C(11)-H(11C)	0.9800
Cl(1)-Zn(1)	2.2100(4)
Cl(2)-Zn(1)	2.2368(4)
N(1)-Zn(1)	2.0275(13)
N(3)-Zn(1)	2.0205(12)

N(1)-C(1)-C(2)	123.08(14)
N(1)-C(1)-H(1)	118.5
C(2)-C(1)-H(1)	118.5
C(1)-C(2)-C(3)	117.98(14)
C(1)-C(2)-H(2)	121.0
C(3)-C(2)-H(2)	121.0
C(4)-C(3)-C(2)	119.67(15)
C(4)-C(3)-H(3)	120.2
C(2)-C(3)-H(3)	120.2
C(3)-C(4)-C(5)	119.69(14)
C(3)-C(4)-H(4)	120.2
C(5)-C(4)-H(4)	120.2
N(1)-C(5)-C(4)	120.40(13)
N(1)-C(5)-N(2)	120.01(13)
C(4)-C(5)-N(2)	119.55(13)
N(3)-C(6)-N(2)	119.67(12)
N(3)-C(6)-C(7)	120.26(13)
N(2)-C(6)-C(7)	120.07(13)
C(8)-C(7)-C(6)	119.34(14)
C(8)-C(7)-H(7)	120.3
C(6)-C(7)-H(7)	120.3
C(7)-C(8)-C(9)	120.33(14)

C(7)-C(8)-H(8)	119.8
C(9)-C(8)-H(8)	119.8
C(10)-C(9)-C(8)	117.24(14)
C(10)-C(9)-H(9)	121.4
C(8)-C(9)-H(9)	121.4
N(3)-C(10)-C(9)	123.44(14)
N(3)-C(10)-H(10)	118.3
C(9)-C(10)-H(10)	118.3
N(2)-C(11)-H(11A)	109.5
N(2)-C(11)-H(11B)	109.5
H(11A)-C(11)-H(11B)	109.5
N(2)-C(11)-H(11C)	109.5
H(11A)-C(11)-H(11C)	109.5
H(11B)-C(11)-H(11C)	109.5
C(5)-N(1)-C(1)	119.06(13)
C(5)-N(1)-Zn(1)	123.38(10)
C(1)-N(1)-Zn(1)	117.47(10)
C(6)-N(2)-C(5)	126.07(12)
C(6)-N(2)-C(11)	115.93(12)
C(5)-N(2)-C(11)	115.10(12)
C(6)-N(3)-C(10)	119.33(12)
C(6)-N(3)-Zn(1)	123.82(10)
C(10)-N(3)-Zn(1)	116.61(10)
N(3)-Zn(1)-N(1)	90.71(5)
N(3)-Zn(1)-Cl(1)	113.58(4)
N(1)-Zn(1)-Cl(1)	114.08(4)
N(3)-Zn(1)-Cl(2)	110.19(4)
N(1)-Zn(1)-Cl(2)	106.55(4)
Cl(1)-Zn(1)-Cl(2)	118.228(15)

Symmetry transformations used to generate equivalent atoms:

Table 4. Anisotropic displacement parameters ($Å^2 x\ 10^3$) for phw0816m. The anisotropic displacement factor exponent takes the form: $-2\pi^2[\ h^2\ a^{*2}U^{11} + ... + 2\ h\ k\ a^*\ b^*\ U^{12}\ ]$

	U^{11}	U^{22}	U^{33}	U^{23}	U^{13}	U^{12}
C(1)	21(1)	23(1)	23(1)	9(1)	6(1)	12(1)

C(2)	21(1)	34(1)	18(1)	9(1)	6(1)	12(1)
C(3)	21(1)	30(1)	17(1)	0(1)	4(1)	9(1)
C(4)	20(1)	19(1)	22(1)	2(1)	5(1)	8(1)
C(5)	15(1)	18(1)	18(1)	4(1)	5(1)	8(1)
C(6)	17(1)	17(1)	17(1)	5(1)	7(1)	9(1)
C(7)	23(1)	18(1)	22(1)	8(1)	9(1)	12(1)
C(8)	24(1)	27(1)	23(1)	13(1)	9(1)	17(1)
C(9)	19(1)	27(1)	20(1)	7(1)	5(1)	11(1)
C(10)	19(1)	18(1)	19(1)	4(1)	4(1)	7(1)
C(11)	26(1)	14(1)	26(1)	6(1)	6(1)	5(1)
Cl(1)	24(1)	22(1)	22(1)	7(1)	8(1)	14(1)
Cl(2)	25(1)	16(1)	28(1)	8(1)	10(1)	8(1)
N(1)	18(1)	17(1)	18(1)	6(1)	5(1)	9(1)
N(2)	20(1)	13(1)	19(1)	4(1)	4(1)	6(1)
N(3)	17(1)	14(1)	18(1)	5(1)	4(1)	8(1)
Zn(1)	19(1)	14(1)	19(1)	5(1)	4(1)	9(1)

Table 5. Hydrogen coordinates (x 10^4) and isotropic displacement parameters ($Å^2$x 10^{3}) for phw0816m.

	x	y	z	U(eq)
H(1)	6911	7203	9928	26
H(2)	8495	9318	11801	29
H(3)	9010	12339	11915	29
H(4)	8005	13144	10141	25
H(7)	4692	12389	6425	23

H(8)	1892	10711	4811	26
H(9)	362	7494	4376	25
H(10)	1828	6099	5522	23
H(11A)	7717	13333	7123	35
H(11B)	9036	13616	8447	35
H(11C)	6986	13771	8344	35

Table 6. Torsion angles [°] for phw0816m.

N(1)-C(1)-C(2)-C(3)	3.2(2)
C(1)-C(2)-C(3)-C(4)	-0.9(2)
C(2)-C(3)-C(4)-C(5)	-2.1(2)
C(3)-C(4)-C(5)-N(1)	3.2(2)
C(3)-C(4)-C(5)-N(2)	-174.38(14)
N(3)-C(6)-C(7)-C(8)	1.3(2)
N(2)-C(6)-C(7)-C(8)	-179.65(13)
C(6)-C(7)-C(8)-C(9)	1.2(2)
C(7)-C(8)-C(9)-C(10)	-2.0(2)
C(8)-C(9)-C(10)-N(3)	0.4(2)
C(4)-C(5)-N(1)-C(1)	-1.1(2)
N(2)-C(5)-N(1)-C(1)	176.50(13)
C(4)-C(5)-N(1)-Zn(1)	175.39(10)
N(2)-C(5)-N(1)-Zn(1)	-7.05(18)
C(2)-C(1)-N(1)-C(5)	-2.2(2)
C(2)-C(1)-N(1)-Zn(1)	-178.84(12)
N(3)-C(6)-N(2)-C(5)	-34.2(2)
C(7)-C(6)-N(2)-C(5)	146.70(14)
N(3)-C(6)-N(2)-C(11)	166.15(13)
C(7)-C(6)-N(2)-C(11)	-12.94(19)
N(1)-C(5)-N(2)-C(6)	42.6(2)
C(4)-C(5)-N(2)-C(6)	-139.82(15)
N(1)-C(5)-N(2)-C(11)	-157.62(13)
C(4)-C(5)-N(2)-C(11)	19.96(19)
N(2)-C(6)-N(3)-C(10)	178.12(13)
C(7)-C(6)-N(3)-C(10)	-2.8(2)
N(2)-C(6)-N(3)-Zn(1)	-7.78(18)
C(7)-C(6)-N(3)-Zn(1)	171.31(10)

C(9)-C(10)-N(3)-C(6)	2.0(2)
C(9)-C(10)-N(3)-Zn(1)	-172.54(12)
C(6)-N(3)-Zn(1)-N(1)	28.00(11)
C(10)-N(3)-Zn(1)-N(1)	-157.75(11)
C(6)-N(3)-Zn(1)-Cl(1)	-88.78(11)
C(10)-N(3)-Zn(1)-Cl(1)	85.47(10)
C(6)-N(3)-Zn(1)-Cl(2)	135.94(10)
C(10)-N(3)-Zn(1)-Cl(2)	-49.80(11)
C(5)-N(1)-Zn(1)-N(3)	-20.33(12)
C(1)-N(1)-Zn(1)-N(3)	156.16(11)
C(5)-N(1)-Zn(1)-Cl(1)	96.01(11)
C(1)-N(1)-Zn(1)-Cl(1)	-87.49(11)
C(5)-N(1)-Zn(1)-Cl(2)	-131.67(11)
C(1)-N(1)-Zn(1)-Cl(2)	44.83(11)

Symmetry transformations used to generate equivalent atoms:

Crystallographic data for $[Zn(Cl)_3(Me\text{-}dpHa)]$

Table 1. Crystal data and structure refinement for akd0802m.

Identification code	akd0802m	
Empirical formula	C11 H12 Cl3 N3 Zn	
Formula weight	357.96	
Temperature	110(2) K	
Wavelength	0.71073 Å	
Crystal system	Orthorhombic	
Space group	Pbca	
Unit cell dimensions	a = 7.5645(5) Å	α= 90°.
	b = 13.4638(9) Å	β= 90°.
	c = 26.8958(17) Å	γ = 90°.
Volume	2739.3(3) $Å^3$	
Z	8	
Density (calculated)	1.736 Mg/m^3	
Absorption coefficient	2.362 mm^{-1}	
F(000)	1440	
Crystal size	0.44 x 0.13 x 0.04 mm^3	

Theta range for data collection	3.03 to 30.01°.
Index ranges	-10<=h<=10, -18<=k<=18, -37<=l<=37
Reflections collected	28940
Independent reflections	3986 [R(int) = 0.0290]
Completeness to theta = 30.01°	99.4 %
Absorption correction	Semi-empirical from equivalents
Max. and min. transmission	0.910 and 0.695
Refinement method	Full-matrix least-squares on F^2
Data / restraints / parameters	3986 / 0 / 168
Goodness-of-fit on F^2	1.121
Final R indices [I>2sigma(I)]	R1 = 0.0254, wR2 = 0.0594
R indices (all data)	R1 = 0.0294, wR2 = 0.0607
Largest diff. peak and hole	0.512 and -0.222 e.$Å^{-3}$

Table 2. Atomic coordinates (x 10^4) and equivalent isotropic displacement parameters ($Å^2$x 10^3) for akd0802m. U(eq) is defined as one third of the trace of the orthogonalized U^{ij} tensor.

	x	y	z	U(eq)
C(1)	2997(2)	1327(1)	4860(1)	17(1)
C(2)	3899(2)	1484(1)	5299(1)	19(1)
C(3)	5722(2)	1388(1)	5299(1)	19(1)
C(4)	6588(2)	1182(1)	4858(1)	18(1)
C(5)	5590(2)	1066(1)	4426(1)	14(1)
C(6)	6175(2)	1419(1)	3554(1)	14(1)
C(7)	5272(2)	2325(1)	3552(1)	16(1)
C(8)	5049(2)	2834(1)	3114(1)	20(1)
C(9)	5740(2)	2454(1)	2672(1)	20(1)
C(10)	6615(2)	1567(1)	2687(1)	18(1)
C(11)	7715(2)	82(1)	3109(1)	19(1)
Cl(1)	534(1)	2024(1)	3648(1)	19(1)
Cl(2)	3192(1)	-201(1)	3242(1)	18(1)
Cl(3)	103(1)	-366(1)	4278(1)	18(1)
N(1)	3813(2)	1106(1)	4427(1)	15(1)
N(2)	6451(2)	860(1)	3974(1)	16(1)
N(3)	6819(2)	1057(1)	3120(1)	15(1)
Zn(1)	2035(1)	662(1)	3876(1)	15(1)

Table 3. Bond lengths [Å] and angles [°] for akd0802m.

C(1)-N(1)	1.3523(19)

C(1)-C(2)	1.379(2)
C(1)-H(1)	0.9500
C(2)-C(3)	1.385(2)
C(2)-H(2)	0.9500
C(3)-C(4)	1.383(2)
C(3)-H(3)	0.9500
C(4)-C(5)	1.394(2)
C(4)-H(4)	0.9500
C(5)-N(1)	1.3451(19)
C(5)-N(2)	1.4065(19)
C(6)-N(3)	1.3572(18)
C(6)-N(2)	1.3732(19)
C(6)-C(7)	1.398(2)
C(7)-C(8)	1.374(2)
C(7)-H(7)	0.9500
C(8)-C(9)	1.396(2)
C(8)-H(8)	0.9500
C(9)-C(10)	1.366(2)
C(9)-H(9)	0.9500
C(10)-N(3)	1.360(2)
C(10)-H(10)	0.9500
C(11)-N(3)	1.478(2)
C(11)-H(11A)	0.9800
C(11)-H(11B)	0.9800
C(11)-H(11C)	0.9800
Cl(1)-Zn(1)	2.2416(4)
Cl(2)-Zn(1)	2.2406(4)
Cl(3)-Zn(1)	2.2857(4)
N(1)-Zn(1)	2.0883(12)
N(2)-H(2A)	0.79(3)

N(1)-C(1)-C(2)	123.04(14)
N(1)-C(1)-H(1)	118.5
C(2)-C(1)-H(1)	118.5
C(1)-C(2)-C(3)	118.62(14)
C(1)-C(2)-H(2)	120.7
C(3)-C(2)-H(2)	120.7
C(4)-C(3)-C(2)	119.35(14)
C(4)-C(3)-H(3)	120.3
C(2)-C(3)-H(3)	120.3

C(3)-C(4)-C(5)	118.68(15)
C(3)-C(4)-H(4)	120.7
C(5)-C(4)-H(4)	120.7
N(1)-C(5)-C(4)	122.40(14)
N(1)-C(5)-N(2)	118.14(13)
C(4)-C(5)-N(2)	119.40(14)
N(3)-C(6)-N(2)	117.24(13)
N(3)-C(6)-C(7)	119.01(13)
N(2)-C(6)-C(7)	123.75(13)
C(8)-C(7)-C(6)	119.97(14)
C(8)-C(7)-H(7)	120.0
C(6)-C(7)-H(7)	120.0
C(7)-C(8)-C(9)	120.05(15)
C(7)-C(8)-H(8)	120.0
C(9)-C(8)-H(8)	120.0
C(10)-C(9)-C(8)	118.56(15)
C(10)-C(9)-H(9)	120.7
C(8)-C(9)-H(9)	120.7
N(3)-C(10)-C(9)	121.38(14)
N(3)-C(10)-H(10)	119.3
C(9)-C(10)-H(10)	119.3
N(3)-C(11)-H(11A)	109.5
N(3)-C(11)-H(11B)	109.5
H(11A)-C(11)-H(11B)	109.5
N(3)-C(11)-H(11C)	109.5
H(11A)-C(11)-H(11C)	109.5
H(11B)-C(11)-H(11C)	109.5
C(5)-N(1)-C(1)	117.76(13)
C(5)-N(1)-Zn(1)	129.14(10)
C(1)-N(1)-Zn(1)	112.40(10)
C(6)-N(2)-C(5)	122.20(13)
C(6)-N(2)-H(2A)	118.0(17)
C(5)-N(2)-H(2A)	115.0(17)
C(6)-N(3)-C(10)	121.02(13)
C(6)-N(3)-C(11)	120.05(13)
C(10)-N(3)-C(11)	118.91(13)
N(1)-Zn(1)-Cl(2)	115.87(4)
N(1)-Zn(1)-Cl(1)	106.63(4)
Cl(2)-Zn(1)-Cl(1)	114.489(16)
N(1)-Zn(1)-Cl(3)	104.41(4)

Cl(2)-Zn(1)-Cl(3)	107.207(16)
Cl(1)-Zn(1)-Cl(3)	107.496(16)

Symmetry transformations used to generate equivalent atoms:

Table 4. Anisotropic displacement parameters ($Å^2 x\ 10^3$) for akd0802m. The anisotropic displacement factor exponent takes the form: $-2\pi^2[\ h^2\ a^{*2}U^{11} + ... + 2\ h\ k\ a^*\ b^*\ U^{12}\ ]$

	U^{11}	U^{22}	U^{33}	U^{23}	U^{13}	U^{12}
C(1)	15(1)	19(1)	17(1)	-1(1)	1(1)	-1(1)
C(2)	22(1)	21(1)	14(1)	-1(1)	2(1)	-1(1)
C(3)	22(1)	21(1)	14(1)	-1(1)	-5(1)	-1(1)
C(4)	15(1)	20(1)	19(1)	-2(1)	-3(1)	1(1)
C(5)	14(1)	15(1)	15(1)	0(1)	-1(1)	0(1)
C(6)	10(1)	19(1)	15(1)	-1(1)	1(1)	-3(1)
C(7)	15(1)	16(1)	18(1)	-3(1)	2(1)	-1(1)
C(8)	18(1)	17(1)	24(1)	1(1)	1(1)	0(1)
C(9)	20(1)	23(1)	18(1)	4(1)	0(1)	-1(1)
C(10)	16(1)	23(1)	15(1)	-1(1)	1(1)	-1(1)
C(11)	19(1)	21(1)	18(1)	-4(1)	-1(1)	6(1)
Cl(1)	19(1)	20(1)	19(1)	0(1)	-2(1)	1(1)
Cl(2)	18(1)	20(1)	17(1)	-3(1)	1(1)	-3(1)
Cl(3)	13(1)	23(1)	17(1)	3(1)	0(1)	-2(1)
N(1)	14(1)	18(1)	13(1)	0(1)	-1(1)	-2(1)
N(2)	12(1)	21(1)	15(1)	-1(1)	0(1)	3(1)
N(3)	11(1)	18(1)	16(1)	-2(1)	0(1)	0(1)
Zn(1)	12(1)	20(1)	13(1)	0(1)	-1(1)	-2(1)

Table 5. Hydrogen coordinates ($x\ 10^4$) and isotropic displacement parameters ($Å^2 x\ 10^{\ 3}$) for akd0802m.

	x	y	z	U(eq)

H(1)	1745	1377	4863	21
H(2)	3284	1653	5595	22
H(3)	6371	1463	5599	23
H(4)	7839	1121	4850	22
H(7)	4813	2588	3853	20
H(8)	4424	3446	3111	23
H(9)	5605	2804	2368	24
H(10)	7092	1300	2388	21
H(11A)	8848	130	3283	29
H(11B)	7921	-116	2763	29
H(11C)	6968	-415	3273	29
H(2A)	7360(30)	575(17)	4000(8)	28(6)

Table 6. Torsion angles [°] for akd0802m.

N(1)-C(1)-C(2)-C(3)	-1.5(2)
C(1)-C(2)-C(3)-C(4)	2.8(2)
C(2)-C(3)-C(4)-C(5)	-0.7(2)
C(3)-C(4)-C(5)-N(1)	-2.9(2)
C(3)-C(4)-C(5)-N(2)	179.78(14)
N(3)-C(6)-C(7)-C(8)	0.0(2)
N(2)-C(6)-C(7)-C(8)	-179.75(15)
C(6)-C(7)-C(8)-C(9)	-0.7(2)
C(7)-C(8)-C(9)-C(10)	0.7(2)
C(8)-C(9)-C(10)-N(3)	0.0(2)
C(4)-C(5)-N(1)-C(1)	4.1(2)
N(2)-C(5)-N(1)-C(1)	-178.47(13)
C(4)-C(5)-N(1)-Zn(1)	-165.44(11)
N(2)-C(5)-N(1)-Zn(1)	11.9(2)
C(2)-C(1)-N(1)-C(5)	-1.9(2)
C(2)-C(1)-N(1)-Zn(1)	169.35(13)
N(3)-C(6)-N(2)-C(5)	-168.59(13)
C(7)-C(6)-N(2)-C(5)	11.1(2)
N(1)-C(5)-N(2)-C(6)	55.4(2)
C(4)-C(5)-N(2)-C(6)	-127.12(16)
N(2)-C(6)-N(3)-C(10)	-179.48(13)

C(7)-C(6)-N(3)-C(10)	0.8(2)
N(2)-C(6)-N(3)-C(11)	2.2(2)
C(7)-C(6)-N(3)-C(11)	-177.54(14)
C(9)-C(10)-N(3)-C(6)	-0.8(2)
C(9)-C(10)-N(3)-C(11)	177.56(15)
C(5)-N(1)-Zn(1)-Cl(2)	9.99(14)
C(1)-N(1)-Zn(1)-Cl(2)	-160.04(9)
C(5)-N(1)-Zn(1)-Cl(1)	-118.74(13)
C(1)-N(1)-Zn(1)-Cl(1)	71.23(11)
C(5)-N(1)-Zn(1)-Cl(3)	127.64(13)
C(1)-N(1)-Zn(1)-Cl(3)	-42.39(11)

Symmetry transformations used to generate equivalent atoms:

Table 7. Hydrogen bonds for akd0802m [Å and °].

D-H...A	d(D-H)	d(H...A)	d(D...A)	<(DHA)
N(2)-H(2A)...Cl(3)#1	0.79(3)	2.54(3)	3.3206(14)	168(2)

Symmetry transformations used to generate equivalent atoms:

#1 x+1,y,z

Crystallographic data for $[Co(Cl)(dpma)_2(H_2O)(CoCl_3)]$

Table 1. Crystal data and structure refinement for phw0905m.

Identification code	phw0905m	
Empirical formula	C22 H24 Cl4 Co2 N6 O	
Formula weight	648.13	
Temperature	110(2) K	
Wavelength	0.71073 Å	
Crystal system	Monoclinic	
Space group	P2(1)/n	
Unit cell dimensions	a = 12.6688(7) Å	α= 90°.
	b = 16.9011(10) Å	β= 109.7950(10)°.
	c = 12.7250(7) Å	γ = 90°.
Volume	2563.6(3) $Å^3$	
Z	4	
Density (calculated)	1.679 Mg/m^3	
Absorption coefficient	1.740 mm^{-1}	
F(000)	1312	
Crystal size	0.14 x 0.12 x 0.06 mm^3	
Theta range for data collection	1.96 to 30.03°.	
Index ranges	-17<=h<=17, -23<=k<=23, -17<=l<=17	
Reflections collected	28948	
Independent reflections	7437 [R(int) = 0.0279]	
Completeness to theta = 30.03°	99.1 %	
Absorption correction	Semi-empirical from equivalents	
Max. and min. transmission	0.901 and 0.797	
Refinement method	Full-matrix least-squares on F^2	
Data / restraints / parameters	7437 / 0 / 324	
Goodness-of-fit on F^2	1.026	
Final R indices [I>2sigma(I)]	R1 = 0.0289, wR2 = 0.0710	
R indices (all data)	R1 = 0.0388, wR2 = 0.0757	
Largest diff. peak and hole	0.614 and -0.358 $e.Å^{-3}$	

Table 2. Atomic coordinates (x 10^4) and equivalent isotropic displacement parameters ($Å^2$x 10^3) for phw0905m. U(eq) is defined as one third of the trace of the orthogonalized U^{ij} tensor.

	x	y	z	U(eq)
C(1)	4414(2)	753(1)	3252(2)	24(1)
C(2)	4639(2)	35(1)	2859(2)	29(1)
C(3)	4123(2)	-635(1)	3081(2)	32(1)
C(4)	3420(2)	-572(1)	3697(2)	28(1)
C(5)	3217(1)	176(1)	4058(1)	20(1)
C(6)	1627(2)	-369(1)	4508(2)	26(1)
C(7)	2737(1)	712(1)	5633(1)	17(1)
C(8)	2499(2)	430(1)	6567(2)	23(1)
C(9)	2768(2)	891(1)	7515(2)	25(1)
C(10)	3288(2)	1618(1)	7539(2)	22(1)
C(11)	3483(2)	1862(1)	6588(1)	20(1)
C(12)	2982(2)	3742(1)	4474(2)	22(1)
C(13)	2564(2)	4449(1)	4714(2)	26(1)
C(14)	1595(2)	4426(1)	4992(2)	28(1)
C(15)	1071(2)	3713(1)	5008(2)	26(1)
C(16)	1528(2)	3022(1)	4727(1)	19(1)
C(17)	351(2)	2187(1)	5469(2)	26(1)
C(18)	723(1)	1793(1)	3771(1)	17(1)
C(19)	-320(2)	1406(1)	3376(2)	23(1)
C(20)	-553(2)	926(1)	2452(2)	25(1)
C(21)	233(2)	838(1)	1922(2)	23(1)
C(22)	1234(2)	1233(1)	2354(1)	20(1)
Cl(1)	5199(1)	2392(1)	5176(1)	20(1)
Cl(2)	7896(1)	3432(1)	5399(1)	22(1)
Cl(3)	6825(1)	1821(1)	3308(1)	24(1)
Cl(4)	5244(1)	3756(1)	3035(1)	25(1)
Co(1)	3198(1)	1973(1)	4146(1)	15(1)
Co(2)	6330(1)	2831(1)	4208(1)	18(1)
N(1)	3693(1)	835(1)	3823(1)	19(1)
N(2)	2481(1)	251(1)	4668(1)	19(1)
N(3)	3190(1)	1432(1)	5635(1)	17(1)
N(4)	2486(1)	3036(1)	4491(1)	19(1)
N(5)	982(1)	2293(1)	4698(1)	20(1)
N(6)	1499(1)	1688(1)	3278(1)	17(1)
O(1)	3325(1)	2491(1)	2683(1)	24(1)

Table 3. Bond lengths [Å] and angles [°] for phw0905m.

C(1)-N(1)	1.352(2)
C(1)-C(2)	1.379(3)
C(1)-H(1)	0.9500
C(2)-C(3)	1.383(3)
C(2)-H(2)	0.9500
C(3)-C(4)	1.375(3)
C(3)-H(3)	0.9500
C(4)-C(5)	1.400(2)
C(4)-H(4)	0.9500
C(5)-N(1)	1.347(2)
C(5)-N(2)	1.405(2)
C(6)-N(2)	1.470(2)
C(6)-H(6A)	0.9800
C(6)-H(6B)	0.9800
C(6)-H(6C)	0.9800
C(7)-N(3)	1.344(2)
C(7)-N(2)	1.397(2)
C(7)-C(8)	1.406(2)
C(8)-C(9)	1.379(3)
C(8)-H(8)	0.9500
C(9)-C(10)	1.388(3)
C(9)-H(9)	0.9500
C(10)-C(11)	1.378(2)
C(10)-H(10)	0.9500
C(11)-N(3)	1.352(2)
C(11)-H(11)	0.9500
C(12)-N(4)	1.352(2)
C(12)-C(13)	1.383(2)
C(12)-H(12)	0.9500
C(13)-C(14)	1.388(3)
C(13)-H(13)	0.9500
C(14)-C(15)	1.379(3)
C(14)-H(14)	0.9500
C(15)-C(16)	1.404(2)
C(15)-H(15)	0.9500
C(16)-N(4)	1.346(2)

C(16)-N(5)	1.407(2)
C(17)-N(5)	1.471(2)
C(17)-H(17A)	0.9800
C(17)-H(17B)	0.9800
C(17)-H(17C)	0.9800
C(18)-N(6)	1.346(2)
C(18)-N(5)	1.396(2)
C(18)-C(19)	1.405(2)
C(19)-C(20)	1.377(3)
C(19)-H(19)	0.9500
C(20)-C(21)	1.386(3)
C(20)-H(20)	0.9500
C(21)-C(22)	1.373(2)
C(21)-H(21)	0.9500
C(22)-N(6)	1.348(2)
C(22)-H(22)	0.9500
Cl(1)-Co(2)	2.3063(5)
Cl(1)-Co(1)	2.5291(5)
Cl(2)-Co(2)	2.2871(5)
Cl(3)-Co(2)	2.2600(5)
Cl(4)-Co(2)	2.2730(5)
Co(1)-N(1)	2.1061(15)
Co(1)-N(3)	2.1076(14)
Co(1)-O(1)	2.1126(13)
Co(1)-N(6)	2.1154(14)
Co(1)-N(4)	2.1230(14)
O(1)-H(1A)	0.81(3)
O(1)-H(1B)	0.66(3)

N(1)-C(1)-C(2)	123.00(18)
N(1)-C(1)-H(1)	118.5
C(2)-C(1)-H(1)	118.5
C(1)-C(2)-C(3)	118.48(18)
C(1)-C(2)-H(2)	120.8
C(3)-C(2)-H(2)	120.8
C(4)-C(3)-C(2)	119.62(18)
C(4)-C(3)-H(3)	120.2
C(2)-C(3)-H(3)	120.2
C(3)-C(4)-C(5)	119.00(19)
C(3)-C(4)-H(4)	120.5

C(5)-C(4)-H(4)	120.5
N(1)-C(5)-C(4)	121.79(16)
N(1)-C(5)-N(2)	118.65(15)
C(4)-C(5)-N(2)	119.55(16)
N(2)-C(6)-H(6A)	109.5
N(2)-C(6)-H(6B)	109.5
H(6A)-C(6)-H(6B)	109.5
N(2)-C(6)-H(6C)	109.5
H(6A)-C(6)-H(6C)	109.5
H(6B)-C(6)-H(6C)	109.5
N(3)-C(7)-N(2)	118.65(14)
N(3)-C(7)-C(8)	121.24(16)
N(2)-C(7)-C(8)	120.09(15)
C(9)-C(8)-C(7)	119.16(17)
C(9)-C(8)-H(8)	120.4
C(7)-C(8)-H(8)	120.4
C(8)-C(9)-C(10)	119.67(16)
C(8)-C(9)-H(9)	120.2
C(10)-C(9)-H(9)	120.2
C(11)-C(10)-C(9)	117.99(17)
C(11)-C(10)-H(10)	121.0
C(9)-C(10)-H(10)	121.0
N(3)-C(11)-C(10)	123.40(16)
N(3)-C(11)-H(11)	118.3
C(10)-C(11)-H(11)	118.3
N(4)-C(12)-C(13)	122.97(17)
N(4)-C(12)-H(12)	118.5
C(13)-C(12)-H(12)	118.5
C(12)-C(13)-C(14)	118.04(17)
C(12)-C(13)-H(13)	121.0
C(14)-C(13)-H(13)	121.0
C(15)-C(14)-C(13)	120.00(17)
C(15)-C(14)-H(14)	120.0
C(13)-C(14)-H(14)	120.0
C(14)-C(15)-C(16)	118.78(17)
C(14)-C(15)-H(15)	120.6
C(16)-C(15)-H(15)	120.6
N(4)-C(16)-C(15)	121.53(16)
N(4)-C(16)-N(5)	118.82(15)
C(15)-C(16)-N(5)	119.65(16)

N(5)-C(17)-H(17A)	109.5
N(5)-C(17)-H(17B)	109.5
H(17A)-C(17)-H(17B)	109.5
N(5)-C(17)-H(17C)	109.5
H(17A)-C(17)-H(17C)	109.5
H(17B)-C(17)-H(17C)	109.5
N(6)-C(18)-N(5)	118.28(15)
N(6)-C(18)-C(19)	121.26(16)
N(5)-C(18)-C(19)	120.46(15)
C(20)-C(19)-C(18)	118.91(16)
C(20)-C(19)-H(19)	120.5
C(18)-C(19)-H(19)	120.5
C(19)-C(20)-C(21)	119.78(17)
C(19)-C(20)-H(20)	120.1
C(21)-C(20)-H(20)	120.1
C(22)-C(21)-C(20)	118.18(17)
C(22)-C(21)-H(21)	120.9
C(20)-C(21)-H(21)	120.9
N(6)-C(22)-C(21)	123.32(16)
N(6)-C(22)-H(22)	118.3
C(21)-C(22)-H(22)	118.3
Co(2)-Cl(1)-Co(1)	120.528(19)
N(1)-Co(1)-N(3)	82.66(5)
N(1)-Co(1)-O(1)	95.16(6)
N(3)-Co(1)-O(1)	175.99(6)
N(1)-Co(1)-N(6)	90.45(6)
N(3)-Co(1)-N(6)	93.25(5)
O(1)-Co(1)-N(6)	90.13(6)
N(1)-Co(1)-N(4)	171.54(6)
N(3)-Co(1)-N(4)	92.80(5)
O(1)-Co(1)-N(4)	89.77(6)
N(6)-Co(1)-N(4)	82.66(6)
N(1)-Co(1)-Cl(1)	92.53(4)
N(3)-Co(1)-Cl(1)	87.95(4)
O(1)-Co(1)-Cl(1)	88.78(4)
N(6)-Co(1)-Cl(1)	176.90(4)
N(4)-Co(1)-Cl(1)	94.44(4)
Cl(3)-Co(2)-Cl(4)	113.40(2)
Cl(3)-Co(2)-Cl(2)	110.092(19)
Cl(4)-Co(2)-Cl(2)	109.057(19)

Cl(3)-Co(2)-Cl(1)	110.867(18)
Cl(4)-Co(2)-Cl(1)	103.016(18)
Cl(2)-Co(2)-Cl(1)	110.200(18)
C(5)-N(1)-C(1)	118.03(15)
C(5)-N(1)-Co(1)	121.69(11)
C(1)-N(1)-Co(1)	119.86(12)
C(7)-N(2)-C(5)	122.36(14)
C(7)-N(2)-C(6)	117.39(14)
C(5)-N(2)-C(6)	117.04(14)
C(7)-N(3)-C(11)	118.39(14)
C(7)-N(3)-Co(1)	121.45(11)
C(11)-N(3)-Co(1)	119.35(11)
C(16)-N(4)-C(12)	118.60(15)
C(16)-N(4)-Co(1)	120.64(11)
C(12)-N(4)-Co(1)	120.76(12)
C(18)-N(5)-C(16)	121.67(14)
C(18)-N(5)-C(17)	117.68(15)
C(16)-N(5)-C(17)	117.47(14)
C(18)-N(6)-C(22)	118.46(15)
C(18)-N(6)-Co(1)	120.11(11)
C(22)-N(6)-Co(1)	119.60(11)
Co(1)-O(1)-H(1A)	118.5(18)
Co(1)-O(1)-H(1B)	124(2)
H(1A)-O(1)-H(1B)	112(3)

Symmetry transformations used to generate equivalent atoms:

Table 4. Anisotropic displacement parameters ($Å^2 x\ 10^3$) for phw0905m. The anisotropic displacement factor exponent takes the form: $-2\pi^2[\ h^2\ a^{*2}U^{11} + ...\ + 2\ h\ k\ a^*\ b^*\ U^{12}\ ]$

	U^{11}	U^{22}	U^{33}	U^{23}	U^{13}	U^{12}
C(1)	17(1)	32(1)	22(1)	-4(1)	6(1)	0(1)
C(2)	22(1)	40(1)	23(1)	-6(1)	5(1)	10(1)
C(3)	36(1)	27(1)	28(1)	-6(1)	5(1)	14(1)
C(4)	34(1)	20(1)	26(1)	-1(1)	5(1)	7(1)
C(5)	20(1)	20(1)	16(1)	0(1)	3(1)	3(1)
C(6)	27(1)	21(1)	28(1)	3(1)	4(1)	-9(1)

C(7)	14(1)	18(1)	20(1)	2(1)	5(1)	2(1)
C(8)	21(1)	23(1)	27(1)	6(1)	11(1)	1(1)
C(9)	27(1)	30(1)	22(1)	6(1)	14(1)	8(1)
C(10)	24(1)	27(1)	18(1)	-1(1)	9(1)	7(1)
C(11)	21(1)	20(1)	20(1)	-1(1)	8(1)	2(1)
C(12)	24(1)	17(1)	21(1)	1(1)	4(1)	-1(1)
C(13)	30(1)	17(1)	26(1)	-2(1)	2(1)	1(1)
C(14)	32(1)	22(1)	25(1)	-5(1)	2(1)	8(1)
C(15)	25(1)	26(1)	24(1)	-5(1)	8(1)	7(1)
C(16)	20(1)	19(1)	16(1)	-1(1)	4(1)	3(1)
C(17)	26(1)	34(1)	24(1)	1(1)	16(1)	4(1)
C(18)	16(1)	18(1)	18(1)	3(1)	6(1)	2(1)
C(19)	17(1)	27(1)	25(1)	5(1)	8(1)	-1(1)
C(20)	21(1)	29(1)	24(1)	3(1)	4(1)	-7(1)
C(21)	26(1)	22(1)	17(1)	1(1)	2(1)	-4(1)
C(22)	22(1)	21(1)	16(1)	1(1)	6(1)	1(1)
Cl(1)	20(1)	21(1)	20(1)	0(1)	8(1)	-3(1)
Cl(2)	20(1)	24(1)	21(1)	0(1)	7(1)	-1(1)
Cl(3)	23(1)	21(1)	30(1)	0(1)	13(1)	1(1)
Cl(4)	23(1)	22(1)	29(1)	9(1)	8(1)	3(1)
Co(1)	16(1)	15(1)	15(1)	-1(1)	6(1)	-1(1)
Co(2)	18(1)	18(1)	20(1)	2(1)	7(1)	1(1)
N(1)	17(1)	22(1)	19(1)	-4(1)	5(1)	0(1)
N(2)	21(1)	16(1)	20(1)	-1(1)	7(1)	-3(1)
N(3)	17(1)	18(1)	17(1)	0(1)	6(1)	0(1)
N(4)	20(1)	17(1)	18(1)	-1(1)	6(1)	1(1)
N(5)	20(1)	21(1)	21(1)	-1(1)	11(1)	1(1)
N(6)	16(1)	18(1)	17(1)	1(1)	5(1)	-1(1)
O(1)	29(1)	29(1)	17(1)	-4(1)	9(1)	-12(1)

Table 5. Hydrogen coordinates (x 10^4) and isotropic displacement parameters ($Å^2$x 10^3) for phw0905m.

	x	y	z	U(eq)
H(1)	4782	1211	3116	28

H(2)	5136	1	2445	35
H(3)	4254	-1136	2809	38
H(4)	3078	-1030	3874	33
H(6A)	1960	-826	4978	40
H(6B)	1350	-532	3723	40
H(6C)	1003	-163	4718	40
H(8)	2156	-72	6545	27
H(9)	2600	713	8148	30
H(10)	3502	1937	8192	27
H(11)	3842	2357	6602	24
H(12)	3648	3753	4289	26
H(13)	2928	4936	4689	31
H(14)	1293	4902	5171	34
H(15)	412	3691	5206	31
H(17A)	-411	2395	5124	39
H(17B)	729	2474	6165	39
H(17C)	315	1623	5631	39
H(19)	-855	1475	3742	27
H(20)	-1251	655	2177	30
H(21)	83	513	1279	28
H(22)	1767	1184	1982	23
H(1A)	3800(20)	2821(15)	2750(20)	29
H(1B)	3190(20)	2305(15)	2200(20)	29

Table 6. Torsion angles [°] for phw0905m.

N(1)-C(1)-C(2)-C(3)	-1.6(3)
C(1)-C(2)-C(3)-C(4)	-1.0(3)
C(2)-C(3)-C(4)-C(5)	1.9(3)
C(3)-C(4)-C(5)-N(1)	-0.2(3)
C(3)-C(4)-C(5)-N(2)	178.63(17)
N(3)-C(7)-C(8)-C(9)	-2.1(3)
N(2)-C(7)-C(8)-C(9)	179.33(16)
C(7)-C(8)-C(9)-C(10)	-1.2(3)
C(8)-C(9)-C(10)-C(11)	2.0(3)
C(9)-C(10)-C(11)-N(3)	0.3(3)
N(4)-C(12)-C(13)-C(14)	0.5(3)

C(12)-C(13)-C(14)-C(15)	-0.9(3)
C(13)-C(14)-C(15)-C(16)	-0.8(3)
C(14)-C(15)-C(16)-N(4)	2.9(3)
C(14)-C(15)-C(16)-N(5)	-177.61(16)
N(6)-C(18)-C(19)-C(20)	-1.5(3)
N(5)-C(18)-C(19)-C(20)	179.18(16)
C(18)-C(19)-C(20)-C(21)	-0.6(3)
C(19)-C(20)-C(21)-C(22)	0.7(3)
C(20)-C(21)-C(22)-N(6)	1.4(3)
Co(2)-Cl(1)-Co(1)-N(1)	82.51(4)
Co(2)-Cl(1)-Co(1)-N(3)	165.07(4)
Co(2)-Cl(1)-Co(1)-O(1)	-12.60(5)
Co(2)-Cl(1)-Co(1)-N(4)	-102.28(4)
Co(1)-Cl(1)-Co(2)-Cl(3)	-71.65(3)
Co(1)-Cl(1)-Co(2)-Cl(4)	49.97(3)
Co(1)-Cl(1)-Co(2)-Cl(2)	166.211(19)
C(4)-C(5)-N(1)-C(1)	-2.2(3)
N(2)-C(5)-N(1)-C(1)	178.91(15)
C(4)-C(5)-N(1)-Co(1)	170.31(13)
N(2)-C(5)-N(1)-Co(1)	-8.6(2)
C(2)-C(1)-N(1)-C(5)	3.2(3)
C(2)-C(1)-N(1)-Co(1)	-169.50(14)
N(3)-Co(1)-N(1)-C(5)	41.71(13)
O(1)-Co(1)-N(1)-C(5)	-141.68(13)
N(6)-Co(1)-N(1)-C(5)	-51.51(13)
Cl(1)-Co(1)-N(1)-C(5)	129.32(13)
N(3)-Co(1)-N(1)-C(1)	-145.90(14)
O(1)-Co(1)-N(1)-C(1)	30.71(14)
N(6)-Co(1)-N(1)-C(1)	120.88(13)
Cl(1)-Co(1)-N(1)-C(1)	-58.29(13)
N(3)-C(7)-N(2)-C(5)	43.7(2)
C(8)-C(7)-N(2)-C(5)	-137.70(17)
N(3)-C(7)-N(2)-C(6)	-157.16(15)
C(8)-C(7)-N(2)-C(6)	21.4(2)
N(1)-C(5)-N(2)-C(7)	-46.5(2)
C(4)-C(5)-N(2)-C(7)	134.62(17)
N(1)-C(5)-N(2)-C(6)	154.32(16)
C(4)-C(5)-N(2)-C(6)	-24.6(2)
N(2)-C(7)-N(3)-C(11)	-177.04(15)
C(8)-C(7)-N(3)-C(11)	4.4(2)

N(2)-C(7)-N(3)-Co(1)	13.3(2)
C(8)-C(7)-N(3)-Co(1)	-165.24(13)
C(10)-C(11)-N(3)-C(7)	-3.5(3)
C(10)-C(11)-N(3)-Co(1)	166.29(14)
N(1)-Co(1)-N(3)-C(7)	-44.33(13)
N(6)-Co(1)-N(3)-C(7)	45.71(13)
N(4)-Co(1)-N(3)-C(7)	128.50(13)
Cl(1)-Co(1)-N(3)-C(7)	-137.15(12)
N(1)-Co(1)-N(3)-C(11)	146.15(13)
N(6)-Co(1)-N(3)-C(11)	-123.81(13)
N(4)-Co(1)-N(3)-C(11)	-41.02(13)
Cl(1)-Co(1)-N(3)-C(11)	53.33(12)
C(15)-C(16)-N(4)-C(12)	-3.2(2)
N(5)-C(16)-N(4)-C(12)	177.23(15)
C(15)-C(16)-N(4)-Co(1)	177.00(13)
N(5)-C(16)-N(4)-Co(1)	-2.5(2)
C(13)-C(12)-N(4)-C(16)	1.6(3)
C(13)-C(12)-N(4)-Co(1)	-178.70(14)
N(3)-Co(1)-N(4)-C(16)	-53.33(13)
O(1)-Co(1)-N(4)-C(16)	129.75(13)
N(6)-Co(1)-N(4)-C(16)	39.59(13)
Cl(1)-Co(1)-N(4)-C(16)	-141.49(12)
N(3)-Co(1)-N(4)-C(12)	126.93(13)
O(1)-Co(1)-N(4)-C(12)	-49.99(14)
N(6)-Co(1)-N(4)-C(12)	-140.15(14)
Cl(1)-Co(1)-N(4)-C(12)	38.77(13)
N(6)-C(18)-N(5)-C(16)	42.7(2)
C(19)-C(18)-N(5)-C(16)	-137.95(17)
N(6)-C(18)-N(5)-C(17)	-157.92(15)
C(19)-C(18)-N(5)-C(17)	21.4(2)
N(4)-C(16)-N(5)-C(18)	-52.0(2)
C(15)-C(16)-N(5)-C(18)	128.45(18)
N(4)-C(16)-N(5)-C(17)	148.59(16)
C(15)-C(16)-N(5)-C(17)	-30.9(2)
N(5)-C(18)-N(6)-C(22)	-177.16(15)
C(19)-C(18)-N(6)-C(22)	3.5(2)
N(5)-C(18)-N(6)-Co(1)	18.3(2)
C(19)-C(18)-N(6)-Co(1)	-160.99(13)
C(21)-C(22)-N(6)-C(18)	-3.6(3)
C(21)-C(22)-N(6)-Co(1)	161.06(14)

N(1)-Co(1)-N(6)-C(18)	127.04(13)
N(3)-Co(1)-N(6)-C(18)	44.37(13)
O(1)-Co(1)-N(6)-C(18)	-137.80(13)
N(4)-Co(1)-N(6)-C(18)	-48.04(12)
N(1)-Co(1)-N(6)-C(22)	-37.31(13)
N(3)-Co(1)-N(6)-C(22)	-119.98(13)
O(1)-Co(1)-N(6)-C(22)	57.85(13)
N(4)-Co(1)-N(6)-C(22)	147.61(13)

Symmetry transformations used to generate equivalent atoms:

Table 7. Hydrogen bonds for phw0905m [Å and °].

D-H...A	d(D-H)	d(H...A)	d(D...A)	<(DHA)
O(1)-H(1B)...Cl(2)#1	0.66(3)	2.52(3)	3.1779(14)	174(3)
O(1)-H(1A)...Cl(4)	0.81(3)	2.35(3)	3.1531(15)	177(2)

Symmetry transformations used to generate equivalent atoms:

#1 x-1/2,-y+1/2,z-1/2

Crystallographic data for $[Co(Cl)_2(dpma)_2]OTf$

Table 1. Crystal data and structure refinement for phw0903m.

Identification code	phw0903m	
Empirical formula	C23 H22 Cl2 Co F3 N6 O3 S	
Formula weight	649.36	
Temperature	110(2) K	
Wavelength	0.71073 Å	
Crystal system	Triclinic	
Space group	P-1	
Unit cell dimensions	a = 8.5150(13) Å	α= 113.239(3)°.
	b = 12.4156(19) Å	β= 91.134(3)°.
	c = 13.291(2) Å	γ = 97.251(3)°.
Volume	1277.0(3) $Å^3$	
Z	2	
Density (calculated)	1.689 Mg/m^3	
Absorption coefficient	1.025 mm^{-1}	
F(000)	660	
Crystal size	0.17 x 0.11 x 0.08 mm^3	
Theta range for data collection	1.67 to 28.29°.	
Index ranges	-11<=h<=11, -16<=k<=16, -17<=l<=17	
Reflections collected	13211	
Independent reflections	6272 [R(int) = 0.0199]	
Completeness to theta = 28.29°	98.6 %	
Absorption correction	Semi-empirical from equivalents	
Max. and min. transmission	0.920 and 0.771	
Refinement method	Full-matrix least-squares on F^2	
Data / restraints / parameters	6272 / 0 / 354	
Goodness-of-fit on F^2	1.019	
Final R indices [I>2sigma(I)]	R1 = 0.0339, wR2 = 0.0812	
R indices (all data)	R1 = 0.0426, wR2 = 0.0861	
Largest diff. peak and hole	0.500 and -0.438 $e.Å^{-3}$	

Table 2. Atomic coordinates (x 10^4) and equivalent isotropic displacement parameters ($Å^2$x 10^3) for phw0903m. U(eq) is defined as one third of the trace of the orthogonalized U^{ij} tensor.

	x	y	z	U(eq)
C(1)	7216(2)	7760(2)	5558(2)	20(1)
C(2)	7214(2)	8210(2)	4767(2)	22(1)
C(3)	5776(3)	8395(2)	4397(2)	24(1)
C(4)	4402(2)	8132(2)	4838(2)	22(1)
C(5)	4490(2)	7717(2)	5673(2)	17(1)
C(6)	1789(2)	8148(2)	6114(2)	22(1)
C(7)	2790(2)	6524(2)	6426(2)	16(1)
C(8)	1223(2)	5970(2)	6349(2)	19(1)
C(9)	946(2)	4987(2)	6593(2)	22(1)
C(10)	2225(2)	4530(2)	6865(2)	21(1)
C(11)	3729(2)	5116(2)	6931(2)	18(1)
C(12)	5391(2)	9510(2)	8034(2)	18(1)
C(13)	4504(2)	10411(2)	8432(2)	21(1)
C(14)	3239(2)	10292(2)	9051(2)	23(1)
C(15)	2948(2)	9291(2)	9266(2)	21(1)
C(16)	3907(2)	8397(2)	8835(2)	17(1)
C(17)	2171(2)	7111(2)	9489(2)	25(1)
C(18)	4991(2)	6902(2)	9270(2)	18(1)
C(19)	5073(3)	6616(2)	10190(2)	22(1)
C(20)	6391(3)	6174(2)	10397(2)	25(1)
C(21)	7599(3)	5998(2)	9688(2)	25(1)
C(22)	7445(2)	6283(2)	8795(2)	22(1)
Cl(1)	8452(1)	8254(1)	7952(1)	21(1)
Cl(2)	7161(1)	5543(1)	6225(1)	21(1)
Co(1)	6067(1)	7118(1)	7293(1)	15(1)
N(1)	5886(2)	7547(1)	6039(1)	16(1)
N(2)	3112(2)	7508(1)	6164(1)	17(1)
N(3)	4007(2)	6134(1)	6771(1)	15(1)
N(4)	5066(2)	8489(1)	8189(1)	15(1)
N(5)	3684(2)	7388(1)	9064(1)	18(1)
N(6)	6165(2)	6726(1)	8579(1)	17(1)
C(23)	10025(3)	1357(2)	7622(2)	24(1)
F(1)	11577(2)	1672(1)	7559(1)	32(1)
F(2)	9886(2)	1225(1)	8569(1)	35(1)
F(3)	9584(2)	309(1)	6805(1)	42(1)

O(1)	9172(2)	2448(1)	6472(1)	25(1)
O(2)	7258(2)	1993(2)	7639(1)	32(1)
O(3)	9527(2)	3534(1)	8455(1)	31(1)
S(1)	8857(1)	2466(1)	7541(1)	20(1)

Table 3. Bond lengths [Å] and angles [°] for phw0903m.

C(1)-N(1)	1.360(2)
C(1)-C(2)	1.372(3)
C(1)-H(1)	0.9500
C(2)-C(3)	1.389(3)
C(2)-H(2)	0.9500
C(3)-C(4)	1.379(3)
C(3)-H(3)	0.9500
C(4)-C(5)	1.400(3)
C(4)-H(4)	0.9500
C(5)-N(1)	1.348(2)
C(5)-N(2)	1.399(2)
C(6)-N(2)	1.472(2)
C(6)-H(6A)	0.9800
C(6)-H(6B)	0.9800
C(6)-H(6C)	0.9800
C(7)-N(3)	1.342(2)
C(7)-N(2)	1.394(2)
C(7)-C(8)	1.405(3)
C(8)-C(9)	1.376(3)
C(8)-H(8)	0.9500
C(9)-C(10)	1.392(3)
C(9)-H(9)	0.9500
C(10)-C(11)	1.374(3)
C(10)-H(10)	0.9500
C(11)-N(3)	1.355(2)
C(11)-H(11)	0.9500
C(12)-N(4)	1.358(2)
C(12)-C(13)	1.365(3)
C(12)-H(12)	0.9500
C(13)-C(14)	1.397(3)
C(13)-H(13)	0.9500

C(14)-C(15)	1.375(3)
C(14)-H(14)	0.9500
C(15)-C(16)	1.405(3)
C(15)-H(15)	0.9500
C(16)-N(4)	1.345(2)
C(16)-N(5)	1.392(2)
C(17)-N(5)	1.473(2)
C(17)-H(17A)	0.9800
C(17)-H(17B)	0.9800
C(17)-H(17C)	0.9800
C(18)-N(6)	1.350(2)
C(18)-N(5)	1.402(2)
C(18)-C(19)	1.405(3)
C(19)-C(20)	1.378(3)
C(19)-H(19)	0.9500
C(20)-C(21)	1.387(3)
C(20)-H(20)	0.9500
C(21)-C(22)	1.374(3)
C(21)-H(21)	0.9500
C(22)-N(6)	1.356(2)
C(22)-H(22)	0.9500
Cl(1)-Co(1)	2.2611(6)
Cl(2)-Co(1)	2.2421(6)
Co(1)-N(3)	1.9468(16)
Co(1)-N(1)	1.9481(16)
Co(1)-N(6)	1.9556(16)
Co(1)-N(4)	1.9623(16)
C(23)-F(3)	1.326(3)
C(23)-F(2)	1.338(2)
C(23)-F(1)	1.344(2)
C(23)-S(1)	1.831(2)
O(1)-S(1)	1.4432(14)
O(2)-S(1)	1.4435(15)
O(3)-S(1)	1.4390(16)

N(1)-C(1)-C(2)	122.88(18)
N(1)-C(1)-H(1)	118.6
C(2)-C(1)-H(1)	118.6
C(1)-C(2)-C(3)	118.56(18)
C(1)-C(2)-H(2)	120.7

C(3)-C(2)-H(2)	120.7
C(4)-C(3)-C(2)	119.42(18)
C(4)-C(3)-H(3)	120.3
C(2)-C(3)-H(3)	120.3
C(3)-C(4)-C(5)	119.28(18)
C(3)-C(4)-H(4)	120.4
C(5)-C(4)-H(4)	120.4
N(1)-C(5)-N(2)	119.00(16)
N(1)-C(5)-C(4)	121.37(17)
N(2)-C(5)-C(4)	119.60(17)
N(2)-C(6)-H(6A)	109.5
N(2)-C(6)-H(6B)	109.5
H(6A)-C(6)-H(6B)	109.5
N(2)-C(6)-H(6C)	109.5
H(6A)-C(6)-H(6C)	109.5
H(6B)-C(6)-H(6C)	109.5
N(3)-C(7)-N(2)	118.53(16)
N(3)-C(7)-C(8)	120.92(17)
N(2)-C(7)-C(8)	120.54(17)
C(9)-C(8)-C(7)	119.18(18)
C(9)-C(8)-H(8)	120.4
C(7)-C(8)-H(8)	120.4
C(8)-C(9)-C(10)	119.53(18)
C(8)-C(9)-H(9)	120.2
C(10)-C(9)-H(9)	120.2
C(11)-C(10)-C(9)	118.43(18)
C(11)-C(10)-H(10)	120.8
C(9)-C(10)-H(10)	120.8
N(3)-C(11)-C(10)	122.49(18)
N(3)-C(11)-H(11)	118.8
C(10)-C(11)-H(11)	118.8
N(4)-C(12)-C(13)	122.72(18)
N(4)-C(12)-H(12)	118.6
C(13)-C(12)-H(12)	118.6
C(12)-C(13)-C(14)	118.62(18)
C(12)-C(13)-H(13)	120.7
C(14)-C(13)-H(13)	120.7
C(15)-C(14)-C(13)	119.35(19)
C(15)-C(14)-H(14)	120.3
C(13)-C(14)-H(14)	120.3

C(14)-C(15)-C(16)	119.29(18)
C(14)-C(15)-H(15)	120.4
C(16)-C(15)-H(15)	120.4
N(4)-C(16)-N(5)	118.08(17)
N(4)-C(16)-C(15)	120.91(17)
N(5)-C(16)-C(15)	121.02(17)
N(5)-C(17)-H(17A)	109.5
N(5)-C(17)-H(17B)	109.5
H(17A)-C(17)-H(17B)	109.5
N(5)-C(17)-H(17C)	109.5
H(17A)-C(17)-H(17C)	109.5
H(17B)-C(17)-H(17C)	109.5
N(6)-C(18)-N(5)	119.09(16)
N(6)-C(18)-C(19)	120.96(18)
N(5)-C(18)-C(19)	119.95(18)
C(20)-C(19)-C(18)	119.07(19)
C(20)-C(19)-H(19)	120.5
C(18)-C(19)-H(19)	120.5
C(19)-C(20)-C(21)	119.85(19)
C(19)-C(20)-H(20)	120.1
C(21)-C(20)-H(20)	120.1
C(22)-C(21)-C(20)	118.47(19)
C(22)-C(21)-H(21)	120.8
C(20)-C(21)-H(21)	120.8
N(6)-C(22)-C(21)	122.8(2)
N(6)-C(22)-H(22)	118.6
C(21)-C(22)-H(22)	118.6
N(3)-Co(1)-N(1)	87.73(7)
N(3)-Co(1)-N(6)	91.22(7)
N(1)-Co(1)-N(6)	177.32(7)
N(3)-Co(1)-N(4)	91.45(7)
N(1)-Co(1)-N(4)	90.16(7)
N(6)-Co(1)-N(4)	87.40(7)
N(3)-Co(1)-Cl(2)	87.47(5)
N(1)-Co(1)-Cl(2)	88.44(5)
N(6)-Co(1)-Cl(2)	93.97(5)
N(4)-Co(1)-Cl(2)	178.27(5)
N(3)-Co(1)-Cl(1)	178.07(5)
N(1)-Co(1)-Cl(1)	94.14(5)
N(6)-Co(1)-Cl(1)	86.89(5)

N(4)-Co(1)-Cl(1)	88.10(5)
Cl(2)-Co(1)-Cl(1)	93.02(2)
C(5)-N(1)-C(1)	118.35(16)
C(5)-N(1)-Co(1)	121.99(12)
C(1)-N(1)-Co(1)	119.52(13)
C(7)-N(2)-C(5)	122.13(16)
C(7)-N(2)-C(6)	118.03(15)
C(5)-N(2)-C(6)	117.60(15)
C(7)-N(3)-C(11)	119.00(16)
C(7)-N(3)-Co(1)	121.68(12)
C(11)-N(3)-Co(1)	118.44(13)
C(16)-N(4)-C(12)	118.86(17)
C(16)-N(4)-Co(1)	121.59(13)
C(12)-N(4)-Co(1)	118.87(13)
C(16)-N(5)-C(18)	120.50(16)
C(16)-N(5)-C(17)	118.09(16)
C(18)-N(5)-C(17)	117.60(16)
C(18)-N(6)-C(22)	118.89(17)
C(18)-N(6)-Co(1)	121.44(13)
C(22)-N(6)-Co(1)	119.66(14)
F(3)-C(23)-F(2)	108.10(17)
F(3)-C(23)-F(1)	107.16(18)
F(2)-C(23)-F(1)	106.98(17)
F(3)-C(23)-S(1)	111.46(15)
F(2)-C(23)-S(1)	111.82(15)
F(1)-C(23)-S(1)	111.07(14)
O(3)-S(1)-O(1)	115.15(10)
O(3)-S(1)-O(2)	115.16(10)
O(1)-S(1)-O(2)	115.26(9)
O(3)-S(1)-C(23)	103.52(10)
O(1)-S(1)-C(23)	102.01(9)
O(2)-S(1)-C(23)	103.05(10)

Symmetry transformations used to generate equivalent atoms:

Table 4. Anisotropic displacement parameters ($Å^2 x\ 10^3$) for phw0903m. The anisotropic displacement factor exponent takes the form: $-2\pi^2[\ h^2\ a^{*2}U^{11} + ... + 2\ h\ k\ a^*\ b^*\ U^{12}\ ]$

	U^{11}	U^{22}	U^{33}	U^{23}	U^{13}	U^{12}
C(1)	15(1)	25(1)	19(1)	8(1)	4(1)	2(1)
C(2)	20(1)	26(1)	22(1)	11(1)	8(1)	2(1)
C(3)	28(1)	28(1)	21(1)	15(1)	5(1)	2(1)
C(4)	18(1)	30(1)	21(1)	14(1)	2(1)	4(1)
C(5)	15(1)	19(1)	15(1)	6(1)	2(1)	1(1)
C(6)	17(1)	29(1)	25(1)	15(1)	4(1)	8(1)
C(7)	14(1)	18(1)	15(1)	6(1)	3(1)	2(1)
C(8)	12(1)	24(1)	22(1)	9(1)	2(1)	2(1)
C(9)	15(1)	23(1)	26(1)	8(1)	3(1)	-1(1)
C(10)	21(1)	18(1)	23(1)	9(1)	3(1)	0(1)
C(11)	17(1)	18(1)	19(1)	7(1)	2(1)	4(1)
C(12)	20(1)	19(1)	16(1)	8(1)	1(1)	-1(1)
C(13)	27(1)	18(1)	19(1)	9(1)	-1(1)	1(1)
C(14)	24(1)	22(1)	20(1)	5(1)	-1(1)	8(1)
C(15)	19(1)	25(1)	18(1)	8(1)	3(1)	4(1)
C(16)	16(1)	20(1)	15(1)	7(1)	0(1)	1(1)
C(17)	22(1)	31(1)	26(1)	15(1)	10(1)	3(1)
C(18)	21(1)	14(1)	19(1)	7(1)	1(1)	0(1)
C(19)	31(1)	18(1)	17(1)	9(1)	2(1)	0(1)
C(20)	37(1)	18(1)	22(1)	11(1)	-8(1)	-3(1)
C(21)	26(1)	22(1)	29(1)	12(1)	-9(1)	0(1)
C(22)	18(1)	23(1)	26(1)	11(1)	-3(1)	1(1)
Cl(1)	14(1)	26(1)	23(1)	12(1)	0(1)	-2(1)
Cl(2)	16(1)	24(1)	23(1)	8(1)	4(1)	6(1)
Co(1)	11(1)	18(1)	16(1)	8(1)	2(1)	2(1)
N(1)	13(1)	19(1)	16(1)	7(1)	2(1)	2(1)
N(2)	11(1)	22(1)	20(1)	12(1)	3(1)	3(1)
N(3)	13(1)	17(1)	16(1)	6(1)	4(1)	2(1)
N(4)	15(1)	17(1)	14(1)	7(1)	1(1)	0(1)
N(5)	17(1)	21(1)	19(1)	10(1)	6(1)	2(1)
N(6)	16(1)	17(1)	19(1)	8(1)	-1(1)	0(1)
C(23)	24(1)	26(1)	23(1)	12(1)	4(1)	3(1)
F(1)	21(1)	48(1)	36(1)	23(1)	7(1)	10(1)
F(2)	40(1)	46(1)	34(1)	30(1)	11(1)	15(1)
F(3)	54(1)	23(1)	42(1)	6(1)	-1(1)	5(1)
O(1)	23(1)	38(1)	21(1)	18(1)	1(1)	0(1)
O(2)	18(1)	53(1)	35(1)	28(1)	6(1)	3(1)
O(3)	39(1)	28(1)	25(1)	9(1)	-2(1)	7(1)

S(1)	18(1)	26(1)	18(1)	13(1)	2(1)	3(1)

Table 5. Hydrogen coordinates (x 10^4) and isotropic displacement parameters ($Å^2$x 10^3) for phw0903m.

	x	y	z	U(eq)
H(1)	8190	7589	5779	24
H(2)	8176	8392	4478	27
H(3)	5740	8701	3846	29
H(4)	3406	8232	4578	26
H(6A)	1158	7719	5411	33
H(6B)	2213	8946	6180	33
H(6C)	1117	8203	6718	33
H(8)	364	6270	6131	23
H(9)	-110	4622	6576	27
H(10)	2061	3830	7001	25
H(11)	4607	4795	7094	22
H(12)	6272	9601	7632	22
H(13)	4742	11104	8290	26
H(14)	2587	10897	9322	27
H(15)	2107	9206	9700	25
H(17A)	2187	7622	10271	38
H(17B)	2025	6279	9393	38
H(17C)	1294	7247	9086	38
H(19)	4231	6725	10663	26
H(20)	6473	5989	11024	31
H(21)	8511	5688	9817	30
H(22)	8271	6164	8309	26

Table 6. Torsion angles [°] for phw0903m.

N(1)-C(1)-C(2)-C(3)	-3.7(3)
C(1)-C(2)-C(3)-C(4)	0.5(3)

C(2)-C(3)-C(4)-C(5)	1.9(3)
C(3)-C(4)-C(5)-N(1)	-1.3(3)
C(3)-C(4)-C(5)-N(2)	176.62(19)
N(3)-C(7)-C(8)-C(9)	-2.5(3)
N(2)-C(7)-C(8)-C(9)	178.77(18)
C(7)-C(8)-C(9)-C(10)	-2.7(3)
C(8)-C(9)-C(10)-C(11)	3.0(3)
C(9)-C(10)-C(11)-N(3)	1.8(3)
N(4)-C(12)-C(13)-C(14)	2.0(3)
C(12)-C(13)-C(14)-C(15)	1.6(3)
C(13)-C(14)-C(15)-C(16)	-1.5(3)
C(14)-C(15)-C(16)-N(4)	-2.2(3)
C(14)-C(15)-C(16)-N(5)	177.80(18)
N(6)-C(18)-C(19)-C(20)	1.4(3)
N(5)-C(18)-C(19)-C(20)	-177.97(18)
C(18)-C(19)-C(20)-C(21)	-1.1(3)
C(19)-C(20)-C(21)-C(22)	0.5(3)
C(20)-C(21)-C(22)-N(6)	0.0(3)
N(2)-C(5)-N(1)-C(1)	-179.65(17)
C(4)-C(5)-N(1)-C(1)	-1.7(3)
N(2)-C(5)-N(1)-Co(1)	-4.0(2)
C(4)-C(5)-N(1)-Co(1)	173.96(15)
C(2)-C(1)-N(1)-C(5)	4.3(3)
C(2)-C(1)-N(1)-Co(1)	-171.48(16)
N(3)-Co(1)-N(1)-C(5)	37.55(15)
N(4)-Co(1)-N(1)-C(5)	-53.89(15)
Cl(2)-Co(1)-N(1)-C(5)	125.08(15)
Cl(1)-Co(1)-N(1)-C(5)	-142.00(14)
N(3)-Co(1)-N(1)-C(1)	-146.85(15)
N(4)-Co(1)-N(1)-C(1)	121.71(15)
Cl(2)-Co(1)-N(1)-C(1)	-59.32(14)
Cl(1)-Co(1)-N(1)-C(1)	33.60(15)
N(3)-C(7)-N(2)-C(5)	35.6(3)
C(8)-C(7)-N(2)-C(5)	-145.61(18)
N(3)-C(7)-N(2)-C(6)	-161.78(17)
C(8)-C(7)-N(2)-C(6)	17.0(3)
N(1)-C(5)-N(2)-C(7)	-42.8(3)
C(4)-C(5)-N(2)-C(7)	139.16(19)
N(1)-C(5)-N(2)-C(6)	154.48(18)
C(4)-C(5)-N(2)-C(6)	-23.5(3)

N(2)-C(7)-N(3)-C(11)	-173.97(17)
C(8)-C(7)-N(3)-C(11)	7.3(3)
N(2)-C(7)-N(3)-Co(1)	17.0(2)
C(8)-C(7)-N(3)-Co(1)	-161.82(14)
C(10)-C(11)-N(3)-C(7)	-7.0(3)
C(10)-C(11)-N(3)-Co(1)	162.41(15)
N(1)-Co(1)-N(3)-C(7)	-44.49(15)
N(6)-Co(1)-N(3)-C(7)	133.05(15)
N(4)-Co(1)-N(3)-C(7)	45.62(15)
Cl(2)-Co(1)-N(3)-C(7)	-133.03(14)
N(1)-Co(1)-N(3)-C(11)	146.38(14)
N(6)-Co(1)-N(3)-C(11)	-36.09(14)
N(4)-Co(1)-N(3)-C(11)	-123.51(14)
Cl(2)-Co(1)-N(3)-C(11)	57.84(14)
N(5)-C(16)-N(4)-C(12)	-174.38(16)
C(15)-C(16)-N(4)-C(12)	5.7(3)
N(5)-C(16)-N(4)-Co(1)	15.2(2)
C(15)-C(16)-N(4)-Co(1)	-164.78(14)
C(13)-C(12)-N(4)-C(16)	-5.6(3)
C(13)-C(12)-N(4)-Co(1)	165.10(15)
N(3)-Co(1)-N(4)-C(16)	46.57(15)
N(1)-Co(1)-N(4)-C(16)	134.30(15)
N(6)-Co(1)-N(4)-C(16)	-44.59(14)
Cl(1)-Co(1)-N(4)-C(16)	-131.56(14)
N(3)-Co(1)-N(4)-C(12)	-123.87(14)
N(1)-Co(1)-N(4)-C(12)	-36.14(14)
N(6)-Co(1)-N(4)-C(12)	144.97(14)
Cl(1)-Co(1)-N(4)-C(12)	58.00(13)
N(4)-C(16)-N(5)-C(18)	39.8(3)
C(15)-C(16)-N(5)-C(18)	-140.24(19)
N(4)-C(16)-N(5)-C(17)	-162.70(17)
C(15)-C(16)-N(5)-C(17)	17.3(3)
N(6)-C(18)-N(5)-C(16)	-48.2(3)
C(19)-C(18)-N(5)-C(16)	131.21(19)
N(6)-C(18)-N(5)-C(17)	154.20(18)
C(19)-C(18)-N(5)-C(17)	-26.4(3)
N(5)-C(18)-N(6)-C(22)	178.40(17)
C(19)-C(18)-N(6)-C(22)	-1.0(3)
N(5)-C(18)-N(6)-Co(1)	-0.7(2)
C(19)-C(18)-N(6)-Co(1)	179.88(14)

C(21)-C(22)-N(6)-C(18)	0.3(3)
C(21)-C(22)-N(6)-Co(1)	179.45(15)
N(3)-Co(1)-N(6)-C(18)	-54.76(15)
N(4)-Co(1)-N(6)-C(18)	36.64(15)
Cl(2)-Co(1)-N(6)-C(18)	-142.31(14)
Cl(1)-Co(1)-N(6)-C(18)	124.88(15)
N(3)-Co(1)-N(6)-C(22)	126.13(15)
N(4)-Co(1)-N(6)-C(22)	-142.48(15)
Cl(2)-Co(1)-N(6)-C(22)	38.58(14)
Cl(1)-Co(1)-N(6)-C(22)	-54.24(14)
F(3)-C(23)-S(1)-O(3)	-178.22(15)
F(2)-C(23)-S(1)-O(3)	60.65(17)
F(1)-C(23)-S(1)-O(3)	-58.79(16)
F(3)-C(23)-S(1)-O(1)	-58.34(16)
F(2)-C(23)-S(1)-O(1)	-179.48(14)
F(1)-C(23)-S(1)-O(1)	61.09(16)
F(3)-C(23)-S(1)-O(2)	61.48(17)
F(2)-C(23)-S(1)-O(2)	-59.66(17)
F(1)-C(23)-S(1)-O(2)	-179.10(14)

Symmetry transformations used to generate equivalent atoms:

Crystallographic data for [{Cu(Cl)$_2$(dpea)}$_2$]

Table 1. Crystal data and structure refinement for phw0916m.

Identification code	phw0916m	
Empirical formula	C24 H26 Cl4 Cu2 N6	
Formula weight	667.39	
Temperature	110(2) K	
Wavelength	0.71073 Å	
Crystal system	Triclinic	
Space group	P-1	
Unit cell dimensions	a = 7.2030(6) Å	α= 110.9320(10)°.
	b = 8.8918(8) Å	β= 91.609(2)°.
	c = 11.7252(10) Å	γ = 112.0740(10)°.
Volume	638.46(10) Å^3	
Z	1	
Density (calculated)	1.736 Mg/m^3	
Absorption coefficient	2.112 mm^{-1}	
F(000)	338	
Crystal size	0.27 x 0.22 x 0.08 mm^3	
Theta range for data collection	1.89 to 28.28°.	
Index ranges	-9<=h<=9, -11<=k<=11, -15<=l<=15	
Reflections collected	6527	
Independent reflections	3120 [R(int) = 0.0142]	
Completeness to theta = 28.28°	98.5 %	
Absorption correction	Semi-empirical from equivalents	
Max. and min. transmission	0.845 and 0.655	
Refinement method	Full-matrix least-squares on F^2	
Data / restraints / parameters	3120 / 0 / 164	
Goodness-of-fit on F^2	1.058	
Final R indices [I>2sigma(I)]	R1 = 0.0244, wR2 = 0.0667	
R indices (all data)	R1 = 0.0259, wR2 = 0.0678	
Largest diff. peak and hole	0.457 and -0.533 e.Å^{-3}	

Table 2. Atomic coordinates (x 10^4) and equivalent isotropic displacement parameters ($Å^2$x 10^3) for phw0916m. U(eq) is defined as one third of the trace of the orthogonalized U^{ij} tensor.

	x	y	z	U(eq)
C(1)	2437(3)	2326(2)	2643(2)	20(1)
C(2)	1441(3)	3133(3)	3472(2)	23(1)
C(3)	2455(3)	4943(3)	4187(2)	24(1)
C(4)	4354(3)	5894(2)	4000(2)	20(1)
C(5)	5238(3)	4993(2)	3107(2)	16(1)
C(6)	6995(2)	3327(2)	-372(2)	16(1)
C(7)	7607(2)	4563(2)	-891(2)	17(1)
C(8)	8044(2)	6314(2)	-148(2)	17(1)
C(9)	7849(2)	6762(2)	1086(2)	17(1)
C(10)	7277(2)	5452(2)	1556(1)	14(1)
C(11)	8410(3)	7704(2)	3708(2)	20(1)
C(12)	10656(3)	8174(2)	3660(2)	26(1)
Cl(1)	5834(1)	770(1)	3021(1)	20(1)
Cl(2)	7477(1)	292(1)	356(1)	17(1)
Cu(1)	5894(1)	1897(1)	1545(1)	14(1)
N(1)	4324(2)	3231(2)	2486(1)	15(1)
N(2)	7115(2)	5872(2)	2826(1)	16(1)
N(3)	6866(2)	3759(2)	839(1)	14(1)

Table 3. Bond lengths [Å] and angles [°] for phw0916m.

C(1)-N(1)	1.352(2)
C(1)-C(2)	1.379(2)
C(1)-H(1)	0.9500
C(2)-C(3)	1.395(3)
C(2)-H(2)	0.9500
C(3)-C(4)	1.384(3)
C(3)-H(3)	0.9500
C(4)-C(5)	1.402(2)
C(4)-H(4)	0.9500
C(5)-N(1)	1.342(2)
C(5)-N(2)	1.401(2)
C(6)-N(3)	1.349(2)
C(6)-C(7)	1.379(2)
C(6)-H(6)	0.9500
C(7)-C(8)	1.390(2)
C(7)-H(7)	0.9500
C(8)-C(9)	1.382(2)
C(8)-H(8)	0.9500
C(9)-C(10)	1.393(2)
C(9)-H(9)	0.9500
C(10)-N(3)	1.345(2)
C(10)-N(2)	1.420(2)
C(11)-N(2)	1.481(2)
C(11)-C(12)	1.520(3)
C(11)-H(11A)	0.9900
C(11)-H(11B)	0.9900
C(12)-H(12A)	0.9800
C(12)-H(12B)	0.9800
C(12)-H(12C)	0.9800
Cl(1)-Cu(1)	2.2830(4)
Cl(2)-Cu(1)	2.2739(4)
Cu(1)-N(1)	2.0114(14)
Cu(1)-N(3)	2.0133(13)

N(1)-C(1)-C(2)	122.45(17)
N(1)-C(1)-H(1)	118.8
C(2)-C(1)-H(1)	118.8
C(1)-C(2)-C(3)	118.07(16)

C(1)-C(2)-H(2)	121.0
C(3)-C(2)-H(2)	121.0
C(4)-C(3)-C(2)	119.91(16)
C(4)-C(3)-H(3)	120.0
C(2)-C(3)-H(3)	120.0
C(3)-C(4)-C(5)	118.65(16)
C(3)-C(4)-H(4)	120.7
C(5)-C(4)-H(4)	120.7
N(1)-C(5)-N(2)	116.70(14)
N(1)-C(5)-C(4)	121.22(15)
N(2)-C(5)-C(4)	122.07(15)
N(3)-C(6)-C(7)	122.64(15)
N(3)-C(6)-H(6)	118.7
C(7)-C(6)-H(6)	118.7
C(6)-C(7)-C(8)	118.76(15)
C(6)-C(7)-H(7)	120.6
C(8)-C(7)-H(7)	120.6
C(9)-C(8)-C(7)	119.10(15)
C(9)-C(8)-H(8)	120.5
C(7)-C(8)-H(8)	120.5
C(8)-C(9)-C(10)	119.01(15)
C(8)-C(9)-H(9)	120.5
C(10)-C(9)-H(9)	120.5
N(3)-C(10)-C(9)	121.96(15)
N(3)-C(10)-N(2)	117.46(13)
C(9)-C(10)-N(2)	120.59(14)
N(2)-C(11)-C(12)	111.58(14)
N(2)-C(11)-H(11A)	109.3
C(12)-C(11)-H(11A)	109.3
N(2)-C(11)-H(11B)	109.3
C(12)-C(11)-H(11B)	109.3
H(11A)-C(11)-H(11B)	108.0
C(11)-C(12)-H(12A)	109.5
C(11)-C(12)-H(12B)	109.5
H(12A)-C(12)-H(12B)	109.5
C(11)-C(12)-H(12C)	109.5
H(12A)-C(12)-H(12C)	109.5
H(12B)-C(12)-H(12C)	109.5
N(1)-Cu(1)-N(3)	85.74(5)
N(1)-Cu(1)-Cl(2)	175.70(4)

N(3)-Cu(1)-Cl(2)	93.60(4)
N(1)-Cu(1)-Cl(1)	89.02(4)
N(3)-Cu(1)-Cl(1)	155.57(4)
Cl(2)-Cu(1)-Cl(1)	93.293(16)
C(5)-N(1)-C(1)	119.42(14)
C(5)-N(1)-Cu(1)	120.41(11)
C(1)-N(1)-Cu(1)	119.45(11)
C(5)-N(2)-C(10)	118.23(13)
C(5)-N(2)-C(11)	117.72(13)
C(10)-N(2)-C(11)	116.54(13)
C(10)-N(3)-C(6)	118.48(13)
C(10)-N(3)-Cu(1)	120.23(11)
C(6)-N(3)-Cu(1)	121.16(11)

Symmetry transformations used to generate equivalent atoms:

Table 4. Anisotropic displacement parameters ($Å^2 x\ 10^3$) for phw0916m. The anisotropic displacement factor exponent takes the form: $-2\pi^2[\ h^2\ a^{*2}U^{11} + ...\ + 2\ h\ k\ a^*\ b^*\ U^{12}\ ]$

	U^{11}	U^{22}	U^{33}	U^{23}	U^{13}	U^{12}
C(1)	19(1)	24(1)	20(1)	12(1)	6(1)	8(1)
C(2)	19(1)	34(1)	23(1)	16(1)	8(1)	14(1)
C(3)	26(1)	34(1)	22(1)	14(1)	11(1)	20(1)
C(4)	25(1)	22(1)	20(1)	9(1)	7(1)	15(1)
C(5)	19(1)	18(1)	15(1)	9(1)	5(1)	10(1)
C(6)	16(1)	15(1)	16(1)	5(1)	3(1)	7(1)
C(7)	17(1)	21(1)	16(1)	8(1)	4(1)	9(1)
C(8)	17(1)	19(1)	21(1)	12(1)	4(1)	8(1)
C(9)	16(1)	13(1)	21(1)	7(1)	4(1)	6(1)
C(10)	13(1)	14(1)	15(1)	5(1)	3(1)	6(1)
C(11)	26(1)	13(1)	16(1)	2(1)	3(1)	8(1)
C(12)	25(1)	21(1)	24(1)	3(1)	1(1)	8(1)
Cl(1)	23(1)	19(1)	20(1)	10(1)	4(1)	9(1)
Cl(2)	17(1)	14(1)	21(1)	6(1)	6(1)	8(1)
Cu(1)	17(1)	11(1)	16(1)	6(1)	6(1)	6(1)
N(1)	16(1)	16(1)	16(1)	8(1)	5(1)	7(1)
N(2)	19(1)	12(1)	14(1)	3(1)	5(1)	6(1)
N(3)	14(1)	12(1)	15(1)	5(1)	4(1)	6(1)

Table 5. Hydrogen coordinates (x 10^4) and isotropic displacement parameters ($Å^2$x 10^{3}) for phw0916m.

	x	y	z	U(eq)
H(1)	1773	1089	2165	24
H(2)	102	2474	3554	27
H(3)	1844	5522	4803	28
H(4)	5044	7133	4466	24
H(6)	6651	2123	-888	19
H(7)	7727	4223	-1742	21
H(8)	8472	7192	-482	21
H(9)	8100	7945	1604	20
H(11A)	8195	7832	4562	24
H(11B)	8000	8536	3503	24
H(12A)	11021	7259	3747	38
H(12B)	11481	9316	4339	38
H(12C)	10916	8250	2862	38

Table 6. Torsion angles [°] for phw0916m.

N(1)-C(1)-C(2)-C(3)	-1.4(3)
C(1)-C(2)-C(3)-C(4)	3.9(3)
C(2)-C(3)-C(4)-C(5)	-1.6(3)
C(3)-C(4)-C(5)-N(1)	-3.3(2)
C(3)-C(4)-C(5)-N(2)	177.31(15)
N(3)-C(6)-C(7)-C(8)	-2.2(2)
C(6)-C(7)-C(8)-C(9)	-0.1(2)
C(7)-C(8)-C(9)-C(10)	1.9(2)
C(8)-C(9)-C(10)-N(3)	-1.5(2)
C(8)-C(9)-C(10)-N(2)	178.24(14)
N(2)-C(5)-N(1)-C(1)	-174.79(14)
C(4)-C(5)-N(1)-C(1)	5.8(2)
N(2)-C(5)-N(1)-Cu(1)	14.97(19)
C(4)-C(5)-N(1)-Cu(1)	-164.47(12)
C(2)-C(1)-N(1)-C(5)	-3.4(2)
C(2)-C(1)-N(1)-Cu(1)	166.94(13)
N(3)-Cu(1)-N(1)-C(5)	-47.81(12)
Cl(1)-Cu(1)-N(1)-C(5)	108.31(12)
N(3)-Cu(1)-N(1)-C(1)	141.95(13)
Cl(1)-Cu(1)-N(1)-C(1)	-61.93(12)
N(1)-C(5)-N(2)-C(10)	47.2(2)
C(4)-C(5)-N(2)-C(10)	-133.36(16)
N(1)-C(5)-N(2)-C(11)	-164.04(14)
C(4)-C(5)-N(2)-C(11)	15.4(2)
N(3)-C(10)-N(2)-C(5)	-58.35(19)
C(9)-C(10)-N(2)-C(5)	121.90(16)
N(3)-C(10)-N(2)-C(11)	152.53(14)
C(9)-C(10)-N(2)-C(11)	-27.2(2)
C(12)-C(11)-N(2)-C(5)	153.14(15)
C(12)-C(11)-N(2)-C(10)	-57.59(19)
C(9)-C(10)-N(3)-C(6)	-0.7(2)
N(2)-C(10)-N(3)-C(6)	179.54(13)
C(9)-C(10)-N(3)-Cu(1)	-176.56(12)
N(2)-C(10)-N(3)-Cu(1)	3.69(19)
C(7)-C(6)-N(3)-C(10)	2.6(2)
C(7)-C(6)-N(3)-Cu(1)	178.39(12)
N(1)-Cu(1)-N(3)-C(10)	37.33(12)
Cl(2)-Cu(1)-N(3)-C(10)	-146.93(11)

Cl(1)-Cu(1)-N(3)-C(10)	-40.80(18)
N(1)-Cu(1)-N(3)-C(6)	-138.40(13)
Cl(2)-Cu(1)-N(3)-C(6)	37.35(12)
Cl(1)-Cu(1)-N(3)-C(6)	143.47(10)

Symmetry transformations used to generate equivalent atoms:

Crystallographic data for $[Zn(Cl)_2(dpea)]$

Table 1. Crystal data and structure refinement for phw1002m.

Identification code	phw1002m	
Empirical formula	C12 H13 Cl2 N3 Zn	
Formula weight	335.52	
Temperature	110(2) K	
Wavelength	0.71073 Å	
Crystal system	Triclinic	
Space group	P-1	
Unit cell dimensions	a = 7.6933(17) Å	α= 91.554(4)°.
	b = 8.1468(18) Å	β= 90.993(4)°.
	c = 11.692(3) Å	γ = 108.414(4)°.
Volume	694.8(3) $Å^3$	
Z	2	
Density (calculated)	1.604 Mg/m^3	
Absorption coefficient	2.136 mm^{-1}	
F(000)	340	
Crystal size	0.33 x 0.17 x 0.12 mm^3	
Theta range for data collection	1.74 to 28.35°.	
Index ranges	-10<=h<=10, -10<=k<=10, -15<=l<=15	
Reflections collected	7094	
Independent reflections	3416 [R(int) = 0.0211]	
Completeness to theta = 28.35°	98.3 %	
Absorption correction	Semi-empirical from equivalents	
Max. and min. transmission	0.774 and 0.602	
Refinement method	Full-matrix least-squares on F^2	
Data / restraints / parameters	3416 / 0 / 164	
Goodness-of-fit on F^2	1.139	
Final R indices [I>2sigma(I)]	R1 = 0.0291, wR2 = 0.0758	
R indices (all data)	R1 = 0.0335, wR2 = 0.0815	
Largest diff. peak and hole	0.447 and -0.385 $e.Å^{-3}$	

Table 2. Atomic coordinates (x 10^4) and equivalent isotropic displacement parameters ($Å^2$x 10^3) for phw1002m. U(eq) is defined as one third of the trace of the orthogonalized U^{ij} tensor.

	x	y	z	U(eq)
C(1)	3623(3)	-817(3)	8646(2)	17(1)
C(2)	3049(3)	408(3)	9227(2)	20(1)
C(3)	4096(3)	2141(3)	9135(2)	21(1)
C(4)	5626(3)	2575(3)	8469(2)	19(1)
C(5)	6130(3)	1268(3)	7910(2)	15(1)
C(6)	6951(3)	-1496(3)	4895(2)	21(1)
C(7)	7675(3)	-520(4)	3969(2)	25(1)
C(8)	8376(4)	1276(4)	4124(2)	25(1)
C(9)	8328(3)	2010(3)	5198(2)	23(1)
C(10)	7647(3)	958(3)	6108(2)	17(1)
C(11)	9192(3)	3289(3)	7512(2)	20(1)
C(12)	9895(4)	3340(4)	8735(2)	26(1)
Cl(1)	8449(1)	-2562(1)	8357(1)	21(1)
Cl(2)	3814(1)	-4623(1)	6833(1)	25(1)
N(1)	5152(3)	-414(3)	8027(2)	16(1)
N(2)	6968(3)	-773(3)	5953(2)	18(1)
N(3)	7693(3)	1656(3)	7231(2)	17(1)
Zn(1)	6110(1)	-2263(1)	7328(1)	17(1)

Table 3. Bond lengths [Å] and angles [°] for phw1002m.

C(1)-N(1)	1.347(3)
C(1)-C(2)	1.379(3)
C(1)-H(1)	0.9500
C(2)-C(3)	1.395(4)
C(2)-H(2)	0.9500
C(3)-C(4)	1.379(3)
C(3)-H(3)	0.9500
C(4)-C(5)	1.395(3)
C(4)-H(4)	0.9500
C(5)-N(1)	1.351(3)
C(5)-N(3)	1.408(3)
C(6)-N(2)	1.354(3)
C(6)-C(7)	1.380(4)
C(6)-H(6)	0.9500
C(7)-C(8)	1.396(4)
C(7)-H(7)	0.9500
C(8)-C(9)	1.382(4)
C(8)-H(8)	0.9500
C(9)-C(10)	1.389(3)
C(9)-H(9)	0.9500
C(10)-N(2)	1.346(3)
C(10)-N(3)	1.411(3)
C(11)-N(3)	1.484(3)
C(11)-C(12)	1.515(4)
C(11)-H(11A)	0.9900
C(11)-H(11B)	0.9900
C(12)-H(12A)	0.9800
C(12)-H(12B)	0.9800
C(12)-H(12C)	0.9800
Cl(1)-Zn(1)	2.2274(7)
Cl(2)-Zn(1)	2.2162(7)
N(1)-Zn(1)	2.034(2)
N(2)-Zn(1)	2.032(2)

N(1)-C(1)-C(2)	123.1(2)
N(1)-C(1)-H(1)	118.5
C(2)-C(1)-H(1)	118.5
C(1)-C(2)-C(3)	117.6(2)

C(1)-C(2)-H(2)	121.2
C(3)-C(2)-H(2)	121.2
C(4)-C(3)-C(2)	120.0(2)
C(4)-C(3)-H(3)	120.0
C(2)-C(3)-H(3)	120.0
C(3)-C(4)-C(5)	119.4(2)
C(3)-C(4)-H(4)	120.3
C(5)-C(4)-H(4)	120.3
N(1)-C(5)-C(4)	120.7(2)
N(1)-C(5)-N(3)	118.1(2)
C(4)-C(5)-N(3)	121.2(2)
N(2)-C(6)-C(7)	122.1(2)
N(2)-C(6)-H(6)	119.0
C(7)-C(6)-H(6)	119.0
C(6)-C(7)-C(8)	118.6(2)
C(6)-C(7)-H(7)	120.7
C(8)-C(7)-H(7)	120.7
C(9)-C(8)-C(7)	118.9(2)
C(9)-C(8)-H(8)	120.5
C(7)-C(8)-H(8)	120.5
C(8)-C(9)-C(10)	119.9(2)
C(8)-C(9)-H(9)	120.0
C(10)-C(9)-H(9)	120.0
N(2)-C(10)-C(9)	120.9(2)
N(2)-C(10)-N(3)	117.7(2)
C(9)-C(10)-N(3)	121.4(2)
N(3)-C(11)-C(12)	111.5(2)
N(3)-C(11)-H(11A)	109.3
C(12)-C(11)-H(11A)	109.3
N(3)-C(11)-H(11B)	109.3
C(12)-C(11)-H(11B)	109.3
H(11A)-C(11)-H(11B)	108.0
C(11)-C(12)-H(12A)	109.5
C(11)-C(12)-H(12B)	109.5
H(12A)-C(12)-H(12B)	109.5
C(11)-C(12)-H(12C)	109.5
H(12A)-C(12)-H(12C)	109.5
H(12B)-C(12)-H(12C)	109.5
C(1)-N(1)-C(5)	119.2(2)
C(1)-N(1)-Zn(1)	122.02(16)

C(5)-N(1)-Zn(1)	118.70(15)
C(10)-N(2)-C(6)	119.5(2)
C(10)-N(2)-Zn(1)	119.30(16)
C(6)-N(2)-Zn(1)	121.11(17)
C(5)-N(3)-C(10)	122.42(19)
C(5)-N(3)-C(11)	117.37(19)
C(10)-N(3)-C(11)	116.32(19)
N(2)-Zn(1)-N(1)	89.95(8)
N(2)-Zn(1)-Cl(2)	110.79(6)
N(1)-Zn(1)-Cl(2)	110.65(6)
N(2)-Zn(1)-Cl(1)	111.99(6)
N(1)-Zn(1)-Cl(1)	111.70(6)
Cl(2)-Zn(1)-Cl(1)	118.26(3)

Symmetry transformations used to generate equivalent atoms:

Table 4. Anisotropic displacement parameters ($Å^2 x\ 10^3$) for phw1002m. The anisotropic displacement factor exponent takes the form: $-2\pi^2[\ h^2\ a^{*2}U^{11} + ... + 2\ h\ k\ a^*\ b^*\ U^{12}\ ]$

	U^{11}	U^{22}	U^{33}	U^{23}	U^{13}	U^{12}
C(1)	16(1)	16(1)	17(1)	2(1)	-1(1)	3(1)
C(2)	15(1)	27(1)	19(1)	0(1)	3(1)	7(1)
C(3)	20(1)	26(1)	20(1)	-5(1)	1(1)	11(1)
C(4)	17(1)	19(1)	20(1)	0(1)	0(1)	6(1)
C(5)	14(1)	15(1)	15(1)	1(1)	0(1)	4(1)
C(6)	23(1)	20(1)	20(1)	-2(1)	-1(1)	9(1)
C(7)	21(1)	38(2)	16(1)	-4(1)	-1(1)	12(1)
C(8)	21(1)	37(2)	18(1)	4(1)	3(1)	8(1)
C(9)	21(1)	24(1)	22(1)	3(1)	2(1)	4(1)
C(10)	12(1)	20(1)	18(1)	0(1)	3(1)	5(1)
C(11)	16(1)	16(1)	25(1)	-1(1)	3(1)	1(1)
C(12)	20(1)	27(1)	26(1)	-3(1)	-1(1)	0(1)
Cl(1)	20(1)	23(1)	21(1)	-1(1)	0(1)	8(1)
Cl(2)	21(1)	17(1)	32(1)	-2(1)	0(1)	-1(1)
N(1)	14(1)	18(1)	16(1)	1(1)	0(1)	4(1)
N(2)	16(1)	20(1)	18(1)	-3(1)	1(1)	5(1)
N(3)	14(1)	15(1)	18(1)	-2(1)	2(1)	2(1)
Zn(1)	17(1)	14(1)	18(1)	-1(1)	2(1)	4(1)

Table 5. Hydrogen coordinates (x 10^4) and isotropic displacement parameters ($Å^2$x 10^3) for phw1002m.

	x	y	z	U(eq)
H(1)	2905	-2000	8684	20
H(2)	1981	83	9673	24
H(3)	3755	3020	9531	25
H(4)	6331	3755	8392	23
H(6)	6423	-2714	4787	25
H(7)	7696	-1059	3241	30
H(8)	8879	1982	3501	30
H(9)	8760	3232	5312	27
H(11A)	8738	4285	7402	24
H(11B)	10212	3398	6984	24
H(12A)	8959	3454	9261	39
H(12B)	11012	4330	8855	39
H(12C)	10169	2267	8881	39

Table 6. Torsion angles [°] for phw1002m.

N(1)-C(1)-C(2)-C(3)	1.6(4)
C(1)-C(2)-C(3)-C(4)	0.9(4)
C(2)-C(3)-C(4)-C(5)	-1.2(4)
C(3)-C(4)-C(5)-N(1)	-1.0(3)
C(3)-C(4)-C(5)-N(3)	-179.4(2)
N(2)-C(6)-C(7)-C(8)	-2.8(4)
C(6)-C(7)-C(8)-C(9)	0.3(4)
C(7)-C(8)-C(9)-C(10)	2.2(4)
C(8)-C(9)-C(10)-N(2)	-2.4(4)
C(8)-C(9)-C(10)-N(3)	175.6(2)
C(2)-C(1)-N(1)-C(5)	-3.8(3)
C(2)-C(1)-N(1)-Zn(1)	173.11(18)
C(4)-C(5)-N(1)-C(1)	3.4(3)
N(3)-C(5)-N(1)-C(1)	-178.1(2)
C(4)-C(5)-N(1)-Zn(1)	-173.62(17)
N(3)-C(5)-N(1)-Zn(1)	4.9(3)
C(9)-C(10)-N(2)-C(6)	0.0(3)
N(3)-C(10)-N(2)-C(6)	-178.1(2)
C(9)-C(10)-N(2)-Zn(1)	176.87(18)
N(3)-C(10)-N(2)-Zn(1)	-1.2(3)
C(7)-C(6)-N(2)-C(10)	2.6(4)
C(7)-C(6)-N(2)-Zn(1)	-174.18(19)
N(1)-C(5)-N(3)-C(10)	51.0(3)
C(4)-C(5)-N(3)-C(10)	-130.5(2)
N(1)-C(5)-N(3)-C(11)	-152.0(2)
C(4)-C(5)-N(3)-C(11)	26.5(3)
N(2)-C(10)-N(3)-C(5)	-53.2(3)
C(9)-C(10)-N(3)-C(5)	128.7(2)
N(2)-C(10)-N(3)-C(11)	149.6(2)
C(9)-C(10)-N(3)-C(11)	-28.5(3)
C(12)-C(11)-N(3)-C(5)	58.0(3)
C(12)-C(11)-N(3)-C(10)	-143.7(2)
C(10)-N(2)-Zn(1)-N(1)	36.37(18)
C(6)-N(2)-Zn(1)-N(1)	-146.83(19)
C(10)-N(2)-Zn(1)-Cl(2)	148.51(16)
C(6)-N(2)-Zn(1)-Cl(2)	-34.69(19)
C(10)-N(2)-Zn(1)-Cl(1)	-77.10(18)
C(6)-N(2)-Zn(1)-Cl(1)	99.70(18)

C(1)-N(1)-Zn(1)-N(2)	144.91(18)
C(5)-N(1)-Zn(1)-N(2)	-38.18(17)
C(1)-N(1)-Zn(1)-Cl(2)	32.64(19)
C(5)-N(1)-Zn(1)-Cl(2)	-150.45(15)
C(1)-N(1)-Zn(1)-Cl(1)	-101.34(17)
C(5)-N(1)-Zn(1)-Cl(1)	75.56(17)

Symmetry transformations used to generate equivalent atoms:

Crystallographic data for [dp(CN)(pyH)Ha][Zn(Cl)$_4$]

Table 1. Crystal data and structure refinement for phw0907m.

Identification code	phw0907m	
Empirical formula	C19 H26 Cl4 N6 O Zn	
Formula weight	561.63	
Temperature	110(2) K	
Wavelength	0.71073 Å	
Crystal system	Triclinic	
Space group	P-1	
Unit cell dimensions	a = 8.5322(3) Å	α= 78.4510(10)°.
	b = 9.9924(4) Å	β= 80.9670(10)°.
	c = 15.6774(6) Å	γ = 75.7830(10)°.
Volume	1261.23(8) Å^3	
Z	2	
Density (calculated)	1.479 Mg/m^3	
Absorption coefficient	1.420 mm^{-1}	
F(000)	576	
Crystal size	0.33 x 0.23 x 0.04 mm^3	
Theta range for data collection	2.13 to 28.29°.	
Index ranges	-11<=h<=11, -13<=k<=13, -20<=l<=20	
Reflections collected	13100	
Independent reflections	6215 [R(int) = 0.0117]	
Completeness to theta = 28.29°	99.1 %	
Absorption correction	Semi-empirical from equivalents	
Max. and min. transmission	0.945 and 0.751	
Refinement method	Full-matrix least-squares on F^2	
Data / restraints / parameters	6215 / 4 / 336	
Goodness-of-fit on F^2	1.052	
Final R indices [I>2sigma(I)]	R1 = 0.0244, wR2 = 0.0656	
R indices (all data)	R1 = 0.0277, wR2 = 0.0677	
Largest diff. peak and hole	0.407 and -0.166 e.Å^{-3}	

Table 2. Atomic coordinates (x 10^4) and equivalent isotropic displacement parameters ($Å^2$x 10^3) for phw0907m. U(eq) is defined as one third of the trace of the orthogonalized U^{ij} tensor.

	x	y	z	U(eq)
C(1)	2474(2)	7241(2)	5332(1)	27(1)
C(2)	3314(2)	7115(2)	6039(1)	28(1)
C(3)	3983(2)	5761(2)	6446(1)	25(1)
C(4)	3823(2)	4600(1)	6139(1)	22(1)
C(5)	2966(2)	4856(1)	5411(1)	21(1)
C(6)	2058(2)	3711(1)	4371(1)	19(1)
C(7)	2157(2)	2442(1)	4085(1)	20(1)
C(8)	1410(2)	2446(1)	3371(1)	20(1)
C(9)	531(2)	3720(1)	2935(1)	23(1)
C(10)	476(2)	4929(1)	3223(1)	23(1)
C(11)	1512(2)	1080(1)	3077(1)	22(1)
C(12)	3732(2)	1543(2)	1865(1)	29(1)
C(13)	4366(2)	1019(2)	999(1)	38(1)
C(14)	3524(2)	-167(2)	999(1)	44(1)
C(15)	2441(2)	-305(2)	1865(1)	35(1)
C(16)	4894(2)	5536(2)	7187(1)	29(1)
N(1)	2291(1)	6136(1)	5018(1)	23(1)
N(2)	2812(1)	3715(1)	5073(1)	21(1)
N(3)	1232(1)	4909(1)	3930(1)	21(1)
N(4)	5653(2)	5336(2)	7756(1)	38(1)
N(5)	2139(1)	1108(1)	2130(1)	23(1)
Cl(2)	5431(1)	9233(1)	3871(1)	28(1)
Cl(3)	9785(1)	8216(1)	3672(1)	28(1)
Cl(4)	7944(1)	11194(1)	2072(1)	30(1)
Cl(5)	7505(1)	7599(1)	1956(1)	37(1)
Zn(1)	7688(1)	9081(1)	2831(1)	23(1)
C(17)	8073(4)	3539(4)	-735(2)	62(1)
C(18)	7503(3)	4598(3)	604(2)	52(1)
C(19)	10085(3)	3057(2)	279(1)	31(1)
N(6)	8636(3)	3688(4)	54(2)	33(1)
O(1)	10669(13)	3190(30)	919(13)	34(2)
C(17A)	6619(11)	4616(13)	84(7)	74(4)
C(18A)	8975(16)	2811(16)	-363(9)	101(6)
C(19A)	9107(9)	3930(7)	814(4)	38(2)
N(6A)	8279(11)	3876(16)	190(7)	33(1)

O(1A)	10430(40)	3190(80)	1000(40)	31(5)

Table 3. Bond lengths [Å] and angles [°] for phw0907m.

C(1)-N(1)	1.3454(18)
C(1)-C(2)	1.382(2)
C(1)-H(1)	0.9500
C(2)-C(3)	1.397(2)
C(2)-H(2)	0.9500
C(3)-C(4)	1.3853(19)
C(3)-C(16)	1.448(2)
C(4)-C(5)	1.3980(18)
C(4)-H(4)	0.9500
C(5)-N(1)	1.3352(17)
C(5)-N(2)	1.3908(17)
C(6)-N(3)	1.3481(17)
C(6)-N(2)	1.3598(17)
C(6)-C(7)	1.4071(18)
C(7)-C(8)	1.3723(18)
C(7)-H(7)	0.9500
C(8)-C(9)	1.4121(18)
C(8)-C(11)	1.5041(18)
C(9)-C(10)	1.3598(19)
C(9)-H(9)	0.9500
C(10)-N(3)	1.3617(17)
C(10)-H(10)	0.9500
C(11)-N(5)	1.4939(17)
C(11)-H(11A)	0.9900
C(11)-H(11B)	0.9900
C(12)-N(5)	1.5001(18)
C(12)-C(13)	1.525(2)
C(12)-H(12A)	0.9900
C(12)-H(12B)	0.9900
C(13)-C(14)	1.529(3)
C(13)-H(13A)	0.9900
C(13)-H(13B)	0.9900
C(14)-C(15)	1.520(2)
C(14)-H(14A)	0.9900

C(14)-H(14B)	0.9900
C(15)-N(5)	1.5023(18)
C(15)-H(15A)	0.9900
C(15)-H(15B)	0.9900
C(16)-N(4)	1.141(2)
N(2)-H(2A)	0.82(2)
N(3)-H(3)	0.834(19)
N(5)-H(5)	0.845(19)
Cl(2)-Zn(1)	2.3151(4)
Cl(3)-Zn(1)	2.2830(4)
Cl(4)-Zn(1)	2.2502(4)
Cl(5)-Zn(1)	2.2563(4)
C(18)-N(6)	1.458(4)
C(18)-H(18A)	0.9800
C(18)-H(18B)	0.9800
C(18)-H(18C)	0.9800
C(17)-N(6)	1.442(3)
C(17)-H(17A)	0.9800
C(17)-H(17B)	0.9800
C(17)-H(17C)	0.9800
C(19)-O(1)	1.23(2)
C(19)-N(6)	1.310(3)
C(19)-H(19)	0.9500
C(18A)-N(6A)	1.460(9)
C(18A)-H(18D)	0.9800
C(18A)-H(18E)	0.9800
C(18A)-H(18F)	0.9800
C(17A)-N(6A)	1.446(8)
C(17A)-H(17D)	0.9800
C(17A)-H(17E)	0.9800
C(17A)-H(17F)	0.9800
C(19A)-O(1A)	1.23(2)
C(19A)-N(6A)	1.310(8)
C(19A)-H(19A)	0.9500

N(1)-C(1)-C(2)	123.40(13)
N(1)-C(1)-H(1)	118.3
C(2)-C(1)-H(1)	118.3
C(1)-C(2)-C(3)	117.30(13)
C(1)-C(2)-H(2)	121.4

C(3)-C(2)-H(2)	121.4
C(4)-C(3)-C(2)	120.85(13)
C(4)-C(3)-C(16)	118.27(13)
C(2)-C(3)-C(16)	120.86(13)
C(3)-C(4)-C(5)	116.79(12)
C(3)-C(4)-H(4)	121.6
C(5)-C(4)-H(4)	121.6
N(1)-C(5)-N(2)	117.95(12)
N(1)-C(5)-C(4)	123.68(12)
N(2)-C(5)-C(4)	118.36(12)
N(3)-C(6)-N(2)	121.26(12)
N(3)-C(6)-C(7)	118.79(12)
N(2)-C(6)-C(7)	119.94(12)
C(8)-C(7)-C(6)	119.73(12)
C(8)-C(7)-H(7)	120.1
C(6)-C(7)-H(7)	120.1
C(7)-C(8)-C(9)	119.79(12)
C(7)-C(8)-C(11)	119.15(12)
C(9)-C(8)-C(11)	121.05(12)
C(10)-C(9)-C(8)	118.93(12)
C(10)-C(9)-H(9)	120.5
C(8)-C(9)-H(9)	120.5
C(9)-C(10)-N(3)	120.59(12)
C(9)-C(10)-H(10)	119.7
N(3)-C(10)-H(10)	119.7
N(5)-C(11)-C(8)	112.42(11)
N(5)-C(11)-H(11A)	109.1
C(8)-C(11)-H(11A)	109.1
N(5)-C(11)-H(11B)	109.1
C(8)-C(11)-H(11B)	109.1
H(11A)-C(11)-H(11B)	107.9
N(5)-C(12)-C(13)	104.04(12)
N(5)-C(12)-H(12A)	110.9
C(13)-C(12)-H(12A)	110.9
N(5)-C(12)-H(12B)	110.9
C(13)-C(12)-H(12B)	110.9
H(12A)-C(12)-H(12B)	109.0
C(12)-C(13)-C(14)	106.00(13)
C(12)-C(13)-H(13A)	110.5
C(14)-C(13)-H(13A)	110.5

C(12)-C(13)-H(13B)	110.5
C(14)-C(13)-H(13B)	110.5
H(13A)-C(13)-H(13B)	108.7
C(15)-C(14)-C(13)	106.13(13)
C(15)-C(14)-H(14A)	110.5
C(13)-C(14)-H(14A)	110.5
C(15)-C(14)-H(14B)	110.5
C(13)-C(14)-H(14B)	110.5
H(14A)-C(14)-H(14B)	108.7
N(5)-C(15)-C(14)	104.02(13)
N(5)-C(15)-H(15A)	111.0
C(14)-C(15)-H(15A)	111.0
N(5)-C(15)-H(15B)	111.0
C(14)-C(15)-H(15B)	111.0
H(15A)-C(15)-H(15B)	109.0
N(4)-C(16)-C(3)	177.88(17)
C(5)-N(1)-C(1)	117.95(12)
C(6)-N(2)-C(5)	128.60(12)
C(6)-N(2)-H(2A)	115.1(13)
C(5)-N(2)-H(2A)	116.3(13)
C(6)-N(3)-C(10)	122.16(12)
C(6)-N(3)-H(3)	117.2(12)
C(10)-N(3)-H(3)	120.6(12)
C(11)-N(5)-C(12)	114.75(11)
C(11)-N(5)-C(15)	112.38(11)
C(12)-N(5)-C(15)	104.36(11)
C(11)-N(5)-H(5)	110.3(12)
C(12)-N(5)-H(5)	104.8(12)
C(15)-N(5)-H(5)	109.8(12)
Cl(4)-Zn(1)-Cl(5)	112.398(16)
Cl(4)-Zn(1)-Cl(3)	108.718(14)
Cl(5)-Zn(1)-Cl(3)	112.804(16)
Cl(4)-Zn(1)-Cl(2)	112.116(14)
Cl(5)-Zn(1)-Cl(2)	108.031(16)
Cl(3)-Zn(1)-Cl(2)	102.381(14)
O(1)-C(19)-N(6)	126.4(9)
O(1)-C(19)-H(19)	116.8
N(6)-C(19)-H(19)	116.8
C(19)-N(6)-C(17)	123.0(3)
C(19)-N(6)-C(18)	120.5(2)

C(17)-N(6)-C(18)	116.5(2)
N(6A)-C(18A)-H(18D)	109.5
N(6A)-C(18A)-H(18E)	109.5
H(18D)-C(18A)-H(18E)	109.5
N(6A)-C(18A)-H(18F)	109.5
H(18D)-C(18A)-H(18F)	109.5
H(18E)-C(18A)-H(18F)	109.5
N(6A)-C(17A)-H(17D)	109.5
N(6A)-C(17A)-H(17E)	109.5
H(17D)-C(17A)-H(17E)	109.5
N(6A)-C(17A)-H(17F)	109.5
H(17D)-C(17A)-H(17F)	109.5
H(17E)-C(17A)-H(17F)	109.5
O(1A)-C(19A)-N(6A)	128(4)
O(1A)-C(19A)-H(19A)	116.0
N(6A)-C(19A)-H(19A)	116.0
C(19A)-N(6A)-C(17A)	125.8(10)
C(19A)-N(6A)-C(18A)	117.6(9)
C(17A)-N(6A)-C(18A)	115.9(10)

Symmetry transformations used to generate equivalent atoms:

Table 4. Anisotropic displacement parameters ($Å^2 x\ 10^3$) for phw0907m. The anisotropic displacement factor exponent takes the form: $-2\pi^2[\ h^2\ a^{*2}U^{11} + ... + 2\ h\ k\ a^*\ b^*\ U^{12}\ ]$

	U^{11}	U^{22}	U^{33}	U^{23}	U^{13}	U^{12}
C(1)	30(1)	21(1)	31(1)	-5(1)	-4(1)	-5(1)
C(2)	29(1)	28(1)	31(1)	-10(1)	-1(1)	-9(1)
C(3)	21(1)	32(1)	23(1)	-7(1)	-1(1)	-9(1)
C(4)	21(1)	25(1)	21(1)	-2(1)	-2(1)	-6(1)
C(5)	20(1)	22(1)	20(1)	-5(1)	0(1)	-6(1)
C(6)	17(1)	21(1)	18(1)	-2(1)	-1(1)	-4(1)
C(7)	19(1)	19(1)	20(1)	-2(1)	-3(1)	-2(1)
C(8)	17(1)	21(1)	21(1)	-5(1)	0(1)	-3(1)
C(9)	21(1)	26(1)	21(1)	-4(1)	-5(1)	-1(1)
C(10)	22(1)	22(1)	21(1)	-1(1)	-5(1)	1(1)
C(11)	23(1)	22(1)	21(1)	-5(1)	-2(1)	-5(1)
C(12)	25(1)	38(1)	24(1)	-6(1)	0(1)	-10(1)
C(13)	33(1)	50(1)	27(1)	-11(1)	4(1)	-7(1)

C(14)	45(1)	52(1)	36(1)	-23(1)	3(1)	-7(1)
C(15)	41(1)	31(1)	35(1)	-18(1)	2(1)	-8(1)
C(16)	27(1)	35(1)	30(1)	-10(1)	-2(1)	-11(1)
N(1)	24(1)	21(1)	24(1)	-4(1)	-3(1)	-4(1)
N(2)	24(1)	17(1)	22(1)	-1(1)	-7(1)	-2(1)
N(3)	21(1)	18(1)	21(1)	-4(1)	-3(1)	-2(1)
N(4)	37(1)	46(1)	37(1)	-9(1)	-11(1)	-12(1)
N(5)	23(1)	25(1)	21(1)	-7(1)	-4(1)	-3(1)
Cl(2)	23(1)	26(1)	28(1)	1(1)	-2(1)	2(1)
Cl(3)	26(1)	21(1)	38(1)	2(1)	-12(1)	-4(1)
Cl(4)	30(1)	25(1)	34(1)	5(1)	-8(1)	-8(1)
Cl(5)	50(1)	32(1)	31(1)	-9(1)	-8(1)	-10(1)
Zn(1)	22(1)	20(1)	25(1)	-2(1)	-4(1)	-3(1)
C(17)	53(2)	95(2)	42(2)	-5(2)	-28(1)	-16(2)
C(18)	37(1)	52(2)	51(2)	0(1)	1(1)	7(1)
C(19)	32(1)	34(1)	25(1)	-1(1)	-7(1)	-6(1)
N(6)	28(1)	40(2)	26(1)	1(1)	-6(1)	-4(1)
O(1)	38(4)	40(2)	25(2)	5(2)	-10(4)	-14(4)
C(17A)	44(5)	107(9)	54(6)	25(6)	-18(4)	-6(5)
C(18A)	83(9)	180(17)	73(8)	-65(10)	-14(7)	-49(10)
C(19A)	49(4)	32(3)	30(3)	4(3)	-6(3)	-10(3)
N(6A)	28(1)	40(2)	26(1)	1(1)	-6(1)	-4(1)
O(1A)	24(6)	37(6)	31(11)	5(7)	-7(7)	-13(6)

Table 5. Hydrogen coordinates (x 10^4) and isotropic displacement parameters ($Å^2$x 10^3) for phw0907m.

	x	y	z	U(eq)
H(1)	2001	8154	5053	33
H(2)	3433	7916	6241	34
H(4)	4274	3675	6409	27
H(7)	2738	1587	4385	24
H(9)	-13	3732	2448	27
H(10)	-96	5794	2928	27
H(11A)	2239	321	3434	26
H(11B)	418	867	3180	26

H(12A)	4494	1105	2310	34
H(12B)	3574	2574	1787	34
H(13A)	5562	670	955	45
H(13B)	4097	1782	499	45
H(14A)	2866	61	501	52
H(14B)	4339	-1052	949	52
H(15A)	1408	-527	1789	42
H(15B)	2996	-1047	2307	42
H(2A)	3230(20)	2940(20)	5327(12)	32(5)
H(3)	1220(20)	5650(20)	4097(12)	29(4)
H(17A)	8930	2912	-1053	93
H(17B)	7805	4459	-1106	93
H(17C)	7101	3144	-583	93
H(18A)	8041	4684	1092	77
H(18B)	6552	4196	835	77
H(18C)	7153	5526	255	77
H(19)	10751	2440	-88	37
H(17D)	6554	5101	-523	112
H(17E)	6269	5302	482	112
H(17F)	5909	3947	220	112
H(18D)	9928	2173	-118	152
H(18E)	9304	3265	-956	152
H(18F)	8161	2281	-386	152
H(19A)	8623	4623	1169	45
H(5)	1480(20)	1698(19)	1814(12)	27(4)

Table 6. Torsion angles [°] for phw0907m.

N(1)-C(1)-C(2)-C(3)	-0.7(2)
C(1)-C(2)-C(3)-C(4)	0.9(2)
C(1)-C(2)-C(3)-C(16)	179.48(13)
C(2)-C(3)-C(4)-C(5)	-0.1(2)
C(16)-C(3)-C(4)-C(5)	-178.69(12)
C(3)-C(4)-C(5)-N(1)	-1.0(2)
C(3)-C(4)-C(5)-N(2)	178.59(12)
N(3)-C(6)-C(7)-C(8)	-0.31(19)
N(2)-C(6)-C(7)-C(8)	-179.27(12)

C(6)-C(7)-C(8)-C(9)	-0.79(19)
C(6)-C(7)-C(8)-C(11)	-179.45(11)
C(7)-C(8)-C(9)-C(10)	1.5(2)
C(11)-C(8)-C(9)-C(10)	-179.86(12)
C(8)-C(9)-C(10)-N(3)	-1.1(2)
C(7)-C(8)-C(11)-N(5)	-126.52(13)
C(9)-C(8)-C(11)-N(5)	54.83(16)
N(5)-C(12)-C(13)-C(14)	-22.80(18)
C(12)-C(13)-C(14)-C(15)	-0.5(2)
C(13)-C(14)-C(15)-N(5)	23.56(18)
N(2)-C(5)-N(1)-C(1)	-178.40(12)
C(4)-C(5)-N(1)-C(1)	1.2(2)
C(2)-C(1)-N(1)-C(5)	-0.3(2)
N(3)-C(6)-N(2)-C(5)	-4.5(2)
C(7)-C(6)-N(2)-C(5)	174.47(12)
N(1)-C(5)-N(2)-C(6)	0.5(2)
C(4)-C(5)-N(2)-C(6)	-179.10(13)
N(2)-C(6)-N(3)-C(10)	179.67(12)
C(7)-C(6)-N(3)-C(10)	0.73(19)
C(9)-C(10)-N(3)-C(6)	0.0(2)
C(8)-C(11)-N(5)-C(12)	53.74(15)
C(8)-C(11)-N(5)-C(15)	172.76(12)
C(13)-C(12)-N(5)-C(11)	161.34(12)
C(13)-C(12)-N(5)-C(15)	37.92(16)
C(14)-C(15)-N(5)-C(11)	-163.20(13)
C(14)-C(15)-N(5)-C(12)	-38.26(16)
O(1)-C(19)-N(6)-C(17)	176.5(13)
O(1)-C(19)-N(6)-C(18)	-3.1(13)
O(1A)-C(19A)-N(6A)-C(17A)	170(4)
O(1A)-C(19A)-N(6A)-C(18A)	1(4)

Symmetry transformations used to generate equivalent atoms:

Table 7. Hydrogen bonds for phw0907m [Å and °].

D-H...A	d(D-H)	d(H...A)	d(D...A)	<(DHA)
N(2)-H(2A)...Cl(2)#1	0.82(2)	2.39(2)	3.2130(12)	175.3(17)
N(3)-H(3)...N(1)	0.834(19)	2.015(18)	2.6643(16)	134.2(17)

N(3)-H(3)...Cl(3)#2	0.834(19)	2.556(19)	3.1969(12)	134.5(15)
N(5)-H(5)...O(1)#2	0.845(19)	1.90(2)	2.716(12)	160.8(18)
N(5)-H(5)...O(1A)#2	0.845(19)	1.90(4)	2.73(3)	167(2)

Symmetry transformations used to generate equivalent atoms:

#1 -x+1,-y+1,-z+1 #2 x-1,y,z

Crystallographic data for [dp(CN)(pyH)Ha][$Co(Cl)_4$]

Table 1. Crystal data and structure refinement for phw0909m.

Identification code	phw0909m	
Empirical formula	C19 H26 Cl4 Co N6 O	
Formula weight	555.19	
Temperature	110(2) K	
Wavelength	0.71073 Å	
Crystal system	Triclinic	
Space group	P-1	
Unit cell dimensions	a = 8.5434(10) Å	α= 78.621(2)°.
	b = 9.9845(12) Å	β= 81.064(2)°.
	c = 15.6817(19) Å	γ = 75.609(2)°.
Volume	1262.2(3) $Å^3$	
Z	2	
Density (calculated)	1.461 Mg/m^3	
Absorption coefficient	1.126 mm^{-1}	
F(000)	570	
Crystal size	0.45 x 0.04 x 0.03 mm^3	
Theta range for data collection	2.14 to 27.11°.	
Index ranges	-10<=h<=10, -12<=k<=12, -20<=l<=20	
Reflections collected	11967	
Independent reflections	5518 [R(int) = 0.0430]	
Completeness to theta = 27.11°	98.9 %	
Absorption correction	None	
Max. and min. transmission	0.9670 and 0.6312	
Refinement method	Full-matrix least-squares on F^2	
Data / restraints / parameters	5518 / 1 / 317	
Goodness-of-fit on F^2	0.987	
Final R indices [I>2sigma(I)]	R1 = 0.0418, wR2 = 0.0849	

R indices (all data)	R1 = 0.0824, wR2 = 0.0975
Largest diff. peak and hole	0.518 and -0.444 e.Å^{-3}

Table 2. Atomic coordinates (x 10^4) and equivalent isotropic displacement parameters ($Å^2$x 10^3) for phw0909m. U(eq) is defined as one third of the trace of the orthogonalized U^{ij} tensor.

	x	y	z	U(eq)
C(1)	2481(4)	7247(3)	5338(2)	28(1)
C(2)	3311(4)	7122(3)	6040(2)	28(1)
C(3)	3988(3)	5768(3)	6448(2)	24(1)
C(4)	3821(3)	4610(3)	6140(2)	22(1)
C(5)	2973(3)	4860(3)	5414(2)	21(1)
C(6)	478(3)	4930(3)	3223(2)	24(1)
C(7)	537(3)	3730(3)	2936(2)	23(1)
C(8)	1408(3)	2452(3)	3368(2)	20(1)
C(9)	2158(3)	2456(3)	4082(2)	20(1)
C(10)	2065(3)	3715(3)	4369(2)	19(1)
C(11)	4898(4)	5537(3)	7190(2)	31(1)
C(12)	1509(4)	1088(3)	3075(2)	23(1)
C(13)	3729(4)	1540(3)	1863(2)	30(1)
C(14)	4353(4)	1007(4)	1003(2)	39(1)
C(15)	3509(4)	-170(4)	1004(2)	46(1)
C(16)	2441(4)	-313(3)	1862(2)	37(1)
N(1)	2292(3)	6145(2)	5019(2)	23(1)
N(2)	2811(3)	3722(3)	5072(2)	21(1)
N(3)	1227(3)	4918(2)	3933(2)	20(1)
N(4)	5659(3)	5334(3)	7760(2)	39(1)
N(5)	2132(3)	1104(3)	2132(2)	25(1)
C(17)	-87(5)	6949(5)	9723(3)	37(1)
C(18)	2490(7)	5399(6)	9408(4)	59(2)
C(19)	1910(7)	6461(7)	10730(3)	67(2)
N(6)	1440(4)	6270(3)	9915(2)	42(1)
O(1)	-675(17)	6810(19)	9087(14)	34(3)
C(17A)	913(19)	6044(16)	9163(10)	37(1)
C(18A)	1000(20)	7310(20)	10320(13)	59(2)
C(19A)	3410(20)	5390(20)	9894(13)	72(7)
N(6A)	1440(4)	6270(3)	9915(2)	42(1)
O(1A)	-390(60)	6820(70)	8970(50)	34(11)
Cl(1)	7948(1)	11188(1)	2065(1)	32(1)
Cl(2)	5422(1)	9229(1)	3874(1)	29(1)
Cl(3)	9773(1)	8231(1)	3680(1)	30(1)
Cl(4)	7501(1)	7597(1)	1953(1)	38(1)

Co(1)	7675(1)	9080(1)	2838(1)	24(1)

Table 3. Bond lengths [Å] and angles [°] for phw0909m.

C(1)-N(1)	1.347(4)
C(1)-C(2)	1.370(4)
C(1)-H(1)	0.9500
C(2)-C(3)	1.399(4)
C(2)-H(2)	0.9500
C(3)-C(4)	1.382(4)
C(3)-C(11)	1.449(4)
C(4)-C(5)	1.393(4)
C(4)-H(4)	0.9500
C(5)-N(1)	1.340(3)
C(5)-N(2)	1.392(4)
C(6)-C(7)	1.348(4)
C(6)-N(3)	1.364(3)
C(6)-H(6)	0.9500
C(7)-C(8)	1.409(4)
C(7)-H(7)	0.9500
C(8)-C(9)	1.375(4)
C(8)-C(12)	1.500(4)
C(9)-C(10)	1.397(4)
C(9)-H(9)	0.9500
C(10)-N(3)	1.351(3)
C(10)-N(2)	1.358(3)
C(11)-N(4)	1.143(4)
C(12)-N(5)	1.490(4)
C(12)-H(12A)	0.9900
C(12)-H(12B)	0.9900
C(13)-N(5)	1.508(4)
C(13)-C(14)	1.517(4)
C(13)-H(13A)	0.9900
C(13)-H(13B)	0.9900
C(14)-C(15)	1.523(5)
C(14)-H(14A)	0.9900
C(14)-H(14B)	0.9900
C(15)-C(16)	1.506(5)

C(15)-H(15A)	0.9900
C(15)-H(15B)	0.9900
C(16)-N(5)	1.506(4)
C(16)-H(16A)	0.9900
C(16)-H(16B)	0.9900
N(2)-H(2A)	0.80(3)
N(3)-H(3)	0.9736
N(5)-H(5)	0.83(3)
C(17)-O(1)	1.230(17)
C(17)-N(6)	1.361(5)
C(17)-H(17A)	0.9500
C(18)-N(6)	1.363(6)
C(18)-H(18D)	0.9800
C(18)-H(18E)	0.9800
C(18)-H(18F)	0.9800
C(19)-N(6)	1.457(6)
C(19)-H(19D)	0.9800
C(19)-H(19E)	0.9800
C(19)-H(19F)	0.9800
C(17A)-O(1A)	1.230(18)
C(17A)-H(17)	0.9500
C(18A)-H(18A)	0.9800
C(18A)-H(18B)	0.9800
C(18A)-H(18C)	0.9800
C(19A)-H(19A)	0.9800
C(19A)-H(19B)	0.9800
C(19A)-H(19C)	0.9800
Cl(1)-Co(1)	2.2595(9)
Cl(2)-Co(1)	2.3122(9)
Cl(3)-Co(1)	2.2830(8)
Cl(4)-Co(1)	2.2640(9)

N(1)-C(1)-C(2)	123.8(3)
N(1)-C(1)-H(1)	118.1
C(2)-C(1)-H(1)	118.1
C(1)-C(2)-C(3)	117.5(3)
C(1)-C(2)-H(2)	121.3
C(3)-C(2)-H(2)	121.3
C(4)-C(3)-C(2)	120.5(3)
C(4)-C(3)-C(11)	118.3(3)

C(2)-C(3)-C(11)	121.3(3)
C(3)-C(4)-C(5)	117.2(3)
C(3)-C(4)-H(4)	121.4
C(5)-C(4)-H(4)	121.4
N(1)-C(5)-N(2)	117.5(2)
N(1)-C(5)-C(4)	123.6(3)
N(2)-C(5)-C(4)	118.9(2)
C(7)-C(6)-N(3)	120.8(3)
C(7)-C(6)-H(6)	119.6
N(3)-C(6)-H(6)	119.6
C(6)-C(7)-C(8)	119.4(3)
C(6)-C(7)-H(7)	120.3
C(8)-C(7)-H(7)	120.3
C(9)-C(8)-C(7)	119.1(3)
C(9)-C(8)-C(12)	119.4(2)
C(7)-C(8)-C(12)	121.4(3)
C(8)-C(9)-C(10)	120.3(2)
C(8)-C(9)-H(9)	119.9
C(10)-C(9)-H(9)	119.9
N(3)-C(10)-N(2)	120.9(3)
N(3)-C(10)-C(9)	118.7(2)
N(2)-C(10)-C(9)	120.4(2)
N(4)-C(11)-C(3)	177.8(4)
N(5)-C(12)-C(8)	112.7(2)
N(5)-C(12)-H(12A)	109.1
C(8)-C(12)-H(12A)	109.1
N(5)-C(12)-H(12B)	109.1
C(8)-C(12)-H(12B)	109.1
H(12A)-C(12)-H(12B)	107.8
N(5)-C(13)-C(14)	103.9(2)
N(5)-C(13)-H(13A)	111.0
C(14)-C(13)-H(13A)	111.0
N(5)-C(13)-H(13B)	111.0
C(14)-C(13)-H(13B)	111.0
H(13A)-C(13)-H(13B)	109.0
C(13)-C(14)-C(15)	106.1(3)
C(13)-C(14)-H(14A)	110.5
C(15)-C(14)-H(14A)	110.5
C(13)-C(14)-H(14B)	110.5
C(15)-C(14)-H(14B)	110.5

H(14A)-C(14)-H(14B)	108.7
C(16)-C(15)-C(14)	106.7(3)
C(16)-C(15)-H(15A)	110.4
C(14)-C(15)-H(15A)	110.4
C(16)-C(15)-H(15B)	110.4
C(14)-C(15)-H(15B)	110.4
H(15A)-C(15)-H(15B)	108.6
C(15)-C(16)-N(5)	103.9(3)
C(15)-C(16)-H(16A)	111.0
N(5)-C(16)-H(16A)	111.0
C(15)-C(16)-H(16B)	111.0
N(5)-C(16)-H(16B)	111.0
H(16A)-C(16)-H(16B)	109.0
C(5)-N(1)-C(1)	117.4(2)
C(10)-N(2)-C(5)	129.1(2)
C(10)-N(2)-H(2A)	113(2)
C(5)-N(2)-H(2A)	118(2)
C(10)-N(3)-C(6)	121.7(2)
C(10)-N(3)-H(3)	119.3
C(6)-N(3)-H(3)	118.7
C(12)-N(5)-C(16)	112.9(2)
C(12)-N(5)-C(13)	114.9(2)
C(16)-N(5)-C(13)	104.1(2)
C(12)-N(5)-H(5)	111(2)
C(16)-N(5)-H(5)	106(2)
C(13)-N(5)-H(5)	107(2)
O(1)-C(17)-N(6)	123.4(9)
O(1)-C(17)-H(17A)	118.3
N(6)-C(17)-H(17A)	118.3
C(17)-N(6)-C(18)	123.5(4)
C(17)-N(6)-C(19)	116.7(4)
C(18)-N(6)-C(19)	119.8(4)
O(1A)-C(17A)-H(17)	122.6
H(18A)-C(18A)-H(18B)	109.5
H(18A)-C(18A)-H(18C)	109.5
H(18B)-C(18A)-H(18C)	109.5
H(19A)-C(19A)-H(19B)	109.5
H(19A)-C(19A)-H(19C)	109.5
H(19B)-C(19A)-H(19C)	109.5
Cl(1)-Co(1)-Cl(4)	111.49(3)

Cl(1)-Co(1)-Cl(3)	108.27(3)
Cl(4)-Co(1)-Cl(3)	113.29(3)
Cl(1)-Co(1)-Cl(2)	113.02(3)
Cl(4)-Co(1)-Cl(2)	108.07(3)
Cl(3)-Co(1)-Cl(2)	102.45(3)

Symmetry transformations used to generate equivalent atoms:

Table 4. Anisotropic displacement parameters ($Å^2 x\ 10^3$) for phw0909m. The anisotropic displacement factor exponent takes the form: $-2\pi^2[\ h^2\ a^{*2}U^{11} + ... + 2\ h\ k\ a^*\ b^*\ U^{12}\ ]$

	U^{11}	U^{22}	U^{33}	U^{23}	U^{13}	U^{12}
C(1)	28(2)	20(2)	34(2)	-5(1)	-1(1)	-5(1)
C(2)	31(2)	24(2)	32(2)	-10(1)	-2(1)	-9(1)
C(3)	21(2)	30(2)	25(2)	-7(1)	0(1)	-8(1)
C(4)	20(2)	24(2)	22(2)	-2(1)	-2(1)	-4(1)
C(5)	20(2)	20(2)	20(2)	-4(1)	1(1)	-3(1)
C(6)	25(2)	23(2)	20(2)	-2(1)	-6(1)	2(1)
C(7)	23(2)	25(2)	20(2)	-6(1)	-4(1)	-1(1)
C(8)	15(1)	20(2)	22(2)	-5(1)	3(1)	-4(1)
C(9)	20(2)	16(1)	23(2)	-1(1)	-4(1)	-2(1)
C(10)	16(1)	20(2)	18(2)	-1(1)	-1(1)	-2(1)
C(11)	28(2)	37(2)	31(2)	-10(2)	0(2)	-12(1)
C(12)	23(2)	25(2)	21(2)	-7(1)	-1(1)	-4(1)
C(13)	26(2)	38(2)	25(2)	-4(1)	-2(1)	-9(1)
C(14)	38(2)	49(2)	28(2)	-9(2)	2(2)	-11(2)
C(15)	48(2)	55(2)	37(2)	-26(2)	3(2)	-5(2)
C(16)	45(2)	32(2)	37(2)	-19(2)	2(2)	-8(2)
N(1)	23(1)	20(1)	26(1)	-4(1)	-4(1)	-2(1)
N(2)	25(1)	16(1)	22(1)	-1(1)	-7(1)	-1(1)
N(3)	22(1)	16(1)	21(1)	-3(1)	-3(1)	-1(1)
N(4)	39(2)	47(2)	37(2)	-10(1)	-11(1)	-13(1)
N(5)	25(1)	26(1)	24(1)	-6(1)	-4(1)	-2(1)
C(17)	41(3)	33(2)	32(3)	1(2)	-5(2)	-6(2)
C(18)	51(3)	59(3)	58(3)	1(3)	-7(3)	1(3)
C(19)	64(4)	95(5)	45(3)	-4(3)	-23(3)	-18(3)
N(6)	48(2)	44(2)	35(2)	6(2)	-18(2)	-11(2)
O(1)	40(5)	43(4)	24(5)	3(3)	-10(6)	-18(3)

C(17A)	41(3)	33(2)	32(3)	1(2)	-5(2)	-6(2)
C(18A)	51(3)	59(3)	58(3)	1(3)	-7(3)	1(3)
C(19A)	46(11)	105(18)	54(12)	35(12)	-29(10)	-20(11)
N(6A)	48(2)	44(2)	35(2)	6(2)	-18(2)	-11(2)
O(1A)	31(14)	31(11)	30(20)	13(9)	-3(14)	-7(11)
Cl(1)	34(1)	25(1)	36(1)	4(1)	-9(1)	-9(1)
Cl(2)	26(1)	25(1)	30(1)	0(1)	-3(1)	3(1)
Cl(3)	29(1)	21(1)	40(1)	2(1)	-14(1)	-4(1)
Cl(4)	54(1)	31(1)	33(1)	-10(1)	-8(1)	-9(1)
Co(1)	24(1)	19(1)	27(1)	-2(1)	-5(1)	-3(1)

Table 5. Hydrogen coordinates (x 10^4) and isotropic displacement parameters ($Å^2$x 10^3) for phw0909m.

	x	y	z	U(eq)
H(1)	2012	8162	5059	33
H(2)	3424	7926	6243	34
H(4)	4266	3684	6413	27
H(6)	-94	5796	2928	29
H(7)	-3	3746	2447	28
H(9)	2740	1599	4382	24
H(12A)	2234	328	3432	28
H(12B)	415	880	3178	28
H(13A)	4495	1106	2306	36
H(13B)	3568	2572	1782	36
H(14A)	5548	650	960	46
H(14B)	4086	1768	503	46
H(15A)	2846	63	508	55
H(15B)	4322	-1057	951	55
H(16A)	3001	-1057	2301	44
H(16B)	1410	-536	1785	44
H(2A)	3220(40)	2960(30)	5300(20)	33(10)
H(3)	1255	5809	4087	24
H(5)	1470(40)	1640(40)	1810(20)	47(11)
H(17A)	-732	7562	10101	44
H(18D)	1908	5205	8971	89
H(18E)	2948	4518	9777	89
H(18F)	3370	5849	9110	89
H(19D)	2855	6887	10601	100
H(19E)	2188	5549	11108	100
H(19F)	1003	7076	11028	100
H(17)	1512	5345	8831	44
H(18A)	-19	7907	10122	89
H(18B)	1844	7848	10201	89
H(18C)	828	6970	10951	89
H(19A)	3602	4660	9532	108
H(19B)	3648	4963	10491	108
H(19C)	4110	6046	9648	108

Table 6. Torsion angles [°] for phw0909m.

N(1)-C(1)-C(2)-C(3)	-0.4(5)
C(1)-C(2)-C(3)-C(4)	0.4(4)
C(1)-C(2)-C(3)-C(11)	179.5(3)
C(2)-C(3)-C(4)-C(5)	0.5(4)
C(11)-C(3)-C(4)-C(5)	-178.6(3)
C(3)-C(4)-C(5)-N(1)	-1.6(4)
C(3)-C(4)-C(5)-N(2)	178.6(3)
N(3)-C(6)-C(7)-C(8)	-1.0(4)
C(6)-C(7)-C(8)-C(9)	1.0(4)
C(6)-C(7)-C(8)-C(12)	179.9(3)
C(7)-C(8)-C(9)-C(10)	-0.5(4)
C(12)-C(8)-C(9)-C(10)	-179.5(3)
C(8)-C(9)-C(10)-N(3)	0.1(4)
C(8)-C(9)-C(10)-N(2)	-179.7(3)
C(4)-C(3)-C(11)-N(4)	61(9)
C(2)-C(3)-C(11)-N(4)	-119(9)
C(9)-C(8)-C(12)-N(5)	-126.4(3)
C(7)-C(8)-C(12)-N(5)	54.7(4)
N(5)-C(13)-C(14)-C(15)	-22.4(3)
C(13)-C(14)-C(15)-C(16)	-0.9(4)
C(14)-C(15)-C(16)-N(5)	23.8(4)
N(2)-C(5)-N(1)-C(1)	-178.5(3)
C(4)-C(5)-N(1)-C(1)	1.6(4)
C(2)-C(1)-N(1)-C(5)	-0.6(4)
N(3)-C(10)-N(2)-C(5)	-5.5(5)
C(9)-C(10)-N(2)-C(5)	174.3(3)
N(1)-C(5)-N(2)-C(10)	1.2(4)
C(4)-C(5)-N(2)-C(10)	-179.0(3)
N(2)-C(10)-N(3)-C(6)	179.7(3)
C(9)-C(10)-N(3)-C(6)	-0.1(4)
C(7)-C(6)-N(3)-C(10)	0.6(4)
C(8)-C(12)-N(5)-C(16)	172.6(2)
C(8)-C(12)-N(5)-C(13)	53.4(3)
C(15)-C(16)-N(5)-C(12)	-163.3(3)
C(15)-C(16)-N(5)-C(13)	-38.1(3)
C(14)-C(13)-N(5)-C(12)	161.5(2)

C(14)-C(13)-N(5)-C(16)	37.5(3)
O(1)-C(17)-N(6)-C(18)	2.0(14)
O(1)-C(17)-N(6)-C(19)	-175.3(13)

Symmetry transformations used to generate equivalent atoms:

Table 7. Hydrogen bonds for phw0909m [Å and °].

D-H...A	d(D-H)	d(H...A)	d(D...A)	<(DHA)
N(5)-H(5)...O(1A)#1	0.83(3)	1.90(6)	2.71(4)	164(4)
N(5)-H(5)...O(1)#1	0.83(3)	1.94(4)	2.724(13)	157(4)

Symmetry transformations used to generate equivalent atoms:

#1 -x,-y+1,-z+1

Crystallographic data for tpzH-$CONH_2$

Table 8. Crystal data and structure refinement for phw0904m.

Identification code	phw0904m	
Empirical formula	C9 H10 N4 O4	
Formula weight	238.21	
Temperature	110(2) K	
Wavelength	0.71073 Å	
Crystal system	Monoclinic	
Space group	P2(1)/c	
Unit cell dimensions	a = 10.1467(8) Å	α= 90°.
	b = 4.9859(4) Å	β= 99.619(2)°.
	c = 19.8568(16) Å	γ = 90°.
Volume	990.44(14) $Å^3$	
Z	4	
Density (calculated)	1.598 Mg/m^3	
Absorption coefficient	0.128 mm^{-1}	
F(000)	496	
Crystal size	0.31 x 0.09 x 0.04 mm^3	
Theta range for data collection	2.04 to 28.28°.	
Index ranges	-13<=h<=13, -6<=k<=6, -26<=l<=26	
Reflections collected	9705	
Independent reflections	2467 [R(int) = 0.0212]	
Completeness to theta = 28.28°	100.0 %	
Absorption correction	Semi-empirical from equivalents	
Max. and min. transmission	1.000 and 0.874	
Refinement method	Full-matrix least-squares on F^2	
Data / restraints / parameters	2467 / 0 / 184	
Goodness-of-fit on F^2	1.053	
Final R indices [I>2sigma(I)]	R1 = 0.0530, wR2 = 0.1561	
R indices (all data)	R1 = 0.0624, wR2 = 0.1657	
Largest diff. peak and hole	0.507 and -0.436 $e.Å^{-3}$	

Table 9. Atomic coordinates (x 10^4) and equivalent isotropic displacement parameters ($Å^2$x 10^3) for phw0904m. U(eq) is defined as one third of the trace of the orthogonalized U^{ij} tensor.

	x	y	z	U(eq)
C(1)	3356(2)	8612(3)	1029(1)	24(1)
C(2)	4429(2)	10439(3)	1094(1)	29(1)
C(3)	4597(2)	12208(4)	1636(1)	35(1)
C(4)	3712(2)	12204(4)	2108(1)	34(1)
C(5)	2661(2)	10431(3)	2049(1)	30(1)
C(6)	2479(2)	8590(3)	1502(1)	23(1)
C(7)	1262(2)	4967(3)	907(1)	21(1)
C(8)	2160(2)	5010(3)	420(1)	21(1)
C(9)	1979(2)	2985(3)	-156(1)	23(1)
N(1)	3163(1)	6796(3)	483(1)	23(1)
N(2)	1444(1)	6774(3)	1427(1)	22(1)
N(3)	255(1)	3266(3)	898(1)	24(1)
N(4)	2790(2)	3082(4)	-616(1)	36(1)
O(1)	4004(2)	6944(3)	74(1)	46(1)
O(2)	615(1)	6688(3)	1878(1)	30(1)
O(3)	1084(1)	1309(3)	-184(1)	35(1)
O(4)	8496(2)	271(4)	1773(1)	41(1)

Table 10. Bond lengths [Å] and angles [°] for phw0904m.

C(1)-C(6)	1.398(2)
C(1)-N(1)	1.401(2)
C(1)-C(2)	1.409(2)
C(2)-C(3)	1.380(3)
C(2)-H(2)	0.9500
C(3)-C(4)	1.401(3)
C(3)-H(3)	0.9500
C(4)-C(5)	1.375(3)
C(4)-H(4)	0.9500
C(5)-C(6)	1.410(2)
C(5)-H(5)	0.9500
C(6)-N(2)	1.376(2)
C(7)-N(3)	1.326(2)

C(7)-N(2)	1.359(2)
C(7)-C(8)	1.436(2)
C(8)-N(1)	1.342(2)
C(8)-C(9)	1.513(2)
C(9)-O(3)	1.228(2)
C(9)-N(4)	1.329(2)
N(1)-O(1)	1.274(2)
N(2)-O(2)	1.3271(18)
N(3)-H(3A)	0.82(2)
N(3)-H(3B)	0.81(3)
N(4)-H(4A)	1.03(4)
N(4)-H(4B)	0.92(3)
O(4)-H(4C)	0.94(6)
O(4)-H(4D)	0.96(5)
O(4)-H(4E)	0.88(8)
O(4)-H(4F)	0.78(8)

C(6)-C(1)-N(1)	119.56(14)
C(6)-C(1)-C(2)	120.77(16)
N(1)-C(1)-C(2)	119.67(16)
C(3)-C(2)-C(1)	118.57(18)
C(3)-C(2)-H(2)	120.7
C(1)-C(2)-H(2)	120.7
C(2)-C(3)-C(4)	120.70(16)
C(2)-C(3)-H(3)	119.6
C(4)-C(3)-H(3)	119.6
C(5)-C(4)-C(3)	121.27(17)
C(5)-C(4)-H(4)	119.4
C(3)-C(4)-H(4)	119.4
C(4)-C(5)-C(6)	118.88(18)
C(4)-C(5)-H(5)	120.6
C(6)-C(5)-H(5)	120.6
N(2)-C(6)-C(1)	119.47(14)
N(2)-C(6)-C(5)	120.74(16)
C(1)-C(6)-C(5)	119.79(15)
N(3)-C(7)-N(2)	116.22(15)
N(3)-C(7)-C(8)	125.02(15)
N(2)-C(7)-C(8)	118.76(14)
N(1)-C(8)-C(7)	120.23(14)
N(1)-C(8)-C(9)	120.52(15)

C(7)-C(8)-C(9)	119.24(14)
O(3)-C(9)-N(4)	122.12(16)
O(3)-C(9)-C(8)	118.97(15)
N(4)-C(9)-C(8)	118.91(15)
O(1)-N(1)-C(8)	123.87(15)
O(1)-N(1)-C(1)	115.69(14)
C(8)-N(1)-C(1)	120.43(14)
O(2)-N(2)-C(7)	117.98(13)
O(2)-N(2)-C(6)	120.45(13)
C(7)-N(2)-C(6)	121.54(14)
C(7)-N(3)-H(3A)	117.8(15)
C(7)-N(3)-H(3B)	116.0(17)
H(3A)-N(3)-H(3B)	126(2)
C(9)-N(4)-H(4A)	123(2)
C(9)-N(4)-H(4B)	123.9(19)
H(4A)-N(4)-H(4B)	113(3)
H(4C)-O(4)-H(4D)	107(4)
H(4C)-O(4)-H(4E)	58(5)
H(4D)-O(4)-H(4E)	143(5)
H(4C)-O(4)-H(4F)	95(6)
H(4D)-O(4)-H(4F)	83(5)
H(4E)-O(4)-H(4F)	128(6)

Symmetry transformations used to generate equivalent atoms:

Table 11. Anisotropic displacement parameters ($Å^2 x\ 10^3$) for phw0904m. The anisotropic displacement factor exponent takes the form: $-2\pi^2[\ h^2\ a^{*2}U^{11} + ... + 2\ h\ k\ a^*\ b^*\ U^{12}\ ]$

	U^{11}	U^{22}	U^{33}	U^{23}	U^{13}	U^{12}
C(1)	25(1)	16(1)	28(1)	2(1)	-5(1)	2(1)
C(2)	28(1)	21(1)	36(1)	6(1)	-5(1)	-1(1)
C(3)	36(1)	19(1)	42(1)	5(1)	-16(1)	-6(1)
C(4)	46(1)	18(1)	31(1)	-2(1)	-15(1)	0(1)
C(5)	41(1)	20(1)	24(1)	-1(1)	-6(1)	4(1)
C(6)	28(1)	15(1)	24(1)	2(1)	-5(1)	3(1)
C(7)	24(1)	16(1)	23(1)	1(1)	-3(1)	3(1)
C(8)	23(1)	16(1)	23(1)	0(1)	-2(1)	2(1)
C(9)	24(1)	19(1)	26(1)	-1(1)	-2(1)	4(1)
N(1)	23(1)	19(1)	28(1)	1(1)	2(1)	1(1)
N(2)	26(1)	18(1)	21(1)	0(1)	1(1)	2(1)
N(3)	25(1)	21(1)	25(1)	-2(1)	3(1)	-2(1)
N(4)	33(1)	37(1)	39(1)	-11(1)	10(1)	-3(1)
O(1)	44(1)	43(1)	55(1)	-6(1)	17(1)	-5(1)
O(2)	36(1)	30(1)	25(1)	-2(1)	7(1)	1(1)
O(3)	43(1)	28(1)	32(1)	-7(1)	4(1)	-9(1)
O(4)	41(1)	51(1)	31(1)	-6(1)	6(1)	2(1)

Table 12. Hydrogen coordinates ($x\ 10^4$) and isotropic displacement parameters ($Å^2 x\ 10^{\ 3}$) for phw0904m.

	x	y	z	U(eq)
H(2)	5024	10453	772	35
H(3)	5320	13443	1690	42
H(4)	3841	13449	2475	41
H(5)	2067	10446	2372	36
H(3A)	-170(20)	3340(40)	1212(11)	22(5)
H(3B)	170(20)	2140(60)	600(14)	41(7)
H(4A)	2740(40)	1730(80)	-1010(20)	102(13)
H(4B)	3540(30)	4150(70)	-574(16)	65(9)
H(4C)	8630(50)	890(110)	2220(30)	49

H(4D)	9230(50)	-900(100)	1730(20)	49
H(4E)	8290(70)	1910(150)	1870(40)	49
H(4F)	8150(70)	-1060(150)	1850(40)	49

Table 13. Torsion angles [°] for phw0904m.

C(6)-C(1)-C(2)-C(3)	0.0(2)
N(1)-C(1)-C(2)-C(3)	179.97(14)
C(1)-C(2)-C(3)-C(4)	-0.6(2)
C(2)-C(3)-C(4)-C(5)	0.6(3)
C(3)-C(4)-C(5)-C(6)	0.0(3)
N(1)-C(1)-C(6)-N(2)	0.4(2)
C(2)-C(1)-C(6)-N(2)	-179.66(14)
N(1)-C(1)-C(6)-C(5)	-179.40(14)
C(2)-C(1)-C(6)-C(5)	0.5(2)
C(4)-C(5)-C(6)-N(2)	179.66(15)
C(4)-C(5)-C(6)-C(1)	-0.6(2)
N(3)-C(7)-C(8)-N(1)	-178.95(14)
N(2)-C(7)-C(8)-N(1)	0.4(2)
N(3)-C(7)-C(8)-C(9)	-0.2(2)
N(2)-C(7)-C(8)-C(9)	179.19(13)
N(1)-C(8)-C(9)-O(3)	177.11(15)
C(7)-C(8)-C(9)-O(3)	-1.6(2)
N(1)-C(8)-C(9)-N(4)	-3.0(2)
C(7)-C(8)-C(9)-N(4)	178.22(15)
C(7)-C(8)-N(1)-O(1)	179.48(15)
C(9)-C(8)-N(1)-O(1)	0.7(2)
C(7)-C(8)-N(1)-C(1)	0.8(2)
C(9)-C(8)-N(1)-C(1)	-177.91(13)
C(6)-C(1)-N(1)-O(1)	179.99(14)
C(2)-C(1)-N(1)-O(1)	0.0(2)
C(6)-C(1)-N(1)-C(8)	-1.2(2)
C(2)-C(1)-N(1)-C(8)	178.81(14)
N(3)-C(7)-N(2)-O(2)	0.2(2)
C(8)-C(7)-N(2)-O(2)	-179.29(13)
N(3)-C(7)-N(2)-C(6)	178.14(13)
C(8)-C(7)-N(2)-C(6)	-1.3(2)
C(1)-C(6)-N(2)-O(2)	178.83(13)

C(5)-C(6)-N(2)-O(2)	-1.4(2)
C(1)-C(6)-N(2)-C(7)	0.9(2)
C(5)-C(6)-N(2)-C(7)	-179.32(14)

Symmetry transformations used to generate equivalent atoms:

Table 14. Hydrogen bonds for phw0904m [Å and °].

D-H...A	d(D-H)	d(H...A)	d(D...A)	<(DHA)
O(4)-H(4D)...O(2)#1	0.96(5)	1.84(5)	2.776(2)	166(4)
O(4)-H(4C)...O(2)#2	0.94(6)	1.86(6)	2.772(2)	163(5)
N(4)-H(4B)...O(1)#3	0.92(3)	2.58(3)	3.251(3)	130(3)
N(4)-H(4B)...O(1)	0.92(3)	1.90(3)	2.557(2)	126(3)
N(4)-H(4A)...O(4)#4	1.03(4)	2.06(4)	2.963(2)	146(3)
N(3)-H(3B)...O(3)#5	0.81(3)	2.22(3)	2.901(2)	142(2)
N(3)-H(3B)...O(3)	0.81(3)	1.98(3)	2.622(2)	136(2)
N(3)-H(3A)...O(4)#6	0.82(2)	2.43(2)	3.079(2)	136.8(19)

Symmetry transformations used to generate equivalent atoms:

#1 x+1,y-1,z #2 -x+1,y-1/2,-z+1/2 #3 -x+1,-y+1,-z

#4 -x+1,-y,-z #5 -x,-y,-z #6 x-1,y,z

Crystallographic data for tpzH

Table 1. Crystal data and structure refinement for phw0915m.

Identification code	phw0915m	
Empirical formula	C8 H10 N4 O3	
Formula weight	210.20	
Temperature	110(2) K	
Wavelength	0.71073 Å	
Crystal system	Monoclinic	
Space group	P2(1)/c	
Unit cell dimensions	a = 7.0011(9) Å	α= 90°.
	b = 18.680(3) Å	β= 91.747(3)°.
	c = 7.2449(10) Å	γ = 90°.
Volume	947.0(2) $Å^3$	
Z	4	
Density (calculated)	1.474 Mg/m^3	
Absorption coefficient	0.116 mm^{-1}	
F(000)	440	
Crystal size	0.23 x 0.13 x 0.06 mm^3	
Theta range for data collection	2.18 to 28.28°.	
Index ranges	-9<=h<=9, -24<=k<=24, -9<=l<=9	
Reflections collected	9677	
Independent reflections	2350 [R(int) = 0.0384]	
Completeness to theta = 28.28°	99.8 %	
Absorption correction	Semi-empirical from equivalents	
Max. and min. transmission	0.993 and 0.773	
Refinement method	Full-matrix least-squares on F^2	
Data / restraints / parameters	2350 / 0 / 160	
Goodness-of-fit on F^2	1.056	
Final R indices [I>2sigma(I)]	R1 = 0.0446, wR2 = 0.1067	
R indices (all data)	R1 = 0.0592, wR2 = 0.1169	
Largest diff. peak and hole	0.291 and -0.247 $e.Å^{-3}$	

Table 2. Atomic coordinates (x 10^4) and equivalent isotropic displacement parameters ($Å^2$x 10^3) for phw0915m. U(eq) is defined as one third of the trace of the orthogonalized U^{ij} tensor.

	x	y	z	U(eq)
C(1)	6331(2)	6203(1)	3480(2)	19(1)
C(2)	5113(2)	7571(1)	3840(2)	18(1)
C(3)	4549(2)	8286(1)	4033(2)	21(1)
C(4)	2807(2)	8425(1)	4778(2)	24(1)
C(5)	1614(2)	7860(1)	5314(2)	23(1)
C(6)	2158(2)	7159(1)	5133(2)	21(1)
C(7)	3956(2)	7008(1)	4409(2)	17(1)
N(1)	4614(2)	6319(1)	4232(2)	18(1)
N(2)	6857(2)	7403(1)	3030(2)	19(1)
N(3)	6947(2)	5538(1)	3278(2)	24(1)
N(4)	7458(2)	6741(1)	2858(2)	20(1)
O(1)	3588(2)	5762(1)	4788(2)	24(1)
O(2)	7867(2)	7897(1)	2400(2)	25(1)
C(8A)	1190(20)	4578(9)	2150(20)	34(2)
C(8B)	1590(30)	4635(14)	1920(30)	42(4)
O(3)	793(2)	5309(1)	2425(2)	27(1)

Table 3. Bond lengths [Å] and angles [°] for phw0915m.

C(1)-N(3)	1.3241(19)
C(1)-N(1)	1.3527(19)
C(1)-N(4)	1.3624(18)
C(2)-C(7)	1.397(2)
C(2)-C(3)	1.402(2)
C(2)-N(2)	1.4061(18)
C(3)-C(4)	1.374(2)
C(3)-H(3)	0.9500
C(4)-C(5)	1.408(2)
C(4)-H(4)	0.9500
C(5)-C(6)	1.372(2)
C(5)-H(5)	0.9500
C(6)-C(7)	1.408(2)
C(6)-H(6)	0.9500

C(7)-N(1)	1.3740(18)
N(1)-O(1)	1.3330(15)
N(2)-O(2)	1.2574(15)
N(2)-N(4)	1.3130(17)
N(3)-H(3A)	0.93(2)
N(3)-H(3B)	0.89(2)
C(8A)-O(3)	1.409(18)
C(8A)-H(8A1)	0.9800
C(8A)-H(8A2)	0.9800
C(8A)-H(8A3)	0.9800
C(8B)-O(3)	1.43(3)
C(8B)-H(8B1)	0.9800
C(8B)-H(8B2)	0.9800
C(8B)-H(8B3)	0.9800
O(3)-H(3C)	0.87(2)

N(3)-C(1)-N(1)	119.40(13)
N(3)-C(1)-N(4)	117.50(13)
N(1)-C(1)-N(4)	123.08(13)
C(7)-C(2)-C(3)	121.35(13)
C(7)-C(2)-N(2)	118.29(13)
C(3)-C(2)-N(2)	120.35(13)
C(4)-C(3)-C(2)	118.45(14)
C(4)-C(3)-H(3)	120.8
C(2)-C(3)-H(3)	120.8
C(3)-C(4)-C(5)	120.49(14)
C(3)-C(4)-H(4)	119.8
C(5)-C(4)-H(4)	119.8
C(6)-C(5)-C(4)	121.42(14)
C(6)-C(5)-H(5)	119.3
C(4)-C(5)-H(5)	119.3
C(5)-C(6)-C(7)	118.74(14)
C(5)-C(6)-H(6)	120.6
C(7)-C(6)-H(6)	120.6
N(1)-C(7)-C(2)	118.58(13)
N(1)-C(7)-C(6)	121.90(13)
C(2)-C(7)-C(6)	119.52(13)
O(1)-N(1)-C(1)	119.38(12)
O(1)-N(1)-C(7)	121.15(12)
C(1)-N(1)-C(7)	119.47(12)

O(2)-N(2)-N(4)	118.14(12)
O(2)-N(2)-C(2)	119.52(12)
N(4)-N(2)-C(2)	122.31(12)
C(1)-N(3)-H(3A)	117.2(12)
C(1)-N(3)-H(3B)	118.2(13)
H(3A)-N(3)-H(3B)	121.7(18)
N(2)-N(4)-C(1)	118.20(12)
O(3)-C(8A)-H(8A1)	109.5
O(3)-C(8A)-H(8A2)	109.5
O(3)-C(8A)-H(8A3)	109.5
O(3)-C(8B)-H(8B1)	109.5
O(3)-C(8B)-H(8B2)	109.5
H(8B1)-C(8B)-H(8B2)	109.5
O(3)-C(8B)-H(8B3)	109.5
H(8B1)-C(8B)-H(8B3)	109.5
H(8B2)-C(8B)-H(8B3)	109.5
C(8A)-O(3)-C(8B)	13.9(11)
C(8A)-O(3)-H(3C)	108.1(17)
C(8B)-O(3)-H(3C)	102.8(19)

Symmetry transformations used to generate equivalent atoms:

Table 4. Anisotropic displacement parameters ($Å^2 x\ 10^3$) for phw0915m. The anisotropic displacement factor exponent takes the form: $-2\pi^2[\ h^2\ a^{*2}U^{11} + ... + 2\ h\ k\ a^*\ b^*\ U^{12}\ ]$

	U^{11}	U^{22}	U^{33}	U^{23}	U^{13}	U^{12}
C(1)	19(1)	20(1)	18(1)	1(1)	0(1)	0(1)
C(2)	17(1)	19(1)	17(1)	0(1)	1(1)	0(1)
C(3)	22(1)	19(1)	23(1)	-1(1)	0(1)	-1(1)
C(4)	26(1)	22(1)	24(1)	-3(1)	0(1)	4(1)
C(5)	19(1)	31(1)	19(1)	-2(1)	2(1)	4(1)
C(6)	17(1)	27(1)	19(1)	0(1)	1(1)	-2(1)
C(7)	17(1)	19(1)	16(1)	1(1)	-2(1)	-1(1)
N(1)	17(1)	18(1)	21(1)	2(1)	2(1)	-3(1)
N(2)	16(1)	18(1)	21(1)	1(1)	3(1)	-1(1)
N(3)	22(1)	19(1)	32(1)	3(1)	7(1)	1(1)
N(4)	19(1)	19(1)	22(1)	1(1)	4(1)	1(1)
O(1)	21(1)	19(1)	31(1)	5(1)	3(1)	-6(1)
O(2)	21(1)	21(1)	35(1)	4(1)	8(1)	-5(1)

C(8A)	33(5)	28(3)	42(3)	-8(2)	-7(3)	9(3)
C(8B)	31(7)	35(6)	59(10)	-25(6)	-18(5)	10(5)
O(3)	22(1)	22(1)	36(1)	-2(1)	0(1)	2(1)

Table 5. Hydrogen coordinates (x 10^4) and isotropic displacement parameters ($Å^2$x 10^3) for phw0915m.

	x	y	z	U(eq)
H(3)	5352	8665	3657	26
H(4)	2403	8907	4932	29
H(5)	407	7967	5813	27
H(6)	1336	6782	5491	25
H(3A)	8200(30)	5478(10)	2930(30)	34(5)
H(3B)	6300(30)	5186(11)	3810(30)	40(5)
H(8A1)	1101	4469	827	51
H(8A2)	267	4286	2805	51
H(8A3)	2486	4471	2625	51
H(8B1)	1619	4315	2996	63
H(8B2)	2895	4707	1503	63
H(8B3)	807	4421	925	63
H(3C)	1640(40)	5479(12)	3200(30)	54(7)

Table 6. Torsion angles [°] for phw0915m.

C(7)-C(2)-C(3)-C(4)	-0.8(2)
N(2)-C(2)-C(3)-C(4)	177.97(13)
C(2)-C(3)-C(4)-C(5)	-0.7(2)
C(3)-C(4)-C(5)-C(6)	0.8(2)
C(4)-C(5)-C(6)-C(7)	0.6(2)
C(3)-C(2)-C(7)-N(1)	-178.12(13)
N(2)-C(2)-C(7)-N(1)	3.06(19)
C(3)-C(2)-C(7)-C(6)	2.2(2)
N(2)-C(2)-C(7)-C(6)	-176.65(12)
C(5)-C(6)-C(7)-N(1)	178.30(13)
C(5)-C(6)-C(7)-C(2)	-2.0(2)
N(3)-C(1)-N(1)-O(1)	1.2(2)
N(4)-C(1)-N(1)-O(1)	179.20(12)
N(3)-C(1)-N(1)-C(7)	-178.69(13)
N(4)-C(1)-N(1)-C(7)	-0.7(2)
C(2)-C(7)-N(1)-O(1)	178.61(12)
C(6)-C(7)-N(1)-O(1)	-1.7(2)
C(2)-C(7)-N(1)-C(1)	-1.51(19)
C(6)-C(7)-N(1)-C(1)	178.19(13)
C(7)-C(2)-N(2)-O(2)	175.51(12)
C(3)-C(2)-N(2)-O(2)	-3.3(2)
C(7)-C(2)-N(2)-N(4)	-2.6(2)
C(3)-C(2)-N(2)-N(4)	178.55(13)
O(2)-N(2)-N(4)-C(1)	-177.67(12)
C(2)-N(2)-N(4)-C(1)	0.5(2)
N(3)-C(1)-N(4)-N(2)	179.26(13)
N(1)-C(1)-N(4)-N(2)	1.2(2)

Symmetry transformations used to generate equivalent atoms:

Table 7. Hydrogen bonds for phw0915m [Å and °].

D-H...A	d(D-H)	d(H...A)	d(D...A)	<(DHA)
O(3)-H(3C)...O(1)	0.87(2)	1.83(2)	2.6962(16)	174(2)
N(3)-H(3B)...O(1)#1	0.89(2)	2.04(2)	2.8347(17)	147.5(19)
N(3)-H(3A)...O(3)#2	0.93(2)	1.89(2)	2.8137(18)	174.5(17)

Symmetry transformations used to generate equivalent atoms:

#1 -x+1,-y+1,-z+1 #2 x+1,y,z

Crystallographic data for [Zn(tpz-CN)$_2$(DMF)]

Table 1. Crystal data and structure refinement for phw0901m.

Identification code	phw0901m	
Empirical formula	C22.83 H21.50 N9.17 O5.50 Zn	
Formula weight	577.72	
Temperature	110(2) K	
Wavelength	0.71073 Å	
Crystal system	Monoclinic	
Space group	P2(1)/n	
Unit cell dimensions	a = 9.8016(12) Å	α= 90°.
	b = 19.346(2) Å	β= 94.274(2)°.
	c = 12.6985(16) Å	γ = 90°.
Volume	2401.3(5) Å^3	
Z	4	
Density (calculated)	1.598 Mg/m^3	
Absorption coefficient	1.082 mm^{-1}	
F(000)	1186.7	
Crystal size	0.28 x 0.07 x 0.04 mm^3	
Theta range for data collection	1.92 to 28.30°.	
Index ranges	-13<=h<=13, -25<=k<=25, -16<=l<=16	
Reflections collected	24425	
Independent reflections	5949 [R(int) = 0.0286]	
Completeness to theta = 28.30°	99.9 %	
Absorption correction	Semi-empirical from equivalents	
Max. and min. transmission	0.958 and 0.847	
Refinement method	Full-matrix least-squares on F^2	
Data / restraints / parameters	5949 / 16 / 380	
Goodness-of-fit on F^2	1.121	
Final R indices [I>2sigma(I)]	R1 = 0.0471, wR2 = 0.1103	
R indices (all data)	R1 = 0.0581, wR2 = 0.1154	
Largest diff. peak and hole	0.929 and -0.484 e.Å^{-3}	

Table 2. Atomic coordinates (x 10^4) and equivalent isotropic displacement parameters ($Å^2$x 10^3) for phw0901m. U(eq) is defined as one third of the trace of the orthogonalized U^{ij} tensor.

	x	y	z	U(eq)
C(1)	8161(3)	1597(1)	4312(2)	23(1)
C(2)	8972(3)	2214(1)	4297(2)	25(1)
C(3)	7021(3)	2929(1)	4356(2)	26(1)
C(4)	6435(3)	3590(1)	4359(2)	33(1)
C(5)	5045(3)	3649(2)	4377(2)	35(1)
C(6)	4213(3)	3057(1)	4374(2)	30(1)
C(7)	4772(3)	2405(1)	4361(2)	25(1)
C(8)	6196(3)	2333(1)	4360(2)	22(1)
C(9)	10414(3)	2149(2)	4247(2)	30(1)
C(10)	6143(2)	-1007(1)	3497(2)	23(1)
C(11)	5306(2)	-1610(1)	3299(2)	22(1)
C(12)	7241(2)	-2338(1)	3251(2)	22(1)
C(13)	7797(3)	-3003(1)	3192(2)	26(1)
C(14)	9188(3)	-3076(1)	3192(2)	27(1)
C(15)	10035(3)	-2488(1)	3231(2)	25(1)
C(16)	9505(2)	-1835(1)	3308(2)	22(1)
C(17)	8084(2)	-1750(1)	3344(2)	20(1)
C(18)	3854(3)	-1539(1)	3182(2)	26(1)
C(19)	8287(3)	-108(1)	6461(2)	27(1)
C(20)	7408(3)	-980(2)	7607(3)	35(1)
C(21)	9690(3)	-447(2)	8028(2)	34(1)
N(1)	6780(2)	1687(1)	4337(2)	22(1)
N(2)	8438(2)	2854(1)	4311(2)	28(1)
N(3)	8615(2)	962(1)	4291(2)	28(1)
N(4)	11557(3)	2036(2)	4229(2)	41(1)
N(5)	7529(2)	-1109(1)	3489(2)	22(1)
N(6)	5814(2)	-2250(1)	3205(2)	21(1)
N(7)	5711(2)	-383(1)	3668(2)	29(1)
N(8)	2699(2)	-1441(1)	3071(2)	37(1)
N(9)	8452(2)	-495(1)	7314(2)	28(1)
O(1)	5976(2)	1127(1)	4322(2)	26(1)
O(2)	9204(2)	3390(1)	4284(2)	40(1)
O(3)	8357(2)	-558(1)	3666(2)	29(1)
O(4)	5028(2)	-2776(1)	3070(2)	28(1)
O(5)	7233(2)	-116(1)	5843(2)	32(1)

Zn(1)	7173(1)	238(1)	4295(1)	25(1)
C(22)	2796(7)	4586(5)	5263(8)	40(2)
C(23)	1644(11)	4864(12)	5857(8)	125(8)
O(6)	453(7)	4940(4)	5159(6)	41(3)
C(24)	-615(11)	5221(10)	5742(10)	100(6)
C(25)	-1886(15)	5320(20)	5011(18)	202(16)
C(26)	783(12)	4896(7)	5361(10)	11(3)
C(27)	-480(20)	4906(14)	3657(11)	77(12)
C(28)	-1492(13)	5370(9)	5350(13)	30(4)
N(10)	-407(15)	5060(11)	4780(10)	130(20)
O(7)	833(17)	5032(8)	6314(10)	53(5)

Table 3. Bond lengths [Å] and angles [°] for phw0901m.

C(1)-N(3)	1.308(3)
C(1)-N(1)	1.368(3)
C(1)-C(2)	1.434(3)
C(2)-N(2)	1.345(4)
C(2)-C(9)	1.425(4)
C(3)-C(4)	1.401(4)
C(3)-N(2)	1.402(4)
C(3)-C(8)	1.409(4)
C(4)-C(5)	1.369(4)
C(4)-H(4)	0.9500
C(5)-C(6)	1.405(4)
C(5)-H(5)	0.9500
C(6)-C(7)	1.377(4)
C(6)-H(6)	0.9500
C(7)-C(8)	1.403(4)
C(7)-H(7)	0.9500
C(8)-N(1)	1.374(3)
C(9)-N(4)	1.144(4)
C(10)-N(7)	1.303(3)
C(10)-N(5)	1.373(3)
C(10)-C(11)	1.437(3)
C(11)-N(6)	1.344(3)
C(11)-C(18)	1.427(3)
C(12)-C(13)	1.401(4)

C(12)-N(6)	1.405(3)
C(12)-C(17)	1.406(3)
C(13)-C(14)	1.370(4)
C(13)-H(13)	0.9500
C(14)-C(15)	1.407(4)
C(14)-H(14)	0.9500
C(15)-C(16)	1.373(4)
C(15)-H(15)	0.9500
C(16)-C(17)	1.406(3)
C(16)-H(16)	0.9500
C(17)-N(5)	1.372(3)
C(18)-N(8)	1.146(3)
C(19)-O(5)	1.250(3)
C(19)-N(9)	1.317(4)
C(19)-H(19)	0.9500
C(20)-N(9)	1.457(4)
C(20)-H(20A)	0.9800
C(20)-H(20B)	0.9800
C(20)-H(20C)	0.9800
C(21)-N(9)	1.463(4)
C(21)-H(21A)	0.9800
C(21)-H(21B)	0.9800
C(21)-H(21C)	0.9800
N(1)-O(1)	1.340(3)
N(2)-O(2)	1.282(3)
N(3)-Zn(1)	1.990(2)
N(3)-H(3)	0.82(4)
N(5)-O(3)	1.348(3)
N(6)-O(4)	1.280(3)
N(7)-Zn(1)	1.989(2)
N(7)-H(7A)	0.84(4)
O(1)-Zn(1)	2.0838(18)
O(3)-Zn(1)	2.1196(19)
O(5)-Zn(1)	2.078(2)
C(22)-C(23)	1.503(5)
C(22)-H(22A)	0.9800
C(22)-H(22B)	0.9800
C(22)-H(22C)	0.9800
C(23)-O(6)	1.419(5)
C(23)-H(23A)	0.9900

C(23)-H(23B)	0.9900
O(6)-C(24)	1.435(5)
C(24)-C(25)	1.510(5)
C(24)-H(24A)	0.9900
C(24)-H(24B)	0.9900
C(25)-H(25A)	0.9800
C(25)-H(25B)	0.9800
C(25)-H(25C)	0.9800
C(26)-O(7)	1.235(5)
C(26)-N(10)	1.371(5)
C(26)-H(26)	0.9500
C(27)-N(10)	1.453(5)
C(27)-H(27A)	0.9800
C(27)-H(27B)	0.9800
C(27)-H(27C)	0.9800
C(28)-N(10)	1.459(5)
C(28)-H(28A)	0.9800
C(28)-H(28B)	0.9800
C(28)-H(28C)	0.9800

N(3)-C(1)-N(1)	117.3(2)
N(3)-C(1)-C(2)	126.3(2)
N(1)-C(1)-C(2)	116.4(2)
N(2)-C(2)-C(9)	118.0(2)
N(2)-C(2)-C(1)	123.3(2)
C(9)-C(2)-C(1)	118.7(2)
C(4)-C(3)-N(2)	120.2(2)
C(4)-C(3)-C(8)	120.7(3)
N(2)-C(3)-C(8)	119.1(2)
C(5)-C(4)-C(3)	119.0(3)
C(5)-C(4)-H(4)	120.5
C(3)-C(4)-H(4)	120.5
C(4)-C(5)-C(6)	120.6(3)
C(4)-C(5)-H(5)	119.7
C(6)-C(5)-H(5)	119.7
C(7)-C(6)-C(5)	121.1(3)
C(7)-C(6)-H(6)	119.5
C(5)-C(6)-H(6)	119.5
C(6)-C(7)-C(8)	119.2(3)
C(6)-C(7)-H(7)	120.4

C(8)-C(7)-H(7)	120.4
N(1)-C(8)-C(7)	120.4(2)
N(1)-C(8)-C(3)	120.2(2)
C(7)-C(8)-C(3)	119.3(2)
N(4)-C(9)-C(2)	173.8(3)
N(7)-C(10)-N(5)	117.9(2)
N(7)-C(10)-C(11)	126.4(2)
N(5)-C(10)-C(11)	115.7(2)
N(6)-C(11)-C(18)	116.9(2)
N(6)-C(11)-C(10)	123.6(2)
C(18)-C(11)-C(10)	119.5(2)
C(13)-C(12)-N(6)	120.0(2)
C(13)-C(12)-C(17)	121.2(2)
N(6)-C(12)-C(17)	118.8(2)
C(14)-C(13)-C(12)	119.1(2)
C(14)-C(13)-H(13)	120.5
C(12)-C(13)-H(13)	120.5
C(13)-C(14)-C(15)	120.1(2)
C(13)-C(14)-H(14)	120.0
C(15)-C(14)-H(14)	120.0
C(16)-C(15)-C(14)	121.4(2)
C(16)-C(15)-H(15)	119.3
C(14)-C(15)-H(15)	119.3
C(15)-C(16)-C(17)	119.4(2)
C(15)-C(16)-H(16)	120.3
C(17)-C(16)-H(16)	120.3
N(5)-C(17)-C(12)	120.4(2)
N(5)-C(17)-C(16)	120.9(2)
C(12)-C(17)-C(16)	118.7(2)
N(8)-C(18)-C(11)	175.8(3)
O(5)-C(19)-N(9)	123.7(2)
O(5)-C(19)-H(19)	118.2
N(9)-C(19)-H(19)	118.2
N(9)-C(20)-H(20A)	109.5
N(9)-C(20)-H(20B)	109.5
H(20A)-C(20)-H(20B)	109.5
N(9)-C(20)-H(20C)	109.5
H(20A)-C(20)-H(20C)	109.5
H(20B)-C(20)-H(20C)	109.5
N(9)-C(21)-H(21A)	109.5

N(9)-C(21)-H(21B)	109.5
H(21A)-C(21)-H(21B)	109.5
N(9)-C(21)-H(21C)	109.5
H(21A)-C(21)-H(21C)	109.5
H(21B)-C(21)-H(21C)	109.5
O(1)-N(1)-C(1)	118.6(2)
O(1)-N(1)-C(8)	119.3(2)
C(1)-N(1)-C(8)	122.1(2)
O(2)-N(2)-C(2)	121.0(2)
O(2)-N(2)-C(3)	120.1(2)
C(2)-N(2)-C(3)	118.9(2)
C(1)-N(3)-Zn(1)	114.77(18)
C(1)-N(3)-H(3)	113(3)
Zn(1)-N(3)-H(3)	132(3)
O(3)-N(5)-C(17)	119.79(19)
O(3)-N(5)-C(10)	118.0(2)
C(17)-N(5)-C(10)	122.2(2)
O(4)-N(6)-C(11)	121.4(2)
O(4)-N(6)-C(12)	119.8(2)
C(11)-N(6)-C(12)	118.8(2)
C(10)-N(7)-Zn(1)	113.07(18)
C(10)-N(7)-H(7A)	117(2)
Zn(1)-N(7)-H(7A)	124(2)
C(19)-N(9)-C(20)	122.1(2)
C(19)-N(9)-C(21)	121.3(2)
C(20)-N(9)-C(21)	116.6(2)
N(1)-O(1)-Zn(1)	109.72(14)
N(5)-O(3)-Zn(1)	107.30(13)
C(19)-O(5)-Zn(1)	123.60(18)
N(7)-Zn(1)-N(3)	156.05(11)
N(7)-Zn(1)-O(5)	98.58(9)
N(3)-Zn(1)-O(5)	105.32(9)
N(7)-Zn(1)-O(1)	96.58(8)
N(3)-Zn(1)-O(1)	79.60(8)
O(5)-Zn(1)-O(1)	103.46(8)
N(7)-Zn(1)-O(3)	79.01(8)
N(3)-Zn(1)-O(3)	95.84(8)
O(5)-Zn(1)-O(3)	98.03(8)
O(1)-Zn(1)-O(3)	158.48(8)
O(6)-C(23)-C(22)	109.7(5)

O(6)-C(23)-H(23A)	109.7
C(22)-C(23)-H(23A)	109.7
O(6)-C(23)-H(23B)	109.7
C(22)-C(23)-H(23B)	109.7
H(23A)-C(23)-H(23B)	108.2
C(23)-O(6)-C(24)	108.3(5)
O(6)-C(24)-C(25)	109.3(5)
O(6)-C(24)-H(24A)	109.8
C(25)-C(24)-H(24A)	109.8
O(6)-C(24)-H(24B)	109.8
C(25)-C(24)-H(24B)	109.8
H(24A)-C(24)-H(24B)	108.3
O(7)-C(26)-N(10)	116.6(6)
O(7)-C(26)-H(26)	121.7
N(10)-C(26)-H(26)	121.7
N(10)-C(27)-H(27A)	109.5
N(10)-C(27)-H(27B)	109.5
H(27A)-C(27)-H(27B)	109.5
N(10)-C(27)-H(27C)	109.5
H(27A)-C(27)-H(27C)	109.5
H(27B)-C(27)-H(27C)	109.5
N(10)-C(28)-H(28A)	109.5
N(10)-C(28)-H(28B)	109.5
H(28A)-C(28)-H(28B)	109.5
N(10)-C(28)-H(28C)	109.5
H(28A)-C(28)-H(28C)	109.5
H(28B)-C(28)-H(28C)	109.5
C(26)-N(10)-C(27)	117.2(6)
C(26)-N(10)-C(28)	116.7(6)
C(27)-N(10)-C(28)	126.1(9)

Symmetry transformations used to generate equivalent atoms:

Table 4. Anisotropic displacement parameters ($Å^2 x\ 10^3$) for phw0901m. The anisotropic displacement factor exponent takes the form: $-2\pi^2[\ h^2\ a^{*2}U^{11} + ... + 2\ h\ k\ a^*\ b^*\ U^{12}\ ]$

	U^{11}	U^{22}	U^{33}	U^{23}	U^{13}	U^{12}
C(1)	23(1)	26(1)	19(1)	-2(1)	-1(1)	-4(1)

C(2)	25(1)	29(1)	22(1)	0(1)	0(1)	-6(1)
C(3)	34(1)	24(1)	21(1)	1(1)	2(1)	-4(1)
C(4)	48(2)	22(1)	29(2)	-1(1)	4(1)	-6(1)
C(5)	53(2)	23(1)	31(2)	0(1)	9(1)	8(1)
C(6)	37(2)	28(1)	25(1)	1(1)	7(1)	7(1)
C(7)	29(1)	24(1)	23(1)	2(1)	3(1)	1(1)
C(8)	28(1)	21(1)	18(1)	0(1)	2(1)	-2(1)
C(9)	30(1)	36(2)	23(1)	0(1)	0(1)	-12(1)
C(10)	19(1)	25(1)	26(1)	0(1)	0(1)	-2(1)
C(11)	20(1)	26(1)	22(1)	0(1)	0(1)	-4(1)
C(12)	22(1)	24(1)	20(1)	0(1)	1(1)	-2(1)
C(13)	30(1)	22(1)	25(1)	0(1)	4(1)	-3(1)
C(14)	29(1)	25(1)	27(1)	0(1)	1(1)	4(1)
C(15)	22(1)	31(1)	23(1)	-2(1)	2(1)	4(1)
C(16)	20(1)	27(1)	20(1)	-1(1)	1(1)	-2(1)
C(17)	20(1)	22(1)	19(1)	0(1)	0(1)	-2(1)
C(18)	23(1)	28(1)	29(1)	-5(1)	2(1)	-5(1)
C(19)	23(1)	21(1)	38(2)	1(1)	7(1)	2(1)
C(20)	33(2)	35(2)	39(2)	4(1)	9(1)	-5(1)
C(21)	33(2)	31(1)	37(2)	4(1)	-3(1)	1(1)
N(1)	22(1)	21(1)	24(1)	1(1)	1(1)	-3(1)
N(2)	35(1)	25(1)	25(1)	0(1)	-1(1)	-10(1)
N(3)	20(1)	26(1)	37(1)	-3(1)	2(1)	-2(1)
N(4)	29(1)	61(2)	31(1)	-2(1)	2(1)	-11(1)
N(5)	18(1)	22(1)	27(1)	-2(1)	2(1)	-3(1)
N(6)	21(1)	24(1)	19(1)	-2(1)	2(1)	-5(1)
N(7)	18(1)	25(1)	44(1)	-5(1)	1(1)	1(1)
N(8)	23(1)	42(1)	47(2)	-13(1)	1(1)	-3(1)
N(9)	25(1)	25(1)	33(1)	3(1)	4(1)	-1(1)
O(1)	21(1)	18(1)	39(1)	0(1)	0(1)	-4(1)
O(2)	43(1)	29(1)	46(1)	0(1)	2(1)	-20(1)
O(3)	20(1)	21(1)	46(1)	-6(1)	4(1)	-6(1)
O(4)	26(1)	26(1)	33(1)	-4(1)	3(1)	-11(1)
O(5)	24(1)	33(1)	38(1)	3(1)	1(1)	0(1)
Zn(1)	21(1)	20(1)	35(1)	-1(1)	0(1)	-1(1)

Table 5. Hydrogen coordinates (x 10^4) and isotropic displacement parameters ($Å^2$x 10^{3}) for phw0901m.

	x	y	z	U(eq)
H(4)	6994	3990	4350	40
H(5)	4638	4094	4390	42
H(6)	3250	3108	4382	36
H(7)	4199	2008	4353	30
H(13)	7219	-3397	3153	31
H(14)	9580	-3524	3166	33
H(15)	10994	-2544	3204	30
H(16)	10092	-1443	3337	27
H(19)	9010	194	6306	32
H(20A)	6609	-949	7097	53
H(20B)	7136	-866	8314	53
H(20C)	7776	-1451	7608	53
H(21A)	10339	-129	7731	51
H(21B)	10109	-906	8115	51
H(21C)	9452	-275	8716	51
H(3)	9450(40)	940(19)	4270(30)	47(11)
H(7A)	4880(40)	-337(17)	3750(30)	38(9)
H(22A)	2487	4535	4515	60
H(22B)	3080	4135	5554	60
H(22C)	3570	4907	5333	60
H(23A)	1454	4543	6436	150
H(23B)	1906	5317	6172	150
H(24A)	-320	5671	6055	120
H(24B)	-812	4904	6323	120
H(25A)	-1625	5437	4303	303
H(25B)	-2439	5695	5276	303
H(25C)	-2421	4891	4978	303
H(26)	1531	4687	5048	13
H(27A)	-1195	4563	3489	115
H(27B)	405	4721	3472	115
H(27C)	-686	5330	3254	115
H(28A)	-1240	5845	5549	45
H(28B)	-1618	5099	5988	45
H(28C)	-2346	5372	4897	45

Table 6. Torsion angles [°] for phw0901m.

N(3)-C(1)-C(2)-N(2)	179.4(3)
N(1)-C(1)-C(2)-N(2)	0.3(4)
N(3)-C(1)-C(2)-C(9)	0.4(4)
N(1)-C(1)-C(2)-C(9)	-178.7(2)
N(2)-C(3)-C(4)-C(5)	178.4(3)
C(8)-C(3)-C(4)-C(5)	0.7(4)
C(3)-C(4)-C(5)-C(6)	-1.0(4)
C(4)-C(5)-C(6)-C(7)	0.4(4)
C(5)-C(6)-C(7)-C(8)	0.6(4)
C(6)-C(7)-C(8)-N(1)	-179.4(2)
C(6)-C(7)-C(8)-C(3)	-0.9(4)
C(4)-C(3)-C(8)-N(1)	178.8(2)
N(2)-C(3)-C(8)-N(1)	1.1(4)
C(4)-C(3)-C(8)-C(7)	0.3(4)
N(2)-C(3)-C(8)-C(7)	-177.4(2)
N(7)-C(10)-C(11)-N(6)	-174.9(3)
N(5)-C(10)-C(11)-N(6)	5.9(4)
N(7)-C(10)-C(11)-C(18)	5.7(4)
N(5)-C(10)-C(11)-C(18)	-173.4(2)
N(6)-C(12)-C(13)-C(14)	177.2(2)
C(17)-C(12)-C(13)-C(14)	-2.1(4)
C(12)-C(13)-C(14)-C(15)	-1.2(4)
C(13)-C(14)-C(15)-C(16)	2.4(4)
C(14)-C(15)-C(16)-C(17)	-0.3(4)
C(13)-C(12)-C(17)-N(5)	-174.5(2)
N(6)-C(12)-C(17)-N(5)	6.2(4)
C(13)-C(12)-C(17)-C(16)	4.1(4)
N(6)-C(12)-C(17)-C(16)	-175.2(2)
C(15)-C(16)-C(17)-N(5)	175.8(2)
C(15)-C(16)-C(17)-C(12)	-2.8(4)
N(3)-C(1)-N(1)-O(1)	-1.1(3)
C(2)-C(1)-N(1)-O(1)	178.1(2)
N(3)-C(1)-N(1)-C(8)	-179.9(2)
C(2)-C(1)-N(1)-C(8)	-0.7(4)
C(7)-C(8)-N(1)-O(1)	-0.3(4)
C(3)-C(8)-N(1)-O(1)	-178.8(2)
C(7)-C(8)-N(1)-C(1)	178.5(2)
C(3)-C(8)-N(1)-C(1)	0.0(4)

C(9)-C(2)-N(2)-O(2)	-0.2(4)
C(1)-C(2)-N(2)-O(2)	-179.2(2)
C(9)-C(2)-N(2)-C(3)	179.8(2)
C(1)-C(2)-N(2)-C(3)	0.8(4)
C(4)-C(3)-N(2)-O(2)	0.8(4)
C(8)-C(3)-N(2)-O(2)	178.5(2)
C(4)-C(3)-N(2)-C(2)	-179.2(2)
C(8)-C(3)-N(2)-C(2)	-1.5(4)
N(1)-C(1)-N(3)-Zn(1)	0.2(3)
C(2)-C(1)-N(3)-Zn(1)	-178.9(2)
C(12)-C(17)-N(5)-O(3)	174.4(2)
C(16)-C(17)-N(5)-O(3)	-4.2(4)
C(12)-C(17)-N(5)-C(10)	-3.3(4)
C(16)-C(17)-N(5)-C(10)	178.1(2)
N(7)-C(10)-N(5)-O(3)	0.5(4)
C(11)-C(10)-N(5)-O(3)	179.7(2)
N(7)-C(10)-N(5)-C(17)	178.2(2)
C(11)-C(10)-N(5)-C(17)	-2.5(4)
C(18)-C(11)-N(6)-O(4)	-3.4(4)
C(10)-C(11)-N(6)-O(4)	177.2(2)
C(18)-C(11)-N(6)-C(12)	176.2(2)
C(10)-C(11)-N(6)-C(12)	-3.2(4)
C(13)-C(12)-N(6)-O(4)	-2.6(3)
C(17)-C(12)-N(6)-O(4)	176.7(2)
C(13)-C(12)-N(6)-C(11)	177.8(2)
C(17)-C(12)-N(6)-C(11)	-3.0(3)
N(5)-C(10)-N(7)-Zn(1)	-17.0(3)
C(11)-C(10)-N(7)-Zn(1)	163.9(2)
O(5)-C(19)-N(9)-C(20)	0.8(4)
O(5)-C(19)-N(9)-C(21)	-177.9(3)
C(1)-N(1)-O(1)-Zn(1)	1.3(3)
C(8)-N(1)-O(1)-Zn(1)	-179.80(18)
C(17)-N(5)-O(3)-Zn(1)	-163.15(18)
C(10)-N(5)-O(3)-Zn(1)	14.6(3)
N(9)-C(19)-O(5)-Zn(1)	-160.0(2)
C(10)-N(7)-Zn(1)-N(3)	98.3(3)
C(10)-N(7)-Zn(1)-O(5)	-77.8(2)
C(10)-N(7)-Zn(1)-O(1)	177.5(2)
C(10)-N(7)-Zn(1)-O(3)	18.8(2)
C(1)-N(3)-Zn(1)-N(7)	83.1(3)

C(1)-N(3)-Zn(1)-O(5)	-100.8(2)
C(1)-N(3)-Zn(1)-O(1)	0.40(19)
C(1)-N(3)-Zn(1)-O(3)	159.2(2)
C(19)-O(5)-Zn(1)-N(7)	150.0(2)
C(19)-O(5)-Zn(1)-N(3)	-28.4(2)
C(19)-O(5)-Zn(1)-O(1)	-111.1(2)
C(19)-O(5)-Zn(1)-O(3)	70.0(2)
N(1)-O(1)-Zn(1)-N(7)	-157.00(16)
N(1)-O(1)-Zn(1)-N(3)	-0.91(16)
N(1)-O(1)-Zn(1)-O(5)	102.52(16)
N(1)-O(1)-Zn(1)-O(3)	-80.3(2)
N(5)-O(3)-Zn(1)-N(7)	-17.55(16)
N(5)-O(3)-Zn(1)-N(3)	-173.90(16)
N(5)-O(3)-Zn(1)-O(5)	79.69(16)
N(5)-O(3)-Zn(1)-O(1)	-97.5(2)
C(22)-C(23)-O(6)-C(24)	-178.6(15)
C(23)-O(6)-C(24)-C(25)	179(2)
O(7)-C(26)-N(10)-C(27)	179.7(13)
O(7)-C(26)-N(10)-C(28)	-0.9(19)

Symmetry transformations used to generate equivalent atoms:

Table 7. Hydrogen bonds for phw0901m [Å and °].

D-H...A	d(D-H)	d(H...A)	d(D...A)	<(DHA)
N(7)-H(7A)...O(5)#1	0.84(4)	2.34(4)	3.148(3)	163(3)

Symmetry transformations used to generate equivalent atoms:

#1 -x+1,-y,-z+1

Crystallographic data for [Cu(tpz-CN)(dpHa)(H_2O)]Cl

Table 1. Crystal data and structure refinement for phw0911ma.

Identification code	phw0911ma	
Empirical formula	C19 H16 Cl Cu N7 O3	
Formula weight	489.38	
Temperature	110(2) K	
Wavelength	0.71073 Å	
Crystal system	Monoclinic	
Space group	P2(1)/c	
Unit cell dimensions	a = 13.7739(5) Å	α= 90°.
	b = 15.9937(6) Å	β= 92.4990(10)°.
	c = 8.6766(3) Å	γ = 90°.
Volume	1909.60(12) $Å^3$	
Z	4	
Density (calculated)	1.702 Mg/m^3	
Absorption coefficient	1.324 mm^{-1}	
F(000)	996	
Crystal size	0.33 x 0.06 x 0.03 mm^3	
Theta range for data collection	1.48 to 28.30°.	
Index ranges	-18<=h<=18, -21<=k<=21, -11<=l<=11	
Reflections collected	25950	
Independent reflections	4749 [R(int) = 0.0344]	
Completeness to theta = 28.30°	100.0 %	
Absorption correction	Semi-empirical from equivalents	
Refinement method	Full-matrix least-squares on F^2	
Data / restraints / parameters	4749 / 0 / 296	
Goodness-of-fit on F^2	1.040	
Final R indices [I>2sigma(I)]	R1 = 0.0312, wR2 = 0.0798	
R indices (all data)	R1 = 0.0375, wR2 = 0.0835	
Largest diff. peak and hole	0.510 and -0.290 $e.Å^{-3}$	

Table 2. Atomic coordinates (x 10^4) and equivalent isotropic displacement parameters ($Å^2$x 10^3) for phw0911ma. U(eq) is defined as one third of the trace of the orthogonalized U^{ij} tensor.

	x	y	z	U(eq)
C(1)	3726(1)	1638(1)	1787(2)	16(1)
C(2)	4476(1)	1898(1)	793(2)	17(1)
C(3)	4140(1)	3333(1)	1235(2)	17(1)
C(4)	4366(1)	4176(1)	1010(2)	21(1)
C(5)	3886(1)	4774(1)	1821(2)	23(1)
C(6)	3170(1)	4539(1)	2848(2)	21(1)
C(7)	2924(1)	3713(1)	3053(2)	18(1)
C(8)	3420(1)	3094(1)	2242(2)	16(1)
C(9)	5086(1)	1296(1)	99(2)	19(1)
C(10)	2719(1)	-912(1)	2753(2)	19(1)
C(11)	2916(1)	-1738(1)	3065(2)	21(1)
C(12)	2610(1)	-2073(1)	4451(2)	21(1)
C(13)	2120(1)	-1571(1)	5439(2)	19(1)
C(14)	1936(1)	-732(1)	5036(2)	16(1)
C(15)	737(1)	1771(1)	4607(2)	21(1)
C(16)	102(1)	2047(1)	5661(2)	22(1)
C(17)	-91(1)	1528(1)	6908(2)	20(1)
C(18)	343(1)	759(1)	7016(2)	19(1)
C(19)	989(1)	514(1)	5880(2)	16(1)
Cu(1)	2282(1)	829(1)	3313(1)	17(1)
N(1)	3218(1)	2261(1)	2438(2)	17(1)
N(2)	4647(1)	2707(1)	462(2)	17(1)
N(3)	3471(1)	871(1)	2119(2)	18(1)
N(4)	5570(1)	789(1)	-389(2)	26(1)
N(5)	2254(1)	-396(1)	3734(2)	17(1)
N(6)	1398(1)	-269(1)	6024(2)	18(1)
N(7)	1202(1)	1018(1)	4709(2)	18(1)
O(1)	2515(1)	2038(1)	3395(2)	21(1)
O(2)	5267(1)	2908(1)	-533(2)	21(1)
O(3)	1259(1)	799(1)	1036(2)	22(1)
Cl(1)	8856(1)	980(1)	634(1)	21(1)

Table 3. Bond lengths [Å] and angles [°] for phw0911ma.

C(1)-N(3)	1.311(2)
C(1)-N(1)	1.355(2)
C(1)-C(2)	1.436(2)
C(2)-N(2)	1.349(2)
C(2)-C(9)	1.428(2)
C(3)-C(4)	1.400(2)
C(3)-C(8)	1.402(2)
C(3)-N(2)	1.407(2)
C(4)-C(5)	1.375(3)
C(4)-H(4)	0.9500
C(5)-C(6)	1.409(3)
C(5)-H(5)	0.9500
C(6)-C(7)	1.377(3)
C(6)-H(6)	0.9500
C(7)-C(8)	1.409(2)
C(7)-H(7)	0.9500
C(8)-N(1)	1.373(2)
C(9)-N(4)	1.142(2)
C(10)-N(5)	1.365(2)
C(10)-C(11)	1.373(3)
C(10)-H(10)	0.9500
C(11)-C(12)	1.398(3)
C(11)-H(11)	0.9500
C(12)-C(13)	1.373(3)
C(12)-H(12)	0.9500
C(13)-C(14)	1.408(2)
C(13)-H(13)	0.9500
C(14)-N(5)	1.343(2)
C(14)-N(6)	1.373(2)
C(15)-N(7)	1.365(2)
C(15)-C(16)	1.366(3)
C(15)-H(15)	0.9500
C(16)-C(17)	1.398(3)
C(16)-H(16)	0.9500
C(17)-C(18)	1.370(3)
C(17)-H(17)	0.9500
C(18)-C(19)	1.411(2)
C(18)-H(18)	0.9500

C(19)-N(7)	1.339(2)
C(19)-N(6)	1.377(2)
Cu(1)-O(1)	1.9614(13)
Cu(1)-N(3)	1.9764(16)
Cu(1)-N(7)	1.9828(15)
Cu(1)-N(5)	1.9928(15)
Cu(1)-O(3)	2.3772(15)
N(1)-O(1)	1.3508(18)
N(2)-O(2)	1.2814(18)
N(3)-H(3)	0.79(3)
N(6)-H(6A)	0.76(3)
O(3)-H(3A)	0.72(3)
O(3)-H(3B)	0.75(3)

N(3)-C(1)-N(1)	116.65(16)
N(3)-C(1)-C(2)	127.53(17)
N(1)-C(1)-C(2)	115.81(15)
N(2)-C(2)-C(9)	116.49(15)
N(2)-C(2)-C(1)	122.81(16)
C(9)-C(2)-C(1)	120.70(16)
C(4)-C(3)-C(8)	121.12(17)
C(4)-C(3)-N(2)	119.99(16)
C(8)-C(3)-N(2)	118.88(15)
C(5)-C(4)-C(3)	118.96(17)
C(5)-C(4)-H(4)	120.5
C(3)-C(4)-H(4)	120.5
C(4)-C(5)-C(6)	120.23(17)
C(4)-C(5)-H(5)	119.9
C(6)-C(5)-H(5)	119.9
C(7)-C(6)-C(5)	121.39(17)
C(7)-C(6)-H(6)	119.3
C(5)-C(6)-H(6)	119.3
C(6)-C(7)-C(8)	118.83(17)
C(6)-C(7)-H(7)	120.6
C(8)-C(7)-H(7)	120.6
N(1)-C(8)-C(3)	119.58(16)
N(1)-C(8)-C(7)	120.97(16)
C(3)-C(8)-C(7)	119.45(16)
N(4)-C(9)-C(2)	176.4(2)
N(5)-C(10)-C(11)	123.56(17)

N(5)-C(10)-H(10)	118.2
C(11)-C(10)-H(10)	118.2
C(10)-C(11)-C(12)	118.33(17)
C(10)-C(11)-H(11)	120.8
C(12)-C(11)-H(11)	120.8
C(13)-C(12)-C(11)	119.18(17)
C(13)-C(12)-H(12)	120.4
C(11)-C(12)-H(12)	120.4
C(12)-C(13)-C(14)	119.39(17)
C(12)-C(13)-H(13)	120.3
C(14)-C(13)-H(13)	120.3
N(5)-C(14)-N(6)	120.96(16)
N(5)-C(14)-C(13)	121.90(16)
N(6)-C(14)-C(13)	117.13(16)
N(7)-C(15)-C(16)	123.63(17)
N(7)-C(15)-H(15)	118.2
C(16)-C(15)-H(15)	118.2
C(15)-C(16)-C(17)	118.37(17)
C(15)-C(16)-H(16)	120.8
C(17)-C(16)-H(16)	120.8
C(18)-C(17)-C(16)	119.29(17)
C(18)-C(17)-H(17)	120.4
C(16)-C(17)-H(17)	120.4
C(17)-C(18)-C(19)	119.18(17)
C(17)-C(18)-H(18)	120.4
C(19)-C(18)-H(18)	120.4
N(7)-C(19)-N(6)	120.93(16)
N(7)-C(19)-C(18)	121.91(16)
N(6)-C(19)-C(18)	117.16(16)
O(1)-Cu(1)-N(3)	81.21(6)
O(1)-Cu(1)-N(7)	87.30(6)
N(3)-Cu(1)-N(7)	167.41(7)
O(1)-Cu(1)-N(5)	165.23(6)
N(3)-Cu(1)-N(5)	98.80(6)
N(7)-Cu(1)-N(5)	90.99(6)
O(1)-Cu(1)-O(3)	98.04(6)
N(3)-Cu(1)-O(3)	92.29(6)
N(7)-Cu(1)-O(3)	94.42(6)
N(5)-Cu(1)-O(3)	96.73(6)
O(1)-N(1)-C(1)	117.29(14)

O(1)-N(1)-C(8)	119.16(14)
C(1)-N(1)-C(8)	123.44(15)
O(2)-N(2)-C(2)	120.76(15)
O(2)-N(2)-C(3)	120.15(15)
C(2)-N(2)-C(3)	119.09(15)
C(1)-N(3)-Cu(1)	112.54(13)
C(1)-N(3)-H(3)	116(2)
Cu(1)-N(3)-H(3)	130(2)
C(14)-N(5)-C(10)	117.54(15)
C(14)-N(5)-Cu(1)	123.86(12)
C(10)-N(5)-Cu(1)	117.82(12)
C(14)-N(6)-C(19)	131.57(16)
C(14)-N(6)-H(6A)	115.7(19)
C(19)-N(6)-H(6A)	112.7(19)
C(19)-N(7)-C(15)	117.55(16)
C(19)-N(7)-Cu(1)	124.50(12)
C(15)-N(7)-Cu(1)	117.24(12)
N(1)-O(1)-Cu(1)	111.03(10)
Cu(1)-O(3)-H(3A)	109(2)
Cu(1)-O(3)-H(3B)	123(2)
H(3A)-O(3)-H(3B)	106(3)

Symmetry transformations used to generate equivalent atoms:

Table 4. Anisotropic displacement parameters ($Å^2 x\ 10^3$) for phw0911ma. The anisotropic displacement factor exponent takes the form: $-2\pi^2[\ h^2\ a^{*2}U^{11} + ... + 2\ h\ k\ a^*\ b^*\ U^{12}\ ]$

	U^{11}	U^{22}	U^{33}	U^{23}	U^{13}	U^{12}
C(1)	16(1)	18(1)	15(1)	1(1)	2(1)	-1(1)
C(2)	17(1)	17(1)	16(1)	0(1)	4(1)	0(1)
C(3)	18(1)	17(1)	16(1)	0(1)	2(1)	-1(1)
C(4)	23(1)	18(1)	22(1)	4(1)	3(1)	-3(1)
C(5)	26(1)	15(1)	26(1)	2(1)	2(1)	-2(1)
C(6)	22(1)	19(1)	21(1)	-2(1)	-1(1)	3(1)
C(7)	18(1)	19(1)	18(1)	-1(1)	2(1)	2(1)
C(8)	17(1)	16(1)	16(1)	1(1)	1(1)	-1(1)
C(9)	18(1)	20(1)	19(1)	2(1)	4(1)	-2(1)
C(10)	21(1)	20(1)	17(1)	-1(1)	5(1)	-1(1)
C(11)	21(1)	21(1)	21(1)	-4(1)	3(1)	1(1)
C(12)	21(1)	17(1)	25(1)	0(1)	-1(1)	2(1)
C(13)	20(1)	18(1)	19(1)	3(1)	2(1)	-1(1)
C(14)	15(1)	17(1)	17(1)	1(1)	1(1)	-1(1)
C(15)	22(1)	18(1)	25(1)	6(1)	7(1)	0(1)
C(16)	20(1)	16(1)	29(1)	1(1)	5(1)	0(1)
C(17)	18(1)	22(1)	21(1)	-4(1)	4(1)	0(1)
C(18)	19(1)	21(1)	17(1)	1(1)	4(1)	-2(1)
C(19)	15(1)	16(1)	17(1)	0(1)	1(1)	-2(1)
Cu(1)	19(1)	15(1)	17(1)	2(1)	6(1)	-1(1)
N(1)	17(1)	17(1)	17(1)	1(1)	6(1)	-2(1)
N(2)	16(1)	19(1)	15(1)	2(1)	3(1)	-2(1)
N(3)	21(1)	15(1)	19(1)	0(1)	7(1)	0(1)
N(4)	25(1)	25(1)	28(1)	2(1)	10(1)	3(1)
N(5)	18(1)	16(1)	17(1)	0(1)	3(1)	-1(1)
N(6)	21(1)	16(1)	15(1)	4(1)	6(1)	0(1)
N(7)	18(1)	17(1)	18(1)	2(1)	4(1)	-1(1)
O(1)	22(1)	18(1)	23(1)	0(1)	13(1)	-3(1)
O(2)	19(1)	24(1)	20(1)	2(1)	9(1)	-3(1)
O(3)	23(1)	22(1)	23(1)	-3(1)	1(1)	0(1)
Cl(1)	26(1)	18(1)	18(1)	3(1)	5(1)	-1(1)

Table 5. Hydrogen coordinates (x 10^4) and isotropic displacement parameters ($Å^2$x 10^3) for phw0911ma.

	x	y	z	U(eq)
H(4)	4844	4332	308	25
H(5)	4038	5349	1689	27
H(6)	2850	4959	3411	25
H(7)	2429	3564	3730	22
H(10)	2918	-687	1804	23
H(11)	3251	-2073	2357	25
H(12)	2741	-2641	4706	25
H(13)	1908	-1789	6386	23
H(15)	863	2123	3757	26
H(16)	-203	2578	5548	26
H(17)	-517	1708	7673	24
H(18)	211	394	7845	22
H(3)	3760(20)	511(18)	1720(30)	38(7)
H(6A)	1298(18)	-477(16)	6790(30)	25(6)
H(3A)	1280(20)	390(20)	690(30)	43(9)
H(3B)	730(30)	916(18)	1030(40)	44(9)

Table 6. Torsion angles [°] for phw0911ma.

N(3)-C(1)-C(2)-N(2)	176.35(18)
N(1)-C(1)-C(2)-N(2)	-2.8(3)
N(3)-C(1)-C(2)-C(9)	-3.7(3)
N(1)-C(1)-C(2)-C(9)	177.14(16)
C(8)-C(3)-C(4)-C(5)	1.5(3)
N(2)-C(3)-C(4)-C(5)	-177.64(17)
C(3)-C(4)-C(5)-C(6)	-0.7(3)
C(4)-C(5)-C(6)-C(7)	-0.8(3)
C(5)-C(6)-C(7)-C(8)	1.5(3)
C(4)-C(3)-C(8)-N(1)	-179.82(17)
N(2)-C(3)-C(8)-N(1)	-0.7(3)
C(4)-C(3)-C(8)-C(7)	-0.7(3)
N(2)-C(3)-C(8)-C(7)	178.40(16)

C(6)-C(7)-C(8)-N(1)	178.31(17)
C(6)-C(7)-C(8)-C(3)	-0.8(3)
N(5)-C(10)-C(11)-C(12)	1.0(3)
C(10)-C(11)-C(12)-C(13)	0.6(3)
C(11)-C(12)-C(13)-C(14)	0.0(3)
C(12)-C(13)-C(14)-N(5)	-2.3(3)
C(12)-C(13)-C(14)-N(6)	176.61(17)
N(7)-C(15)-C(16)-C(17)	-0.4(3)
C(15)-C(16)-C(17)-C(18)	-1.5(3)
C(16)-C(17)-C(18)-C(19)	1.2(3)
C(17)-C(18)-C(19)-N(7)	1.0(3)
C(17)-C(18)-C(19)-N(6)	-179.16(17)
N(3)-C(1)-N(1)-O(1)	1.5(2)
C(2)-C(1)-N(1)-O(1)	-179.20(15)
N(3)-C(1)-N(1)-C(8)	177.77(17)
C(2)-C(1)-N(1)-C(8)	-2.9(2)
C(3)-C(8)-N(1)-O(1)	-179.14(15)
C(7)-C(8)-N(1)-O(1)	1.8(3)
C(3)-C(8)-N(1)-C(1)	4.7(3)
C(7)-C(8)-N(1)-C(1)	-174.42(17)
C(9)-C(2)-N(2)-O(2)	6.0(2)
C(1)-C(2)-N(2)-O(2)	-173.98(15)
C(9)-C(2)-N(2)-C(3)	-173.37(16)
C(1)-C(2)-N(2)-C(3)	6.6(3)
C(4)-C(3)-N(2)-O(2)	-5.0(2)
C(8)-C(3)-N(2)-O(2)	175.86(16)
C(4)-C(3)-N(2)-C(2)	174.41(17)
C(8)-C(3)-N(2)-C(2)	-4.7(2)
N(1)-C(1)-N(3)-Cu(1)	7.0(2)
C(2)-C(1)-N(3)-Cu(1)	-172.14(15)
O(1)-Cu(1)-N(3)-C(1)	-9.32(13)
N(7)-Cu(1)-N(3)-C(1)	-33.7(4)
N(5)-Cu(1)-N(3)-C(1)	-174.37(13)
O(3)-Cu(1)-N(3)-C(1)	88.46(13)
N(6)-C(14)-N(5)-C(10)	-175.08(16)
C(13)-C(14)-N(5)-C(10)	3.8(3)
N(6)-C(14)-N(5)-Cu(1)	15.3(2)
C(13)-C(14)-N(5)-Cu(1)	-165.84(13)
C(11)-C(10)-N(5)-C(14)	-3.2(3)
C(11)-C(10)-N(5)-Cu(1)	167.09(15)

O(1)-Cu(1)-N(5)-C(14)	56.9(3)
N(3)-Cu(1)-N(5)-C(14)	145.78(14)
N(7)-Cu(1)-N(5)-C(14)	-26.28(15)
O(3)-Cu(1)-N(5)-C(14)	-120.85(14)
O(1)-Cu(1)-N(5)-C(10)	-112.7(2)
N(3)-Cu(1)-N(5)-C(10)	-23.84(15)
N(7)-Cu(1)-N(5)-C(10)	164.10(14)
O(3)-Cu(1)-N(5)-C(10)	69.54(14)
N(5)-C(14)-N(6)-C(19)	8.6(3)
C(13)-C(14)-N(6)-C(19)	-170.35(18)
N(7)-C(19)-N(6)-C(14)	-10.2(3)
C(18)-C(19)-N(6)-C(14)	170.00(18)
N(6)-C(19)-N(7)-C(15)	177.34(17)
C(18)-C(19)-N(7)-C(15)	-2.8(3)
N(6)-C(19)-N(7)-Cu(1)	-12.6(2)
C(18)-C(19)-N(7)-Cu(1)	167.24(13)
C(16)-C(15)-N(7)-C(19)	2.6(3)
C(16)-C(15)-N(7)-Cu(1)	-168.22(16)
O(1)-Cu(1)-N(7)-C(19)	-140.32(15)
N(3)-Cu(1)-N(7)-C(19)	-116.2(3)
N(5)-Cu(1)-N(7)-C(19)	25.00(15)
O(3)-Cu(1)-N(7)-C(19)	121.82(15)
O(1)-Cu(1)-N(7)-C(15)	29.78(14)
N(3)-Cu(1)-N(7)-C(15)	53.9(4)
N(5)-Cu(1)-N(7)-C(15)	-164.90(14)
O(3)-Cu(1)-N(7)-C(15)	-68.08(14)
C(1)-N(1)-O(1)-Cu(1)	-9.25(18)
C(8)-N(1)-O(1)-Cu(1)	174.33(13)
N(3)-Cu(1)-O(1)-N(1)	9.82(11)
N(7)-Cu(1)-O(1)-N(1)	-175.35(12)
N(5)-Cu(1)-O(1)-N(1)	101.0(2)
O(3)-Cu(1)-O(1)-N(1)	-81.26(11)

Symmetry transformations used to generate equivalent atoms:

Table 7. Hydrogen bonds for phw0911ma [Å and °].

D-H...A	d(D-H)	d(H...A)	d(D...A)	<(DHA)

O(3)-H(3B)...Cl(1)#1	0.75(3)	2.59(3)	3.3250(17)	166(3)
O(3)-H(3A)...Cl(1)#2	0.72(3)	2.48(3)	3.1942(17)	172(3)
N(6)-H(6A)...Cl(1)#3	0.76(3)	2.39(3)	3.1487(16)	172(2)
N(3)-H(3)...N(4)#2	0.79(3)	2.57(3)	3.350(2)	171(3)

Symmetry transformations used to generate equivalent atoms:

#1 x-1,y,z #2 -x+1,-y,-z #3 -x+1,-y,-z+1

Crystallographic data for $[Zn(tpzH\text{-}CN)(dpHa)(MeOH)]BF_4$

Table 1. Crystal data and structure refinement for phw1010m.

Identification code	phw1010m	
Empirical formula	C20 H18 B F4 N7 O3 Zn	
Formula weight	556.59	
Temperature	110(2) K	
Wavelength	0.71073 Å	
Crystal system	Monoclinic	
Space group	P2(1)/n	
Unit cell dimensions	a = 7.5622(8) Å	α= 90°.
	b = 16.4939(18) Å	β= 99.859(2)°.
	c = 17.7364(19) Å	γ = 90°.
Volume	2179.6(4) $Å^3$	
Z	4	
Density (calculated)	1.696 Mg/m^3	
Absorption coefficient	1.202 mm^{-1}	
F(000)	1128	
Crystal size	0.28 x 0.06 x 0.04 mm^3	
Theta range for data collection	1.70 to 28.35°.	
Index ranges	-10<=h<=10, -21<=k<=22, -23<=l<=23	
Reflections collected	22248	
Independent reflections	5420 [R(int) = 0.0559]	
Completeness to theta = 28.35°	99.6 %	
Absorption correction	Semi-empirical from equivalents	
Max. and min. transmission	0.953 and 0.724	
Refinement method	Full-matrix least-squares on F^2	
Data / restraints / parameters	5420 / 0 / 338	
Goodness-of-fit on F^2	1.019	
Final R indices [I>2sigma(I)]	R1 = 0.0436, wR2 = 0.0896	
R indices (all data)	R1 = 0.0697, wR2 = 0.1009	
Largest diff. peak and hole	0.442 and -0.623 $e.Å^{-3}$	

Table 2. Atomic coordinates (x 10^4) and equivalent isotropic displacement parameters ($Å^2$x 10^3) for phw1010m. U(eq) is defined as one third of the trace of the orthogonalized U^{ij} tensor.

	x	y	z	U(eq)
B(1A)	2556(4)	339(2)	1812(2)	24(1)
C(1)	1306(3)	4547(2)	845(1)	18(1)
C(2)	1594(3)	5399(2)	757(1)	18(1)
C(3)	-917(3)	5743(2)	1325(2)	20(1)
C(4)	-2046(4)	6329(2)	1561(2)	23(1)
C(5)	-3485(4)	6084(2)	1878(2)	26(1)
C(6)	-3816(4)	5250(2)	1971(2)	27(1)
C(7)	-2722(4)	4671(2)	1745(2)	25(1)
C(8)	-1240(4)	4911(2)	1418(1)	20(1)
C(9)	3019(4)	5667(2)	387(2)	21(1)
C(10)	4171(4)	2450(2)	-113(2)	22(1)
C(11)	5053(4)	2202(2)	-689(2)	24(1)
C(12)	4209(4)	1640(2)	-1215(2)	26(1)
C(13)	2550(4)	1342(2)	-1136(2)	24(1)
C(14)	1743(3)	1619(2)	-526(2)	20(1)
C(15)	-1760(4)	1909(2)	1188(2)	24(1)
C(16)	-3051(4)	1336(2)	1227(2)	24(1)
C(17)	-3262(4)	714(2)	685(2)	24(1)
C(18)	-2194(4)	702(2)	134(2)	22(1)
C(19)	-910(3)	1316(2)	129(2)	19(1)
C(20)	3172(5)	2921(2)	2422(2)	46(1)
F(1)	2755(3)	751(1)	1162(1)	38(1)
F(2)	1104(3)	-165(1)	1669(1)	56(1)
F(3)	4085(3)	-146(1)	2024(1)	69(1)
F(4)	2419(2)	885(1)	2388(1)	33(1)
N(1)	-128(3)	4341(1)	1180(1)	20(1)
N(2)	535(3)	5977(1)	984(1)	20(1)
N(3)	2233(3)	3952(1)	613(1)	20(1)
N(4)	4177(3)	5821(1)	73(1)	28(1)
N(5)	2516(3)	2184(1)	-32(1)	19(1)
N(6)	99(3)	1289(1)	-453(1)	22(1)
N(7)	-692(3)	1915(1)	647(1)	20(1)
O(1)	-491(3)	3553(1)	1249(1)	25(1)
O(2)	823(3)	6733(1)	868(1)	26(1)
O(3)	2829(3)	2442(1)	1742(1)	29(1)

Zn(1)	1219(1)	2832(1)	725(1)	20(1)

Table 3. Bond lengths [Å] and angles [°] for phw1010m.

B(1A)-F(2)	1.365(4)
B(1A)-F(1)	1.369(4)
B(1A)-F(4)	1.380(3)
B(1A)-F(3)	1.403(4)
C(1)-N(3)	1.313(3)
C(1)-N(1)	1.365(3)
C(1)-C(2)	1.434(3)
C(2)-N(2)	1.351(3)
C(2)-C(9)	1.425(4)
C(3)-N(2)	1.396(3)
C(3)-C(4)	1.400(4)
C(3)-C(8)	1.409(4)
C(4)-C(5)	1.368(4)
C(4)-H(4)	0.9500
C(5)-C(6)	1.411(4)
C(5)-H(5)	0.9500
C(6)-C(7)	1.368(4)
C(6)-H(6)	0.9500
C(7)-C(8)	1.403(4)
C(7)-H(7)	0.9500
C(8)-N(1)	1.375(3)
C(9)-N(4)	1.144(3)
C(10)-N(5)	1.357(3)
C(10)-C(11)	1.375(4)
C(10)-H(10)	0.9500
C(11)-C(12)	1.390(4)
C(11)-H(11)	0.9500
C(12)-C(13)	1.376(4)
C(12)-H(12)	0.9500
C(13)-C(14)	1.407(4)
C(13)-H(13)	0.9500
C(14)-N(5)	1.342(3)
C(14)-N(6)	1.384(3)
C(15)-N(7)	1.356(3)

C(15)-C(16)	1.370(4)
C(15)-H(15)	0.9500
C(16)-C(17)	1.395(4)
C(16)-H(16)	0.9500
C(17)-C(18)	1.371(4)
C(17)-H(17)	0.9500
C(18)-C(19)	1.405(4)
C(18)-H(18)	0.9500
C(19)-N(7)	1.339(3)
C(19)-N(6)	1.386(3)
C(20)-O(3)	1.427(4)
C(20)-H(20A)	0.9800
C(20)-H(20B)	0.9800
C(20)-H(20C)	0.9800
N(1)-O(1)	1.339(3)
N(2)-O(2)	1.288(3)
N(3)-Zn(1)	2.024(2)
N(3)-H(3)	0.81(3)
N(5)-Zn(1)	2.088(2)
N(6)-H(6A)	0.81(3)
N(7)-Zn(1)	2.080(2)
O(1)-Zn(1)	2.0891(19)
O(3)-Zn(1)	2.097(2)
O(3)-H(3A)	0.76(4)

F(2)-B(1A)-F(1)	110.3(2)
F(2)-B(1A)-F(4)	112.0(3)
F(1)-B(1A)-F(4)	109.4(2)
F(2)-B(1A)-F(3)	107.6(3)
F(1)-B(1A)-F(3)	107.7(3)
F(4)-B(1A)-F(3)	109.7(2)
N(3)-C(1)-N(1)	117.2(2)
N(3)-C(1)-C(2)	126.8(2)
N(1)-C(1)-C(2)	116.0(2)
N(2)-C(2)-C(9)	116.9(2)
N(2)-C(2)-C(1)	123.4(2)
C(9)-C(2)-C(1)	119.7(2)
N(2)-C(3)-C(4)	120.3(2)
N(2)-C(3)-C(8)	119.0(2)
C(4)-C(3)-C(8)	120.7(2)

C(5)-C(4)-C(3)	119.2(3)
C(5)-C(4)-H(4)	120.4
C(3)-C(4)-H(4)	120.4
C(4)-C(5)-C(6)	120.3(3)
C(4)-C(5)-H(5)	119.8
C(6)-C(5)-H(5)	119.8
C(7)-C(6)-C(5)	121.2(3)
C(7)-C(6)-H(6)	119.4
C(5)-C(6)-H(6)	119.4
C(6)-C(7)-C(8)	119.3(3)
C(6)-C(7)-H(7)	120.3
C(8)-C(7)-H(7)	120.3
N(1)-C(8)-C(7)	120.5(2)
N(1)-C(8)-C(3)	120.2(2)
C(7)-C(8)-C(3)	119.3(2)
N(4)-C(9)-C(2)	174.7(3)
N(5)-C(10)-C(11)	123.8(3)
N(5)-C(10)-H(10)	118.1
C(11)-C(10)-H(10)	118.1
C(10)-C(11)-C(12)	118.2(3)
C(10)-C(11)-H(11)	120.9
C(12)-C(11)-H(11)	120.9
C(13)-C(12)-C(11)	119.4(3)
C(13)-C(12)-H(12)	120.3
C(11)-C(12)-H(12)	120.3
C(12)-C(13)-C(14)	119.0(3)
C(12)-C(13)-H(13)	120.5
C(14)-C(13)-H(13)	120.5
N(5)-C(14)-N(6)	120.7(2)
N(5)-C(14)-C(13)	122.0(2)
N(6)-C(14)-C(13)	117.3(2)
N(7)-C(15)-C(16)	123.8(3)
N(7)-C(15)-H(15)	118.1
C(16)-C(15)-H(15)	118.1
C(15)-C(16)-C(17)	118.1(3)
C(15)-C(16)-H(16)	120.9
C(17)-C(16)-H(16)	120.9
C(18)-C(17)-C(16)	119.4(3)
C(18)-C(17)-H(17)	120.3
C(16)-C(17)-H(17)	120.3

C(17)-C(18)-C(19)	119.1(2)
C(17)-C(18)-H(18)	120.5
C(19)-C(18)-H(18)	120.5
N(7)-C(19)-N(6)	121.1(2)
N(7)-C(19)-C(18)	122.1(2)
N(6)-C(19)-C(18)	116.8(2)
O(3)-C(20)-H(20A)	109.5
O(3)-C(20)-H(20B)	109.5
H(20A)-C(20)-H(20B)	109.5
O(3)-C(20)-H(20C)	109.5
H(20A)-C(20)-H(20C)	109.5
H(20B)-C(20)-H(20C)	109.5
O(1)-N(1)-C(1)	118.2(2)
O(1)-N(1)-C(8)	119.3(2)
C(1)-N(1)-C(8)	122.5(2)
O(2)-N(2)-C(2)	120.7(2)
O(2)-N(2)-C(3)	120.3(2)
C(2)-N(2)-C(3)	119.0(2)
C(1)-N(3)-Zn(1)	114.84(18)
C(1)-N(3)-H(3)	117.6(19)
Zn(1)-N(3)-H(3)	127.3(19)
C(14)-N(5)-C(10)	117.5(2)
C(14)-N(5)-Zn(1)	125.09(18)
C(10)-N(5)-Zn(1)	116.51(17)
C(14)-N(6)-C(19)	132.4(2)
C(14)-N(6)-H(6A)	112(2)
C(19)-N(6)-H(6A)	115(2)
C(19)-N(7)-C(15)	117.5(2)
C(19)-N(7)-Zn(1)	125.79(18)
C(15)-N(7)-Zn(1)	116.67(18)
N(1)-O(1)-Zn(1)	111.07(14)
C(20)-O(3)-Zn(1)	123.50(19)
C(20)-O(3)-H(3A)	112(3)
Zn(1)-O(3)-H(3A)	116(3)
N(3)-Zn(1)-N(7)	158.12(9)
N(3)-Zn(1)-N(5)	100.14(9)
N(7)-Zn(1)-N(5)	89.01(8)
N(3)-Zn(1)-O(1)	78.32(8)
N(7)-Zn(1)-O(1)	88.15(8)
N(5)-Zn(1)-O(1)	166.53(8)

N(3)-Zn(1)-O(3)	100.97(9)
N(7)-Zn(1)-O(3)	97.44(9)
N(5)-Zn(1)-O(3)	97.44(8)
O(1)-Zn(1)-O(3)	95.98(8)

Symmetry transformations used to generate equivalent atoms:

Table 4. Anisotropic displacement parameters ($Å^2 x\ 10^3$) for phw1010m. The anisotropic displacement factor exponent takes the form: $-2\pi^2[\ h^2\ a^{*2}U^{11} + ... + 2\ h\ k\ a^*\ b^*\ U^{12}\ ]$

	U^{11}	U^{22}	U^{33}	U^{23}	U^{13}	U^{12}
B(1A)	28(2)	19(1)	24(2)	-3(1)	6(1)	-6(1)
C(1)	19(1)	16(1)	17(1)	-1(1)	2(1)	-2(1)
C(2)	18(1)	15(1)	20(1)	-2(1)	4(1)	-1(1)
C(3)	19(1)	23(1)	18(1)	1(1)	2(1)	3(1)
C(4)	26(1)	20(1)	23(1)	-1(1)	3(1)	5(1)
C(5)	27(2)	29(2)	23(1)	-1(1)	6(1)	9(1)
C(6)	27(2)	33(2)	24(1)	2(1)	10(1)	5(1)
C(7)	25(2)	24(1)	26(1)	3(1)	9(1)	3(1)
C(8)	22(1)	21(1)	17(1)	0(1)	4(1)	1(1)
C(9)	24(1)	12(1)	25(1)	-2(1)	0(1)	-1(1)
C(10)	23(1)	15(1)	29(1)	4(1)	4(1)	1(1)
C(11)	20(1)	20(1)	33(2)	6(1)	9(1)	4(1)
C(12)	29(2)	22(1)	30(2)	3(1)	14(1)	6(1)
C(13)	31(2)	18(1)	25(1)	-2(1)	8(1)	2(1)
C(14)	20(1)	15(1)	25(1)	4(1)	4(1)	1(1)
C(15)	26(2)	24(1)	22(1)	-1(1)	6(1)	-3(1)
C(16)	21(1)	26(1)	25(1)	3(1)	6(1)	-5(1)
C(17)	21(1)	20(1)	31(2)	4(1)	4(1)	-3(1)
C(18)	22(1)	17(1)	25(1)	-2(1)	1(1)	-2(1)
C(19)	19(1)	17(1)	23(1)	2(1)	3(1)	3(1)
C(20)	61(2)	45(2)	30(2)	-6(2)	-2(2)	5(2)
F(1)	50(1)	31(1)	36(1)	2(1)	16(1)	-5(1)
F(2)	69(1)	61(1)	46(1)	-29(1)	34(1)	-44(1)
F(3)	79(2)	57(1)	60(2)	-12(1)	-19(1)	35(1)
F(4)	36(1)	32(1)	33(1)	-12(1)	9(1)	-9(1)
N(1)	22(1)	16(1)	23(1)	1(1)	7(1)	0(1)
N(2)	23(1)	16(1)	21(1)	-2(1)	2(1)	1(1)

N(3)	19(1)	18(1)	25(1)	-2(1)	9(1)	-3(1)
N(4)	29(1)	19(1)	37(1)	-1(1)	9(1)	-4(1)
N(5)	21(1)	14(1)	23(1)	4(1)	4(1)	0(1)
N(6)	26(1)	18(1)	23(1)	-6(1)	6(1)	-5(1)
N(7)	21(1)	19(1)	21(1)	0(1)	4(1)	-2(1)
O(1)	29(1)	14(1)	36(1)	2(1)	14(1)	-1(1)
O(2)	30(1)	13(1)	34(1)	0(1)	7(1)	-1(1)
O(3)	38(1)	16(1)	30(1)	0(1)	0(1)	-1(1)
Zn(1)	21(1)	15(1)	25(1)	-2(1)	7(1)	-2(1)

Table 5. Hydrogen coordinates (x 10^4) and isotropic displacement parameters ($Å^2$x 10^3) for phw1010m.

	x	y	z	U(eq)
H(4)	-1816	6889	1502	28
H(5)	-4265	6476	2036	31
H(6)	-4816	5089	2194	33
H(7)	-2963	4112	1808	29
H(10)	4754	2829	250	27
H(11)	6207	2409	-727	29
H(12)	4773	1463	-1625	31
H(13)	1959	955	-1489	29
H(15)	-1603	2328	1562	28
H(16)	-3781	1360	1612	29
H(17)	-4138	304	698	29
H(18)	-2320	283	-239	26
H(20A)	4357	3175	2465	70
H(20B)	3142	2574	2868	70
H(20C)	2252	3343	2399	70
H(3)	3080(40)	4070(16)	414(15)	12(7)
H(6A)	-230(40)	953(19)	-780(17)	24(8)
H(3A)	2780(50)	1990(20)	1830(20)	43(11)

Table 6. Torsion angles [°] for phw1010m.

N(3)-C(1)-C(2)-N(2)	177.2(2)
N(1)-C(1)-C(2)-N(2)	-0.1(4)
N(3)-C(1)-C(2)-C(9)	-0.3(4)
N(1)-C(1)-C(2)-C(9)	-177.6(2)
N(2)-C(3)-C(4)-C(5)	178.5(2)
C(8)-C(3)-C(4)-C(5)	-0.7(4)
C(3)-C(4)-C(5)-C(6)	0.5(4)
C(4)-C(5)-C(6)-C(7)	-0.4(4)
C(5)-C(6)-C(7)-C(8)	0.3(4)
C(6)-C(7)-C(8)-N(1)	-179.4(3)

C(6)-C(7)-C(8)-C(3)	-0.5(4)
N(2)-C(3)-C(8)-N(1)	0.4(4)
C(4)-C(3)-C(8)-N(1)	179.6(2)
N(2)-C(3)-C(8)-C(7)	-178.5(2)
C(4)-C(3)-C(8)-C(7)	0.6(4)
N(2)-C(2)-C(9)-N(4)	-168(3)
C(1)-C(2)-C(9)-N(4)	10(3)
N(5)-C(10)-C(11)-C(12)	-0.7(4)
C(10)-C(11)-C(12)-C(13)	-1.1(4)
C(11)-C(12)-C(13)-C(14)	0.4(4)
C(12)-C(13)-C(14)-N(5)	2.2(4)
C(12)-C(13)-C(14)-N(6)	-178.2(2)
N(7)-C(15)-C(16)-C(17)	1.0(4)
C(15)-C(16)-C(17)-C(18)	-0.5(4)
C(16)-C(17)-C(18)-C(19)	0.0(4)
C(17)-C(18)-C(19)-N(7)	0.1(4)
C(17)-C(18)-C(19)-N(6)	-178.2(2)
N(3)-C(1)-N(1)-O(1)	0.1(3)
C(2)-C(1)-N(1)-O(1)	177.6(2)
N(3)-C(1)-N(1)-C(8)	-177.4(2)
C(2)-C(1)-N(1)-C(8)	0.2(3)
C(7)-C(8)-N(1)-O(1)	1.2(4)
C(3)-C(8)-N(1)-O(1)	-177.8(2)
C(7)-C(8)-N(1)-C(1)	178.6(2)
C(3)-C(8)-N(1)-C(1)	-0.3(4)
C(9)-C(2)-N(2)-O(2)	-0.2(4)
C(1)-C(2)-N(2)-O(2)	-177.7(2)
C(9)-C(2)-N(2)-C(3)	177.7(2)
C(1)-C(2)-N(2)-C(3)	0.2(4)
C(4)-C(3)-N(2)-O(2)	-1.6(4)
C(8)-C(3)-N(2)-O(2)	177.6(2)
C(4)-C(3)-N(2)-C(2)	-179.5(2)
C(8)-C(3)-N(2)-C(2)	-0.3(4)
N(1)-C(1)-N(3)-Zn(1)	4.6(3)
C(2)-C(1)-N(3)-Zn(1)	-172.7(2)
N(6)-C(14)-N(5)-C(10)	176.5(2)
C(13)-C(14)-N(5)-C(10)	-3.8(4)
N(6)-C(14)-N(5)-Zn(1)	-14.6(3)
C(13)-C(14)-N(5)-Zn(1)	164.99(19)
C(11)-C(10)-N(5)-C(14)	3.2(4)

C(11)-C(10)-N(5)-Zn(1)	-166.6(2)
N(5)-C(14)-N(6)-C(19)	-12.5(4)
C(13)-C(14)-N(6)-C(19)	167.8(3)
N(7)-C(19)-N(6)-C(14)	23.0(4)
C(18)-C(19)-N(6)-C(14)	-158.7(3)
N(6)-C(19)-N(7)-C(15)	178.5(2)
C(18)-C(19)-N(7)-C(15)	0.3(4)
N(6)-C(19)-N(7)-Zn(1)	-4.3(3)
C(18)-C(19)-N(7)-Zn(1)	177.52(18)
C(16)-C(15)-N(7)-C(19)	-0.8(4)
C(16)-C(15)-N(7)-Zn(1)	-178.3(2)
C(1)-N(1)-O(1)-Zn(1)	-4.4(3)
C(8)-N(1)-O(1)-Zn(1)	173.13(18)
C(1)-N(3)-Zn(1)-N(7)	47.7(3)
C(1)-N(3)-Zn(1)-N(5)	161.14(18)
C(1)-N(3)-Zn(1)-O(1)	-5.24(18)
C(1)-N(3)-Zn(1)-O(3)	-99.16(19)
C(19)-N(7)-Zn(1)-N(3)	102.9(3)
C(15)-N(7)-Zn(1)-N(3)	-79.8(3)
C(19)-N(7)-Zn(1)-N(5)	-12.5(2)
C(15)-N(7)-Zn(1)-N(5)	164.8(2)
C(19)-N(7)-Zn(1)-O(1)	154.3(2)
C(15)-N(7)-Zn(1)-O(1)	-28.40(19)
C(19)-N(7)-Zn(1)-O(3)	-109.9(2)
C(15)-N(7)-Zn(1)-O(3)	67.4(2)
C(14)-N(5)-Zn(1)-N(3)	-138.0(2)
C(10)-N(5)-Zn(1)-N(3)	30.91(19)
C(14)-N(5)-Zn(1)-N(7)	22.0(2)
C(10)-N(5)-Zn(1)-N(7)	-169.08(18)
C(14)-N(5)-Zn(1)-O(1)	-55.9(4)
C(10)-N(5)-Zn(1)-O(1)	113.1(3)
C(14)-N(5)-Zn(1)-O(3)	119.4(2)
C(10)-N(5)-Zn(1)-O(3)	-71.70(19)
N(1)-O(1)-Zn(1)-N(3)	5.05(16)
N(1)-O(1)-Zn(1)-N(7)	-157.65(17)
N(1)-O(1)-Zn(1)-N(5)	-79.7(4)
N(1)-O(1)-Zn(1)-O(3)	105.06(16)
C(20)-O(3)-Zn(1)-N(3)	48.3(3)
C(20)-O(3)-Zn(1)-N(7)	-119.8(3)
C(20)-O(3)-Zn(1)-N(5)	150.2(3)

C(20)-O(3)-Zn(1)-O(1)	-30.9(3)

Symmetry transformations used to generate equivalent atoms:

Table 7. Hydrogen bonds for phw1010m [Å and °].

D-H...A	d(D-H)	d(H...A)	d(D...A)	<(DHA)
O(3)-H(3A)...F(1)	0.76(4)	2.37(4)	2.970(3)	137(3)
O(3)-H(3A)...F(4)	0.76(4)	2.12(4)	2.851(3)	163(4)
N(6)-H(6A)...F(2)#1	0.81(3)	2.06(3)	2.872(3)	176(3)
N(3)-H(3)...N(4)#2	0.81(3)	2.39(3)	3.182(3)	169(3)

Symmetry transformations used to generate equivalent atoms:

#1 -x,-y,-z #2 -x+1,-y+1,-z

Crystallographic data for [Cu(Cl)(tpz-$CONH_2$)(dpHa)]

Crystal Submitted by:

Emma Dux

Crystal Submitted on:

21/06/11

Data Collected on:

27/06/11

Structure Solved by:

Rob Thatcher

Table 1: Crystal data and structure refinement for phw1110

Identification code	phw1110
Empirical formula	$C_{19}H_{18}ClCuN_7O_4$
Formula weight	507.39
Temperature / K	110.0
Crystal system	triclinic
Space group	P-1
a / Å, b / Å, c / Å	8.5102(6), 9.2014(5), 13.9166(10)
α/°, β/°, γ/°	71.147(5), 89.498(6), 72.581(5)
Volume / $Å^3$	979.31(11)
Z	2
ρ_{calc} / mg mm^{-3}	1.721
μ / mm^{-1}	1.298
F(000)	518
Crystal size / mm^3	0.2143 × 0.0672 × 0.038
2Θ range for data collection	6.18 to 55.92°
Index ranges	$-10 \leq h \leq 10$, $-12 \leq k \leq 12$, $-18 \leq l \leq 18$
Reflections collected	13185

Independent reflections	4127[R(int) = 0.0326]
Data/restraints/parameters	4127/0/313
Goodness-of-fit on F^2	1.061
Final R indexes [I>2σ (I)]	R_1 = 0.0309, wR_2 = 0.0676
Final R indexes [all data]	R_1 = 0.0371, wR_2 = 0.0707
Largest diff. peak/hole / e $Å^{-3}$	0.419/-0.420

Table 2 Fractional Atomic Coordinates ($\times 10^4$) and Equivalent Isotropic Displacement Parameters ($Å^2 \times 10^3$) for phw1110. U_{eq} is defined as 1/3 of of the trace of the orthogonalised U_{IJ} tensor.

Atom	***x***	***y***	***z***	**U(eq)**
C1	3062(3)	4575(2)	587.2(16)	10.6(4)
C2	2388(3)	4812(3)	-427.5(16)	12.1(4)
C3	4679(3)	2573(3)	-497.7(16)	12.7(4)
C4	5469(3)	1543(3)	-1025.7(17)	17.0(5)
C5	6979(3)	399(3)	-618.8(17)	18.4(5)
C6	7703(3)	266(3)	315.1(18)	19.5(5)
C7	6932(3)	1254(3)	849.0(17)	15.4(5)
C8	5388(3)	2425(3)	443.2(16)	12.6(4)
C9	808(3)	6167(3)	-889.2(17)	14.2(5)
C10	607(3)	6738(3)	2786.5(16)	13.3(4)
C11	-513(3)	8098(3)	2863.1(16)	15.5(5)
C12	86(3)	9206(3)	3109.2(17)	16.6(5)
C13	1762(3)	8854(3)	3319.7(16)	14.5(5)
C14	2832(3)	7385(3)	3279.7(15)	11.4(4)
C15	5745(3)	5531(3)	3793.3(15)	11.7(4)
C16	7235(3)	5368(3)	4306.0(16)	14.6(5)
C17	8519(3)	3958(3)	4508.0(16)	15.8(5)
C18	8293(3)	2693(3)	4238.7(16)	15.0(5)
C19	6800(3)	2921(3)	3758.9(16)	14.2(4)

Cl1	2630.2(6)	2316.0(6)	3751.8(4)	16.68(12)
Cu1	3729.0(3)	4684.8(3)	2487.90(19)	11.71(8)
N1	4562(2)	3426(2)	950.1(13)	11.6(4)
N2	3164(2)	3792(2)	-916.7(13)	13.3(4)
N3	2415(2)	5361(2)	1202.2(14)	13.7(4)
N4	407(3)	6556(3)	-1885.2(15)	18.9(4)
N5	2272(2)	6380(2)	2968.8(13)	11.5(4)
N6	4491(2)	6988(2)	3572.1(14)	12.4(4)
N7	5537(2)	4334(2)	3508.8(13)	11.6(4)
O1	5252.8(18)	3282.6(18)	1864.6(11)	14.6(3)
O2	2599(2)	3869.1(19)	-1797.8(11)	18.6(3)
O3	-18.6(18)	6888.2(19)	-357.4(12)	18.0(4)
O4	5746(2)	9306(2)	3922.7(15)	21.1(4)

Table 3 Anisotropic Displacement Parameters ($Å^2 \times 10^3$) for phw1110. The Anisotropic displacement factor exponent takes the form: $-2\pi^2[h^2a^{*2}U_{11}+...+2hka\times b\times U_{12}]$

Atom	**U_{11}**	**U_{22}**	**U_{33}**	**U_{23}**	**U_{13}**	**U_{12}**
C1	11.1(10)	7.9(10)	13.1(10)	-1.9(8)	0.9(8)	-5.0(8)
C2	11.2(10)	12.4(10)	13.6(10)	-2.9(9)	0.6(8)	-6.4(9)
C3	14.4(10)	13.5(11)	11.3(10)	-2.5(9)	1.6(9)	-7.6(9)
C4	24.9(12)	18.1(11)	12.1(10)	-6.2(9)	5.7(9)	-11.4(10)
C5	23.2(12)	14.4(11)	17.9(11)	-6.4(10)	9(1)	-5.7(10)
C6	17.6(12)	14.8(11)	23.2(12)	-5.4(10)	3.9(10)	-2.3(9)
C7	14.9(11)	14.9(11)	15.9(11)	-3.8(9)	0.7(9)	-5.2(9)
C8	14.4(10)	12.6(10)	14.2(11)	-5.6(9)	3.0(9)	-7.7(9)
C9	12.4(10)	13.6(11)	17.0(11)	-2.6(9)	0.0(9)	-7.5(9)
C10	13.6(10)	15.0(11)	13(1)	-4.9(9)	0.9(9)	-6.7(9)
C11	13.4(10)	17.3(11)	13.6(11)	-3.2(9)	-1.3(9)	-3.4(9)
C12	20.3(12)	12.1(11)	14.9(11)	-4.6(9)	1.5(9)	-1.3(9)

C13	19.7(11)	12.7(11)	12.7(10)	-5.7(9)	1.0(9)	-6.0(9)
C14	14.4(10)	12.9(10)	8(1)	-2.9(8)	1.0(8)	-6.2(9)
C15	14.1(10)	13.1(11)	8.3(10)	-2.5(8)	3.0(8)	-6.2(9)
C16	16.9(11)	17.7(11)	11.6(10)	-5.5(9)	0.6(9)	-8.1(9)
C17	14.9(11)	20.7(12)	11.8(10)	-3.8(9)	-0.9(9)	-7.2(9)
C18	15.1(11)	15.1(11)	12.7(10)	-4.9(9)	0.2(9)	-1.3(9)
C19	18.5(11)	12(1)	13.2(11)	-5.1(9)	3.1(9)	-5.2(9)
Cl1	15.6(3)	12.3(3)	20.8(3)	-4.5(2)	-1.7(2)	-3.5(2)
Cu1	11.48(14)	12.26(14)	12.89(14)	-7.12(11)	-0.52(10)	-2.65(10)
N1	13.0(9)	13.0(9)	9.8(8)	-5.1(7)	-0.7(7)	-3.9(7)
N2	16.7(9)	16.2(9)	9.7(9)	-3.7(8)	1.8(7)	-9.7(8)
N3	11.3(9)	12.0(9)	15.6(10)	-4.6(8)	-1.6(8)	-0.2(8)
N4	15.3(10)	20.9(11)	15.9(10)	-2.8(9)	-2.2(9)	-2.8(9)
N5	12.9(9)	12.1(9)	10.5(9)	-4.2(7)	1.0(7)	-4.8(7)
N6	15.0(9)	10.4(9)	14.8(9)	-6.3(8)	0.3(7)	-5.9(8)
N7	12.5(9)	12.9(9)	11.1(9)	-5.9(7)	1.6(7)	-4.3(7)
O1	14.6(8)	18.5(8)	11.0(7)	-8.4(7)	-3.6(6)	-1.9(6)
O2	22.6(8)	24.0(9)	10.9(7)	-7.8(7)	-3.6(6)	-7.6(7)
O3	15.3(8)	17.8(8)	18.0(8)	-5.9(7)	-1.1(7)	-1.3(7)
O4	21.8(9)	14.8(9)	25.8(10)	-9.3(8)	-4.1(8)	-1.4(8)

Table 4 Bond Lengths for phw1110.

Atom	**Atom**	**Length/Å**	**Atom**	**Atom**	**Length/Å**
C1	C2	1.453(3)	C12	C13	1.376(3)
C1	N1	1.364(3)	C13	C14	1.404(3)
C1	N3	1.308(3)	C14	N5	1.340(3)
C2	C9	1.507(3)	C14	N6	1.378(3)
C2	N2	1.347(3)	C15	C16	1.405(3)
C3	C4	1.396(3)	C15	N6	1.383(3)
C3	C8	1.395(3)	C15	N7	1.342(3)

C3	N2	1.409(3)	C16	C17	1.370(3)
C4	C5	1.377(3)	C17	C18	1.396(3)
C5	C6	1.397(3)	C18	C19	1.367(3)
C6	C7	1.371(3)	C19	N7	1.358(3)
C7	C8	1.407(3)	Cl1	Cu1	2.7263(6)
C8	N1	1.365(3)	Cu1	N3	1.9334(19)
C9	N4	1.334(3)	Cu1	N5	1.9804(17)
C9	O3	1.229(3)	Cu1	N7	1.9839(18)
C10	C11	1.362(3)	Cu1	O1	1.9495(14)
C10	N5	1.361(3)	N1	O1	1.357(2)
C11	C12	1.399(3)	N2	O2	1.294(2)

Table 5 Bond Angles for phw1110.

Atom	**Atom**	**Atom**	**Angle/°**	**Atom**	**Atom**	**Atom**	**Angle/°**
N1	C1	C2	117.36(18)	C17	C16	C15	119.1(2)
N3	C1	C2	127.72(19)	C16	C17	C18	119.3(2)
N3	C1	N1	114.91(19)	C19	C18	C17	118.5(2)
C1	C2	C9	118.77(18)	N7	C19	C18	123.1(2)
N2	C2	C1	119.32(18)	N3	Cu1	Cl1	104.18(6)
N2	C2	C9	121.88(19)	N3	Cu1	N5	95.21(7)
C4	C3	N2	120.30(19)	N3	Cu1	N7	161.38(8)
C8	C3	C4	120.6(2)	N3	Cu1	O1	81.88(7)
C8	C3	N2	119.14(18)	N5	Cu1	Cl1	93.19(5)
C5	C4	C3	119.3(2)	N5	Cu1	N7	89.75(7)
C4	C5	C6	120.3(2)	N7	Cu1	Cl1	93.42(5)
C7	C6	C5	121.1(2)	O1	Cu1	Cl1	95.47(5)
C6	C7	C8	119.2(2)	O1	Cu1	N5	171.30(7)
C3	C8	C7	119.57(19)	O1	Cu1	N7	90.56(6)
N1	C8	C3	119.01(19)	C1	N1	C8	123.44(18)
N1	C8	C7	121.42(19)	O1	N1	C1	117.58(16)

N4	C9	C2	116.89(19)	O1	N1	C8	118.98(16)
O3	C9	C2	119.92(19)	C2	N2	C3	121.40(18)
O3	C9	N4	123.2(2)	O2	N2	C2	123.11(18)
N5	C10	C11	123.4(2)	O2	N2	C3	115.49(17)
C10	C11	C12	118.1(2)	C1	N3	Cu1	114.68(15)
C13	C12	C11	119.6(2)	C10	N5	Cu1	117.75(14)
C12	C13	C14	118.9(2)	C14	N5	C10	118.23(18)
N5	C14	C13	121.49(19)	C14	N5	Cu1	122.75(14)
N5	C14	N6	120.20(18)	C14	N6	C15	130.31(19)
N6	C14	C13	118.31(19)	C15	N7	C19	118.05(18)
N6	C15	C16	117.70(19)	C15	N7	Cu1	122.78(14)
N7	C15	C16	121.73(19)	C19	N7	Cu1	117.65(14)
N7	C15	N6	120.56(19)	N1	O1	Cu1	110.66(11)

Table 6 Hydrogen Bonds for phw1110.

D	**H**	**A**	**d(D-H)/Å**	**d(H-A)/Å**	**d(D-A)/Å**	**D-H-A/°**
N3	H3	O3	0.78(3)	2.06(3)	2.709(2)	140(2)
N4	H4A	O2	0.87(3)	1.85(3)	2.580(3)	140(3)
N6	H6A	O4	0.80(3)	2.03(3)	2.823(3)	173(3)

Table 7 Torsion Angles for phw1110.

A	**B**	**C**	**D**	**Angle/°**
C1	C2	C9	N4	166.8(2)
C1	C2	C9	O3	-11.1(3)
C1	C2	N2	C3	-4.7(3)
C1	C2	N2	O2	176.37(18)
C1	N1	O1	Cu1	5.8(2)
C2	C1	N1	C8	-4.9(3)
C2	C1	N1	O1	175.26(17)
C2	C1	N3	Cu1	-179.36(17)
C3	C4	C5	C6	0.4(3)

C3	C8	N1	C1	0.2(3)
C3	C8	N1	O1	-179.93(18)
C4	C3	C8	C7	1.7(3)
C4	C3	C8	N1	-178.4(2)
C4	C3	N2	C2	-179.2(2)
C4	C3	N2	O2	-0.2(3)
C4	C5	C6	C7	0.4(4)
C5	C6	C7	C8	-0.3(3)
C6	C7	C8	C3	-0.8(3)
C6	C7	C8	N1	179.3(2)
C7	C8	N1	C1	-179.9(2)
C7	C8	N1	O1	0.0(3)
C8	C3	C4	C5	-1.5(3)
C8	C3	N2	C2	-0.1(3)
C8	C3	N2	O2	178.95(19)
C8	N1	O1	Cu1	-174.03(15)
C9	C2	N2	C3	177.17(19)
C9	C2	N2	O2	-1.8(3)
C10	C11	C12	C13	-3.5(3)
C11	C10	N5	C14	2.8(3)
C11	C10	N5	Cu1	-164.62(17)
C11	C12	C13	C14	0.1(3)
C12	C13	C14	N5	5.1(3)
C12	C13	C14	N6	-174.8(2)
C13	C14	N5	C10	-6.4(3)
C13	C14	N5	Cu1	160.33(16)
C13	C14	N6	C15	166.1(2)
C15	C16	C17	C18	-2.7(3)
C16	C15	N6	C14	-164.9(2)

C16	C15	N7	C19	2.0(3)
C16	C15	N7	Cu1	-163.55(16)
C16	C17	C18	C19	1.4(3)
C17	C18	C19	N7	1.7(3)
C18	C19	N7	C15	-3.4(3)
C18	C19	N7	Cu1	162.94(17)
Cl1	Cu1	N3	C1	-90.53(16)
Cl1	Cu1	N5	C10	-64.04(15)
Cl1	Cu1	N5	C14	129.12(16)
Cl1	Cu1	N7	C15	-126.54(16)
Cl1	Cu1	N7	C19	67.82(15)
Cl1	Cu1	O1	N1	98.91(12)
N1	C1	C2	C9	-174.72(18)
N1	C1	C2	N2	7.1(3)
N1	C1	N3	Cu1	-0.8(2)
N2	C2	C9	N4	-15.0(3)
N2	C2	C9	O3	167.1(2)
N2	C3	C4	C5	177.6(2)
N2	C3	C8	C7	-177.47(19)
N2	C3	C8	N1	2.4(3)
N3	C1	C2	C9	3.8(3)
N3	C1	C2	N2	-174.4(2)
N3	C1	N1	C8	176.4(2)
N3	C1	N1	O1	-3.5(3)
N3	Cu1	N5	C10	40.52(17)
N3	Cu1	N5	C14	-126.32(17)
N3	Cu1	N7	C15	72.4(3)
N3	Cu1	N7	C19	-93.3(3)
N3	Cu1	O1	N1	-4.68(13)

N5	C10	C11	C12	2.2(3)
N5	C14	N6	C15	-13.7(3)
N5	Cu1	N3	C1	174.84(16)
N5	Cu1	N7	C15	-33.36(17)
N5	Cu1	N7	C19	161.00(16)
N6	C14	N5	C10	173.41(19)
N6	C14	N5	Cu1	-19.8(3)
N6	C15	C16	C17	-177.98(19)
N6	C15	N7	C19	-179.06(19)
N6	C15	N7	Cu1	15.3(3)
N7	C15	C16	C17	1.0(3)
N7	C15	N6	C14	16.1(3)
N7	Cu1	N3	C1	70.0(3)
N7	Cu1	N5	C10	-157.46(16)
N7	Cu1	N5	C14	35.71(17)
N7	Cu1	O1	N1	-167.60(13)
O1	Cu1	N3	C1	3.09(16)
O1	Cu1	N7	C15	137.95(16)
O1	Cu1	N7	C19	-27.69(16)

Table 8 Hydrogen Atom Coordinates ($Å \times 10^4$) and Isotropic Displacement Parameters ($Å^2 \times 10^3$) for phw1110.

Atom	***x***	***y***	***z***	**U(eq)**
H4	4970	1631	-1659	20
H5	7529	-302	-975	22
H6	8749	-523	585	23
H7	7435	1150	1485	18
H10	205	6002	2596	16
H11	-1668	8288	2752	19
H12	-659	10194	3131	20

H13	2188	9594	3489	17
H16	7351	6224	4510	18
H17	9551	3843	4828	19
H18	9158	1696	4385	18
H19	6638	2050	3593	17
H3	1570.0(3)	6020.0(3)	957(19)	16(7)
H4A	1030.0(4)	5900.0(4)	-2160.0(2)	34(8)
H4B	-500.0(3)	7180.0(3)	-2120.0(2)	19(7)
H6A	4780.0(3)	7660.0(3)	3704(19)	19(7)
H4C	5060.0(4)	10050.0(4)	3870.0(2)	41(10)
H4D	6110.0(4)	8980.0(4)	4510.0(3)	33(9)

[RSC Journal Format]

Experimental

Single crystals of $C_{19}H_{18}ClCuN_7O_4$ [phw1110] were recrystallised from [solvents] mounted in inert oil and transferred to the cold gas stream of the diffractometer.

Crystal structure determination of [phw1110]

Crystal Data. $C_{19}H_{18}ClCuN_7O_4$, M =507.39, triclinic, a = 8.5102(6) Å, b = 9.2014(5) Å, c = 13.9166(10) Å, α = 71.147(5)°, β = 89.498(6)°, γ = 72.581(5)°, U = 979.31(11) Å^3, T = 110.0, space group P-1 (no. 2), Z = 2, μ(Mo Kα) = 1.298, 13185 reflections measured, 4127 unique (R_{int} = 0.0326) which were used in all calculations. The final $wR(F_2)$ was 0.0707 (all data).

This report has been created with Olex2, compiled on 2011.02.15 svn.r1672. Please let us know if there are any errors or if you would like to have additional featrues.

Crystallographic data for [Cu(tpz)(dpHa)(MeOH)]Cl

Table 1. Crystal data and structure refinement for phw0914m.

Identification code	phw0914m	
Empirical formula	C18.60 H20.42 Cl Cu N7 O3.60	
Formula weight	498.75	
Temperature	110(2) K	
Wavelength	0.71073 Å	
Crystal system	Triclinic	
Space group	P-1	
Unit cell dimensions	a = 9.2226(5) Å	α= 91.4310(10)°.
	b = 14.8803(8) Å	β= 92.7400(10)°.
	c = 15.4862(9) Å	γ = 98.8030(10)°.
Volume	2096.7(2) $Å^3$	
Z	4	
Density (calculated)	1.580 Mg/m^3	
Absorption coefficient	1.209 mm^{-1}	
F(000)	1023.3	
Crystal size	0.44 x 0.13 x 0.03 mm^3	
Theta range for data collection	1.39 to 28.31°.	
Index ranges	-12<=h<=12, -19<=k<=19, -20<=l<=20	
Reflections collected	21456	
Independent reflections	10332 [R(int) = 0.0223]	
Completeness to theta = 28.31°	98.8 %	
Absorption correction	Semi-empirical from equivalents	
Max. and min. transmission	0.965 and 0.70	
Refinement method	Full-matrix least-squares on F^2	
Data / restraints / parameters	10332 / 0 / 610	
Goodness-of-fit on F^2	1.028	
Final R indices [I>2sigma(I)]	R1 = 0.0360, wR2 = 0.0881	
R indices (all data)	R1 = 0.0470, wR2 = 0.0937	
Largest diff. peak and hole	0.779 and -0.484 $e.Å^{-3}$	

Table 2. Atomic coordinates (x 10^4) and equivalent isotropic displacement parameters ($Å^2$x 10^3) for phw0914m. U(eq) is defined as one third of the trace of the orthogonalized U^{ij} tensor.

	x	y	z	U(eq)
C(1)	8438(2)	2505(1)	7946(1)	18(1)
C(2)	9929(2)	4098(1)	8662(1)	20(1)
C(3)	10647(2)	4903(1)	9063(1)	22(1)
C(4)	10613(2)	5709(1)	8652(2)	25(1)
C(5)	9888(3)	5712(2)	7834(2)	28(1)
C(6)	9196(3)	4918(2)	7422(2)	28(1)
C(7)	9210(2)	4098(1)	7851(1)	22(1)
C(8)	5634(2)	111(1)	6615(1)	21(1)
C(9)	4553(2)	-635(1)	6604(1)	24(1)
C(10)	3248(2)	-609(1)	6114(1)	25(1)
C(11)	3098(2)	151(1)	5655(1)	23(1)
C(12)	4238(2)	895(1)	5709(1)	19(1)
C(13)	7529(3)	2962(2)	4845(1)	27(1)
C(14)	7234(3)	3416(2)	4115(2)	29(1)
C(15)	5788(3)	3316(2)	3784(2)	29(1)
C(16)	4715(3)	2748(2)	4173(1)	26(1)
C(17)	5109(2)	2277(1)	4899(1)	20(1)
C(18)	9877(3)	854(2)	6471(2)	45(1)
Cu(1)	6991(1)	1982(1)	6404(1)	20(1)
N(1)	8534(2)	3283(1)	7496(1)	23(1)
N(2)	9926(2)	3253(1)	9058(1)	19(1)
N(3)	7620(2)	1789(1)	7591(1)	19(1)
N(4)	9201(2)	2488(1)	8728(1)	18(1)
N(5)	5482(2)	883(1)	6190(1)	19(1)
N(6)	4048(2)	1658(1)	5253(1)	22(1)
N(7)	6484(2)	2405(1)	5247(1)	22(1)
O(1)	7871(2)	3237(1)	6692(1)	31(1)
O(2)	10637(2)	3235(1)	9771(1)	23(1)
O(3)	8985(2)	1341(2)	5938(1)	48(1)
C(19)	5877(2)	5564(1)	9188(1)	16(1)
C(20)	4976(2)	3913(1)	8376(1)	18(1)
C(21)	4557(2)	3056(1)	7965(1)	24(1)
C(22)	3405(3)	2943(2)	7363(2)	30(1)
C(23)	2662(3)	3676(2)	7162(2)	29(1)
C(24)	3071(2)	4520(1)	7553(1)	23(1)

C(25)	4259(2)	4652(1)	8171(1)	17(1)
C(26)	2701(2)	7777(1)	8113(1)	19(1)
C(27)	1442(2)	8113(1)	7873(1)	21(1)
C(28)	823(2)	8620(1)	8488(2)	24(1)
C(29)	1502(2)	8790(1)	9291(1)	21(1)
C(30)	2836(2)	8462(1)	9480(1)	17(1)
C(31)	7292(2)	8296(1)	10335(1)	20(1)
C(32)	7924(2)	8818(1)	11036(1)	22(1)
C(33)	7026(2)	9299(1)	11514(1)	23(1)
C(34)	5580(2)	9266(1)	11251(1)	20(1)
C(35)	5012(2)	8721(1)	10521(1)	17(1)
C(36)	7442(2)	7405(2)	7814(1)	25(1)
Cu(2)	5007(1)	7250(1)	9207(1)	15(1)
N(8)	4736(2)	5465(1)	8589(1)	16(1)
N(9)	6125(2)	4053(1)	9017(1)	18(1)
N(10)	6241(2)	6365(1)	9569(1)	18(1)
N(11)	6582(2)	4843(1)	9404(1)	19(1)
N(12)	3389(2)	7932(1)	8907(1)	17(1)
N(13)	3561(2)	8716(1)	10261(1)	18(1)
N(14)	5846(2)	8220(1)	10085(1)	17(1)
O(4)	4095(2)	6207(1)	8422(1)	20(1)
O(5)	6738(2)	3390(1)	9245(1)	25(1)
O(6)	6334(2)	7902(1)	8084(1)	22(1)
Cl(1)	9175(1)	8323(1)	5657(1)	32(1)
Cl(2)	2139(1)	127(1)	1420(1)	21(1)
O(7)	8941(3)	6239(2)	5870(2)	58(1)
C(37)	8347(6)	5794(3)	5136(3)	91(2)
O(8)	6251(9)	5308(6)	6662(6)	36(3)
C(38)	5720(13)	4629(8)	6046(9)	36(3)

Table 3. Bond lengths [Å] and angles [°] for phw0914m.

C(1)-N(3)	1.301(3)
C(1)-N(1)	1.359(2)
C(1)-N(4)	1.374(3)
C(2)-C(7)	1.392(3)
C(2)-C(3)	1.393(3)
C(2)-N(2)	1.411(2)
C(3)-C(4)	1.375(3)
C(3)-H(3)	0.9500
C(4)-C(5)	1.405(3)
C(4)-H(4)	0.9500
C(5)-C(6)	1.379(3)
C(5)-H(5)	0.9500
C(6)-C(7)	1.406(3)
C(6)-H(6)	0.9500
C(7)-N(1)	1.365(3)
C(8)-N(5)	1.360(3)
C(8)-C(9)	1.372(3)
C(8)-H(8)	0.9500
C(9)-C(10)	1.398(3)
C(9)-H(9)	0.9500
C(10)-C(11)	1.373(3)
C(10)-H(10)	0.9500
C(11)-C(12)	1.402(3)
C(11)-H(11)	0.9500
C(12)-N(5)	1.341(3)
C(12)-N(6)	1.382(3)
C(13)-N(7)	1.358(3)
C(13)-C(14)	1.368(3)
C(13)-H(13)	0.9500
C(14)-C(15)	1.391(3)
C(14)-H(14)	0.9500
C(15)-C(16)	1.372(3)
C(15)-H(15)	0.9500
C(16)-C(17)	1.402(3)
C(16)-H(16)	0.9500
C(17)-N(7)	1.338(3)
C(17)-N(6)	1.382(3)
C(18)-O(3)	1.425(3)

C(18)-H(18A)	0.9800
C(18)-H(18B)	0.9800
C(18)-H(18C)	0.9800
Cu(1)-N(3)	1.9429(18)
Cu(1)-O(1)	1.9509(15)
Cu(1)-N(7)	1.9714(18)
Cu(1)-N(5)	1.9881(17)
Cu(1)-O(3)	2.3323(19)
N(1)-O(1)	1.355(2)
N(2)-O(2)	1.261(2)
N(2)-N(4)	1.307(2)
N(3)-H(3A)	0.80(3)
N(6)-H(6A)	0.76(3)
O(3)-H(3B)	0.78(4)
C(19)-N(10)	1.305(2)
C(19)-N(8)	1.357(2)
C(19)-N(11)	1.377(2)
C(20)-C(21)	1.402(3)
C(20)-C(25)	1.404(3)
C(20)-N(9)	1.404(3)
C(21)-C(22)	1.367(3)
C(21)-H(21)	0.9500
C(22)-C(23)	1.408(3)
C(22)-H(22)	0.9500
C(23)-C(24)	1.372(3)
C(23)-H(23)	0.9500
C(24)-C(25)	1.407(3)
C(24)-H(24)	0.9500
C(25)-N(8)	1.359(2)
C(26)-N(12)	1.355(3)
C(26)-C(27)	1.371(3)
C(26)-H(26)	0.9500
C(27)-C(28)	1.396(3)
C(27)-H(27)	0.9500
C(28)-C(29)	1.365(3)
C(28)-H(28)	0.9500
C(29)-C(30)	1.413(3)
C(29)-H(29)	0.9500
C(30)-N(12)	1.341(3)
C(30)-N(13)	1.369(3)

C(31)-N(14)	1.358(3)
C(31)-C(32)	1.371(3)
C(31)-H(31)	0.9500
C(32)-C(33)	1.400(3)
C(32)-H(32)	0.9500
C(33)-C(34)	1.369(3)
C(33)-H(33)	0.9500
C(34)-C(35)	1.407(3)
C(34)-H(34)	0.9500
C(35)-N(14)	1.342(2)
C(35)-N(13)	1.378(3)
C(36)-O(6)	1.423(3)
C(36)-H(36A)	0.9800
C(36)-H(36B)	0.9800
C(36)-H(36C)	0.9800
Cu(2)-N(10)	1.9437(16)
Cu(2)-N(12)	1.9736(16)
Cu(2)-N(14)	1.9981(17)
Cu(2)-O(4)	2.0005(14)
Cu(2)-O(6)	2.3215(15)
N(8)-O(4)	1.3548(19)
N(9)-O(5)	1.259(2)
N(9)-N(11)	1.307(2)
N(10)-H(10A)	0.83(2)
N(13)-H(13A)	0.74(3)
O(6)-H(6B)	0.72(3)
O(7)-C(37)	1.350(4)
O(7)-H(7)	0.91(4)
C(37)-H(37A)	0.9800
C(37)-H(37B)	0.9800
C(37)-H(37C)	0.9800
O(8)-C(38)	1.389(14)
O(8)-H(8A)	0.8400
C(38)-H(38A)	0.9800
C(38)-H(38B)	0.9800
C(38)-H(38C)	0.9800

N(3)-C(1)-N(1)	116.69(18)
N(3)-C(1)-N(4)	122.62(18)
N(1)-C(1)-N(4)	120.67(17)

C(7)-C(2)-C(3)	121.07(19)
C(7)-C(2)-N(2)	117.73(18)
C(3)-C(2)-N(2)	121.19(18)
C(4)-C(3)-C(2)	118.9(2)
C(4)-C(3)-H(3)	120.6
C(2)-C(3)-H(3)	120.6
C(3)-C(4)-C(5)	120.3(2)
C(3)-C(4)-H(4)	119.9
C(5)-C(4)-H(4)	119.9
C(6)-C(5)-C(4)	121.4(2)
C(6)-C(5)-H(5)	119.3
C(4)-C(5)-H(5)	119.3
C(5)-C(6)-C(7)	118.2(2)
C(5)-C(6)-H(6)	120.9
C(7)-C(6)-H(6)	120.9
N(1)-C(7)-C(2)	117.91(18)
N(1)-C(7)-C(6)	121.97(19)
C(2)-C(7)-C(6)	120.12(19)
N(5)-C(8)-C(9)	123.23(19)
N(5)-C(8)-H(8)	118.4
C(9)-C(8)-H(8)	118.4
C(8)-C(9)-C(10)	118.4(2)
C(8)-C(9)-H(9)	120.8
C(10)-C(9)-H(9)	120.8
C(11)-C(10)-C(9)	119.13(19)
C(11)-C(10)-H(10)	120.4
C(9)-C(10)-H(10)	120.4
C(10)-C(11)-C(12)	119.27(19)
C(10)-C(11)-H(11)	120.4
C(12)-C(11)-H(11)	120.4
N(5)-C(12)-N(6)	119.91(18)
N(5)-C(12)-C(11)	121.99(18)
N(6)-C(12)-C(11)	118.10(18)
N(7)-C(13)-C(14)	123.1(2)
N(7)-C(13)-H(13)	118.4
C(14)-C(13)-H(13)	118.4
C(13)-C(14)-C(15)	118.2(2)
C(13)-C(14)-H(14)	120.9
C(15)-C(14)-H(14)	120.9
C(16)-C(15)-C(14)	119.8(2)

C(16)-C(15)-H(15)	120.1
C(14)-C(15)-H(15)	120.1
C(15)-C(16)-C(17)	118.8(2)
C(15)-C(16)-H(16)	120.6
C(17)-C(16)-H(16)	120.6
N(7)-C(17)-N(6)	119.53(18)
N(7)-C(17)-C(16)	121.74(19)
N(6)-C(17)-C(16)	118.72(19)
O(3)-C(18)-H(18A)	109.5
O(3)-C(18)-H(18B)	109.5
H(18A)-C(18)-H(18B)	109.5
O(3)-C(18)-H(18C)	109.5
H(18A)-C(18)-H(18C)	109.5
H(18B)-C(18)-H(18C)	109.5
N(3)-Cu(1)-O(1)	83.02(7)
N(3)-Cu(1)-N(7)	169.93(7)
O(1)-Cu(1)-N(7)	86.93(7)
N(3)-Cu(1)-N(5)	99.79(7)
O(1)-Cu(1)-N(5)	160.39(7)
N(7)-Cu(1)-N(5)	89.48(7)
N(3)-Cu(1)-O(3)	89.04(7)
O(1)-Cu(1)-O(3)	102.52(8)
N(7)-Cu(1)-O(3)	93.78(7)
N(5)-Cu(1)-O(3)	96.95(8)
O(1)-N(1)-C(1)	117.94(16)
O(1)-N(1)-C(7)	120.45(16)
C(1)-N(1)-C(7)	121.53(18)
O(2)-N(2)-N(4)	118.18(16)
O(2)-N(2)-C(2)	118.55(16)
N(4)-N(2)-C(2)	123.26(16)
C(1)-N(3)-Cu(1)	112.17(14)
C(1)-N(3)-H(3A)	114(2)
Cu(1)-N(3)-H(3A)	132(2)
N(2)-N(4)-C(1)	118.25(16)
C(12)-N(5)-C(8)	117.88(17)
C(12)-N(5)-Cu(1)	122.53(13)
C(8)-N(5)-Cu(1)	119.24(14)
C(17)-N(6)-C(12)	128.08(18)
C(17)-N(6)-H(6A)	113(2)
C(12)-N(6)-H(6A)	115(2)

C(17)-N(7)-C(13)	118.20(19)
C(17)-N(7)-Cu(1)	122.76(14)
C(13)-N(7)-Cu(1)	118.31(14)
N(1)-O(1)-Cu(1)	109.37(11)
C(18)-O(3)-Cu(1)	124.76(16)
C(18)-O(3)-H(3B)	110(3)
Cu(1)-O(3)-H(3B)	122(3)
N(10)-C(19)-N(8)	116.95(17)
N(10)-C(19)-N(11)	121.68(18)
N(8)-C(19)-N(11)	121.34(17)
C(21)-C(20)-C(25)	121.46(19)
C(21)-C(20)-N(9)	120.66(18)
C(25)-C(20)-N(9)	117.88(17)
C(22)-C(21)-C(20)	118.72(19)
C(22)-C(21)-H(21)	120.6
C(20)-C(21)-H(21)	120.6
C(21)-C(22)-C(23)	120.3(2)
C(21)-C(22)-H(22)	119.8
C(23)-C(22)-H(22)	119.8
C(24)-C(23)-C(22)	121.5(2)
C(24)-C(23)-H(23)	119.2
C(22)-C(23)-H(23)	119.2
C(23)-C(24)-C(25)	119.04(19)
C(23)-C(24)-H(24)	120.5
C(25)-C(24)-H(24)	120.5
N(8)-C(25)-C(20)	118.19(18)
N(8)-C(25)-C(24)	122.89(17)
C(20)-C(25)-C(24)	118.91(18)
N(12)-C(26)-C(27)	123.25(19)
N(12)-C(26)-H(26)	118.4
C(27)-C(26)-H(26)	118.4
C(26)-C(27)-C(28)	118.10(19)
C(26)-C(27)-H(27)	120.9
C(28)-C(27)-H(27)	120.9
C(29)-C(28)-C(27)	119.67(18)
C(29)-C(28)-H(28)	120.2
C(27)-C(28)-H(28)	120.2
C(28)-C(29)-C(30)	119.25(19)
C(28)-C(29)-H(29)	120.4
C(30)-C(29)-H(29)	120.4

N(12)-C(30)-N(13)	121.10(17)
N(12)-C(30)-C(29)	121.08(19)
N(13)-C(30)-C(29)	117.81(18)
N(14)-C(31)-C(32)	123.42(19)
N(14)-C(31)-H(31)	118.3
C(32)-C(31)-H(31)	118.3
C(31)-C(32)-C(33)	118.00(19)
C(31)-C(32)-H(32)	121.0
C(33)-C(32)-H(32)	121.0
C(34)-C(33)-C(32)	119.6(2)
C(34)-C(33)-H(33)	120.2
C(32)-C(33)-H(33)	120.2
C(33)-C(34)-C(35)	119.13(19)
C(33)-C(34)-H(34)	120.4
C(35)-C(34)-H(34)	120.4
N(14)-C(35)-N(13)	120.56(18)
N(14)-C(35)-C(34)	121.64(18)
N(13)-C(35)-C(34)	117.80(17)
O(6)-C(36)-H(36A)	109.5
O(6)-C(36)-H(36B)	109.5
H(36A)-C(36)-H(36B)	109.5
O(6)-C(36)-H(36C)	109.5
H(36A)-C(36)-H(36C)	109.5
H(36B)-C(36)-H(36C)	109.5
N(10)-Cu(2)-N(12)	167.01(7)
N(10)-Cu(2)-N(14)	96.25(7)
N(12)-Cu(2)-N(14)	90.20(7)
N(10)-Cu(2)-O(4)	81.50(6)
N(12)-Cu(2)-O(4)	91.05(6)
N(14)-Cu(2)-O(4)	174.50(6)
N(10)-Cu(2)-O(6)	100.11(6)
N(12)-Cu(2)-O(6)	90.54(6)
N(14)-Cu(2)-O(6)	94.82(6)
O(4)-Cu(2)-O(6)	90.53(6)
O(4)-N(8)-C(19)	117.51(15)
O(4)-N(8)-C(25)	121.28(16)
C(19)-N(8)-C(25)	121.21(16)
O(5)-N(9)-N(11)	117.77(17)
O(5)-N(9)-C(20)	119.19(16)
N(11)-N(9)-C(20)	123.03(16)

C(19)-N(10)-Cu(2)	114.05(13)
C(19)-N(10)-H(10A)	114.9(15)
Cu(2)-N(10)-H(10A)	130.9(15)
N(9)-N(11)-C(19)	118.31(17)
C(30)-N(12)-C(26)	118.44(16)
C(30)-N(12)-Cu(2)	123.14(13)
C(26)-N(12)-Cu(2)	118.01(13)
C(30)-N(13)-C(35)	129.95(18)
C(30)-N(13)-H(13A)	113.4(19)
C(35)-N(13)-H(13A)	113.7(19)
C(35)-N(14)-C(31)	118.05(17)
C(35)-N(14)-Cu(2)	122.88(14)
C(31)-N(14)-Cu(2)	118.50(13)
N(8)-O(4)-Cu(2)	109.85(11)
C(36)-O(6)-Cu(2)	113.78(13)
C(36)-O(6)-H(6B)	107(2)
Cu(2)-O(6)-H(6B)	116(2)
C(37)-O(7)-H(7)	103(3)
O(7)-C(37)-H(37A)	109.5
O(7)-C(37)-H(37B)	109.5
H(37A)-C(37)-H(37B)	109.5
O(7)-C(37)-H(37C)	109.5
H(37A)-C(37)-H(37C)	109.5
H(37B)-C(37)-H(37C)	109.5
C(38)-O(8)-H(8A)	109.5
O(8)-C(38)-H(38A)	109.5
O(8)-C(38)-H(38B)	109.5
H(38A)-C(38)-H(38B)	109.5
O(8)-C(38)-H(38C)	109.5
H(38A)-C(38)-H(38C)	109.5
H(38B)-C(38)-H(38C)	109.5

Symmetry transformations used to generate equivalent atoms:

Table 4. Anisotropic displacement parameters ($Å^2 x\ 10^3$) for phw0914m. The anisotropic displacement factor exponent takes the form: $-2\pi^2[\ h^2\ a^{*2}U^{11} + ... + 2\ h\ k\ a^*\ b^*\ U^{12}\ ]$

	U^{11}	U^{22}	U^{33}	U^{23}	U^{13}	U^{12}

C(1)	17(1)	17(1)	19(1)	3(1)	1(1)	3(1)
C(2)	18(1)	17(1)	23(1)	3(1)	1(1)	2(1)
C(3)	18(1)	23(1)	24(1)	-1(1)	1(1)	0(1)
C(4)	23(1)	19(1)	30(1)	0(1)	3(1)	-2(1)
C(5)	31(1)	18(1)	34(1)	7(1)	1(1)	-1(1)
C(6)	35(1)	22(1)	25(1)	7(1)	-6(1)	-3(1)
C(7)	22(1)	17(1)	25(1)	2(1)	-2(1)	-1(1)
C(8)	25(1)	19(1)	20(1)	2(1)	-1(1)	4(1)
C(9)	30(1)	17(1)	24(1)	1(1)	3(1)	3(1)
C(10)	27(1)	20(1)	26(1)	-2(1)	3(1)	-4(1)
C(11)	21(1)	24(1)	22(1)	-1(1)	-1(1)	0(1)
C(12)	22(1)	20(1)	17(1)	0(1)	4(1)	5(1)
C(13)	30(1)	25(1)	24(1)	4(1)	1(1)	-2(1)
C(14)	37(1)	25(1)	23(1)	6(1)	5(1)	-1(1)
C(15)	40(1)	25(1)	22(1)	6(1)	0(1)	6(1)
C(16)	30(1)	27(1)	22(1)	4(1)	-1(1)	7(1)
C(17)	25(1)	18(1)	19(1)	-1(1)	1(1)	6(1)
C(18)	38(2)	59(2)	42(2)	5(1)	7(1)	21(1)
Cu(1)	23(1)	17(1)	19(1)	3(1)	-2(1)	-1(1)
N(1)	30(1)	18(1)	20(1)	5(1)	-6(1)	-2(1)
N(2)	16(1)	20(1)	20(1)	1(1)	0(1)	5(1)
N(3)	23(1)	14(1)	20(1)	2(1)	0(1)	1(1)
N(4)	19(1)	16(1)	19(1)	1(1)	0(1)	4(1)
N(5)	22(1)	17(1)	18(1)	0(1)	1(1)	3(1)
N(6)	18(1)	25(1)	23(1)	4(1)	-1(1)	3(1)
N(7)	24(1)	19(1)	21(1)	1(1)	1(1)	0(1)
O(1)	45(1)	21(1)	23(1)	7(1)	-13(1)	-6(1)
O(2)	21(1)	26(1)	23(1)	2(1)	-6(1)	5(1)
O(3)	36(1)	85(2)	30(1)	14(1)	11(1)	29(1)
C(19)	14(1)	18(1)	17(1)	3(1)	3(1)	4(1)
C(20)	20(1)	16(1)	19(1)	2(1)	4(1)	4(1)
C(21)	31(1)	14(1)	27(1)	0(1)	6(1)	4(1)
C(22)	40(1)	18(1)	29(1)	-3(1)	0(1)	1(1)
C(23)	36(1)	23(1)	26(1)	-4(1)	-8(1)	2(1)
C(24)	27(1)	20(1)	22(1)	-1(1)	-4(1)	5(1)
C(25)	20(1)	15(1)	17(1)	2(1)	3(1)	3(1)
C(26)	19(1)	15(1)	22(1)	3(1)	2(1)	3(1)
C(27)	19(1)	18(1)	25(1)	4(1)	-3(1)	1(1)
C(28)	15(1)	16(1)	41(1)	4(1)	-2(1)	3(1)
C(29)	18(1)	16(1)	32(1)	2(1)	5(1)	7(1)

C(30)	16(1)	12(1)	24(1)	4(1)	3(1)	2(1)
C(31)	19(1)	16(1)	26(1)	2(1)	1(1)	4(1)
C(32)	20(1)	19(1)	27(1)	2(1)	-3(1)	2(1)
C(33)	26(1)	18(1)	23(1)	-1(1)	-1(1)	0(1)
C(34)	25(1)	14(1)	22(1)	-1(1)	5(1)	3(1)
C(35)	19(1)	13(1)	20(1)	2(1)	3(1)	2(1)
C(36)	22(1)	28(1)	24(1)	-1(1)	4(1)	4(1)
Cu(2)	15(1)	12(1)	19(1)	0(1)	0(1)	5(1)
N(8)	18(1)	12(1)	19(1)	1(1)	0(1)	5(1)
N(9)	19(1)	14(1)	24(1)	3(1)	4(1)	4(1)
N(10)	17(1)	16(1)	21(1)	0(1)	-2(1)	5(1)
N(11)	17(1)	14(1)	26(1)	4(1)	2(1)	5(1)
N(12)	16(1)	13(1)	21(1)	2(1)	2(1)	4(1)
N(13)	19(1)	17(1)	22(1)	-3(1)	5(1)	7(1)
N(14)	17(1)	13(1)	21(1)	1(1)	3(1)	3(1)
O(4)	21(1)	13(1)	26(1)	1(1)	-5(1)	9(1)
O(5)	24(1)	14(1)	39(1)	6(1)	0(1)	10(1)
O(6)	20(1)	18(1)	27(1)	0(1)	5(1)	2(1)
Cl(1)	23(1)	41(1)	33(1)	12(1)	3(1)	7(1)
Cl(2)	24(1)	16(1)	25(1)	1(1)	3(1)	8(1)
O(7)	78(2)	39(1)	55(1)	18(1)	-12(1)	4(1)
C(37)	137(4)	65(3)	65(3)	-3(2)	-28(3)	11(3)
O(8)	27(4)	39(5)	45(5)	-4(4)	8(4)	11(4)
C(38)	29(6)	31(6)	48(8)	-12(5)	12(5)	-1(5)

Table 5. Hydrogen coordinates (x 10^4) and isotropic displacement parameters ($Å^2$x 10^3) for phw0914m.

	x	y	z	U(eq)
H(3)	11152	4896	9612	27
H(4)	11081	6265	8922	29
H(5)	9874	6274	7557	34
H(6)	8724	4926	6864	34
H(8)	6532	86	6934	26
H(9)	4689	-1156	6922	28
H(10)	2474	-1111	6100	30

H(11)	2232	174	5303	27
H(13)	8512	3040	5081	32
H(14)	7997	3789	3842	34
H(15)	5544	3640	3290	35
H(16)	3722	2676	3954	31
H(18A)	10870	1200	6548	67
H(18B)	9924	260	6195	67
H(18C)	9451	767	7036	67
H(3A)	7630(30)	1340(20)	7856(19)	37(8)
H(6A)	3290(30)	1640(20)	5033(19)	38(8)
H(3B)	9390(40)	1500(20)	5520(20)	57
H(21)	5064	2564	8101	29
H(22)	3103	2366	7079	36
H(23)	1859	3584	6745	35
H(24)	2560	5008	7409	28
H(26)	3111	7418	7701	22
H(27)	1004	8004	7305	25
H(28)	-66	8845	8349	28
H(29)	1082	9126	9717	25
H(31)	7898	7971	10007	24
H(32)	8940	8852	11193	26
H(33)	7418	9646	12018	28
H(34)	4968	9607	11558	24
H(36A)	8118	7338	8308	37
H(36B)	7988	7732	7360	37
H(36C)	6985	6801	7589	37
H(10A)	6990(30)	6420(15)	9896(15)	14(5)
H(13A)	3190(30)	9023(17)	10528(16)	18(6)
H(6B)	6670(30)	8370(20)	8150(19)	38(9)
H(7)	9040(50)	6840(30)	5720(30)	90(14)
H(37A)	7564	6104	4894	136
H(37B)	7939	5168	5266	136
H(37C)	9108	5788	4716	136
H(8A)	6845	5710	6438	54
H(38A)	6500	4273	5918	54
H(38B)	5399	4905	5516	54
H(38C)	4887	4228	6268	54

Table 6. Torsion angles [°] for phw0914m.

C(7)-C(2)-C(3)-C(4)	1.2(3)
N(2)-C(2)-C(3)-C(4)	-179.73(19)
C(2)-C(3)-C(4)-C(5)	-1.2(3)
C(3)-C(4)-C(5)-C(6)	0.0(4)
C(4)-C(5)-C(6)-C(7)	1.1(4)
C(3)-C(2)-C(7)-N(1)	179.77(19)
N(2)-C(2)-C(7)-N(1)	0.7(3)
C(3)-C(2)-C(7)-C(6)	0.0(3)
N(2)-C(2)-C(7)-C(6)	-179.1(2)
C(5)-C(6)-C(7)-N(1)	179.1(2)
C(5)-C(6)-C(7)-C(2)	-1.1(3)
N(5)-C(8)-C(9)-C(10)	1.8(3)
C(8)-C(9)-C(10)-C(11)	0.8(3)
C(9)-C(10)-C(11)-C(12)	-2.0(3)
C(10)-C(11)-C(12)-N(5)	0.8(3)
C(10)-C(11)-C(12)-N(6)	-178.83(19)
N(7)-C(13)-C(14)-C(15)	1.6(4)
C(13)-C(14)-C(15)-C(16)	-2.3(3)
C(14)-C(15)-C(16)-C(17)	-0.2(3)
C(15)-C(16)-C(17)-N(7)	3.6(3)
C(15)-C(16)-C(17)-N(6)	-175.5(2)
N(3)-C(1)-N(1)-O(1)	-5.0(3)
N(4)-C(1)-N(1)-O(1)	173.79(18)
N(3)-C(1)-N(1)-C(7)	171.8(2)
N(4)-C(1)-N(1)-C(7)	-9.5(3)
C(2)-C(7)-N(1)-O(1)	-177.15(19)
C(6)-C(7)-N(1)-O(1)	2.7(3)
C(2)-C(7)-N(1)-C(1)	6.2(3)
C(6)-C(7)-N(1)-C(1)	-174.0(2)
C(7)-C(2)-N(2)-O(2)	176.36(18)
C(3)-C(2)-N(2)-O(2)	-2.7(3)
C(7)-C(2)-N(2)-N(4)	-4.8(3)
C(3)-C(2)-N(2)-N(4)	176.16(19)
N(1)-C(1)-N(3)-Cu(1)	9.4(2)
N(4)-C(1)-N(3)-Cu(1)	-169.36(15)
O(1)-Cu(1)-N(3)-C(1)	-8.16(15)
N(7)-Cu(1)-N(3)-C(1)	-11.9(5)
N(5)-Cu(1)-N(3)-C(1)	-168.54(14)
O(3)-Cu(1)-N(3)-C(1)	94.58(15)

O(2)-N(2)-N(4)-C(1)	-179.34(17)
C(2)-N(2)-N(4)-C(1)	1.8(3)
N(3)-C(1)-N(4)-N(2)	-176.03(18)
N(1)-C(1)-N(4)-N(2)	5.3(3)
N(6)-C(12)-N(5)-C(8)	-178.69(18)
C(11)-C(12)-N(5)-C(8)	1.7(3)
N(6)-C(12)-N(5)-Cu(1)	8.1(3)
C(11)-C(12)-N(5)-Cu(1)	-171.57(15)
C(9)-C(8)-N(5)-C(12)	-3.0(3)
C(9)-C(8)-N(5)-Cu(1)	170.45(16)
N(3)-Cu(1)-N(5)-C(12)	143.45(16)
O(1)-Cu(1)-N(5)-C(12)	46.7(3)
N(7)-Cu(1)-N(5)-C(12)	-32.58(16)
O(3)-Cu(1)-N(5)-C(12)	-126.33(16)
N(3)-Cu(1)-N(5)-C(8)	-29.70(16)
O(1)-Cu(1)-N(5)-C(8)	-126.4(2)
N(7)-Cu(1)-N(5)-C(8)	154.26(16)
O(3)-Cu(1)-N(5)-C(8)	60.52(16)
N(7)-C(17)-N(6)-C(12)	-26.8(3)
C(16)-C(17)-N(6)-C(12)	152.4(2)
N(5)-C(12)-N(6)-C(17)	30.6(3)
C(11)-C(12)-N(6)-C(17)	-149.7(2)
N(6)-C(17)-N(7)-C(13)	174.79(19)
C(16)-C(17)-N(7)-C(13)	-4.4(3)
N(6)-C(17)-N(7)-Cu(1)	-15.2(3)
C(16)-C(17)-N(7)-Cu(1)	165.63(16)
C(14)-C(13)-N(7)-C(17)	1.8(3)
C(14)-C(13)-N(7)-Cu(1)	-168.70(18)
N(3)-Cu(1)-N(7)-C(17)	-120.7(4)
O(1)-Cu(1)-N(7)-C(17)	-124.40(17)
N(5)-Cu(1)-N(7)-C(17)	36.31(17)
O(3)-Cu(1)-N(7)-C(17)	133.24(17)
N(3)-Cu(1)-N(7)-C(13)	49.3(5)
O(1)-Cu(1)-N(7)-C(13)	45.60(17)
N(5)-Cu(1)-N(7)-C(13)	-153.69(17)
O(3)-Cu(1)-N(7)-C(13)	-56.76(17)
C(1)-N(1)-O(1)-Cu(1)	-2.0(2)
C(7)-N(1)-O(1)-Cu(1)	-178.82(16)
N(3)-Cu(1)-O(1)-N(1)	5.38(14)
N(7)-Cu(1)-O(1)-N(1)	-175.27(15)

N(5)-Cu(1)-O(1)-N(1)	105.0(2)
O(3)-Cu(1)-O(1)-N(1)	-82.07(14)
N(3)-Cu(1)-O(3)-C(18)	12.5(2)
O(1)-Cu(1)-O(3)-C(18)	95.1(2)
N(7)-Cu(1)-O(3)-C(18)	-177.2(2)
N(5)-Cu(1)-O(3)-C(18)	-87.3(2)
C(25)-C(20)-C(21)-C(22)	-1.3(3)
N(9)-C(20)-C(21)-C(22)	178.1(2)
C(20)-C(21)-C(22)-C(23)	0.3(3)
C(21)-C(22)-C(23)-C(24)	0.4(4)
C(22)-C(23)-C(24)-C(25)	-0.1(4)
C(21)-C(20)-C(25)-N(8)	-179.24(18)
N(9)-C(20)-C(25)-N(8)	1.4(3)
C(21)-C(20)-C(25)-C(24)	1.6(3)
N(9)-C(20)-C(25)-C(24)	-177.80(18)
C(23)-C(24)-C(25)-N(8)	180.0(2)
C(23)-C(24)-C(25)-C(20)	-0.9(3)
N(12)-C(26)-C(27)-C(28)	-1.7(3)
C(26)-C(27)-C(28)-C(29)	2.1(3)
C(27)-C(28)-C(29)-C(30)	1.0(3)
C(28)-C(29)-C(30)-N(12)	-4.8(3)
C(28)-C(29)-C(30)-N(13)	173.92(18)
N(14)-C(31)-C(32)-C(33)	-0.3(3)
C(31)-C(32)-C(33)-C(34)	-2.7(3)
C(32)-C(33)-C(34)-C(35)	2.3(3)
C(33)-C(34)-C(35)-N(14)	1.2(3)
C(33)-C(34)-C(35)-N(13)	-178.66(19)
N(10)-C(19)-N(8)-O(4)	1.5(3)
N(11)-C(19)-N(8)-O(4)	179.30(16)
N(10)-C(19)-N(8)-C(25)	-178.72(18)
N(11)-C(19)-N(8)-C(25)	-0.9(3)
C(20)-C(25)-N(8)-O(4)	179.96(17)
C(24)-C(25)-N(8)-O(4)	-0.9(3)
C(20)-C(25)-N(8)-C(19)	0.2(3)
C(24)-C(25)-N(8)-C(19)	179.32(19)
C(21)-C(20)-N(9)-O(5)	-2.9(3)
C(25)-C(20)-N(9)-O(5)	176.46(18)
C(21)-C(20)-N(9)-N(11)	178.20(19)
C(25)-C(20)-N(9)-N(11)	-2.4(3)
N(8)-C(19)-N(10)-Cu(2)	1.6(2)

N(11)-C(19)-N(10)-Cu(2)	-176.25(14)
N(12)-Cu(2)-N(10)-C(19)	52.9(4)
N(14)-Cu(2)-N(10)-C(19)	172.20(14)
O(4)-Cu(2)-N(10)-C(19)	-2.73(14)
O(6)-Cu(2)-N(10)-C(19)	-91.76(15)
O(5)-N(9)-N(11)-C(19)	-177.16(17)
C(20)-N(9)-N(11)-C(19)	1.7(3)
N(10)-C(19)-N(11)-N(9)	177.67(18)
N(8)-C(19)-N(11)-N(9)	0.0(3)
N(13)-C(30)-N(12)-C(26)	-173.50(18)
C(29)-C(30)-N(12)-C(26)	5.2(3)
N(13)-C(30)-N(12)-Cu(2)	14.1(3)
C(29)-C(30)-N(12)-Cu(2)	-167.18(14)
C(27)-C(26)-N(12)-C(30)	-1.9(3)
C(27)-C(26)-N(12)-Cu(2)	170.83(15)
N(10)-Cu(2)-N(12)-C(30)	88.6(3)
N(14)-Cu(2)-N(12)-C(30)	-31.38(16)
O(4)-Cu(2)-N(12)-C(30)	143.26(15)
O(6)-Cu(2)-N(12)-C(30)	-126.20(15)
N(10)-Cu(2)-N(12)-C(26)	-83.8(4)
N(14)-Cu(2)-N(12)-C(26)	156.21(15)
O(4)-Cu(2)-N(12)-C(26)	-29.16(15)
O(6)-Cu(2)-N(12)-C(26)	61.39(14)
N(12)-C(30)-N(13)-C(35)	18.8(3)
C(29)-C(30)-N(13)-C(35)	-159.94(19)
N(14)-C(35)-N(13)-C(30)	-19.1(3)
C(34)-C(35)-N(13)-C(30)	160.74(19)
N(13)-C(35)-N(14)-C(31)	175.73(18)
C(34)-C(35)-N(14)-C(31)	-4.1(3)
N(13)-C(35)-N(14)-Cu(2)	-13.1(3)
C(34)-C(35)-N(14)-Cu(2)	167.03(14)
C(32)-C(31)-N(14)-C(35)	3.7(3)
C(32)-C(31)-N(14)-Cu(2)	-167.83(16)
N(10)-Cu(2)-N(14)-C(35)	-137.79(15)
N(12)-Cu(2)-N(14)-C(35)	30.91(16)
O(6)-Cu(2)-N(14)-C(35)	121.47(15)
N(10)-Cu(2)-N(14)-C(31)	33.33(16)
N(12)-Cu(2)-N(14)-C(31)	-157.98(15)
O(6)-Cu(2)-N(14)-C(31)	-67.42(15)
C(19)-N(8)-O(4)-Cu(2)	-3.6(2)

C(25)-N(8)-O(4)-Cu(2)	176.61(14)
N(10)-Cu(2)-O(4)-N(8)	3.33(12)
N(12)-Cu(2)-O(4)-N(8)	-165.98(12)
O(6)-Cu(2)-O(4)-N(8)	103.48(12)
N(10)-Cu(2)-O(6)-C(36)	13.03(15)
N(12)-Cu(2)-O(6)-C(36)	-159.48(14)
N(14)-Cu(2)-O(6)-C(36)	110.27(14)
O(4)-Cu(2)-O(6)-C(36)	-68.43(14)

Symmetry transformations used to generate equivalent atoms:

Table 7. Hydrogen bonds for phw0914m [Å and °].

D-H...A	d(D-H)	d(H...A)	d(D...A)	<(DHA)
O(8)-H(8A)...O(7)	0.84	2.21	2.984(9)	154
O(7)-H(7)...Cl(1)	0.91(4)	2.20(4)	3.102(2)	168(4)
O(6)-H(6B)...Cl(2)#1	0.72(3)	2.40(3)	3.1135(17)	172(3)
N(13)-H(13A)...Cl(2)#2	0.74(3)	2.46(3)	3.1980(18)	175(2)
N(10)-H(10A)...O(2)#3	0.83(2)	2.21(2)	2.975(2)	155(2)
O(3)-H(3B)...Cl(1)#4	0.78(4)	2.30(4)	3.071(2)	167(3)
N(6)-H(6A)...Cl(1)#1	0.76(3)	2.48(3)	3.232(2)	177(3)
N(3)-H(3A)...Cl(2)#5	0.80(3)	2.51(3)	3.3028(18)	174(3)

Symmetry transformations used to generate equivalent atoms:

#1 -x+1,-y+1,-z+1 #2 x,y+1,z+1 #3 -x+2,-y+1,-z+2

#4 -x+2,-y+1,-z+1 #5 -x+1,-y,-z+1

Crystallographic data for $[Co(tpz\text{-}CN)(dpHa)_2](BF_4)_2$

Table 1. Crystal data and structure refinement for phw0913m.

Identification code	phw0913m	
Empirical formula	C29 H23 B2 Co F8 N10 O2	
Formula weight	776.12	
Temperature	110(2) K	
Wavelength	0.71073 Å	
Crystal system	Triclinic	
Space group	P-1	
Unit cell dimensions	a = 11.9399(10) Å	α= 90.789(2)°.
	b = 12.6855(11) Å	β= 107.803(2)°.
	c = 14.2855(12) Å	γ = 107.775(2)°.
Volume	1948.0(3) $Å^3$	
Z	2	
Density (calculated)	1.323 Mg/m^3	
Absorption coefficient	0.518 mm^{-1}	
F(000)	784	
Crystal size	0.41 x 0.33 x 0.20 mm^3	
Theta range for data collection	1.51 to 28.31°.	
Index ranges	-15<=h<=15, -16<=k<=16, -19<=l<=19	
Reflections collected	20042	
Independent reflections	9561 [R(int) = 0.0159]	
Completeness to theta = 28.31°	98.6 %	
Absorption correction	Semi-empirical from equivalents	
Max. and min. transmission	0.904 and 0.764	
Refinement method	Full-matrix least-squares on F^2	
Data / restraints / parameters	9561 / 56 / 573	
Goodness-of-fit on F^2	1.046	
Final R indices [I>2sigma(I)]	R1 = 0.0389, wR2 = 0.1065	
R indices (all data)	R1 = 0.0428, wR2 = 0.1097	
Largest diff. peak and hole	0.573 and -0.555 $e.Å^{-3}$	

Table 2. Atomic coordinates (x 10^4) and equivalent isotropic displacement parameters ($Å^2$x 10^3) for phw0913m. U(eq) is defined as one third of the trace of the orthogonalized U^{ij} tensor.

	x	y	z	U(eq)
C(1)	6347(1)	4928(1)	2409(1)	25(1)
C(2)	5087(1)	4199(1)	2067(1)	28(1)
C(3)	5152(2)	3883(1)	3718(1)	30(1)
C(4)	4548(2)	3388(2)	4379(1)	36(1)
C(5)	5191(2)	3626(2)	5381(1)	39(1)
C(6)	6417(2)	4352(2)	5727(1)	37(1)
C(7)	7022(2)	4835(1)	5080(1)	33(1)
C(8)	6386(2)	4597(1)	4062(1)	28(1)
C(9)	4425(1)	3987(1)	1036(1)	30(1)
C(10)	9294(2)	8197(1)	1484(1)	36(1)
C(11)	9331(2)	8675(2)	635(1)	48(1)
C(12)	9037(2)	7987(2)	-237(1)	47(1)
C(13)	8788(2)	6865(2)	-209(1)	37(1)
C(14)	8804(1)	6428(1)	689(1)	30(1)
C(15)	9714(2)	4728(1)	3219(1)	37(1)
C(16)	9972(2)	3758(2)	3100(2)	45(1)
C(17)	9718(2)	3268(2)	2144(2)	49(1)
C(18)	9245(2)	3779(2)	1349(2)	43(1)
C(19)	9036(2)	4784(1)	1518(1)	33(1)
C(20)	11269(2)	7354(1)	3426(1)	36(1)
C(21)	12407(2)	7805(2)	4149(2)	46(1)
C(22)	12443(2)	8241(2)	5066(2)	52(1)
C(23)	11373(2)	8294(2)	5195(1)	43(1)
C(24)	10251(2)	7873(1)	4409(1)	33(1)
C(25)	6889(2)	7686(1)	2143(1)	31(1)
C(26)	6172(2)	8280(2)	2313(1)	38(1)
C(27)	6450(2)	8765(2)	3277(2)	43(1)
C(28)	7452(2)	8668(2)	4010(1)	39(1)
C(29)	8171(2)	8065(1)	3784(1)	31(1)
Co(1)	8595(1)	6430(1)	2640(1)	25(1)
N(1)	6944(1)	5077(1)	3390(1)	26(1)
N(2)	4503(1)	3680(1)	2687(1)	31(1)
N(3)	6990(1)	5469(1)	1868(1)	26(1)
N(4)	3989(1)	3866(1)	191(1)	39(1)
N(5)	8986(1)	7074(1)	1514(1)	27(1)

N(6)	8598(1)	5303(1)	715(1)	33(1)
N(7)	9238(1)	5238(1)	2436(1)	30(1)
N(8)	10189(1)	7344(1)	3559(1)	29(1)
N(9)	9203(2)	8016(1)	4517(1)	35(1)
N(10)	7864(1)	7548(1)	2869(1)	27(1)
O(1)	8163(1)	5758(1)	3721(1)	30(1)
O(2)	3393(1)	3028(1)	2362(1)	43(1)
B(1A)	2889(6)	6372(6)	1568(4)	36(2)
F(1A)	3554(5)	5679(4)	1899(3)	68(1)
F(2A)	1635(3)	5832(2)	1143(2)	55(1)
F(3A)	3156(12)	7182(8)	2300(6)	58(2)
F(4A)	3115(8)	6840(5)	762(4)	119(2)
B(1B)	2858(13)	6482(12)	1566(10)	71(7)
F(1B)	3112(18)	5503(10)	1648(11)	186(6)
F(2B)	1615(7)	6032(11)	1471(9)	213(7)
F(3B)	3347(16)	7151(11)	2426(9)	44(2)
F(4B)	3335(5)	6911(8)	828(5)	80(3)
B(2A)	9031(6)	9132(6)	6808(6)	37(1)
F(5A)	8560(9)	8088(7)	6354(8)	46(2)
F(6A)	9866(2)	9797(2)	6395(2)	56(1)
F(7A)	8002(3)	9492(2)	6607(2)	71(1)
F(8A)	9665(14)	9194(9)	7817(6)	47(2)
B(2B)	9453(9)	9198(9)	6872(9)	35(2)
F(5B)	8781(15)	8138(10)	6342(13)	47(3)
F(6B)	10531(5)	9267(5)	6672(5)	92(2)
F(7B)	9096(5)	10084(3)	6499(2)	60(2)
F(8B)	9450(20)	9154(16)	7840(10)	49(4)

Table 3. Bond lengths [Å] and angles [°] for phw0913m.

C(1)-N(3)	1.3094(19)
C(1)-N(1)	1.3446(19)
C(1)-C(2)	1.430(2)
C(2)-N(2)	1.3483(19)
C(2)-C(9)	1.419(2)
C(3)-C(8)	1.400(2)
C(3)-C(4)	1.402(2)
C(3)-N(2)	1.416(2)
C(4)-C(5)	1.380(3)
C(4)-H(4)	0.9500
C(5)-C(6)	1.399(3)
C(5)-H(5)	0.9500
C(6)-C(7)	1.380(2)
C(6)-H(6)	0.9500
C(7)-C(8)	1.399(2)
C(7)-H(7)	0.9500
C(8)-N(1)	1.3769(19)
C(9)-N(4)	1.146(2)
C(10)-N(5)	1.363(2)
C(10)-C(11)	1.370(2)
C(10)-H(10)	0.9500
C(11)-C(12)	1.397(3)
C(11)-H(11)	0.9500
C(12)-C(13)	1.366(3)
C(12)-H(12)	0.9500
C(13)-C(14)	1.401(2)
C(13)-H(13)	0.9500
C(14)-N(5)	1.346(2)
C(14)-N(6)	1.375(2)
C(15)-N(7)	1.359(2)
C(15)-C(16)	1.376(3)
C(15)-H(15)	0.9500
C(16)-C(17)	1.397(3)
C(16)-H(16)	0.9500
C(17)-C(18)	1.371(3)
C(17)-H(17)	0.9500
C(18)-C(19)	1.404(2)
C(18)-H(18)	0.9500

C(19)-N(7)	1.346(2)
C(19)-N(6)	1.374(2)
C(20)-N(8)	1.356(2)
C(20)-C(21)	1.375(3)
C(20)-H(20)	0.9500
C(21)-C(22)	1.398(3)
C(21)-H(21)	0.9500
C(22)-C(23)	1.366(3)
C(22)-H(22)	0.9500
C(23)-C(24)	1.403(2)
C(23)-H(23)	0.9500
C(24)-N(8)	1.350(2)
C(24)-N(9)	1.371(2)
C(25)-N(10)	1.361(2)
C(25)-C(26)	1.370(2)
C(25)-H(25)	0.9500
C(26)-C(27)	1.400(3)
C(26)-H(26)	0.9500
C(27)-C(28)	1.367(3)
C(27)-H(27)	0.9500
C(28)-C(29)	1.410(2)
C(28)-H(28)	0.9500
C(29)-N(10)	1.344(2)
C(29)-N(9)	1.371(2)
Co(1)-N(3)	1.9022(13)
Co(1)-O(1)	1.9059(11)
Co(1)-N(5)	1.9337(13)
Co(1)-N(8)	1.9422(14)
Co(1)-N(7)	1.9484(14)
Co(1)-N(10)	1.9484(13)
N(1)-O(1)	1.3745(16)
N(2)-O(2)	1.2645(18)
N(3)-H(3)	0.87(2)
N(6)-H(6A)	0.79(3)
N(9)-H(9)	0.79(3)
B(1A)-F(3A)	1.348(8)
B(1A)-F(1A)	1.354(7)
B(1A)-F(4A)	1.365(7)
B(1A)-F(2A)	1.373(6)
B(1B)-F(3B)	1.341(12)

B(1B)-F(1B)	1.364(13)
B(1B)-F(2B)	1.380(12)
B(1B)-F(4B)	1.388(11)
B(2A)-F(5A)	1.339(8)
B(2A)-F(6A)	1.384(6)
B(2A)-F(7A)	1.390(6)
B(2A)-F(8A)	1.396(9)
B(2B)-F(7B)	1.378(10)
B(2B)-F(6B)	1.380(9)
B(2B)-F(8B)	1.384(12)
B(2B)-F(5B)	1.403(11)

N(3)-C(1)-N(1)	116.02(13)
N(3)-C(1)-C(2)	127.02(14)
N(1)-C(1)-C(2)	116.96(13)
N(2)-C(2)-C(9)	118.13(14)
N(2)-C(2)-C(1)	122.56(14)
C(9)-C(2)-C(1)	119.30(13)
C(8)-C(3)-C(4)	120.96(15)
C(8)-C(3)-N(2)	119.26(13)
C(4)-C(3)-N(2)	119.77(15)
C(5)-C(4)-C(3)	118.59(16)
C(5)-C(4)-H(4)	120.7
C(3)-C(4)-H(4)	120.7
C(4)-C(5)-C(6)	120.57(15)
C(4)-C(5)-H(5)	119.7
C(6)-C(5)-H(5)	119.7
C(7)-C(6)-C(5)	121.20(16)
C(7)-C(6)-H(6)	119.4
C(5)-C(6)-H(6)	119.4
C(6)-C(7)-C(8)	118.95(16)
C(6)-C(7)-H(7)	120.5
C(8)-C(7)-H(7)	120.5
N(1)-C(8)-C(7)	120.95(14)
N(1)-C(8)-C(3)	119.30(14)
C(7)-C(8)-C(3)	119.73(14)
N(4)-C(9)-C(2)	173.91(17)
N(5)-C(10)-C(11)	122.64(16)
N(5)-C(10)-H(10)	118.7
C(11)-C(10)-H(10)	118.7

C(10)-C(11)-C(12)	118.83(17)
C(10)-C(11)-H(11)	120.6
C(12)-C(11)-H(11)	120.6
C(13)-C(12)-C(11)	119.24(16)
C(13)-C(12)-H(12)	120.4
C(11)-C(12)-H(12)	120.4
C(12)-C(13)-C(14)	119.23(16)
C(12)-C(13)-H(13)	120.4
C(14)-C(13)-H(13)	120.4
N(5)-C(14)-N(6)	119.56(14)
N(5)-C(14)-C(13)	121.84(15)
N(6)-C(14)-C(13)	118.58(15)
N(7)-C(15)-C(16)	122.23(17)
N(7)-C(15)-H(15)	118.9
C(16)-C(15)-H(15)	118.9
C(15)-C(16)-C(17)	119.10(18)
C(15)-C(16)-H(16)	120.5
C(17)-C(16)-H(16)	120.5
C(18)-C(17)-C(16)	119.20(18)
C(18)-C(17)-H(17)	120.4
C(16)-C(17)-H(17)	120.4
C(17)-C(18)-C(19)	119.07(18)
C(17)-C(18)-H(18)	120.5
C(19)-C(18)-H(18)	120.5
N(7)-C(19)-N(6)	119.73(15)
N(7)-C(19)-C(18)	121.87(16)
N(6)-C(19)-C(18)	118.40(16)
N(8)-C(20)-C(21)	122.65(17)
N(8)-C(20)-H(20)	118.7
C(21)-C(20)-H(20)	118.7
C(20)-C(21)-C(22)	118.42(19)
C(20)-C(21)-H(21)	120.8
C(22)-C(21)-H(21)	120.8
C(23)-C(22)-C(21)	119.62(18)
C(23)-C(22)-H(22)	120.2
C(21)-C(22)-H(22)	120.2
C(22)-C(23)-C(24)	118.98(18)
C(22)-C(23)-H(23)	120.5
C(24)-C(23)-H(23)	120.5
N(8)-C(24)-N(9)	120.04(15)

N(8)-C(24)-C(23)	121.56(17)
N(9)-C(24)-C(23)	118.40(16)
N(10)-C(25)-C(26)	122.96(15)
N(10)-C(25)-H(25)	118.5
C(26)-C(25)-H(25)	118.5
C(25)-C(26)-C(27)	118.59(17)
C(25)-C(26)-H(26)	120.7
C(27)-C(26)-H(26)	120.7
C(28)-C(27)-C(26)	119.20(17)
C(28)-C(27)-H(27)	120.4
C(26)-C(27)-H(27)	120.4
C(27)-C(28)-C(29)	119.50(16)
C(27)-C(28)-H(28)	120.2
C(29)-C(28)-H(28)	120.2
N(10)-C(29)-N(9)	119.99(15)
N(10)-C(29)-C(28)	121.30(16)
N(9)-C(29)-C(28)	118.71(15)
N(3)-Co(1)-O(1)	84.07(5)
N(3)-Co(1)-N(5)	94.08(5)
O(1)-Co(1)-N(5)	178.10(5)
N(3)-Co(1)-N(8)	173.54(5)
O(1)-Co(1)-N(8)	89.47(5)
N(5)-Co(1)-N(8)	92.38(5)
N(3)-Co(1)-N(7)	87.59(6)
O(1)-Co(1)-N(7)	89.62(6)
N(5)-Co(1)-N(7)	89.88(6)
N(8)-Co(1)-N(7)	92.63(6)
N(3)-Co(1)-N(10)	89.82(6)
O(1)-Co(1)-N(10)	87.22(5)
N(5)-Co(1)-N(10)	93.21(5)
N(8)-Co(1)-N(10)	89.62(6)
N(7)-Co(1)-N(10)	176.10(5)
C(1)-N(1)-O(1)	117.30(12)
C(1)-N(1)-C(8)	123.13(13)
O(1)-N(1)-C(8)	119.56(12)
O(2)-N(2)-C(2)	121.11(14)
O(2)-N(2)-C(3)	120.15(13)
C(2)-N(2)-C(3)	118.74(13)
C(1)-N(3)-Co(1)	112.76(10)
C(1)-N(3)-H(3)	116.2(14)

Co(1)-N(3)-H(3)	129.4(14)
C(14)-N(5)-C(10)	117.84(13)
C(14)-N(5)-Co(1)	121.30(11)
C(10)-N(5)-Co(1)	120.26(10)
C(19)-N(6)-C(14)	126.94(14)
C(19)-N(6)-H(6A)	114.3(18)
C(14)-N(6)-H(6A)	113.7(18)
C(19)-N(7)-C(15)	118.46(14)
C(19)-N(7)-Co(1)	120.95(11)
C(15)-N(7)-Co(1)	119.67(12)
C(24)-N(8)-C(20)	118.18(15)
C(24)-N(8)-Co(1)	120.42(11)
C(20)-N(8)-Co(1)	120.89(11)
C(29)-N(9)-C(24)	127.49(14)
C(29)-N(9)-H(9)	113.9(18)
C(24)-N(9)-H(9)	114.9(18)
C(29)-N(10)-C(25)	118.27(14)
C(29)-N(10)-Co(1)	120.71(11)
C(25)-N(10)-Co(1)	120.17(11)
N(1)-O(1)-Co(1)	109.31(8)
F(3A)-B(1A)-F(1A)	109.6(7)
F(3A)-B(1A)-F(4A)	109.6(7)
F(1A)-B(1A)-F(4A)	112.3(6)
F(3A)-B(1A)-F(2A)	113.0(7)
F(1A)-B(1A)-F(2A)	113.8(6)
F(4A)-B(1A)-F(2A)	98.1(5)
F(3B)-B(1B)-F(1B)	112.7(13)
F(3B)-B(1B)-F(2B)	103.7(11)
F(1B)-B(1B)-F(2B)	96.2(12)
F(3B)-B(1B)-F(4B)	114.4(11)
F(1B)-B(1B)-F(4B)	102.2(12)
F(2B)-B(1B)-F(4B)	126.1(13)
F(5A)-B(2A)-F(6A)	110.7(7)
F(5A)-B(2A)-F(7A)	103.7(6)
F(6A)-B(2A)-F(7A)	108.8(5)
F(5A)-B(2A)-F(8A)	112.7(8)
F(6A)-B(2A)-F(8A)	107.1(8)
F(7A)-B(2A)-F(8A)	113.9(7)
F(7B)-B(2B)-F(6B)	106.8(8)
F(7B)-B(2B)-F(8B)	109.9(11)

F(6B)-B(2B)-F(8B)	119.0(14)
F(7B)-B(2B)-F(5B)	117.5(11)
F(6B)-B(2B)-F(5B)	94.7(10)
F(8B)-B(2B)-F(5B)	108.6(13)

Symmetry transformations used to generate equivalent atoms:

Table 4. Anisotropic displacement parameters ($Å^2 x\ 10^3$) for phw0913m. The anisotropic displacement factor exponent takes the form: $-2\pi^2[\ h^2\ a^{*2}U^{11} + ... + 2\ h\ k\ a^*\ b^*\ U^{12}\ ]$

	U^{11}	U^{22}	U^{33}	U^{23}	U^{13}	U^{12}
C(1)	28(1)	22(1)	25(1)	6(1)	10(1)	9(1)
C(2)	29(1)	26(1)	26(1)	7(1)	10(1)	7(1)
C(3)	33(1)	30(1)	28(1)	10(1)	13(1)	9(1)
C(4)	36(1)	37(1)	37(1)	14(1)	18(1)	9(1)
C(5)	45(1)	42(1)	35(1)	19(1)	21(1)	15(1)
C(6)	44(1)	43(1)	29(1)	16(1)	15(1)	16(1)
C(7)	36(1)	34(1)	27(1)	12(1)	10(1)	10(1)
C(8)	33(1)	27(1)	27(1)	11(1)	13(1)	11(1)
C(9)	27(1)	29(1)	31(1)	7(1)	11(1)	4(1)
C(10)	46(1)	28(1)	27(1)	3(1)	18(1)	-1(1)
C(11)	68(1)	34(1)	32(1)	6(1)	24(1)	-5(1)
C(12)	59(1)	45(1)	29(1)	7(1)	24(1)	-3(1)
C(13)	37(1)	45(1)	27(1)	-2(1)	17(1)	1(1)
C(14)	26(1)	34(1)	28(1)	0(1)	12(1)	5(1)
C(15)	34(1)	31(1)	37(1)	1(1)	2(1)	9(1)
C(16)	41(1)	34(1)	51(1)	3(1)	-2(1)	14(1)
C(17)	46(1)	36(1)	59(1)	-6(1)	3(1)	19(1)
C(18)	40(1)	37(1)	46(1)	-8(1)	5(1)	16(1)
C(19)	28(1)	32(1)	35(1)	-3(1)	7(1)	9(1)
C(20)	33(1)	34(1)	36(1)	3(1)	9(1)	6(1)
C(21)	33(1)	44(1)	49(1)	2(1)	5(1)	7(1)
C(22)	46(1)	51(1)	37(1)	2(1)	-5(1)	6(1)
C(23)	50(1)	41(1)	26(1)	3(1)	5(1)	4(1)
C(24)	42(1)	27(1)	24(1)	7(1)	10(1)	3(1)
C(25)	40(1)	29(1)	27(1)	7(1)	14(1)	11(1)
C(26)	45(1)	36(1)	38(1)	8(1)	16(1)	16(1)
C(27)	58(1)	37(1)	46(1)	5(1)	29(1)	19(1)

C(28)	56(1)	34(1)	30(1)	3(1)	23(1)	12(1)
C(29)	42(1)	26(1)	25(1)	7(1)	17(1)	6(1)
Co(1)	28(1)	22(1)	22(1)	4(1)	9(1)	5(1)
N(1)	27(1)	25(1)	25(1)	7(1)	9(1)	5(1)
N(2)	30(1)	31(1)	30(1)	8(1)	11(1)	5(1)
N(3)	28(1)	25(1)	23(1)	6(1)	8(1)	6(1)
N(4)	35(1)	45(1)	30(1)	7(1)	10(1)	5(1)
N(5)	29(1)	27(1)	24(1)	2(1)	13(1)	3(1)
N(6)	35(1)	35(1)	28(1)	-5(1)	8(1)	11(1)
N(7)	28(1)	27(1)	31(1)	2(1)	5(1)	7(1)
N(8)	32(1)	25(1)	26(1)	5(1)	10(1)	4(1)
N(9)	47(1)	35(1)	20(1)	3(1)	15(1)	7(1)
N(10)	36(1)	25(1)	22(1)	6(1)	14(1)	7(1)
O(1)	28(1)	29(1)	25(1)	9(1)	7(1)	1(1)
O(2)	29(1)	50(1)	37(1)	11(1)	10(1)	-3(1)
B(1A)	51(4)	27(3)	21(3)	-4(2)	4(3)	7(3)
F(1A)	102(3)	77(2)	60(2)	23(2)	38(2)	65(2)
F(2A)	51(1)	60(2)	39(1)	-16(1)	21(1)	-8(1)
F(3A)	65(4)	51(2)	51(4)	-18(3)	18(3)	9(2)
F(4A)	213(6)	97(4)	39(2)	21(2)	30(3)	51(4)
B(1B)	87(13)	59(10)	58(11)	7(7)	30(9)	6(8)
F(1B)	267(16)	110(6)	163(10)	-64(7)	30(9)	80(8)
F(2B)	57(4)	334(15)	163(8)	-175(10)	12(4)	-21(5)
F(3B)	54(4)	44(3)	23(2)	5(2)	10(2)	3(2)
F(4B)	30(2)	142(6)	36(3)	15(3)	20(2)	-28(2)
B(2A)	56(4)	34(2)	26(2)	10(2)	21(3)	16(2)
F(5A)	44(2)	48(2)	33(3)	5(2)	10(1)	1(1)
F(6A)	70(2)	51(1)	46(1)	20(1)	32(1)	4(1)
F(7A)	88(2)	88(2)	70(2)	26(1)	41(1)	58(2)
F(8A)	80(5)	36(2)	28(2)	11(2)	21(2)	20(3)
B(2B)	58(7)	25(3)	25(3)	3(2)	19(4)	11(4)
F(5B)	88(9)	34(4)	29(4)	3(3)	26(5)	24(4)
F(6B)	70(3)	101(4)	125(5)	22(3)	63(3)	26(3)
F(7B)	104(4)	33(2)	36(2)	10(1)	7(2)	30(2)
F(8B)	80(8)	38(3)	20(3)	1(2)	25(3)	-2(3)

Table 5. Hydrogen coordinates (x 10^4) and isotropic displacement parameters ($Å^2$x 10^{3}) for phw0913m.

	x	y	z	U(eq)
H(4)	3714	2898	4143	43
H(5)	4797	3293	5840	46
H(6)	6840	4515	6420	45
H(7)	7857	5322	5323	39
H(10)	9491	8666	2075	43
H(11)	9552	9462	639	57
H(12)	9012	8296	-842	56
H(13)	8605	6387	-791	45
H(15)	9874	5052	3869	44
H(16)	10317	3426	3661	54
H(17)	9872	2590	2046	59
H(18)	9061	3456	693	51
H(20)	11238	7037	2809	43
H(21)	13151	7819	4028	55
H(22)	13208	8500	5596	62
H(23)	11389	8610	5807	52
H(25)	6698	7355	1488	37
H(26)	5500	8362	1787	46
H(27)	5949	9157	3422	52
H(28)	7662	9003	4666	46
H(3)	6580(20)	5455(18)	1248(17)	37(5)
H(6A)	8470(20)	4970(20)	195(19)	48(6)
H(9)	9300(20)	8310(20)	5037(19)	50(7)

Table 6. Torsion angles [°] for phw0913m.

N(3)-C(1)-C(2)-N(2)	-179.79(15)
N(1)-C(1)-C(2)-N(2)	0.4(2)
N(3)-C(1)-C(2)-C(9)	1.7(2)
N(1)-C(1)-C(2)-C(9)	-178.18(14)
C(8)-C(3)-C(4)-C(5)	0.6(3)
N(2)-C(3)-C(4)-C(5)	-178.10(16)
C(3)-C(4)-C(5)-C(6)	0.4(3)
C(4)-C(5)-C(6)-C(7)	-1.0(3)

C(5)-C(6)-C(7)-C(8)	0.6(3)
C(6)-C(7)-C(8)-N(1)	178.78(15)
C(6)-C(7)-C(8)-C(3)	0.4(2)
C(4)-C(3)-C(8)-N(1)	-179.38(15)
N(2)-C(3)-C(8)-N(1)	-0.7(2)
C(4)-C(3)-C(8)-C(7)	-1.0(2)
N(2)-C(3)-C(8)-C(7)	177.70(15)
N(2)-C(2)-C(9)-N(4)	-171.0(17)
C(1)-C(2)-C(9)-N(4)	7.6(18)
N(5)-C(10)-C(11)-C(12)	0.2(3)
C(10)-C(11)-C(12)-C(13)	-3.5(3)
C(11)-C(12)-C(13)-C(14)	1.4(3)
C(12)-C(13)-C(14)-N(5)	4.0(3)
C(12)-C(13)-C(14)-N(6)	-177.50(17)
N(7)-C(15)-C(16)-C(17)	-1.1(3)
C(15)-C(16)-C(17)-C(18)	1.4(3)
C(16)-C(17)-C(18)-C(19)	0.4(3)
C(17)-C(18)-C(19)-N(7)	-2.8(3)
C(17)-C(18)-C(19)-N(6)	178.02(18)
N(8)-C(20)-C(21)-C(22)	1.8(3)
C(20)-C(21)-C(22)-C(23)	-5.3(3)
C(21)-C(22)-C(23)-C(24)	2.0(3)
C(22)-C(23)-C(24)-N(8)	5.1(3)
C(22)-C(23)-C(24)-N(9)	-174.45(17)
N(10)-C(25)-C(26)-C(27)	-0.2(3)
C(25)-C(26)-C(27)-C(28)	2.4(3)
C(26)-C(27)-C(28)-C(29)	-1.1(3)
C(27)-C(28)-C(29)-N(10)	-2.6(3)
C(27)-C(28)-C(29)-N(9)	177.23(16)
N(3)-C(1)-N(1)-O(1)	-1.18(19)
C(2)-C(1)-N(1)-O(1)	178.70(12)
N(3)-C(1)-N(1)-C(8)	177.73(13)
C(2)-C(1)-N(1)-C(8)	-2.4(2)
C(7)-C(8)-N(1)-C(1)	-175.78(14)
C(3)-C(8)-N(1)-C(1)	2.6(2)
C(7)-C(8)-N(1)-O(1)	3.1(2)
C(3)-C(8)-N(1)-O(1)	-178.52(13)
C(9)-C(2)-N(2)-O(2)	-0.5(2)
C(1)-C(2)-N(2)-O(2)	-179.01(15)
C(9)-C(2)-N(2)-C(3)	179.94(14)

C(1)-C(2)-N(2)-C(3)	1.4(2)
C(8)-C(3)-N(2)-O(2)	179.20(15)
C(4)-C(3)-N(2)-O(2)	-2.1(2)
C(8)-C(3)-N(2)-C(2)	-1.2(2)
C(4)-C(3)-N(2)-C(2)	177.50(15)
N(1)-C(1)-N(3)-Co(1)	-4.46(17)
C(2)-C(1)-N(3)-Co(1)	175.68(12)
O(1)-Co(1)-N(3)-C(1)	6.20(11)
N(5)-Co(1)-N(3)-C(1)	-174.23(11)
N(8)-Co(1)-N(3)-C(1)	4.0(6)
N(7)-Co(1)-N(3)-C(1)	96.07(11)
N(10)-Co(1)-N(3)-C(1)	-81.02(11)
N(6)-C(14)-N(5)-C(10)	174.39(15)
C(13)-C(14)-N(5)-C(10)	-7.1(2)
N(6)-C(14)-N(5)-Co(1)	-14.4(2)
C(13)-C(14)-N(5)-Co(1)	164.10(13)
C(11)-C(10)-N(5)-C(14)	5.0(3)
C(11)-C(10)-N(5)-Co(1)	-166.29(16)
N(3)-Co(1)-N(5)-C(14)	-48.18(13)
O(1)-Co(1)-N(5)-C(14)	-35.2(17)
N(8)-Co(1)-N(5)-C(14)	132.02(13)
N(7)-Co(1)-N(5)-C(14)	39.39(13)
N(10)-Co(1)-N(5)-C(14)	-138.23(13)
N(3)-Co(1)-N(5)-C(10)	122.82(13)
O(1)-Co(1)-N(5)-C(10)	135.8(16)
N(8)-Co(1)-N(5)-C(10)	-56.98(14)
N(7)-Co(1)-N(5)-C(10)	-149.61(13)
N(10)-Co(1)-N(5)-C(10)	32.77(14)
N(7)-C(19)-N(6)-C(14)	29.8(2)
C(18)-C(19)-N(6)-C(14)	-150.96(17)
N(5)-C(14)-N(6)-C(19)	-29.4(2)
C(13)-C(14)-N(6)-C(19)	152.07(17)
N(6)-C(19)-N(7)-C(15)	-177.66(15)
C(18)-C(19)-N(7)-C(15)	3.1(2)
N(6)-C(19)-N(7)-Co(1)	13.3(2)
C(18)-C(19)-N(7)-Co(1)	-165.87(14)
C(16)-C(15)-N(7)-C(19)	-1.2(3)
C(16)-C(15)-N(7)-Co(1)	167.94(15)
N(3)-Co(1)-N(7)-C(19)	55.25(13)
O(1)-Co(1)-N(7)-C(19)	139.32(13)

N(5)-Co(1)-N(7)-C(19)	-38.84(13)
N(8)-Co(1)-N(7)-C(19)	-131.22(13)
N(10)-Co(1)-N(7)-C(19)	103.6(8)
N(3)-Co(1)-N(7)-C(15)	-113.62(13)
O(1)-Co(1)-N(7)-C(15)	-29.55(13)
N(5)-Co(1)-N(7)-C(15)	152.29(13)
N(8)-Co(1)-N(7)-C(15)	59.91(13)
N(10)-Co(1)-N(7)-C(15)	-65.3(8)
N(9)-C(24)-N(8)-C(20)	170.98(15)
C(23)-C(24)-N(8)-C(20)	-8.6(2)
N(9)-C(24)-N(8)-Co(1)	-17.1(2)
C(23)-C(24)-N(8)-Co(1)	163.32(13)
C(21)-C(20)-N(8)-C(24)	5.1(3)
C(21)-C(20)-N(8)-Co(1)	-166.75(14)
N(3)-Co(1)-N(8)-C(24)	-44.1(6)
O(1)-Co(1)-N(8)-C(24)	-46.25(12)
N(5)-Co(1)-N(8)-C(24)	134.17(12)
N(7)-Co(1)-N(8)-C(24)	-135.84(12)
N(10)-Co(1)-N(8)-C(24)	40.97(12)
N(3)-Co(1)-N(8)-C(20)	127.6(5)
O(1)-Co(1)-N(8)-C(20)	125.40(13)
N(5)-Co(1)-N(8)-C(20)	-54.18(13)
N(7)-Co(1)-N(8)-C(20)	35.81(13)
N(10)-Co(1)-N(8)-C(20)	-147.38(13)
N(10)-C(29)-N(9)-C(24)	26.7(2)
C(28)-C(29)-N(9)-C(24)	-153.08(17)
N(8)-C(24)-N(9)-C(29)	-25.8(2)
C(23)-C(24)-N(9)-C(29)	153.71(17)
N(9)-C(29)-N(10)-C(25)	-175.03(14)
C(28)-C(29)-N(10)-C(25)	4.8(2)
N(9)-C(29)-N(10)-Co(1)	15.47(19)
C(28)-C(29)-N(10)-Co(1)	-164.72(12)
C(26)-C(25)-N(10)-C(29)	-3.4(2)
C(26)-C(25)-N(10)-Co(1)	166.14(13)
N(3)-Co(1)-N(10)-C(29)	133.31(12)
O(1)-Co(1)-N(10)-C(29)	49.24(12)
N(5)-Co(1)-N(10)-C(29)	-132.62(12)
N(8)-Co(1)-N(10)-C(29)	-40.25(12)
N(7)-Co(1)-N(10)-C(29)	85.0(8)
N(3)-Co(1)-N(10)-C(25)	-35.99(12)

O(1)-Co(1)-N(10)-C(25)	-120.06(12)
N(5)-Co(1)-N(10)-C(25)	58.08(12)
N(8)-Co(1)-N(10)-C(25)	150.45(12)
N(7)-Co(1)-N(10)-C(25)	-84.3(8)
C(1)-N(1)-O(1)-Co(1)	6.07(15)
C(8)-N(1)-O(1)-Co(1)	-172.89(11)
N(3)-Co(1)-O(1)-N(1)	-6.47(9)
N(5)-Co(1)-O(1)-N(1)	-19.5(17)
N(8)-Co(1)-O(1)-N(1)	173.28(10)
N(7)-Co(1)-O(1)-N(1)	-94.09(10)
N(10)-Co(1)-O(1)-N(1)	83.64(10)

Symmetry transformations used to generate equivalent atoms:

Table 7. Hydrogen bonds for phw0913m [Å and °].

D-H...A	d(D-H)	d(H...A)	d(D...A)	<(DHA)
N(3)-H(3)...N(4)#1	0.87(2)	2.23(2)	3.048(2)	156.8(19)

Symmetry transformations used to generate equivalent atoms:

#1 -x+1,-y+1,-z

Crystallographic data for $[Co(tpz\text{-}CONH_2)(dpHa)_2]2NO_3$

Crystal Submitted by:

Emma Dux

Crystal Submitted on:

7/6/11

Data Collected on:

9/6/11

Structure Solved by:

ACW/SJH

Table 1: Crystal data and structure refinement for phw1109

Identification code	phw1109
Empirical formula	$C_{33}H_{35}CoN_{12}O_{10}$
Formula weight	818.66
Temperature / K	110.0
Crystal system	triclinic
Space group	P-1
a / Å, b / Å, c / Å	10.371(2), 12.715(3), 14.053(3)
α/°, β/°, γ/°	74.64(2), 76.945(18), 81.408(19)
Volume / $Å^3$	1732.9(6)
Z	2
ρ_{calc} / mg mm^{-3}	1.569
μ / mm^{-1}	0.574
F(000)	848
Crystal size / mm^3	0.32 × 0.1834 × 0.0798
2Θ range for data collection	6.28 to 57.62°
Index ranges	$-13 \leq h \leq 7$, $-17 \leq k \leq 16$, $-18 \leq l \leq 17$
Reflections collected	11512

Independent reflections	7448[R(int) = 0.0280]
Data/restraints/parameters	7448/38/542
Goodness-of-fit on F^2	1.049
Final R indexes [I>2σ (I)]	R_1 = 0.0595, wR_2 = 0.1406
Final R indexes [all data]	R_1 = 0.0817, wR_2 = 0.1558
Largest diff. peak/hole / e $Å^{-3}$	1.018/-0.444

Table 2 Fractional Atomic Coordinates ($\times 10^4$) and Equivalent Isotropic Displacement Parameters ($Å^2 \times 10^3$) for phw1109. U_{eq} is defined as 1/3 of of the trace of the orthogonalised U_{IJ} tensor.

Atom	***x***	***y***	***z***	**U(eq)**
C1	5979(3)	445(3)	1626(2)	23.3(7)
C2	7091(3)	856(3)	1786(3)	32.5(8)
C3	8325(4)	345(4)	1506(3)	40.0(9)
C4	8500(4)	-542(4)	1132(3)	42.4(10)
C5	7395(4)	-969(3)	953(3)	38.8(9)
C6	6137(3)	-460(3)	1215(2)	26.5(7)
C7	3788(3)	-366(3)	1315(2)	24.9(7)
C8	3634(3)	583(2)	1722(2)	17.1(6)
C9	2588(4)	-792(3)	1194(3)	29.9(8)
C10	4228(3)	3560(3)	645(3)	26.2(7)
C11	4562(4)	4012(3)	-363(3)	30.6(8)
C12	3625(4)	4127(3)	-956(3)	33.7(8)
C13	2399(3)	3785(3)	-517(3)	27.8(7)
C14	2126(3)	3315(3)	515(2)	23.9(7)
C15	194(3)	2967(3)	1887(3)	24.4(7)
C16	-1196(3)	3118(3)	2044(3)	31.2(8)
C17	-1901(4)	3188(3)	2974(3)	36.1(9)
C18	-1236(4)	3139(3)	3741(3)	35.6(9)
C19	127(3)	2964(3)	3547(3)	28.1(8)

C20	2740(3)	4577(3)	2562(2)	24.8(7)
C21	3125(4)	5449(3)	2797(3)	30.0(8)
C22	3939(4)	5243(3)	3501(3)	30.1(8)
C23	4284(4)	4186(3)	3964(3)	27.1(7)
C24	3815(3)	3326(3)	3721(2)	21.8(7)
C25	3333(3)	1405(3)	4446(2)	21.9(7)
C26	3429(3)	557(3)	5304(3)	27.2(7)
C27	2657(4)	-294(3)	5529(3)	30.1(8)
C28	1776(3)	-292(3)	4920(3)	28.9(8)
C29	1739(3)	556(3)	4092(3)	25.5(7)
Co1	2720.7(4)	2344.4(3)	2479.7(3)	19.42(13)
N1	4718(3)	933(2)	1864.3(19)	20.6(6)
N2	5019(3)	-846(2)	1064(2)	28.9(7)
N3	2515(3)	1158(2)	1979(2)	21.6(6)
N4	2773(5)	-1694(3)	829(3)	41.0(9)
N5	3021(3)	3199(2)	1096(2)	21.1(6)
N6	887(3)	2956(2)	941(2)	26.3(6)
N7	839(3)	2843(2)	2643(2)	22.7(6)
N8	3102(3)	3517(2)	2998.2(19)	20.0(6)
N9	4091(3)	2274(2)	4254(2)	22.2(6)
N10	2520(3)	1393(2)	3836(2)	21.0(6)
O1	4531(2)	1810.3(18)	2293.8(17)	23.0(5)
O2	5272(3)	-1679(2)	665(2)	45.3(7)
O3	1512(3)	-328(2)	1432(2)	43.2(7)
C30	167(8)	2071(9)	6450(7)	85(3)
C30A	-180.0(3)	2430.0(2)	6700.0(2)	85(3)
C31	1398(8)	2630(8)	6356(7)	82(2)
C31A	670.0(3)	3330.0(2)	6180(19)	82(2)
C32	1323(11)	3482(8)	6914(7)	104(3)

C32A	0.0(3)	4430.0(2)	5738(17)	104(3)
C33	2649(9)	3835(8)	6790(6)	89(3)
C33A	1020.0(2)	4580.0(3)	4858(16)	89(3)
O10	-728(6)	2836(8)	5898(4)	110(3)
O10A	-330.0(2)	1720.0(2)	6090.0(2)	111(8)
N11	3947(3)	-1916(2)	3792(2)	27.3(6)
O4	4688(3)	-1172(2)	3433(2)	45.4(7)
O5	3984(3)	-2513(2)	4653.4(19)	34.4(6)
O6	3160(3)	-2072(2)	3306(2)	43.2(7)
N12	1203(3)	6213(3)	640(2)	34.2(7)
O7	549(3)	5424(2)	1092(3)	49.1(8)
O8	618(3)	7168(2)	427(2)	40.8(7)
O9	2412(3)	6069(3)	388(2)	51.7(8)

Table 3 Anisotropic Displacement Parameters ($Å^2 \times 10^3$) for phw1109. The Anisotropic displacement factor exponent takes the form: $-2\pi^2[h^2a^{*2}U_{11}+...+2hka \times b \times U_{12}]$

Atom	**U_{11}**	**U_{22}**	**U_{33}**	**U_{23}**	**U_{13}**	**U_{12}**
C1	18.2(16)	28.1(17)	20.8(16)	-2.4(13)	-2.9(12)	-0.8(14)
C2	18.3(18)	42(2)	31.5(19)	1.8(16)	-4.8(14)	-5.5(16)
C3	21.3(19)	52(3)	46(2)	-6(2)	-8.3(16)	-6.5(18)
C4	18.8(19)	48(2)	61(3)	-16(2)	-6.7(17)	1.1(17)
C5	38(2)	33(2)	40(2)	-10.4(17)	-2.3(17)	8.8(18)
C6	26.1(18)	27.7(18)	23.3(17)	-4.2(14)	-5.0(13)	2.0(15)
C7	29.4(18)	23.4(17)	24.1(17)	-3.2(14)	-8.9(14)	-8.6(14)
C8	18.9(15)	18.6(15)	15.3(14)	-2.4(12)	-5.3(11)	-6.2(12)
C9	28(2)	33.3(19)	31.4(19)	-6.4(16)	-10.3(15)	-7.7(16)
C10	17.9(17)	29.8(18)	30.5(18)	-7.5(15)	-2.9(13)	-4.1(14)
C11	25.2(18)	36(2)	29.0(18)	-6.6(16)	0.5(14)	-8.6(16)
C12	36(2)	37(2)	25.6(18)	-3.5(16)	-3.2(15)	-4.9(17)

C13	26.9(18)	31.5(19)	26.6(17)	-7.0(15)	-9.6(14)	-1.5(15)
C14	18.5(16)	25.0(17)	28.8(17)	-8.9(14)	-3.4(13)	-1.5(14)
C15	21.0(17)	18.1(15)	32.7(18)	-3.1(14)	-4.2(13)	-4.3(13)
C16	21.4(18)	26.3(18)	46(2)	-4.5(16)	-8.9(15)	-5.0(15)
C17	17.6(18)	28.8(19)	56(3)	-4.8(18)	-0.3(16)	-3.4(15)
C18	30(2)	29.0(19)	41(2)	-7.3(17)	3.0(16)	-2.2(16)
C19	25.0(18)	23.6(17)	31.6(19)	-4.5(14)	0.5(14)	-1.9(14)
C20	24.5(18)	24.0(17)	22.8(16)	-3.4(13)	-2.1(13)	-0.2(14)
C21	39(2)	20.1(17)	29.8(18)	-4.7(14)	-6.1(15)	-2.5(15)
C22	40(2)	22.8(17)	31.1(19)	-9.2(15)	-7.2(15)	-7.3(16)
C23	31.9(19)	26.6(17)	25.1(17)	-7.9(14)	-6.5(14)	-5.4(15)
C24	19.4(16)	22.6(16)	23.3(16)	-9.2(13)	1.3(12)	-3.0(13)
C25	19.0(16)	19.9(16)	25.6(16)	-6.7(13)	-1.1(13)	-0.9(13)
C26	27.0(18)	26.3(17)	29.1(18)	-5.2(14)	-8.6(14)	-2.9(15)
C27	32(2)	25.5(18)	29.0(18)	0.9(15)	-5.7(15)	-3.5(15)
C28	25.0(18)	25.1(18)	34.4(19)	-4.5(15)	-1.1(14)	-7.2(15)
C29	21.9(17)	25.9(17)	28.6(18)	-4.5(14)	-4.7(13)	-5.5(14)
Co1	16.2(2)	20.1(2)	22.0(2)	-5.13(17)	-3.28(16)	-2.41(17)
N1	18.6(14)	21.8(14)	23.1(14)	-6.8(11)	-5.4(11)	-2.0(11)
N2	37.3(18)	25.0(15)	26.3(15)	-10.2(12)	-6.0(13)	-1.3(13)
N3	15.1(15)	26.0(15)	27.2(15)	-7.1(12)	-7.8(12)	-6.0(12)
N4	55(2)	39(2)	39(2)	-5.3(15)	-21.9(18)	-23.5(19)
N5	18.2(14)	22.8(14)	22.7(14)	-6.6(11)	-3(1)	-3.0(11)
N6	21.4(15)	29.0(15)	30.7(16)	-5.5(12)	-9.0(12)	-5.8(12)
N7	17.0(14)	21.2(14)	27.6(15)	-3.8(11)	-1.6(11)	-2.1(11)
N8	20.4(14)	19.7(13)	19.2(13)	-5.9(11)	-1.2(10)	-1.7(11)
N9	23.9(15)	19.6(13)	23.9(14)	-3.3(11)	-7.6(11)	-3.2(11)
N10	18.6(14)	20.5(13)	24.3(14)	-6.7(11)	-3.2(11)	-2.3(11)
O1	18.9(12)	24.4(12)	30.1(12)	-13(1)	-6.0(9)	-2.3(9)

O2	51.2(18)	38.4(16)	54.1(18)	-27.5(14)	-11.2(14)	2.0(14)
O3	34.0(16)	43.8(17)	59.7(19)	-20.8(15)	-13.5(13)	-6.2(13)
C30	44(5)	139(9)	73(6)	-48(6)	5(4)	-1(5)
C30A	44(5)	139(9)	73(6)	-48(6)	5(4)	-1(5)
C31	70(6)	96(7)	78(5)	-35(5)	4(4)	-6(4)
C31A	70(6)	96(7)	78(5)	-35(5)	4(4)	-6(4)
C32	148(9)	103(7)	65(5)	-36(5)	7(5)	-42(6)
C32A	148(9)	103(7)	65(5)	-36(5)	7(5)	-42(6)
C33	98(6)	138(8)	55(4)	-38(5)	-16(4)	-54(6)
C33A	98(6)	138(8)	55(4)	-38(5)	-16(4)	-54(6)
O10	66(4)	196(9)	60(4)	1(4)	-8(3)	-51(5)
O10A	84(14)	119(17)	180.0(2)	-88(17)	-61(15)	-4(14)
N11	27.2(16)	24.4(15)	32.6(16)	-7.8(13)	-9.0(12)	-2.3(13)
O4	52.1(18)	48.9(17)	37.6(16)	2.5(13)	-13.4(13)	-29.1(15)
O5	38.5(15)	31.7(14)	30.0(14)	1.2(11)	-9.1(11)	-6.0(12)
O6	46.4(17)	40.8(16)	52.5(18)	-9.2(14)	-28.7(14)	-10.4(13)
N12	30.4(18)	33.4(18)	42.9(19)	-7.4(15)	-19.1(14)	-1.3(15)
O7	36.8(16)	31.4(15)	81(2)	-4.3(15)	-22.9(15)	-7.0(13)
O8	39.5(16)	31.9(15)	56.7(18)	-7.1(13)	-25.6(13)	-2.8(13)
O9	34.9(17)	55(2)	59(2)	-3.0(16)	-11.8(14)	-1.4(15)

Table 4 Bond Lengths for phw1109.

Atom	**Atom**	**Length/Å**	**Atom**	**Atom**	**Length/Å**
C1	C2	1.419(5)	C23	C24	1.408(5)
C1	C6	1.392(5)	C24	N8	1.338(4)
C1	N1	1.369(4)	C24	N9	1.372(4)
C2	C3	1.370(5)	C25	C26	1.399(5)
C3	C4	1.339(6)	C25	N9	1.385(4)
C4	C5	1.434(6)	C25	N10	1.337(4)
C5	C6	1.384(5)	C26	C27	1.370(5)

C6	N2	1.403(5)	C27	C28	1.385(5)
C7	C8	1.440(4)	C28	C29	1.365(5)
C7	C9	1.489(5)	C29	N10	1.357(4)
C7	N2	1.343(5)	Co1	N3	1.882(3)
C8	N1	1.342(4)	Co1	N5	1.941(3)
C8	N3	1.307(4)	Co1	N7	1.941(3)
C9	N4	1.347(5)	Co1	N8	1.948(3)
C9	O3	1.203(4)	Co1	N10	1.953(3)
C10	C11	1.365(5)	Co1	O1	1.883(2)
C10	N5	1.356(4)	N1	O1	1.373(3)
C11	C12	1.384(5)	N2	O2	1.292(4)
C12	C13	1.362(5)	C30	C31	1.516(11)
C13	C14	1.395(5)	C30	O10	1.437(11)
C14	N5	1.337(4)	C30A	C31A	1.481(19)
C14	N6	1.379(4)	C30A	O10A	1.446(17)
C15	C16	1.399(5)	C31	C32	1.481(10)
C15	N6	1.363(4)	C31A	C32A	1.500(18)
C15	N7	1.344(4)	C32	C33	1.469(10)
C16	C17	1.365(5)	C32A	C33A	1.425(17)
C17	C18	1.389(6)	N11	O4	1.237(4)
C18	C19	1.373(5)	N11	O5	1.252(4)
C19	N7	1.352(4)	N11	O6	1.242(4)
C20	C21	1.373(5)	N12	O7	1.240(4)
C20	N8	1.359(4)	N12	O8	1.266(4)
C21	C22	1.390(5)	N12	O9	1.224(4)
C22	C23	1.363(5)			

Table 5 Bond Angles for phw1109.

Atom	**Atom**	**Atom**	**Angle/°**	**Atom**	**Atom**	**Atom**	**Angle/°**
C6	C1	C2	121.0(3)	N3	Co1	N7	93.02(12)

N1	C1	C2	121.0(3)	N3	Co1	N8	174.75(12)
N1	C1	C6	118.0(3)	N3	Co1	N10	89.71(12)
C3	C2	C1	117.8(4)	N3	Co1	O1	84.32(11)
C4	C3	C2	122.3(4)	N5	Co1	N7	90.59(11)
C3	C4	C5	121.1(4)	N5	Co1	N8	93.36(11)
C6	C5	C4	118.0(4)	N5	Co1	N10	175.43(11)
C1	C6	N2	119.7(3)	N7	Co1	N8	92.19(11)
C5	C6	C1	119.8(3)	N7	Co1	N10	92.93(11)
C5	C6	N2	120.4(3)	N8	Co1	N10	89.41(11)
C8	C7	C9	119.5(3)	O1	Co1	N5	89.08(11)
N2	C7	C8	118.6(3)	O1	Co1	N7	177.33(11)
N2	C7	C9	121.9(3)	O1	Co1	N8	90.47(10)
N1	C8	C7	118.9(3)	O1	Co1	N10	87.26(11)
N3	C8	C7	126.2(3)	C1	N1	O1	119.2(3)
N3	C8	N1	115.0(3)	C8	N1	C1	123.4(3)
N4	C9	C7	117.6(4)	C8	N1	O1	117.4(2)
O3	C9	C7	118.9(3)	C7	N2	C6	121.4(3)
O3	C9	N4	123.4(4)	O2	N2	C6	115.0(3)
N5	C10	C11	123.0(3)	O2	N2	C7	123.6(3)
C10	C11	C12	119.0(3)	C8	N3	Co1	113.6(2)
C13	C12	C11	119.1(3)	C10	N5	Co1	120.4(2)
C12	C13	C14	119.1(3)	C14	N5	C10	117.4(3)
N5	C14	C13	122.4(3)	C14	N5	Co1	121.5(2)
N5	C14	N6	119.4(3)	C15	N6	C14	126.5(3)
N6	C14	C13	118.2(3)	C15	N7	C19	118.6(3)
N6	C15	C16	118.4(3)	C15	N7	Co1	120.4(2)
N7	C15	C16	121.2(3)	C19	N7	Co1	120.7(2)
N7	C15	N6	120.3(3)	C20	N8	Co1	119.6(2)
C17	C16	C15	119.2(4)	C24	N8	C20	118.0(3)

C16	C17	C18	119.8(3)	C24	N8	Co1	122.1(2)
C19	C18	C17	118.3(3)	C24	N9	C25	126.6(3)
N7	C19	C18	122.7(3)	C25	N10	C29	118.2(3)
N8	C20	C21	122.9(3)	C25	N10	Co1	121.0(2)
C20	C21	C22	118.8(3)	C29	N10	Co1	119.5(2)
C23	C22	C21	119.1(3)	N1	O1	Co1	109.54(17)
C22	C23	C24	119.5(3)	O10	C30	C31	108.2(9)
N8	C24	C23	121.5(3)	O10A	C30A	C31A	115(2)
N8	C24	N9	120.2(3)	C32	C31	C30	119.5(8)
N9	C24	C23	118.3(3)	C30A	C31A	C32A	118(3)
N9	C25	C26	118.0(3)	C33	C32	C31	110.2(8)
N10	C25	C26	121.4(3)	C33A	C32A	C31A	92(2)
N10	C25	N9	120.6(3)	O4	N11	O5	119.9(3)
C27	C26	C25	119.2(3)	O4	N11	O6	120.5(3)
C26	C27	C28	119.7(3)	O6	N11	O5	119.7(3)
C29	C28	C27	118.1(3)	O7	N12	O8	120.1(3)
N10	C29	C28	123.4(3)	O9	N12	O7	120.2(3)
N3	Co1	N5	87.21(12)	O9	N12	O8	119.7(3)

Table 6 Torsion Angles for phw1109.

A	**B**	**C**	**D**	**Angle/**°
C1	C2	C3	C4	-2.8(6)
C1	C6	N2	C7	-0.6(5)
C1	C6	N2	O2	179.0(3)
C1	N1	O1	Co1	177.4(2)
C2	C1	C6	C5	-0.2(5)
C2	C1	C6	N2	-179.9(3)
C2	C1	N1	C8	179.5(3)
C2	C1	N1	O1	-2.1(4)
C2	C3	C4	C5	3.5(7)

C3	C4	C5	C6	-2.4(6)
C4	C5	C6	C1	0.8(5)
C4	C5	C6	N2	-179.6(3)
C5	C6	N2	C7	179.8(3)
C5	C6	N2	O2	-0.6(5)
C6	C1	C2	C3	1.2(5)
C6	C1	N1	C8	0.0(5)
C6	C1	N1	O1	178.4(3)
C7	C8	N1	C1	1.2(5)
C7	C8	N1	O1	-177.3(3)
C7	C8	N3	Co1	-179.8(3)
C8	C7	C9	N4	-178.7(3)
C8	C7	C9	O3	0.5(5)
C8	C7	N2	C6	1.7(5)
C8	C7	N2	O2	-177.8(3)
C8	N1	O1	Co1	-4.1(3)
C9	C7	C8	N1	177.4(3)
C9	C7	C8	N3	-2.4(5)
C9	C7	N2	C6	-177.7(3)
C9	C7	N2	O2	2.8(5)
C10	C11	C12	C13	-0.2(5)
C11	C10	N5	C14	-1.1(5)
C11	C10	N5	Co1	169.4(3)
C11	C12	C13	C14	-0.8(5)
C12	C13	C14	N5	0.8(5)
C12	C13	C14	N6	-178.9(3)
C13	C14	N5	C10	0.1(5)
C13	C14	N5	Co1	-170.3(3)
C13	C14	N6	C15	-146.7(3)

C15	C16	C17	C18	1.8(5)
C16	C15	N6	C14	147.9(3)
C16	C15	N7	C19	-5.8(5)
C16	C15	N7	Co1	167.6(3)
C16	C17	C18	C19	-3.2(6)
C17	C18	C19	N7	0.2(5)
C18	C19	N7	C15	4.3(5)
C18	C19	N7	Co1	-169.1(3)
C20	C21	C22	C23	-2.6(5)
C21	C20	N8	C24	3.1(5)
C21	C20	N8	Co1	-171.3(3)
C21	C22	C23	C24	0.2(5)
C22	C23	C24	N8	4.2(5)
C22	C23	C24	N9	-175.0(3)
C23	C24	N8	C20	-5.7(5)
C23	C24	N8	Co1	168.6(2)
C23	C24	N9	C25	151.4(3)
C25	C26	C27	C28	-1.3(5)
C26	C25	N9	C24	-154.1(3)
C26	C25	N10	C29	2.8(4)
C26	C25	N10	Co1	-163.6(2)
C26	C27	C28	C29	1.8(5)
C27	C28	C29	N10	0.1(5)
C28	C29	N10	C25	-2.4(5)
C28	C29	N10	Co1	164.3(3)
N1	C1	C2	C3	-178.3(3)
N1	C1	C6	C5	179.3(3)
N1	C1	C6	N2	-0.3(5)
N1	C8	N3	Co1	0.3(4)

N2	C7	C8	N1	-2.0(4)
N2	C7	C8	N3	178.2(3)
N2	C7	C9	N4	0.7(5)
N2	C7	C9	O3	180.0(3)
N3	C8	N1	C1	-179.0(3)
N3	C8	N1	O1	2.6(4)
N3	Co1	N5	C10	-113.4(3)
N3	Co1	N5	C14	56.7(3)
N3	Co1	N7	C15	-49.3(3)
N3	Co1	N7	C19	123.9(3)
N3	Co1	N10	C25	135.0(2)
N3	Co1	N10	C29	-31.2(2)
N3	Co1	O1	N1	3.25(19)
N5	C10	C11	C12	1.1(5)
N5	C14	N6	C15	33.6(5)
N5	Co1	N3	C8	87.3(2)
N5	Co1	N7	C15	37.9(3)
N5	Co1	N7	C19	-148.9(3)
N5	Co1	N8	C20	35.3(3)
N5	Co1	N8	C24	-138.9(2)
N5	Co1	O1	N1	-84.04(19)
N6	C14	N5	C10	179.8(3)
N6	C14	N5	Co1	9.4(4)
N6	C15	C16	C17	-176.6(3)
N6	C15	N7	C19	173.6(3)
N6	C15	N7	Co1	-13.0(4)
N7	C15	C16	C17	2.9(5)
N7	C15	N6	C14	-31.5(5)
N7	Co1	N3	C8	177.7(2)

N7	Co1	N5	C10	153.6(3)
N7	Co1	N5	C14	-36.3(3)
N7	Co1	N8	C20	-55.5(3)
N7	Co1	N8	C24	130.4(2)
N7	Co1	N10	C25	-132.0(2)
N7	Co1	N10	C29	61.8(2)
N8	C20	C21	C22	1.0(5)
N8	C24	N9	C25	-27.8(5)
N8	Co1	N5	C10	61.4(3)
N8	Co1	N5	C14	-128.5(2)
N8	Co1	N7	C15	131.3(3)
N8	Co1	N7	C19	-55.5(3)
N8	Co1	N10	C25	-39.8(2)
N8	Co1	N10	C29	153.9(2)
N8	Co1	O1	N1	-177.39(19)
N9	C24	N8	C20	173.4(3)
N9	C24	N8	Co1	-12.3(4)
N9	C25	C26	C27	177.8(3)
N9	C25	N10	C29	-176.0(3)
N9	C25	N10	Co1	17.6(4)
N10	C25	C26	C27	-1.0(5)
N10	C25	N9	C24	24.8(5)
N10	Co1	N3	C8	-89.4(2)
N10	Co1	N7	C15	-139.2(2)
N10	Co1	N7	C19	34.0(3)
N10	Co1	N8	C20	-148.4(2)
N10	Co1	N8	C24	37.4(3)
N10	Co1	O1	N1	93.23(19)
O1	Co1	N3	C8	-2.1(2)

O1	Co1	N5	C10	-29.1(2)
O1	Co1	N5	C14	141.1(2)
O1	Co1	N8	C20	124.4(2)
O1	Co1	N8	C24	-49.8(2)
O1	Co1	N10	C25	50.7(2)
O1	Co1	N10	C29	-115.6(2)
C30	C31	C32	C33	174.7(9)
C30A	C31A	C32A	C33A	-139(2)
O10	C30	C31	C32	73.1(12)
O10A	C30A	C31A	C32A	95(3)

Table 7 Hydrogen Atom Coordinates ($Å \times 10^4$) and Isotropic Displacement Parameters ($Å^2 \times 10^3$) for phw1109.

Atom	***x***	***y***	***z***	**U(eq)**
H2	6983	1465	2078	39
H3	9084	630	1580	48
H4	9369	-895	982	51
H5	7524	-1582	664	47
H10	4870	3495	1048	31
H11	5423	4243	-654	37
H12	3835	4441	-1658	40
H13	1739	3865	-909	33
H16	-1642	3172	1510	37
H17	-2846	3271	3097	43
H18	-1710	3224	4382	43
H19	588	2927	4069	34
H20	2196	4720	2072	30
H21	2840	6179	2485	36
H22	4249	5832	3657	36
H23	4838	4031	4448	33

H26	4023	571	5724	33
H27	2724	-883	6101	36
H28	1214	-865	5075	35
H29	1135	560	3673	31
H3A	2000.0(4)	1010.0(3)	1890.0(3)	23(12)
H4A	3690.0(5)	-2050.0(4)	610.0(3)	49
H4B	2200.0(5)	-1830.0(4)	760.0(4)	54(17)
H6	505	2695	565	32
H9	4825	2139	4500	27
H30C	412	1413	6173	102
H30D	-265	1839	7166	102
H30A	195	1983	7284	102
H30B	-1076	2756	6966	102
H31C	2100	2052	6565	98
H31D	1704	2967	5633	98
H31A	1325	3094	5630	98
H31B	1171	3438	6664	98
H32C	712	4118	6659	125
H32D	966	3186	7637	125
H32A	-881	4388	5599	125
H32B	-54	4977	6137	125
H33D	2956	4205	6085	134
H33E	3271	3194	6986	134
H33F	2604	4342	7217	134
H33A	1686	3945	4911	134
H33B	1452	5242	4795	134
H33C	636	4668	4265	134
H10B	-1502	2642	6105	165
H10A	-450	1089	6458	166

[RSC Journal Format]

Experimental

Single crystals of $C_{33}H_{35}CoN_{12}O_{10}$ [phw1109] were recrystallised from [solvents] mounted in inert oil and transferred to the cold gas stream of the diffractometer.

Crystal structure determination of [phw1109]

Crystal Data. $C_{33}H_{35}CoN_{12}O_{10}$, M =818.66, triclinic, a = 10.371(2) Å, b = 12.715(3) Å, c = 14.053(3) Å, α = 74.64(2)°, β = 76.945(18)°, γ = 81.408(19)°, U = 1732.9(6) Å^3, T = 110.0, space group P-1 (no. 2), Z = 2, μ(Mo Kα) = 0.574, 11512 reflections measured, 7448 unique (R_{int} = 0.0280) which were used in all calculations. The final $wR(F_2)$ was 0.1558 (all data).

This report has been created with Olex2, compiled on 2011.02.15 svn.r1672. Please let us know if there are any errors or if you would like to have additional featrues.

Crystallographic data for $[Co(tpz)(dpHa)_2](BF_4)_2$

Table 1. Crystal data and structure refinement for phw1008m.

Identification code	phw1008m	
Empirical formula	C27 H25 B2 Co F8 N10 O3	
Formula weight	770.12	
Temperature	110(2) K	
Wavelength	0.71073 Å	
Crystal system	Triclinic	
Space group	P-1	
Unit cell dimensions	a = 10.8037(13) Å	α= 82.644(2)°.
	b = 12.7848(15) Å	β= 68.882(2)°.

	c = 13.1991(16) Å γ = 66.186(2)°.
Volume	1555.5(3) $Å^3$
Z	2
Density (calculated)	1.644 Mg/m^3
Absorption coefficient	0.650 mm^{-1}
F(000)	780
Crystal size	0.29 x 0.24 x 0.22 mm^3
Theta range for data collection	1.65 to 28.33°.
Index ranges	-14<=h<=14, -17<=k<=17, -17<=l<=17
Reflections collected	21600
Independent reflections	7719 [R(int) = 0.0258]
Completeness to theta = 28.33°	99.2 %
Absorption correction	Semi-empirical from equivalents
Max. and min. transmission	0.870 and 0.773
Refinement method	Full-matrix least-squares on F^2
Data / restraints / parameters	7719 / 12 / 525
Goodness-of-fit on F^2	1.045
Final R indices [I>2sigma(I)]	R1 = 0.0372, wR2 = 0.0895
R indices (all data)	R1 = 0.0436, wR2 = 0.0938
Largest diff. peak and hole	0.721 and -0.331 $e.Å^{-3}$

Table 2. Atomic coordinates (x 10^4) and equivalent isotropic displacement parameters ($Å^2$x 10^3) for phw1008m. U(eq) is defined as one third of the trace of the orthogonalized U^{ij} tensor.

	x	y	z	U(eq)
C(1)	11447(2)	5698(1)	6049(1)	17(1)
C(2)	14098(2)	4146(1)	5998(1)	20(1)
C(3)	15457(2)	3333(2)	5945(2)	26(1)
C(4)	15835(2)	3141(2)	6860(2)	28(1)
C(5)	14864(2)	3750(2)	7832(2)	27(1)
C(6)	13533(2)	4567(2)	7891(2)	23(1)
C(7)	13139(2)	4770(1)	6959(1)	19(1)
C(8)	7079(2)	8035(2)	9621(1)	20(1)
C(9)	6582(2)	8307(2)	10703(1)	24(1)
C(10)	7495(2)	8464(2)	11139(1)	26(1)
C(11)	8823(2)	8417(2)	10466(1)	23(1)
C(12)	9240(2)	8197(1)	9351(1)	18(1)
C(13)	10861(2)	8498(1)	7572(1)	18(1)
C(14)	11874(2)	9006(2)	7111(2)	23(1)
C(15)	12155(2)	9317(2)	6046(2)	25(1)
C(16)	11443(2)	9119(2)	5438(1)	22(1)
C(17)	10504(2)	8589(1)	5924(1)	19(1)
C(18)	7118(2)	9396(1)	7219(1)	18(1)
C(19)	6057(2)	10143(2)	6844(1)	20(1)
C(20)	5381(2)	9710(2)	6380(1)	21(1)
C(21)	5761(2)	8550(2)	6350(1)	20(1)
C(22)	6828(2)	7827(1)	6780(1)	17(1)
C(23)	7588(2)	5912(1)	7557(1)	20(1)
C(24)	7233(2)	4945(2)	7777(2)	27(1)
C(25)	7623(2)	4208(2)	8559(2)	30(1)
C(26)	8351(2)	4444(2)	9128(2)	27(1)
C(27)	8700(2)	5387(2)	8858(1)	23(1)
Co(1)	9211(1)	7227(1)	7521(1)	15(1)
N(1)	11846(1)	5555(1)	6937(1)	18(1)
N(2)	13651(2)	4367(1)	5089(1)	19(1)
N(3)	10160(2)	6444(1)	6147(1)	17(1)
N(4)	12386(1)	5105(1)	5094(1)	19(1)
N(5)	10229(1)	8254(1)	6977(1)	17(1)
N(6)	10513(2)	8263(1)	8663(1)	21(1)
N(7)	8418(1)	7936(1)	8948(1)	17(1)

N(8)	7539(1)	8238(1)	7163(1)	16(1)
N(9)	7127(2)	6672(1)	6803(1)	19(1)
N(10)	8347(2)	6110(1)	8062(1)	18(1)
O(1)	10872(1)	6199(1)	7844(1)	19(1)
O(2)	14519(1)	3832(1)	4205(1)	25(1)
B(1)	8631(2)	7464(2)	3636(2)	27(1)
F(1)	9129(2)	6325(1)	3401(2)	70(1)
F(2)	8960(2)	7643(2)	4506(1)	52(1)
F(3)	7144(1)	7921(1)	3888(1)	44(1)
F(4)	9261(2)	8005(1)	2739(1)	38(1)
O(3)	1373(2)	8875(2)	2603(2)	45(1)
B(2A)	3426(10)	8345(8)	9766(7)	33(1)
F(5A)	4427(3)	7244(3)	9829(3)	59(1)
F(6A)	2120(4)	8241(4)	9954(3)	44(1)
F(7A)	3248(3)	9040(3)	10580(2)	60(1)
F(8A)	4084(11)	8676(7)	8808(6)	78(3)
B(2B)	3440(20)	8056(17)	9527(16)	49(4)
F(5B)	3644(8)	7093(6)	9044(8)	123(3)
F(6B)	1974(7)	8772(6)	9803(6)	46(2)
F(7B)	3783(7)	7896(7)	10454(5)	76(3)
F(8B)	3855(16)	8820(8)	8751(8)	38(2)

Table 3. Bond lengths [Å] and angles [°] for phw1008m.

C(1)-N(3)	1.300(2)
C(1)-N(1)	1.356(2)
C(1)-N(4)	1.377(2)

C(2)-C(3)	1.398(2)
C(2)-C(7)	1.401(2)
C(2)-N(2)	1.405(2)
C(3)-C(4)	1.372(3)
C(3)-H(3)	0.9500
C(4)-C(5)	1.407(3)
C(4)-H(4)	0.9500
C(5)-C(6)	1.376(2)
C(5)-H(5)	0.9500
C(6)-C(7)	1.403(2)
C(6)-H(6)	0.9500
C(7)-N(1)	1.360(2)
C(8)-N(7)	1.361(2)
C(8)-C(9)	1.368(2)
C(8)-H(8)	0.9500
C(9)-C(10)	1.394(2)
C(9)-H(9)	0.9500
C(10)-C(11)	1.370(2)
C(10)-H(10)	0.9500
C(11)-C(12)	1.404(2)
C(11)-H(11)	0.9500
C(12)-N(7)	1.345(2)
C(12)-N(6)	1.378(2)
C(13)-N(5)	1.343(2)
C(13)-N(6)	1.377(2)
C(13)-C(14)	1.408(2)
C(14)-C(15)	1.369(3)
C(14)-H(14)	0.9500
C(15)-C(16)	1.397(3)
C(15)-H(15)	0.9500
C(16)-C(17)	1.370(2)
C(16)-H(16)	0.9500
C(17)-N(5)	1.362(2)
C(17)-H(17)	0.9500
C(18)-N(8)	1.365(2)
C(18)-C(19)	1.369(2)
C(18)-H(18)	0.9500
C(19)-C(20)	1.396(2)
C(19)-H(19)	0.9500
C(20)-C(21)	1.372(2)

C(20)-H(20)	0.9500
C(21)-C(22)	1.407(2)
C(21)-H(21)	0.9500
C(22)-N(8)	1.341(2)
C(22)-N(9)	1.377(2)
C(23)-N(10)	1.336(2)
C(23)-N(9)	1.379(2)
C(23)-C(24)	1.404(2)
C(24)-C(25)	1.370(3)
C(24)-H(24)	0.9500
C(25)-C(26)	1.396(3)
C(25)-H(25)	0.9500
C(26)-C(27)	1.373(3)
C(26)-H(26)	0.9500
C(27)-N(10)	1.364(2)
C(27)-H(27)	0.9500
Co(1)-O(1)	1.9059(12)
Co(1)-N(3)	1.9077(14)
Co(1)-N(8)	1.9314(14)
Co(1)-N(7)	1.9361(14)
Co(1)-N(10)	1.9385(14)
Co(1)-N(5)	1.9494(14)
N(1)-O(1)	1.3650(17)
N(2)-O(2)	1.2668(18)
N(2)-N(4)	1.309(2)
N(3)-H(3A)	0.83(2)
N(6)-H(6A)	0.78(2)
N(9)-H(9A)	0.80(2)
B(1)-F(1)	1.367(3)
B(1)-F(2)	1.386(3)
B(1)-F(4)	1.391(2)
B(1)-F(3)	1.393(2)
O(3)-H(3B)	0.87(3)
O(3)-H(3C)	0.82(3)
B(2A)-F(8A)	1.320(12)
B(2A)-F(7A)	1.392(7)
B(2A)-F(6A)	1.400(9)
B(2A)-F(5A)	1.401(10)
B(2B)-F(5B)	1.359(17)
B(2B)-F(7B)	1.371(18)

B(2B)-F(6B)	1.40(2)
B(2B)-F(8B)	1.40(2)

N(3)-C(1)-N(1)	116.24(14)
N(3)-C(1)-N(4)	122.72(15)
N(1)-C(1)-N(4)	121.00(14)
C(3)-C(2)-C(7)	121.04(16)
C(3)-C(2)-N(2)	121.06(16)
C(7)-C(2)-N(2)	117.90(14)
C(4)-C(3)-C(2)	118.78(17)
C(4)-C(3)-H(3)	120.6
C(2)-C(3)-H(3)	120.6
C(3)-C(4)-C(5)	120.31(17)
C(3)-C(4)-H(4)	119.8
C(5)-C(4)-H(4)	119.8
C(6)-C(5)-C(4)	121.52(17)
C(6)-C(5)-H(5)	119.2
C(4)-C(5)-H(5)	119.2
C(5)-C(6)-C(7)	118.49(17)
C(5)-C(6)-H(6)	120.8
C(7)-C(6)-H(6)	120.8
N(1)-C(7)-C(2)	117.28(15)
N(1)-C(7)-C(6)	122.89(15)
C(2)-C(7)-C(6)	119.83(15)
N(7)-C(8)-C(9)	122.68(15)
N(7)-C(8)-H(8)	118.7
C(9)-C(8)-H(8)	118.7
C(8)-C(9)-C(10)	118.71(16)
C(8)-C(9)-H(9)	120.6
C(10)-C(9)-H(9)	120.6
C(11)-C(10)-C(9)	119.38(16)
C(11)-C(10)-H(10)	120.3
C(9)-C(10)-H(10)	120.3
C(10)-C(11)-C(12)	119.14(16)
C(10)-C(11)-H(11)	120.4
C(12)-C(11)-H(11)	120.4
N(7)-C(12)-N(6)	119.86(14)
N(7)-C(12)-C(11)	121.34(15)
N(6)-C(12)-C(11)	118.80(15)
N(5)-C(13)-N(6)	120.11(15)

N(5)-C(13)-C(14)	121.55(15)
N(6)-C(13)-C(14)	118.34(15)
C(15)-C(14)-C(13)	118.97(16)
C(15)-C(14)-H(14)	120.5
C(13)-C(14)-H(14)	120.5
C(14)-C(15)-C(16)	119.64(16)
C(14)-C(15)-H(15)	120.2
C(16)-C(15)-H(15)	120.2
C(17)-C(16)-C(15)	118.55(16)
C(17)-C(16)-H(16)	120.7
C(15)-C(16)-H(16)	120.7
N(5)-C(17)-C(16)	122.71(15)
N(5)-C(17)-H(17)	118.6
C(16)-C(17)-H(17)	118.6
N(8)-C(18)-C(19)	122.51(15)
N(8)-C(18)-H(18)	118.7
C(19)-C(18)-H(18)	118.7
C(18)-C(19)-C(20)	119.09(16)
C(18)-C(19)-H(19)	120.5
C(20)-C(19)-H(19)	120.5
C(21)-C(20)-C(19)	119.03(15)
C(21)-C(20)-H(20)	120.5
C(19)-C(20)-H(20)	120.5
C(20)-C(21)-C(22)	119.24(15)
C(20)-C(21)-H(21)	120.4
C(22)-C(21)-H(21)	120.4
N(8)-C(22)-N(9)	120.17(15)
N(8)-C(22)-C(21)	121.65(15)
N(9)-C(22)-C(21)	118.18(14)
N(10)-C(23)-N(9)	119.87(15)
N(10)-C(23)-C(24)	121.71(16)
N(9)-C(23)-C(24)	118.41(15)
C(25)-C(24)-C(23)	119.26(17)
C(25)-C(24)-H(24)	120.4
C(23)-C(24)-H(24)	120.4
C(24)-C(25)-C(26)	119.16(17)
C(24)-C(25)-H(25)	120.4
C(26)-C(25)-H(25)	120.4
C(27)-C(26)-C(25)	118.88(17)
C(27)-C(26)-H(26)	120.6

C(25)-C(26)-H(26)	120.6
N(10)-C(27)-C(26)	122.35(16)
N(10)-C(27)-H(27)	118.8
C(26)-C(27)-H(27)	118.8
O(1)-Co(1)-N(3)	84.49(5)
O(1)-Co(1)-N(8)	178.34(5)
N(3)-Co(1)-N(8)	94.00(6)
O(1)-Co(1)-N(7)	89.94(5)
N(3)-Co(1)-N(7)	174.40(6)
N(8)-Co(1)-N(7)	91.57(6)
O(1)-Co(1)-N(10)	88.62(6)
N(3)-Co(1)-N(10)	88.77(6)
N(8)-Co(1)-N(10)	90.65(6)
N(7)-Co(1)-N(10)	91.70(6)
O(1)-Co(1)-N(5)	86.88(5)
N(3)-Co(1)-N(5)	89.73(6)
N(8)-Co(1)-N(5)	93.82(6)
N(7)-Co(1)-N(5)	89.37(6)
N(10)-Co(1)-N(5)	175.37(6)
C(1)-N(1)-C(7)	122.27(14)
C(1)-N(1)-O(1)	117.62(13)
C(7)-N(1)-O(1)	120.05(13)
O(2)-N(2)-N(4)	117.49(14)
O(2)-N(2)-C(2)	118.70(14)
N(4)-N(2)-C(2)	123.80(14)
C(1)-N(3)-Co(1)	112.28(11)
C(1)-N(3)-H(3A)	117.4(16)
Co(1)-N(3)-H(3A)	129.9(16)
N(2)-N(4)-C(1)	117.60(14)
C(13)-N(5)-C(17)	118.40(14)
C(13)-N(5)-Co(1)	120.61(11)
C(17)-N(5)-Co(1)	120.18(11)
C(13)-N(6)-C(12)	127.03(14)
C(13)-N(6)-H(6A)	115.2(16)
C(12)-N(6)-H(6A)	115.0(16)
C(12)-N(7)-C(8)	118.22(14)
C(12)-N(7)-Co(1)	120.79(11)
C(8)-N(7)-Co(1)	120.39(11)
C(22)-N(8)-C(18)	118.24(14)
C(22)-N(8)-Co(1)	121.15(11)

C(18)-N(8)-Co(1)	120.44(10)
C(22)-N(9)-C(23)	126.60(14)
C(22)-N(9)-H(9A)	115.0(16)
C(23)-N(9)-H(9A)	113.0(16)
C(23)-N(10)-C(27)	118.50(15)
C(23)-N(10)-Co(1)	120.96(11)
C(27)-N(10)-Co(1)	119.70(11)
N(1)-O(1)-Co(1)	109.04(9)
F(1)-B(1)-F(2)	111.65(19)
F(1)-B(1)-F(4)	109.52(17)
F(2)-B(1)-F(4)	108.13(17)
F(1)-B(1)-F(3)	107.98(18)
F(2)-B(1)-F(3)	109.54(16)
F(4)-B(1)-F(3)	110.02(17)
H(3B)-O(3)-H(3C)	104(3)
F(8A)-B(2A)-F(7A)	109.8(6)
F(8A)-B(2A)-F(6A)	119.5(7)
F(7A)-B(2A)-F(6A)	108.8(6)
F(8A)-B(2A)-F(5A)	102.2(8)
F(7A)-B(2A)-F(5A)	109.3(6)
F(6A)-B(2A)-F(5A)	106.7(6)
F(5B)-B(2B)-F(7B)	115.9(16)
F(5B)-B(2B)-F(6B)	107.7(11)
F(7B)-B(2B)-F(6B)	107.4(14)
F(5B)-B(2B)-F(8B)	111.1(14)
F(7B)-B(2B)-F(8B)	119.0(12)
F(6B)-B(2B)-F(8B)	92.3(14)

Symmetry transformations used to generate equivalent atoms:

Table 4. Anisotropic displacement parameters ($Å^2 x\ 10^3$) for phw1008m. The anisotropic displacement factor exponent takes the form: $-2\pi^2[\ h^2\ a^{*2}U^{11} + ... + 2\ h\ k\ a^*\ b^*\ U^{12}\ ]$

	U^{11}	U^{22}	U^{33}	U^{23}	U^{13}	U^{12}
C(1)	19(1)	17(1)	18(1)	0(1)	-5(1)	-10(1)
C(2)	19(1)	18(1)	27(1)	-1(1)	-9(1)	-9(1)
C(3)	20(1)	19(1)	39(1)	-4(1)	-10(1)	-7(1)
C(4)	22(1)	19(1)	46(1)	4(1)	-18(1)	-8(1)
C(5)	26(1)	27(1)	36(1)	9(1)	-19(1)	-14(1)

C(6)	23(1)	26(1)	24(1)	4(1)	-11(1)	-12(1)
C(7)	18(1)	17(1)	24(1)	2(1)	-9(1)	-8(1)
C(8)	18(1)	22(1)	20(1)	-1(1)	-6(1)	-9(1)
C(9)	20(1)	29(1)	20(1)	-1(1)	-3(1)	-11(1)
C(10)	26(1)	35(1)	17(1)	-4(1)	-6(1)	-10(1)
C(11)	23(1)	30(1)	20(1)	-3(1)	-9(1)	-10(1)
C(12)	18(1)	18(1)	19(1)	0(1)	-7(1)	-6(1)
C(13)	16(1)	19(1)	19(1)	-2(1)	-6(1)	-6(1)
C(14)	18(1)	28(1)	28(1)	-1(1)	-8(1)	-12(1)
C(15)	17(1)	25(1)	31(1)	3(1)	-5(1)	-10(1)
C(16)	18(1)	23(1)	22(1)	3(1)	-5(1)	-6(1)
C(17)	17(1)	19(1)	18(1)	0(1)	-7(1)	-5(1)
C(18)	17(1)	19(1)	17(1)	-2(1)	-4(1)	-8(1)
C(19)	19(1)	17(1)	20(1)	-1(1)	-3(1)	-6(1)
C(20)	17(1)	23(1)	20(1)	2(1)	-6(1)	-6(1)
C(21)	19(1)	26(1)	18(1)	-1(1)	-7(1)	-9(1)
C(22)	16(1)	21(1)	14(1)	-2(1)	-3(1)	-8(1)
C(23)	19(1)	19(1)	19(1)	-2(1)	-4(1)	-8(1)
C(24)	31(1)	26(1)	30(1)	1(1)	-12(1)	-17(1)
C(25)	36(1)	23(1)	35(1)	4(1)	-11(1)	-17(1)
C(26)	32(1)	22(1)	25(1)	5(1)	-9(1)	-10(1)
C(27)	26(1)	24(1)	19(1)	1(1)	-8(1)	-10(1)
Co(1)	15(1)	17(1)	14(1)	-1(1)	-5(1)	-7(1)
N(1)	17(1)	18(1)	17(1)	-1(1)	-6(1)	-6(1)
N(2)	17(1)	18(1)	23(1)	-4(1)	-5(1)	-8(1)
N(3)	19(1)	19(1)	15(1)	-1(1)	-7(1)	-7(1)
N(4)	17(1)	20(1)	20(1)	-3(1)	-5(1)	-7(1)
N(5)	15(1)	18(1)	17(1)	-1(1)	-5(1)	-6(1)
N(6)	19(1)	29(1)	19(1)	-2(1)	-9(1)	-12(1)
N(7)	17(1)	19(1)	16(1)	-1(1)	-5(1)	-8(1)
N(8)	15(1)	18(1)	15(1)	-1(1)	-4(1)	-7(1)
N(9)	21(1)	19(1)	22(1)	-2(1)	-10(1)	-10(1)
N(10)	20(1)	18(1)	18(1)	0(1)	-6(1)	-8(1)
O(1)	18(1)	22(1)	15(1)	-3(1)	-6(1)	-5(1)
O(2)	19(1)	28(1)	25(1)	-12(1)	-3(1)	-8(1)
B(1)	30(1)	24(1)	23(1)	2(1)	-6(1)	-7(1)
F(1)	58(1)	26(1)	96(1)	-5(1)	11(1)	-17(1)
F(2)	44(1)	93(1)	26(1)	12(1)	-20(1)	-28(1)
F(3)	30(1)	61(1)	35(1)	-4(1)	-14(1)	-8(1)
F(4)	58(1)	50(1)	27(1)	13(1)	-21(1)	-37(1)

O(3)	33(1)	39(1)	70(1)	-11(1)	-23(1)	-12(1)
B(2A)	30(2)	49(4)	33(3)	19(3)	-19(2)	-27(3)
F(5A)	42(2)	56(2)	82(2)	29(2)	-32(2)	-22(1)
F(6A)	35(2)	74(3)	38(1)	8(2)	-21(1)	-30(2)
F(7A)	73(2)	101(3)	37(1)	6(1)	-21(1)	-62(2)
F(8A)	77(4)	107(5)	50(3)	37(2)	-14(2)	-53(4)
B(2B)	47(6)	66(11)	55(9)	19(7)	-29(6)	-38(7)
F(5B)	113(6)	64(4)	190(9)	-35(5)	-68(6)	-8(4)
F(6B)	28(2)	64(4)	48(3)	-14(3)	-15(2)	-14(3)
F(7B)	63(4)	122(7)	74(4)	70(4)	-53(3)	-60(4)
F(8B)	65(5)	25(2)	18(3)	7(2)	-7(3)	-19(2)

Table 5. Hydrogen coordinates (x 10^4) and isotropic displacement parameters ($Å^2$x 10^3) for phw1008m.

	x	y	z	U(eq)
H(3)	16107	2922	5288	31
H(4)	16756	2593	6837	33
H(5)	15134	3594	8463	32
H(6)	12895	4984	8548	28
H(8)	6464	7911	9328	24
H(9)	5633	8387	11148	28
H(10)	7199	8602	11897	31
H(11)	9452	8533	10749	28
H(14)	12354	9131	7533	28
H(15)	12831	9665	5722	30
H(16)	11607	9348	4703	27
H(17)	10025	8449	5510	22
H(18)	7578	9695	7530	21
H(19)	5785	10945	6898	24
H(20)	4669	10212	6089	25
H(21)	5310	8238	6043	24
H(24)	6727	4803	7387	32
H(25)	7402	3545	8713	36
H(26)	8601	3959	9692	32
H(27)	9206	5542	9239	27
H(3A)	9910(20)	6563(19)	5600(19)	30(6)

H(6A)	10970(20)	8365(18)	8950(18)	24(5)
H(9A)	6690(20)	6480(19)	6535(18)	24(5)
H(3B)	1800(30)	8880(30)	1910(30)	54
H(3C)	740(30)	8640(20)	2670(20)	54

Table 6. Torsion angles [°] for phw1008m.

C(7)-C(2)-C(3)-C(4)	1.0(3)
N(2)-C(2)-C(3)-C(4)	-179.27(16)
C(2)-C(3)-C(4)-C(5)	0.2(3)
C(3)-C(4)-C(5)-C(6)	-1.4(3)
C(4)-C(5)-C(6)-C(7)	1.4(3)
C(3)-C(2)-C(7)-N(1)	179.10(15)
N(2)-C(2)-C(7)-N(1)	-0.6(2)
C(3)-C(2)-C(7)-C(6)	-1.1(3)
N(2)-C(2)-C(7)-C(6)	179.20(15)
C(5)-C(6)-C(7)-N(1)	179.71(16)
C(5)-C(6)-C(7)-C(2)	-0.1(3)
N(7)-C(8)-C(9)-C(10)	-1.4(3)
C(8)-C(9)-C(10)-C(11)	4.3(3)
C(9)-C(10)-C(11)-C(12)	-0.8(3)
C(10)-C(11)-C(12)-N(7)	-5.7(3)
C(10)-C(11)-C(12)-N(6)	173.64(17)
N(5)-C(13)-C(14)-C(15)	3.8(3)
N(6)-C(13)-C(14)-C(15)	-175.47(16)
C(13)-C(14)-C(15)-C(16)	-0.4(3)
C(14)-C(15)-C(16)-C(17)	-1.7(3)
C(15)-C(16)-C(17)-N(5)	0.5(3)
N(8)-C(18)-C(19)-C(20)	-0.3(2)
C(18)-C(19)-C(20)-C(21)	2.4(2)
C(19)-C(20)-C(21)-C(22)	-0.4(2)
C(20)-C(21)-C(22)-N(8)	-3.8(2)
C(20)-C(21)-C(22)-N(9)	175.99(15)
N(10)-C(23)-C(24)-C(25)	2.6(3)
N(9)-C(23)-C(24)-C(25)	-176.98(17)
C(23)-C(24)-C(25)-C(26)	0.7(3)
C(24)-C(25)-C(26)-C(27)	-2.3(3)
C(25)-C(26)-C(27)-N(10)	0.8(3)
N(3)-C(1)-N(1)-C(7)	177.25(15)
N(4)-C(1)-N(1)-C(7)	-4.8(2)
N(3)-C(1)-N(1)-O(1)	0.1(2)
N(4)-C(1)-N(1)-O(1)	178.01(13)
C(2)-C(7)-N(1)-C(1)	3.6(2)
C(6)-C(7)-N(1)-C(1)	-176.23(16)
C(2)-C(7)-N(1)-O(1)	-179.30(14)

C(6)-C(7)-N(1)-O(1)	0.9(2)
C(3)-C(2)-N(2)-O(2)	-1.6(2)
C(7)-C(2)-N(2)-O(2)	178.13(14)
C(3)-C(2)-N(2)-N(4)	179.03(15)
C(7)-C(2)-N(2)-N(4)	-1.2(2)
N(1)-C(1)-N(3)-Co(1)	4.09(18)
N(4)-C(1)-N(3)-Co(1)	-173.80(12)
O(1)-Co(1)-N(3)-C(1)	-5.05(12)
N(8)-Co(1)-N(3)-C(1)	175.65(12)
N(7)-Co(1)-N(3)-C(1)	1.1(7)
N(10)-Co(1)-N(3)-C(1)	-93.78(12)
N(5)-Co(1)-N(3)-C(1)	81.84(12)
O(2)-N(2)-N(4)-C(1)	-179.19(14)
C(2)-N(2)-N(4)-C(1)	0.2(2)
N(3)-C(1)-N(4)-N(2)	-179.42(15)
N(1)-C(1)-N(4)-N(2)	2.8(2)
N(6)-C(13)-N(5)-C(17)	174.32(15)
C(14)-C(13)-N(5)-C(17)	-4.9(2)
N(6)-C(13)-N(5)-Co(1)	-16.0(2)
C(14)-C(13)-N(5)-Co(1)	164.80(13)
C(16)-C(17)-N(5)-C(13)	2.8(2)
C(16)-C(17)-N(5)-Co(1)	-166.97(13)
O(1)-Co(1)-N(5)-C(13)	-49.07(12)
N(3)-Co(1)-N(5)-C(13)	-133.57(13)
N(8)-Co(1)-N(5)-C(13)	132.43(12)
N(7)-Co(1)-N(5)-C(13)	40.90(12)
N(10)-Co(1)-N(5)-C(13)	-62.6(7)
O(1)-Co(1)-N(5)-C(17)	120.46(12)
N(3)-Co(1)-N(5)-C(17)	35.96(12)
N(8)-Co(1)-N(5)-C(17)	-58.03(12)
N(7)-Co(1)-N(5)-C(17)	-149.56(12)
N(10)-Co(1)-N(5)-C(17)	106.9(7)
N(5)-C(13)-N(6)-C(12)	-26.2(3)
C(14)-C(13)-N(6)-C(12)	153.02(17)
N(7)-C(12)-N(6)-C(13)	25.2(3)
C(11)-C(12)-N(6)-C(13)	-154.12(17)
N(6)-C(12)-N(7)-C(8)	-170.85(15)
C(11)-C(12)-N(7)-C(8)	8.5(2)
N(6)-C(12)-N(7)-Co(1)	18.0(2)
C(11)-C(12)-N(7)-Co(1)	-162.65(13)

C(9)-C(8)-N(7)-C(12)	-4.9(3)
C(9)-C(8)-N(7)-Co(1)	166.24(14)
O(1)-Co(1)-N(7)-C(12)	44.94(13)
N(3)-Co(1)-N(7)-C(12)	38.8(7)
N(8)-Co(1)-N(7)-C(12)	-135.75(13)
N(10)-Co(1)-N(7)-C(12)	133.56(13)
N(5)-Co(1)-N(7)-C(12)	-41.94(13)
O(1)-Co(1)-N(7)-C(8)	-126.00(13)
N(3)-Co(1)-N(7)-C(8)	-132.1(6)
N(8)-Co(1)-N(7)-C(8)	53.31(13)
N(10)-Co(1)-N(7)-C(8)	-37.38(13)
N(5)-Co(1)-N(7)-C(8)	147.12(13)
N(9)-C(22)-N(8)-C(18)	-173.98(14)
C(21)-C(22)-N(8)-C(18)	5.8(2)
N(9)-C(22)-N(8)-Co(1)	10.8(2)
C(21)-C(22)-N(8)-Co(1)	-169.40(12)
C(19)-C(18)-N(8)-C(22)	-3.8(2)
C(19)-C(18)-N(8)-Co(1)	171.49(12)
O(1)-Co(1)-N(8)-C(22)	27.1(19)
N(3)-Co(1)-N(8)-C(22)	52.03(13)
N(7)-Co(1)-N(8)-C(22)	-128.50(12)
N(10)-Co(1)-N(8)-C(22)	-36.78(12)
N(5)-Co(1)-N(8)-C(22)	142.02(12)
O(1)-Co(1)-N(8)-C(18)	-148.0(18)
N(3)-Co(1)-N(8)-C(18)	-123.09(12)
N(7)-Co(1)-N(8)-C(18)	56.38(12)
N(10)-Co(1)-N(8)-C(18)	148.10(12)
N(5)-Co(1)-N(8)-C(18)	-33.10(12)
N(8)-C(22)-N(9)-C(23)	30.6(2)
C(21)-C(22)-N(9)-C(23)	-149.17(16)
N(10)-C(23)-N(9)-C(22)	-28.2(2)
C(24)-C(23)-N(9)-C(22)	151.46(17)
N(9)-C(23)-N(10)-C(27)	175.42(15)
C(24)-C(23)-N(10)-C(27)	-4.2(2)
N(9)-C(23)-N(10)-Co(1)	-15.1(2)
C(24)-C(23)-N(10)-Co(1)	165.33(13)
C(26)-C(27)-N(10)-C(23)	2.5(2)
C(26)-C(27)-N(10)-Co(1)	-167.16(14)
O(1)-Co(1)-N(10)-C(23)	-139.47(13)
N(3)-Co(1)-N(10)-C(23)	-54.96(13)

N(8)-Co(1)-N(10)-C(23)	39.04(13)
N(7)-Co(1)-N(10)-C(23)	130.62(13)
N(5)-Co(1)-N(10)-C(23)	-126.0(7)
O(1)-Co(1)-N(10)-C(27)	29.91(13)
N(3)-Co(1)-N(10)-C(27)	114.43(13)
N(8)-Co(1)-N(10)-C(27)	-151.58(13)
N(7)-Co(1)-N(10)-C(27)	-59.99(13)
N(5)-Co(1)-N(10)-C(27)	43.4(8)
C(1)-N(1)-O(1)-Co(1)	-4.13(16)
C(7)-N(1)-O(1)-Co(1)	178.64(12)
N(3)-Co(1)-O(1)-N(1)	4.84(10)
N(8)-Co(1)-O(1)-N(1)	29.8(19)
N(7)-Co(1)-O(1)-N(1)	-174.56(10)
N(10)-Co(1)-O(1)-N(1)	93.73(10)
N(5)-Co(1)-O(1)-N(1)	-85.18(10)

Symmetry transformations used to generate equivalent atoms:

Table 7. Hydrogen bonds for phw1008m [Å and °].

D-H...A	d(D-H)	d(H...A)	d(D...A)	<(DHA)
N(3)-H(3A)...F(2)	0.83(2)	2.11(2)	2.8802(19)	153(2)
N(6)-H(6A)...F(6B)#1	0.78(2)	2.05(2)	2.822(7)	174(2)
N(6)-H(6A)...F(6A)#1	0.78(2)	2.07(2)	2.828(4)	164(2)
N(9)-H(9A)...O(2)#2	0.80(2)	2.06(2)	2.8639(19)	174(2)
O(3)-H(3B)...F(7A)#3	0.87(3)	1.94(3)	2.753(3)	156(3)
O(3)-H(3B)...F(7B)#3	0.87(3)	2.30(3)	3.057(8)	145(3)
O(3)-H(3C)...F(4)#4	0.82(3)	2.04(3)	2.860(2)	177(3)

Symmetry transformations used to generate equivalent atoms:

#1 x+1,y,z #2 -x+2,-y+1,-z+1 #3 x,y,z-1 #4 x-1,y,z